

BioMed Research International

Biologic Activity and Biotechnological Development of Natural Products 2014

Guest Editors: José Carlos Tavares Carvalho, Fabio Ferreira Perazzo,
Leandro Rocha, and Didier Bereau





**Biologic Activity and Biotechnological
Development of Natural Products 2014**

BioMed Research International

Biologic Activity and Biotechnological Development of Natural Products 2014

Guest Editors: José Carlos Tavares Carvalho,
Fabio Ferreira Perazzo, Leandro Rocha,
and Didier Bereau



Copyright © 2014 Hindawi Publishing Corporation. All rights reserved.

This is a special issue published in “BioMed Research International.” All articles are open access articles distributed under the Creative Commons Attribution License, which permits unrestricted use, distribution, and reproduction in any medium, provided the original work is properly cited.

Contents

Antioxidant Properties of Mushroom Mycelia Obtained by Batch Cultivation and Tocopherol Content Affected by Extraction Procedures, Emanuel Vamanu

Volume 2014, Article ID 974804, 8 pages

Plant-Derived Antimicrobials Reduce *E. coli* O157:H7 Virulence Factors Critical for Colonization in Cattle Gastrointestinal Tract *In Vitro*, Sangeetha Ananda Baskaran and Kumar Venkitanarayanan

Volume 2014, Article ID 212395, 10 pages

Antibacterial Activity of Leaf Extracts of *Baeckea frutescens* against Methicillin-Resistant *Staphylococcus aureus*, Somayeh Razmavar, Mahmood Ameen Abdulla,

Salmah Binti Ismail, and Pouya Hassandarvish

Volume 2014, Article ID 521287, 5 pages

Jacobsen Catalyst as a Cytochrome P450 Biomimetic Model for the Metabolism of Monensin A,

Bruno Alves Rocha, Anderson Rodrigo Moraes de Oliveira, Murilo Pazin, Daniel Junqueira Dorta, Andresa Piacezzi Nascimento Rodrigues, Andresa Aparecida Berretta, Ana Paula Ferranti Peti, Luiz Alberto Beraldo de Moraes, Norberto Peoporine Lopes, Stanislav Pospíšil, Paul Jonathan Gates, and Marilda das Dores Assis

Volume 2014, Article ID 152102, 8 pages

Glioprotective Effects of Ashwagandha Leaf Extract against Lead Induced Toxicity, Praveen Kumar, Raghavendra Singh, Arshed Nazmi, Dinesh Lakhanpal, Hardeep Kataria, and Gurcharan Kaur

Volume 2014, Article ID 182029, 15 pages

Production and Enhancement of Omega-3 Fatty Acid from *Mortierella alpina* CFR-GV15: Its Food and Therapeutic Application, Ganesan Vadivelan and Govindarajulu Venkateswaran

Volume 2014, Article ID 657414, 9 pages

Potent Protein Glycation Inhibition of Plantagosome in *Plantago major* Seeds, Nobuyasu Matsuura, Tadashi Aradate, Chihiro Kurosaka, Makoto Ubukata, Shiho Kittaka, Yuri Nakaminami, Kanae Gamo, Hiroyuki Kojima, and Mitsuharu Ohara

Volume 2014, Article ID 208539, 5 pages

Watermelon (*Citrullus lanatus* (Thunb.) Matsum. and Nakai) Juice Modulates Oxidative Damage Induced by Low Dose X-Ray in Mice, Mohd Khairul Amran Mohammad, Muhamad Idham Mohamed, Ainul Mardhiyah Zakaria, Hairil Rashmizal Abdul Razak, and Wan Mazlina Md. Saad

Volume 2014, Article ID 512834, 6 pages

***In Vivo* Antistress and Antioxidant Effects of Fermented and Germinated Mung Bean**, Swee Keong Yeap, Boon Kee Beh, Norlaily Mohd Ali, Hamidah Mohd Yusof, Wan Yong Ho, Soo Peng Koh, Noorjahan Banu Alitheen, and Kamariah Long

Volume 2014, Article ID 694842, 6 pages

A Review on Antibacterial, Antiviral, and Antifungal Activity of Curcumin,

Soheil Zorofchian Moghadamtousi, Habsah Abdul Kadir, Pouya Hassandarvish, Hassan Tajik, Sazaly Abubakar, and Keivan Zandi

Volume 2014, Article ID 186864, 12 pages

The Interaction Pattern between a Homology Model of 40S Ribosomal S9 Protein of *Rhizoctonia solani* and 1-Hydroxyphenazine by Docking Study, Seema Dharni, Sanchita, Abdul Samad, Ashok Sharma, and Dharani Dhar Patra

Volume 2014, Article ID 682946, 6 pages

Biodegradation and Utilization of Organophosphorus Pesticide Malathion by Cyanobacteria,

Wael M. Ibrahim, Mohamed A. Karam, Reda M. El-Shahat, and Asmaa A. Adway

Volume 2014, Article ID 392682, 6 pages

Production and Cytotoxicity of Extracellular Insoluble and Droplets of Soluble Melanin by *Streptomyces*

lusitanus DMZ-3, D. N. Madhusudhan, Bi Bi Zainab Mazhari, Syed G. Dastager, and Dayanand Agsar

Volume 2014, Article ID 306895, 11 pages

In Vitro and In Vivo Leishmanicidal Activity of *Astronium fraxinifolium* (Schott) and *Plectranthus amboinicus* (Lour.) Spreng against *Leishmania* (*Viannia*) *braziliensis*,

Silvio César Gomes de Lima, Maria Jania Teixeira, José Evaldo Gonçalves Lopes Júnior, Selene Maia de Morais, Alba Fabiola Torres,

Milena Aguiar Braga, Raphael Oliveira Rodrigues, Gilvandete Maria Pinheiro Santiago,

Alice Costa Martins, and Aparecida Tiemi Nagao-Dias

Volume 2014, Article ID 848293, 7 pages

Biologic Propensities and Phytochemical Profile of *Vangueria madagascariensis* J. F. Gmelin (Rubiaceae): An Underutilized Native Medicinal Food Plant from Africa,

Nelvana Ramalingum and M. Fawzi Mahomoodally

Volume 2014, Article ID 681073, 15 pages

***Arrabidaea chica* Hexanic Extract Induces Mitochondrion Damage and Peptidase Inhibition on**

Leishmania spp., Igor A. Rodrigues, Mariana M. B. Azevedo, Francisco C. M. Chaves, Celuta S. Alviano,

Daniela S. Alviano, and Alane B. Vermelho

Volume 2014, Article ID 985171, 7 pages

Antioxidant Activity of Essential Oil and Extracts of *Valeriana jatamansi* Roots,

Sakshima Thusoo, Sahil Gupta, Rasleen Sudan, Jaspreet Kour, Sahil Bhagat, Rashid Hussain, and Madhulika Bhagat

Volume 2014, Article ID 614187, 4 pages

Antioxidants, Phytochemicals, and Cytotoxicity Studies on *Phaleria macrocarpa* (Scheff.) Boerl Seeds,

Ma Ma Lay, Saiful Anuar Karsani, Behrooz Banisalam, Sadegh Mohajer, and Sri Nurestri Abd Malek

Volume 2014, Article ID 410184, 13 pages

Mitogenic Effects of Phosphatidylcholine Nanoparticles on MCF-7 Breast Cancer Cells,

Yamila B. Gándola, Sebastián E. Pérez, Pablo E. Irene, Ana I. Sotelo, Johanna G. Miquet,

Gerardo R. Corradi, Adriana M. Carlucci, and Lorena Gonzalez

Volume 2014, Article ID 687037, 13 pages

Chemical Constituents from the Fruits of *Forsythia suspensa* and Their Antimicrobial Activity,

Ping-Chung Kuo, Guo-Feng Chen, Mei-Lin Yang, Ya-Hua Lin, and Chi-Chung Peng

Volume 2014, Article ID 304830, 7 pages

Antioxidant Activity of Extract and Its Major Constituents from Okra Seed on Rat Hepatocytes Injured by Carbon Tetrachloride,

Lianmei Hu, Wenlan Yu, Ying Li, Nagendra Prasad, and Zhaoxin Tang

Volume 2014, Article ID 341291, 9 pages

Research Article

Antioxidant Properties of Mushroom Mycelia Obtained by Batch Cultivation and Tocopherol Content Affected by Extraction Procedures

Emanuel Vamanu

Department of Industrial Biotechnology, University of Agronomical Sciences and Veterinary Medicine Bucharest, Faculty of Biotechnology, 59 Marasti Boulevard, 011464 Bucharest, Romania

Correspondence should be addressed to Emanuel Vamanu; email@emanuelvamanu.ro

Received 7 February 2014; Revised 21 June 2014; Accepted 25 June 2014; Published 10 July 2014

Academic Editor: Didier Bereau

Copyright © 2014 Emanuel Vamanu. This is an open access article distributed under the Creative Commons Attribution License, which permits unrestricted use, distribution, and reproduction in any medium, provided the original work is properly cited.

The determination of the antioxidant potential of lyophilized mushroom mycelia from 5 strains of the species *Pleurotus ostreatus* and *Coprinus comatus* (obtained by submerged cultivation in batch system) was analyzed as ethanolic extracts by evaluating ABTS and the hydroxyl scavenging activity, FRAP method, the chelating capacity, the inhibition of human erythrocyte hemolysis, and the inhibition of xanthine oxidase activity. The main compounds present in all extracts were determined by HPLC chromatography. Overall, results demonstrated that the biologically active substances content is modulated by the extraction method used. The most beneficial extract, characterized by determining the EC_{50} value, was that of *C. comatus* M8102, followed by *P. ostreatus* PQMZ91109. Significant amount of α -tocopherol (179.51 ± 1.51 mg/100 g extract) was determined as well as flavones such as rutin and apigenin. In the *P. ostreatus* PQMZ91109 extract, 4.8 ± 0.05 mg/100 g extract of tocopherol acetate known to play a significant role as an antioxidant in skin protection against oxidative stress generated by UV rays was determined. The various correlations ($r^2 = 0.7665$ – 0.9426 for tocopherol content) assessed and the composition of extracts in fluidized bed from the mycelia of the tested species depicted a significant pharmacological potential as well as the possibility of usage in the development of new functional products.

1. Introduction

Medicinal mushrooms are an effective alternative in the prevention and treatment of many modern diseases. *P. ostreatus* and *C. comatus* are used as a food source; however, due to their high content in therapeutic biomolecules, *P. ostreatus* and *C. comatus* are also a source of biologically active compounds. Fungal mycelia can easily be acquired in sufficient quantities by fermentation. Due to an increase in demand for the extraction of bioactive molecules in order to produce biologically active supplements, the determination of an effective and efficient method of extraction is thus required. The submerged cultivation method is an acceptable method; however increased efficiency is very important. The extractive efficiency depends mainly on the species used, on the nutrient sources in the culture medium, and on the cultivation parameters [1].

Mycelia extracts prevent free radical attack known to initiate membrane lipid peroxidation, resulting in an overall

increased ability in defense against cellular malignization. Free radicals react with various molecules at the cellular level via oxidative stress and, as a result, bring about a perturbation of the normal cellular cycle. Free radicals are also known to accelerate the aging process, therefore disrupting various known natural defense mechanisms. Thus, taking supplements with such extracts is an alternative means against oxidative stress [2]. In addition, the presence of tocopherols is shown to be associated with the protection of low density lipoproteins (LDL) against oxidative stress. Oxidized LDL has been correlated with high plasma cholesterol levels [3]. Thus, the use of this mycelia extract may offer protection against the risk of developing cardiovascular disease, preventing atherosclerosis, and ultimately eliminating the risk of developing myocardial infarction.

Fungal fermentation in liquid medium ensures a high uniform quantitative biomass production as well as a high biological value, thus representing an alternative means to

obtaining the various potential medicinal products. The fermentation technology has a role in maximizing the production of biomass and the level of biologically active components it contains [4]. *In vitro* antioxidant activity has been correlated with phenolic components (i.e., amounts of anthocyanins and of tocopherols) [5]. The phenolic concentrations of the extracts depend on the species used, on the method used in obtaining the extracts (the process of extraction and conditioning), and on the evaluation method [6]. As a large amount of tocopherols was identified following the fluidized bed extraction from dried fruit bodies of the oyster mushroom (data not yet published), a similar amount is expected in the same type of extract from the mycelia of the *P. ostreatus* species. Thus, the aim of this study was to assess the antioxidant activity of lyophilized mycelia (submitted to extraction in fluidized bed) from 5 strains of *P. ostreatus* and *C. comatus* and to both correlate and identify the key molecules (by HPLC chromatographic analysis), which determine these antioxidative activities. The mycelium of each species was obtained by submerged cultivation in a batch system.

2. Materials and Methods

2.1. Chemicals. All chemicals and reagents were purchased from Sigma Aldrich GmbH (Steinheim, Germany). All other unlabelled chemicals and reagents were of analytical grade [7].

2.2. Microorganism, Media, Fermentations Conditions, and Fluidized Bed Extraction Process. Mushrooms belonging to *P. ostreatus* PQMZ91109, *Pleurotus ostreatus* PBS281009, *P. ostreatus* PSI101109, *P. ostreatus* M2191, and *C. comatus* M8102 were obtained from the collection of the Faculty of Biotechnology, Bucharest, Romania. The mycelia were kept in Nalgene cryotubes grown on barley grains, in 20% glycerol, at -80°C . The mycelia were revitalized on the medium of potato dextrose agar (PDA) at 4°C . The inoculum was prepared by growing the mushrooms on a LabTech rotary shaker at 150 rpm, for five days, at 25°C , in 500 mL Erlenmeyer flasks containing 250 mL of the culture medium containing 6.0 g glucose, 100.0 g malt extract, 20.0 g yeast extract, 1.0 g KH_2PO_4 , and 0.5 g $\text{MgSO}_4 \times 7\text{H}_2\text{O}$, per liter. The medium was adjusted to a pH of 5.5 with 0.2 M NaOH [6, 7].

The second inoculum was performed in a 500 mL flask containing 300 mL of the medium after inoculating with 10% (v/v) of the first inoculum culture under the conditions described above. The fermentation medium (KH_2PO_4 0.2%, CaSO_4 0.5%, MgSO_4 0.05%, Na_2HPO_4 0.01%, and corn extract (dry substance 40%, as nitrogen source) 1% in 5% solution of corn starch) was inoculated with 10% (v/v) of the second inoculum culture and then cultivated in a 5-L New Brunswick BioFlo 310 bioreactor. Fermentations were conducted under the following conditions: temperature 25°C , aeration rate 1 vvm, agitation speed 150 rpm, pH 5.5–6, and working volume 4 L. The inoculum culture was then

transferred to the fermentation medium and cultivated for 10 days [7].

The mycelium was recovered from the liquid medium by centrifugation at $4000 \times g$ (Centurion C2041 centrifuge) for 15 min. Next, the obtained mycelia were washed 3 times with distilled water and freeze-dried in an Alpha 1-2 LD freeze-dryer in the absence of a cryoprotective agent [6].

A quantity consisting of 50 g of the freeze-dried mycelia and 150 mL ethanol 70% was used to generate an extract using a fluidized bed extractor (fexIKA 200, IKA Labortechnik), after two extraction cycles. The alcohol extracts were concentrated in a rotary evaporator (Buchi R 210) with vacuum controller at 50°C , 175 mbar, and 200 rpm. The elected concentrated solution was freeze-dried in a Martin Christ Alpha 1-2 LD, to obtain the solid substance. The dried fractions were then redissolved in 80% ethanol to yield solutions containing 0.2–1.0 mg of extract per mL [8].

2.3. Antioxidant Activity Determinations

2.3.1. ABTS (2,2'-Azino-bis(3-ethylbenzothiazoline-6-sulphonic Acid)) Radical Scavenging Activity. Radical scavenging assay ABTS radical cations are produced by reacting ABTS (7 mM) and potassium persulfate (2.45 mM) on incubating the mixture at room temperature in darkness for 16 h. The solution thus obtained was further diluted with phosphate buffered saline to give an absorbance of 1.000. Different concentrations of the extracts (0.2–1 mg/mL), 50 μL , were added to 950 μL of the ABTS working solution to give a final volume of 1 mL. The absorbance was recorded immediately at 734 nm with the Helios λ spectrophotometer. The percentage of inhibition was calculated with the following equation: % inhibition = [(Absorbance of control – Absorbance of test sample)/Absorbance control] \times 100. Ascorbic acid was used as standard [9].

2.3.2. Determination of Hydroxyl Radical Scavenging Activity. Quantities consisting of 0.2 mL of 0.1 mM $\text{FeSO}_4/0.1$ mM EDTA-2Na, 0.2 mL 2-deoxyribose (10 mM), 0.2 mL sample (different concentration 0.2–1 mg/mL), and 1.2 mL phosphate buffer (0.1 M; pH 7.4) were mixed. After the addition of 0.2 mL H_2O_2 (10 mM), the mixture was incubated at 37°C for 4 h, and the reaction stopped by addition of a 1 mL trichloroacetic acid (2.8%) solution. Thiobarbituric acid/50 mM NaOH (1%; 1 mL) was then added and the mixtures heated at 100°C for 10 min, followed by rapid cooling and measurement of OD_{532} [10].

2.3.3. Ferrous Ion Chelating Activity. To determine the Fe ion chelating ability, first, 1 mL of each polysaccharide (0.2–1 mg/mL) was mixed with 3.7 mL of ultrapure water, following which the mixture was reacted with ferrous chloride (2 mmol/L, 0.1 mL) and ferrozine (5 mmol/L, 0.2 mL) for 20 min. The absorbance at 562 nm was determined spectrophotometrically. EDTA was used as positive control. The chelating activity on the ferrous ion was calculated using the following equation: Chelating Activity (%) = [(Ab – As)/Ab] \times 100, where Ab is the absorbance of the blank without the

sample or ascorbic acid and A_s is the absorbance in the presence of the extract or EDTA [7, 11].

2.3.4. Inhibition of Human Erythrocyte Hemolysis. The capacity to inhibit human erythrocyte hemolysis was based on the method described by Barros et al., 2007 [12]. Blood was obtained by harvesting from the first author. Blood tubes were immediately centrifuged at 3000 rpm for 10 min in a cooled Heidolff 320R centrifuge, with cooling at 9°C. The sediment was washed three times with 0.9% NaCl, and the reunited final sediments were brought into a 10% solution in 7.4 phosphate buffer [13]. The reaction mixture consisted of 0.1 mL of 10% human erythrocytes suspension, 0.2 mL of 200 mL 2,2'-azo-bis(2-amidinopropane) dihydrochloride, and 0.1 mL sample of extract (0.2–1 mg/mL). Test tubes were maintained at 37°C for 3 h. For dilution, 8 mL phosphate buffer pH 7.4 was added and each sample was centrifuged at 3000 rpm for 10 min. Finally, absorbance was read at 540 nm, and the inhibition of human erythrocyte hemolysis was calculated following the equation $[(A_C - A_S)/A_C] \times 100$, where A_C represents the absorbance of the control sample without extract and A_S is the absorbance of the sample containing the extract. TBHQ was used as standard. The EC_{50} value (mg extract/mL), that is, the effective concentration at which the inhibition of human erythrocyte hemolysis is 50%, was obtained [14].

2.3.5. Ferric Reducing Antioxidant Power (FRAP) Assay. The FRAP reagent was prepared by adding 2.5 ml of 10 mM TPTZ into 40 mM HCl. After dissolving TPTZ in HCl, 2.5 ml of 20 mM $FeCl_3$ was added and 25 ml of 0.3 M acetate buffer pH 3.6. Then, approximately 3 ml of the FRAP reagent was added to 100 μ L of mushroom extract and 300 μ L of distilled water. The absorbance was measured at 593 nm against the blank after 4 minutes. FRAP value was calculated and expressed as mM Fe^{2+} equivalent (FE) per 100 g sample using the calibration curve of Fe^{2+} [15].

2.4. Xanthine Oxidase Inhibition Assay. Xanthine oxidase activity was determined by measuring the formation of uric acid from xanthine. All extracts were prepared in 50 mM phosphate buffer solution (pH 7.0). 2 mL of the sample was mixed with solution containing xanthine oxidase (2 mL, 0.4 U/mL) and xanthine (100 μ M). After incubating at room temperature (24°C) for 3 minutes, uric acid production was determined by measuring the absorbance at 295 nm. The inhibition percentage of xanthine oxidase activity was calculated according to the formula $[(A_{control} - A_{sample})/A_{control}] \times 100\%$ [16].

2.5. Determination of Antioxidant Component

2.5.1. Determination of Total Phenolic Content. The content of total phenols was determined by spectrophotometry, using gallic acid as standard, according to the method described by the International Organization for Standardization (ISO) 14502-1. Briefly, an aliquot of the diluted sample extract (1.0 mL) was transferred in duplicate to separate tubes

containing a 1/10 dilution of Folin-Ciocalteu's reagent in water (5.0 mL). Then, a sodium carbonate solution (4.0 mL, 7.5% w/v) was added. The tubes were then allowed to stand at room temperature for 60 min before absorbance at 765 nm was measured against water. The content of total phenols was expressed as mg/g biomass. The concentration of polyphenols in samples was derived from a standard curve of gallic acid ranging from 10 to 50 μ g/mL (Pearson's correlation coefficient: $r^2 = 0.9996$) [6, 17].

2.5.2. Determination of Total Flavonoids. Sample (0.25 mL of the extracts) was added to a tube containing distilled water (1 mL). Next, 5% $NaNO_2$ (0.075 mL), 10% $AlCl_3$ (0.075 mL), and 1 M NaOH (0.5 mL) were added sequentially at 0, 5, and 6 min. Finally, the volume of the reacting solution was adjusted to 2.5 mL with double-distilled water. The absorbance of the solution at a wavelength of 410 nm was detected using the Helios λ spectrophotometers. Quercetin is a ubiquitous flavonoid, present in many natural extracts, used as standard to quantify the total flavonoid content. Results were expressed in mg/g biomass [6, 18].

2.5.3. Determination of β -Carotene and Lycopene. For β -carotene and lycopene determination, the dried ethanolic extract (100 mg) was vigorously shaken with an acetone-hexane mixture (4 : 6, 10 mL) for 1 min and filtered through Whatman number 1 filter paper. The absorbance of the filtrate was measured at 453, 505, and 663 nm. β -Carotene and lycopene content were calculated according to the following equations: lycopene (mg/100 mL) = $-0.0458 \times A_{663} + 0.372 \times A_{505} - 0.0806 \times A_{453}$; β -carotene (mg/100 mL) = $0.216 \times A_{663} - 0.304 \times A_{505} + 0.452 \times A_{453}$. The results are expressed as mg of carotenoid/g of extract [6, 12].

2.5.4. Determination of Ascorbic Acid. Determination of ascorbic acid was determined by the method described by Barros et al., 2007. Content of ascorbic acid was calculated on the basis of the calibration curve of L-ascorbic acid, and the results were expressed as mg of ascorbic acid/g extract [12].

2.5.5. Determination of the Total Quantity of Polyphenol Carboxylic Acids, Flavones, and Tocopherols. Determination of the total quantity of polyphenol carboxylic acids, flavones, and tocopherols was determined by means of chromatography using high-pressure liquid chromatograph (HPLC) ELITE-LaChrom, with DAD detector, and presented in a previous study [5].

2.6. Statistical Analysis. All the assays for fermentation and antioxidant activity were assessed in triplicate, and the results were expressed as mean \pm SD values of the three sets of observations ($P < 0.05$). The mean values and standard deviation were calculated using the EXCEL program from Microsoft Office 2010 package [7].

3. Results and Discussion

3.1. Mycelium Growth and Total Phenols and Flavonoids Accumulation in the Biomass. The maximum amount of biomass

accumulation was achieved by maintaining optimal conditions of pH, temperature, and stirring. The profile of the growth curve showed a steady rollout after the eighth day with a maximum following the tenth day of submerged fermentation in a batch system. It was also observed that, in the biomass samples taken during the fermentative processes, the accumulation of the antioxidant compounds was directly proportional to the increase in biomass amount (data not shown) with the exception of *C. comatus* M8102 (45.37 ± 3.43 g/L/day biomass) and *P. ostreatus* PSI101109 (16.63 ± 0.77 g/L/day biomass), which showed a decrease in the total amount of phenols and flavonoids with entry into the stationary phase (Table 1). The decrease did not exceed 10% and remained constant until the end of the fermentative process. This observation was also supported by the carbon source depletion. The maximum growth rate was calculated for *P. ostreatus* PQMZ91109 (0.56 ± 0.09 h⁻¹). For the other species, the determined differences are the result of an exponential growth phase of the mycelia which stretched over a longer period of time.

The gradual depletion in carbon source and the change in ratio between amount of carbon and nitrogen sources are a possible explanation as this behavior is typical of the cultivated species. This behavior occurred when the carbon source was depleted in favor of the nitrogen source resulting in a direct reduction in the growth rate of the mycelia and of the sizes; however, the density of mushroom pellets is increased. Thus, there was an increase in total amount of phenols and flavonoids present in the biomass produced by batch fermentation compared with the cultivation in stirred flasks (inoculum), in which growth was at least 20% in *C. comatus* M8102. The accumulation of these secondary metabolites can also be explained as a mushroom response to the stress as determined by the inversely proportional decrease of the amount of carbon source in the case of batch cultivation. Such a behavior has been previously demonstrated both in plants and in other fungi (*Russula griseocarnosa*) [1].

The accumulation of secondary compounds showed much higher values than the cultivation in other conditions (in Erlenmeyer flasks), ranging between 20% and 50%. The highest amount was found in the mycelium of *P. ostreatus* PSI101109 (98.60 ± 1.85 mg/g biomass). The least productive species was *P. ostreatus* PBS281009 (35.40 ± 6.75 mg/g biomass), with no more than 65% of the other tested species (Table 1). The flavonoids are the most important group of phenolic compounds, representing over 50% of the total registered amount with the exception noted by *C. comatus* M8102 with a rate of only 34%. If we consider the accumulation of biomass in the course of the batch fermentative process, the correlation with the total amount of polyphenols showed positive correlations ($r^2 = 0.514$ – 0.689) which also corresponded to the amount of determined flavonoids ($r^2 = 0.679$ – 0.861), according to species. Thus, it has been shown that the synthesis of these secondary metabolites occurs during different periods of the mycelia growth phases in a batch system. A marked accumulation of flavonoids was also noted toward the end of the exponential phase of growth and with entry into the stationary phase. This behavior has

been observed in both *P. ostreatus* PSI101109 and *P. ostreatus* PBS281009, where the amount of flavonoids in the total phenolic compounds was highest, by at least 70%.

The quantities of phenolic compounds in the obtained extracts were lower than expected possibly due to their concentration levels being below the limit of detection of the high performance liquid (HPLC) chromatographic method used. An additional problem may be due to extraction procedure used, which favors the extraction of other active compounds (tocopherols), possibly as a result of a significant decrease in the amount of total phenolic compounds. This is the first published investigation known to show the effect of ethanol extraction in fluidized bed on the phenolic composition of lyophilized mycelium extract. Even though the presence of these molecules is indicated by the Folin Ciocalteu method, the concentrations may be influenced by interaction with other active ingredients, as has been shown by recent studies [19]. This observation has also been depicted in the case of fluidized bed extraction from the fruit body of the same species, as well as some wild ones such as *Tuber melanosporum*, *Marasmius oreades*, or *Craterellus cornucopioides*—data yet to be published.

The main phenolic acids determined were homogentisic acid (0.14 ± 0.001 – 35.18 ± 0.4 mg/100 g of extract) and gallic acid (0.82 ± 0.01 – 16.21 ± 0.16 mg/100 g of extract) compounds that were found present in all extracts from the mycelium. In addition, a small amount of chlorogenic acid in the *P. ostreatus* M2191 mycelium extract was also detected (Table 2). A significant number of flavones were also identified, indicative of the presence of rutin in *C. comatus* M8102 extract and also the lack of catechin, except for the *P. ostreatus* PQMZ91109 mycelium extract. Another novel finding was the presence of apigenin (0.034 ± 0.00 mg/100 g extract) in the *C. comatus* M8102 extract, which is responsible for the inhibition of membrane lipid peroxidation [20]. An additional finding as a result of the chromatographic analysis was the identification of pyrogallol in the *P. ostreatus* PBS281009 mycelium extract, which has not been identified for this species in previous studies [19].

While most studies focus mainly on the phenolic profile, the tocopherol composition has not been analyzed as much in medicinal mushroom mycelia extracts. As such, the fluidized bed extraction process of the present study resulted in the identification of significant amounts of α -tocopherol, with the greatest significant amount determined in the *C. comatus* M8102 extract. A third novel finding of this study was the presence of tocopherol acetate in the extract of *P. ostreatus* PQMZ91109. Tocopherol acetate is the ester moiety formed between acetic acid and α -tocopherol (4.8 ± 0.05 mg/100 g of extract), which is known for its inhibitory effect on tyrosinase, which has an important physiological significant role in controlling melanin production.

In addition to the phenolic compounds, following the extraction in fluidized bed from the mycelium, a significantly similar amount of ascorbic acid was obtained in the analyzed extracts (Table 2). A similar trend was observed for the accumulation of β -carotene and lycopene for the four species of *Pleurotus*. In the *C. comatus* M8102 mycelium extracts, an amount of β -carotene determined to be 88.5% higher was

TABLE 1: Biomass production and total phenols and flavonoids accumulation in the submerged culture of mushrooms mycelia after 10 days of batch fermentation.

Mushroom species	Biomass productivity (g/L/day)	Total phenols (mg/g biomass)	Total flavonoids (mg/g biomass)	Product yield (g biomass/g carbon source)	Maximum growth speed (h ⁻¹)
<i>P. ostreatus</i> PQMZ91109	22.50 ± 1.50	63.40 ± 4.30	34.35 ± 1.67	45.05 ± 1.69	0.56 ± 0.09
<i>P. ostreatus</i> PSII01109	16.63 ± 0.77	98.60 ± 1.85	69.75 ± 3.52	38.04 ± 1.51	0.74 ± 0.01
<i>P. ostreatus</i> PBS281009	35.16 ± 1.71	35.40 ± 6.75	28.00 ± 5.70	50.22 ± 2.40	0.63 ± 0.12
<i>P. ostreatus</i> M2191	26.25 ± 0.81	70.00 ± 3.91	45.00 ± 2.89	29.16 ± 0.88	0.65 ± 0.05
<i>C. comatus</i> M8102	45.37 ± 3.43	72.60 ± 8.67	24.75 ± 1.28	37.80 ± 2.93	0.59 ± 0.1

TABLE 2: The main compounds with antioxidant effect identified in the fluidized bed extracts of lyophilized mycelium.

Compound (mg/100 g extract)	<i>P. ostreatus</i> PQMZ91109	<i>P. ostreatus</i> PSII01109	<i>P. ostreatus</i> PBS281009	<i>P. ostreatus</i> M2191	<i>C. comatus</i> M8102
Gallic acid	9.39 ± 0.1	16.21 ± 0.16	0.82 ± 0.01	10.56 ± 0.11	11 ± 0.1
Homogentisic acid	17.78 ± 0.2	35.18 ± 0.4	0.14 ± 0.001	10.93 ± 0.1	7.96 ± 0.08
Chlorogenic acid	—	—	—	0.0436 ± 0.0004	—
Catechin	0.67 ± 0.007	—	—	—	—
Rutin	—	—	—	—	0.19 ± 0.002
Myricetin	1.6 ± 0.02	1.32 ± 0.01	—	—	—
Apigenin	—	—	—	—	0.034 ± 0.00
Pyrogallol	—	—	64.67 ± 0.6	—	—
Ascorbic acid	0.94 ± 0.02	0.93 ± 0.04	0.93 ± 0.01	0.92 ± 0.02	0.94 ± 0.32
β-Carotene	0.02 ± 0.01	0.03 ± 0.02	0.02 ± 0.002	0.03 ± 0.002	0.13 ± 0.09
Lycopene	0.01 ± 0.004	—	0.01 ± 0.002	0.03 ± 0.001	0.09 ± 0.05
α-Tocopherol	14.52 ± 0.15	23.4 ± 0.2	30.47 ± 0.35	24.56 ± 0.56	179.51 ± 1.51
Tocopherol acetate	4.8 ± 0.05	—	—	—	—

identified, and 3 times more lycopene was also determined in comparison to the *P. ostreatus* mycelia extracts. Results depict the specific characteristic behaviors of the two species in the case of cultivation in the bioreactor, under steady conditions. In this manner, the fermentative batch process may be used in order to obtain a mycelium rich in the most important secondary metabolites of biological activity.

3.2. Evaluation of Antioxidant Activity of Extracts in Fluidized Bed from Mycelium Obtained by Batch Cultivation. The evaluation results of the antioxidant activity of lyophilized mycelia of all five fungal strains are presented as EC₅₀ values in Table 3. The evaluation of free radical scavenging activity was performed by using ABTS and hydroxyl radicals. Compared to other methods used to assess free radical activity, the ABTS scavenging activity assessment results in greater accuracy. As both the hydrophilic antioxidant component and the lipophilic components of the extract are known to react in the assessment [21], the free radical scavenging activities were as follows (in increasing order): *C. comatus* M8102 < *P. ostreatus* PSII01109 < *P. ostreatus* M2191 < *P. ostreatus* PQMZ91109 < *P. ostreatus* PBS281009. Hydroxyl radicals are among the most reactive of reactive oxygen species and can cause increased oxidative damage to DNA, lipids, and proteins [6]. Thus, for the hydroxyl radical

scavenging activity, the increasing order of EC₅₀ value was as follows: *P. ostreatus* PBS281009 < *P. ostreatus* M2191 < *C. comatus* M8102 < *P. ostreatus* PQMZ91109 < *P. ostreatus* PSII01109.

Chelating agents are known to prevent the generation of oxyradicals. For that purpose, a chelating method was used to evaluate antioxidant activity [22]. Human erythrocytes represent an ideal *in vitro* model which is very useful due to their membranes which contain polyunsaturated fatty acids which are extremely susceptible to free radical attack following the decomposition of AAPH [23]. The direct relationship therefore between both methods is a precise indicator of the ability to prevent lipid peroxidation, expressed as peroxyl radicals scavenging activity. In both cases, the increasing order was as follows: *C. comatus* M8102 < *P. ostreatus* PQMZ91109 < *P. ostreatus* PSII01109 < *P. ostreatus* M2191 < *P. ostreatus* PBS281009.

The FRAP method is an accurately known method used to quantify the antioxidant potential of an extract. The methodology is based on the reaction of the extracts of antioxidant components with inactivated oxidants. The reducing power exerted by the antioxidant molecules from the analyzed extract is associated with the interruption of free radical formation [24]. The results obtained as EC₅₀ values demonstrated a ferric ion reducing capacity of 25% higher on average, compared with the standard (ascorbic acid). These

TABLE 3: The antioxidant activity (expressed as EC₅₀ value in mg/mL) of the extracts of lyophilized mycelium.

Mushroom species	ABTS scavenging activity	Hydroxyl scavenging activity	Chelating effect	AAPH	FRAP	XO
<i>P. ostreatus</i> PQMZ91109	0.63 ± 0.02	1.65 ± 0.04	0.17 ± 0.05	2.63 ± 0.13	1.76 ± 0.05	0.9 ± 0.21
<i>P. ostreatus</i> PSI101109	0.25 ± 0.01	1.48 ± 0.07	0.22 ± 0.02	2.65 ± 0.20	1.51 ± 0.04	1.8 ± 0.65
<i>P. ostreatus</i> PBS281009	1.78 ± 0.04	4.54 ± 0.01	3.67 ± 0.01	6.96 ± 0.28	4.77 ± 0.17	2.45 ± 0.54
<i>P. ostreatus</i> M2191	0.45 ± 0.11	2.20 ± 0.20	0.64 ± 0.01	4.15 ± 0.24	3.77 ± 0.04	1.41 ± 0.22
<i>C. comatus</i> M8102	0.10 ± 0.05	1.87 ± 0.03	0.12 ± 0.03	2.27 ± 0.15	0.72 ± 0.01	0.78 ± 0.08

values were up to 10 times lower than the methanol extracts of edible wild species (*Russula nigricans*, *Amanita rubescens* var. *Rubescens*, *P. dryinus*, or *Leccinum scabrum*) [25].

For the assessments of such extracts in the prevention and/or support of conventional treatments to inhibit the inflammatory processes caused by the formation of uric acid, the inhibition of xanthine oxidase is a widely accepted *in vitro* model. For evaluation of the mycelium, the inhibition of formation of uric acid (a substance which causes the disease gout) grew and produced the following results: *C. comatus* M8102 > *P. ostreatus* PQMZ91109 > *P. ostreatus* M2191 > *P. ostreatus* PSI101109 > *P. ostreatus* PBS281009. Thus, due to the biological activity of the mycelium extract, it is recommended as an additive or as part of the composition of some products which protect the liver, thus fulfilling also a possible additional detoxifying role by increasing the efficiency of the removal function, favoring the inhibition of excess uric acid production. The presence of apigenin in the extract of *C. comatus* M8102 can confirm probable anti-inflammatory effects of mycelium. This flavonoid is known to inhibit the physiological process of formation of uric acid [26].

The bioreactor cultivation of mycelia is a reproducible method in obtaining a valuable substrate from extracts with high biological activity. The mycelia contain antioxidant compounds that differ from those present in the fructification body of the fungus. An example is the presence of intracellular and extracellular polysaccharides significantly contributing to an increase in the biological activity of the obtained mycelia. As the molecular weight is directly proportional to the bioactivity, the fermentation process is the most important in the synthesis of polysaccharides resulting in molecular weight as high as possible. This occurs with a depletion of the carbon source and the entry into the stationary phase. Thus, as a result, it was determined that while the proliferation of the mycelia grown in batch culture is related to the carbon source, the amount of antioxidant compounds from the mycelia is to a larger extent related to the source of nitrogen and to the maintenance of an appropriate pH level [7]. A smaller size of the mushroom pellets resulted in a greater accumulation of compounds with antioxidant activity. This observation was supported by the results shown in Table 1, for the strains *C. comatus* M8102, *P. ostreatus* M2191, and *P. ostreatus* PQMZ91109. An increase in the amount of the secondary compounds, of approximately 35%, was registered compared to the ethanol

extracts in fluidized bed from the fruiting body of the *P. ostreatus* species [27]. If the rheological properties of the medium can represent a direct indication of the synthesis of a specific metabolite such as exopolysaccharides, the morphological aspect is significant enough to achieve mycelia rich in functional compounds. Changing the parameters of the fermentative process by increasing the stirrer speed does not result in increased efficiency of production of such compounds in the mycelia. Moreover, only a decrease in the amount of biomass was noted, with a direct effect on its composition [7].

Freeze drying is the most effective in retaining the maximum amount of compounds with antioxidant activity in an extract. As such, freeze drying was therefore used to obtain a valuable substrate for the later stage of the extraction. The ethanol and water mixture is believed to be the solvent mix that ensures appropriate extraction efficiency, expressed as the amount of antioxidants/g of substrate. This was shown in the case of *Agaricus brasiliensis* mycelium [28]. By using the extraction in fluidized-bed from the lyophilized mycelia of *P. ostreatus* and *C. comatus*, an increase in antioxidant potential of the lyophilized extract was determined. A comparison was made with the mycelia obtained by submerged cultivation in Erlenmeyer flasks and submitted to a simple extraction (also a lyophilized mycelium) [6]. Extraction in fluidized bed favored the presence of tocopherols, which represents a novelty, compared to most studies in which various phenolic compounds predominate. Results may lead to the possibility of modulating the composition of the active compounds in the final extract by the extraction method used. This possibility is novel as simple extractions in previous studies have not led to similar results for the same species [29]. The significance in our findings is supported both by the determined amount and by the localization within the cell membrane of mainly α -tocopherol.

Extracts from the mycelia of *P. ostreatus* and *C. comatus* showed relatively similar capabilities of free radical scavenging and of ferric ion chelation; however a lower capacity (EC₅₀ value greater on average by 60%) for the protection of lipid peroxidation by the peroxy radicals was noted. Compared with the extracts from *Leucopaxillus giganteus*, *Sarcodon imbricatus*, and *Agaricus arvensis*, the mycelia of the two mushrooms submitted to extraction in fluidized bed, a product with superior capabilities for the protection of the erythrocyte membrane against radical attack generated by AAPH, which may cause hemolysis, were determined [12].

These antioxidant capabilities are all considered to mainly be linked with the phenolic components of the extracts, resulting in significant medicinal efficacy, thus supporting the idea of using such compounds as active ingredients in functional products. The data is in contradiction with the effects of the herb *Hypericum perforatum* extracts which contain phenolic compounds and flavonoids with low affinity for the peroxy radicals, thus validating the significance of the composition of the active components (mainly phenolic compounds) that are involved in the scavenging effect [30]. Besides the significant antioxidant efficacy, the mycelium extracts in fluidized bed demonstrated an anti-inflammatory effect. This property is also directly expressed by the total amount of phenolic acids and flavonoids, as noted by the *in vitro* inhibition of xanthine oxidase by *C. comatus* M8102 extracts.

The types and amounts of phenolic compounds varied with the same culture conditions of the species; however, similar antioxidant activity was observed. It can therefore be concluded that other components may be involved in these antioxidative properties as mentioned in previous studies [7, 31]. According to published data with respect to the relationships between the concentration of phenolic compounds and the antioxidant activity there is much controversy. Moreover, antioxidant properties have also been shown to be influenced by the content of tocopherols, anthocyanins, and carotenoids compounds [32].

A positive correlation expressed by *in vitro* analysis between the amount of biologically active compounds and the different antioxidative properties of each separate extract was determined. With respect to the α -tocopherol content, the r^2 value (0.7665–0.9426) was greatest for the inhibition of xanthine oxidase, the inhibition of erythrocyte hemolysis, and the FRAP method for the evaluation of the reducing power ($P < 0.0001$). As for the inhibition of the two species of free radicals, the value of the correlation index with the tocopherol content was moderate.

The polyphenolic content had a medium degree of correlation, with the largest correlation related to the capacity to inhibit the erythrocyte hemolysis ($r^2 = 0.476$ – 0.9773). The greatest correlations r^2 were expressed for the species *C. comatus* M8102, *P. ostreatus* PQMZ91109, and *P. ostreatus* PSII01109 ($P < 0.0001$). With regard to the inhibition of xanthine oxidase, the FRAP method as well as the ability of chelation and the correlations with respect to the polyphenolic content were moderate. The ability to inhibit free radical species in pyrogallol of *P. ostreatus* PBS281009 was determined to be highly correlated. Overall, pyrogallol presence to the expression does not exceed 50% of the antioxidant potential. A similar behavior was also observed in *C. comatus* M8102 when the rutin and apigenin content were also considered. An increase of the r^2 value was also observed for the inhibition of hemolysis and xanthine oxidase and for the chelating capacity. This activity was also determined for the strains *P. ostreatus* PQMZ91109 and *P. ostreatus* PSII01109, where myricetin and catechin were present ($P < 0.004$).

In conclusion, choosing the appropriate extraction procedure allowing for the modulation of the biological value of

the extract allows for new and improved technological implications. This is the first study known to evaluate the antioxidant capacity of a fluidized bed extract from mushroom mycelium. Regardless, the current results do not invalidate the pharmacological value of such preparations in alleviating the oxidative properties. The relevance of these *in vitro* results must be supported by future *in vivo* studies. Moreover, *in vivo* studies should be performed in the determination of antioxidant capacity and level of assimilation after passage through the human gastrointestinal tract.

Conflict of Interests

The author declares that there is no conflict of interests regarding the publication of this paper.

Acknowledgments

This work was supported by the Executive Agency for Higher Education, Research, Development and Innovation Funding, Human Resources, Theme 9/2010 (<http://proiecte9.freewb.ro/>; <http://mushroomextracts.freewb.ro/>). Chromatograms were realised in the Department of Physical-Chemical Analysis and Quality Control from National Institute for Chemical-Pharmaceutical Research and Development, ICCF Bucharest, Chief of the Department, Ph.D. Chem., Sultana Nita, as a result of Research Projects 3035/3.04.2012 and 3063/26.06.2012.

References

- [1] J. Dong, M. Zhang, L. Lu, L. Sun, and M. Xu, "Nitric oxide fumigation stimulates flavonoid and phenolic accumulation and enhances antioxidant activity of mushroom," *Food Chemistry*, vol. 135, no. 3, pp. 1220–1225, 2012.
- [2] D. Barreca, G. Laganà, S. Ficarra et al., "Evaluation of the antioxidant and cytoprotective properties of the exotic fruit *Annona cherimola* Mill. (Annonaceae)," *Food Research International*, vol. 44, no. 7, pp. 2302–2310, 2011.
- [3] 2014, <http://www.sanathon.ro>.
- [4] A. Gregori, M. Švagelj, and J. Pohleven, "Cultivation techniques and medicinal properties of *Pleurotus spp.*," *Food Technology and Biotechnology*, vol. 45, no. 3, pp. 238–249, 2007.
- [5] E. Vamanu and S. Nita, "Antioxidant capacity and the correlation with major phenolic compounds, anthocyanin, and tocopherol content in various extracts from the wild edible *Boletus edulis* mushroom," *BioMed Research International*, vol. 2013, Article ID 313905, 11 pages, 2013.
- [6] E. Vamanu, "In Vitro antimicrobial and antioxidant activities of ethanolic extract of lyophilized mycelium of *Pleurotus ostreatus* PQMZ91109," *Molecules*, vol. 17, no. 4, pp. 3653–3671, 2012.
- [7] E. Vamanu, "Biological activities of the polysaccharides produced in submerged culture of two edible *Pleurotus ostreatus* mushrooms," *Journal of Biomedicine and Biotechnology*, vol. 2012, Article ID 565974, 8 pages, 2012.
- [8] V. Emanue, V. Adrian, N. Sultana, and C. Svetlana, "Antioxidant and antimicrobial activities of ethanol extracts of *Cynara scolymus* (*Cynarae folium*, *asteraceae* family)," *Tropical Journal of Pharmaceutical Research*, vol. 10, no. 6, pp. 777–783, 2011.

- [9] T. E. Kwape and P. Chaturvedi, "Anti-oxidant activities of leaf extracts of *Ziziphus mucronata*," *International Journal of Food, Agriculture & Veterinary Sciences*, vol. 2, pp. 62–69, 2012.
- [10] S.-I. Lim, C.-W. Cho, U.-K. Choi, and Y.-C. Kim, "Antioxidant activity and ginsenoside pattern of fermented white ginseng," *Journal of Ginseng Research*, vol. 34, no. 3, pp. 168–174, 2010.
- [11] V. O. Oyetayo, C. H. Dong, and Y. J. Yao, "Antioxidant and antimicrobial properties of aqueous extract from *Dictyophora indusiata*," *Open Mycology Journal*, vol. 3, pp. 20–26, 2009.
- [12] L. Barros, M. Ferreira, B. Queirós, I. C. F. R. Ferreira, and P. Baptista, "Total phenols, ascorbic acid, β -carotene and lycopene in Portuguese wild edible mushrooms and their antioxidant activities," *Food Chemistry*, vol. 103, no. 2, pp. 413–419, 2007.
- [13] H.-F. Chang and L.-L. Yang, "Radical-scavenging and rat liver mitochondria lipid peroxidative inhibitory effects of natural flavonoids from traditional medicinal herbs," *Journal of Medicinal Plants Research*, vol. 6, no. 6, pp. 997–1006, 2012.
- [14] S. S. Sakat, A. R. Juvekar, and M. N. Gambhire, "In-vitro antioxidant and anti-inflammatory activity of methanol extract of *Oxalis corniculata* linn," *International Journal of Pharmacy and Pharmaceutical Sciences*, vol. 2, no. 1, pp. 146–155, 2010.
- [15] H. S. Yim, F. Y. Chye, C. T. Tan, Y. C. Ng, and C. W. Ho, "Antioxidant activities and total phenolic content of aqueous extract of *Pleurotus ostreatus* (Cultivated Oyster Mushroom)," *Malaysian Journal of Nutrition*, vol. 16, no. 2, pp. 281–291, 2010.
- [16] G. Sahgal, S. Ramanathan, S. Sasidharan, M. N. Mordi, S. Ismail, and S. M. Mansor, "In vitro antioxidant and xanthine oxidase inhibitory activities of methanolic *Swietenia mahagoni* seed extracts," *Molecules*, vol. 14, no. 11, pp. 4476–4485, 2009.
- [17] C. Anesini, G. E. Ferraro, and R. Filip, "Total polyphenol content and antioxidant capacity of commercially available tea (*Camellia sinensis*) in Argentina," *Journal of Agricultural and Food Chemistry*, vol. 56, no. 19, pp. 9225–9229, 2008.
- [18] I. Kim, M. Yang, O. Lee, and S. Kang, "Antioxidant activities of hot water extracts from various spices," *The International Journal of Molecular Sciences*, vol. 12, no. 6, pp. 4120–4131, 2011.
- [19] I. Palacios, M. Lozano, C. Moro et al., "Antioxidant properties of phenolic compounds occurring in edible mushrooms," *Food Chemistry*, vol. 128, no. 3, pp. 674–678, 2011.
- [20] J. Prince Vijeya Singh, K. Selvendiran, S. Mumtaz Banu, R. Padmavathi, and D. Sakthisekaran, "Protective role of Apigenin on the status of lipid peroxidation and antioxidant defense against hepatocarcinogenesis in Wistar albino rats," *Phytomedicine*, vol. 11, no. 4, pp. 309–314, 2004.
- [21] P. Li, L. Huo, W. Su et al., "Free radical-scavenging capacity, antioxidant activity and phenolic content of *Pouzolzia zeylanica*," *Journal of the Serbian Chemical Society*, vol. 76, no. 5, pp. 709–717, 2011.
- [22] B. Tepe, C. Sarikurku, S. Berk, A. Alim, and H. A. Akpulat, "Chemical composition, radical scavenging and antimicrobial activity of the essential oils of *Thymus boveii* and *Thymus hyemalis*," *Records of Natural Products*, vol. 5, no. 3, pp. 208–220, 2011.
- [23] Z. Asghar and Z. Masood, "Evaluation of antioxidant properties of silymarin and its potential to inhibit peroxy radicals *in vitro*," *Pakistan Journal of Pharmaceutical Sciences*, vol. 21, no. 3, pp. 249–254, 2008.
- [24] M. Irshad, M. Zafaryab, M. Singh, and M. M. A. Rizvi, "Comparative analysis of the antioxidant activity of *Cassia fistula* extracts," *International Journal of Medicinal Chemistry*, vol. 2012, Article ID 157125, 6 pages, 2012.
- [25] A. Keles, I. Koca, and H. Genccelep, "Antioxidant properties of wild edible mushrooms," *Journal of Food Processing & Technology*, vol. 2, article 130, 2011.
- [26] T. P. A. Devasagayam, J. C. Tilak, K. K. Bloor, K. S. Sane, S. S. Ghaskadbi, and R. D. Lele, "Free radicals and antioxidants in human health: Current status and future prospects," *Journal of Association of Physicians of India*, vol. 52, pp. 794–804, 2004.
- [27] E. Vamanu and S. Nita, "Biological activity of ethanolic fluidized bed extracts from several edible mushrooms," *Food Science and Biotechnology*. Accepted Paper.
- [28] A. E. S. S. Carvajal, E. A. Koehnlein, A. A. Soares et al., "Bioactives of fruiting bodies and submerged culture mycelia of *Agaricus brasiliensis* (*A. blazei*) and their antioxidant properties," *Food Science and Technology*, vol. 46, no. 2, pp. 493–499, 2012.
- [29] E. Vamanu, E. Mihaela, D. Peunesco, I. Sarbu, A. Vamanu, and S. Nita, "Determination of antioxidant and antimicrobial properties of alcoholic extract from *Pleurotus ostreatus* M2191 mycelium obtained in the presence of various nitrogen sources," *Revista de Chimie*, vol. 62, no. 12, pp. 1189–1194, 2011.
- [30] B. A. Silva, J. O. Malva, and A. C. P. Dias, "St. John's Wort (*Hypericum perforatum*) extracts and isolated phenolic compounds are effective antioxidants in several *in vitro* models of oxidative stress," *Food Chemistry*, vol. 110, no. 3, pp. 611–619, 2008.
- [31] E. Vamanu, "Antioxidant properties and chemical compositions of various extracts of the edible commercial mushroom, *Pleurotus ostreatus*, in Romanian markets," *Revista de Chimie*, vol. 64, no. 1, pp. 49–54, 2013.
- [32] N. Gursoy, C. Sarikurku, M. Cengiz, and M. H. Solak, "Antioxidant activities, metal contents, total phenolics and flavonoids of seven *Morchella* species," *Food and Chemical Toxicology*, vol. 47, no. 9, pp. 2381–2388, 2009.

Research Article

Plant-Derived Antimicrobials Reduce *E. coli* O157:H7 Virulence Factors Critical for Colonization in Cattle Gastrointestinal Tract *In Vitro*

Sangeetha Ananda Baskaran¹ and Kumar Venkitanarayanan²

¹ Department of Poultry Science, Texas A&M University, College Station, TX 77843, USA

² Department of Animal Science, University of Connecticut, Storrs, CT 06269, USA

Correspondence should be addressed to Kumar Venkitanarayanan; kumar.venkitanarayanan@uconn.edu

Received 19 February 2014; Accepted 31 May 2014; Published 19 June 2014

Academic Editor: José Carlos Tavares Carvalho

Copyright © 2014 S. Ananda Baskaran and K. Venkitanarayanan. This is an open access article distributed under the Creative Commons Attribution License, which permits unrestricted use, distribution, and reproduction in any medium, provided the original work is properly cited.

This study investigated the effect of subinhibitory concentrations (SIC) of five plant-derived antimicrobials (PDAs), namely, trans cinnamaldehyde, eugenol, carvacrol, thymol, and β -resorcylic acid, on *E. coli* O157:H7 (EHEC) attachment and invasion of cultured bovine colonic (CO) and rectoanal junction (RAJ) epithelial cells. In addition, PDAs' effect on EHEC genes critical for colonization of cattle gastrointestinal tract (CGIT) was determined in bovine rumen fluid (RF) and intestinal contents (BICs). Primary bovine CO and RAJ epithelial cells were established and were separately inoculated with three EHEC strains with or without (control) SIC of each PDA. Following incubation, EHEC that attached and invaded the cells were determined. Furthermore, the expression of EHEC genes critical for colonization in cattle was investigated using real-time, quantitative polymerase chain reaction in RF and BICs. All the PDAs decreased EHEC invasion of CO and RAJ epithelial cells ($P < 0.05$). The PDAs also downregulated ($P < 0.05$) the expression of EHEC genes critical for colonization in CGIT. Results suggest that the PDAs could potentially be used to control EHEC colonization in cattle; however follow-up *in vivo* studies in cattle are warranted.

1. Introduction

Enterohemorrhagic *Escherichia coli* O157:H7 (EHEC) is a major food-borne pathogen that causes disease conditions in humans, ranging from diarrhea to hemorrhagic colitis and hemolytic-uremic syndrome [1]. Cattle are the principal reservoir of EHEC [2–5], with fecal contamination of carcass being an important source of human infection. In addition, fecal shedding of EHEC imposes a risk of direct zoonotic and environmental transmission of the pathogen to humans, especially children [6].

The primary site of EHEC colonization in cattle is the terminal rectum, particularly an anatomical area within the terminal rectum referred to as the rectoanal junction (RAJ) [3, 4]. The EHEC carriage at RAJ in cattle is associated with high levels of pathogen excretion in feces as well as long-duration of fecal shedding [3, 7–9]. Besides feces, rectal,

colonic, and rumen contents were also found as sources of EHEC in cattle [4].

Previous research has revealed that EHEC colonization in cattle gastrointestinal tract (CGIT) is mediated by several factors. First, the bacterial colonization of CGIT is facilitated by its attachment to the gastrointestinal epithelial cells [10–12]. In addition, ethanolamine (EA) utilization, which is mediated by the induction of ethanolamine utilization genes (*eutB*, *eutC*, and *eutR*), is also critical for EHEC colonization [13]. Ethanolamine present in the CGIT could be selectively utilized by EHEC as an energy substrate. In addition, Hughes et al. [14] demonstrated the role of quorum sensing in EHEC colonization of CGIT. The pathogen produces SdiA protein, a LuxR homolog that senses acyl-homoserine lactones (AHLs) produced by endogenous microflora in the rumen. This SdiA-AHL chemical signaling regulates the expression of *gad* acid resistance system and locus of enterocyte effacement

(LEE) genes in EHEC, which are essential for colonization in cattle [14]. Also, this signaling facilitates a commensal lifestyle in cattle gut. Furthermore, EHEC colonization is mediated by catabolism of complex oligosaccharides, namely, L-fucose, D-galactose, sialic acids, *N*-acetylgalactosamine, and *N*-acetylglucosamine, present in the intestinal mucus of cattle [15, 16]. Therefore, catabolism of rectal mucin-derived sugars, mainly *N*-acetylgalactosamine and L-fucose, plays a role in the colonization of EHEC in the bovine rectum. Hence, inhibiting SdiA-mediated colonization and minimizing EA and mucus carbohydrate utilization would aid in limiting EHEC colonization and shedding in cattle and, consequently, the food-borne transmission of EHEC.

The use of plant-derived antimicrobials (PDAs) for controlling pathogenic microorganisms has received increased attention in recent years due to concerns for toxicity of synthetic chemicals and emerging antimicrobial resistance in bacteria [17–20]. The PDAs represent a group of natural antimicrobials that have been traditionally used to preserve foods as well as enhance food flavor. The antimicrobial properties of several plant-derived essential oils have been demonstrated [21–23], and a variety of active components of these oils have been identified. *trans*-Cinnamaldehyde (TC) is an aromatic aldehyde present as a major component of bark extract of cinnamon (*Cinnamomum verum*) [22]. Eugenol (EG) is an active ingredient in the oil from cloves (*Eugenia caryophyllus*) [24]. Carvacrol (CR) and thymol (TH) are antimicrobial ingredients in oregano oil obtained from *Origanum glandulosum* [25], whereas β -resorcylic acid (BR; 2,4 dihydroxybenzoic acid) is a phytophenolic compound widely distributed among the angiosperms and is a secondary metabolite that plays a key role in the biochemistry and physiology of plants [26]. All the aforementioned compounds are classified as GRAS (generally recognized as safe) by the US Food and Drug Administration [26–28].

This study was undertaken to determine the effect of subinhibitory concentrations (SIC, the highest concentration below MIC that does not inhibit bacterial growth) of PDAs on EHEC invasion of cultured bovine colonic (CO) and rectoanal junction (RAJ) epithelial cells. In addition, the effect of PDAs on EHEC genes that are critical for colonization in CGIT was determined in bovine rumen fluid (RF) and intestinal contents (BICs) for potential future application as a dietary supplement for reducing EHEC carriage in cattle.

2. Materials and Methods

2.1. Bacterial Culture and Media. Three isolates of EHEC, namely, E10 (meat), E16 (meat), and E22 (calf feces), were used in this study. Each EHEC strain was individually cultured in 10 mL of tryptic soy broth (TSB, Becton-Dickinson, Sparks, MD) at 37°C for 24 h with agitation (150 rpm). Following incubation, the cultures were sedimented by centrifugation (3,600 \times g for 15 min), washed twice, and resuspended in 10 mL of sterile phosphate-buffered saline (PBS, pH 7.2). To determine the bacterial population in each culture, 0.1 mL portions of appropriately diluted culture were surface-plated on tryptic soy agar (TSA, Becton-Dickinson, Sparks, MD)

and incubated at 37°C for 24 h. Appropriate dilutions of each isolate were made in PBS, and 0.1 mL (~6.0 log CFU) was used as the inoculum.

2.2. Determination of SIC of PDAs. The SIC of TC, EG, CR, TH, and BR against three EHEC strains was determined, as reported previously [28, 29]. Tryptic soy broth containing each of the aforementioned PDAs in the range of 0 to 0.05% (vol/vol) in increments of 0.001% was inoculated with each strain of EHEC at 6.0 log₁₀ CFU/mL and incubated at 37°C for 24 h. Control samples containing TSB without any added PDAs were included. After 24 h of incubation, the samples were serially diluted (1:10) in PBS and bacterial counts were determined on TSA. The highest concentration of each plant compound that did not significantly reduce bacterial growth after incubation at 37°C for 24 h was taken as the SIC of the PDA.

2.3. Primary Cell Cultures of Bovine Colon and Rectal-Anal Junction Epithelial Cells. The bovine colonocytes and RAJ epithelial cells were isolated, as previously described [30, 31]. Fresh bovine colonic and RAJ tissues were obtained from a local slaughterhouse. The tissues were immediately transferred to the laboratory in cold isotonic NaCl solution supplemented with 100 U/mL penicillin, 100 μ g/mL streptomycin, 2.5 μ g/mL gentamicin, and 2.5 μ g/mL amphotericin. The epithelium was scraped from the underlying tissue and triturated in Hank's balanced salt solution (HBSS). The cell suspension was centrifuged at 130 g for 5 min and the pellet was resuspended in cold HBSS. The washing was repeated three times. The final pellet was resuspended in "dissociation solution" containing 10 mL HBSS, 10 mL Dulbecco's modified Eagle's medium (DMEM), 100 U/mL penicillin, 100 μ g/mL streptomycin, 2.5 μ g/mL gentamicin, 2.5 μ g/mL amphotericin, and 100 U/mL collagenase I. The cells were incubated with shaking for 45 min at 37°C. After digestion, the cell material was centrifuged through a 2% sorbitol gradient in DMEM at 50 g for 5 min, and the pellet was resuspended in 2% sorbitol gradient. This procedure was repeated until the supernatant was clear, and the resulting pellet was resuspended in an aliquot of DMEM. The identity of bovine colon and RAJ epithelial cells was confirmed by detecting the basal level expression of pan-cytokeratin gene (KRT7) [32] and absence of expression of vimentin gene (VIM, [32]) to rule out contamination of fibroblasts, by RT-qPCR.

2.4. Culture Medium. The culture medium used for growing cattle colonocytes and RAJ epithelial cells was DMEM supplemented with 100 U/mL penicillin, 100 μ g/mL streptomycin, 2.5 μ g/mL gentamicin, 2.5 μ g/mL amphotericin, 2.5% fetal bovine serum (FBS; Gibco Invitrogen), 30 ng/mL epidermal growth factor (EGF; Sigma-Aldrich), and 0.25 U/mL insulin (Sigma-Aldrich) [32].

2.5. Effect of PDAs on EHEC Adherence to Bovine Colon and RAJ Epithelial Cells. *E. coli* O157:H7 adherence to bovine colonic and RAJ epithelial cells was assayed, as described

by Sheng et al. [32], with slight modifications. The cells were cultivated at 37°C under 5% CO₂ atmosphere in a cell culture flask. Polystyrene (24-well) plates were seeded with cells at a density of 1 × 10⁵ cells per well and allowed to form a monolayer. The cell monolayer was washed three times with DMEM and each EHEC strain (6 log CFU/mL) was separately added and treated with the respective SIC of TC, EG, CR, TH, or BR. The cells were incubated for 2 h and washed three times with PBS. The cells were then lysed by treating with 0.1% triton X-100 for 15 min, and adherent EHEC population was quantified by plating on TSA. Each treatment was assayed in duplicate and the entire experiment was repeated three times.

2.6. Effect of PDAs on EHEC Invasion of Bovine Colon and RAJ Epithelial Cells. The invasion assay was performed as described previously by Sheng et al. [32]. The cells were cultivated at 37°C under 5% CO₂ atmosphere in a cell culture flask. Polystyrene plates were seeded with cells at a density of 1 × 10⁵ cells per well and allowed to form a monolayer. The monolayer was washed three times with DMEM and each EHEC inoculum containing 6 log CFU/mL was added and treated with the SIC of each PDA. The cells were incubated for 2 h and washed three times with PBS. The cell monolayer was treated with 100 µg of gentamicin per mL in culture medium for 2 h to kill all extracellular bacteria. Intracellular EHEC was enumerated after lysis with 0.1% triton X-100 and plating on TSA.

2.7. Effect of PDAs on EHEC Ability to Survive in Minimal Medium Containing EA. The ability of EHEC to survive/grow by using EA as sole nitrogen source was studied in M9 minimal medium [13] supplemented with EA hydrochloride (30 mM) and SIC of TC, EG, CR, TH, or BR. The minimal medium was inoculated with ~4 log CFU/mL of each EHEC strain, and bacterial counts were determined at 24 h of incubation at 37°C.

2.8. Bovine Rumen Fluid and Intestinal Contents. Rumen fluid (RF) was collected from cattle that were housed at the University of Connecticut beef barn. Bovine intestinal contents (BICs) were collected from a local slaughterhouse. Both RF and BIC were filtered through a cheese cloth and centrifuged at 10,000 g for 15 min [13]. The supernatant obtained after centrifugation was filter-sterilized through 0.2 µm filter. Sterile RF and BICs obtained were used for the experiment.

2.9. Effect of PDAs on EHEC Colonization Genes. The effect of TC, EG, CR, TH, and BR at their respective SICs on EHEC genes, namely, *gadA*, *gadC*, *gadX*, *ler*, *sdiA*, *ea*, *eutB*, *eutC*, *eutR*, *agaA*, *fucA*, and *fucO*, that are essential for its colonization in CGIT was investigated in RF and BICs as *in vitro* models.

2.9.1. RNA Isolation. Sterile RF and BICs with or without SICs of the PDAs were inoculated with each EHEC strain (6.0 log CFU/mL) separately and incubated at 39°C for 4 h

in an anaerobic chamber. Total RNA was extracted using RNeasy mini kit (Qiagen).

2.9.2. cDNA Synthesis and Real-Time Quantitative PCR (RT-qPCR). The RNA was converted to cDNA using the Super-script II reverse transcriptase kit (Invitrogen, Grand Island, NY). The cDNA was used as the template for real-time PCR amplification of the abovementioned cattle colonization genes. Primers specific for each of the aforementioned genes were designed from published GenBank sequences using Primer Express software (Applied Biosystems, Foster City, CA) (Table 1). Relative gene expression of the aforementioned genes was determined using a 7500 fast real-time PCR system (Applied Biosystems) with SYBR Green reagents. Data were normalized to the endogenous control, 16S rRNA, and the level of gene expression between treated and control samples was analyzed using the comparative threshold cycle method (C_T). Each treatment had two samples and the experiment was replicated two times.

2.10. Statistical Analysis. For each treatment, data from independent replicate experiments were pooled and analyzed using PROC MIXED of SAS version (SAS Institute, Cary, NC, U.S.A.). Variation among replicates was used as the error term. Data were expressed as least squares means, and differences were considered significant at $P < 0.05$. Data comparisons for the gene expression study were made by using Student's *t*-test. Differences were considered significant when the *P* value was less than 0.05.

3. Results

The RT-qPCR results revealed that the colon and RAJ epithelial cells constitutively expressed the pan-cytokeratin gene KRT7, thereby validating their identity (data not shown). In addition, the VIM gene encoding vimentin was not detected in both cell types, thus confirming that the isolated primary epithelial cells were devoid of any fibroblast contamination. Although the effect of PDAs on EHEC adhesion and invasion of colon and RAJ epithelial cells was investigated on three different strains of the pathogen, only results obtained with E16 strain are presented, since the effect of PDAs was not significantly different among the three EHEC strains ($P > 0.05$). The SIC of TC, EG, and BR was 0.75 mM (0.01%), 1.85 mM (0.03%), and 2.60 mM (0.04%), respectively, whereas that of CR and TH was 0.65 mM (0.01%). The SIC of PDAs obtained in TSB was similar in RF and BICs. The effect PDAs on EHEC adhesion and invasion of bovine colonocytes is provided in Figures 1(a) and 1(b). In the adhesion assay, all the PDAs reduced EHEC adhesion by ~20% ($P < 0.05$) compared to control (Figure 1(a)). The PDAs were also effective in inhibiting the invasive ability of EHEC to colonocytes by 40–80% ($P < 0.05$). Thymol was found to be more effective in reducing EHEC invasion of colonocytes ($P < 0.05$). The effect of PDAs on EHEC adhesion and invasion of RAJ epithelial cells is depicted in Figures 2(a) and 2(b). As observed with the colonocytes, PDAs significantly reduced adhesion and

TABLE 1: List of primers used in this study.

Gene	Forward primer sequence (5'-3')	Reverse primer sequence (5'-3')
<i>sdiA</i>	TGGCGGACGGGTGAGTA	CCGGAGTTATCCCCAACTTACA
<i>eae</i>	GTTGTTGCCGGCGTTACAC	CGCGATAATTGCTTTGAAAAGA
<i>ler</i>	GCGGTCAACCGTTCCA	TGAGGCTCGTGAGGAATACGA
<i>gadA</i>	TCGGACCATTGTAGTCATCTTGA	CACAAATTCGGCATGCAGTT
<i>gadC</i>	CGCAGCTCCGCATGATATT	GATTATCCGCGGACCAACTAAG
<i>gadX</i>	TCTCCGCCTGCAAGTCCTA	TCGATTTTCATCCGCGTGT
<i>eutB</i>	GCGTGGATCCGCATGAAT	GCATCCGCAGCACTTTGAAT
<i>eutC</i>	CGTCGTCATCCAGGATTGC	TGCTATGGCTTTCCTTCTTTT
<i>eutR</i>	CTACAGCTGGGATTGCGGTAA	TGCTTGCGGATGCGATT
<i>agaA</i>	AATGTAACAGACACGGTCTCACAAA	TCCCTAATCTATCCGCCTGAAG
<i>fucA</i>	CGAAAGTACAAGCGGAGACTATCA	GTTTCTGCAAAAGCATCATCTGA
<i>fucO</i>	AAAGCAGCTGAAAACAATAATGGA	CACGCGCAACTTCGGTATT

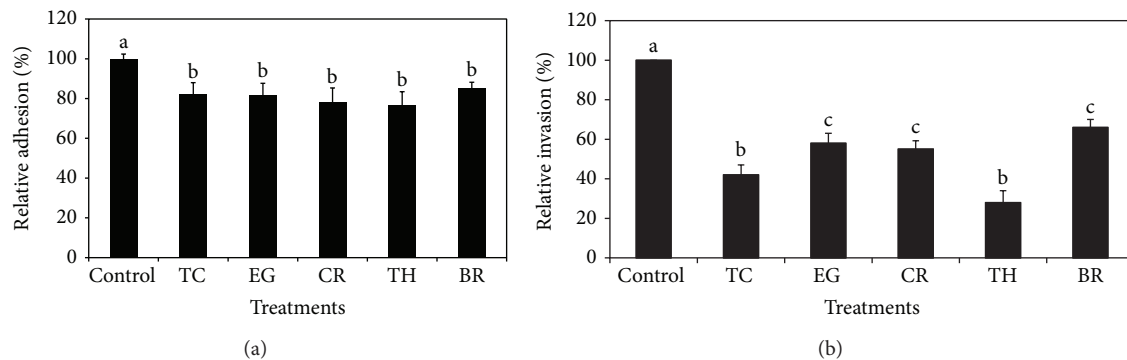


FIGURE 1: (a) Effect of PDAs on EHEC adhesion of bovine colonic epithelial cells. Treatments include control (0 mM), TC (0.75 mM), EG (1.85 mM), CR (0.65 mM), TH (0.65 mM), and BR (2.6 mM). Error bars represent SEM ($n = 3$). Bars with a common letter are not significantly different ($P > 0.05$). (b) Effect of PDAs on EHEC invasion of bovine colonic epithelial cells. Treatments include control (0 mM), TC (0.75 mM), EG (1.85 mM), CR (0.65 mM), TH (0.65 mM), and BR (2.6 mM). Error bars represent SEM ($n = 3$). Bars with a common letter are not significantly different ($P > 0.05$).

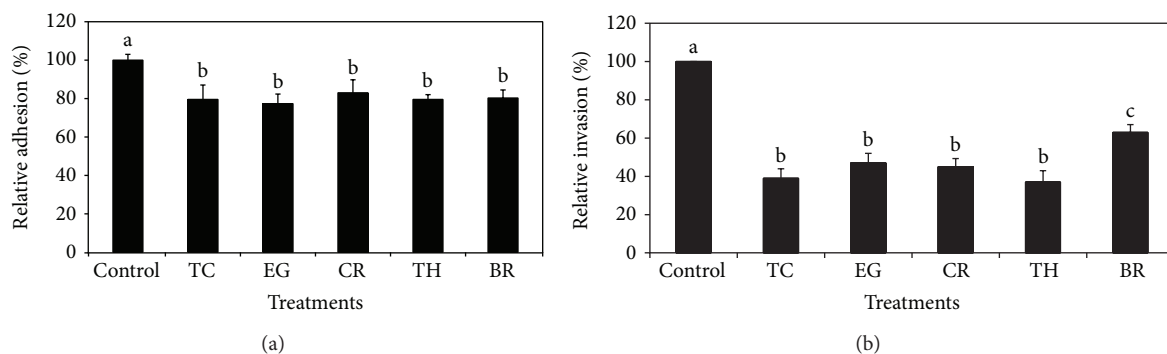


FIGURE 2: (a) Effect of PDAs on EHEC adhesion to bovine RAJ epithelial cells. Treatments include control (0 mM), TC (0.75 mM), EG (1.85 mM), CR (0.65 mM), TH (0.65 mM), and BR (2.6 mM). Error bars represent SEM ($n = 3$). Bars with a common letter are not significantly different ($P > 0.05$). (b) Effect of PDAs on EHEC invasion of bovine RAJ epithelial cells. Treatments include control (0 mM), TC (0.75 mM), EG (1.85 mM), CR (0.65 mM), TH (0.65 mM), and BR (2.6 mM). Error bars represent SEM ($n = 3$). Bars with a common letter are not significantly different ($P > 0.05$).

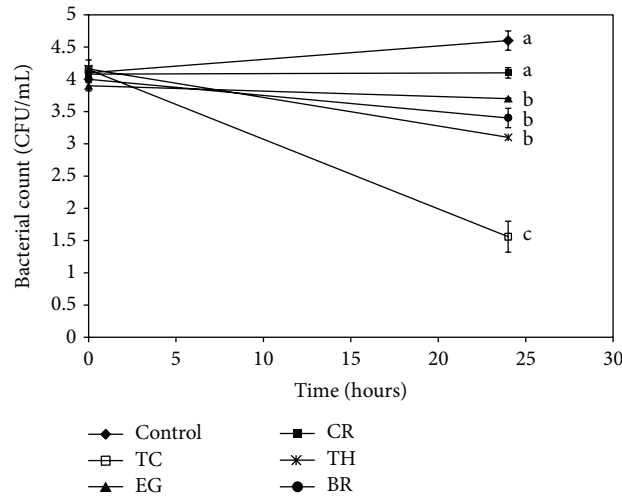


FIGURE 3: Effect of PDAs on EHEC ability to utilize ethanolamine in minimal medium. Treatments include control (0 mM), TC (0.75 mM), EG (1.85 mM), CR (0.65 mM), TH (0.65 mM), and BR (2.6 mM). Error bars represent SEM ($n = 3$). Lines with a common letter are not significantly different ($P > 0.05$).

invasion of EHEC to RAJ cells by ~20% and 60%, respectively (Figure 2(a)).

The effect of PDAs on EHEC ability to survive/grow by utilizing EA as a nitrogen source is shown in Figure 3. The control and all PDA treatments had a bacterial population of ~4 log CFU/mL at the start of the assay. After 24 h, EHEC grew by 0.5 log CFU/mL in control samples devoid of any PDA, whereas the bacterial count in samples containing PDAs except EG decreased significantly ($P < 0.05$). Among the various PDAs tested, TC was most effective in reducing EHEC's ability to survive, where the pathogen counts were reduced to ~1.5 log CFU/mL. To elucidate the mechanism of action of PDAs on EHEC ability to utilize EA as energy source, an RT-qPCR was performed on RNA obtained from EHEC grown in RF and BICs, using primers specific for ethanolamine utilization genes, namely, *eutB*, *eutC*, and *eutR*. The results are given in Figures 4-5. The results revealed that all the PDAs significantly downregulated ($P < 0.05$) the expression of the three EA utilization genes. *beta*-Resorcylic acid was most effective in reducing *eutC* expression in RF (Figure 5), whereas TC brought about maximal reductions in all three EA utilization genes in BICs, which concurred with the findings from the survival assay (Figure 3). Similarly, RT-qPCR data indicated that the PDAs, except BR in RF and EG and TH in BICs, downregulated *agaA*, *fucA*, and *fucO* involved in EHEC mucin utilization in cattle ($P < 0.05$) (Figures 6 and 7). Likewise, the expression of SdiA-controlled EHEC colonization genes was also decreased by the PDAs except EG ($P < 0.05$) (Figures 8 and 9).

4. Discussion

Since cattle serve as the principal reservoir of EHEC, decreasing the carriage of *E. coli* O157:H7 in the cattle gastrointestinal tract would potentially lead to decreased fecal shedding,

which in turn would improve farm and animal hygiene and reduce contamination of food products such as beef, raw milk, and fresh produce [33–35]. Thus, there is a critical need for effective preharvest interventional approaches to decrease *E. coli* O157:H7 carriage and shedding by cattle [36].

In ruminants, rumen microorganisms utilize feeds to produce volatile fatty acids and protein as an energy and protein supply for the animals, respectively [37]. This fermentation process, however, potentially results in energy and protein inefficiencies by loss of methane and ammonia, respectively [38], thereby leading to reduced performance of the animal and release of methane into the environment [39]. In cattle, therefore, supplementation of antibiotic ionophores in feed has been reported as a useful strategy for reducing energy and nitrogen losses in the rumen [40]. However, the use of antibiotics in feeds has been prohibited in many countries due to potential residues in foods and the emergence of antibiotic resistant bacteria. This has led to exploring alternative approaches to antibiotics, including supplementing antimicrobial plant extracts, for modulating rumen fermentation [37, 41]. This study investigated the potential of several plant-derived antimicrobials for attenuating EHEC virulence factors that are critical for colonization in CGIT. Since subinhibitory concentrations of antimicrobials, including antibiotics, can modulate bacterial physicochemical functions, including that of genes, they are used for studying the effect of antimicrobials on bacterial gene expression and virulence [42–44]. Therefore, we investigated the potential inhibitory effect of SIC of TC, EG, CR, TH, and BR on EHEC virulence factors critical for intestinal colonization in cattle. Moreover, since the intended application of the PDAs is as dietary supplements in cattle to control EHEC colonization, lowest effective concentrations of the plant molecules are advantageous for economical and palatability reasons.

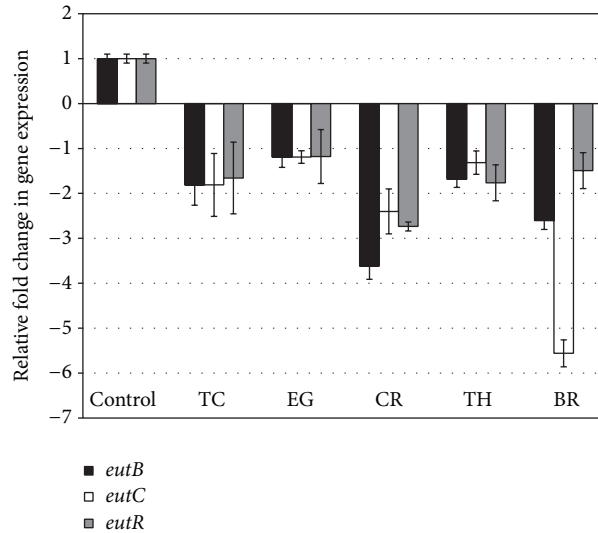


FIGURE 4: Effect of PDAs on EHEC ethanolamine utilization genes in RF. Treatments include control (0 mM), TC (0.75 mM), EG (1.85 mM), CR (0.65 mM), TH (0.65 mM), and BR (2.6 mM). Error bars represent SEM ($n = 3$). * All the treatments are significantly different from control at $P < 0.05$.

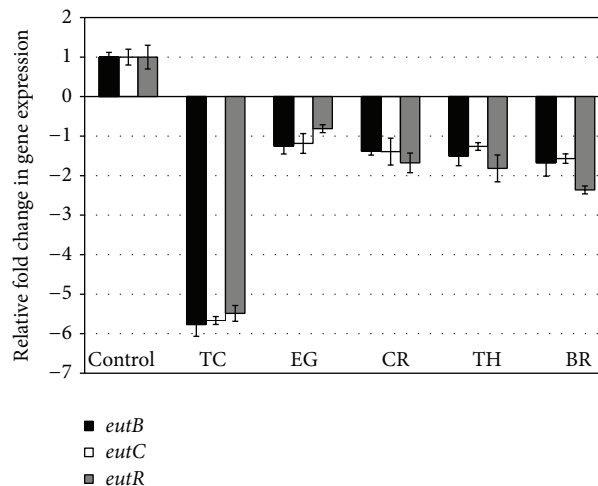


FIGURE 5: Effect of PDAs on EHEC ethanolamine utilization genes in BICs. Treatments include control (0 mM), TC (0.75 mM), EG (1.85 mM), CR (0.65 mM), TH (0.65 mM), and BR (2.6 mM). Error bars represent SEM ($n = 3$). * All the treatments are significantly different from control at $P < 0.05$.

It is demonstrated that EHEC primarily colonizes the terminal rectum, especially the rectoanal junction in bovines, besides colon [3, 4]. In addition, Sheng et al. [32] demonstrated that EHEC was internalized by RAJ epithelial cells, which plays a major role in the persistence of this bacterium in cattle. Hence, we first investigated the effect of PDAs on adherence and invasion of EHEC in bovine colonic and RAJ epithelial cells. To accomplish this, primary cells from bovine colonocytes and RAJ epithelial cells were isolated and their identity was confirmed by detecting markers specific to the epithelial cells. The results from the cell culture studies revealed that all the PDAs significantly reduced the adhesive and invasive abilities of EHEC to both primary epithelial cell lines (Figures 1(a) and 1(b) and Figures 2(a)

and 2(b)). The reduced adhesive and invasive abilities of EHEC observed in the cell culture studies were supported by RT-qPCR data, where the results revealed that the PDAs significantly downregulated the expression of *eae* and *ler* ($P < 0.05$), which play a critical role in bacterial colonization in CGIT [14, 45, 46].

In addition, we determined the effect of the PDAs on EHEC ability to utilize ethanolamine for survival, since Bertin et al. [13] demonstrated the presence of ethanolamine in the gastrointestinal tract of cattle and EHEC ability to metabolize it for energy. This gives a competitive edge to EHEC to utilize EA as a source of nitrogen, which is not used by resident microbiota, since they lack the genes for EA utilization, thus favoring EHEC persistence in the bovine

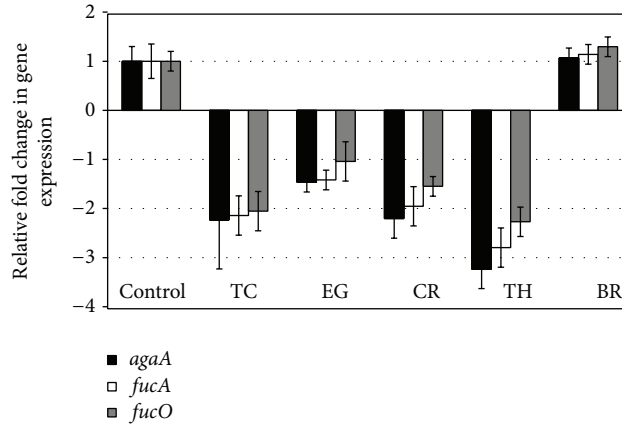


FIGURE 6: Effect of PDAs on EHEC mucus utilization genes in RF. Treatments include control (0 mM), TC (0.75 mM), EG (1.85 mM), CR (0.65 mM), TH (0.65 mM), and BR (2.6 mM). Error bars represent SEM ($n = 3$). * All the treatments except BR are significantly different from control at $P < 0.05$.

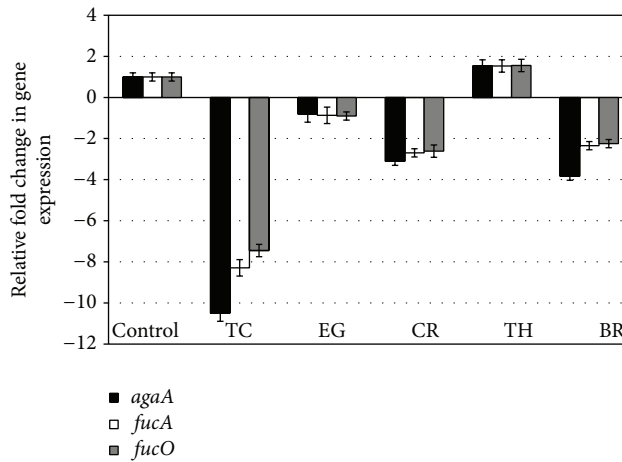


FIGURE 7: Effect of PDAs on EHEC mucus utilization genes in BICs. Treatments include control (0 mM), TC (0.75 mM), EG (1.85 mM), CR (0.65 mM), TH (0.65 mM), and BR (2.6 mM). Error bars represent SEM ($n = 3$). * All the treatments except TH are significantly different from control at $P < 0.05$.

intestine [13]. Hence, gastrointestinal contents, namely, RF and BICs, were used as *in vitro* models for determining the effect of PDAs on EHEC’s ability to persist by utilizing EA. The results revealed that TC, CR, TH, and BR significantly reduced the pathogen’s ability to persist when EA was the primary nitrogen source in the growth medium (Figure 3). These results concurred with the gene expression studies, where a significant downregulation in majority of the EA utilization genes was brought about by the PDAs (Figures 4 and 5).

The mucins present in the intestinal mucus of cattle consist of proteins extensively glycosylated by O-linked oligosaccharides [15]. The intestinal mucins provide a substrate for energy and can be utilized by EHEC for its growth. Snider et al. [16] showed that two major sugars present in mucin, namely, N-acetyl-galactosamine and fucose, play a critical role in EHEC colonization in cattle. Hence, we studied

the PDAs’ effect on mucus carbohydrate utilization genes in EHEC. Among the tested PDAs, TC was found to be consistently effective in decreasing the expression of *agaA*, *fucA*, and *fucO* both in RF and BICs ($P < 0.05$).

Besides EA utilization, SdiA-mediated chemical sensing plays a major role in EHEC colonization in the bovine gastrointestinal tract [14, 47]. Hughes et al. [14] demonstrated the importance of SdiA-mediated chemical sensing in reducing EHEC colonization in the bovine gastrointestinal tract. These investigators found that an *sdiA* mutant of EHEC was defective for colonization in CGIT and concluded that interventions targeting SdiA in EHEC are a potential strategy to control the pathogen in cattle. Our results show that the PDAs significantly reduced the expression of not only *sdiA*, but also several other SdiA-controlled genes critical for colonization in cattle, including the *gad* acid resistance system, *eae*, and *ler* (Figures 8 and 9).

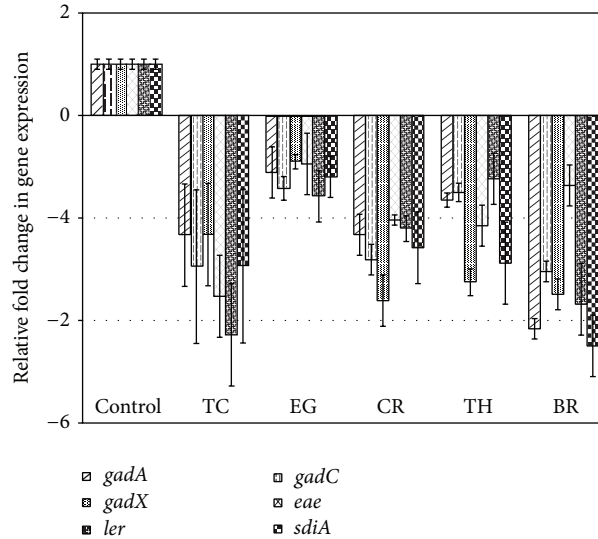


FIGURE 8: Effect of PDAs on EHEC SdiA-mediated colonization genes in RE. Treatments include control (0 mM), TC (0.75 mM), EG (1.85 mM), CR (0.65 mM), TH (0.65 mM), and BR (2.6 mM). Error bars represent SEM ($n = 3$). * All the treatments are significantly different from control at $P < 0.05$.

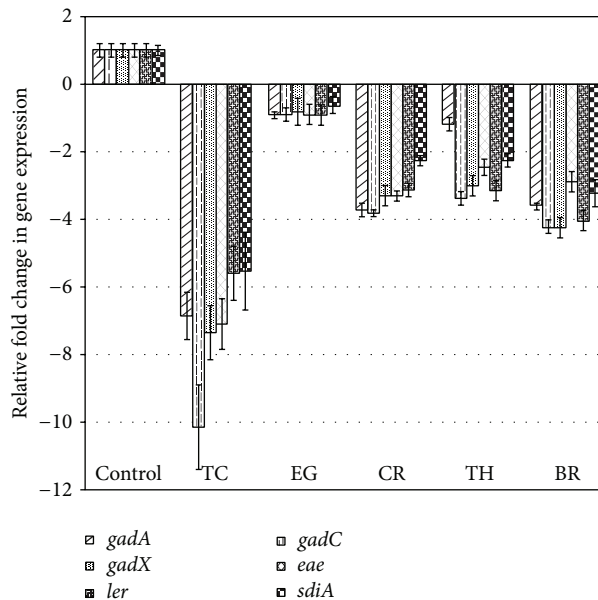


FIGURE 9: Effect of PDAs on EHEC SdiA-mediated colonization genes in BICs. Treatments include control (0 mM), TC (0.75 mM), EG (1.85 mM), CR (0.65 mM), TH (0.65 mM), and BR (2.6 mM). Error bars represent SEM ($n = 3$). * All the treatments are significantly different from control at $P < 0.05$.

In conclusion, the results from this study suggest the potential efficacy of one or more of the PDAs, especially TC, as a dietary supplement for reducing EHEC shedding in cattle, but extensive follow-up studies in cattle are needed for validating their use.

Conflict of Interests

The authors declare that there is no conflict of interests regarding the publishing of this paper.

References

- [1] D. Law, "Virulence factors of *Escherichia coli* O157 and other Shiga toxin-producing *E. coli*," *Journal of Applied Microbiology*, vol. 88, no. 5, pp. 729–745, 2000.
- [2] P. A. Chapman, C. A. Siddons, D. J. Wright, P. Norman, J. Fox, and E. Crick, "Cattle as a possible source of verocytotoxin-producing *Escherichia coli* O157 infections in man," *Epidemiology and Infection*, vol. 111, no. 3, pp. 439–447, 1993.
- [3] J. C. Low, I. J. McKendrick, C. McKechnie et al., "Rectal carriage of enterohemorrhagic *Escherichia coli* O157 in slaughtered

- cattle," *Applied and Environmental Microbiology*, vol. 71, no. 1, pp. 93–97, 2005.
- [4] S. W. Naylor, J. C. Low, T. E. Besser et al., "Lymphoid follicle-dense mucosa at the terminal rectum is the principal site of colonization of enterohemorrhagic *Escherichia coli* O157:H7 in the bovine host," *Infection and Immunity*, vol. 71, no. 3, pp. 1505–1512, 2003.
- [5] J. A. Shere, K. J. Bartlett, and C. W. Kaspar, "Longitudinal study of *Escherichia coli* O157:H7 dissemination on four dairy farms in Wisconsin," *Applied and Environmental Microbiology*, vol. 64, no. 4, pp. 1390–1399, 1998.
- [6] P. A. Chapman, J. Cornell, and C. Green, "Infection with verocytotoxin-producing *Escherichia coli* O157 during a visit to an inner city open farm," *Epidemiology and Infection*, vol. 125, no. 3, pp. 531–536, 2000.
- [7] R. N. Cobbold, D. D. Hancock, D. H. Rice et al., "Rectoanal junction colonization of feedlot cattle by *Escherichia coli* O157:H7 and its association with supershedders and excretion dynamics," *Applied and Environmental Microbiology*, vol. 73, no. 5, pp. 1563–1568, 2007.
- [8] M. A. Davis, D. H. Rice, H. Sheng et al., "Comparison of cultures from rectoanal-junction mucosal swabs and feces for detection of *Escherichia coli* O157 in dairy heifers," *Applied and Environmental Microbiology*, vol. 72, no. 5, pp. 3766–3770, 2006.
- [9] J. Y. Lim, J. Li, H. Sheng, T. E. Besser, K. Potter, and C. J. Hovde, "*Escherichia coli* O157:H7 colonization at the rectoanal junction of long-duration culture-positive cattle," *Applied and Environmental Microbiology*, vol. 73, no. 4, pp. 1380–1382, 2007.
- [10] E. A. Dean-Nystrom, W. C. Stoffregen, B. T. Bosworth, H. W. Moon, and J. F. Pohlenz, "Early attachment sites for shiga-toxigenic *Escherichia coli* O157:H7 in experimentally inoculated weaned calves," *Applied and Environmental Microbiology*, vol. 74, no. 20, pp. 6378–6384, 2008.
- [11] S. J. Elliott, L. A. Wainwright, T. K. McDaniel et al., "The complete sequence of the locus of enterocyte effacement (LEE) from enteropathogenic *Escherichia coli* E2348/69," *Molecular Microbiology*, vol. 28, no. 1, pp. 1–4, 1998.
- [12] J. P. Nataro and J. B. Kaper, "Diarrheagenic *Escherichia coli*," *Clinical Microbiology Reviews*, vol. 11, no. 1, pp. 142–201, 1998.
- [13] Y. Bertin, J. P. Girardeau, F. Chaucheyras-Durand et al., "Enterohaemorrhagic *Escherichia coli* gains a competitive advantage by using ethanolamine as a nitrogen source in the bovine intestinal content," *Environmental Microbiology*, vol. 13, no. 2, pp. 365–377, 2011.
- [14] D. T. Hughes, D. A. Terekhova, L. Liou et al., "Chemical sensing in mammalian host-bacterial commensal associations," *Proceedings of the National Academy of Sciences of the United States of America*, vol. 107, no. 21, pp. 9831–9836, 2010.
- [15] C. Robbe, C. Capon, B. Coddeville, and J.-C. Michalski, "Structural diversity and specific distribution of O-glycans in normal human mucins along the intestinal tract," *The Biochemical Journal*, vol. 384, no. 2, pp. 307–316, 2004.
- [16] T. A. Snider, A. J. Fabich, T. Conway, and K. D. Clinkenbeard, "*E. coli* O157:H7 catabolism of intestinal mucin-derived carbohydrates and colonization," *Veterinary Microbiology*, vol. 136, no. 1–2, pp. 150–154, 2009.
- [17] P. Domadia, S. Swarup, A. Bhunia, J. Sivaraman, and D. Dasgupta, "Inhibition of bacterial cell division protein FtsZ by cinnamaldehyde," *Biochemical Pharmacology*, vol. 74, no. 6, pp. 831–840, 2007.
- [18] M. T. Gahart and J. E. Lansburgh, *Antibiotic Resistance: Federal Agencies Need to Better Focus Efforts to Address Risk to Humans from Antibiotics Use in Animals*, U.S. Government Accountability Office, 2004, <http://www.gao.gov/new.items/d04490.pdf>.
- [19] E. M. Ribot, R. K. Wierzbza, F. J. Angulo, and T. J. Barrett, "*Salmonella enterica* serotype Typhimurium DT104 isolated from humans, United States, 1985, 1990, and 1995," *Emerging Infectious Diseases*, vol. 8, no. 4, pp. 387–391, 2002.
- [20] K. E. Smith, J. M. Besser, C. W. Hedberg et al., "Quinolone-resistant *Campylobacter jejuni* infections in Minnesota, 1992–1998," *The New England Journal of Medicine*, vol. 340, no. 20, pp. 1525–1532, 1999.
- [21] K. S. Bilgrami, K. K. Sinha, and A. K. Sinha, "Inhibition of aflatoxin production and growth of *Aspergillus flavus* by eugenol and onion and garlic extracts," *Indian Journal of Medical Research*, vol. 96, pp. 171–175, 1992.
- [22] S. A. Burt, R. Vlieland, H. P. Haagsman, and E. J. A. Veldhuizen, "Increase in activity of essential oil components carvacrol and thymol against *Escherichia coli* O157:H7 by addition of food stabilizers," *Journal of Food Protection*, vol. 68, no. 5, pp. 919–926, 2005.
- [23] R. A. Holley and D. Patel, "Improvement in shelf-life and safety of perishable foods by plant essential oils and smoke antimicrobials," *Food Microbiology*, vol. 22, no. 4, pp. 273–292, 2005.
- [24] S. M. Ali, A. A. Khan, I. Ahmed et al., "Antimicrobial activities of Eugenol and Cinnamaldehyde against the human gastric pathogen *Helicobacter pylori*," *Annals of Clinical Microbiology and Antimicrobials*, vol. 4, article 20, pp. 20–26, 2005.
- [25] M. Bendahou, A. Muselli, M. Grignon-Dubois et al., "Antimicrobial activity and chemical composition of *Origanum glandulosum* Desf. essential oil and extract obtained by microwave extraction: comparison with hydrodistillation," *Food Chemistry*, vol. 106, no. 1, pp. 132–139, 2008.
- [26] M. Friedman, P. R. Henika, and R. E. Mandrell, "Antibacterial activities of phenolic benzaldehydes and benzoic acids against *Campylobacter jejuni*, *Escherichia coli*, *Listeria monocytogenes*, and *Salmonella enterica*," *Journal of Food Protection*, vol. 66, no. 10, pp. 1811–1821, 2003.
- [27] A. Kollanoor-Johny, S. A. Baskaran, A. S. Charles et al., "Prophylactic supplementation of caprylic acid in feed reduces *Salmonella enteritidis* colonization in commercial broiler chicks," *Journal of Food Protection*, vol. 72, no. 4, pp. 722–727, 2009.
- [28] A. Kollanoor-Johny, T. Hoagland, and K. Venkitanarayanan, "Effect of subinhibitory concentrations of plant-derived molecules in increasing the sensitivity of multidrug-resistant *Salmonella enterica* serovar Typhimurium DT104 to antibiotics," *Foodborne Pathogens and Disease*, vol. 7, no. 10, pp. 1165–1170, 2010.
- [29] M. A. R. Amalaradjou and K. Venkitanarayanan, "Effect of trans-cinnamaldehyde on inhibition and inactivation of *Cronobacter sakazakii* biofilm on abiotic surfaces," *Journal of Food Protection*, vol. 74, no. 2, pp. 200–208, 2011.
- [30] W. Föllmann and S. Birkner, "The use of cultured primary bovine colon epithelial cells as a screening model to detect genotoxic effects of heterocyclic aromatic amines in the comet assay," *Journal of Toxicology and Environmental Health A*, vol. 71, no. 13–14, pp. 947–953, 2008.
- [31] W. Föllmann, S. Weber, and S. Birkner, "Primary cell cultures of bovine colon epithelium: isolation and cell culture of colonocytes," *Toxicology in Vitro*, vol. 14, no. 5, pp. 435–445, 2000.
- [32] H. Sheng, J. Wang, J. Y. Lim, C. Davitt, S. A. Minnich, and C. J. Hovde, "Internalization of *Escherichia coli* O157:H7 by bovine rectal epithelial cells," *Frontiers in Microbiology*, vol. 2, article 32, 2011.

- [33] M. M. Brashears, D. Jaroni, and J. Trimble, "Isolation, selection, and characterization of lactic acid bacteria for a competitive exclusion product to reduce shedding of *Escherichia coli* O157:H7 in cattle," *Journal of Food Protection*, vol. 66, no. 3, pp. 355–363, 2003.
- [34] A. de Vaux, M. Morrison, and R. W. Hutkins, "Displacement of *Escherichia coli* O157:H7 from rumen medium containing prebiotic sugars," *Applied and Environmental Microbiology*, vol. 68, no. 2, pp. 519–524, 2002.
- [35] T. Zhao, M. P. Doyle, B. G. Harmon, C. A. Brown, P. O. E. Mueller, and A. H. Parks, "Reduction of carriage of enterohemorrhagic *Escherichia coli* O157:H7 in cattle by inoculation with probiotic bacteria," *Journal of Clinical Microbiology*, vol. 36, no. 3, pp. 641–647, 1998.
- [36] United States Department of Agriculture Food Safety Inspection Service, 2010, http://www.fsis.usda.gov/PDF/Reducing_Ecoli_Shedding_In_Cattle_0510.pdf.
- [37] S. Calsamiglia, M. Busquet, P. W. Cardozo, L. Castillejos, and A. Ferret, "Invited review: essential oils as modifiers of rumen microbial fermentation," *Journal of Dairy Science*, vol. 90, no. 6, pp. 2580–2595, 2007.
- [38] C. J. van Nevel and D. I. Demeyer, "Manipulation of rumen fermentation," in *The Rumen Microbial Ecosystem*, P. N. Hobson, Ed., pp. 387–443, Elsevier Science, Essex, UK, 1988.
- [39] S. Tamminga, "A review on environmental impacts of nutritional strategies in ruminants," *Journal of Animal Science*, vol. 74, no. 12, pp. 3112–3124, 1996.
- [40] R. K. McGuffey, L. F. Richardson, and J. I. D. Wilkinson, "Tonophores for dairy cattle: current status and future outlook," *Journal of Dairy Science*, vol. 84, supplement, pp. E194–E203, 2001.
- [41] M. Busquet, S. Calsamiglia, A. Ferret, and C. Kamel, "Screening for effects of plant extracts and active compounds of plants on dairy cattle rumen microbial fermentation in a continuous culture system," *Animal Feed Science and Technology*, vol. 123–124, part 2, pp. 597–613, 2005.
- [42] A. P. Fonseca, C. Extremina, A. F. Fonseca, and J. C. Sousa, "Effect of subinhibitory concentration of piperacillin/tazobactam on *Pseudomonas aeruginosa*," *Journal of Medical Microbiology*, vol. 53, no. 9, pp. 903–910, 2004.
- [43] E.-B. Goh, G. Yim, W. Tsui, J. McClure, M. G. Surette, and J. Davies, "Transcriptional modulation of bacterial gene expression by subinhibitory concentrations of antibiotics," *Proceedings of the National Academy of Sciences of the United States of America*, vol. 99, no. 26, pp. 17025–17030, 2002.
- [44] W. H. W. Tsui, G. Yim, H. H. Wang, J. E. McClure, M. G. Surette, and J. Davies, "Dual effects of MLS antibiotics: transcriptional modulation and interactions on the ribosome," *Chemistry and Biology*, vol. 11, no. 9, pp. 1307–1316, 2004.
- [45] F. Dziva, P. M. van Diemen, M. P. Stevens, A. J. Smith, and T. S. Wallis, "Identification of *Escherichia coli* O157:H7 genes influencing colonization of the bovine gastrointestinal tract using signature-tagged mutagenesis," *Microbiology*, vol. 150, no. 11, pp. 3631–3645, 2004.
- [46] H. Sheng, J. Y. Lim, H. J. Knecht, J. Li, and C. J. Hovde, "Role of *Escherichia coli* O157:H7 virulence factors in colonization at the bovine terminal rectal mucosa," *Infection and Immunity*, vol. 74, no. 8, pp. 4685–4693, 2006.
- [47] V. Sperandio, "SdiA sensing of acyl-homoserine lactones by enterohemorrhagic *E. coli* (EHEC) serotype O157:H7 in the bovine rumen," *Gut Microbes*, vol. 1, no. 6, pp. 432–435, 2010.

Research Article

Antibacterial Activity of Leaf Extracts of *Baeckea frutescens* against Methicillin-Resistant *Staphylococcus aureus*

Somayeh Razmavar, Mahmood Ameen Abdulla, Salmah Binti Ismail, and Pouya Hassandarvish

Department of Molecular Medicine, Faculty of Medicine, University of Malaya, Malaysia

Correspondence should be addressed to Somayeh Razmavar; enteha.tanhaee@yahoo.com

Received 3 February 2014; Accepted 16 April 2014; Published 16 June 2014

Academic Editor: Fabio Ferreira Perazzo

Copyright © 2014 Somayeh Razmavar et al. This is an open access article distributed under the Creative Commons Attribution License, which permits unrestricted use, distribution, and reproduction in any medium, provided the original work is properly cited.

This study was based on screening antibacterial activity of the ethanol extract of *Baeckea frutescens* L. against MRSA clinical isolates, analyzes the potential antibacterial compound, and assesses the cytotoxicity effect of the extract in tissue culture. Leaves of *Baeckea frutescens* L. were shade dried, powdered, and extracted using solvent ethanol. Preliminary phytochemical screening of the crude extracts revealed the presence of alkaloids, flavonoids, steroids, terpenoids, phenols, and carbohydrates. The presence of these bioactive constituents is related to the antibacterial activity of the plant. Disc diffusion method revealed a high degree of activity against microorganisms. The results confirm that *Baeckea frutescens* L. can be used as a source of drugs to fight infections caused by susceptible bacteria.

1. Introduction

In recent years, there has been an increasing awareness about the importance of medicinal plants. Drugs from these plants are easily available, inexpensive, safe, efficient, and rarely accompanied by side effects. Plants which have been selected for medical use over thousands of years constitute the most obvious starting point for new therapeutically effective drugs such as anticancer drugs [1] and antimicrobial drugs [2]. Recently, medicinal plants usage has increased in spite of the advances made in the field of chemotherapy. The reasons proposed [3] are the use of medicinal plants as materials for the extraction of active pharmacological agents or as precursors for chemicopharmaceutical hemisynthesis. There is also the increased use of medicinal plants in industrialized countries for galenic preparations and herbal medicines.

Baeckea frutescens L. of the family Myrtaceae and subfamily Myrtoideae is a medicinal plant that has an essential oil which has been used as a traditional drug in South East Asia. *Baeckea frutescens* L. is a small tree found in mountainous areas of South China, Hong Kong, South East Asia, and Australia. The local Malay name of this plant is “Cucur Atap.”

The needle-like leaves are small and narrow in only about 6–15 mm long. When crushed, the leaves give off a resinous aromatic fragrance. The tiny fruits split, releasing minute angular seeds. Tea made from these leaves is used to treat fever in China [4]. It is one of the traditional folk medicine in Indonesia [4]. Packets of leaves are burned under the bed of colic sufferers.

The essential oil has been used for aromatherapy and is inhaled for mental clarity and to ease mental distress [5]. The oil is also used when massaging aching muscles and to treat pain on the surface of the body in addition to its use as a bath or tonic [5].

This paper presents a preliminary phytochemical investigation of *Baeckea frutescens* L., which is responsible for the antibacterial activity of the extracts of the leaves on methicillin-resistant *Staphylococcus aureus* (MRSA) bacterial species.

2. Materials and Methods

2.1. Preparation of Plant Extracts. Test plant was first collected from the Rimba Ilmu, University of Malaya. All parts

of the plant except the roots were oven-dried at 56°C for several days until fully dried and then ground to fine powder with a blender machine. The extraction was done at room temperature. The powder was soaked in absolute ethanol at a 1:20 ratio for 7 days and then filtered by Whatman filter paper number 1. The filtrate was collected and evaporated under vacuum using the BUCHI Switzerland Rotary Evaporator to obtain concentrated, powdered extracts. All extracts were stored at 4°C for further use. The ranged yield of extracts is 5–20% (w/w).

2.2. Bacterial Culture. A bacterial culture is a method of bacteria organisms by allowing them to reproduce in predetermined culture media under controlled laboratory conditions. For any bacterial culture, it is necessary to provide the suitable environmental and nutritional conditions that exist in its natural habitat.

The methicillin-resistant *Staphylococcus aureus* (MRSA) pure isolates used in this study were kindly provided by Professor Dr. Yassim of the Microbiology Laboratory of University Malaya Medical Centre. The streak plate method is the most common way of separating bacterial cells on the agar surface.

Confirmation of the identity of working strains was done by colony morphology and gram staining as described in the Textbook of Diagnostic Microbiology [6]. The bacterial isolate was maintained in Brain Heart Infusion (BHI) agar (Pronadisa, Spain) slants at 4°C.

2.3. Disc Diffusion Method. Disc diffusion method was used for antibacterial activity. A stock solution of extract was prepared by dissolving 0.1 g of extract with 100 mL of their respective solvents (distilled water and absolute ethanol) to produce a final concentration of 100 mg/mL. The stock solution was then diluted to concentrations of 2.5, 5, 10, 20, 50, and 100 mg/mL of extract. 20 µL of each dilution was impregnated into sterile, blank discs 6 mm in diameter. 5 µL of extract was spotted alternately on both sides of the discs and allowed to dry before the next 5 µL was spotted to ensure precise impregnation. Distilled water and ethanol-loaded discs were used as negative controls for aqueous and ethanol extracts, respectively. All discs were fully dried before the application on bacterial lawn. The positive controls used were vancomycin antibiotic discs (Becton-Dickinson, USA) for all *S. aureus* strains. Antibacterial activity was evaluated by measuring the diameter of the inhibition zone (IZ) around the discs. The assay was repeated thrice. Antibacterial activity was expressed as the mean zone of inhibition diameters (mm) produced by the leaf extract.

2.4. Column Chromatography (CC) Spectral Analysis. The sample is dissolved in a solvent and applied to the front of the column (wet packing) or alternatively adsorbed on a coarse silica gel (dry packing). Using a ratio of 100 g of silica gel/g of crude sample allows for relatively easy separation. The solvent elutes the sample through the column, allowing the components to separate. The ethanol soluble phase was subjected to silica gel column chromatography using AcOH-MeOH (90:10) solvent system.

TABLE 1: Result of the phytochemical screening of ethanol extracts of leaves of *Baeckea frutescens* L.

S. number	Phytochemical compounds	Leaves of crude extracts
1	Flavonoids	+
2	Glycosides	+
3	Phenolic	+

2.5. HPLC Analysis. A HPLC test was performed using an Agilent Zorbax column (Xdb-C18 Type MG 5 µm, 4.6 × 250 mm). The detection wavelengths were 200, 230, 254, and 320 nm. Elution was carried out with CH₃CN-H₂O at the flow rate of 1.2 mL/min. The injection volume was 100 µm. Samples were mixed and vacuum dried to 29.6 mg. Then the samples were dissolved in 1.0 mL of distilled water. A stock solution (12,00 ppm) was prepared by adding 405.4 µL of sample solution (29.6 mg/mL) to 594.6 µL of distilled water, which was kept refrigerated at 4°C. The samples were filtered using a SRP-4 membrane 0.45 µM before they were injected into HPLC. The fractions were collected and subjected to profiling.

2.6. Liquid Chromatography-Mass Spectrometry. Liquid chromatography-mass spectrometry (LC-MS, or alternatively HPLC-MS) is an analytical chemistry technique that combines the physical separation capabilities of liquid chromatography (or HPLC) with the mass analysis capabilities of mass spectrometry. LC-MS is a powerful technique used for many applications which has very high sensitivity and selectivity.

2 mg of sample was prepared by dissolving in 2 mL methanol in volumetric flask. Solution was then filtered by using SRP-4 membrane 0.45 mm. Stock solution 1 mg/mL was kept in fridge at 4°C.

LCMS was performed with an Acquity BEH C18, 2.1 × 50 mm, 1.7 µm UPLC columns. Elution was carried out with %H₂O + 0.1% F.A at the flow rate 0.5 mL/min. The injection volume was 3 µL.

3. Results and Discussion

Phytochemical screening of the crude extracts of *Baeckea frutescens* L. revealed the presence of flavonoids and phenolic compounds (Table 1).

The presence of alkaloid is interesting as significant quantities are used as antimalarial, analgesics, and stimulants [7]. Flavonoids, which are known to prevent tumor growth and also used to protect against gastrointestinal infections, are of pharmacognostic importance thus lending credence to the use of the plant in ethnomedicine [8]. Some of these bioactive compounds that are synthesized as secondary metabolites as the plant grows are also used to protect the plant against microbial attacks and predation by animals [8].

According to the results of disc diffusion assay, this plant has active compounds that are effective for the prevention of infections caused by MRSA.

There are a number of factors that could influence the results of the disc diffusion assay. Firstly, the diameter of the

TABLE 2: Antibacterial activity of ethanol extract of *Baekea frutescens* in different solvents against MRSA.

S. number	Zone of inhibition (mm) against MRSA				Solvents in CC
	Rep. 1	Rep. 2	Rep. 3	Mean	
1	10	8	12	10	Ethyl acetate and hexane
2	20	22	18	20	
3	16	16	16	16	
4	20	18	22	20	
5	6	8	4	6	
6	14	10	18	14	
7	8	6	10	8	
8	16	18	14	16	
9	10	10	10	10	
10	15	10	20	15	
1	0	0	0	0	Acid acetic and methanol
2	10	12	18	10	
3	30	25	35	30	
Ethyl ACETATE	0	0	0	0	Control
Hexane	0	0	0	0	
Acid acetic	0	0	0	0	
Methanol	0	0	0	0	

TABLE 3: Liquid chromatography-mass spectrometry.

Mass [M + H]	Molecular formula [M]	Number of hits [M]
118.0874	C ₅ H ₁₁ N _O ₂	665
136.0623	C ₅ H ₅ N ₅	140
120.082	C ₈ H ₉ N	148

zones is affected by the rate of diffusion of the antimicrobial compound [9, 10] and thus may not exactly represent the potency of the extract's antimicrobial activity. Where studies of plant extracts are concerned, the disc preparation technique could present with another problem wherein the extract was not properly and evenly impregnated into the paper discs. Another important factor is the standardization of the inoculum size to 0.5 McFarland turbidity. This inoculum size is important to ensure confluent or almost confluent lawn growth as a smaller inoculum size (such that single colonies are seen) may produce falsely large inhibition zones while a bigger inoculum size (thick bacterial lawn) may produce falsely smaller zones instead [11].

The ethyl acetate, methanol, and acid acetic solvents were more effective than other solvents to show inhibition zone against MRSA (Table 2).

The zone produced by the plant extract against the MRSA was from acid acetic and methanol solvents were the largest zone. The lowest zone of growth inhibition was ethyl acetate and hexane.

To determine the chemical constituents of the biological activity in ethyl acetate:normal-hexane and acid acetic:methanol soluble phases, HPLC analysis was performed (Figure 1).

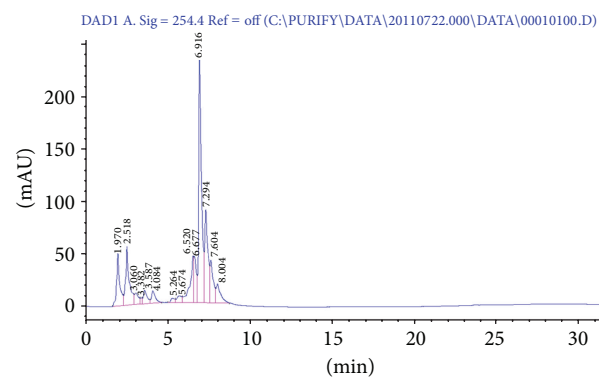


FIGURE 1: HPLC profiling of samples by UV 254 nm. Indicating the compounds shown in Figure 2.

One principal peak and several lesser peaks were observed in the ethyl acetate (EtOAc):normal-hexane soluble phases. Compound 1 was isolated from the EtOAc soluble phase by repeated column chromatography on silica gel.

The molecular formula of the main peak was determined to be C₅H₁₁NO₂, C₅H₅N₅ or C₈H₉N by liquid chromatography-mass spectrometry (Table 3 and Figure 2).

Results obtained for antibacterial activity against MRSA for 3 main peaks were in Table 4.

From the results of the disc diffusion screening, *B. frutescens* is shown to clearly possess antibacterial properties against MRSA. As *B. frutescens* seems to give appreciable antibacterial activity against all gram-positive staphylococcal strains, this may indicate that the plant extract acts specifically against the gram-positive cell wall, particularly the staphylococcal cell wall [12] because they have a much

TABLE 4: Antibacterial activity of liquid chromatography-mass spectrometry results against MRSA.

Number	Molecular formula [M]	Zone of inhibition (mm) against MRSA			Mean
		Rep. 1	Rep. 2	Rep. 3	
1	C ₅ H ₁₁ N _O ₂	10	11	10	10.33
2	C ₅ H ₅ N ₅	11	12	12	11.66
3	C ₈ H ₉ N	10	10	10	10

TABLE 5: Zone of inhibition against some bacteria strains by ethanol extract of *Baeckea frutescens* L.

Bacteria strain	Zone of inhibition (mm)				Gram	Shape
	Conc. of extract (mg/mL)					
	100	50	20	10		
MRSA ST/0903-24	14.0	11.5	9.5	7.5	Positive	Cocci
MRSA ST/0904-25	12.0	8.5	7.0	—	Positive	Cocci
MRSA ST/0904-28	14.5	11.5	8.0	7.5	Positive	Cocci
MRSA ST/0904-30	12.0	8.5	—	—	Positive	Cocci
<i>S.aureus</i>	13.0	11.5	7.5	—	Positive	Cocci
<i>E.coli</i>	8.5	7.5	7.0	7.5	Negative	Bacilli
<i>Klebsiella</i> sp.	—	—	—	—	Negative	Diplococci
<i>Bacillus</i> sp.	9.5	8.5	7.0	7.0	Positive	Bacilli
<i>P. aeruginosa</i>	—	—	—	—	Negative	Bacilli

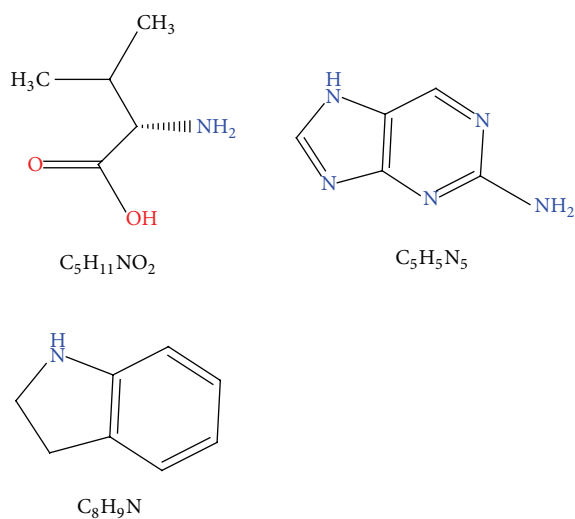


FIGURE 2: Chemical structures of compounds.

thicker peptidoglycan layer than gram-negative bacteria. This outer membrane is composed of lipopolysaccharides that give gram-negative bacteria extra resistance against antibiotics that cannot penetrate it, for example, glycopeptides like vancomycin [13].

Antibacterial activity of ethanol extract of *B. frutescens* leaf has been assessed by measuring the diameters of zones of growth inhibition on some strain of bacteria and the results are presented as shown in Table 5.

Inhibition growth of the highest zone has been shown by ethanol extract against gram-positive bacteria like MRSA (14.5 mm), *Staphylococcus aureus* (13 mm), and *Bacillus* (9.5 mm). The growth inhibition was moderately active

against gram-negative bacteria *Escherichia coli* (8.5 mm) and *Klebsiella* (0 mm).

4. Conclusion

The result of this study showed that *Baeckea frutescens* L. extract contains phytochemical components. Potentially, these compounds have the most important applications against human pathogens, including those that cause enteric infections. The results of various screening tests indicate that the leaves have some measurable inhibitory action against gram-positive bacteria such as *Staphylococcus aureus* (MRSA).

Conflict of Interests

All authors have nothing to disclose and have no commercial or financial interests in the products described in this paper.

References

- [1] P. M. Dewick, "Tumor inhibitor from plants," in *Trease and Evans' Pharmacognosy*, Elsevier Health Sciences, Philadelphia, Pa, USA, 1996.
- [2] J. D. Phillipson and C. W. Wright, "Plants with antiprotozoal activity," in *Trease and Evans' Pharmacognosy*, W.B.Saunders company, London, UK, 14th edition, 1996.
- [3] R. Magherini, "Le piante edicinalie aromatiche oggi Possibilita di coltivazione delle piante medicinali aromatiche," *Litalia Agricola*, vol. 3, 1998.
- [4] S. Mardiswojo and H. Rajakmangunsudarso, *Cabe Puyang Warisan Nenek Moyang*, Balai Pustaka, Jakarta, Indonesia, 1985.
- [5] W. N. Setzer, B. Vogler, J. M. Schmidt, J. G. Leahy, and R. Rives, "Antimicrobial activity of *Artemisia douglasiana* leaf essential oil," *Fitoterapia*, vol. 75, no. 2, pp. 192–200, 2003.

- [6] J. F. Hindler and J. K. Jorgensen, "Antimicrobial susceptibility testing: procedures in antimicrobial susceptibility testing," in *Textbook of Diagnostic Microbiology*, C. R. Mahon, D. C. Lehman, and G. Manuselis, Eds., pp. 319–353, Saunders Elsevier, Beijing, China, 2007.
- [7] J. A. Duke and E. S. Ayensu, *Medicinal Plants of China*, vol. 4 of *Medicinal Plants of the World*, Reference Publications, Algonac, Mich, USA, 1985.
- [8] L. Cathrine and N. P. Nagarajan, "Preliminary phytochemical analysis and antibacterial activity of leaf extracts of *Vitex leucocylon* L.F.," *International Journal of Current Pharmaceutical Research*, vol. 3, no. 2, 2010.
- [9] I. M. S. Eldeen, E. E. Elgorashi, and J. van Staden, "Antibacterial, anti-inflammatory, anti-cholinesterase and mutagenic effects of extracts obtained from some trees used in South African traditional medicine," *Journal of Ethnopharmacology*, vol. 102, no. 3, pp. 457–464, 2005.
- [10] J. D. Turnidge, M. J. Ferraro, and J. H. Jorgensen, "Susceptibility test methods: general considerations," in *Manual of Clinical Microbiology*, P. R. Murray, E. J. Baron, J. H. Jorgensen, M. L. Landry, and M. A. Pfaller, Eds., pp. 1146–1151, ASM press, Washington, DC, USA, 9th edition, 2007.
- [11] J. H. Jorgensen and J. P. Turnidge, "Susceptibility test methods: dilution and disk diffusion methods," in *Manual of Clinical Microbiology*, P. R. Murray, E. J. Baron, J. H. Jorgensen, M. L. Landry, and M. A. Pfaller, Eds., pp. 1152–1172, ASM press, Washington, DC, USA, 9th edition, 2007.
- [12] A. N. Sudjana, C. D'Orazio, V. Ryan et al., "Antimicrobial activity of commercial *Olea europaea* (olive) leaf extract," *International Journal of Antimicrobial Agents*, vol. 33, no. 5, pp. 461–463, 2009.
- [13] A. Sheldon, "Antibiotic mechanisms of action and resistance," in *Textbook of Diagnostic Microbiology*, C. R. Mahon, D. C. Lehman, and G. Mansuselis, Eds., pp. 303–317, Saunders Elsevier, Beijing, China, 3rd edition, 2007.

Research Article

Jacobsen Catalyst as a Cytochrome P450 Biomimetic Model for the Metabolism of Monensin A

Bruno Alves Rocha,¹ Anderson Rodrigo Moraes de Oliveira,¹ Murilo Pazin,² Daniel Junqueira Dorta,¹ Andresa Piacezzi Nascimento Rodrigues,³ Andresa Aparecida Berretta,³ Ana Paula Ferranti Peti,¹ Luiz Alberto Beraldo de Moraes,¹ Norberto Peporine Lopes,⁴ Stanislav Pospíšil,⁵ Paul Jonathan Gates,⁶ and Marilda das Dores Assis¹

¹ Departamento de Química, Faculdade de Filosofia, Ciências e Letras de Ribeirão Preto, Universidade de São Paulo, 14040-901 Ribeirão Preto, SP, Brazil

² Departamento de Análises Clínicas, Toxicológicas e Bromatológicas, Faculdade de Ciências Farmacêuticas de Ribeirão Preto, Universidade de São Paulo, 14040-903 Ribeirão Preto, SP, Brazil

³ Laboratório de Pesquisa, Desenvolvimento e Inovação, Apis Flora Industrial e Comercial LTDA, 140120-670 Ribeirão Preto, SP, Brazil

⁴ Núcleo de Pesquisas em Produtos Naturais e Sintéticos, Faculdade de Ciências Farmacêuticas de Ribeirão Preto, Universidade de São Paulo, 14040-903 Ribeirão Preto, SP, Brazil

⁵ Institute of Microbiology, Academy of Sciences of the Czech Republic, Videňská, CZ-142 20 Prague, Czech Republic

⁶ School of Chemistry, University of Bristol, Bristol BS8 1TS, UK

Correspondence should be addressed to Marilda das Dores Assis; mddassis@usp.br

Received 21 February 2014; Accepted 11 May 2014; Published 28 May 2014

Academic Editor: Fabio Ferreira Perazzo

Copyright © 2014 Bruno Alves Rocha et al. This is an open access article distributed under the Creative Commons Attribution License, which permits unrestricted use, distribution, and reproduction in any medium, provided the original work is properly cited.

Monensin A is a commercially important natural product isolated from *Streptomyces cinnamonensis* that is primarily employed to treat coccidiosis. Monensin A selectively complexes and transports sodium cations across lipid membranes and displays a variety of biological properties. In this study, we evaluated the Jacobsen catalyst as a cytochrome P450 biomimetic model to investigate the oxidation of monensin A. Mass spectrometry analysis of the products from these model systems revealed the formation of two products: 3-O-demethyl monensin A and 12-hydroxy monensin A, which are the same ones found in *in vivo* models. Monensin A and products obtained in biomimetic model were tested in a mitochondrial toxicity model assessment and an antimicrobial bioassay against *Staphylococcus aureus*, *S. aureus* methicillin-resistant, *Staphylococcus epidermidis*, *Pseudomonas aeruginosa*, and *Escherichia coli*. Our results demonstrated the toxicological effects of monensin A in isolated rat liver mitochondria but not its products, showing that the metabolism of monensin A is a detoxification metabolism. In addition, the antimicrobial bioassay showed that monensin A and its products possessed activity against Gram-positive microorganisms but not for Gram-negative microorganisms. The results revealed the potential of application of this biomimetic chemical model in the synthesis of drug metabolites, providing metabolites for biological tests and other purposes.

1. Introduction

Monensin A (Figure 1) is the main representative drug of the class of polyether ionophore antibiotics of natural origin, isolated from strains of *actinomycetes*. The chemical and biological properties of monensin A are related to their

ability to form complexes with cations, especially sodium, and transport the complex formed through cell membranes, thus modifying the normal concentration gradient of Na^+/K^+ and thus leading to cell death [1–4].

Since its discovery, monensin A has been widely studied due to its wide spectrum of biological properties such as

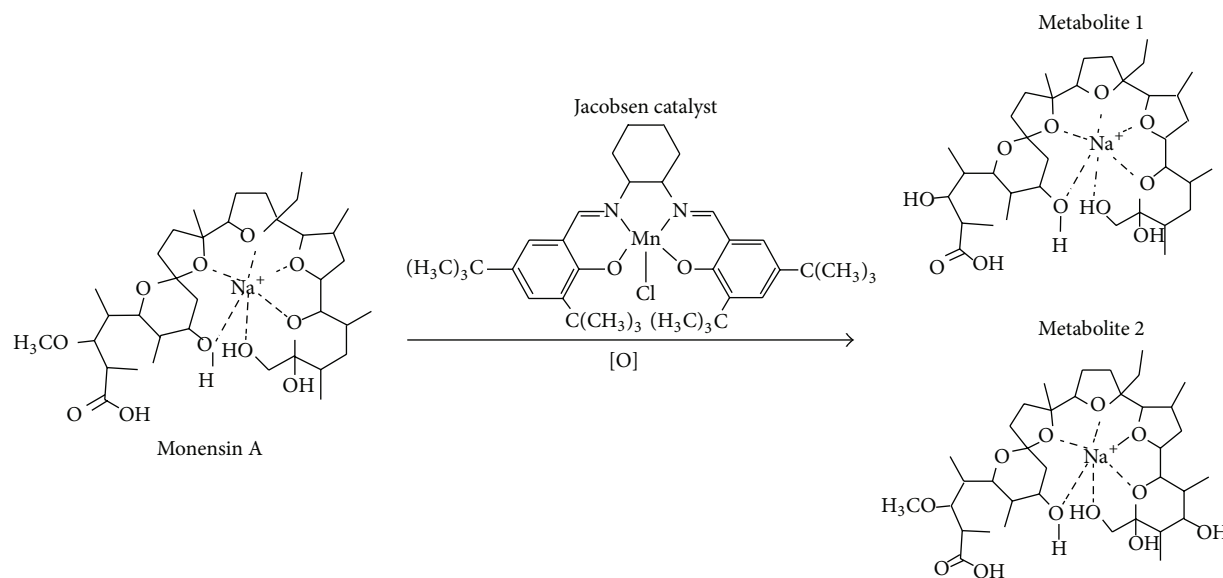


FIGURE 1: Chemical structures of monensin A, metabolite 1, metabolite 2, and Jacobsen catalyst.

antimicrobial (especially against Gram-positive bacteria), antiparasitic, antimalarial, and antiviral activities. Furthermore, recent studies on biological properties for cancer therapy have focused on studies of the metabolism of this drug in humans [3–6].

Another important area of concern is the recent reports of the presence of significant levels of waste monensin A in poultry meat and eggs [7–9]. The presence of monensin A in processed food leads to the real eventuality of interaction with other drugs, since monensin A is metabolized by enzymes of the cytochrome P450 3A family (CYP450), resulting in human health problems, such as resistance to antibiotics and poisoning [10–12]. The need to know the actions of monensin A and its metabolites on organisms and the risk of toxicity associated with these compounds exemplifies the need for models that simulate the metabolism of this compound leading to an increased understanding of its mechanism of action, toxicity, and pharmacokinetics in humans.

Cytochrome P450 is a superfamily of enzymes responsible for the oxidative metabolism of a wide variety of xenobiotics in living organisms and they are involved in the metabolism of a wide variety of xenobiotics [13, 14]. In the presence of oxygen donors, Jacobsen catalyst (Figure 1) is known to mimic various reactions of CYP450 enzymes, such as oxidation and oxygenation. Some recent examples in the literature include studies on drugs such as primidone [15], carbamazepine [16], and other synthetic drugs [14], as well as other active natural products such as lapachol [17] and grandisin [18].

In vitro studies of drug metabolism using chemical models such as Jacobsen catalyst have several advantages: (1) oxidation products are obtained in relatively large amounts, enabling their use in the identification of *in vivo* metabolites, not to mention the possibility of employing them as standards in pharmacological assays; (2) drug toxicity and action mechanisms can be more easily established; (3) the use of

animals for toxicological and pharmacological tests can be reduced [19, 20].

In this context, the aim of this work was to investigate the *in vitro* metabolism of monensin A by applying the Jacobsen catalyst as biomimetical model of CYP450 in order to improve the information available for preclinical pharmacokinetic studies and also to evaluate the toxicity of the products in mitochondrial models compared to monensin A. To conclude, a study of the antimicrobial activity of monensin A and its metabolites was carried out in some Gram-positive and Gram-negative microorganisms in order to evaluate the biological activity of the metabolites generated.

2. Materials and Methods

Monensin A (95%) was sourced from Sigma-Aldrich Chemical Co. The Jacobsen catalyst, 3-chloroperoxybenzoic acid (*m*-CPBA), and *tert*-butyl hydroperoxide (*t*-BOOH, 70% solution in water) were all acquired from Acros-Organics. Hydrogen peroxide (30% in water) was supplied by Fluka and stored at 5°C, and it was periodically titrated to confirm its purity. Iodosylbenzene (PhIO) was obtained through iodosyl benzenediacetate hydrolysis and its purity was measured by iodometric assay.

2.1. Oxidation Reactions and Isolation of Metabolites.

Based on the previous studies by this laboratory [22], the oxidation reactions were performed in an Eppendorf tube (2 mL), under mechanical stirring (Vibrax VXR agitator) at room temperature for 24 h. The ideal molar ratio obtained for the reaction was 1:20:20 (for catalyst : oxidant : monensin A). This was achieved by adding $0.3 \text{ mmol}\cdot\text{L}^{-1} : 6 \text{ mmol}\cdot\text{L}^{-1} : 6 \text{ mmol}\cdot\text{L}^{-1}$ in the 0.5 mL of reaction medium (CH_2Cl_2). The oxidants were *m*-CPBA, PhIO, *t*-BOOH, and H_2O_2 . The products from monensin

A oxidation were analyzed by HPLC-ESI-MS. Control reactions were carried out in the absence of catalyst under the same conditions as the catalytic runs and no products were detected.

The oxidation reaction in preparative scale was performed in a Falcon tube (50 mL), under mechanical stirring (Vibrax VXR agitator) at room temperature for 24 h. The ideal molar ratio obtained for the reaction was 1:20:20 (for Jacobsen catalyst: PhIO: monensin A). This was 1:20:20 achieved by adding 0.3 mM:6 mM:6 mM in the 25 mL of reaction medium (CH_2Cl_2). After that, the separation of products was performed by silica gel preparative TLC using a mixture of CHCl_3 :MeOH (93:7 v/v) as eluent. After elution, the borders of the plates were revealed with solution of vanillin-sulfuric acid (1% vanillin and 1% H_2SO_4 in ethanol) for visualization of the metabolites and its further isolation.

2.2. Quantification of Monensin A Oxidation by HPLC-ESI-MS Analysis. LC-ESI-MS analyses were performed on a Varian LC-MS 1200L triple quadrupole apparatus coupled to a mass spectrometer with ESI ionization in the positive mode (Varian Medical Systems Inc., Palo Alto, CA). The chromatographic analysis was performed using an injection volume of 10 μL , sample concentration 50 $\mu\text{g}\cdot\text{mL}^{-1}$ in an Xterra analytical column MS C-18 (150 \times 2.1 mm, 5 μm) (Waters) and following gradient (MeOH:H₂O): 0.1 min 70% MeOH, 20.0 min 98% MeOH, 21.0 min 30% MeOH, and 30.0 min 70% MeOH. The MS conditions were capillary voltage 3.2 kV, cone voltage 40 V, source temperature 40°C, and N₂ desolvation temperature 350°C. The percentage of monensin A oxidation was determined by using a calibration curve of 10–100 $\mu\text{g}\cdot\text{mL}^{-1}$. The resulting mass spectra were monitored over a *m/z* range of 610 to 800.

2.3. Identification of Metabolites. The product ion spectra (see Figures S1–S3 in Supplementary Material available online at <http://dx.doi.org/10.1155/2014/152102>) were obtained using a micrOTOF-Q II hybrid quadrupole time-of-flight (Qq-TOF) mass spectrometer (Bruker Daltonics Inc., Billerica, MA) using positive ion electrospray (ESI) ionization. Monensin A and the metabolites were directly infused into the instrument by syringe pump (Cole-Palmer) at a flow rate of 300 $\text{mL}\cdot\text{h}^{-1}$. The instrument settings were capillary temperature 250°C, capillary voltage 4.0 kV, and source cone potential 30 V. The nebulizer and drying gas were N₂ and the collision gas was argon. Tandem mass spectrometry (MS/MS) analysis was achieved on isolated precursor ions using collision induced dissociation (CID) with argon as collision gas at 80 eV.

2.4. Antimicrobial Activity Bioassay. The bioassays were carried out using the strains *Staphylococcus aureus* ATCC 25923, *Staphylococcus aureus* ATCC 43300 (MRSA-methicillin resistant), *Staphylococcus epidermidis* ATCC 14990, *Pseudomonas aeruginosa* ATCC 27853, and *Escherichia coli* ATCC 25922 all acquired from the American Type Culture Collection (ATCC). Approximately 5×10^5 microorganisms $\cdot\text{mL}^{-1}$ were incubated in Muller Hinton

broth in 96-well microtiter plates containing the samples to be tested. The compounds (monensin A, metabolite 1, and metabolite 2) were dissolved in dimethylsulfoxide (DMSO) and diluted into the medium to give 100, 50, 25, 12.5, 6.3, 3.1, 1.6, 0.8, 0.4, 0.2, 0.1, and 0.05 $\mu\text{g}\cdot\text{mL}^{-1}$, as their final concentrations. The plates were incubated at 37°C and the bioassays were performed in triplicate. The cell death was determined by a MTT colorimetric method which was described by Andrews [23] and Furtado et al. [24]. The DMSO solution and chloramphenicol were used as controls of the experiment.

2.5. Evaluation of Toxicity of Monensin A and Products 1 and 2 Using Mitochondrial Model. Monensin A was diluted in ethanol to concentrations 0.01, 0.1, and 1 μM . All assays were performed in three replicates. Rat liver mitochondria were isolated by standard differential centrifugation according to Pereira et al. [25] and the mitochondrial protein content was determined by the biuret method.

Mitochondrial respiration was monitored polarographically with an oxygraph (Hansatech) equipped with a Clark-type oxygen electrode [26]. The mitochondria (1.0 mg protein) were incubated at 30°C in 1 mL of the respiratory medium containing 125 mM sucrose, 65 mM KCl, 10 mM HEPES-KOH, 0.5 mM EGTA, and 10 mM K₂HPO₄; pH 7.2. 5 mM glutamate and malate were used as the oxidizable substrates for complex I; and mitochondrial oxidative phosphorylation (state 3) was initiated using 400 nmol ADP.

Mitochondrial Membrane potential ($\Delta\psi$) was monitored spectrofluorimetrically using 10 μM safranin-o as a probe in a F-4500 spectrofluorometer (Hitachi) with the 495/586 nm excitation/emission wavelength pair [25]. The mitochondria (1.0 mg protein $\cdot\text{mL}^{-1}$) were incubated at 30°C in 2 mL of the standard reaction medium containing 125 mM sucrose, 65 mM KCl, and 10 mM HEPES-KOH, and CCCP (carbonyl cyanide 3-chlorophenylhydrazone) was added at the end of each experiment for the complete dissipation of the membrane potential.

Mitochondrial swelling was estimated from the decrease in apparent absorbance at 540 nm performed with a Model DU-70 spectrophotometer (Beckman). The mitochondria were incubated using 30°C in 2 mL of the standard reaction medium.

Mitochondrial reactive oxygen species (ROS) production was monitored spectrofluorimetrically with 2',7'-dichlorodihydrofluorescein diacetate (H₂DCFDA) with the 503/529 nm excitation/emission wavelength pair, both using the standard reaction medium [27].

2.6. Statistical Analysis of Mitochondrial Assays. The experimental data were evaluated by analysis of variance (ANOVA), followed by the post hoc of Tukey, to compare which groups are different from each other and their control using the program GraphPad Prism, version 5.1 for Windows. Results with *P* < 0.05 were considered statistically significant.

3. Results and Discussion

Under optimized reaction conditions chosen, the efficiency of the various oxidants PhIO, *m*-CPBA, H₂O₂, and *t*-BOOH in the oxidation of monensin A catalysed by Jacobsen catalyst can be measured through the monensin conversion of 36, 27, 26, and 14%, respectively. PhIO was used as an oxygen donor because it is considered as a standard and simple oxidant which contains a single oxygen atom and is well-adapted for the selective and clean formation of metal-oxo intermediates, Mn^V(O)-salen, more efficient and selective in transferring oxygen to the substrate [13–16]. When using hydroperoxides and peracids as the oxidative agent it is possible for two competing oxygen activation mechanisms to occur. One involves homolytic cleavage of the O–O bond, leading to the formation of the less reactive intermediate Mn^{IV}(OH) salen, as well as RO· radicals resulting in reduced yields. The other mechanism involves a heterolytic cleavage of the non-symmetrical O–O bond, leading to the formation of the active specie Mn^V(O) salen that result in higher yields of oxidation products [13–16]. Considering the monensin A conversion %, the PhIO was chosen as the standard oxidant in order to isolate the oxidative products in preparative scale.

Monensin A oxidation with this biomimetic model leads to the formation of two main products, product 1 (*m/z* 679) and product 2 (*m/z* 709). Other reaction media were also tested with little significant influence on the efficiency of oxidation. These two products were isolated by preparative TLC and characterized by ESI-HRMS and MS/MS.

ESI-HRMS was used to determine the molecular formula of these products. The analysis resulted in the [M + Na]⁺ signal at *m/z* 679.4008 for product 1 (3-*O*-demethyl monensin A) and *m/z* 709.4134 for product 2 (12-hydroxy monensin A) confirming the molecular formula (mass error < 5 ppm) the same as observed for the products obtained from *in vitro* metabolism of monensin A by human liver microsomes and microbial transformation by fungi of *Cunninghamella* genus [21]. Additionally, products 1 and 2 displayed an identical low-resolution product ion spectrum (Supplementary Materials) as well as having the same retention times as those observed in the previous studies [21, 22]. The major ion formed in the MS/MS studies results from a Grob-Wharton type fragmentation and/or H₂O, followed by CO elimination, as previously proposed for monensin A and its metabolites (Table 1) [21, 22, 28, 29].

Another part of the study was to assess if products 1 and 2 still had toxic activity against the mitochondrial organelle as observed for monensin A. After isolation of the products, they were evaluated to test whether they could damage the mammalian mitochondria. Mitochondria are intracellular structures primarily responsible for transforming the energy from food into useful and transportable energy to the cells through the molecule adenosine 5-triphosphate (ATP). In this way, mitochondria are fundamental to cellular life of most eukaryotic organisms [30]. Since mitochondrial damage may be associated with various tissue injuries or diseases, this organelle has become an important tool for toxicological studies. These studies should help increase the understanding and enable prediction of any adverse effects of various

TABLE 1: Major product ions (*m/z*) observed in the MS/MS spectra of monensin A and its products (these ions are in accordance with Rocha et al. 2014 [21]).

Monensin A (<i>m/z</i>)	Product 1 (<i>m/z</i>)	Product 2 (<i>m/z</i>)
693	679	709
507	507	523
479	479	495
461	461	477
443	443	459
—	—	441
343	343	343
303	303	303
675	661	691
657	643	673
—	—	655
675	661	691
501	501	517
483	483	499
383	383	441

xenobiotics [31, 32]. Often, xenobiotics have different effects on mitochondrial function. Therefore, the use of isolated mitochondria can be considered as a good experimental model to evaluate the toxicological effect of compounds [33, 34].

The results of this study demonstrated that a concentration of only 1 μM for monensin A affected the mitochondrial parameters. Monensin A was observed to increase state 4 of oxygen consumption by 44.11% and consequently decreased the respiratory control ratio (RCR) by 32.59%. It also caused a 47.73% reduction in ADP/O, leading to a decrease mitochondrial respiratory efficiency (Table 2). The products 1 and 2 demonstrated none of these detrimental effects in the study.

Figures 2(a), 2(b), and 2(c) show the effects of monensin A and its products (1 μM) on mitochondrial membrane potential ($P = 0.0036$), swelling ($P < 0.0001$), and ROS accumulation ($P < 0.0001$), respectively. In this study of these three parameters, significant effects were only observed for the mitochondria incubated with monensin A.

The increase on mitochondrial state 4 respiration is an indicative of the uncoupler activity of monensin A which leads to the observed decrease of 23.29% on the mitochondrial membrane potential. These effects were probably due to the fact that monensin A has the capacity to cause exchange of H⁺ ions, which is primarily responsible for the formation of the mitochondrial membrane potential [35]. Mitochondrial swelling is also related to the effect on these parameters, reaching 54.61% effect on the apparent turbidity, and it is shown on the literature that monensin A also interferes with the Na⁺ and Ca²⁺ mitochondrial regulation, which affects the osmotic balance causing a swelling in this organelle [36].

Monensin A (1 μM) also affected mitochondrial oxidative stress, increasing by 12.14% accumulation of free radicals, which is in accordance with Ketola et al. [37] which observed the same effect in a strain of prostate cancer cells. The ROS production may occur due to the fact that monensin A

TABLE 2: Values of the effect caused by monensin A and its products (1 μ M) on respiratory parameters.

	V3	V4	RCR	ADP/O
Control	66.107 \pm 2.45 ^a	9.798 \pm 0.32 ^a	6.747 \pm 0.12 ^a	2.874 \pm 0.03 ^a
Monensin A	64.097 \pm 2.35 ^a	14.12 \pm 0.97 ^b	4.548 \pm 0.16 ^b	1.498 \pm 0.01 ^b
Metabolite 1	66.363 \pm 2.29 ^a	10.02 \pm 0.11 ^a	6.623 \pm 0.27 ^a	2.757 \pm 0.09 ^a
Metabolite 2	66.730 \pm 1.95 ^a	9.832 \pm 0.07 ^a	6.786 \pm 0.15 ^a	2.728 \pm 0.06 ^a

*Respiration rates in nmol O₂/mg protein/min were performed in mitochondria isolated from rat liver (1.0 mg protein·mL⁻¹) incubated.

*Different letters represent significant differences between treatments according to Tukey's test ($P < 0,05$).

*V3 = state 3; V4 = state 4; RCR = respiratory control ratio; ADP/O = phosphorylation efficiency.

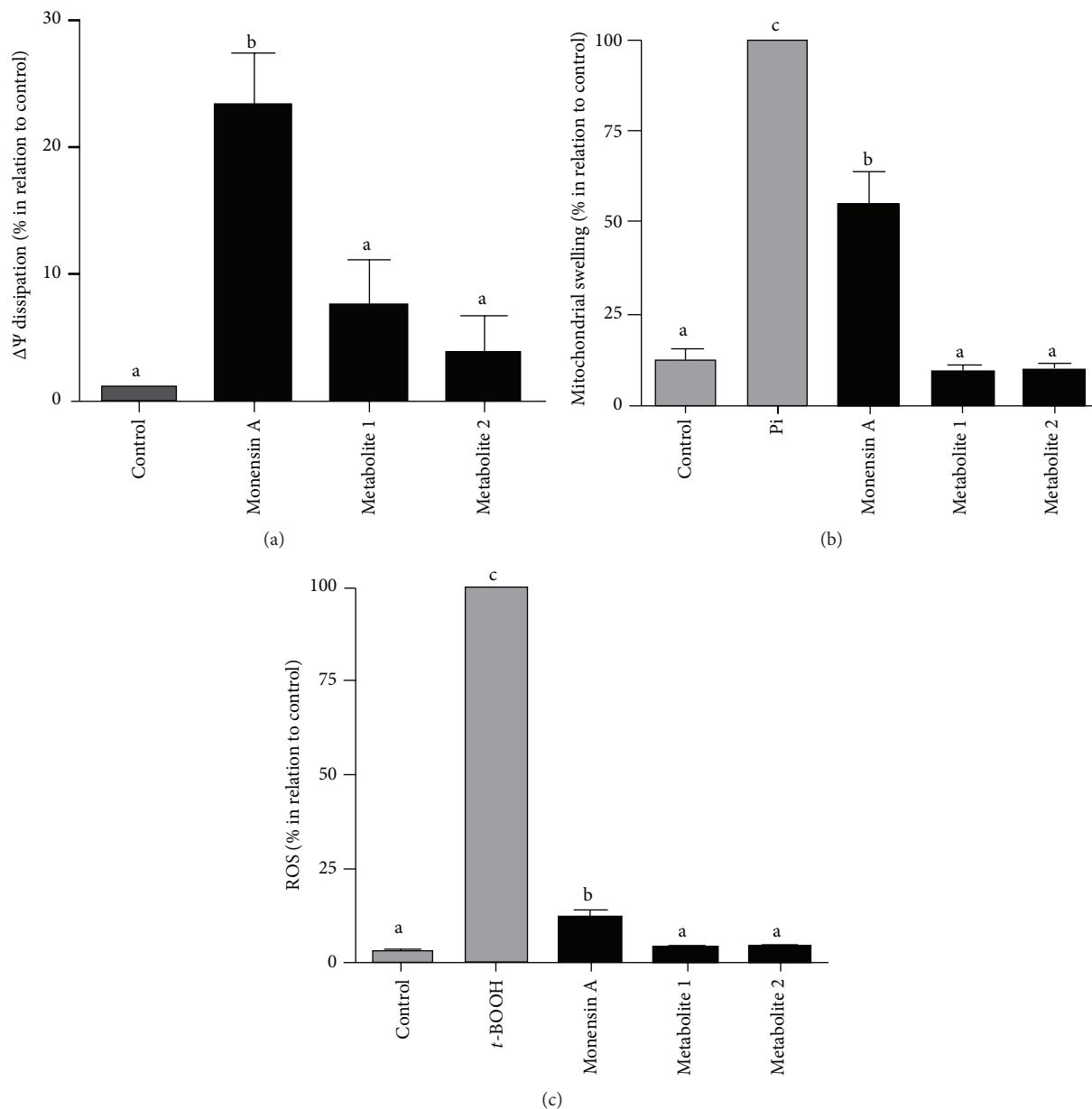


FIGURE 2: (a) Effect of monensin A (1 μ M), metabolite 1 (1 μ M), and metabolite 2 (1 μ M) on the dissipation of the mitochondrial membrane potential. (b) Effect of monensin A (1 μ M), metabolite 1 (1 μ M), and metabolite 2 (1 μ M) on mitochondrial swelling. (c) Effect of monensin A (1 μ M), metabolite 1 (1 μ M), and metabolite 2 (1 μ M) on mitochondrial production of free radicals. All experiments were performed in mitochondria isolated from rat liver (1.0 mg protein·mL⁻¹) incubated as described in Section 2. Points represent the mean \pm SEM of three determinations with different mitochondrial preparations, relative to the control in the absence of the compound. *Different letters represent significant differences between treatments according to Tukey's test ($P < 0.05$).

TABLE 3: Minimal bactericidal concentration of monensin A, metabolite 1, and metabolite 2 and the controls against *Staphylococcus aureus* ATCC 25923, *Staphylococcus aureus* ATCC 43300, *Staphylococcus epidermidis* ATCC 14990, *Pseudomonas aeruginosa* ATCC 27853, and *Escherichia coli* ATCC 25922. Results are expressed in $\mu\text{g}\cdot\text{mL}^{-1}$.

Microorganisms	Samples				
	Monensin A	Product 1	Product 2	DMSO	Chloramphenicol
<i>S. aureus</i> 25923	3.1	25.0	>100	>100	6.3
<i>S. aureus</i> 43300	6.3	50.0	>100	>100	8.3
<i>S. epidermidis</i>	25.0	>100	>100	>100	6.3
<i>E. coli</i>	>100	>100	>100	>100	3.1
<i>P. aeruginosa</i>	>100	>100	>100	>100	100.0

caused the deregulation of mitochondrial bioenergetic states arising from ionic alterations, besides having the ability to cause peroxidation of membrane lipids due to the free radical accumulation [38].

It is noteworthy to observe that the products (1 and 2) showed no effect in any of the studied parameters, indicating that metabolism of monensin A prevents its toxic effects to the mitochondria. The toxic effects observed for the interaction of monensin A with isolated rat liver isolated mitochondria can compromise the ATP production as described by Mollenhauer et al. [36]. This occurs because the ATP depletion is one of the early events of compound-induced toxicity resulting from the observed effects on oxygen consumption, dissipation of the mitochondrial membrane potential, and the generation of reactive oxygen species [39, 40]. Other studies about biological activity of product 1 have indicated that it has a much lower antimicrobial, anticoccidial, cardiotoxic, and cytotoxic activity relative to the parent compound [41, 42].

In order to evaluate antimicrobial behavior of monensin A and products 1 and 2, their effects on three Gram-positive and two Gram-negative microorganisms were investigated. The results demonstrated monensin A were efficient against the Gram-positive strains; however, products 1 and 2 presented a reduction in its activity and an inactivation, respectively. These results obtained for monensin A corroborate those in the study by Łowicki and Huczyński [4] that studied monensin A and some semisynthetic analogues (modifications in hydroxyl and carboxyl groups). The semisynthetic esters of monensin A demonstrated antimicrobial action against Gram-positive bacteria, with the results for monensin A against *S. aureus* 25923 being very similar to that presented in this study [2, 4].

Monensin A is extensively metabolized and converted to numerous metabolites by cattle, pigs, and rats. *O*-demethylation and hydroxylation appear to be the major metabolic pathways. Sassman and Lee [42] evaluated antimicrobial activity of *O*-demethyl monensin A by bioautography against *Bacillus subtilis* and by turbidimetric assay against *Streptococcus faecalis*. In these systems 3-*O*-demethyl monensin A was only 5% as active as monensin, suggesting that the monensin is metabolized to products with little or without antimicrobial activity.

The results found for monensin A against *S. aureus* ATCC 25923, $3.1 \mu\text{g}\cdot\text{mL}^{-1}$ (Table 3), was practically identical to that one related by Łowicki and Huczyński [4] who

found $2.9 \mu\text{g}\cdot\text{mL}^{-1}$ for the same strain, suggesting that the methodology used in this work is reliable. The data found by Łowicki and Huczyński for *S. epidermidis*, however, were different (2.9 and $5.8 \mu\text{g}\cdot\text{mL}^{-1}$ for strains ATCC 12228 and ATCC 35984, resp.) from our results using the same bacteria (Table 3) which can be explained by the different strains used for these authors.

Others studies of the biological activity of product 1 reported on the literature has indicated that this compound has much lower antimicrobial, anticoccidial, cardiotoxic, and cytotoxic activities relative to the parent compound [41, 42], results corroborated by our team, since product 1 presented 25.0 and $50.0 \mu\text{g}\cdot\text{mL}^{-1}$, for *S. aureus* and *S. aureus* MRSA, and product 2 presented $>100 \mu\text{g}\cdot\text{mL}^{-1}$.

The biological activity of monensin A depends on the complex formed with cations exhibiting a polar interior and a nonpolar highly hydrophobic exterior which enables free movement across lipid bilayers of cells to exchange cations [3, 4]. This action results in ion imbalance and subsequent biological and toxicological activities [3, 4, 43]. Our results demonstrated that product 1 and product 2 were less active than monensin A for all microorganisms in the conditions studied. Thus, the first step in the metabolism of monensin A is related to the production of more polar metabolites than monensin A, and then, acting like a detoxification step. It can be concluded that the metabolism of monensin A leads to a reduction in the toxicity of this compound in the organism, but that some bactericidal activity for Gram-positive microorganisms remains.

4. Conclusion

This work has demonstrated the ability of the Jacobsen catalyst to mimic the action of P450 in monensin A metabolism, with formation of two main products found in the *in vivo* systems: 3-*O*-demethyl monensin A (product 1) and 12-hydroxy monensin A (product 2). The results also revealed the potential of application of this biomimetic chemical model in the synthesis of drug metabolites, providing metabolites for biological tests and other purposes. This was demonstrated in this work allowing interesting information which can help the elucidation of *in vivo* drug metabolism, thus overcoming the difficulty in working with *in vivo* or *in vitro* enzymes systems such as those used in microsomes. The biological tests showed

that the products of monensin A have much lower activity or toxicity in all parameters tested. Thus, the first step in monensin A metabolism appears to eliminate or decrease the effects in biological parameters tested and that this effect might be ascribed to greater polarity of product 1 and product 2 that can hamper their transport through membranes.

Conflict of Interests

The authors declare that there is no conflict of interests regarding the publication of this paper.

Acknowledgments

The authors gratefully acknowledge Fundação de Amparo à Pesquisa do Estado de São Paulo (Grant nos. 2011/05800-0 and 2013/17658-9) and Conselho Nacional de Desenvolvimento Científico e Tecnológico (CNPq) for financial support and for granting research fellowships.

References

- [1] A. Huczynski, J. Stefańska, P. Przybylski, B. Brzezinski, and F. Bartl, "Synthesis and antimicrobial properties of Monensin A esters," *Bioorganic and Medicinal Chemistry Letters*, vol. 18, no. 8, pp. 2585–2589, 2008.
- [2] A. Huczynski, M. Ratajczak-Sitarz, J. Stefańska, A. Katrusiak, B. Brzezinski, and F. Bartl, "Reinvestigation of the structure of monensin A phenylurethane sodium salt based on X-ray crystallographic and spectroscopic studies, and its activity against hospital strains of methicillin-resistant *S. epidermidis* and *S. aureus*," *Journal of Antibiotics*, vol. 64, no. 3, pp. 249–256, 2011.
- [3] A. Huczynski, "Polyether ionophores—promising bioactive molecules for cancer therapy," *Bioorganic and Medicinal Chemistry Letters*, vol. 22, no. 23, pp. 7002–7010, 2012.
- [4] D. Łowicki and A. Huczynski, "Structure and antimicrobial properties of monensin a and its derivatives: summary of the achievements," *BioMed Research International*, vol. 2013, Article ID 742149, 14 pages, 2013.
- [5] J. Adovelande and J. Schrével, "Carboxylic ionophores in malaria chemotherapy: the effects of monensin and nigericin on *Plasmodium falciparum* in vitro and *Plasmodium vinckei petteri* in vivo," *Life Sciences*, vol. 59, no. 20, pp. PL309–PL315, 1996.
- [6] R. Suroliá, M. Pachauri, and P. C. Ghosh, "Preparation and characterization of monensin loaded PLGA nanoparticles: in vitro anti-malarial activity against *Plasmodium falciparum*," *Journal of Biomedical Nanotechnology*, vol. 8, no. 1, pp. 172–181, 2012.
- [7] J. Rosén, "Efficient and sensitive screening and confirmation of residues of selected polyether ionophore antibiotics in liver and eggs by liquid chromatography-electrospray tandem mass spectrometry," *Analyst*, vol. 126, no. 11, pp. 1990–1995, 2001.
- [8] M. Rokka and K. Peltonen, "Simultaneous determination of four coccidiostats in eggs and broiler meat: validation of an LC-MS/MS method," *Food Additives and Contaminants A: Chemistry Analysis Control Exposure & Risk Assessment*, vol. 23, no. 5, pp. 470–478, 2006.
- [9] M. Moloney, L. Clarke, J. O'Mahony, A. Gadaj, R. O'Kennedy, and M. Danaher, "Determination of 20 coccidiostats in egg and avian muscle tissue using ultra high performance liquid chromatography-tandem mass spectrometry," *Journal of Chromatography A*, vol. 1253, pp. 94–104, 2012.
- [10] C. Caldeira, W. S. Neves, P. M. Curry, P. Serrano, M. A. S. F. Baptista, and E. A. Burdmann, "Rhabdomyolysis, acute renal failure, and death after monensin ingestion," *The American Journal of Kidney Diseases*, vol. 38, no. 5, pp. 1108–1112, 2001.
- [11] J. A. Kouyoumdjian, M. Da Penha Ananias Morita, A. K. Sato, and A. F. Pissolatti, "Fatal rhabdomyolysis after acute sodium monensin (Rumensin) toxicity: case report," *Arquivos de Neuro-Psiquiatria*, vol. 59, no. 3, pp. 596–598, 2001.
- [12] A. C. Souza, F. S. Machado, M. R. N. Celes et al., "Mitochondrial damage as an early event of monensin-induced cell injury in cultured fibroblasts L929," *Journal of Veterinary Medicine Series A: Physiology Pathology Clinical Medicine*, vol. 52, no. 5, pp. 230–237, 2005.
- [13] D. Mansuy, "Brief historical overview and recent progress on cytochromes P450: adaptation of aerobic organisms to their chemical environment and new mechanisms of prodrug bioactivation," *Annales Pharmaceutiques Francaises*, vol. 69, no. 1, pp. 62–69, 2011.
- [14] P. R. Ortiz-Montellano, *Cytochrome P450: Structure, Mechanism, and Biochemistry*, Plenum Press, New York, NY, USA, 2004.
- [15] T. C. O. Mac Leod, A. L. Faria, V. P. Barros, M. E. C. Queiroz, and M. D. Assis, "Primidone oxidation catalyzed by metalloporphyrins and Jacobsen catalyst," *Journal of Molecular Catalysis A: Chemical*, vol. 296, no. 1-2, pp. 54–60, 2008.
- [16] T. C. O. M. Leod, V. P. Barros, A. L. Faria et al., "Jacobsen catalyst as a P450 biomimetic model for the oxidation of an antiepileptic drug," *Journal of Molecular Catalysis A: Chemical*, vol. 273, no. 1-2, pp. 259–264, 2007.
- [17] M. Niehues, V. P. Barros, F. D. S. Emery, M. Dias-Baruffi, M. D. D. Assis, and N. P. Lopes, "Biomimetic in vitro oxidation of lapachol: a model to predict and analyse the in vivo phase I metabolism of bioactive compounds," *European Journal of Medicinal Chemistry*, vol. 54, pp. 804–812, 2012.
- [18] L. De Santis Ferreira, D. R. Callejon, A. Engemann et al., "In vitro metabolism of grandisin, a lignan with anti-chagasic activity," *Planta Medica*, vol. 78, no. 18, pp. 1939–1941, 2012.
- [19] J. Bernadou and B. Meunier, "Biomimetic chemical catalysts in the oxidative activation of drugs," *Advanced Synthesis and Catalysis*, vol. 346, no. 2-3, pp. 171–184, 2004.
- [20] W. Lohmann and U. Karst, "Biomimetic modeling of oxidative drug metabolism: strategies, advantages and limitations," *Analytical and Bioanalytical Chemistry*, vol. 391, no. 1, pp. 79–96, 2008.
- [21] B. A. Rocha, M. D. Assis, A. P. F. Peti et al., "In vitro metabolism of monensin A: microbial and human liver microsomes models," *Xenobiotica*, vol. 44, pp. 326–335, 2014.
- [22] J. N. Sousa-Junior, B. A. Rocha, M. D. Assis et al., "Biomimetic oxidation studies of monensin A catalyzed by metalloporphyrins: identification of hydroxyl derivative product by electrospray tandem mass spectrometry," *Brazilian Journal of Pharmacognosy*, vol. 23, pp. 621–629, 2013.
- [23] J. M. Andrews, "Determination of minimum inhibitory concentrations," *Journal of Antimicrobial Chemotherapy*, vol. 48, pp. 5–16, 2001.
- [24] N. A. J. C. Furtado, S. Said, I. Y. Ito, and J. K. Bastos, "The antimicrobial activity of *Aspergillus fumigatus* is enhanced by a pool of bacteria," *Microbiological Research*, vol. 157, no. 3, pp. 207–211, 2002.

- [25] L. C. Pereira, A. O. De Souza, and D. J. Dorta, "Polybrominated diphenyl ether congener (BDE-100) induces mitochondrial impairment," *Basic and Clinical Pharmacology and Toxicology*, vol. 112, no. 6, pp. 418–424, 2013.
- [26] B. Chance and G. R. Williams, "The respiratory chain and oxidative phosphorylation," *Advances in Enzymology and Related Subjects of Biochemistry*, vol. 17, pp. 65–134, 1956.
- [27] R. Cathcart, E. Schwiers, and B. N. Ames, "Detection of picomole levels of hydroperoxides using a fluorescent dichlorofluorescein assay," *Analytical Biochemistry*, vol. 134, no. 1, pp. 111–116, 1983.
- [28] N. P. Lopes, C. B. W. Stark, P. J. Gates, and J. Staunton, "Fragmentation studies on monensin A by sequential electrospray mass spectrometry," *Analyst*, vol. 127, no. 4, pp. 503–506, 2002.
- [29] N. P. Lopes, C. B. W. Stark, H. Hong, P. J. Gates, and J. Staunton, "Fragmentation studies on monensin A and B by accurate mass electrospray tandem mass spectrometry," *Rapid Communications in Mass Spectrometry*, vol. 16, no. 5, pp. 414–420, 2002.
- [30] H. Otera, C. Wang, M. M. Cleland et al., "Mff is an essential factor for mitochondrial recruitment of Drp1 during mitochondrial fission in mammalian cells," *Journal of Cell Biology*, vol. 191, no. 6, pp. 1141–1158, 2010.
- [31] J. J. Lemasters, "Mechanisms of hepatic toxicity. V. Necroptosis and the mitochondrial permeability transition: shared pathways to necrosis and apoptosis," *The American Journal of Physiology—Gastrointestinal and Liver Physiology*, vol. 276, no. 1, pp. 1–6, 1999.
- [32] A. Rana, M. Rera, and D. W. Walker, "Parkin overexpression during aging reduces proteotoxicity, alters mitochondrial dynamics, and extends lifespan," *Proceedings of the National Academy of Sciences of the United States of America*, vol. 110, no. 21, pp. 8638–8643, 2013.
- [33] A. F. Garcia, H. C. D. Medeiros, M. A. Maioli et al., "Comparative effects of lantadene A and its reduced metabolite on mitochondrial bioenergetics," *Toxicol*, vol. 55, no. 7, pp. 1331–1337, 2010.
- [34] L. C. Pereira, A. O. Souza, M. Pazin et al., "Mitocôndria como alvo para avaliação de toxicidade de xenobiótico," *Revista Brasileira de Toxicologia*, vol. 25, pp. 1–14, 2012.
- [35] E. M. Garrison and G. Arrizabalaga, "Disruption of a mitochondrial MutS DNA repair enzyme homologue confers drug resistance in the parasite *Toxoplasma gondii*," *Molecular Microbiology*, vol. 72, no. 2, pp. 425–441, 2009.
- [36] H. H. Mollenhauer, D. J. Morr e, and L. D. Rowe, "Alteration of intracellular traffic by monensin; mechanism, specificity and relationship to toxicity," *Biochimica et Biophysica Acta*, vol. 1031, no. 2, pp. 225–246, 1990.
- [37] K. Ketola, P. Vainio, V. Fey, O. Kallioniemi, and K. Iljin, "Monensin is a potent inducer of oxidative stress and inhibitor of androgen signaling leading to apoptosis in prostate cancer cells," *Molecular Cancer Therapeutics*, vol. 9, no. 12, pp. 3175–3185, 2010.
- [38] M. Singh, N. R. Kalla, and S. N. Sanyal, "Effect of monensin, a Na⁺-specific carboxylic ionophore on the oxidative defense system in rat testis," *Pharmacological Reports*, vol. 59, no. 4, pp. 456–461, 2007.
- [39] F. E. Mingatto, T. Rodrigues, A. A. Pigoso, S. A. Uyemura, C. Curti, and A. C. Santos, "The critical role of mitochondrial energetic impairment in the toxicity of nimesulide to hepatocytes," *Journal of Pharmacology and Experimental Therapeutics*, vol. 303, no. 2, pp. 601–607, 2002.
- [40] A. J. Kowaltowski, R. F. Castilho, and A. E. Vercesi, "Mitochondrial permeability transition and oxidative stress," *FEBS Letters*, vol. 495, no. 1–2, pp. 12–15, 2001.
- [41] A. L. Donoho, "Biochemical studies on the fate of monensin in animals and in the environment," *Journal of Animal Science*, vol. 58, no. 6, pp. 1528–1539, 1984.
- [42] S. A. Sassman and L. S. Lee, "Sorption and degradation in soils of veterinary ionophore antibiotics: monensin and lasalocid," *Environmental Toxicology and Chemistry*, vol. 26, no. 8, pp. 1614–1621, 2007.
- [43] D. C. Johnson and P. G. Spear, "Monensin inhibits the processing of herpes simplex virus glycoproteins, their transport to the cell surface, and the egress of virions from infected cells," *Journal of Virology*, vol. 43, no. 3, pp. 1102–1112, 1982.

Research Article

Glioprotective Effects of Ashwagandha Leaf Extract against Lead Induced Toxicity

Praveen Kumar, Raghavendra Singh, Arshed Nazmi, Dinesh Lakhanpal, Hardeep Kataria, and Gurcharan Kaur

Department of Biotechnology, Guru Nanak Dev University, Amritsar, Punjab 143005, India

Correspondence should be addressed to Gurcharan Kaur; kgurcharan.neuro@yahoo.com

Received 13 February 2014; Revised 24 April 2014; Accepted 24 April 2014; Published 28 May 2014

Academic Editor: José Carlos Tavares Carvalho

Copyright © 2014 Praveen Kumar et al. This is an open access article distributed under the Creative Commons Attribution License, which permits unrestricted use, distribution, and reproduction in any medium, provided the original work is properly cited.

Withania somnifera (Ashwagandha), also known as Indian Ginseng, is a well-known Indian medicinal plant due to its antioxidative, antistress, antigenotoxic, and immunomodulatory properties. The present study was designed to assess and establish the cytoprotective potential of Ashwagandha leaf aqueous extract against lead induced toxicity. Pretreatment of C6 cells with 0.1% Ashwagandha extract showed cytoprotection against 25 μ M to 400 μ M concentration of lead nitrate. Further pretreatment with Ashwagandha extract to lead nitrate exposed cells (200 μ M) resulted in normalization of glial fibrillary acidic protein (GFAP) expression as well as heat shock protein (HSP70), mortalin, and neural cell adhesion molecule (NCAM) expression. Further, the cytoprotective efficacy of Ashwagandha extract was studied *in vivo*. Administration of Ashwagandha extract provided significant protection to lead induced antioxidant defense that may significantly compromise normal cellular function. Ashwagandha also provided a significant protection to lipid peroxidation (LPx) levels, catalase, and superoxide dismutase (SOD) but not reduced glutathione (GSH) contents in brain tissue as well as peripheral organs, liver and kidney, suggesting its ability to act as a free radical scavenger protecting cells against toxic insult. These results, thus, suggest that Ashwagandha water extract may have the potential therapeutic implication against lead poisoning.

1. Introduction

There is a growing interest in the use of herbal plants for their different medicinal properties due to their natural origin, cost effectiveness, and negligible side effects [1]. *Withania somnifera* (Ashwagandha) is very popular in traditional Indian medicine system, Ayurveda. It is considered to be Indian Ginseng due to its rejuvenating effects on the body such as antioxidative, antistress, antigenotoxic, and immunomodulatory properties [2, 3]. Among the herbs classified as brain tonics or rejuvenators in the traditional Indian medicine system, Ashwagandha is the most important plant whose extracts make a significant component to the daily supplements for body and brain health. Although a variety of Ashwagandha extracts have displayed neuroprotective, neuroregenerative, and anticancer potentials in recent *in vitro* studies [4–7] using brain-derived cells, potentials of water extract of leaves of Ashwagandha (ASH-WEX) remain largely unexplored.

Lead, although one of the most useful metals, is also one of the most toxic environmental pollutant which is detected in almost all phases of biological systems. The mechanisms of lead induced neurotoxicity are complex. Oxidative stress, membrane biophysics alterations, deregulation of cell signalling, and the impairment of neurotransmission are considered as key aspects involved in lead neurotoxicity. The mechanism involves toxicity by oxidative stress [8] and free radical damage via two separate, albeit related, pathways: (a) the generation of reactive oxygen species (ROS), including hydroperoxides, singlet oxygen, and hydrogen peroxide, and (b) the direct depletion of antioxidant reserves [9].

Astroglial cells are the most abundant cells in the CNS and are believed to play a key role in the brain and spinal cord pathologies. Furthermore, it is established that glial cells and their resident protein GFAP integrate neuronal signals and modulate synaptic activity by formation of cytoskeletal filaments [10]. GFAP is the cytoskeletal protein of astrocytes

which is involved in controlling movement and shape of astrocytes, differentiation marker of glial cells/and increased GFAP expression which has been associated with aging [11, 12]. Astrocytes are important target of lead toxicity and take up lead to store it intracellularly and, by sequestering lead, astrocytes may protect more sensitive neurons [13]. It is well established on getting exposed to stress; the glial cells react by upregulating GFAP expression known as reactive gliosis [14, 15]. It is necessary for CNS morphogenesis as it provides structural support to neurons [16] and hence it is considered as a marker of glial plasticity which controls structure, proliferation, and adhesion of astrocytes, neuron glia interactions, and CNS mechanisms. Therefore, glial cell loss may contribute to the impairment of learning and memory. Therapeutic approaches to combat human neurodegenerative diseases thus need to restore the function of both neurons and glial cells [10].

Various cellular proteins are altered upon challenge of lead induced oxidative stress and many undesired side effects of lead induced toxicity are known which include neurological [16], behavioural [17], immunological [18], renal [19], and hepatic [20] dysfunctions. We examined the expression of several proteins including HSP70, mortalin protein, immunoglobulin superfamily protein NCAM, and an intermediate filament protein GFAP to assess Ashwagandha mediated rejuvenating effects on characteristics like proliferation, adhesion, and differentiation. Lead toxicity is well known for causing oxidative stress in brain cells which can lead to damage and eventual cell death. HSP70 acts as molecular chaperon and assists in the correct folding of the target proteins and it is induced under various environmental stresses [21]. To further study the protective effect of Ashwagandha in tissues other than the brain, HSP70 expression was also studied in the peripheral organs: liver, kidney, and heart. Mortalin has been shown to regulate the homeostasis of Ca^{++} in the mitochondria that are very important for neuron functioning [22]. NCAM regulates cell adhesion and neurite outgrowth by means of homophilic binding and subsequent activation and intracellular signalling through mitogen activated protein kinase (MAPK) pathway [23]. NCAM is neuronal plasticity marker involved in cell adhesion, migration, and neurite extension [24]. The low-level lead exposure has been shown to attenuate the expression of all three major NCAM isoforms and induced reductions in neuronal growth and survival [25].

Nervous tissues have high lipid contents, thus possess high aerobic metabolic activity, which makes it more susceptible to oxidative damage [26]. C6 glioma cell line is well-established *in vitro* model system for toxicity studies due to its astroglial origin. The present study was aimed at evaluating the cytoprotective potential of Ashwagandha leaf water extract against lead induced toxicity using both *in vitro* and *in vivo* model systems. To achieve these objectives, protein and mRNA expression of markers of differentiation such as GFAP and NCAM as well as cytoprotection like HSP70 and mortalin were studied. Further protective effects of Ashwagandha leaf extract were evaluated in the brain and peripheral organs in lead intoxicated animal model system.

2. Material and Methods

2.1. Preparation of Water Extract of Ashwagandha Leaves (ASH-WEX). The Ashwagandha leaf extract was prepared by suspending 10 g of dry leaf powder in 100 mL of double distilled water. The suspension was stirred at $45 \pm 5^\circ\text{C}$ overnight and filtered. The filtrate so obtained was treated as 100% water extract.

2.2. C6 Glioma Cell Culture and Its Treatment. C6 glioma cell line was obtained from National Centre for Cell Science (NCCS), Pune, India. The cell line was maintained on DMEM supplemented with streptomycin (100 U/mL), penicillin (100 U/mL), gentamycin (100 $\mu\text{g/mL}$), and 10% (FBS) at 37°C and 5% CO_2 . For 2-(3,5 dimethylthiazol-2 yl)-4, 5 dimethyltetrazolium bromide (MTT) assay, C6 cells were seeded in 96-well plate and were given 24 hours pretreatment of 0.1% ASH-WEX followed by treatment with different concentrations (25 μM –400 μM) of lead nitrate for 72 hrs. 2 hr prior to the completion of the experiment, MTT (0.5 mg/mL) was added and incubated at 37°C for 2 hr. The medium was discarded and 100 μL dimethylsulfoxide was added per well to dissolve the formazons. The absorbance was recorded at 550 nm. To further evaluate the effect of lead and Ashwagandha on C6 cells, the cultures were divided into four groups: control group without any treatment (C), control group with (0.1%) ASH-WEX treatment (CA), lead nitrate treatment group (LN), and combined lead nitrate and ASH-WEX treatment (LN + AS) group. 10 mM lead nitrate filter sterilized stock solution was prepared. The cells were seeded along with 0.1% ASH-WEX. Cells were allowed to grow for 24 hours followed by lead nitrate (200 μM) treatment for 72 hrs.

2.3. Experimental Animals. The Wistar strain young male albino rats in age group 2-3 months weighing 100–150 mg were taken. All procedures for animals care were carried out strictly in accordance with the guidelines of Institutional Animal Ethical Committee. The animals were divided into three groups, namely, group C, LN, and LN + AS, each having 4-5 rats and were kept in single cage and provided water and food ad libitum. Animals of group C were kept as control (fed equal volume of vehicle), group LN was treated with lead nitrate (40 mg/kg body weight) intraperitoneally, and group LN + AS was fed orally ASH-WEX (1gm/kg body weight) and injected lead nitrate (40 mg/kg body weight) intraperitoneally for 15 days simultaneously.

2.4. Immunostaining. The C6 cells were seeded in multiwell plates on polylysine coated cover slips. After the completion of treatment, the cells were washed with ice cold PBS three times for 5 minutes. Cells were fixed with chilled 4% PFA for 15 minutes. After washing with PBS for 3x5 minutes, cells were permeabilized with 0.3% PBST for 15 minutes. Blocking was carried out with 5% NGS and 1% BSA in 0.1% PBST for 2 hours at room temperature. Cells were incubated in primary antibody (prepared in blocking solution) GFAP (1:500, Sigma), HSP70 (1:1000, Sigma, clone BRM-22), mortalin (1:500, gift sample from Dr. Renu Wadhwa), and NCAM (1:500, Abcys) for 48 hours at 4°C . After washings with

PBST (0.1%), cells were incubated in FITC/TRITC conjugated secondary antibody (1:200) for 2 hours at room temperature. Cover slips were mounted with antifading medium. The cells were observed under fluorescent microscope (Nikon E600) and images were captured and analyzed using Image-Pro Plus software, version 4.5.1.

2.5. Immunohistochemistry. Brains from animals of all three groups control, lead nitrate, and lead nitrate with Ashwagandha treated rats ($N = 4-5$ for each groups) were perfused transcardially with 4% paraformaldehyde in phosphate buffer saline (PBS) (0.1M) and then cryopreserved in 20% and 30% sucrose in phosphate buffer saline each for 24 hrs at 4°C. 30 μm coronal sections of brain were cut using cryostat microtome set at -20°C and sections were washed in 1X PBS (3X for 15 min). Sections were then permeabilized in 0.3% PBS-Triton X-100 (pH 7.4, 0.1M) for 30 min. Then, sections were washed with 0.1% PBST for 15 min. After washing sections were preincubated for 1 hr at room temperature in blocking solution 5% NGS in PBS with 0.32% Triton X-100 for blocking nonspecific binding sites. The sections were then incubated in the primary antibody anti-IgG for GFAP with appropriate dilution (1:500) in 0.32% PBST for 48 hrs at 4°C. Sections were then washed in 0.1% PBST and incubated with fluorescent conjugated secondary antibody (anti-mouse IgG FITC diluted 1:200 for GFAP) in 0.3% PBST for 2 hrs. Sections were then mounted on the glass slide and covered with antifading mounting fluoromount medium for capturing fluorescent images using Nikon E600 fluorescent microscope and CoolSnap CCD camera. GFAP immunostaining was observed in hippocampus, hypothalamus, and cortex regions of brain. Quantitative image analysis for immunostaining intensity measurement was done using Image-ProPlus version 4.5.1 (Media Cybernetics, USA). Intensity of immunoreactivity and the number of GFAP positive cells were quantified in random selected fields in each section using the count/size command of Image-Pro Plus software.

2.6. Western Blotting

2.6.1. Sample Preparation. After 72 hr of treatment, the cells were washed with PBS and were harvested with PBS-EDTA (1 mM). The pellets were homogenized for 2 minutes and the homogenate so produced was centrifuged at 10,000 rpm for 15 minutes at 4°C. Supernatant was collected and the protein was estimated using Bradford's method.

For *in vivo* studies, animals from all three groups ($n = 3$ for each group) control, lead nitrate, and lead nitrate with Ashwagandha were sacrificed by cervical dislocation and decapitated. Brain was dissected, and brain regions, hippocampus (HC), hypothalamus (HT), and cortex were separated. Different brain regions and peripheral organs such as liver, kidney, and heart were homogenized in 5 vol. of chilled homogenizing buffer containing 20 mM Tris, 150 mM NaCl, 10 mM NaF, 1 mM NaVO_4 , 0.01 mM PMSE, DTT, and 1% tritonX-100 and centrifuged for 10 min at 10,000 rpm. Protein content in supernatant was determined by the Bradford method. Each homogenate was then diluted in

homogenization buffer so as to equilibrate the protein content in all the samples.

2.6.2. SDS-PAGE and Chemiluminescence Detection. The SDS-PAGE electrophoresis was carried out under standard denaturing conditions at 15 mA. After electrophoresis, the resolved proteins were transferred (semidry transfer) to blot PVDF membrane Immobilon P (Millipore). The transfer was carried out at 25 V for 2 hr. After transfer, the membrane was put in nonfat protein (5% skimmed milk in 0.1% TBST) for 2 hr at room temperature. The membrane was incubated with monoclonal antibody for GFAP (1:2500), HSP70 (1:5000), and mortalin (1:1000) in blocking solution overnight at 4°C. Membrane was subjected to three washings with 0.1% TBST each for 5 min followed by incubation with 1:7000 diluted HRP conjugated goat anti-mouse IgG for 2 hr at room temperature. Enhanced chemiluminescence (ECL) was used for the detection of protein bands of interest. The developed blots were subjected to analysis by intensity measurement using Alpha Imager Software.

2.7. qRT-PCR. Total RNA was extracted from cells by the TRI reagent (Sigma) according to the manufacturer's instruction. The integrity of the isolated RNA was checked by nondenaturing agarose gel electrophoresis. Equal amounts of RNA were used for cDNA synthesis. cDNAs were synthesized in 20 μL reactions containing 200 units M-MLV reverse transcriptase, 4 μL 5X first strand buffer, 2 μL DTT (0.1 M) (Invitrogen), 5 μg of total RNA, 1 mM each of dNTPs (Amersham), 20 units of ribonuclease inhibitor (Sigma), and 250 ng pd(N)₆ random hexamers (MBI, Fermentas).

2 μL of cDNA was amplified in a 50 μL PCR reaction mixture containing two units Taq polymerase, 5 μL 10X PCR buffer, 1.5 μL of 50 mM MgCl_2 (Invitrogen), 1 μL of 10 mM dNTP mix (Amersham), and 20pM respective primers as listed in Table 1. Cycling conditions comprised an initial denaturation of 3 min at 94°C followed by 35 cycles of amplification (at 94°C for 40 sec, 55°C for 45 sec, and 72°C for 1 min) and final elongation step at 72°C for 10 min. To control the PCR reaction components and the integrity of the RNA, 2 μL of each cDNA sample was amplified separately for β -actin specific primer.

2.8. Estimation of Activities of Antioxidative Enzyme and Levels of Antioxidants

2.8.1. Preparation of Sample. Animals from all three groups ($n = 5$ for each group) control, lead nitrate, and lead nitrate along with Ashwagandha were sacrificed by cervical dislocation and decapitated. Brain was dissected, and brain regions, hippocampus (HC), hypothalamus (HT), and cortex were separated. Different brain regions and peripheral organs such as liver and kidney were homogenized in 10 volume of chilled homogenizing buffer containing 250 mM sucrose, 12 mM Tris-HCl, and 0.1 mM DDT, at pH 7.4. Homogenates were centrifuged at 10,000 rpm and used for further estimation of antioxidative enzymes.

TABLE 1: Primer sequences used for semiquantitative RT-PCR.

Number	mRNA		Primer sequence	Expected product size
1	GFAP	F	5'GGC GCT CAA TGC TGG CTT CA3'	326 bp
		R	5'TCT GCC TCC AGC CTC AGG TT3'	
2	HSP70	F	5'GAG TTC AAG CGC AAA CAC AA3'	428 bp
		R	5'CTC AGA CTT GTC GCC AAT GA3'	
3	NCAM	F	5'GCC AAG GAG AAA TCA GCG TTG GAG AGT C3'	651 bp
		R	5'ATG CTC TTC AGG GTC AAG GAG GAC ACA C3'	
4	Mortalin	F	5'CAG TCT TCT GGT GGA TTA AG3'	420 bp
		R	5'ATT AGC ACC GTC ACG TAA CAC CTC3'	
5	β -Actin	F	5'TCACCCACACTGTGCCCATCTACGA3'	285 bp
		R	5'CAGCGGAACCGCTCATTGCCAATGG3'	

2.8.2. Estimation of Catalase. Catalase activity was measured according to the method of Aebi [27]. The reaction mixture (1 mL) contained 0.8 mL phosphate buffer (0.2 M, pH 7.0) having 12 mM H₂O₂ vol. substrate, 100 μ L enzyme sample to make up the volume. The change in absorbance/minute was taken at 240 nm against H₂O₂-phosphate buffer as blank. Enzyme activity was determined as one unit of catalase equal to decomposition of 1 μ m of H₂O₂ per min at pH 7.0 at 25°C.

2.8.3. Estimation of Cu-Zn SOD. Activity of superoxide dismutase (SOD) was estimated according to the method of Kono [28]. The principle involved the inhibitory effects of SOD on the reduction of nitro blue tetrazolium (NBT) dye by superoxide radicals, which are generated by the autoxidation of hydroxylamine hydrochloride. Briefly, the reaction mixture contained 1.3 mL sodium carbonate buffer (50 mM), pH 10.0, 500 μ L NBT (96 μ M), and 100 μ L Triton X-100 (0.6%). The reaction was initiated by addition of 100 μ L of hydroxylamine hydrochloride (20 mM), pH 6.0. After 2 min, 50 μ L enzyme sample was added and the percentage of inhibition in the rate of NBT reduction was recorded. One unit of enzyme activity was expressed as inverse of the amount of mg protein required to inhibit the reduction of NBT by 50%. The reduction of NBT was followed by an absorbance increase at 540 nm.

2.8.4. Assay of Glutathione Peroxides (GSH) Content. The GSH content in the samples was determined as described by Sedlak and Lindsay [29]. 100 μ L of enzyme sample of all the groups (distilled water in the case of blank) was mixed with 4.4 mL of (0.01 M) EDTA and 500 μ L of trichloroacetic acid (50% w/v). The contents were centrifuged at 3000 g for 15 minutes. The supernatant so obtained was mixed with 50 μ L of 5-5'-dithiobis (2-nitrobenzoic acid) (0.01 M). The yellow color formed was read at 412 nm.

2.8.5. Estimation of Lipid Peroxidation (LPx). Method of Buege and Aust [30] was followed to measure the lipid peroxidation level. 100 μ L sample was incubated with 100 μ L each of FeSO₄ (1 mM), ascorbic acid (1.5 mM), and Tris-HCl buffer (150 mM, pH 7.1) in a final volume made to 1 mL, made up by DDW, for 15 minutes at 37°C. The reaction was

stopped by adding 1 mL of trichloroacetic acid (10% w/v). This was followed by addition of 2 mL thiobarbituric acid (0.375% w/v). After being kept in boiling water bath for 15 min, contents were cooled off and then centrifuged. The absorbance of supernatant so obtained was measured at 532 nm. The extent of lipid peroxidation was expressed as nanomoles of malondialdehyde consumed per minute at 25°C.

2.9. Statistical Analysis. Data of MTT, immunostaining intensity, Western blotting, and RT-PCR was analyzed statistically using Sigma Stat for Windows (version 3.5). The results were analyzed using one way ANOVA to determine the significance of the mean between the groups followed by post hoc comparison using Bonferroni test. Values of $P \leq 0.05$ were considered significant. The means of the data are presented together with the standard error mean (SEM).

3. Results

3.1. ASH-WEX Modulates Lead Induced Morphological Changes as well as Viability in C6 Glioma Cells. There was significant decrease in cell viability as compared to control with an increase in lead nitrate concentrations (50 μ M onwards). The IC₅₀ value was found to be around 200 μ M lead nitrate concentration, which was used for further experiments. The ASH-WEX pretreated group (LN + AS) showed significantly higher survival rate as compared to LN group ($P < 0.001$) at 50, 100, and 200 μ M lead concentrations. Results are presented in Figure 1(a). No such protective effect was observed at 400 μ M lead concentrations in the presence of ASH-WEX.

The control and 0.1% Ashwagandha pretreated cultures were found to be confluent with typical morphology of C6 cells. Most of the cells in LN group showed rounding up and altered morphology as compared to control cells. Cells grown with 0.1% Ashwagandha and treated with 200 μ M concentrations of lead nitrate (LN + AS) showed differentiated morphology (Figure 1(b)). No significant difference was observed in the viability of the cells in the control and CA group whereas with increase in concentration of lead nitrate the number of cells decreased. The Hoechst 33258 staining further supported the cell viability assay results as there were

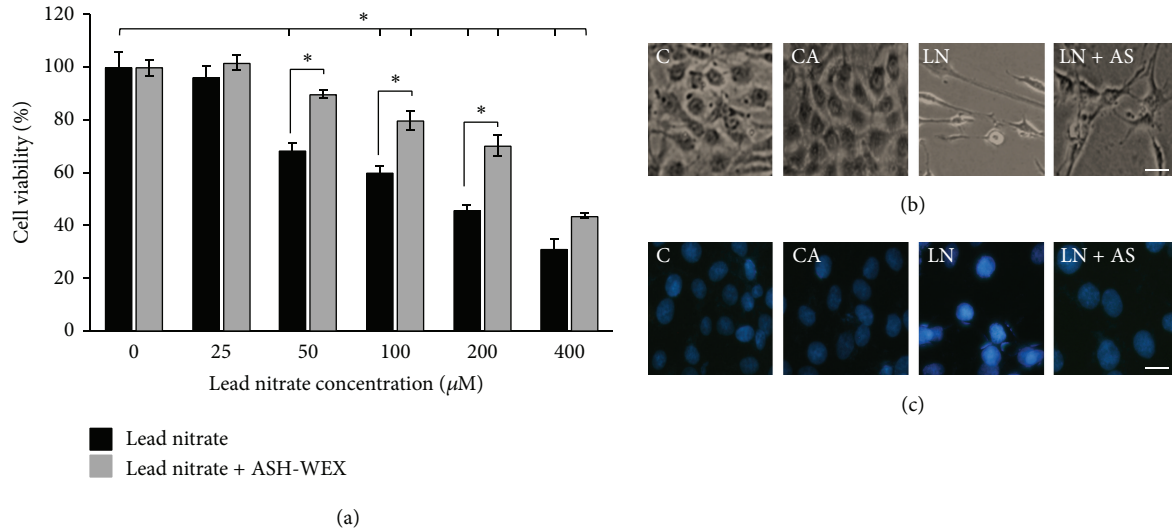


FIGURE 1: ASH-WEX protects against lead induced toxicity. (a) Relative cell viability of C6 glioma cells after lead induced toxicity as assessed by MTT assay. C6 cells were grown and pretreated with ASH-WEX (0.1%) 24 hours before exposure to lead nitrate (25–400 μM) and grown for 48–72 h. Lead nitrate significantly reduced the viable cells at 50 μM and higher concentrations. ASH-WEX treated cells were significantly higher in viability as compared to respective lead nitrate treated groups (in 50, 100, and 200 μM). Data are representative of four different experiments and are expressed as mean ± SEM. (b) Representative phase contrast pictures of control (C), control with ASH-WEX (0.1%) pretreatment (CA), lead nitrate 200 μM (LN), and lead nitrate after pretreatment with ASH-WEX (LN + AS) treatment. Images were captured using Nikon TE-2000 microscope. There was a significant difference in the cell number and morphology in lead nitrate treated cells as compared to control cells which appeared to be normalized by ASH-WEX pretreatment in LN + AS group. (c) Cell death observed by Hoechst 33258 staining. After the cells were treated with lead nitrate and ASH-WEX, Hoechst 33258 staining was used to observe the morphological changes of cell nucleus such as condensation of chromatin and nuclear fragmentations and higher intensity of stain were found clearly in lead nitrate treated group as compared to control and LN + AS group.

most of the cell nuclei in LN group appeared to be with higher intensity of stain due to chromatin condensation and nuclear fragmentation as compared to control cell nuclei. No such difference was observed in the LN + AS group nuclei (Figure 1(c)).

3.2. ASH-WEX Normalizes GFAP Expression, Stress Response Proteins, and NCAM In Vitro after Acute Lead Exposure. GFAP, HSP70, and mortalin protein expression was analysed using immunostaining and Western blotting. GFAP expression was lower in the control group as compared to CA group. Upon lead treatment, the expression increased significantly (Figures 2(a) and 2(b)) and was normalised upon Ashwagandha treatment in LN + AS group ($P < 0.05$). The immunostaining results were further supported by Western blotting analysis for GFAP (Figure 2(c)). RT-PCR results for GFAP mRNA also showed similar results with maximum expression in LN group and normalization upon Ashwagandha treatment (Figure 2(d)). Similarly HSP70 protein expression was enhanced in LN group upon lead treatment which was significantly reduced ($P < 0.05$) in LN + AS group as compared to LN group (Figures 3(a) and 3(b)). Western blotting and RT-PCR results for HSP70 protein further revealed similar trend as shown in Figures 3(c) and 3(d). The mitochondrial Mortalin (the mitochondrial HSP70) was perinuclear in control cells which is a characteristic pattern of transformed cells. Upon 0.1% Ashwagandha treatment, the localization of mortalin seemed

to be redistributed in the cytoplasm. The mortalin protein expression was significantly increased in the LN group and was normalized in the LN + AS group. The results are shown in Figures 4(a) and 4(b). The protein expression as analysed by Western blotting further revealed significant increase in mortalin expression upon lead exposure (Figure 4(c)) which was normalized in the presence of ASH-WEX (LN + AS group). Similarly, there was increase in mortalin mRNA expression upon lead treatment in LN group. Ashwagandha treatment leads to decline in the mortalin mRNA expression in the LN + AS group as compared to LN group (Figure 4(d)). Lead nitrate treatment apparently reduced NCAM expression in the LN group as compared to control and CA groups. Ashwagandha treatment of lead exposed C6 cells showed enhanced NCAM expression in the LN + AS group as shown by immunostaining in Figure 5(a). These results were further supported by semiquantitative RT-PCR data (Figure 5(b)). The rescue of C6 cells by ASH-WEX is also apparent from the morphology of cells in LN + AS group as the cells showed long processes with distinct NCAM cell surface on both the cell bodies and processes.

3.3. ASH-WEX Modulates GFAP Expression in Brain Regions after Lead Exposure. GFAP is excellent marker of astrocytes activation, which responds to CNS damage with reactive gliosis, induced by many neurotoxic agents. Immunohistochemical staining was done to localize the GFAP protein expression

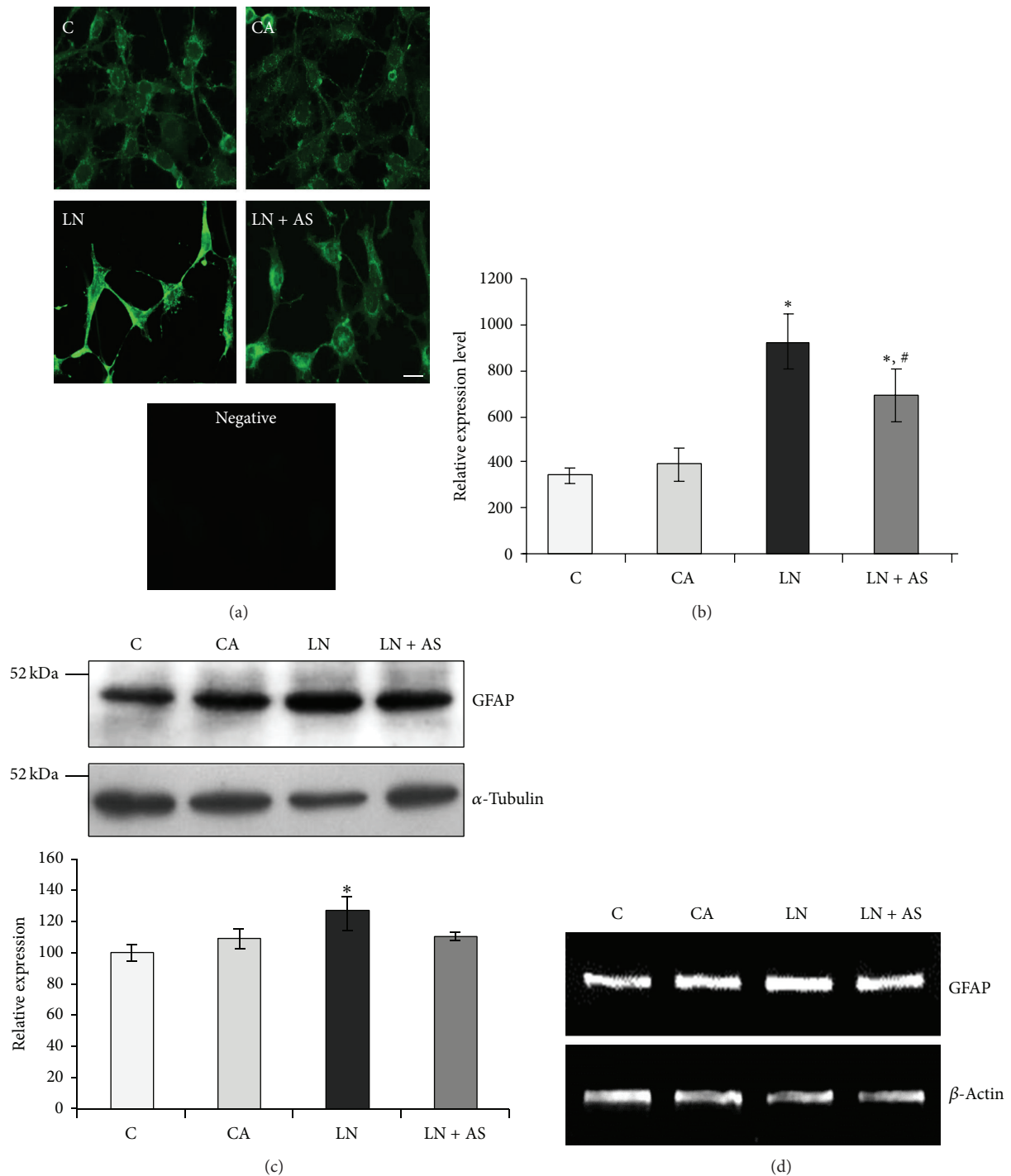


FIGURE 2: Expression of GFAP after treatment with ASH-WEX and lead nitrate. Control (C), control with ASH-WEX (0.1%) pretreatment (CA), lead nitrate 200 μ M (LN), and lead nitrate after pretreatment with ASH-WEX (LN + AS) cells were used for GFAP immunostaining (a) protein expression by Western blotting (c) and mRNA expression by RT-PCR (d). (b) depicts GFAP expression levels as analysed by immunostaining using intensity measurement command of Image-Pro Plus software. GFAP protein expression levels in control cells were taken as 100% to plot the histogram with relative level of expression of GFAP in C, CA, LN, and LN + AS groups. Data are calculated from three independent experiments and represented as the mean \pm SEM. Value of $P \leq 0.05$ was considered to be significant. *Significant difference as compared to control, #significant difference between LN and LN + AS groups. *Significant difference between C and other groups and #significant difference between LN and LN + AS groups.

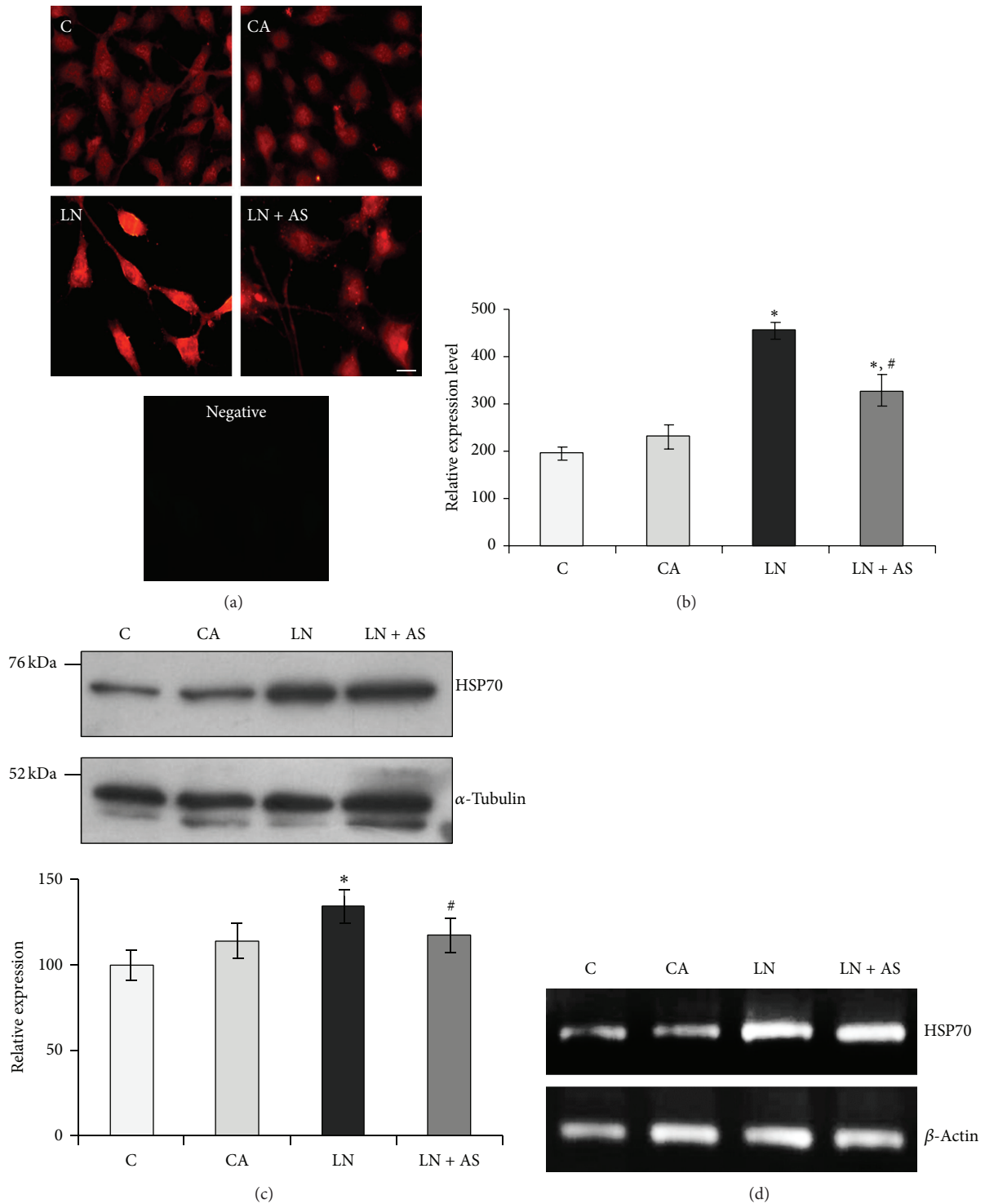


FIGURE 3: (a) Immunostaining of HSP70 in control (C), ASH-WEX (0.1%) pretreatment (CA), lead nitrate 200 μM (LN), and lead nitrate after pretreatment with ASH-WEX (LN + AS) treated C6 cells. (b) Histogram depicts staining intensity measurement of HSP70 immunofluorescence indicating HSP70 expression levels in the cells from different treatment groups. (c) Representative Western blots and relative expression levels as analysed by densitometry and normalized against α-tubulin expression levels. The data represents mean ± SEM from three independent experiments. (d) Representative RT-PCR products of HSP70 and β-actin (internal control) mRNA in different treatment groups. Value of $P \leq 0.05$ was considered to be significant. “*” represents significant difference in comparison to control; “#” represents significant difference between LN and LN + AS groups.

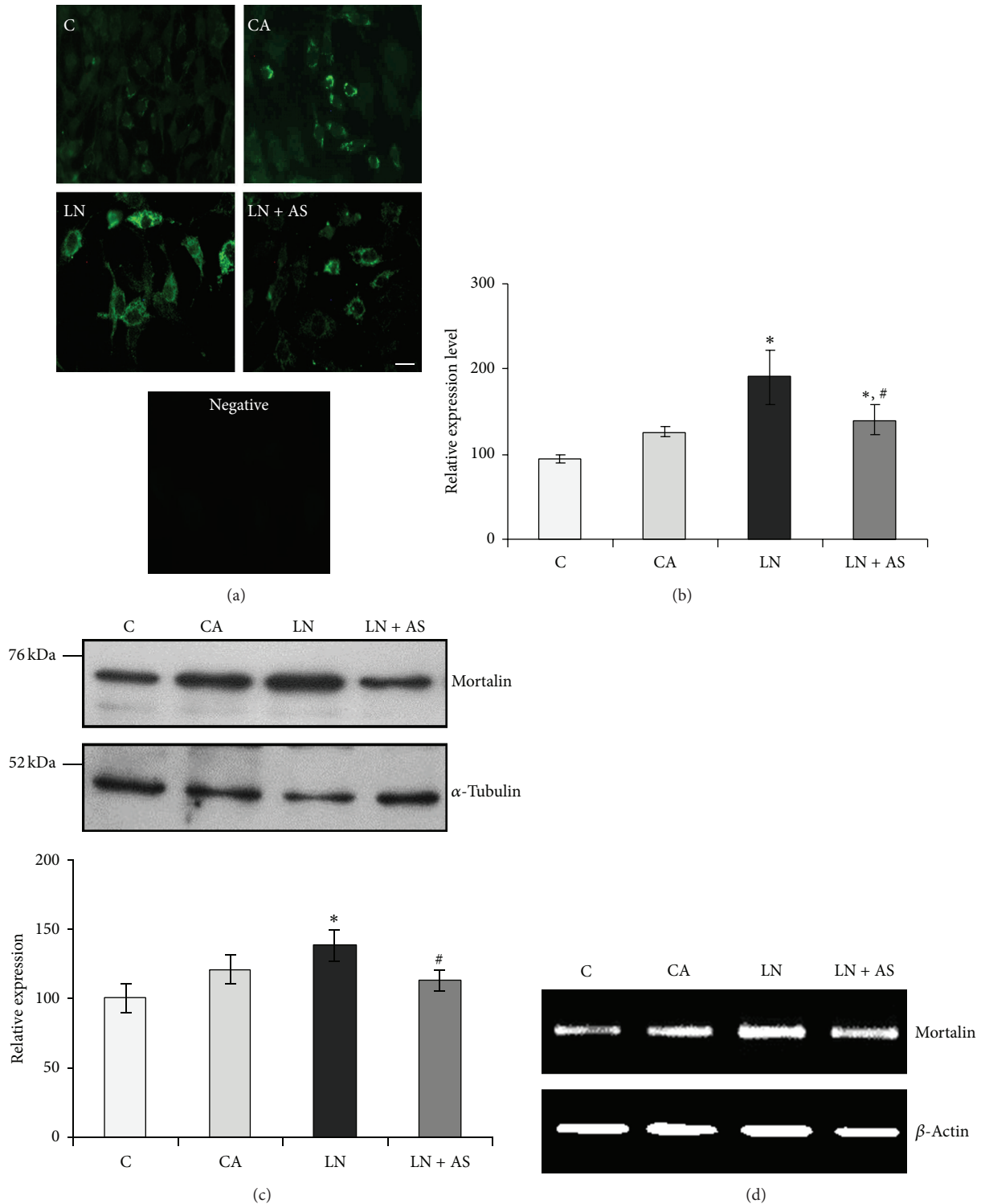


FIGURE 4: ASH-WEX pretreatment normalizes lead induced changes in mortalin expression levels. (a) Immunostaining of mortalin in C6 cells from control (C), ASH-WEX (0.1%) pretreatment (CA), lead nitrate 200 μ M (LN), and lead nitrate after pretreatment with ASH-WEX (LN + AS) treated groups. (b) Histogram shows expression levels of mortalin as analysed by intensity measurement using Image-Pro Plus software. (c) Representative Western blot of mortalin expression and histogram depicts relative expression levels of mortalin normalized against α -tubulin in C, CA, LN, and LN + AS groups as analysed by densitometry. Data are calculated from three independent experiments and represented as the mean \pm SEM. (d) Representative RT-PCR products of mortalin and β -actin mRNA in all the groups under study. Mortalin expression levels were significantly lowered down by ASH-WEX pretreatment in LN + AS group as compared to LN group as shown by immunostaining, Western blotting, and RT-PCR. Value of $P \leq 0.05$ was considered to be significant. “*” represents significant difference in comparison to control; “#” represents significant difference between LN and LN + AS groups.

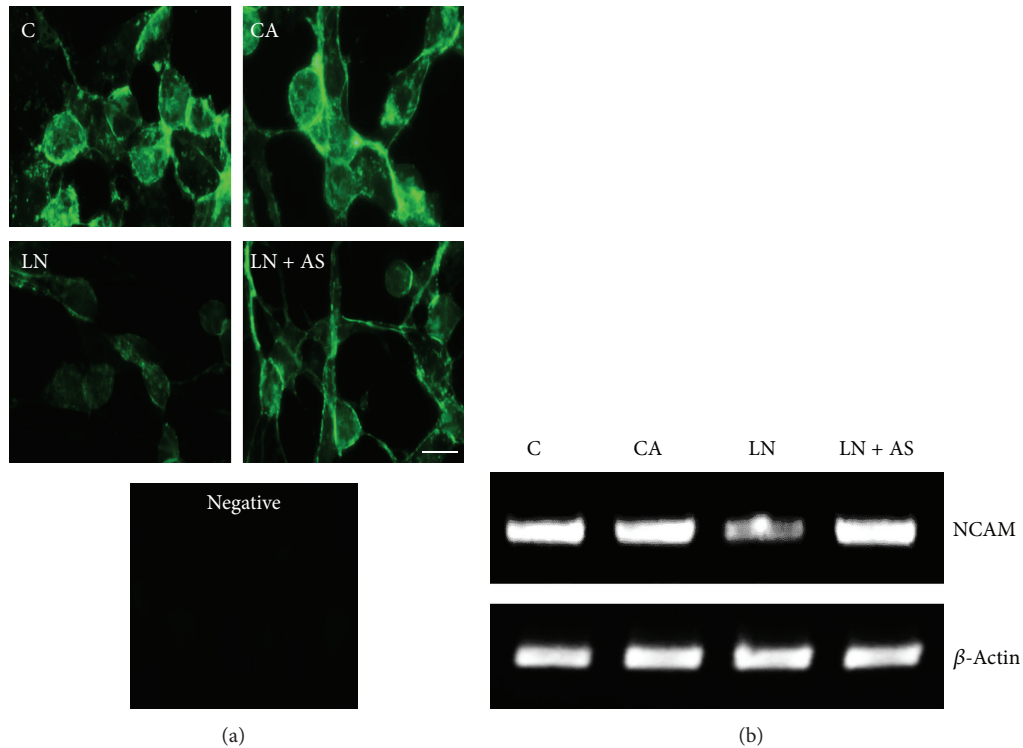


FIGURE 5: (a) NCAM protein expression levels were determined by immunostaining in control (C), ASH-WEX (0.1%) pretreatment (CA), lead nitrate (200 μ M, LN), and lead nitrate after pretreatment with ASH-WEX (LN + AS) treated groups. Lead treatment resulted in decreased expression of NCAM in LN group which was normalized by ASH-WEX pretreatment as shown in LN + AS group cells. These changes were also evident at transcription levels. (b) depicts representative RT-PCR products for the mRNA expression levels of NCAM and β -actin.

in brain regions. Lead nitrate treated group showed a considerable increase in expression of GFAP in the brain regions like hippocampus ($P < 0.001$), hypothalamus ($P < 0.001$), and piriform cortex ($P < 0.05$) (Figure 6(a)). Simultaneous lead nitrate and Ashwagandha treatment showed considerable decrease of GFAP expression in hypothalamus ($P < 0.001$, Figure 6(c)) and piriform cortex ($P < 0.05$, Figure 6(d)), but there was no statistical significant difference in hippocampus (Figure 5(b)). No specific signal was observed in the negative control immunostaining (Figure 6(f)).

GFAP expression was further confirmed by Western blotting. Lead nitrate treatment showed a significant increase in GFAP expression from different regions of brain-hippocampus ($P < 0.01$), hypothalamus ($P < 0.01$), and cortex ($P < 0.05$). Simultaneous lead nitrate and Ashwagandha treatment resulted in decrease of GFAP expression in hypothalamus ($P < 0.001$) and cortex ($P < 0.05$) regions only. Hippocampus region showed no significant decrease in GFAP level upon ASH-WEX treatment. Results are shown in Figure 6(e).

3.4. ASH-WEX Was Able to Normalize HSP70 Levels in Brain Regions and Peripheral Organs. HSP70 expression was analyzed in brain regions such as hippocampus, hypothalamus, and cortex. Hippocampus, hypothalamus, and cortex regions showed significant increase in HSP70 level when

treated with lead nitrate alone. Treatment of ASH-WEX with lead nitrate led to a significant decrease in HSP70 levels both in hypothalamus ($P < 0.05$) and cortex ($P < 0.001$) as compared to lead nitrate treatment group. The HSP70 expression remained significantly higher in LN + AS group as compared to control and no significant change in HSP70 levels was observed as compared to LN group. In order to account for potential variation and sample loading, expression of each sample was compared to that of α -tubulin. Results are shown in Figure 7(a).

The HSP70 levels were also examined in peripheral organs: heart, kidney, and liver. Heart ($P < 0.001$) and kidney ($P < 0.05$) showed a marked increase in HSP70 level upon lead nitrate treatment alone. Simultaneous ASH-WEX and lead nitrate treatment showed considerable reduction in HSP70 level of heart ($P < 0.05$) and kidney ($P < 0.01$) as compared to lead nitrate treatment, thereby indicating that ASH-WEX treatment counteracts lead induced stress. Administration of lead nitrate and Ashwagandha in LN + AS group showed significantly decreased HSP70 in liver ($P < 0.02$) as compared to lead nitrate treatment. Of note, HSP70 protein bands for both constitutive and induced form can be observed in the blots. In order to account for potential variation and sample loading, expression of each sample was normalized to that of α -tubulin. Results are shown in Figure 7(b).

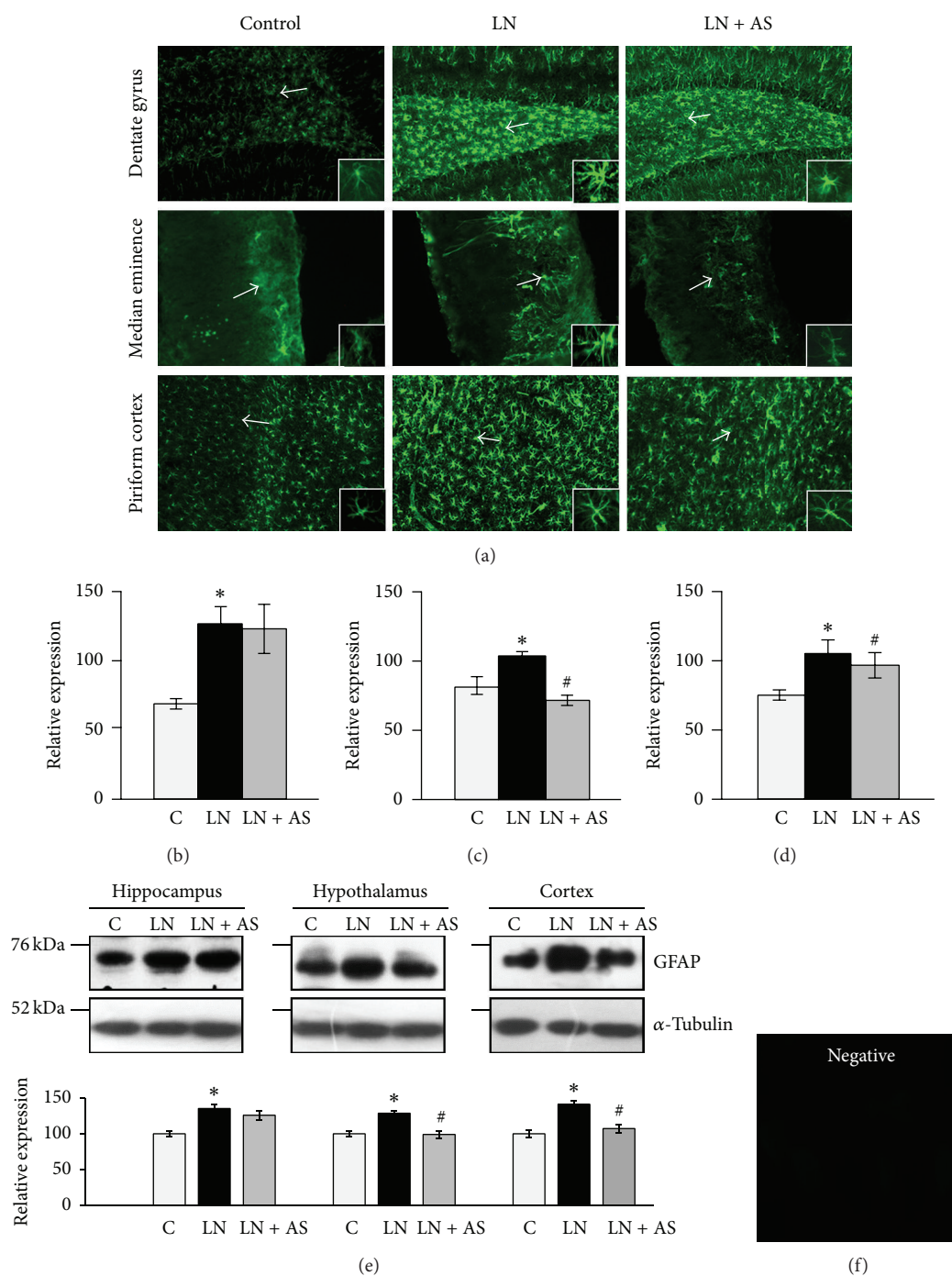


FIGURE 6: (a) Representative immunofluorescent images of 30 μ m thick coronal sections showing GFAP expression in dentate gyrus region of hippocampus, median eminence region of hypothalamus, and piriform cortex in vehicle control (C), lead nitrate (LN), and simultaneous lead nitrate and ASH-WEX (LN + AS) treated animal brains ($N = 4-5$). A marked increase in expression of GFAP was observed in the animals treated with lead nitrate as compared to control. The lead nitrate and ASH-WEX treated group showed normalization in expression of GFAP levels. Relative expression levels of GFAP were analysed using intensity measurement command of Image-Pro Plus software in hippocampus (b), hypothalamus (c), and cortex (d) shown as histograms. (e) Representative Western blot for GFAP and α -tubulin expression levels for different brain regions—hippocampus, hypothalamus, and cortex from C, LN, and LN + AS treated animals. GFAP protein expression levels were normalized against α -tubulin and data was plotted as histograms. Bar shows the mean \pm SEM values. (f) depicts specific immunostaining for GFAP shown above as no specific signal was visible in the secondary antibody control group. $P < 0.05$ was considered significant. “*” represents significant difference between C and other groups and “#” represents significant difference between LN and LN + AS groups.

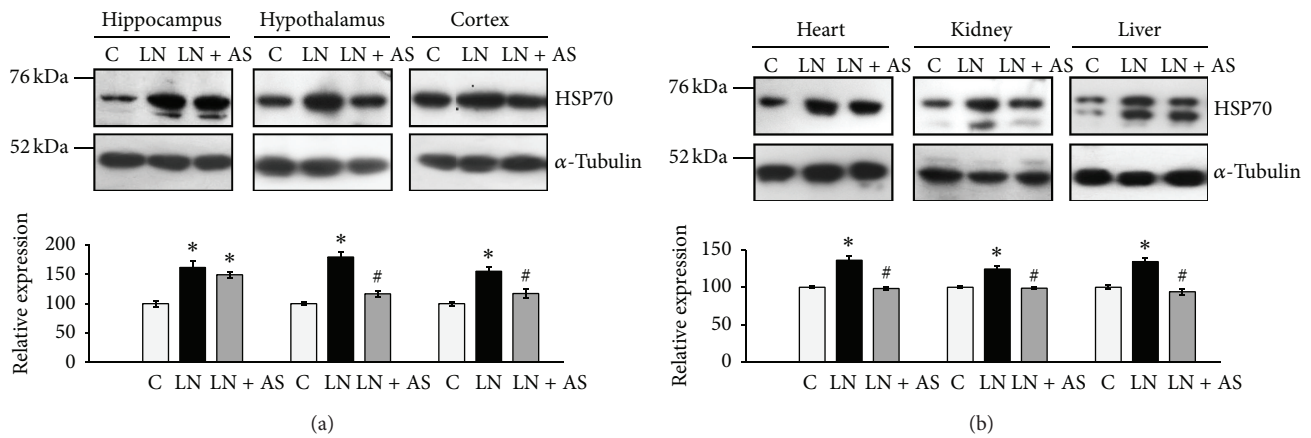


FIGURE 7: (a) Representative Western blots for HSP-70 expression and α -tubulin for different brain regions hippocampus, hypothalamus, and cortex from control (C), lead nitrate (LN), and lead nitrate and Ashwagandha (LN + AS) treated rats. Relative expression levels of HSP-70 normalized against α -tubulin were plotted as histograms. (b) Representative Western blots for HSP-70 expression and α -tubulin from different peripheral organs: heart, kidney, and liver from control and treatment groups. Histograms represent expression levels of HSP-70 normalized against α -tubulin. Data are calculated and represented as the mean \pm SEM ($N = 4-5$). $P < 0.05$ was considered significant. “*” represents significant difference between C and other groups and “#” represents significant difference between LN and LN + AS groups.

3.5. ASH-WEX Interferes with Antioxidant Defence Status in Acute Lead Toxicity

3.5.1. Catalase Activity. A statistical significant decrease ($P < 0.002$) in the CAT activity was seen after lead nitrate treatment from all the brain regions studied. Similarly, a significant decrease was observed in CAT activity in peripheral organs kidney ($P < 0.05$) as well as increase in liver ($P < 0.02$) upon lead nitrate treatment as compared to control group. Catalase activity upon feeding of ASH-WEX with lead nitrate treatment showed significant increase ($P < 0.05$) in enzyme activity in kidney, liver cortex, and hypothalamus regions of brain with no significant changes in hippocampus region of brain as compared to LN group (Table 2).

3.5.2. Superoxide Dismutase (SOD). Lead nitrate treatment alone showed significant decrease ($P < 0.001$) in SOD activity in all regions of brain as well as in kidney and liver ($P < 0.02$) as compared to control group. Treatment of ASH-WEX with lead nitrate showed no significant change on SOD in liver and hippocampus and cortex regions of brain, while hypothalamus and kidney showed significant increase in SOD activity as compared to LN group (Table 2).

3.5.3. Lipid Peroxidation (LPx). The lead nitrate exposed rats exhibited a significant increase in LPx in hippocampus ($P < 0.05$), hypothalamus ($P < 0.02$), and cortex regions of brain as well as kidney, but liver tissue showed nonsignificant increase as compared to control. Simultaneous lead nitrate and Ash-WEX treatment (LN + AS group) showed statistical significant decrease in LPx in hippocampus and hypothalamus, respectively, and also in peripheral organs as compared to LN group (Table 2).

3.5.4. Glutathione Content. Lead nitrate treatment showed slight decrease in GSH content in hippocampus and hypothalamus regions of brain as well as liver. There was no significant change in kidney glutathione content. Ashwagandha treated rats showed increase in level of GSH in all the tissues under study, but the changes were not statistically significant (Table 2).

4. Discussion

CNS is the principal target of the neurotoxic effects of lead; however, there are no effective treatments or interventions available to counteract it. Ashwagandha is a popular Ayurvedic plant with a variety of medicinal properties and is also widely used as a nerve tonic [3]. Ashwagandha leaf extract is a potential agent in treating oxidative damage and physiological abnormalities seen in mouse model of Parkinson’s disease [31]. In the light of aforementioned CNS related beneficial properties of Ashwagandha, the present study was designed to evaluate the beneficial effects of its aqueous leaf extract against lead nitrate neurotoxicity using *in vitro* (C6 glioma cells) and further analysing it *in vivo* rat model system. 0.1% ASH-WEX was able to prevent the toxic effects of lead treatment in LN + AS group as evident by normal cell morphology and viability, providing evidence for cytoprotective role of this important Indian herb.

In the present study, the upregulation of GFAP expression was observed upon lead treatment both *in vitro* and *in vivo* systems. Lead alone induced reactive gliosis which is apparent from the significantly higher expression of GFAP in all brain regions under study. Morphological changes in astrocytes coupled with immunostaining for GFAP expression showed a marked increase in its level after lead nitrate treatment. Simultaneous Ashwagandha treatment of lead

TABLE 2: Effects of Ashwagandha water extract on lead induced oxidative damage to CAT, SOD, GSH, and LPx in rat brain regions, liver, and kidney.

Groups	Kidney	Liver	Hippocampus	Hypothalamus	Cortex
Catalase (CAT)—units/minute/g					
C	10.05 ± 1.37	3.72 ± 1.20	18.80 ± 1.95	11.47 ± 0.47	10.24 ± 1.52
LN	3.80 ± 1.68*	4.95 ± 1.68*	10.57 ± 1.83*	4.58 ± 0.84*	5.35 ± 1.20*
LN + AS	12.37 ± 4.26 [#]	7.00 ± 1.71 [#]	9.56 ± 1.07*	9.31 ± 1.17 [#]	11.37 ± 1.95 [#]
Cu-Zn (SOD)—units/mg					
C	13.44 ± 2.83	10.89 ± 2.64	21.25 ± 4.55	19.88 ± 3.58	13.60 ± 4.61
LN	9.21 ± 1.59	6.74 ± 1.31*	12.37 ± 1.88*	11.52 ± 1.03*	8.66 ± 2.09*
LN + AS	13.03 ± 0.09 [#]	7.26 ± 1.43	12.07 ± 2.51*	22.13 ± 3.03 [#]	9.86 ± 2.54*
Glutathione (GSH)—units/minute/g					
C	3.34 ± 0.09	4.11 ± 0.13	3.48 ± 0.09	3.71 ± 0.11	3.22 ± 0.39
LN	3.28 ± 0.07	3.69 ± 0.16	3.29 ± 0.05	3.16 ± 0.12	3.45 ± 0.21
LN + AS	3.56 ± 0.09	3.92 ± 0.13	3.59 ± 0.05	3.54 ± 0.11	3.89 ± 0.31
Lipid peroxidation (LPx)—nmoles MDA/mL					
C	10.43 ± 2.31	20.07 ± 1.87	4.78 ± 0.23	5.29 ± 0.22	10.76 ± 0.53
LN	23.66 ± 1.75*	22.30 ± 0.53*	13.75 ± 1.71*	12.05 ± 1.03*	18.97 ± 1.65*
LN + AS	11.42 ± 0.83 [#]	14.61 ± 0.67 [#]	09.82 ± 1.04 [#]	06.39 ± 0.67 [#]	14.61 ± 0.82 [#]

Data are expressed as mean ± SEM. $P < 0.05$ was considered significant. * represents significant difference compared to control group. [#] represents significant difference compared to lead treated animals (LN group).

exposed cultures showed significant abatement in GFAP expression and also normalizing the morphology of astrocytes. Previous studies have reported association of increased GFAP levels and hypertrophic changes with susceptibility to toxic insult in C6 rat glioma cells [32]. The acute lead exposure is accompanied by astrocyte activation associated with the enhanced expression of GFAP as an indicator of lead induced neuronal injury [15]. Ashwagandha has been shown to antagonize the DNA damage and oxidative stress induced by lead [21]. Recently, it has been shown that Ashwagandha extract and its bioactive component Withanone was able to revert scopolamine induced changes in GFAP expression in the neuronal cells as well as animal model [33]. Normalization of GFAP expression by Ashwagandha extract in glutamate induced neurodegeneration in RA differentiated cultures has been shown in a recent study from our lab [34]. Thus, downregulation of GFAP expression by ASH-WEX treatment under both *in vitro* as well as *in vivo* conditions could be attributed to protective properties of Ashwagandha.

We further evaluated the levels of HSP70 expression after lead and Ashwagandha treatment. Our results have shown an increase in HSP70 expression in the LN treated cells in response to lead induced stress, whereas, its expression level was significantly reduced in the ASH-WEX pretreated group in C6 cells. Further *in vivo* studies suggested that Ashwagandha leaf extract treatment decapitated the expression of HSP70 significantly as compared to LN treatment group in hypothalamus and cortex regions of brain, thus debilitating the cytotoxic effects of lead nitrate *in vivo*. These palliative results suggested that Ashwagandha leaf extract has a potential cytoprotective effect on different brain regions and can curtail cytotoxicity caused due to exposure of lead. Lead exposure has been implicated in induction of prenatal and postnatal induction of HSP70 in astrocytes [35]. The antibody

used in present study for HSP70 (clone BRM-22) recognises both HSP70 and HSC70. Although HSP70 is known to be cytoplasmic in control cells, it is well documented that HSP70 is present in the nucleus predominantly during S-phase and at low levels during remaining cell cycle [36]. Moreover, nuclear translocation of stress protein Hsc70 during S phase in rat C6 glioma cells has also been reported [37]. So nuclear staining of HSP70 could be attributed to its cell cycle regulatory or other roles.

Furthermore, expression of mitochondrial HSP70, mortalin, was perinuclear in the control group which shifted to pancytoplasmic in case of LN group and in LN + AS group. Mortalin is nonheat inducible molecular chaperon which is induced by different environmental stresses [38]. Mortalin has been implicated in Alzheimer's (AD) and Parkinson's (PD) diseases, with proteomic studies consistently identifying oxidatively damaged mortalin as potential biomarker [29]. Significantly higher expression of mortalin as an adaptive response has been reported as a result of Ashwagandha treatment [39]. Thus, current results showing increase in mortalin in Ashwagandha treated group indicate role of mortalin in cytoprotective mechanism induced in glial cells and elucidation of molecular mechanism(s) of these functions requires further studies.

Lead nitrate treatment caused significant increase in HSP70 expression in all these organs as shown by Western blotting, which was significantly reduced after oral feeding of the animals with Ashwagandha extract. Increased expression of HSPs in liver at both transcriptional and translational levels has been associated with the early phase of liver regeneration [40]. Previously, HSP72 (inducible form of HSP70) has been shown to be upregulated during kidney injury in rats, which partially protected human kidney proximal tubule cell lines HK-2 and HKC from triptolide-induced injury [41]. Thus,

normalization of HSP 70 levels in the present study after Ashwagandha treatment *in vitro* as well as *in vivo* further confirms the protective effects of Ashwagandha against lead induced toxicity.

Another important neuronal marker NCAM was found to be downregulated in C6 glioma cells after lead exposure. The low level maternal lead exposure has been shown to decrease the expression of NCAM and its glycosylated form in hippocampus of rat pups [42, 43]. Consistent with these reports, expression of NCAM was found to decrease in lead nitrate exposed C6 cells, whereas Ashwagandha treatment was observed to augment the lead mediated downregulation of NCAM partially as shown by immunostaining and RT-PCR. A recent study on Ashwagandha treatment in C6 glioma cells has shown significant increase in expression of NCAM [39] and also increase in NCAM expression after Ashwagandha treatment has been associated with protection against glutamate induced damage in RA differentiated neuronal cultures [34].

As recent studies point to the fact that at least some of the effects may occur as a consequence of lead propensity for disrupting the delicate prooxidant/antioxidant balance that exists within mammalian cells [44], we further investigated the possible mechanism of Ashwagandha induced neuroprotection against lead toxicity by analysing the cellular antioxidant defense system. Lead exposure leads to induction of ROS production, oxidative stress, and expression of proapoptotic genes and cell death [45]. The present results have shown that Ashwagandha extract does have antioxidant properties as it resulted in a decrease of lead induced rise in lipid peroxidation in all the brain regions under study as well as peripheral organs kidney and liver. In relation to the levels of SOD, here too mostly beneficial effects were seen in the brain regions. There was a nonsignificant increase in the level of SOD in the liver and cortex while the kidney and hypothalamus SOD levels were normalized. These results are consistent with the data reported by different studies with root extracts of Ashwagandha [2, 46] where an overall increase in the level of SOD and decrease in the lipid peroxidation was observed after administration of Ashwagandha extracts. Chaudhary et al. [47] has reported Ashwagandha root extract enhancing the antiperoxidation of hepatic tissue.

In contrast to the above results, there was a consistent decrease in the levels of catalase in all the regions of the brain and peripheral organs after lead treatment which was normalized by Ashwagandha extract treatment. This is in line with the effect of the root powder and extracts which have been shown to induce an increase in the catalase activity in previous studies. Bhattacharya et al. [2] have shown an increase in catalase activity in rat brain frontal cortex and striatum after treatment with roots of Ashwagandha. Panda and Kar [46] also have reported an increase in the level of catalase after treatment with roots of Ashwagandha. Similarly, Jain et al. [48] have shown that *Withania somnifera* reverses the chronic footshock induced changes, which include an increase in SOD and lipid peroxidation and decrease in catalase activity in the rat frontal brain cortex and striatum.

Administration of Ashwagandha did not show significant change in GSH in all regions understudied and is supported by the study of Bhattacharya et al., [2], in which the administration of Ashwagandha inhibits lipid peroxidation which follows a different mechanism without modifying the glutathione system, which is a main antioxidant system. GSH, selenium containing tetrameric enzyme, is the primary low molecular-weight thiol in the cytoplasm and is a major reserve for cysteine. SOD converts O_2^- into H_2O_2 and GSH in conjunction with the reductant NADPH that can reduce lipid peroxides, free radicals, and H_2O_2 [49]. So, an increase in SOD in our study would indirectly indicate lowering of the free radical levels and thus point towards the antioxidant effect of the aqueous leaf extract of Ashwagandha.

The current data of protection against lead induced cytotoxicity is also consistent with several previously reported neuroprotective activities in both *in vivo* and *in vitro* models using this important medicinal plant. Recently, we reported that water extract of Ashwagandha leaves confers protection to neuronal cells against glutamate excitotoxicity [34]. Preliminary data from our lab also showed that ASH-WEX has six different water soluble molecules which may be associated with neuroprotective activity either alone or combined [39]. The bioactive components sitoindosides VII-X and withaferin A have been shown to have neuroprotective activity by binding with cholinergic receptors [48]. Modulation of release of three neurotransmitters, that is, acetylcholine, glutamate, and serotonin by Ashwagandha has been proposed to contribute to inhibition of nNOS in extract treated stressed mice [5]. Neuroregeneration of both axons and dendrites as well as reconstruction of pre- and postsynapses in the neurons was induced by withanolide A from the Ashwagandha extract which is considered to be an important candidate for the treatment of neurodegenerative diseases [50]. Based on the present findings, it may be suggested that ASH-WEX plays neuromodulatory role to rescue the glial cells against lead toxicity by suppression of stress response and upregulation of plasticity marker proteins such as GFAP and NCAM.

5. Conclusion

In view of our present results, we hypothesize that water soluble extract of Ashwagandha is able to partially reverse the effect of lead induced toxicity as is shown in both *in vitro* and *in vivo* systems. Detailed mechanistic studies are required to understand the mechanisms underlying the beneficial effects of Ashwagandha and to explore the optimum dosage and duration of treatment to implement the same in clinical perspectives.

Conflict of Interests

The authors declare that there is no conflict of interests regarding the publication of this paper.

Authors' Contribution

Praveen Kumar and Dinesh Lakhanpal performed cell culture (*in vitro*) experiments and Raghavendra Singh and Arshed

Nazmi performed *in vivo* experiments and analysed data. Dinesh Lakhanpal, Hardeep Kataria, and Gurcharan Kaur contributed to the paper preparation. Gurcharan Kaur contributed to reagents/materials/analysis tools. Praveen Kumar and Raghavendra Singh contributed equally towards this paper.

Acknowledgment

Dinesh Lakhanpal and Hardeep Kataria are thankful to the Council of Scientific and Industrial Research, India, for providing Junior and Senior Research Fellowship during the course of this study.

References

- [1] G. H. Naik, K. I. Priyadarsini, J. G. Satav et al., "Comparative antioxidant activity of individual herbal components used in ayurvedic medicine," *Phytochemistry*, vol. 63, no. 1, pp. 97–104, 2003.
- [2] S. K. Bhattacharya, K. S. Satyan, and S. Ghosal, "Antioxidant activity of glycowithanolides from *Withania somnifera*," *Indian Journal of Experimental Biology*, vol. 35, pp. 236–239, 1997.
- [3] S. K. Kulkarni and A. Dhir, "*Withania somnifera*: an Indian ginseng," *Progress in Neuro-Psychopharmacology and Biological Psychiatry*, vol. 32, no. 5, pp. 1093–1105, 2008.
- [4] M. Bhatnagar, D. Sharma, and M. Salvi, "Neuroprotective effects of *Withania somnifera* dunal: a possible mechanism," *Neurochemical Research*, vol. 34, no. 11, pp. 1975–1983, 2009.
- [5] S. RajaSankar, T. Manivasagam, V. Sankar et al., "*Withania somnifera* root extract improves catecholamines and physiological abnormalities seen in a Parkinson's disease model mouse," *Journal of Ethnopharmacology*, vol. 125, no. 3, pp. 369–373, 2009.
- [6] C. Tohda and E. Joyashiki, "Sominone enhances neurite outgrowth and spatial memory mediated by the neurotrophic factor receptor, RET," *British Journal of Pharmacology*, vol. 157, no. 8, pp. 1427–1440, 2009.
- [7] N. Shah, H. Kataria, S. C. Kaul, T. Ishii, G. Kaur, and R. Wadhwa, "Effect of the alcoholic extract of Ashwagandha leaves and its components on proliferation, migration, and differentiation of glioblastoma cells: combinational approach for enhanced differentiation," *Cancer Science*, vol. 100, no. 9, pp. 1740–1747, 2009.
- [8] I. A. Bergdahl and S. Skerfving, "Biomonitoring of lead exposure—alternatives to blood," *Journal of Toxicology and Environmental Health A: Current Issues*, vol. 71, no. 18, pp. 1235–1243, 2008.
- [9] T. Sanders, Y. Liu, V. Buchner, and P. B. Tchounwou, "Neurotoxic effects and biomarkers of lead exposure: a review," *Reviews on Environmental Health*, vol. 24, no. 1, pp. 15–45, 2009.
- [10] P. Kurosinski and J. Götz, "Glial cells under physiologic and pathologic conditions," *Archives of Neurology*, vol. 59, no. 10, pp. 1524–1528, 2002.
- [11] E. Galea, P. Dupouey, and D. L. Feinstein, "Glial fibrillary acidic protein mRNA isoforms: expression in vitro and in vivo," *Journal of Neuroscience Research*, vol. 41, no. 4, pp. 452–461, 1995.
- [12] M. Kaur, S. Sharma, and G. Kaur, "Age-related impairments in neuronal plasticity markers and astrocytic GFAP and their reversal by late-onset short term dietary restriction," *Biogerontology*, vol. 9, no. 6, pp. 441–454, 2008.
- [13] D. Holtzman, C. DeVries, and H. Nguyen, "Maturation of resistance to lead encephalopathy: cellular and subcellular mechanisms," *NeuroToxicology*, vol. 5, no. 3, pp. 97–124, 1984.
- [14] J. P. O'Callaghan, K. F. Jensen, and D. B. Miller, "Quantitative aspects of drug and toxicant-induced astrogliosis," *Neurochemistry International*, vol. 26, no. 2, pp. 115–124, 1995.
- [15] L. Struyska, I. Bubko, M. Walski, and U. Rafalowska, "Astroglial reaction during the early phase of acute lead toxicity in the adult rat brain," *Toxicology*, vol. 165, no. 2-3, pp. 121–131, 2001.
- [16] D. C. Bellinger, "Very low lead exposures and children's neurodevelopment," *Current Opinion in Pediatrics*, vol. 20, no. 2, pp. 172–177, 2008.
- [17] M. de Marco, R. Halpern, and H. M. T. Barros, "Early behavioral effects of lead perinatal exposure in rat pups," *Toxicology*, vol. 211, no. 1-2, pp. 49–58, 2005.
- [18] N. Ercal, R. Neal, P. Treeratphan et al., "A role for oxidative stress in suppressing serum immunoglobulin levels in lead-exposed fisher 344 rats," *Archives of Environmental Contamination and Toxicology*, vol. 39, no. 2, pp. 251–256, 2000.
- [19] S. Rastogi, "Renal effects of environmental and occupational lead exposure," *Indian Journal of Occupational and Environmental Medicine*, vol. 12, no. 3, pp. 103–106, 2008.
- [20] D. Y. Yu, W. F. Li, B. Deng, and X. F. Mao, "Effects of lead on hepatic antioxidant status and transcription of superoxide dismutase gene in pigs," *Biological Trace Element Research*, vol. 126, no. 1-3, pp. 121–128, 2008.
- [21] S. Khanam and K. Devi, "Effect of *Withania somnifera* root extract on lead-induced DNA damage," *International Journal of Food, Agriculture and Environment*, vol. 3, pp. 31–33, 2005.
- [22] C. C. Deocaris, S. C. Kaul, and R. Wadhwa, "From proliferative to neurological role of an hsp70 stress chaperone, mortalin," *Biogerontology*, vol. 9, no. 6, pp. 391–403, 2008.
- [23] D. K. Ditlevsen, G. K. Povlsen, V. Berezin, and E. Bock, "NCAM-induced intracellular signaling revisited," *Journal of Neuroscience Research*, vol. 86, no. 4, pp. 727–743, 2008.
- [24] C.-M. Chuong and G. M. Edelman, "Alterations in neural cell adhesion molecules during development of different regions of the nervous system," *Journal of Neuroscience*, vol. 4, no. 9, pp. 2354–2368, 1984.
- [25] Q. Hu, H. Fu, H. Song et al., "Low-level lead exposure attenuates the expression of three major isoforms of neural cell adhesion molecule," *NeuroToxicology*, vol. 32, no. 2, pp. 255–260, 2011.
- [26] R. P. Singh, S. Sharad, and S. Kapur, "Free radicals and oxidative stress in neurodegenerative diseases: relevance of dietary antioxidants," *Journal Indian Academy of Clinical Medicine*, vol. 5, no. 3, pp. 218–225, 2004.
- [27] H. Aebi, *Catalase in Vitro: Methods in Enzymology*, vol. 105, Academic Press, New York, NY, USA, 1984.
- [28] Y. Kono, "Generation of superoxide radical during autoxidation of hydroxylamine and an assay for superoxide dismutase," *Archives of Biochemistry and Biophysics*, vol. 186, no. 1, pp. 189–195, 1978.
- [29] J. Sedlak and R. H. Lindsay, "Estimation of total, protein-bound, and nonprotein sulfhydryl groups in tissue with Ellman's reagent," *Analytical Biochemistry*, vol. 25, pp. 192–205, 1968.
- [30] J. A. Buege and S. D. Aust, "Microsomal lipid peroxidation," *Methods in Enzymology*, vol. 52, pp. 302–310, 1978.
- [31] S. RajaSankar, T. Manivasagam, and S. Surendran, "Ashwagandha leaf extract: a potential agent in treating oxidative damage and physiological abnormalities seen in a mouse model of Parkinson's disease," *Neuroscience Letters*, vol. 454, no. 1, pp. 11–15, 2009.

- [32] C. Mead and V. W. Pentreath, "Hypertrophy and increased glial fibrillary acidic protein are coupled to increased protection against cytotoxicity in glioma cell lines," *Toxicology in Vitro*, vol. 12, no. 2, pp. 141–152, 1998.
- [33] A. Konar, N. Shah, R. Singh et al., "Protective role of Ashwagandha leaf extract and its component withanone on scopolamine-induced changes in the brain and brain-derived cells," *PLoS ONE*, vol. 6, no. 11, Article ID e27265, 2011.
- [34] H. Kataria, R. Wadhwa, S. C. Kaul, and G. Kaur, "Water extract from the leaves of *Withania somnifera* protect ra differentiated c6 and IMR-32 cells against glutamate-induced excitotoxicity," *PLoS ONE*, vol. 7, no. 5, Article ID e37080, 2012.
- [35] A. Selvin-Testa, F. Capani, C. F. Loidl, E. M. Lopez, and J. Pecci-Saavedra, "Prenatal and postnatal lead exposure induces 70 kDa heat shock protein in young rat brain prior to changes in astrocyte cytoskeleton," *Neurotoxicology*, vol. 18, pp. 805–817, 1997.
- [36] K. L. Milarski and R. I. Morimoto, "Expression of human HSP70 during the synthetic phase of the cell cycle," *Proceedings of the National Academy of Sciences of the United States of America*, vol. 83, no. 24, pp. 9517–9521, 1986.
- [37] E. Zeise, N. Kühl, J. Kunz, and L. Rensing, "Nuclear translocation of stress protein Hsc70 during S phase in rat C6 glioma cells," *Cell Stress Chaperones*, vol. 3, no. 2, pp. 94–99, 1998.
- [38] R. Wadhwa, K. Taira, and S. C. Kaul, "An HSP70 family chaperone, mortalin/mthsp70/PBP74/Grp75, what, when, and where?" *Cell Stress Chaperones*, vol. 7, pp. 309–316, 2002.
- [39] H. Kataria, N. Shah, S. C. Kaul, R. Wadhwa, and G. Kaur, "Water extract of Ashwagandha leaves limits proliferation and migration, and induces differentiation in glioma cells," *Evidence-Based Complementary and Alternative Medicine*, vol. 2011, Article ID 267614, 12 pages, 2011.
- [40] Q. Shi, Z. Dong, and H. Wei, "The involvement of heat shock proteins in murine liver regeneration," *Cellular & Molecular Immunology*, vol. 4, no. 1, pp. 53–57, 2007.
- [41] Z. Wang, H. Jin, C. Li, Y. Hou, Q. Mei, and D. Fan, "Heat shock protein 72 protects kidney proximal tubule cells from injury induced by triptolide by means of activation of the MEK/ERK pathway," *International Journal of Toxicology*, vol. 28, no. 3, pp. 177–189, 2009.
- [42] P. M. Dey, J. Burger, M. Gochfeld, and K. R. Reuhl, "Developmental lead exposure disturbs expression of synaptic neural cell adhesion molecules in herring gull brains," *Toxicology*, vol. 146, no. 2-3, pp. 137–147, 2000.
- [43] Q. Hu, H. Fu, T. Ren et al., "Maternal low-level lead exposure reduces the expression of PSA-NCAM and the activity of sialyltransferase in the hippocampi of neonatal rat pups," *NeuroToxicology*, vol. 29, no. 4, pp. 675–681, 2008.
- [44] W. E. Donaldson and S. O. Knowles, "Is lead toxicosis a reflection of altered fatty acid composition of membranes?" *Comparative Biochemistry and Physiology C: Pharmacology Toxicology and Endocrinology*, vol. 104, no. 3, pp. 377–379, 1993.
- [45] K. M. Savolainen, J. Loikkanen, S. Eerikainen, and J. Naarala, "Glutamate-stimulated ROS production in neuronal cultures: interactions with lead and the cholinergic system," *NeuroToxicology*, vol. 19, no. 4-5, pp. 669–674, 1998.
- [46] S. Panda and A. Kar, "Evidence for free radical scavenging activity of Ashwagandha root powder in mice," *Indian Journal of Physiology and Pharmacology*, vol. 41, no. 4, pp. 424–426, 1997.
- [47] G. Chaudhary, U. Sharma, N. R. Jagannathan, and Y. K. Gupta, "Evaluation of *Withania somnifera* in a middle cerebral artery occlusion model of stroke in rats," *Clinical and Experimental Pharmacology and Physiology*, vol. 30, no. 5-6, pp. 399–404, 2003.
- [48] S. Jain, S. D. Shukla, K. Sharma, and M. Bhatnagar, "Neuroprotective effects of *Withania somnifera* Dunn. in hippocampal subregions of female albino rat," *Phytotherapy Research*, vol. 15, no. 6, pp. 544–548, 2001.
- [49] N. A. Simonian and J. T. Coyle, "Oxidative stress in neurodegenerative diseases," *Annual Review of Pharmacology and Toxicology*, vol. 36, pp. 83–106, 1996.
- [50] T. Kuboyama, C. Tohda, and K. Komatsu, "Neuritic regeneration and synaptic reconstruction induced by withanolide A," *British Journal of Pharmacology*, vol. 144, no. 7, pp. 961–971, 2005.

Research Article

Production and Enhancement of Omega-3 Fatty Acid from *Mortierella alpina* CFR-GV15: Its Food and Therapeutic Application

Ganesan Vadivelan and Govindarajulu Venkateswaran

Food Microbiology Department, Central Food Technological Research Institute, Mysore, Karnataka 570020, India

Correspondence should be addressed to Govindarajulu Venkateswaran; venkatcftri@gmail.com

Received 21 February 2014; Revised 25 April 2014; Accepted 25 April 2014; Published 21 May 2014

Academic Editor: Leandro Rocha

Copyright © 2014 G. Vadivelan and G. Venkateswaran. This is an open access article distributed under the Creative Commons Attribution License, which permits unrestricted use, distribution, and reproduction in any medium, provided the original work is properly cited.

Mortierella sp. has been known to produce polyunsaturated fatty acids (PUFAs) such as GLA and AA under normal growth medium conditions. Similarly, under the stress condition, this fungus produces EPA and DHA in their mycelial biomass. Among the 67 soil samples screened from the Western Ghats of India, 11 *Mortierella* isolates showed the presence of omega-6 and omega-3 fatty acid, mainly GLA, AA, EPA, and DHA in starch, yeast-extract medium. Nile red and TTC strains were used for screening their qualitative oleaginesity. Among the representative isolates, when *Mortierella* sp. is grown in a fat-producing basal medium, a maximum lipid content of $42.0 \pm 1.32\%$ in its mycelia, $6.72 \pm 0.5\%$ EPA, and $4.09 \pm 0.1\%$ DHA was obtained. To understand the *Mortierella* sp. CFR-GV15, to the species level, its morphology was seen under the light microscope and scanning electron microscope, respectively. These microscopic observations showed that isolate *Mortierella* sp. CFR-GV15 produced coenocytic hyphae. Later on, its 18S rRNA and the internal transcribed spacer (ITS) sequences were cloned, sequenced, and analyzed phylogenetically to 18S rRNA and ITS1 and ITS4 sequences of related fungi. This newly isolated *Mortierella alpina* CFR-GV15 was found to be promising culture for the development of an economical method for commercial production of omega-3 fatty acid for food and therapeutical application.

1. Introduction

The pathogenesis of lifestyle-related diseases such as obesity, hyperlipidemia, arteriosclerosis, diabetes mellitus, and hypertension is complicated and the precise mechanisms underlying their development have not yet been elucidated. However, there is now much evidence to suggest that specific fatty acids have beneficial effects on human health which could contribute to the prevention of many chronic diseases in humans [1]. In particular, polyunsaturated fatty acids (PUFAs), such as linoleic acid (18:2, n-6), α -linolenic acid (LNA, 18:3, n-3), and arachidonic acid (20:4, n-6), are very important for maintaining biofunctions in mammals as essential fatty acids [2]. Polyunsaturated fatty acids (PUFAs), a group of fatty acids containing double bonds at omega-3 position, including alpha-linolenic acid (ALA), eicosapentaenoic acid (EPA), and docosahexaenoic acid (DHA), have many specialized health benefits. PUFAs are found to be helpful in treating hypertension, Crohn's disease, rheumatoid

arthritis, and asthma. Preview reported reducing the risk of primary cardiac arrest and coronary artery disease and reducing serum triglycerides. Also, encouraging data supports a role of omega-3 fatty acids in the prevention of breast and lung cancer [3]. Recent evidence suggests that omega-3 fatty acids may also have beneficial effects on mood disorders, including major depression and bipolar disorder, schizophrenia, and dementia, and reduce serum triglycerides [4].

As these essential fatty acids cannot be accumulated and synthesized in the human body, they must be derived from dietary sources. Current dietary sources of omega-3 PUFAs (EPA and DHA) from animals include fatty fish species, such as Herring, Mackerel, Sardine, and Salmon [5, 6]. The quality of the fish oil, however, is changing and depends on the type of fish, seasonal time, and place of fishing. The applications of fish oil in foods, infant formulas, or pharmaceuticals have some disadvantages because of their contamination by environmental pollution such as heavy metal accumulation

and regular fishy smell and unpleasant taste. Moreover, the majority of the PUFAs in their body emerge from their food though they had some capacity for de novo biosynthesis of omega-3 fatty acids. The plant sources include green leaves and a variety of vegetable oils like flax, hemp, rapeseed (canola), soybean, and walnut, which are quite rich in alpha-linolenic acid (ALA). The ALA is the “parent” fatty acid of EPA and DHA and human body converts ALA rapidly into EPA and more slowly into DHA [7]. However, since the production building and downstream processing of oils from plants and fishes are cost-effective and time-consuming, it is likely that methods for the microbial production of oils are more convenient and should be focused on in the near future. Although marine algae and fungi are used in commercial production, the difficulties in cultivation and adaptation of marine microorganisms have changed the situation from conventional marine sources into nonmarine microorganisms. One such fungus, *Mortierella*, a member of the family *Mortierellaceae*, is the most promising microorganism for the industrial production of omega-6 or omega-3 PUFAs. Major members of the genus include *M. alliacea*, *M. alpina*, *M. polycephala*, *M. elongata*, and *M. spinosa*. One of the *M. alpina* has gained importance due to its higher production of lipids. Apart from being the major producer of arachidonic acid, *M. alpina* also produces other PUFAs such as linolenic acid (LA), gamma-linolenic acid (GLA), and dihomo-gamma-linolenic acid (DGLA); EPA and DHA, in fewer amounts, [8, 9] suggest that this fungus is a potential producer of many biologically important PUFAs, both omega-3 and omega-6. More enhancement of omega-3 fatty acid production by *M. alpina* would be significant since they are playing a major role in brain development and the prevention of depression-related disorders. Hence the physiology of *M. alpina* can be appropriately altered by several means, for example, induced mutation, chemical inhibitors, stress conditions, cultural changes, and so on, in order to enhance the biosynthesis of omega-3 fatty acids (EPA and DHA) instead of omega-6 fatty acids (GLA and AA). We report in this paper the production of omega-3 fatty acids by *Mortierella alpina* CFR-GV15 by specific cultural methods and their application in food and therapeutic purpose.

2. Material and Method

2.1. Soil Sampling. Collection of saprophytic soil samples from various locations in South India, mostly from Tamil Nadu, Kerala, and Karnataka of the Western Ghats area, was performed. Selectively untouched soil samples were collected from the bottom of 5 to 10 cm, sealed in sterile sampling polythene bags, and brought to the laboratory for further analysis.

2.2. Screening and Isolation of *Mortierella* sp. The soil samples were screened by spread plate techniques by the following method. 10.0 gm of soil sample was suspended in 90 mL sterile saline water, serial 10-fold dilutions of that suspension were made [10], and then 0.1 mL of saline water from the 10^{-2} dilution was spread evenly on the surface of MEA (malt extract agar) medium. The plate was then incubated at

6°C in a cellular refrigerator. After 8–12 days of incubation, the selective fungal white colonies were transferred to fresh potato dextrose agar and incubated at room temperature ($28^{\circ}\text{C} \pm 1$) for further purification. Then the absolute cultures were identified, maintained on the PDA plate or slants at 4°C, and subcultured once every 2 months.

2.3. Cultural Method and Cultivation. *M. alpina* cultures were maintained on potato dextrose agar slants at 4°C and subcultured every 2 months [11]. The seed culture was prepared in 50 mL medium containing (g/L) glucose, 20; yeast extract, 10; the pH was adjusted to 6.0 and cultures were incubated for 48 h at 28°C. The fermentation medium composition was as follows (g/L): starch, 20 g; yeast extract, 5 g; KNO_3 , 10 g; KH_2PO_4 , 1 g; and MgSO_4 , 0.5 g. The final pH was adjusted to 6.5 and sterilized at 121°C for 15 min. The culture medium was then incubated for 7 days at 20°C temperature on a rotary shaker at 230 rpm.

2.4. Dry Biomass Determination and Lipid Extraction. Harvest and extraction of lipids from biomass were performed according to the procedure of Nisha et al. [11]. Biomass production was determined by harvesting the cells by suction filtration followed by drying at 55–60°C overnight. The dry biomass was ground to fine powder and packed into a thimble, macerated with 0.1N HCl for 20 min. 1 g of fungal dry powder was blended with 40 mL of chloroform/methanol (2:1), the mixtures were agitated for 20 min in an orbital shaker at 20°C and then filtered with Whatman paper number 1, and 0.9% sodium chloride solution was added. The chloroform solvent containing total fatty acid then evaporated and dried under N_2 vacuum.

2.5. Analytical Method

2.5.1. Methyl Ester Preparation and Fatty Acid Analysis. Fatty acid methyl esters (FAME) were prepared as described by Nisha and Venkateswaran [12] and were used for gas chromatographic analysis. FAME was prepared by using methanolic HCl in the ratio of 95:5 as the methylating agent and 14% BF_3 . The derivatized lipids in the hexane layer were evaporated under N_2 and dissolved in 1 mL of benzene, and any solids were removed by centrifuging at 10,000 (rpm) for 2 min. Lipids were analyzed by gas chromatography (Shimadzu 2010 system, Japan) using RTX-2330 (fused silica) 30 m capillary column of 0.25 μm internal diameter and df (μm) 0.20 μm . The column was operated at an initial temperature of 160°C–250°C at the rate of 5°C/min and was to hold for 10 min. The injector and detector temperature were 240°C and 250°C, respectively. Carrier gas (nitrogen) was supplied at a total flow rate of 50 mL/min with a split ratio of 20:0 and fatty acids were identified by comparison with standards (Sigma).

2.6. Triphenyltetrazolium Chloride (TTC) Staining. The two-day fresh mycelium of *Mortierella* fungus was harvested by suction filtration, and the staining procedure was done according to Zhu et al.'s [10] method with slight modification;

1 mL of 0.6% triphenyltetrazolium chloride (TTC) solution in 0.5 mol-1 phosphate buffer (pH 7.8) was added to 0.1g of fresh mycelia in a scrub cap tube and incubated in the dark for one hour at room temperature. Mycelia were then rinsed twice with sterile water and homogenized by mortal postal grinding. Then the red triphenylformazan (TF) formed in mycelia was extracted three times with 2 mL of ethyl acetate at room temperature using fresh solvent each time. The staining level was quantified by measuring absorbance of TF in the ethyl acetate solvent at 485 nm wavelengths.

2.7. Genomic DNA Extraction, Sequencing, and Data Analysis. The total genomic DNA extraction was performed according to the protocol followed by Michaelson et al. [13]. The total DNA precipitation was concentrated with ethanol, dissolved, and stored in TE buffer. A DNA segment containing the 3' end of 18S rRNA, internal transcribed spacer 1 (ITS1), 5.8S rRNA, and internal transcribed spacer 4 (ITS4) and the 5' end of 28S rRNA was amplified by using a forward primer ITS1 (5'GGAAGTAAAAGTCGTAACAAGG) and a reverse primer ITS4 (5'TCCCGCTTATTGATATGC) [14]. DNA amplification by PCR was performed in a total volume of 50 μ L. The PCR conditions were followed by the Ho et al. [9] method with slight modification by using ITS1 and ITS4 primer, with initial denaturation at 94°C for 5 min followed by 30 cycles at 94°C for 45 s, 57°C for 45 s, and 72°C for 1 min and a final extension at 72°C for 5 min. After the amplified products were separated on electrophoresis using 0.8% agarose gel and detected by staining with ethidium bromide, all PCR products were amplified from strains of *M. horticola* CFR-GV10, *M. exigus* CFR-GV11, *M. elongata* CFR-GV12, *Mortierella* sp. CFR-GV13, *Mortierella* sp. CFR-GV14, *M. alpina* CFR-GV15, *M. alpina* CFR-GVM15, *M. elongata* CFR-GV16, *M. elongata* CFR-GV17, *M. elongata* CFR-GV18, and *M. elongata* CFR GV19 and standard culture of *M. alpina* CBS 528.72 and *M. alpina* 6344 genomic DNA showed only one band. The PCR products were purified by using Qiagen and DNA Gel Band Purification Kit following the instructions of the manufacturer (Qiagen Biosciences, Germany). The final amplified PCR products were then sequenced by automatic sequencer (Chromos Biotech, Bangalore, India). The standard culture and sequences of *M. alpina* CBS 528.72, *M. alpina* MTCC 6344, recently isolated *Mortierella* sp., *M. horticola* CFR-GV10, *M. exigus* CFR-GV11, *M. elongata* CFR-GV12, *Mortierella* sp. CFR-GV13, *Mortierella* sp. CFR-GV14, *M. alpina* CFR-GV15, *M. alpina* CFR-GVM15, *M. elongata* CFR-GV16, *M. elongata* CFR-GV17, *M. elongata* CFR-GV18, and *M. elongata* CFR GV19 were submitted to GenBank, with accession numbers KF743701, KF743702, KF743703, KF798172, KF798173, KF561137, KF683921, KF568909, KF679986, and KF679987, respectively. Standard sequence was obtained by GenBank. The sequences were aligned by using the phylogeny tree program [15], and the alignment was corrected manually. A character's matrix was calculated by the program of phylogeny tree.

2.8. Statistical Analysis. Data obtained from three independent analyses was expressed as mean (3SD). Experimental

TABLE 1: Collection of saprophytic soil samples from the different species of *Mortierella* growing in the Western Ghats regions of Tamil Nadu, Kerala, and Karnataka. The total cultivable fungi and the total specific species of *Mortierella* (state-wise).

Sl number	Place of collection	Number of soil samples	Total number of fungi	Total <i>Mortierella</i> species
1	Mysore			
	Bandipur wild forest	02	20	0
2	Tamil Nadu			
	Mudumalai wild forest	20	15	02
	Nilambur-Gudalur road	12	20	08
3	Kerala			
	Nilambur road	04	15	04
	Vazhikkadavu	03	12	04
	Karimpuzha bridge	03	08	02
	Payyavoor road	02	11	0
	Chemperi road	02	16	0
4	Karnataka			
	Sullia	03	15	02
	Puttur	03	14	03
	Ujere	04	10	03
	Dharmasthala	02	5	0
	Subramanya	01	14	0
	W.G* 1-W.G7	16	34	1
	W.G8	03	35	0
	W.G10	03	25	02
	W.G11	03	26	02
	W.G12	03	38	05
	W.G13	04	34	0
	Sakleshpur	04	12	0
Total		67	379	37

W.G*: Western Ghats.

data was subjected to analysis of variance and Duncan's multiple range test ($P \leq 0.05$) using the Statistical Analysis System [16].

3. Results and Discussion

Sixty-seven soil (Table 1) samples have been screened on MEA medium for isolation of *Mortierella* sp. for the production of omega-3 fatty acids. After the incubation period of 8–12 days at low temperature, a few white colonies were grown and these white colonies were microscopically observed for their morphological identity (Figures 1 and 2) and further confirmed with fluorescence microscope (Figures 3 and 4). Nile red staining had helped the presence of oil or lipid globules and was further observed under scanning electron microscope (SEM) for their confirmation. The morphologies of mycelial structure and sporangiophores of all the isolates

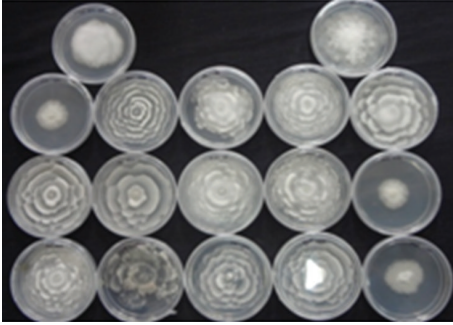


FIGURE 1: *Mortierella* sp. from soil source of roselle petal growth on PDA plate.

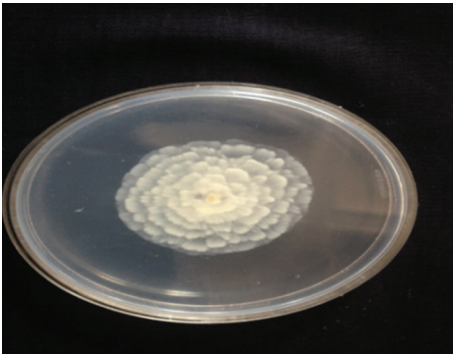


FIGURE 2: Selective isolated *M. alpina* CFR-GV15.

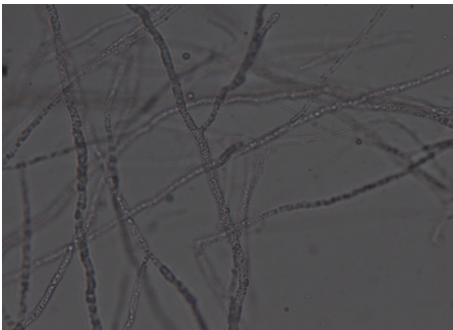


FIGURE 3: Light microscopy image of *M. alpina* CFR-GV15 mycelia.

were compared with the standard culture obtained from *M. alpina* MTCC 6344 and *M. alpina* CBS 528.72 cultures. Most of the features were in compliance with the standard cultures. This initial screening confirmed that most of the white colonies grown on the MEA medium were *Mortierella* sp. [17, 18]. It was also observed that all the sporangiophores were unbranched structure measuring the length between 20 and 120 μm with an irregular and wide swollen base. At this stage, though all the isolated sporangiophores were very much in concomitance with *Mortierella alpina*, they were placed *Mortierella* sp. [9, 19]. Later on, 18S rRNA sequence was also compared with MTCC and CBS standard cultures.

Different growth temperatures play an important role in the formation of roselle petal growth pattern on the growth agar media. Initially a loop of inoculums was placed in the

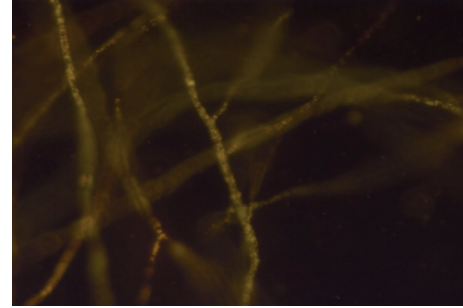


FIGURE 4: Nile red staining of *M. alpina* CFR-GV15 under fluorescence microscope.

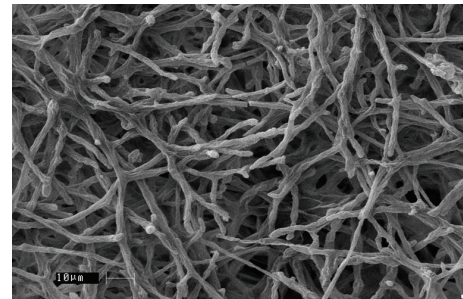


FIGURE 5: Mycelial hyphae of *M. alpina* CFR-GV15 under SEM image.

middle of agar culture plate and incubated at 19°C for 5–7 days. While colonial growth was observed on PDA plate, later on these plates were incubated at 28°C for another 3–4 days. Vigorous growth was observed on PDA plate and roselle petal clearly formed in the plate (Figures 1 and 2). More carbon and low nitrogen content in the medium play a vital role in the formation of roselle petal in the PDA plate. All *Mortierella* sp. were saprophytic and proteolytic in nature, and they grew faster on the nutrient-rich medium compared to the other fungi, *Mucor* sp. and *Pythium* sp. Milky white with cotton colonies with pure white or milky growth, in morphological structure similar to *Mortierella* sp. (standard culture) were tentatively identified as per the fungi manual and were taken further for 18S rRNA sequence studies. Septate coenocytic mycelium, swollen sporangiophores, and morphological characters similar to *Mortierella* sp. were observed in our study (Figures 5 and 6). All the morphological characters were additionally compared with standard culture and the Gilman manual [17]. Based on the above observations, 11 species of *Mortierella* were selected and named as CFR-GV11 to CFR-GV19. In these selective isolates *M. alpina* CFR-GV15 was screened and stained with TTC to measure the relation between staining degree and lipid content, especially with omega-6 and omega-3 fatty acid. The results were presented in Table 2. Staining degree was found maximum in *M. alpina* CFR-GV15 observed as 1.541 at 458 nm. Total lipid in mycelial structure and higher AA increased during the course of production time. The reduction of TTC [10, 20] is mostly used as a biochemical marker for the viability of living cells. It is generally thought

TABLE 2: Biomass production and lipid content of 11 isolates of *Mortierella* sp. after 7 days of cultivation.

Fungal isolates	Strains identified	Genebank accession number	Staining degree (A485 nm)	Dry biomass (g/L)	Total lipid content (%)
MV1	<i>Mortierella horticola</i> CFR-GV10	KF743701	0.812 ± 0.66 ^c	8.52 ± 0.30 ^c	34.60 ± 5.10 ^c
M08	<i>Mortierella exigus</i> CFR-GV11	KF743702	0.761 ± 0.00 ^c	8.24 ± 2.30 ^c	39.00 ± 3.60 ^{ab}
2aS2	<i>Mortierella elongata</i> CFR-GV12	KF743703	0.528 ± 0.04 ^h	7.85 ± 0.01 ^d	38.70 ± 0.20 ^b
M01	<i>Mortierella</i> sp. CFR-GV13	KF798172	0.706 ± 0.03 ^f	5.83 ± 4.05 ^g	41.02 ± 0.80 ^a
S2	<i>Mortierella</i> sp. CFR-GV14	KF798173	0.936 ± 0.35 ^c	6.37 ± 0.60 ^f	38.89 ± 0.70 ^b
M05	<i>Mortierella alpina</i> CFR-GV15	KF561137	1.541 ± 0.02^a	10.82 ± 1.9^a	39.05 ± 0.40^{ab}
M06	<i>Mortierella alpina</i> CFR-GVM15	KF683921	1.099 ± 0.04 ^b	7.85 ± 0.80 ^d	40.00 ± 2.30 ^a
M02	<i>Mortierella elongata</i> CFR-GV16	KF561138	0.641 ± 0.21 ^g	8.42 ± 3.01 ^c	37.90 ± 0.54 ^{bc}
M27	<i>Mortierella elongata</i> CFR-GV17	KF568908	0.683 ± 0.25 ^g	9.02 ± 1.10 ^b	28.98 ± 0.40 ^c
M07	<i>Mortierella elongata</i> CFR-GV18	KF679986	0.941 ± 0.45 ^c	8.45 ± 0.20 ^c	35.62 ± 0.12 ^c
M21	<i>Mortierella elongata</i> CFR-GV19	KF679987	0.329 ± 0.14 ⁱ	7.42 ± 4.02 ^{de}	38.36 ± 0.71 ^{bc}
MA1	<i>Mortierella alpina</i> MTCC 6344	KC018186	0.688 ± 0.58 ^g	4.30 ± 0.20 ^j	29.07 ± 0.50 ^e
MA2	<i>Mortierella alpina</i> CBS 528.72	AJ271629	0.845 ± 0.41 ^d	6.52 ± 5.08 ^f	37.42 ± 0.20 ^{bc}

Culture conditions: starch-yeast extract medium; pH: 6.5 and incubated at 20°C; carbon source: 2% starch, 0.5% yeast extract; 1% KNO₃; 0.1% KH₂PO₄ and MgSO₄·7H₂O 0.05%; 230 rpm; cultivation period: 7-day values of means ± SD, n-3. Values in the same column that do not share the same alphabetic superscripts are significantly different at $P \leq 0.05$ levels according to Duncan's multiple range test.



FIGURE 6: Sporangiospores of *M. alpina* CFR-GV15 under SEM image.

that TTC is reduced by dehydrogenases and it is absorbed by living cells [20], where it reacts with hydrogen atoms released by the dehydrogenase enzymes during cellular respiration [21]. Although there are many dehydrogenases in fungi, only AA-producing fungus *M. alpina* could be stained red. Similarly positive strain of *M. alpina* CFR-GV15 observed maximum amount as 1.541 at 458 nm spectrophotometrically. *Mucor* which is not producing AA could not be stained red, and this indicated that the enzyme dehydrogenase is specific for *Mortierella* sp. and not for *Mucor*. The fatty acid profiles of all 11 selective isolates of *Mortierella* species and two *M. alpina* MTCC and CBS standard strains are shown (Table 3). *M. alpina* CFR-GV15, the total fatty acid content significantly increased maximum of 53.86% AA, 4.87% EPA, and 3.94% DHA whereas the standard culture MTCC 6344 accumulated less amount of total fatty acid content 38.69% AA, 2.65% EPA, and 2.45% DHA. Similarly *M. alpina* CFR-GV15, *M. alpina* CFR-GVM15, and *M. horticola* CFR-GV10 had a higher content of AA, EPA, and DHA. However, *M. elongata* CFR-GV16 and CFR-GV17 and *M. exigus* CFR-GV11 had low yield. A few of our isolates had very negligible

amount of these fatty acids. Therefore, *M. alpina* CFR-GV15 was chosen for further study.

3.1. Molecular Identification and Phylogenetic Tree Prediction of *Mortierella* sp. The 11 selective isolates of *Mortierella* sp. were sequenced and sent to NCBI GenBank. Accession numbers have been shown in Table 2. A total of 37 isolated DNA were amplified with 18S-28S ribosomal gene internal transcribed spacer (ITS1-rDNA-ITS4 DNA) regions of *Mortierella* sp. from three different locations (Western Ghats of Tamil Nadu, Kerala, and Karnataka, India), sequenced, and investigated. Out of the 11 selective *Mortierella* sp., three closely related species (*M. alpina*, *M. horticola*, and *M. exigus*) showed the most similar sequence identity, were isolated from the Western Ghats of Karnataka soil sample compared to the Western Ghats of Tamil Nadu, and were found to have the highest nucleotide diversities. Omega-6 and omega-3 fatty acid production by different strains of *Mortierella* sp. (*M. alpina*, *Mortierella elongata*, *Mortierella horticola*, and *Mortierella exigus*) were detected. One of the isolates, *Mortierella alpina* CFR-GV15, was found to be producing the highest amount of omega-6 and omega-3 fatty acids (AA, EPA, and DHA). Molecular characterization of *M. alpina* CFR-GV15 was carried out for taxonomic identifications using 18S rRNA gene sequences. The genomic DNA extracted from *M. alpina* CFR-GV15 by a modified method was found to be of good quality (Figure 7). The rRNA gene amplicon obtained by PCR was 614 bps as expected (Figure 7) and was subjected to sequencing. The gene sequence of the PCR product obtained represents part of the 18S rRNA, ITS1, 5.8S rRNA, ITS4, and 28S rRNA regions. On BLAST analysis, *M. alpina* CFR-GV15 exhibited 76% homology with *M. alpina* CBS 528.72 (accession number AJ271629). *M. alpina* CFR-GV15 was further confirmed as a new strain of *M. alpina* through molecular phylogenetic analysis. It was subsequently

TABLE 3: Total fatty acid profile of newly isolated *Mortierella* sp.

Strain	C14:0	C16:1	C18:0	C18:1	C18:2	C18:3	C20:3	C20:4	C20:5	C22:6
CFR-GV11	0.96 ± 0.2 ^d	23.14 ± 0.2 ^{ab}	5.67 ± 0.8 ^{fg}	29.78 ± 0.1 ^b	7.17 ± 0.2 ^a	3.86 ± 0.3 ^d	3.00 ± 0.8 ^d	32.03 ± 0.0 ^f	1.34 ± 0.8 ^g	1.56 ± 0.2 ^{bcd}
CFR-GV12	0.62 ± 0.4 ^f	21.02 ± 0.1 ^d	4.56 ± 0.1 ⁱ	32.02 ± 0.8 ^a	6.45 ± 0.1 ^{bcd}	4.62 ± 0.2 ^c	4.20 ± 0.5 ^a	32.54 ± 0.2 ^f	3.65 ± 0.2 ^b	3.48 ± 0.5 ^{ab}
CFR-GV13	0.68 ± 0.1 ^f	18.52 ± 0.3 ^e	4.98 ± 0.4 ⁱ	24.52 ± 0.1 ^e	5.23 ± 0.4 ^{ef}	3.26 ± 0.0 ^f	1.98 ± 0.6 ^b	28.32 ± 0.6 ^g	3.12 ± 0.1 ^c	2.36 ± 0.1 ^{abcd}
CFR-GV14	0.86 ± 0.2 ^e	16.35 ± 0.2 ^f	5.68 ± 0.3 ^{fg}	23.16 ± 0.7 ^f	5.68 ± 0.3 ^e	3.35 ± 0.4 ^{ef}	2.45 ± 0.1 ^{ef}	27.56 ± 0.4 ^h	3.26 ± 0.6 ^c	1.78 ± 0.3 ^{bcd}
CFR-GV15	0.48 ± 0.0 ^h	10.66 ± 0.4 ⁱ	5.05 ± 0.3 ^h	6.21 ± 0.5 ⁱ	6.07 ± 0.5 ^d	5.58 ± 0.2 ^a	3.37 ± 0.3 ^c	53.86 ± 0.2 ^a	4.87 ± 0.0 ^a	3.94 ± 0.6 ^b
CFR-GVM15	0.54 ± 0.7 ^g	9.85 ± 0.2 ⁱ	4.58 ± 0.7 ⁱ	6.00 ± 0.1 ⁱ	5.21 ± 0.2 ^e	5.24 ± 0.6 ^b	2.75 ± 0.6 ^e	48.25 ± 0.1 ^b	2.35 ± 0.6 ^{de}	3.68 ± 0.2 ^{ab}
CFR-GV16	1.92 ± 0.3 ^c	20.87 ± 0.8 ^d	5.58 ± 0.1 ^f	29.58 ± 0.4 ^c	6.37 ± 0.1 ^{bcd}	4.58 ± 0.5 ^c	1.89 ± 0.7 ^h	26.11 ± 0.3 ⁱ	1.91 ± 0.4 ^f	0.68 ± 0.8 ^d
CFR-GV17	2.30 ± 0.4 ^b	22.81 ± 0.1 ^c	7.11 ± 0.5 ^{cd}	30.27 ± 0.1 ^b	6.15 ± 0.6 ^d	3.15 ± 0.3 ^f	2.56 ± 0.6 ^{ef}	22.03 ± 0.9 ⁱ	2.02 ± 0.3 ^{ef}	0.65 ± 0.6 ^d
CFR-GV18	1.89 ± 0.2 ^c	22.01 ± 0.9 ^c	6.89 ± 0.9 ^e	27.52 ± 0.6 ^d	4.25 ± 0.4 ^g	2.87 ± 0.4 ^g	2.15 ± 0.1 ^g	37.12 ± 0.7 ^d	0.78 ± 0.0 ^h	0.68 ± 0.5 ^d
CFR-GV19	2.03 ± 0.1 ^a	23.75 ± 0.0 ^a	7.50 ± 0.8 ^c	30.35 ± 0.8 ^b	6.33 ± 0.2 ^{cd}	3.46 ± 0.1 ^{de}	2.77 ± 0.6 ^e	22.01 ± 0.6 ^k	1.31 ± 0.3 ^g	0.88 ± 0.3 ^{cd}
MTCC 6344	0.45 ± 0.2 ^h	14.25 ± 0.4 ^g	11.25 ± 0.1 ^a	24.00 ± 0.9 ^e	6.90 ± 0.8 ^b	1.05 ± 0.1 ^h	3.90 ± 0.4 ^b	38.69 ± 0.5 ^c	2.65 ± 0.1 ^d	2.45 ± 0.2 ^{abcd}
CBS528.72	0.57 ± 0.4 ^g	13.01 ± 0.2 ^h	10.65 ± 0.6 ^b	18.53 ± 0.4 ^g	6.61 ± 0.9 ^{bc}	0.84 ± 0.2 ⁱ	3.70 ± 0.0 ^b	34.86 ± 0.1 ^e	3.29 ± 0.5 ^{bc}	4.04 ± 0.0 ^a

Culture conditions: starch-yeast extract medium; pH: 6.5 and incubated at 20°C; carbon source: 2% starch, 0.5% yeast extract; 1% KNO₃; 0.1% KH₂PO₄ and MgSO₄·7H₂O 0.05%; 230 rpm; cultivation period: 7-day values of means ± SD, n=3. Values in the same column that do not share the same alphabetic superscripts are significantly different at P ≤ 0.05 levels according to Duncan's multiple range test.

TABLE 4: Effect of temperature on enhancement of biomass, total lipid, and EPA and DHA production by *M. alpina* CFR-GV15.

Temperature	Dry biomass g/L	Total lipid % w/w	ARA content %	EPA content %	DHA content %
20°C for 4 days and 12°C for 5 days*	11.82 ± 0.21 ^a	42.01 ± 0.25 ^b	23.56 ± 0.81 ^e	6.79 ± 0.41 ^a	4.09 ± 0.40 ^b
12°C	8.41 ± 0.10 ^d	38.34 ± 0.11 ^d	30.54 ± 0.52 ^d	5.90 ± 0.01 ^b	4.50 ± 0.56 ^a
15°C	9.80 ± 0.25 ^c	40.20 ± 0.25 ^c	47.20 ± 0.85 ^c	4.21 ± 0.49 ^d	4.20 ± 0.72 ^a
20°C	10.45 ± 0.52 ^b	41.89 ± 0.52 ^b	53.70 ± 0.07 ^b	4.80 ± 0.14 ^c	3.92 ± 0.45 ^c
28°C	10.86 ± 0.22 ^b	44.25 ± 0.78 ^a	56.82 ± 0.24 ^a	3.46 ± 0.75 ^d	4.30 ± 0.90 ^a

Culture conditions: starch-yeast extract medium; pH: 6.5; carbon source: 2% starch, 0.5% yeast extract; 1% KNO₃; 0.1% KH₂PO₄ and MgSO₄·7H₂O 0.05%; 230 rpm; cultivation period: 7-day values of means ± SD, n-3. * Cultivation period: 9-day values of means ± SD, n-3. Values in the same column that do not share the same alphabetic superscripts are significantly different at $P \leq 0.05$ levels according to Duncan's multiple range tests.



DNA ladder: 100 bp to 5 kb marker
 Lane 1: CFR-GV10;594 bp
 Lane 2: CFR-GV11;577 bp
 Lane 3: CFR-GV12;581 bp
 Lane 4: CFR-GV13;597 bp
 Lane 5: CFR-GV14;571 bp
 Lane 6: CFR-GV15;614 bp
 Lane 7: CFR-GVM15; 624 bp
 Lane 8: CFR-GV16; 573 bp
 Lane 9: CFR-GV17; 584 bp

FIGURE 7: 18S rRNA, ITS1 and ITS4 primer, and selective PCR amplified products.

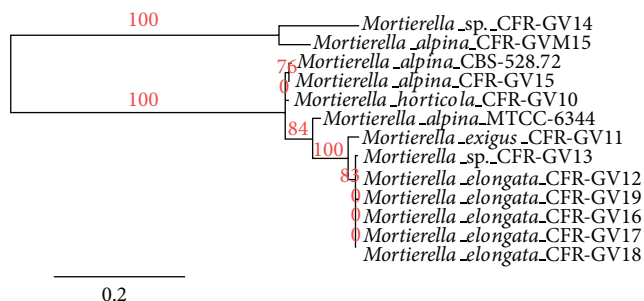


FIGURE 8: Neighbor-joining phylogenetic analyses of putative isolated PUFAs producing *Mortierella* sp.

subjected to DNA sequencing and BLAST analysis. The phylogenetic tree of ITS amplified sequence generated by phylogenic.org [15] showed that *M. alpina* CFR-GV15 was clustered with *Mortierella* sp. (Figure 8).

3.2. Effect of Temperature and Enhanced Production of Omega-3 Fatty Acids. The cultivation temperature is one of the most important environmental factors affecting the growth of microorganisms and causing changes in many biosynthetic pathways. In the present study, profuse growth of *M. alpina* CFR-GV15 was observed at a temperature ranging from 12°C to 28°C with enhanced lipid production (Table 4).

The cultivation temperature had a statistically significant difference and was selected based on temperature enhancing the omega-3 fatty acid production in the strain investigated. A significant difference ($P \leq 0.05$) in higher amount of total biomass 8.41 g/L, total lipid 38.43%, and ARA, EPA, and DHA 30.54%, 5.90%, 4.50%, respectively, obtained at 12°C, whereas significant increase of biomass (11.05 g/L), total lipid (42%), EPA (6.79%), and DHA (4.09%) were obtained first time at 20°C for 4 days and 12°C in 5 days. A study indicated that, at a lower temperature, the fungus produced more eicosapentaenoic acid [18, 19]. *M. alpina* 1S-4 produces EPA (approximately 10% of total fatty acids) below the growth temperature of 20°C through n-3 fatty acid pathway and direct ω -3 desaturation of AA [22]. The strain produced levels of EPA of more than 0.3 g/L at 12°C. The strain exhibits higher EPA production on the addition of α -linolenic acid (18:3n ω -3) containing oils, such as linseed oil, to the medium [23]. By using a Δ^{12} desaturase-defective mutant, Mut48, derived from *M. alpina* 1S-4, an EPA-rich oil with a low level of AA was obtained. Like the wild-type strain, Mut48 converted exogenous ALA to EPA [24]. The amount of EPA accumulated reached 1.88 g/L (66.6 mg/g dry mycelia) on cultivation of *M. alpina* 1S-4 with 3% linseed oil at 12°C [25] and, in another report, basal medium was 2.0% of soluble starch and 1.0% of linseed oil as carbon source at initial pH 6.0 and incubated at 20°C for 7 days [26], with the yield of EPA 3.56% and DHA 0.18%. This result can be attributed to the proposed adaptive role of PUFAs in membrane stabilization under stress conditions of low temperatures. PUFAs including ARA, EPA, and DHA may play a vital role in the regulation of membrane fluidity in this organism, thereby compensating for the decreased functionality of the biomembranes under cold stress conditions. The regulation of fatty acid saturation by desaturase enzymes is known as homeoviscous adaptation, wherein the organism adjusts the membrane fluidity to maintain the optimal function of biological membranes. Another possible explanation is that, at a lower temperature, more dissolved oxygen is available in the culture medium for desaturase enzymes that are oxygen dependent [27], thereby resulting in production of more unsaturated fatty acids.

3.3. Production and Enhancement of Fatty Acid Content of *M. alpina* CFR-GV15 at 7- and 9-Day Cultivation. The changes of fatty acid content of *M. alpina* CFR-GV15 in 7-day cultivation are shown in Figure 9. From days 1 to 11, in contrast, the

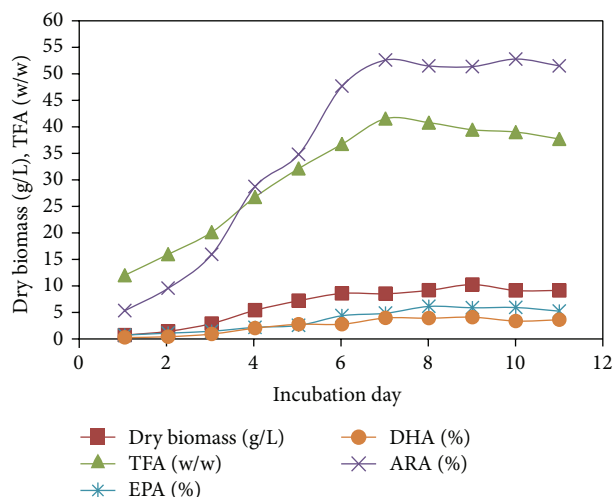


FIGURE 9: Growth curve of *M. alpina* CFR-GV15 in starch-yeast extract medium.

content of AA in cell dry weight increased from 5.2% to 53.25% from days 1 to 7. High contents of OA and AA further implicated that the starch and potassium nitrate (of which 25% is OA and 58% is AA) [28] were absorbed by *M. alpina* CFR-GV15 at the beginning of cultivation. In addition, the correlation coefficients between contents of C18:1 and AA suggest that there were enzymatic conversions of OA and LA to AA in the fungus *M. alpina* CFR-GV15 during fermentation. In the *M. alpina* PUFA enzymatic process, OA is first converted to LA by Δ^{12} desaturations, which is then converted to GLA (C18:3, n-6) by ω -6 desaturation. Two carbon atoms are then added to the GLA by ω -6 specific elongation to form DGLA (C20:3, n-6) which is ultimately converted to AA by ω -5 desaturation [8]. The PUFAs content of DGLA, AA, EPA, and DHA in cell dry weight, the significant differences ($P \leq 0.05$) increased from days 4 to 7 (from 2.75% to 3.78%, from 29% to 53%, from 2.4% to 4.7%, and from 1.84% to 3.8%, resp.). In the stress condition, 2% starch and 0.5% yeast extract and the temperature at 12°C 4 days and 20°C 5 day with the cold adaptation stress condition *M. alpina* CFR-GV15 and further activation of Δ^{17} desaturase converted DGLA to ETA and AA to EPA and further DHA accumulation (data not shown). Previous studies [29, 30] showed that arachidonic acid (Ara) fungi belonging to genus *Mortierella* accumulate EPA in their mycelia when grown in the usual media containing glucose as the major carbon source at low temperature of 6°C–20°C. This phenomenon is probably due to activation of methyl-end-directed desaturation Δ^{17} -desaturation of Ara, formed through n-6 fatty acid route, to EPA at low temperature [31]. Particularly at 20°C temperature, AA accumulations are stimulated in *Mortierella* [8]. In lower temperature of 5°C, a temperature-sensitive Δ^{17} desaturase is activated which catalyses the formation of eicosapentaenoic acid [20:5 (ω -3)] from 20:4 (ω -6) [32]. All significant PUFAs producers (LA, GLA, DGLA, AA, EPA, and DHA) are valuable fatty acids and are beneficial to human health, suggesting that the PUFA-rich oil produced by *M. alpina* CFR-GV15 would

have high potential in food and therapeutic application. Together with the amount of fatty acid unsaturation changes, these findings suggested that the fatty acid compositions were tightly regulated in the fungus during different phases of cultivation.

4. Conclusion

In conclusion, 37 strains and 11 selective native isolates of *Mortierella* sp. were isolated from soil of the Western Ghats of India and were shown to be a potential PUFA producer including a higher amount of AA producers. In the cultivation media, temperature had a statistically significant difference in biomass and omega-3 fatty acid production in the selective strain, and the significantly highest PUFA-containing strain in this study was identified as *M. alpina* CFR-GV15, which was also confirmed as a new strain of *Mortierella* through the ITS region. It is suitable for distinguishing *Mortierella* species identification and other closely related species for comparison. *M. alpina* CFR-GV15 produced the highest levels of biomass and lipid content at stationary phase (day 7 and day 9), whereas fatty acid contents were continuously changed during cultivation. This study would also contribute to the improvement and supplement of some additional nutrient for the PUFA production and add to our understanding of fatty acid metabolism in this fungus *M. alpina*. Nowadays, renewable sources of EPA from algae, yeast, fungi, and other microorganisms are available. Microorganism-based processes seem to be reliable and economically attractive source of omega-3 fatty acid especially EPA and DHA and can provide an efficient way for large-scale production.

Conflict of Interests

The authors declare that there is no conflict of interests regarding the publication of this paper.

Acknowledgments

The authors thank the Directors of CFTRI for their encouraging support. G. Vadivelan greatly acknowledges the grant of Research Fellowship by Indian Council of Medical Research, New Delhi, India. Mr. Shivasamy and Ms. Asha have been acknowledged for their technical assistance in GC.

References

- [1] C. M. Williams, "Dietary fatty acids and human health," *Annales de Zootechnie*, vol. 49, pp. 165–180, 2000.
- [2] N. V. Bhagavan, *Medical Biochemistry*, Jones and Bartlett Publishers International, London, UK, 2nd edition, 1978.
- [3] N. Merendino, L. Costantini, L. Manzi, R. Molinari, D. D'Eliseo, and F. Velotti, "Dietary ω -3 polyunsaturated fatty acid DHA: a potential adjuvant in the treatment of cancer," *BioMed Research International*, vol. 2013, Article ID 310186, 11 pages, 2013.
- [4] M. P. Freeman, "Omega-3 fatty acids in psychiatry: a review," *Annals of Clinical Psychiatry*, vol. 12, no. 3, pp. 159–165, 2000.

- [5] F. D. Gunstone, *Fatty Acid and Lipid Chemistry*, Blackie Academic, London, UK, 1996.
- [6] L. Sijtsma and M. E. de Swaaf, "Biotechnological production and applications of the ω -3 polyunsaturated fatty acid docosahexaenoic acid," *Applied Microbiology and Biotechnology*, vol. 64, no. 2, pp. 146–153, 2004.
- [7] H. Gerster, "Can adults adequately convert α -linolenic acid (18:3n-3) to eicosapentaenoic acid (20:5n-3) and docosahexaenoic acid (22:6n-3)?" *International Journal for Vitamin and Nutrition Research*, vol. 68, no. 3, pp. 159–173, 1998.
- [8] P. K. Bajpai, P. Bajpai, and O. P. Ward, "Production of arachidonic acid by *Mortierella alpina* ATCC 32222," *Journal of Industrial Microbiology*, vol. 8, no. 3, pp. 179–185, 1991.
- [9] S.-Y. Ho, Y. Jiang, and F. Chen, "PUFAs contents of the fungus *M. alpina* isolated from soil," *Journal of Agricultural and Food Chemistry*, vol. 55, no. 10, pp. 3960–3966, 2007.
- [10] M. Zhu, L. J. Yu, Z. Liu, and H. B. Xu, "Isolating *Mortierella alpina* strains of high yield of arachidonic acid," *Letters in Applied Microbiology*, vol. 39, no. 4, pp. 332–335, 2004.
- [11] A. Nisha, S. P. Muthukumar, and G. Venkateswaran, "Safety evaluation of arachidonic acid rich *Mortierella alpina* biomass in albino rats-a subchronic study," *Regulatory Toxicology and Pharmacology*, vol. 53, no. 3, pp. 186–194, 2009.
- [12] A. Nisha and G. Venkateswaran, "Effect of culture variables on mycelial arachidonic acid production by *Mortierella alpina*," *Food and Bioprocess Technology*, vol. 4, no. 2, pp. 232–240, 2011.
- [13] L. V. Michaelson, C. M. Lazarus, G. Griffiths, J. A. Napier, and A. K. Stobart, "Isolation of a Δ 5-fatty acid desaturase gene from *Mortierella alpina*," *Journal of Biological Chemistry*, vol. 273, no. 30, pp. 19055–19059, 1998.
- [14] T. J. White, T. Bruns, S. Lee, and J. Taylor, "Amplification and direct sequencing of fungal ribosomal RNA genes for phylogenetics," in *PCR Protocols: A Guide to Methods and Applications*, M. A. Innis, D. H. Gelfand, J. J. Sninsky, and T. J. White, Eds., pp. 315–322, Academic Press, San Diego, Calif, USA, 1990.
- [15] A. Dereeper, V. Guignon, G. Blanc et al., "Phylogeny.fr: robust phylogenetic analysis for the non-specialist," *Nucleic Acids Research*, vol. 36, pp. W465–W469, 2008.
- [16] K. H. Domsch, W. Gams, and T. H. Anderson, *Compendium of Soil Fungi*, vol. 1, Academic Press, London, UK, 1980.
- [17] C. J. Gilman, *Manual Soil Fungi*, Biotech Books, Delhi, India, 1998.
- [18] W. Gams, "A key to the species of *Mortierella*," *Persoonia*, vol. 9, pp. 381–391, 1977.
- [19] K. Higashiyama, S. Fujikawa, E. Y. Park, and S. Shimizu, "Production of arachidonic acid by *Mortierella* fungi," *Biotechnology and Bioprocess Engineering*, vol. 7, pp. 252–262, 2002.
- [20] J. P. Palta, J. Levitt, and E. J. Stadelmann, "Plant viability assay," *Cryobiology*, vol. 15, pp. 249–255, 1978.
- [21] D. A. Musser and A. R. Oseroff, "The use of tetrazolium salts to determine sites of damage to the mitochondrial electron transport chain in intact cells following in vitro photodynamic therapy with photofrin II," *Photochemistry and Photobiology*, vol. 59, no. 6, pp. 621–626, 1994.
- [22] H. C. Chen, C. C. Chang, and C. X. Chen, "Optimization of Arachidonic acid production by *Mortierella alpina* Wji-H4 Isolate," *Journal of the American Oil Chemists' Society*, vol. 74, pp. 569–578, 1997.
- [23] H.-D. Jang, Y.-Y. Lin, and S.-S. Yang, "Effect of culture media and conditions on polyunsaturated fatty acids production by *Mortierella alpina*," *Bioresource Technology*, vol. 96, no. 15, pp. 1633–1644, 2005.
- [24] J. Ogawa, E. Sakuradan, S. Kishino, K. Yokozeki, and S. Shimizu, "Polyunsaturated fatty Acids production and transformation by *Mortierella alpina* and anaerobic bacteria," *European Journal of Lipid Science and Technology*, vol. 114, pp. 1107–1113, 2012.
- [25] S. Shimizu, H. Kawashima, K. Akimoto, Y. Shinmen, and H. Yamada, "Conversion of linseed oil to an eicosapentaenoic acid-containing oil by *Mortierella alpina* 1S-4 at low temperature," *Applied Microbiology and Biotechnology*, vol. 32, no. 1, pp. 1–4, 1989.
- [26] S. Jareonkitmongkol, S. Shimizu, and H. Yamada, "Production of an eicosapentaenoic acid-containing oil by a Δ 12 desaturase-defective mutant of *Mortierella alpina* 1S-4," *Journal of the American Oil Chemists' Society*, vol. 70, no. 2, pp. 119–123, 1993.
- [27] Z. Cohen, A. Vonshak, and A. Richmond, "Fatty acid composition of *Spirulina* strains grown under various environmental conditions," *Phytochemistry*, vol. 26, no. 8, pp. 2255–2258, 1987.
- [28] S. M. Innis, "Essential fatty acids in growth and development," *Progress in Lipid Research*, vol. 30, no. 1, pp. 39–103, 1991.
- [29] S. Shimizu, Y. Shinmen, H. Kawashima, K. Akimoto, and H. Yamada, "Fungal mycelia as a novel source of eicosapentaenoic acid: activation of enzymes) involved in Eicosapentaenoic acid production at low temperature," *Biochemical and Biophysical Research Communications*, vol. 150, pp. 335–341, 1988.
- [30] S. Shimizu, Y. Shinmen, H. Kawashima, K. Akimoto, and H. Yamada, "production of eicosapentaenoic acid by *Mortierella* fungi," *Journal of the American Oil Chemists' Society*, vol. 65, pp. 1455–1459, 1998.
- [31] S. Shimizu, H. Kawashima, K. Akimoto, Y. Shinmen, and H. Yamada, "Conversion of linseed oil to an eicosapentaenoic acid-containing oil by *Mortierella alpina* 1S-4 at low temperature," *Applied Microbiology and Biotechnology*, vol. 32, no. 1, pp. 1–4, 1989.
- [32] A. Botha, I. Paul, C. Roux et al., "An isolation procedure for arachidonic acid producing *Mortierella* species," *Antonie van Leeuwenhoek*, vol. 75, no. 3, pp. 253–256, 1999.

Research Article

Potent Protein Glycation Inhibition of Plantagoside in *Plantago major* Seeds

Nobuyasu Matsuura,¹ Tadashi Aradate,² Chihiro Kurosaka,³
Makoto Ubukata,⁴ Shiho Kittaka,¹ Yuri Nakaminami,¹ Kanae Gamo,^{1,5}
Hiroyuki Kojima,⁶ and Mitsuharu Ohara⁶

¹ Department of Life Science, Faculty of Science, Okayama University of Science, 1-1 Ridai-cho, Kita-ku, Okayama 700-0005, Japan

² University of Toyama, 2630 Sugitani, Toyama 930-0194, Japan

³ Biotechnology Research Center, Toyama Prefectural University, 5180 Kurokawa, Kosugi-machi, Imizu-gun, Toyama 939-0398, Japan

⁴ Graduate School of Agriculture, Hokkaido University, Kita-9, Nishi-9, Kita-ku, Sapporo 060-8589, Japan

⁵ Department of Pharmaceutical Science, Graduate School of Medicine, Dentistry and Pharmaceutical Sciences, Okayama University, 1-1-1 Tsushima-naka, Kita-ku, Okayama 700-8530, Japan

⁶ Ichimaru Pharcos Co., Ltd., 318-1 Asagi, Motosu-shi, Gifu 501-0475, Japan

Correspondence should be addressed to Nobuyasu Matsuura; nobuyasu@dls.ous.ac.jp

Received 21 February 2014; Accepted 25 April 2014; Published 7 May 2014

Academic Editor: José Carlos Tavares Carvalho

Copyright © 2014 Nobuyasu Matsuura et al. This is an open access article distributed under the Creative Commons Attribution License, which permits unrestricted use, distribution, and reproduction in any medium, provided the original work is properly cited.

Plantagoside (5,7,4',5'-tetrahydroxyflavanone-3'-O-glucoside) and its aglycone (5,7,3',4',5'-pentahydroxyflavanone), isolated from a 50% ethanol extract of *Plantago major* seeds (Plantaginaceae), were established to be potent inhibitors of the Maillard reaction. These compounds also inhibited the formation of advanced glycation end products in proteins in physiological conditions and inhibited protein cross-linking glycation. These results indicate that *P. major* seeds have potential therapeutic applications in the prevention of diabetic complications.

1. Introduction

Nonenzymatic protein glycation in the body leads to vascular and renal complications of diabetes [1]. Diabetic patients tend to accumulate glycated proteins in their body tissues because their blood glucose concentration is higher than that in healthy individuals. The initial chemical modification step is the reaction between the free amino group of proteins and carbonyl group of glucose, which leads to the formation of fructosamines via Schiff bases, followed by the Amadori rearrangement. The fructosamines are successively oxidized, dehydrated, and condensed to form cross-linked proteins and eventually advanced glycation end products (AGEs). Some AGEs have been isolated, and their structures have been elucidated (e.g., pyrraline [2], N^ε-(carboxymethyl)lysine [3], pentosidine [4], 2-(2-furoyl)-4(5)-(2-furanyl)-1H-imidazole [5], and crossline [6]).

Various attempts have been made to identify effective glycation inhibitors. Aminoguanidine has the capacity to prevent the diabetes-induced formation of AGEs, including the inhibition of protein cross-linking [7]. Aspirin [8] as well as vitamin B₆ [9], taurine [10], quercetin [11], and other natural inhibitors have also been reported. To identify effective glycation inhibitors, we devised an improved screening system, which was reported in a previous study [12]. In the present report, we describe the screening results and the differences in the inhibitory mechanisms of plantagoside and aminoguanidine.

2. Materials and Methods

2.1. Materials. *Plantago major* seeds were purchased from Ichimaru Pharcos Co., Ltd. (Gifu Japan). Plantagoside

(5,7,4',5'-tetrahydroxyflavanone-3'-*O*-glucoside) (**1**) and its aglycone (5,7,3',4',5'-pentahydroxyflavanone) (**2**) were isolated from a 50% ethanol extract of *P. major* seeds (Plantaginaceae). 5,7-Dihydroxy-3',4',5'-trimethoxyflavone (**3**), myricetin (5,7,3',4',5'-pentahydroxyflavonol) (**6**), and dihydromyricetin (5,7,3',4',5'-pentahydroxyflavanonol) (**7**) were purchased from Funakoshi Co., Ltd. (Japan). Aminoguanidine hydrochloride, N- α -acetyl-lysine, and N- α -acetyl-arginine were purchased from Sigma-Aldrich (USA). Cell-matrix type I-C collagen was purchased from Asahi Techno Glass (Japan). All the other chemicals were purchased from Nakarai Tesque, Inc. (Japan).

2.2. Evaluation of Glycation

2.2.1. Fluorometric Analysis. Our improved Maillard reaction inhibitor screening system was used for bioassay-guided fractionation and for isolating active compounds in the present study [12]. In brief, a reaction mixture (500 μ L) was prepared in a plastic tube (1.5 mL) that comprised bovine serum albumin (BSA) (400 μ g) and glucose (200 mM), with/without an inhibitor or plant extract (10 μ L), in 50 mM phosphate buffer, pH 7.4. The reaction mixture was heated at 60°C on a heating block for 30 h. The blank sample and the unreacted solution without an inhibitor or plant extract were maintained at 4°C until measurement. After cooling, an aliquot (100 μ L) was transferred to a new plastic tube (1.5 mL), and 100% w/v trichloroacetic acid (TCA) (10 μ L) was added to each tube. The supernatant containing glucose, inhibitor, and interfering substances was discarded after agitation and centrifugation (15,000 rpm, 4°C, 4 min). The precipitate containing AGEs-BSA was then dissolved in alkaline PBS (400 μ L). Alkaline PBS contained NaCl (137 mM), Na₂HPO₄ (8.1 mM), KCl (2.68 mM), and KH₂PO₄ (1.47 mM) and was adjusted to pH 10 with 0.25 N NaOH. The fluorescence intensity (ex. 360 nm, em. 460 nm) related to AGEs-protein was measured using a Cytofluor II fluorescence multiwell plate reader (PersSeptive Biosystems, USA). The true inhibition activity was estimated by subtracting the quenching effect from the apparent inhibitory activity. The apparent inhibitory activity was calculated using the method described above. The quenching effect was measured using the same sample dissolved in alkaline PBS after TCA treatment of the mixed plant extract solution (2 and 100 μ L) after incubating the control solution for 30 h without the inhibitor or plant extract. The Maillard reaction was performed for 96 h without TCA precipitation using N- α -acetyl-lysine or N- α -acetyl-arginine instead of BSA as the substrate.

2.2.2. Protein Cross-Linking. The reaction mixtures (1 mL each), containing lysozyme (5.0 mg) and ribose (20 mM), were prepared in phosphate buffer (100 mM, pH 7.4). Each reaction mixture was sterile filtered into a plastic tube and placed in an incubator at 37°C for 1 week. Sodium dodecyl sulfate polyacrylamide gel electrophoresis (SDS-PAGE) was performed according to the method described by Laemmli [13]. Aliquots (10 μ L each) of the reaction mixtures were heated at 95°C with a buffer (2 μ L) containing 4% SDS,

10% β -mercaptomethanol, 20% glycerol, 0.2 M glycine, and 1% methylene blue in 0.5 M Tris buffer (pH 6.7). After electrophoresis, the gel was stained with Coomassie Brilliant Blue (CBB), destained, and dried.

2.3. Purification and Structural Determination of Plantagoside and 5,7,3',4',5'-Pentahydroxyflavanone. *P. major* seeds (213 g) were extracted with 50% ethanol (2.2 L) for 1 week at room temperature. A crude extract (7.6 g) was obtained by concentration *in vacuo* and was suspended in H₂O (1 L) before the solution was extracted with chloroform (1 L). The aqueous layer was further extracted with ethylacetate (2 L). The resulting extracts were concentrated to produce a crude oil (0.64 g), which was subjected to reversed-phase high-performance liquid chromatography (HPLC). The HPLC conditions were as follows: flow rate: 4.6 mL/min; detector: UV 210 nm; solvent: methanol:H₂O (30:70); column oven temperature: 40°C; and column: Mightysil RP-18, 10 \times 250 mm. Two active fractions (fractions 1 and 2) were obtained. Further purification of the active fractions using HPLC yielded plantagoside (**1**) (148 mg) and 5,7,3',4',5'-pentahydroxyflavanone (**2**) (23 mg).

Plantagoside (**1**): negative-ion FAB-MS *m/z*: 465 [M-H]⁺; ¹H-NMR (400 MHz, DMSO-*d*₆ + D₂O) δ : 2.70 (1H, dd, *J* = 17 and 3 Hz, H-3), 3.07 (1H, dd, *J* = 17 and 12 Hz, H-3), 4.64 (1H, d, *J* = 8 Hz, H-1 of glucose), 5.32 (1H, dd, *J* = 12 and 3 Hz, H-2), 5.81 (1H, d, *J* = 2 Hz, H-6), 5.82 (1H, d, *J* = 2 Hz, H-8), 6.56 (1H, d, *J* = 2 Hz, H-6'), 6.70 (1H, d, *J* = 2 Hz, H-2'); ¹³C-NMR (100 MHz, DMSO-*d*₆ + D₂O) δ : 41.9 (C-3), 60.7 (glc-6), 69.8 (glc-4), 73.3 (glc-2), 75.9 (glc-5), 77.1 (glc-3), 78.4 (C-2), 95.0 (C-8), 95.8 (C-6), 101.7 (C-10), 102.4 (glc-1), 106.4 (C-6'), 109.2 (C-2'), 128.6 (C-1'), 135.2 (C-4'), 145.7 (C-3'), 145.8 (C-5'), 162.8 (C-9), 163.4 (C-5), 166.7 (C-7), 196.1 (C-4).

5,7,3',4',5'-Pentahydroxyflavanone (**2**): negative-ion FAB-MS *m/z*: 303 [M-H]⁺; ¹H-NMR (400 MHz, DMSO-*d*₆) δ : 2.70 (1H, dd, *J* = 17 and 3 Hz, H-3), 3.07 (1H, dd, *J* = 17 and 12 Hz, H-3), 5.32 (1H, dd, *J* = 12 and 3 Hz, H-2), 5.81 (1H, d, *J* = 2 Hz, H-6), 5.82 (1H, d, *J* = 2 Hz, H-8), 6.56 (2H, s, H-2' and 6').

2.4. Synthesis of 5,7,3',4',5'-Pentahydroxyflavone (4**).** 5,7-Dihydroxy-3',4',5'-trimethoxyflavone (**3**; 15 mg) was added to AlCl₃ (8 g) and NaCl (1.4 g) and melted by heating at 180°C. After 10 min, the reaction mixture was cooled and dissolved in 2 N HCl, and **3** (2 mg) was extracted with ethylacetate. ¹H-NMR (400 MHz, acetone-*d*₆) δ : 6.20 (1H, s, H-3), 6.46 (2H, brs, H-6, 8), 7.10 (2H, s, H-2', 6'), 12.98 (1H, brs, C₅-OH).

3. Results and Discussion

We examined 200 natural plant extracts to determine their inhibitory effects on the Maillard reaction and obtained satisfactory results with an extract of *P. major* seeds. The active compounds were characterized as plantagoside (**1**) and its aglycone (**2**) after analyzing the FAB-MS, ¹H-NMR, and ¹³C-NMR spectral data (Figure 1). Flavanones **1** and **2** were first isolated from *P. asiatica* var. *japonica* [14] and *Helichrysum*

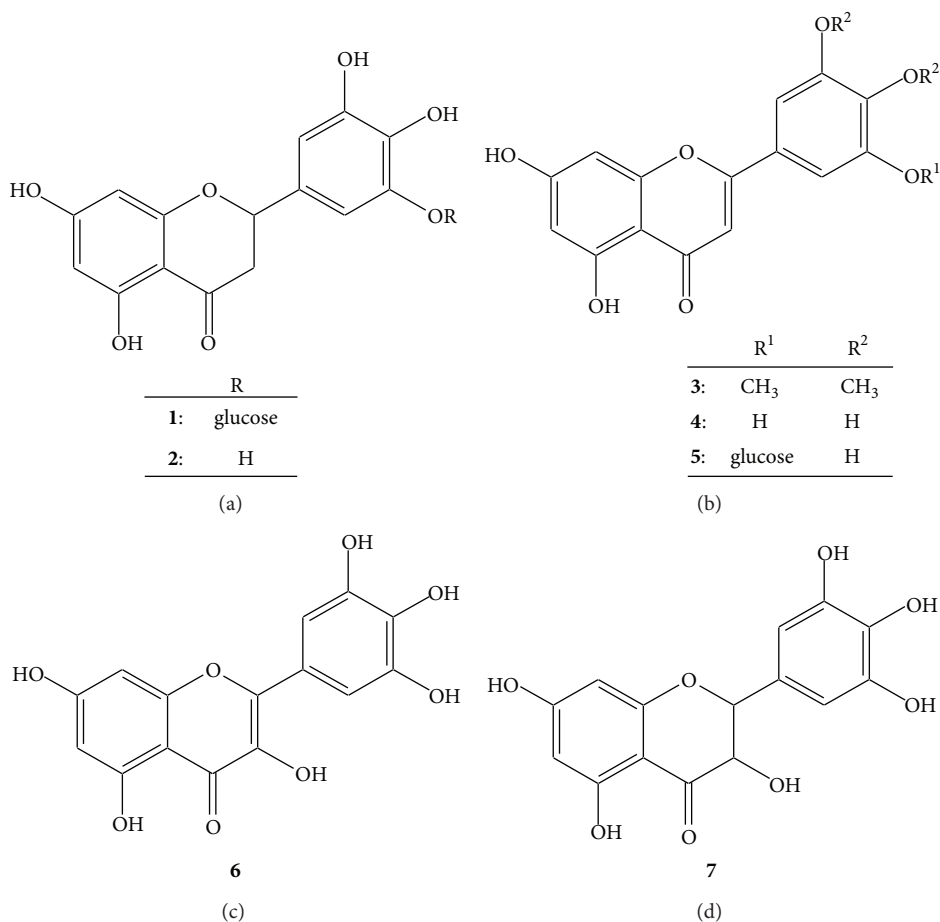


FIGURE 1: The structures of the flavonoids that inhibited glycation. **1**: Plantagoside (R = glucose), **2**: 5,7,3',4',5'-pentahydroxyflavanone (R = H), **3**: 5,7-dihydroxy-3',4',5'-trimethoxyflavone (R¹ = R² = CH₃), **4**: 5,7,3',4',5'-pentahydroxyflavone (R¹ = R² = H), **5**: 5,7,4',5'-tetrahydroxyflavone-3'-O-glucoside (R¹ = glucose, R² = H), **6**: myricetin, and **7**: dihydromyricetin.

bracteatum [15]. α -Mannosidase inhibitory activity has also been reported for **1** [16]. The Maillard reaction inhibitory activities of **1** (IC₅₀, 1.2 μ M) and **2** (IC₅₀, 18.0 μ M) were approximately 83- and 5.5-times stronger, respectively, than that of aminoguanidine (IC₅₀, 100 μ M), which was used as a known Maillard reaction inhibitor [17] in our established assay system [12]. It has been reported that some natural flavonoids, that is, baicalin, baicalein [17], quercetin [11], and maritimein [18], inhibit the Maillard reaction, and these compounds also showed inhibitory activities when our assay system was used (baicalin (IC₅₀, 25.0 μ M), baicalein (IC₅₀ > 100 μ M), quercetin (IC₅₀, 1.4 μ M), and maritimein (IC₅₀, 10.0 μ M)). These results indicated that **1** had the highest inhibitory activity among the known isolated natural products.

To clarify the inhibitory activities of **1** and **2** in physiological conditions, collagen, one of the major proteins in the human body, was used as a substrate instead of BSA. The incubation temperature was changed to 37°C from 60°C. The inhibitory activities (IC₅₀) were 14 μ M for **1**, 42 μ M for **2**, and 2500 μ M for aminoguanidine. The inhibitory activity of each compound was 2–25-times lower than that obtained using the original conditions. When BSA was used as the substrate

and the reaction temperature was high, the rank order of the inhibitory activity of each compound remained unchanged. These results demonstrated that our improved Maillard reaction inhibitor screening method is very useful for bioassay-guided isolation of effective compounds and evaluation of the inhibitory activities of such compounds. Plantagoside was identified using this assay, and it was found to inhibit the formation of AGEs in physiological conditions at a lower concentration.

For evaluating the inhibitory activity of plantagoside against glycation-dependent cross-link formation, each inhibitor, that is, plantagoside and aminoguanidine, which inhibit cross-link formation by linking with the carbonyl groups of Amadori products [7], or NaCNBH₃, which inhibits by reducing Amadori products to a secondary amine [19], was incubated at 37°C with lysozyme and ribose in phosphate buffer. Figure 2 presents the effects of plantagoside against glycation-dependent cross-link formation. A dimer of lysozyme (ca. 29 kDa) was clearly observed after 1 week (lane 1). It was found that 100 mM aminoguanidine (lane 2) and 100 mM NaCNBH₃ (lane 3) inhibited the dimerization of lysozyme, while 12.5–200 μ M plantagoside also caused

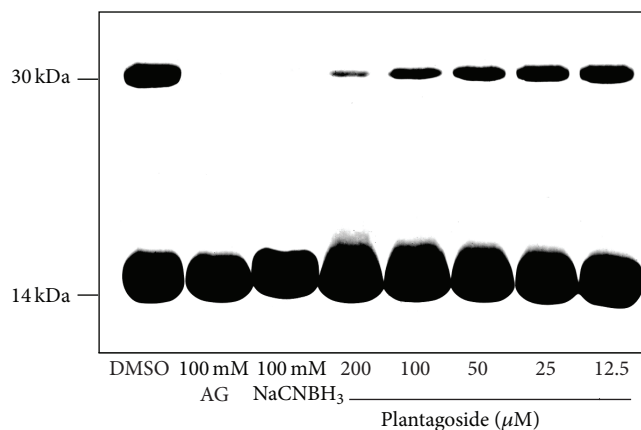


FIGURE 2: Inhibition of cross-link formation by plantagoside (1). This assay was performed at pH 7.4 in phosphate buffer, which contained 20 mM ribose, 5 mg/mL lysozyme, 100 mM of aminoguanidine or NaCNBH₃, or the indicated concentration of plantagoside dissolved in dimethylsulfoxide, for 1 week at 37°C. Each sample was then subjected to 17.5% SDS-PAGE and stained with Coomassie Brilliant Blue. DMSO: dimethylsulfoxide containing no inhibitor; AG: aminoguanidine.

inhibition in a concentration-dependent manner (lanes 4–8). The results showed that plantagoside can inhibit the formation of protein-protein cross-links via glycation and the formation of AGEs in proteins.

To investigate the change in the inhibitory activity due to the formation of AGEs by plantagoside with different types of amino acids as the substrate, we performed assays using either N- α -acetyllysine or N- α -acetylarginine. Plantagoside with N- α -acetyllysine and N- α -acetylarginine as the substrate possessed 46% and 73% inhibitory activities, respectively, (Δ , 27%) at a concentration of 25 μ M and strongly inhibited the formation of AGEs with N- α -acetylarginine (Figure 3). In contrast, aminoguanidine possessed 91% and 80% of the inhibitory activities (Δ , 11%) at a concentration of 10 μ M, while there was no major selectivity of the inhibitory activity. These results indicate that the inhibitory mechanism employed by plantagoside differed from that employed by aminoguanidine.

To develop a more effective inhibitor, we investigated the relationship between the skeletal structures of the aglycones of plantagoside (flavone, 4; flavonol, 6; flavanone, 2; and flavanonol, 7; Figure 1) and their inhibitory activity. The results showed that the order of the inhibitory activity of the compounds (highest first) was 5,7,3',4',5'-pentahydroxyflavone, 4 (7.5 μ M); myricetin, 6 (7.9 μ M); 5,7,3',4',5'-pentahydroxyflavanone, 2 (18.0 μ M); and dihydromyricetin, 7 (45.0 μ M); 5,7,3',4',5'-pentahydroxyflavone possessed the highest activity among the aglycones. The results suggested that the putative compound 5,7,4',5'-tetrahydroxyflavone-3'-O-glucoside (5) would possess a potent inhibitory activity at a submicromolar concentration, given that the inhibitory activity was 15-times higher after 3'-O-glycosylation of 5,7,3',4',5'-pentahydroxyflavanone (2). Therefore, we intend to synthesize 5, which has not been obtained from natural resources.

In this study, we demonstrated the inhibitory activity of plantagoside and its aglycone against the Maillard reaction.

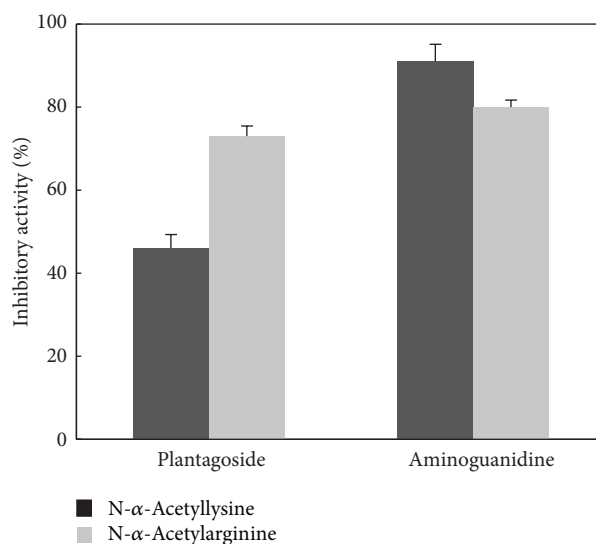


FIGURE 3: Differences in AGE formation inhibitory activity with different types of amino acids as the substrate. The inhibitory activities were determined at concentrations of 25 μ M plantagoside and 10 mM aminoguanidine using N- α -acetyllysine or N- α -acetylarginine as the substrate for glycation. The inhibitory activity was examined by measuring the increase in the fluorescence intensity because of the formation of AGEs. Each value represents the mean \pm standard error of three experiments.

In Europe and the USA, the *P. major* seeds that contain these flavanones are known as “Shazenshi,” which is a well-known crude drug. The seed of *P. asiatica* is used as a diuretic in traditional Chinese medicine. There are no reports on the treatment or prevention of diabetic complications using this drug; however, the present study suggests that Shazenshi has potential as a therapeutic agent to combat diabetic complications.

Abbreviations

BSA:	Bovine serum albumin
dd:	Double doublet
DMSO:	Dimethylsulfoxide
FAB-MS:	Fast atom bombardment mass spectrum
glc:	Glucose
PBS:	Phosphate-buffered saline
SDS-PAGE:	Sodium dodecyl sulfate polyacrylamide gel electrophoresis.

Conflict of Interests

The authors declare that there is no conflict of interests regarding the publication of this paper.

Acknowledgment

This work was supported by a matched fund subsidy for private universities from the Ministry of Education, Culture, Sports, Science and Technology (MEXT).

References

- [1] M. Brownlee, A. Cerami, and H. Vlassara, "Advanced glycosylation end products in tissue and the biochemical basis of diabetic complications," *The New England Journal of Medicine*, vol. 318, no. 20, pp. 1315–1321, 1988.
- [2] F. Hayase, R. H. Nagaraj, S. Miyata, F. G. Njoroge, and V. M. Monnier, "Aging of proteins: immunological detection of a glucose-derived pyrrole formed during Maillard reaction in vivo," *Journal of Biological Chemistry*, vol. 264, no. 7, pp. 3758–3764, 1989.
- [3] M. U. Ahmed, S. R. Thorpe, and J. W. Baynes, "Identification of N(ϵ)-carboxymethyllysine as a degradation product of fructoselysine in glycated protein," *Journal of Biological Chemistry*, vol. 261, no. 11, pp. 4889–4894, 1986.
- [4] D. G. Dyer, J. A. Blackledge, S. R. Thorpe, and J. W. Baynes, "Formation of pentosidine during nonenzymatic browning of proteins by glucose: Identification of glucose and other carbohydrates as possible precursors of pentosidine in vivo," *Journal of Biological Chemistry*, vol. 266, no. 18, pp. 11654–11660, 1991.
- [5] V. M. Monnier, R. R. Kohn, and A. Cerami, "Accelerated age-related browning of human collagen in diabetes mellitus," *Proceedings of the National Academy of Sciences of the United States of America*, vol. 81, no. 2 I, pp. 583–587, 1984.
- [6] H. Obayashi, K. Nakano, H. Shigeta et al., "Formation of cross-line as a fluorescent advanced glycation end product in vitro and in vivo," *Biochemical and Biophysical Research Communications*, vol. 226, no. 1, pp. 37–41, 1996.
- [7] M. Brownlee, H. Vlassara, and A. Kooney, "Aminoguanidine prevents diabetes-induced arterial wall protein cross-linking," *Science*, vol. 232, no. 4758, pp. 1629–1632, 1986.
- [8] R. Huby and J. J. Harding, "Non-enzymic glycosylation (glycation) of lens proteins by galactose and protection by aspirin and reduced glutathione," *Experimental Eye Research*, vol. 47, no. 1, pp. 53–59, 1988.
- [9] A. A. Booth, R. G. Khalifah, and B. G. Hudson, "Thiamine pyrophosphate and pyridoxamine inhibit the formation of antigenic advanced glycation end-products: comparison with aminoguanidine 1," *Biochemical and Biophysical Research Communications*, vol. 220, no. 1, pp. 113–119, 1996.
- [10] J. I. Malone, S. Lowitt, and W. R. Cook, "Nonosmotic diabetic cataracts," *Pediatric Research*, vol. 27, no. 3, pp. 293–296, 1990.
- [11] Y. Morimitsu, K. Yoshida, S. Esaki, and A. Hirota, "Protein glycation inhibitors from thyme (*Thymus vulgaris*)," *Bioscience, Biotechnology and Biochemistry*, vol. 59, no. 11, pp. 2018–2021, 1995.
- [12] N. Matsuura, T. Aradate, C. Sasaki et al., "Screening system for the Maillard reaction inhibitor from natural product extracts," *Journal of Health Science*, vol. 48, no. 6, pp. 520–526, 2002.
- [13] U. K. Laemmli, "Cleavage of structural proteins during the assembly of the head of bacteriophage T4," *Nature*, vol. 227, no. 5259, pp. 680–685, 1970.
- [14] T. Endo, H. Taguchi, and I. Yosioka, "The Glycosides of *Plantago major* var. *japonica* NAKAI. A New Flavanone Glycoside, Plantagoside," *Chemical & Pharmaceutical Bulletin*, vol. 29, pp. 1000–1004, 1981.
- [15] G. Forkmann, "5,7,3',4',5'-pentahydroxyflavanone in the bracts of *Helichrysum bracteatum*," *Zeitschrift für Naturforschung*, vol. 38, pp. 891–893, 1983.
- [16] H. Yamada, T. Nagai, N. Takemoto et al., "Plantagoside, a novel α -mannosidase inhibitor isolated from the seeds of *Plantago asiatica*, suppresses immune response," *Biochemical and Biophysical Research Communications*, vol. 165, no. 3, pp. 1292–1298, 1989.
- [17] M. Ohara, H. Kojima, and N. Matsuura, "Maillard reaction products-degrading preparations containing rosmarinic acid, epigallocatechin, etc.," *Japanese Kokai Tokkyo Koho*, JP2007210956, 2007.
- [18] H. Takahashi, K. Kimura, M. Yoshihama, K. Shinoda, S. Negeishi, and K. Seri, "Maillard reaction inhibitors containing aurone derivatives," *Japanese Kokai Tokkyo Koho*, JP09241165, 1997.
- [19] N. Jentoft and D. G. Dearborn, "Labeling of proteins by reductive methylation using sodium cyanoborohydride," *Journal of Biological Chemistry*, vol. 254, no. 11, pp. 4359–4365, 1979.

Research Article

Watermelon (*Citrullus lanatus* (Thunb.) Matsum. and Nakai) Juice Modulates Oxidative Damage Induced by Low Dose X-Ray in Mice

Mohd Khairul Amran Mohammad,¹ Muhamad Idham Mohamed,¹
Ainul Mardiyah Zakaria,¹ Hairil Rashmizal Abdul Razak,² and Wan Mazlina Md. Saad¹

¹ Department of Medical Laboratory Technology, Faculty of Health Sciences, Universiti Teknologi MARA, UiTM Puncak Alam, 42300 Bandar Puncak Alam, Selangor, Malaysia

² Department of Medical Imaging, Faculty of Health Sciences, Universiti Teknologi MARA, UiTM Puncak Alam, 42300 Bandar Puncak Alam, Selangor, Selangor, Malaysia

Correspondence should be addressed to Wan Mazlina Md. Saad; wanzmaz755@salam.uitm.edu.my

Received 20 February 2014; Revised 8 April 2014; Accepted 8 April 2014; Published 29 April 2014

Academic Editor: José Carlos Tavares Carvalho

Copyright © 2014 Mohd Khairul Amran Mohammad et al. This is an open access article distributed under the Creative Commons Attribution License, which permits unrestricted use, distribution, and reproduction in any medium, provided the original work is properly cited.

Watermelon is a natural product that contains high level of antioxidants and may prevent oxidative damage in tissues due to free radical generation following an exposure to ionizing radiation. The present study aimed to investigate the radioprotective effects of watermelon (*Citrullus lanatus* (Thunb.) Matsum. and Nakai) juice against oxidative damage induced by low dose X-ray exposure in mice. Twelve adult male ICR mice were randomly divided into two groups consisting of radiation (Rx) and supplementation (Tx) groups. Rx received filtered tap water, while Tx was supplemented with 50% (v/v) watermelon juice for 28 days *ad libitum* prior to total body irradiation by 100 μ Gy X-ray on day 29. Brain, lung, and liver tissues were assessed for the levels of malondialdehyde (MDA), apurinic/aprimidinic (AP) sites, glutathione (GSH), and superoxide dismutase (SOD) inhibition activities. Results showed significant reduction of MDA levels and AP sites formation of Tx compared to Rx ($P < 0.05$). Mice supplemented with 50% watermelon juice restore the intracellular antioxidant activities by significantly increased SOD inhibition activities and GSH levels compared to Rx. These findings may postulate that supplementation of 50% watermelon (*Citrullus lanatus* (Thunb.) Matsum. and Nakai) juice could modulate oxidative damage induced by low dose X-ray exposure.

1. Introduction

A variety of highly reactive chemical entities known as reactive oxygen species (ROS) are produced by respiring cells as a small amount of the consumed oxygen is reduced [1]. ROS has dual roles, in which it can be beneficial and/or deleterious [2]. In normal biological system, the cellular functions depend on redox balance which may be defined as reduction and oxidation of prooxidants and antioxidants [2, 3]. Any distortion in the redox balance may promote oxidative stress and lead to a series of pathological condition [4].

X-ray has been clinically used as diagnostic and therapeutic tools [5]. Despite its usefulness, X-ray may also induce

direct or indirect harmful effects on cellular constituents and deoxyribonucleic acid (DNA) [6, 7]. X-ray has a high penetrating power due to its low linear energy transfer (LET) and exposure to X-ray could result in generation of free radicals through radiolysis process [8]. When these free radicals interact with biological molecules, it may cause cellular lipid peroxidation and DNA damage [9].

Lipid peroxidation can be defined as the oxidative deterioration of lipids containing carbon-carbon double bonds that yield a large number of toxic byproducts [10]. Membrane lipids are highly susceptible to free radical damage [11]. The highly damaging chain reaction occurs as the lipids react with free radicals and this can lead to a production of various end products including malondialdehyde (MDA), the main

carbonyl compound [11, 12]. Free radicals especially hydroxyl radicals react with DNA molecules through several mechanisms producing a broad spectrum of structural damage [13, 14]. These structural DNA damages include oxidative base modification, single strand break (SSB), double strand break (DSB), cross-links, clustered base damage, and mismatch repair (MMR) that may affect the cell's ability to transcribe the genes which are encoded by affected DNA [13].

An antioxidant is known as a molecule that acts as free radical scavenger and protects the body from oxidative damage [15]. A study by Srinivasan et al. [16] reveals that an antioxidant defense mechanism is applied to maintain redox balance, and appropriate antioxidants may reduce the free radical toxicity and protect from radiation damage [17]. Defense mechanism such as superoxide dismutase (SOD) is responsible for catalyzing the dismutation of the superoxide anion (O_2^-) into oxygen and hydrogen peroxide (H_2O_2) [18], while glutathione (GSH) provides protection against oxidative damage by participating in the cellular defense system and its intracellular level may be assessed as an indicator of oxidative stress [19].

The dietary guidelines recommended by A. V. Rao and L. G. Rao [20] suggest to increase the consumption of plant-based food that are rich in carotenoids, a bright coloured microcomponent, which is present in fruits and vegetables. Watermelon (*Citrullus lanatus*) contains a high level of carotenoids such as lycopene, beta-cryptoxanthin, beta-carotene, and vitamin E and it is proven to scavenge free radicals [21]. *Citrullus lanatus* (Thunb.) Matsum. and Nakai is the most polymorphic among all *Citrullus* species which has wild, cultivated, and feral forms [22]. Altaş et al. [23] demonstrate that the nature of chemicals present in watermelon is responsible for the reduction of lipid peroxidation.

Thus, the aim of this study was to evaluate the antioxidant capacity of watermelon juice and its protective effect on low dose X-ray-induced oxidative damage in mice model.

2. Materials and Methods

2.1. Chemicals. Oxiselect Total Glutathione Assay Kit, Oxiselect TBARS Assay Kit (MDA Quantification), Oxiselect Superoxide Dismutase Activity Assay, and Oxiselect Oxidative DNA Damage (AP Sites) were purchased from Cell Biolab, Inc. (San Diego, CA), while Invisorb Spin Tissue Mini Kit was purchased from Stratec Molecular (Berlin, Germany).

2.2. A 50% (v/v) Watermelon Juice Preparation. A locally harvested, red seedless, watermelon juice was freshly prepared on a daily basis. The watermelon was cleaned with filtered tap water and peeled to obtain the red flesh. The flesh was then processed with a commercial juice maker which automatically separated the pulp and the juice. A 50% concentration was prepared by diluting a pure watermelon juice with filtered tap water in the ratio of 1:1 (v/v).

2.3. Animal Handling and Study Design. All animal studies were conducted in accordance with the criteria of the

investigations and Universiti Teknologi MARA Committee of Animal Research and Ethics (UiTM CARE) guidelines concerning the use of experimental animals.

Twelve, healthy, four-week-old male ICR mice, each weighing about 30 grams, were obtained from Laboratory Animal Facility and Management (LAFAM), Faculty of Pharmacy, UiTM Puncak Alam Campus. The animals underwent acclimatization period for 14 days and normal mouse diet along with filtered tap water was given *ad libitum*.

The study involved two groups of seven-week-old male ICR mice and each weighting 31.3 grams which consisted of radiation group (Rx) and watermelon juice supplementation group (Tx) with six animals in each group. Mice from Tx were supplemented with 50% watermelon juice as the sole liquid source *ad libitum* for 28 days, while the Rx were only given filtered tap water. All the mice were fed with normal mouse diet. Watermelon juices were changed twice/day and the volume of watermelon juice consumed by each mouse was recorded. On day 29, both groups were exposed to a total body irradiation of a single dose X-ray.

2.4. Irradiation and Tissues Collection. Both groups were placed in cages under Philips Bucky DIAGNOST X-ray machine and treated with single fractionated of 100 μ Gy X-ray for total body irradiation. This low dose irradiation was performed by a qualified radiographer at Medical Imaging Laboratory, Faculty of Health Sciences, UiTM Puncak Alam Campus. All the mice were sacrificed by cervical dislocation within 12 hours following total body irradiation. The brain, lung, and liver tissues were excised immediately and stored at -80°C prior to analysis.

2.5. Lipid Peroxidation Product, MDA Assay. Tissue samples were resuspended at 100 mg/mL in PBS containing 1X butylated hydroxytoluene (BHT). Five grams of the tissue samples was homogenized on ice, spun at 10,000 g for five min. The supernatant was collected and assayed directly for its TBARS level. MDA in samples and standards was interacted with thiobarbituric acid (TBA) at 95°C and incubated and then read spectrophotometrically at 532 nm with POLARstar Omega Reader. MDA levels were determined by comparison with predetermined MDA standard curve.

2.6. Oxidative DNA Damage (AP Sites). Genomic DNAs of brain, lung, and liver were isolated with Invisorb Spin Tissue Mini Kit (Stratec Molecular, Berlin) following the manufacturer's protocol. DNA Damage Quantification Kit (AP Sites) was used to quantitate apurinic/apyrimidinic (AP) sites in tissue of interest. The aldehyde reactive probe (ARP) that reacts specifically with an aldehyde group on the opening form of AP sites (ARP-derived DNA) was detected with Streptavidin-Enzyme Conjugate. The quantity of AP sites in unknown DNA sample of brain, lung, and liver was determined using POLARstar Omega Reader at 450 nm by comparing standard curve of predetermined AP sites. All unknown DNA samples and standard were assayed in duplicate.

2.7. SOD Activity Assay. The activity of SOD was determined by using Oxiselect Superoxide Dismutase Activity Assay. Tissues were homogenized on ice using mortar and pestle in 7 mL of cold 1X Lysis Buffer per gram tissue followed by centrifugation at 12000 ×g for 10 minutes. The supernatant of tissue lysate was then collected and kept at -80°C until further analysis. Superoxide anions generated by Xanthine/Xanthine Oxidase system were detected with a Chromagen Solution by measuring the absorbance reading at 490 nm using POLARstar Omega Reader. The activity of SOD was determined as the inhibition percentage of chromagen reduction.

2.8. GSH Antioxidant Assay. Tissues were blot-dried and weighed. Ice-cold 5% metaphosphoric acid (MPA) was added and homogenized using mortar and pestle and then centrifuged at 12,000 rpm for 15 min at 4°C. The supernatant was collected. The levels of GSH were measured kinetically with a spectrophotometric kit (Oxiselect Total Glutathione Assay) according to the manufacturer's protocol. The chromogen that reacted with the thiol group of GSH produced colored compound which was then detected with POLARstar Omega Reader at 405 nm. The total GSH content in the samples was determined by comparison with GSH standard curve.

2.9. Statistical Analysis. All mean ± SEM (standard error of mean) values were calculated and statistical analysis was done using SPSS version 18.0 (SPSS Inc., Chicago, IL, USA) for Windows. Data were analyzed by one-way analysis of variance (ANOVA), followed by *post hoc* Tukey test for multiple comparison of mean. The difference was considered significant when *P* value was less than 0.05 (*P* < 0.05).

3. Results

3.1. Dietary Supplementation of 50% Watermelon (*Citrullus lanatus* (Thunb.) Matsum. and Nakai) Juice Conferred Remarkable Radioprotection against Lipid Peroxidation. The results obtained from the experimental analysis of MDA levels in mice brain, lung, and liver tissues are presented in Figure 1. There was no significant reduction of MDA levels in brain tissues of Tx compared to Rx. However, MDA levels in lung and liver tissues of Tx were significantly reduced compared to Rx with *P* = 0.004 and *P* = 0.01, respectively. The average MDA levels in lung tissues of Tx and Rx were 25.28 ± 0.45 μM and 30.05 ± 0.94 μM, respectively, while the average MDA level in liver tissues of Tx was 20.20 ± 0.73 μM and Rx was 25.63 ± 1.43 μM.

3.2. Dietary Supplementation of 50% Watermelon (*Citrullus lanatus* (Thunb.) Matsum. and Nakai) Juice Conferred Remarkable Radioprotection against Oxidative DNA Damage by Mitigating Number of AP Sites. The radioprotective effects of 50% watermelon [*Citrullus lanatus* (Thunb.) Matsum. and Nakai] juice against oxidative DNA damage (AP sites) in mice tissues are shown in Figure 2. The generation of noncoding AP sites in brain showed significant differences between Tx and Rx with *P* = 0.029. The average numbers of AP sites per

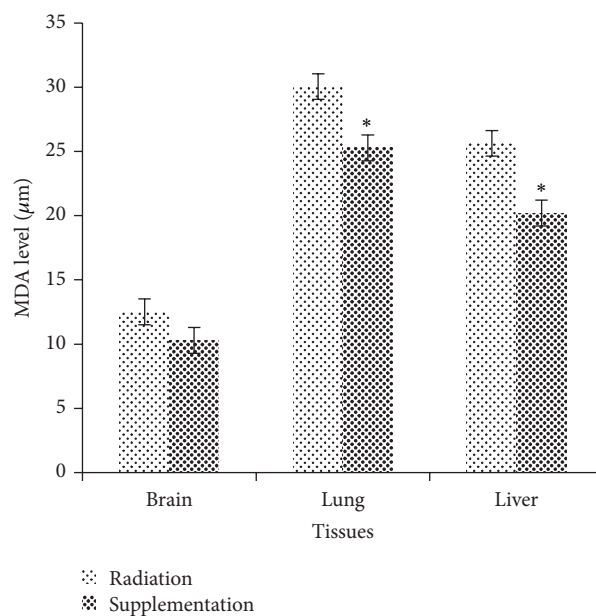


FIGURE 1: Radioprotective effects of 50% watermelon (*Citrullus lanatus* (Thunb.) Matsum. and Nakai) juice against lipid peroxidation in mice tissues. The bar chart shows the levels of MDA in brain, lung, and liver tissues of Rx and Tx. Values were expressed as mean ± SEM (*n* = 6). *Significant difference between Rx and Tx (*P* < 0.05).

10^5 base pairs in Tx and Rx were 26.48 ± 0.81 and 28.96 ± 0.43, respectively. As shown in Figure 2, lung DNA revealed significantly reduced number of abasic sites per 10^5 base pairs in Tx (31.38 ± 0.58) compared to Rx (34.98 ± 0.73) with *P* = 0.018. Meanwhile, the number of AP sites generated per 10^5 base pairs in liver of Tx showed significantly reduced number compared to Rx (*P* = 0.05). The average AP sites generated in Tx and Rx were 28.44 ± 1.17 and 33.37 ± 0.94, respectively.

3.3. Dietary Supplementation of 50% Watermelon (*Citrullus lanatus* (Thunb.) Matsum. and Nakai) Juice Conferred Remarkable Radioprotection against Oxidative Stress by Mitigating SOD Activities. Figure 3 referred to the mean value of SOD inhibition activities in Tx and Rx for mice brain, lung, and liver tissues. There were significant differences between brain SOD inhibition activities in Tx (80.02 ± 1.69%) and Rx (52.79 ± 2.03%) with *P* = 0.001. Meanwhile, SOD activities increased significantly in lung tissues of Tx compared to Rx (*P* = 0.001). The average SOD activities in lung tissues of Tx and Rx were 79.90 ± 1.91% and 42.06 ± 1.24%, respectively. In liver tissue, there was a significant difference between Tx (68.50 ± 1.82%) and Rx (59.13 ± 2.0%) with *P* = 0.04.

3.4. Dietary Supplementation of 50% Watermelon (*Citrullus lanatus* (Thunb.) Matsum. and Nakai) Juice Conferred Remarkable Radioprotection against Oxidative Stress by Mitigating GSH Levels. Figure 4 shows the levels of GSH content in mice brain, lung, and liver tissues. In the present study, GSH levels in brain tissues of Tx (0.18 ± 0.0085 μM) showed

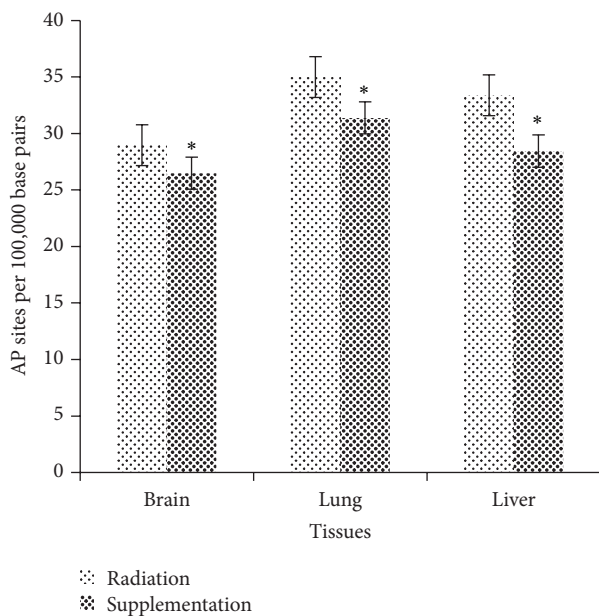


FIGURE 2: Radioprotective effects of 50% watermelon (*Citrullus lanatus* (Thunb.) Matsum. and Nakai) juice against oxidative DNA damage (AP sites). The bar chart shows the number of AP sites per 10^5 base pairs in brain, lung, and liver tissues of Rx and Tx. Values were expressed as mean \pm SEM ($n = 6$). *Significant difference between Rx and Tx ($P < 0.05$).

significant increment compared to Rx ($0.07 \pm 0.006 \mu\text{M}$) with $P = 0.001$. GSH levels in lung tissues of mice supplemented with watermelon juice (Tx) increased compared to Rx but no significant differences ($P > 0.05$) were observed. However, GSH levels in liver tissues of Tx were significantly increased compared to Rx ($P = 0.003$). The average GSH levels in Tx and Rx were $0.06 \pm 0.001 \mu\text{M}$ and $0.04 \pm 0.002 \mu\text{M}$, respectively.

4. Discussion

Oxygen radicals react with PUFA residues in phospholipids resulting in end products that are mostly reactive towards protein and DNA. One of the most abundant carbonyl products of lipid peroxidation is MDA [24]. Low dose X-ray might cause lipid peroxidation and the finding of this present study has shown that mice supplemented with 50% watermelon juice (Tx) resulted in a marked reduction in MDA levels in lung and liver tissues compared to Rx (Figure 1). Supplementation with 50% watermelon juice restored the activities of intracellular antioxidant enzymes in mice lung and liver tissues following exposure to low dose X-ray. Thus, phytochemical antioxidants contents in 50% watermelon juice may possibly contribute to the efficacy of intracellular antioxidant defense system by providing a puissant consumer of free radicals which induced oxidative damage. This was in agreement with the study conducted by Asita and Molise [1] which reveals that watermelon contains higher content of carotenoids such as lycopene and has proven to scavenge free radicals thus inhibit lipid peroxidation.

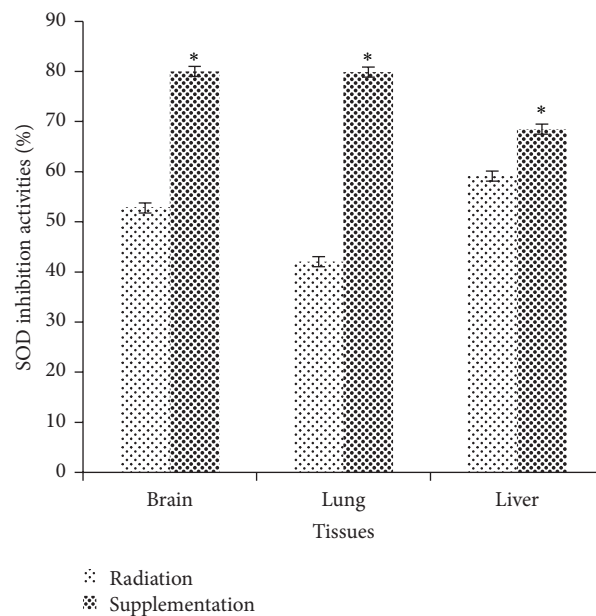


FIGURE 3: Radioprotective effects of 50% watermelon (*Citrullus lanatus* (Thunb.) Matsum. and Nakai) juice on SOD activities. The bar chart shows the percentage SOD inhibition activity in mice brain, lung, and liver tissues of Rx and Tx. Values were expressed as mean \pm SEM ($n = 6$). *Significant difference between Rx and Tx ($P < 0.05$).

DNA continuously generates sites of missing bases termed as abasic or apurinic/aprimidinic (AP) sites through exposure to endogenous and exogenous sources which are capable to induce oxidative DNA damage [25]. This study demonstrated that low dose X-ray exposure induced oxidative DNA damage was indeed positively correlated with AP sites formation. Here, these results show that mice supplemented with 50% watermelon juice in the presence of low dose X-ray exposure significantly prevented progressive increase of AP sites formation in brain, lung, and liver tissues compared to mice irradiated with low dose X-ray alone (Figure 2). It is seen possible to suggest that these results are mainly due to synergistic interaction between micronutrients content in watermelon juice and intracellular antioxidant enzymes could modulate oxidative DNA damage induced by low dose X-ray exposure. The present finding seems to be consistent with a previous study by Shokrzadeh et al. [26] which showed that mice preadministered with *Citrullus colocynthis* (L.) extract or locally known as watermelon for seven consecutive days via intraperitoneal injection followed by injection with 70 mg/kg body weight of cyclophosphamide- (CP-) induced DNA damage significantly reduced the number of micronucleated polychromatic erythrocytes (MnPCEs), an index of oxidative DNA damage.

SOD plays an important role in reducing the effect of free radicals attack, and SOD is the only enzymatic system quenching O_2^- to oxygen and H_2O_2 and plays a significant role against oxidant stress [18]. Referring to Figure 3, the percentage of SOD inhibition activities in brain, lung, and liver tissues of Tx showed significant increment compared to Rx. It seems possible to suggest that these results are mainly due to

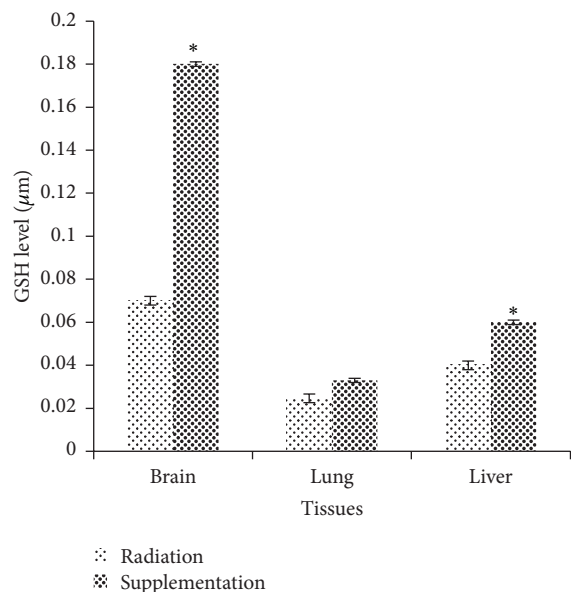


FIGURE 4: Radioprotective effects of 50% watermelon (*Citrullus lanatus* (Thunb.) Matsum. and Nakai) juice on GSH levels. The bar chart shows the GSH levels in brain, lung, and liver tissues in Rx and Tx. Values were expressed as mean \pm SEM ($n = 6$). *Significant difference between Rx and Tx ($P < 0.05$).

watermelon containing high level of phytonutrients including lycopene [27]. Perkins-Veazie et al. [28] point out that lycopene is a highly effective antioxidant because it acts as a strong free radical scavenger compared to carotenoids including beta-carotene, alpha carotene, lutein, beta-cryptoxanthin and astaxanthin in biological systems. In this context, the micronutrient antioxidant contents, especially lycopene, in 50% watermelon (*Citrullus lanatus* (Thunb.) Matsum. and Nakai) juice, accumulate in the tissues and counteract the deleterious effects of free radicals generated by low dose X-ray through activation of oxygen molecules.

GSH has been reported to have protective roles against oxidative stress through scavenging hydroxyl radical and singlet oxygen directly detoxifying H_2O_2 and lipid peroxides and also regenerate important antioxidants, Vitamins C and E, back to their active forms [2]. In the present study, the GSH levels in brain and liver tissues of Tx showed significant increment compared to Rx but no significant increment in lung. This phenomenon may suggest that the supplementation of antioxidant in 50% watermelon juice has successfully elevated the levels of GSH in both brain and liver tissues. Present results were in line with a study by Saada et al. [29] which emphasized that pretreatment with lycopene, which is rich in watermelon, significantly improved the oxidant/antioxidant status and helped in reducing oxidative damage due to radiation.

5. Conclusion

This study clarifies that the supplementation of 50% watermelon juice possesses benefits in modulating the oxidative

damage induced by low dose X-ray exposure in terms of suppressing the levels of MDA and noncoding AP sites formation while enhancing the levels of SOD and GSH activities.

Conflict of Interests

The authors declare that there is no conflict of interests that would prejudice the impartiality of this scientific work.

Acknowledgments

The authors gratefully acknowledge the (1) Faculty of Health Sciences, Universiti Teknologi MARA (UiTM) Puncak Alam and UiTM Research Management Institute (RAGS: 600-RMI/RAGS 5/3 (120/2012) for funding the study, (2) Miss Mazriazie Mohamed Isa and Miss Nurhanisa Ghazali for their laboratory assistance, and (3) Department of Medical Laboratory Technology, Department of Medical Imaging, Postgraduate Department, Integrative Pharmacogenomics Institute (iPROMISE), and Forest Research Institute Malaysia (FRIM) for providing facilities throughout this study.

References

- [1] A. O. Asita and T. Molise, "Antimutagenic effects of red apple and watermelon juices on cyclophosphamide-induced genotoxicity in mice," *African Journal of Biotechnology*, vol. 10, no. 77, pp. 17763–17768, 2011.
- [2] M. Valko, D. Leibfritz, J. Moncol, M. T. D. Cronin, M. Mazur, and J. Telser, "Free radicals and antioxidants in normal physiological functions and human disease," *International Journal of Biochemistry and Cell Biology*, vol. 39, no. 1, pp. 44–84, 2007.
- [3] M. Valko, C. J. Rhodes, J. Moncol, M. Izakovic, and M. Mazur, "Free radicals, metals and antioxidants in oxidative stress-induced cancer," *Chemico-Biological Interactions*, vol. 160, no. 1, pp. 1–40, 2006.
- [4] J. G. Scandalios, "Oxidative stress: molecular perception and transduction of signals triggering antioxidant gene defenses," *Brazilian Journal of Medical and Biological Research*, vol. 38, no. 7, pp. 995–1014, 2005.
- [5] M. Srinivasan, N. Devipriya, K. B. Kalpana, and V. P. Menon, "Lycopene: an antioxidant and radioprotector against γ -radiation-induced cellular damages in cultured human lymphocytes," *Toxicology*, vol. 262, no. 1, pp. 43–49, 2009.
- [6] S. Georgieva, B. Popov, and G. Bonev, "Radioprotective effect of *Haberlea rhodopensis* (Friv.) leaf extract on gamma-radiation-induced DNA damage, lipid peroxidation and antioxidant levels in rabbit blood," *Indian Journal of Experimental Biology*, vol. 51, no. 1, pp. 29–36, 2013.
- [7] C. L. Bladen, D. J. Kozlowski, and W. S. Dynan, "Effects of low-dose ionizing radiation and menadione, an inducer of oxidative stress, alone and in combination in a vertebrate embryo model," *Radiation Research*, vol. 178, no. 5, pp. 499–503, 2012.
- [8] S. S. Puthran, K. Sudha, G. M. Rao, and B. V. Shetty, "Oxidative stress and low dose ionizing radiation," *Indian Journal of Physiology and Pharmacology*, vol. 53, no. 2, pp. 181–184, 2009.
- [9] K. S. Azab, M. Bashandy, M. Salem, O. Ahmed, Z. Tawfik, and H. Helal, "Royal jelly modulates oxidative stress and tissue injury

- in gamma irradiated male Wister Albino rats," *North American Journal of Medical Sciences*, vol. 3, no. 6, pp. 268–276, 2011.
- [10] T. P. A. Devasagayam, K. K. Bloor, and T. Ramasarma, "Methods for estimating lipid peroxidation: an analysis of merits and demerits," *Indian Journal of Biochemistry and Biophysics*, vol. 40, no. 5, pp. 300–308, 2003.
- [11] T. P. A. Devasagayam, J. C. Tilak, K. K. Bloor, K. S. Sane, S. S. Ghaskadbi, and R. D. Lele, "Free radicals and antioxidants in human health: current status and future prospects," *Journal of Association of Physicians of India*, vol. 52, pp. 794–804, 2004.
- [12] J. F. Kergonou, P. Bernard, M. Braquet, and G. Rocquet, "Effect of whole-body gamma irradiation on lipid peroxidation in rat tissues," *Biochimie*, vol. 63, no. 6, pp. 555–559, 1981.
- [13] L. M. Martin, B. Marples, M. Coffey et al., "DNA mismatch repair and the DNA damage response to ionizing radiation: making sense of apparently conflicting data," *Cancer Treatment Reviews*, vol. 36, no. 7, pp. 518–527, 2010.
- [14] M. Dizdaroglu, "Oxidatively induced DNA damage: mechanisms, repair and disease," *Cancer Letters*, vol. 327, no. 1–2, pp. 26–47, 2012.
- [15] P. M. Hanson, R. Yang, J. Wu et al., "Variation for antioxidant activity and antioxidants in tomato," *Journal of the American Society for Horticultural Science*, vol. 129, no. 5, pp. 704–711, 2004.
- [16] M. Srinivasan, A. R. Sudheer, K. R. Pillai, P. R. Kumar, P. R. Sudhakaran, and V. P. Menon, "Lycopene as a natural protector against γ -radiation induced DNA damage, lipid peroxidation and antioxidant status in primary culture of isolated rat hepatocytes in vitro," *Biochimica et Biophysica Acta—General Subjects*, vol. 1770, no. 4, pp. 659–665, 2007.
- [17] H. F. Waer and F. M. Shalaby, "Structural studies on the radioprotective effect of lycopene (tomato supplementation) against hepatic cellular injury induced by chronic doses of gamma radiation," *Journal of Cytology and Histology*, vol. 3, article 145, 2012.
- [18] D. Meydan, B. Gursel, B. Bilgici, B. Can, and N. Ozbek, "Protective effect of lycopene against radiation-induced hepatic toxicity in rats," *Journal of International Medical Research*, vol. 39, no. 4, pp. 1239–1252, 2011.
- [19] M. I. Mohamed, M. K. A. Mohammad, A. M. Zakaria et al., "Induction of oxidative stress following low dose ionizing radiation in ICR mice," *World Journal of Medical Sciences*, vol. 10, no. 2, pp. 198–203, 2014.
- [20] A. V. Rao and L. G. Rao, "Carotenoids and human health," *Pharmacological Research*, vol. 55, no. 3, pp. 207–216, 2007.
- [21] M. P. Pinto, C. N. dos Santos, C. Henriquesa, G. Lima, and F. Quedas, "Lycopene content and antioxidant capacity of Portuguese watermelon fruits," *Electronic Journal of Environmental, Agricultural and Food Chemistry*, vol. 10, no. 4, pp. 2090–2097, 2011.
- [22] K. Wasylkova and M. van der Veen, "An archaeobotanical contribution to the history of watermelon, *Citrullus lanatus* (Thunb.) Matsum. & Nakai (syn. *C. vulgaris* Schrad.)," *Vegetation History and Archaeobotany*, vol. 13, no. 4, pp. 213–217, 2004.
- [23] S. Altaş, G. Kızıl, M. Kızıl, A. Ketani, and P. I. Haris, "Protective effect of Diyarbakır watermelon juice on carbon tetrachloride-induced toxicity in rats," *Food and Chemical Toxicology*, vol. 49, no. 9, pp. 2433–2438, 2011.
- [24] L. J. Marnett, "Oxy radicals, lipid peroxidation and DNA damage," *Toxicology*, vol. 181–182, pp. 219–222, 2002.
- [25] D. M. Wilson and D. Barsky, "The major human abasic endonuclease: formation, consequences and repair of abasic lesions in DNA," *Mutation Research—DNA Repair*, vol. 485, no. 4, pp. 283–307, 2001.
- [26] M. Shokrzadeh, A. Chabra, F. Naghshvar, and A. Ahmadi, "The mitigating effect of *Citrullus colocynthis* (L.) fruit extract against genotoxicity induced by cyclophosphamide in mice bone marrow cells," *The Scientific World Journal*, vol. 2013, Article ID 980480, 8 pages, 2013.
- [27] M. P. Tarazona-Díaz, J. Viegas, M. Moldao-Martins, and E. Aguayo, "Bioactive compounds from flesh and by-product of fresh-cut watermelon cultivars," *Journal of the Science of Food and Agriculture*, vol. 91, no. 5, pp. 805–812, 2011.
- [28] P. Perkins-Veazie, J. K. Collins, S. D. Pair, and W. Roberts, "Lycopene content differs among red-fleshed watermelon cultivars," *Journal of the Science of Food and Agriculture*, vol. 81, no. 10, pp. 983–987, 2001.
- [29] H. N. Saada, R. G. Rezk, and N. A. Eltahawy, "Lycopene protects the structure of the small intestine against gamma-radiation-induced oxidative stress," *Phytotherapy Research*, vol. 24, supplement 2, pp. S204–S208, 2010.

Research Article

In Vivo Antistress and Antioxidant Effects of Fermented and Germinated Mung Bean

Swee Keong Yeap,¹ Boon Kee Beh,² Norlaily Mohd Ali,³ Hamidah Mohd Yusof,³ Wan Yong Ho,⁴ Soo Peng Koh,⁵ Noorjahan Banu Alitheen,³ and Kamariah Long⁵

¹ Institute of Bioscience, Universiti Putra Malaysia, 43400 Serdang, Selangor, Malaysia

² Department of Bioprocess Technology, Faculty of Biotechnology and Biomolecular Science, Universiti Putra Malaysia, 43400 Serdang, Selangor, Malaysia

³ Department of Cell and Molecular Biology, Faculty of Biotechnology and Biomolecular Science, Universiti Putra Malaysia, 43400 Serdang, Selangor, Malaysia

⁴ School of Biomedical Sciences, The University of Nottingham, Malaysia Campus, Jalan Broga, 43500 Semenyih, Selangor, Malaysia

⁵ Biotechnology Research Centre, Malaysian Agricultural Research and Development Institute (MARDI), 43400 Serdang, Selangor, Malaysia

Correspondence should be addressed to Kamariah Long; amai@mardi.gov.my

Received 6 December 2013; Accepted 7 April 2014; Published 29 April 2014

Academic Editor: Didier Bereau

Copyright © 2014 Swee Keong Yeap et al. This is an open access article distributed under the Creative Commons Attribution License, which permits unrestricted use, distribution, and reproduction in any medium, provided the original work is properly cited.

Mung bean has been traditionally used to alleviate heat stress. This effect may be contributed by the presence of flavonoids and γ -aminobutyric acid (GABA). On the other hand, fermentation and germination have been practised to enhance the nutritional and antioxidant properties of certain food products. The main focus of current study was to compare the antistress effect of none-process, fermented and germinated mung bean extracts. Acute and chronic restraint stresses were observed to promote the elevation of serum biochemical markers including cholesterol, triglyceride, total protein, liver enzymes, and glucose. Chronic cold restraint stress was observed to increase the adrenal gland weight, brain 5-hydroxytryptamine (5-HT), and malondialdehyde (MDA) level while reducing brain antioxidant enzyme level. However, these parameters were found reverted in mice treated with diazepam, high concentration of fermented mung bean and high concentration of germinated mung bean. Moreover, enhanced level of antioxidant on the chronic stress mice was observed in fermented and germinated mung bean treated groups. In comparison between germinated and fermented mung bean, fermented mung bean always showed better antistress and antioxidant effects throughout this study.

1. Introduction

Stress response is a behaviour survival mechanism that helps fortify the physical and mental condition [1]. Neurotransmitters including noradrenaline (NA), dopamine (DA), and 5-hydroxytryptamine (5-HT) are the important biogenic monoamines. Under stress condition, NA and 5-HT will be highly elevated [2, 3]. However, extreme stress can cause impaired dopamine neurons [1] and collapse the homeostasis which may lead to various psychotic disorders including immunosuppression, hypertension, anxiety, endocrine disorder, and behaviour disorder [4]. Besides, restraints stress

can be associated with the production of reactive oxygen species that may contribute to tissue damage [2]. Various drugs including diazepam, amphetamines, caffeine, and some anabolic steroids have been used and misused currently to overcome stress. The overdependence or misuse of these drugs often is associated with issues of toxicity and side effects [4].

Herbal medicines have been proposed as a cheaper and safer potential antistress agent. For examples, *Withania somnifera*, *Piper longum*, *Momordica charantia*, and *Asparagus racemosus* have been reported to have adaptogenic effect [2, 3, 5]. Legumes have also received great attention due to

the presence of phytochemicals and their bioactivities. Mung bean (*Vigna radiata*) is a type of legume that is commonly consumed in Asian countries as a source of carbohydrate [6]. It has now been becoming another popular functional food for promoting good health. In Asian countries, mung bean beverages are often used to prevent or eliminate heatstroke. Flavonoids including vitexin and isovitexin have been proven as the major contributor to this protective effect against heat stress and to reduction of oxidative stress [7]. Other than its antioxidant property, mung bean also possessed anti-inflammatory [6, 8], antityrosinase [9], and antiproliferative [10] effects. Fermentation and germination have been proposed as processes that can improve the quality of cereal and legume seeds. For instance, functional nutrients including γ -aminobutyric acid (GABA) and antioxidants compounds were enhanced through germination [11, 12] and fermentation processes [13]. Although the protective effect against heat stress of mung bean has been reported, the effect of mung bean as potential antistress agent on restraint stress is yet unknown.

The purpose of this study was to compare the antistress activity of none-process, fermented and germinated mung bean extracts on acute and chronic restraint stress. Regulations of brain NA, DA, 5-HT, and antioxidant level under chronic stress condition were also examined.

2. Materials and Methods

2.1. Preparation of Fermented Mung Bean Extracts. Mung bean seeds were purchased in October 2010 from a local store in Serdang, Selangor. It was dehulled, washed, and soaked in chilled water at room temperature for 18 hours before being steamed for 40 minutes. Then, the steamed mung bean was fermented using *Rhizopus sp.* strain of 5351 inoculums under solid-state condition at 30°C for another 48 hours. The fermented mung bean was dried, ground into powder, and extracted with deionised water for 30 minutes at room temperature [13]. Finally, the water extract was freeze-dried (yield 25%, w/w) and subjected to GABA determination.

2.2. Detection of GABA Content in Fermented Mung Bean Extracts. GABA content of freeze-dried fermented mung bean was determined using Waters Acquity UPLC system with UV-PDA detector set at wavelength of 260 nm. Acquity UPLC AccQ Tag Ultra Column (2.1 mm i.d. \times 100 mm \times 1.7 μ m particle size) was used together with operating oven column temperature of 55°C and flow rate at 0.7 mL/min. Mobile phase consisted of AccQ Tag Ultra Eluent A (mobile phase A) and AccQ Tag Ultra Eluent B (mobile phase B) that were used under linear gradient condition as follows: 0.1% Eluent B under isocratic flow for 0.54 minutes and increased from 0.1% to 9.1% Eluent B for 5.20 minutes. Eluent B was then increased to 21.2% for another 2 minutes followed by another increment to 59.6% Eluent B for 1.06 minutes before reverting back to 0.1% Eluent B for 2.1 minutes. Finally, reconditioning the column with 0.1% Eluent B with isocratic flow for 0.30 min, data collected was analyzed using Waters Empower 2 software [14].

2.3. Animals. Male Balb/c mice (aged 8 weeks with average body weight of 25 ± 2 g) obtained from Animal Housing Department, Institute of Bioscience, Universiti Putra Malaysia, were used for all the tests below. Mice were kept in prebedded plastic cages under controlled conditions of $22 \pm 1^\circ\text{C}$ and standard 12 hours of dark/light day cycles with food and water *ad libitum*. Procedures for this study were carried out according to the guideline of National Institute of Health for the Care and Use of Laboratory Animals. This study was approved by the Animal Care and Use Committee, Universiti Putra Malaysia (UPM).

2.4. Acute Restraint Stress. Mice were randomly divided into 8 groups with 8 animals each. Group 1 (nonstress control) and group 2 (untreated control) were fed with 0.2% sodium carboxymethyl cellulose in saline, group 3 (positive control) received 2 mg/kg of diazepam, group 4 received 1000 mg/kg of none process mung bean extracts, groups 5 and 6 received 250 or 1000 mg/kg of fermented mung bean extracts, and groups 7 and 8 received 250 or 1000 mg/kg of germinated mung bean extracts. All treatments were given p.o. for 7 days. On the 7th day, mice were tied and immobilized with adhesive tape for 2 hours. At the end of the test, mice were sacrificed and blood was collected to obtain serum for determination of glucose, total cholesterol, triglyceride (TG), alkaline phosphatase (ALP), and alanine aminotransferase (ALT) (Biovision, USA) level according to the manufacturers' protocol [15].

2.5. Chronic Cold Restraint Stress. Mice were randomly divided into 8 groups with 8 animals each and the grouping was the same as the acute restraint stress test. All treatments were given p.o. for 21 days. After that, all mice except for group 1 (nonstress control) were exposed to cold restraint stress (placed under 4°C for 1 hour) continuously for another 7 days. Treatments were continued during this period. On the last day of the experiment, mice were treated, exposed to cold restraint stress, and sacrificed and blood was collected to obtain serum for determination of glucose, total cholesterol, triglyceride (TG) (Biovision, USA), and corticosterone (Cayman, USA) level according to the manufacturers' protocol. Moreover, adrenal gland was removed and weighted. Brains were frozen in liquid nitrogen and homogenized in mixture of HCl (0.01 N) and butanol. The aqueous phase acid extract was recovered by centrifugation and concentrations of dopamine (DA) (IBL, Hamburg, Germany) and 5-hydroxytryptamine (5-HT) (IBL, Hamburg, Germany) were quantified using ELISA [15] while brain superoxide dismutase (SOD) and malondialdehyde (MDA) levels were quantified according to the literature [16].

2.6. Statistical Analysis. Results from all the above tests were presented as mean \pm standard deviation values. One-way analysis of variance (ANOVA) with post hoc Duncan test was used to evaluate statistical significance of the above results. *P* values < 0.05 were considered as significant.

TABLE 1: Effect of fermented and nonfermented mung bean extracts on serum biochemical profile under acute restraint stress.

	Chol (mmol/L)	Trig (mmol/L)	Total protein (g/dL)	Glucose (mmol/L)
Untreated normal control	6.23 ± 0.27*	3.96 ± 0.78*	138.78 ± 6.70*	6.93 ± 0.51*
Untreated stress control	8.32 ± 0.87	5.43 ± 0.30	157.88 ± 13.15	7.85 ± 0.07
Diazepam (2 mg/kg)	5.32 ± 0.86*	2.55 ± 0.49*	104.78 ± 25.03*	5.40 ± 0.26*
None-process mung bean (1000 mg/kg)	7.21 ± 0.77*	3.96 ± 0.35*	147.24 ± 4.14	6.14 ± 1.66*
Fermented mung bean (250 mg/kg)	6.58 ± 0.66*	4.18 ± 0.65*	142.54 ± 1.06	6.07 ± 0.92*
Fermented mung bean (1000 mg/kg)	5.27 ± 0.92*	3.14 ± 0.81*	108.48 ± 10.82*	5.47 ± 0.35*
Germinated mung bean (250 mg/kg)	8.73 ± 0.85	5.86 ± 0.33	155.43 ± 11.16	7.51 ± 0.13
Germinated mung bean (1000 mg/kg)	5.54 ± 0.74	2.34 ± 0.62	100.02 ± 21.63	5.59 ± 0.38

* $P > 0.05$ versus untreated stress control for acute restraint test.

3. Results

3.1. GABA Content in Fermented and Germinated Mung Bean Extracts. The concentrations of GABA in fermented and germinated mung bean extracts were 0.131 ± 0.015 and 0.502 ± 0.035 g/100 g, respectively [17].

3.2. Acute Restraint Stress. Acute restraint stress significantly raised the level of serum cholesterol, TG, total protein, and glucose as compared to untreated normal control. The effects of fermented and germinated mung bean extracts were comparable to diazepam in the reduction of mice serum biochemical profiles under acute restraint stress condition (Table 1).

3.3. Chronic Restraint Stress. Chronic cold restraint stress has significantly increased the serum biochemical levels (cholesterol, TG, total protein, glucose, and corticosterone), adrenal gland weight, and brain MDA level. On the other hand, it also reduced brain antioxidant enzyme level (SOD), brain serotonin (5-HT), and spleen weight (Table 2). Fermented and germinated mung bean extracts (both at 1000 mg/kg concentration) and diazepam were able to restore these parameters back to nonstress normal control level. The antistress effects of fermented and germinated mung bean extracts were in a dosage dependent manner where low dosage of these extracts especially from germinated mung bean possessed the lowest antistress effect among all the tested samples. However, no statistical significance was observed in brain dopamine (DA) level of all the control and treated groups.

4. Discussion

Adaptation is a common central neurotransmission response toward stress and this event can help strengthen the organisms to handle stress [2]. Under stress condition, various adrenal hormones are released and these hormones will induce insulin resistance which results in the elevation of plasma glucose level. Furthermore, the release of NA and corticosteroid will also stimulate hyperinsulinemia and thus raise the synthesis of cholesterol. These changes affect the mobilisation of stored fat and carbohydrate reserves that eventually raise the level of blood cholesterol, TG, total protein, and glucose [15, 18]. Thus, the depletion of

monoamines (NA and DA) was often associated with high level of serum biochemical profiles under overstress condition. According to American Academy of Family Physicians, stress related problems including insomnia and depression have contributed to large percentage of cases in primary health care [19]. Various antistress and antidepressant drugs have been developed; however, the associations of toxicity and side effects issues have limited their therapeutic practice [4]. Thus, food base natural products may be a better and more convenient alternative to assist in stress management in primary health care.

Mung bean was found to be an excellent dietary source of natural antioxidants for health promotion [10] and this antioxidant effect has contributed to its antiheat stress activity [7]. In this study, we evaluated the antistress effect of fermented and germinated mung bean extracts toward acute restraint stress and chronic cold restraint stress. Diazepam, a nonspecific antistress agent [15], was used as positive control in this study. Overall reduction of cholesterol, TG, total protein, and glucose levels may be contributed by the reduction of corticosteroid level in the fermented mung bean extracts treated group. Fermented food such as fermented rice bran has been reported as antistress and antifatigue agent [20]. Our results showed that fermented and germinated mung bean extracts possessed better antistress effect in a dosage dependent manner for both acute and chronic stress model than none-process mung bean extracts. This effect may be contributed by the presence of GABA in both fermented and germinated mung bean extracts. GABA is a nonprotein amino acid that works as an inhibitor to neurotransmission [21]. It plays an important role in central integration of hypothalamic-pituitary-adrenocortical (HPA) stress reaction. None adequate level of GABA in plasma has been related to the development of acute posttraumatic stress disorder [21, 22]. On the other hand, previous study has reported that ethanol extract of *Rubia cordifolia* can stimulate the brain GABA level that subsequently reduced the dopamine and plasma corticosterone levels [18]. The GABA contents of our fermented and germinated mung bean (0.131 ± 0.015 and 0.502 ± 0.035 g/100 g, resp.) were recorded to be higher than those detected in germinated brown rice (0.0818 ± 0.0072 g/100 g). This may be contributed by the different level of GABA-synthesizing enzyme that is present in different plants [23]. In this study, germinated mung bean

TABLE 2: Effect of fermented and nonfermented mung bean extracts on serum biochemical profile, adrenal gland weight, brain 5-hydroxytryptamine (5-HT), superoxide dismutase (SOD), and malondialdehyde (MDA) levels under chronic cold restraint stress.

	Chol (mmol/L)	Trig (mmol/L)	Total protein (g/dL)	Glucose (mmol/L)	Corticosterone (μ g/100 mL)	Adrenal gland weight (mg/100 g)	Brain 5-HT level (μ g/g)	Brain SOD (U/mg protein)	Brain MDA (nmol/g of protein)
Untreated normal control	5.11 \pm 0.56*	2.82 \pm 0.30*	97.90 \pm 8.10	5.32 \pm 0.71*	8.58 \pm 0.75*	31.07 \pm 2.43*	0.08 \pm 0.07*	11.35 \pm 1.22*	2.37 \pm 0.71*
Untreated stress control	5.87 \pm 0.54	3.19 \pm 0.88	118.37 \pm 22.04	9.60 \pm 0.14	14.74 \pm 0.35	35.13 \pm 3.09	2.20 \pm 0.07	4.58 \pm 1.83	15.63 \pm 1.44
Diazepam (2 mg/kg)	4.06 \pm 0.90*	1.70 \pm 0.49*	92.43 \pm 12.42*	5.07 \pm 0.49*	8.81 \pm 0.49*	30.62 \pm 3.33*	0.73 \pm 0.09*	8.32 \pm 1.67*	8.49 \pm 1.51*
None-process mung bean (1000 mg/kg)	4.83 \pm 0.11*	3.62 \pm 0.36	99.52 \pm 6.47	9.04 \pm 0.45*	8.90 \pm 0.14*	27.53 \pm 2.12*	1.72 \pm 0.05*	6.33 \pm 1.25*	11.57 \pm 1.11*
Fermented mung bean (250 mg/kg)	5.15 \pm 0.16*	2.98 \pm 0.19	97.00 \pm 2.83*	9.40 \pm 1.56	9.52 \pm 0.51*	30.05 \pm 2.75*	2.10 \pm 0.09	7.16 \pm 1.15*	9.64 \pm 2.10*
Fermented mung bean (1000 mg/kg)	4.19 \pm 0.08*	3.16 \pm 0.70	91.05 \pm 7.71*	8.13 \pm 0.99*	7.43 \pm 0.31*	26.06 \pm 1.50*	1.20 \pm 0.03*	9.14 \pm 2.36*	7.32 \pm 1.86*
Germinated mung bean (250 mg/kg)	4.66 \pm 0.70*	3.20 \pm 0.65*	98.30 \pm 6.53*	10.00 \pm 1.05	15.01 \pm 0.64	36.70 \pm 1.50	1.70 \pm 0.06*	5.79 \pm 1.28	10.46 \pm 0.36*
Germinated mung bean (1000 mg/kg)	4.77 \pm 0.13*	3.33 \pm 0.99*	96.17 \pm 10.61*	9.04 \pm 0.61*	8.90 \pm 0.14*	26.97 \pm 1.49*	1.65 \pm 0.06*	7.81 \pm 1.47*	10.17 \pm 0.49*

* $P > 0.05$ versus untreated stress control for chronic cold restraint test.

extracts contained higher level of GABA as compared to fermented mung bean extracts. However, fermented mung bean extracts gave the best antistress effect in all the experiments in a dosage dependent manner while germinated mung bean extracts only possessed slightly better effect as compared to none-process mung bean extracts. This phenomenon may be contributed by the strong antioxidant activity found in fermented mung bean extracts which concurrently protected the damage induced by stress [17]. Stress also promotes the development of reactive oxygen species and free radicals that lead to the formation of lipid peroxides. Nervous system is very sensitive to peroxidative damage during restraints stress due to the increase of oxygen tension and reduction of antioxidant level [24]. Thus, effective antioxidants that can inhibit lipid oxidation may help prevent organ damage during stress conditions. Previous study has shown that polyphenol from oolong tea was able to reduce the stress and the stress-induced lipid peroxide levels on women loaded with vigil [25]. To correlate the antistress capability with the antioxidant effects of fermented mung bean extracts, the levels of antioxidant SOD enzyme and lipid peroxidation in the brain were determined. In this study, we found that mice under chronic cold restraint stress contained high level of MDA with depletion of SOD level (Table 2). The decreased SOD level was significantly raised by fermented mung bean extracts in a dosage dependent manner. This effect was associated with mark reduction of MDA level.

High incidence of stress related mental illness has been recorded in primary health care nowadays. Healthy functional food is a more convenient and better choice in stress management. This study has demonstrated that fermented and germinated mung bean extracts possessed antistress activity in both acute and chronic stress mice. It also reverts the antioxidant level in brain under stress condition. Thus, fermented mung bean extracts exhibited great potential to be developed into functional foods or nutraceutical ingredients for reducing oxidative stress and as alternative antistress agent for primary mental health problem.

Conflict of Interests

The authors declare that they have no conflict of interests.

Acknowledgment

This project was supported by Science Fund under Ministry of Agriculture, Malaysia.

References

- [1] L. Pani, A. Porcella, and G. L. Gessa, "The role of stress in the pathophysiology of the dopaminergic system," *Molecular Psychiatry*, vol. 5, no. 1, pp. 14–21, 2000.
- [2] T. Joshi, S. P. Sah, and A. Singh, "Antistress activity of ethanolic of *Asparagus racemosus* Willd roots in mice," *Indian Journal of Experimental Biology*, vol. 50, pp. 419–424, 2012.
- [3] C. N. Kavitha, S. M. Babu, and M. E. B. Rao, "Influence of *Momordica charantia* on oxidative stress-induced perturbations in brain monoamines and plasma corticosterone in albino rats," *Indian Journal of Pharmacology*, vol. 43, no. 4, pp. 424–428, 2011.
- [4] S. K. Desai, S. M. Desai, S. Navdeep, P. Arya, and T. Pooja, "Antistress activity of *Boerhaavia diffusa* root extract and a polyherbal formulation containing *Boerhaavia diffusa* using cold restraint stress model," *International Journal of Pharmacy and Pharmaceutical Sciences*, vol. 3, no. 1, pp. 130–132, 2011.
- [5] M. N. Khan, J. Suresh, K. S. H. Yadav, and J. Ahuja, "Formulation and evaluation of antistress polyherbal capsule," *Der Pharmacia Sinica*, vol. 3, pp. 177–184, 2012.
- [6] S.-J. Lee, J. H. Lee, H.-H. Lee et al., "Effect of mung bean ethanol extract on pro-inflammatory cytokines in LPS stimulated macrophages," *Food Science and Biotechnology*, vol. 20, no. 2, pp. 519–524, 2011.
- [7] D. Cao, H. Li, J. Yi et al., "Antioxidant properties of the mung bean flavonoids on alleviating heat stress," *PLoS ONE*, vol. 6, no. 6, Article ID e21071, 2011.
- [8] G. S. M. Ismail, "Protective role of nitric oxide against arsenic-induced damages in germinating mung bean seeds," *Acta Physiologiae Plantarum*, vol. 34, pp. 1303–1311, 2012.
- [9] Y. Yao, X. Cheng, L. Wang, S. Wang, and G. Ren, "Mushroom tyrosinase inhibitors from mung bean (*Vigna radiatae* L.) extracts," *International Journal of Food Sciences and Nutrition*, vol. 63, no. 3, pp. 358–361, 2012.
- [10] B. Xu and S. K. C. Chang, "Comparative study on antiproliferation properties and cellular antioxidant activities of commonly consumed food legumes against nine human cancer cell lines," *Food Chemistry*, vol. 134, pp. 1287–1296, 2012.
- [11] R. Fernandez-Orozco, J. Frias, H. Zielinski, M. K. Piskula, H. Kozłowska, and C. Vidal-Valverde, "Kinetic study of the antioxidant compounds and antioxidant capacity during germination of *Vigna radiata* cv. emerald, *Glycine max* cv. jutro and *Glycine max* cv. merit," *Food Chemistry*, vol. 111, no. 3, pp. 622–630, 2008.
- [12] J. Sutharut and J. Sudarat, "Total anthocyanin content and antioxidant activity of germinated colored rice," *International Food Research Journal*, vol. 19, no. 1, pp. 215–221, 2012.
- [13] J. S. Tsai, Y. S. Lin, B. S. Pan, and T. J. Chen, "Antihypertensive peptides and γ -aminobutyric acid from prozyme 6 facilitated lactic acid bacteria fermentation of soymilk," *Process Biochemistry*, vol. 41, no. 6, pp. 1282–1288, 2006.
- [14] Y. Guo, H. Chen, Y. Song, and Z. Gu, "Effects of soaking and aeration treatment on γ -aminobutyric acid accumulation in germinated soybean (*Glycine max* L.)," *European Food Research and Technology*, vol. 232, no. 5, pp. 787–795, 2011.
- [15] M. Kulkarni and A. Juvekar, "Attenuation of acute and chronic restraint stress-induced perturbations in experimental animals by *Nelumbo nucifera* Gaertn," *Indian Journal of Pharmaceutical Sciences*, vol. 70, no. 3, pp. 327–332, 2008.
- [16] W. Y. Ho, W. S. Liang, S. K. Yeap, B. K. Beh, A. H. N. Yousr, and N. B. Alitheen, "In vitro and in vivo antioxidant activity of *Vernonia amygdalina* water extract," *African Journal of Biotechnology*, vol. 11, no. 17, pp. 4090–4094, 2012.
- [17] N. M. Ali, H. M. Yusof, K. Long et al., "Antioxidant and hepatoprotective effect of aqueous extract of germinated and fermented mung bean on ethanol-mediated liver damage," *BioMed Research International*, vol. 2013, Article ID 693613, 9 pages, 2013.
- [18] R. D. Kenjale, R. K. Shah, and S. S. Sathaye, "Anti-stress and antioxidant effects of roots of *chlorophytum borivilianum* santa pau & fernandes," *Indian Journal of Experimental Biology*, vol. 45, no. 11, pp. 974–979, 2007.

- [19] American Academy of Family Physicians, "Mental health care services by family physicians (Position paper)," <http://www.aafp.org/online/en/home/policy/policies/m/mentalhealthcareservices.html>.
- [20] K. M. Kim, K. W. Yu, D. H. Kang, J. H. Koh, B. S. Hong, and H. J. Suh, "Anti-stress and anti-fatigue effects of fermented rice bran," *Bioscience, Biotechnology and Biochemistry*, vol. 65, no. 10, pp. 2294–2296, 2001.
- [21] G. Vaiva, P. Thomas, F. Ducrocq et al., "Low posttrauma GABA plasma levels as a predictive factor in the development of acute posttraumatic stress disorder," *Biological Psychiatry*, vol. 55, no. 3, pp. 250–254, 2004.
- [22] N. B. Patel, V. J. Galani, and B. G. Patel, "Antistress activity of *Argyreia speciosa* roots in experimental animals," *Journal of Ayurveda and Integrative Medicine*, vol. 2, no. 3, pp. 129–136, 2011.
- [23] S. Thitinunsomboon, S. Keeratipibul, and A. Boonsiriwit, "Enhancing gamma-aminobutyric acid content in germinated brown rice by repeated treatment of soaking and incubation," *Food Science and Technology International*, vol. 19, pp. 25–33, 2013.
- [24] D. Metodiewa and C. Koska, "Reactive oxygen species and reactive nitrogen species: relevance to cyto (neuro) toxic events and neurologic disorders. An overview," *Neurotoxicity Research*, vol. 1, pp. 197–233, 2000.
- [25] H. Kurihara, L. Chen, B.-F. Zhu et al., "Anti-stress effect of oolong tea in women loaded with vigil," *Journal of Health Science*, vol. 49, no. 6, pp. 436–443, 2003.

Review Article

A Review on Antibacterial, Antiviral, and Antifungal Activity of Curcumin

Soheil Zorofchian Moghadamtousi,¹ Habsah Abdul Kadir,¹
Pouya Hassandarvish,² Hassan Tajik,³ Sazaly Abubakar,² and Keivan Zandi^{2,4}

¹ Biomolecular Research Group, Biochemistry Program, Institute of Biological Sciences, Faculty of Science, University of Malaya, 50603 Kuala Lumpur, Malaysia

² Tropical Infectious Disease Research and Education Center (TIDREC), Department of Medical Microbiology, Faculty of Medicine, University of Malaya, 50603 Kuala Lumpur, Malaysia

³ Department of Chemistry, Faculty of Sciences, Guilan University, Rasht, Iran

⁴ Persian Gulf Marine Biotechnology Research Center, Bushehr University of Medical Sciences, Bushehr 3631, Iran

Correspondence should be addressed to Keivan Zandi; keivan@um.edu.my

Received 21 January 2014; Accepted 28 March 2014; Published 29 April 2014

Academic Editor: José Carlos Tavares Carvalho

Copyright © 2014 Soheil Zorofchian Moghadamtousi et al. This is an open access article distributed under the Creative Commons Attribution License, which permits unrestricted use, distribution, and reproduction in any medium, provided the original work is properly cited.

Curcuma longa L. (Zingiberaceae family) and its polyphenolic compound curcumin have been subjected to a variety of antimicrobial investigations due to extensive traditional uses and low side effects. Antimicrobial activities for curcumin and rhizome extract of *C. longa* against different bacteria, viruses, fungi, and parasites have been reported. The promising results for antimicrobial activity of curcumin made it a good candidate to enhance the inhibitory effect of existing antimicrobial agents through synergism. Indeed, different investigations have been done to increase the antimicrobial activity of curcumin, including synthesis of different chemical derivatives to increase its water solubility as well as cell uptake of curcumin. This review aims to summarize previous antimicrobial studies of curcumin towards its application in the future studies as a natural antimicrobial agent.

1. Introduction

Curcumin or diferuloylmethane with chemical formula of (1,7-bis(4-hydroxy-3-methoxyphenyl)-1,6-heptadiene-3,5-dione) (Figure 1) and other curcuminoids constitute the main phytochemicals of *Curcuma longa* L. (Zingiberaceae family) rhizome with the common name of turmeric [1]. This polyphenolic compound due to a variety of biological activities has been gained significant attention of researchers all over the world [2–5]. Turmeric, an ancient coloring spice of Asia, as the main source of curcumin is traditionally used for many remedies [6]. As shown in Figure 2, curcumin due to a variety of specific characterizations is in interest of scientists in recent years. As many other plant materials, there are differences in the curcumin content for the *Curcuma longa* from different geographical regions and it could be due

to hybridization with other *Curcuma* species which could be important fact to choose the plant with higher content of curcumin [4].

Curcuma longa rhizome has been traditionally used as antimicrobial agent as well as an insect repellent [7]. Several studies have reported the broad-spectrum antimicrobial activity for curcumin including antibacterial, antiviral, antifungal, and antimalarial activities. Because of the extended antimicrobial activity of curcumin and safety property even at high doses (12 g/day) assessed by clinical trials in human, it was used as a structural sample to design the new antimicrobial agents with modified and increased antimicrobial activities through the synthesis of various derivatives related to curcumin [8, 9]. It was even studied as an antimicrobial agent suitable for textile materials. Results showed that curcumin in combination with aloe vera and chitosan could

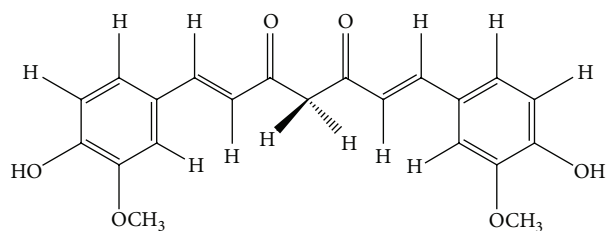


FIGURE 1: Chemical structure of curcumin.

be a potential suppressor for microbial growth in cotton, wool, and rabbit hair assessed by the exhaustion method [10]. Either the continuous or batch dyeing process with curcumin provided textiles with antimicrobial properties beside the color. Curcumin finished wool had semidurable antimicrobial activity, less durable to light exposure than home laundering with 45% and 30% inhibition rates against *Staphylococcus aureus* and *Escherichia coli*, respectively, after 30 cycles of home laundering [11]. Mixture of curcumin with other antimicrobial agents is used for the development of antimicrobial skin gels and emulsions with improved skin protection and wound dressing properties [12]. Composition of curcumin with hydrogel silver nanoparticles is used to increase the function of hydrogel silver nanocomposites as marked substances for antimicrobial applications and wound dressing [12]. Curcumin-loaded myristic acid microemulsion with the 0.86 $\mu\text{g}/\text{mL}$ of curcumin suitable for skin consumption inhibited 50% of the *S. epidermidis* growth as one of the nosocomial infectious agents. It showed 12-fold stronger inhibitory effect compared to curcumin activity dissolved in dimethyl sulfoxide (DMSO) [13].

2. Antibacterial Activity

Bacterial infections are among the important infectious diseases. Hence, over 50 years of extensive researches have been launched for achieving new antimicrobial medicines isolated from different sources. Despite progress in development of antibacterial agents, there are still special needs to find new antibacterial agents due to development of multidrug resistant bacteria [14]. The antibacterial study on aqueous extract of *C. longa* rhizome demonstrated the MIC (minimum inhibitory concentration) value of 4 to 16 g/L and MBC (minimum bactericidal concentration) value of 16 to 32 g/L against *S. epidermidis* ATCC 12228, *Staph. aureus* ATCC 25923, *Klebsiella pneumoniae* ATCC 10031, and *E. coli* ATCC 25922 [15]. The methanol extract of turmeric revealed MIC values of 16 $\mu\text{g}/\text{mL}$ and 128 $\mu\text{g}/\text{mL}$ against *Bacillus subtilis* and *Staph. aureus*, respectively [16]. The study of hexane and ethanol turmeric extract and curcuminoids (from ethyl acetate extract of curcuminoids isolated from *C. longa* with 86.5% curcumin value) against 24 pathogenic bacteria isolated from the chicken and shrimp showed the highest antimicrobial activity for ethanol extract with the MIC value of 3.91 to 125 ppt [17]. The hexane and methanol extracts of *C. longa* demonstrated antibacterial effect against

13 bacteria, namely, *Vibrio harveyi*, *V. alginolyticus*, *V. vulnificus*, *V. parahaemolyticus*, *V. cholerae*, *Bacillus subtilis*, *B. cereus*, *Aeromonas hydrophila*, *Streptococcus agalactiae*, *Staph. aureus*, *Staph. intermedius*, *Staph. epidermidis*, and *Edwardsiella tarda*. However, curcuminoids elicited inhibitory activities against 8 bacteria of *Str. agalactiae*, *Staph. intermedius*, *Staph. epidermidis*, *Staph. aureus*, *A. hydrophila*, *B. subtilis*, *B. cereus*, and *Ed. tarda*. Hexane extract and curcuminoids exhibited the MIC values of 125 to 1000 ppt and 3.91 to 500 ppt, respectively [17]. Indeed, it was shown that the addition of 0.3% (w/v) of aqueous curcumin extract to the cheese caused the reduction in bacterial counts of *Salmonella typhimurium*, *Pseudomonas aeruginosa*, and *E. coli* O157:H7. Moreover, it has decreased the *Staph. aureus*, *B. cereus*, and *Listeria monocytogenes* contamination after 14 days of cold storage period [18]. Turmeric oil as a byproduct from curcumin manufacture also was found effective against *B. subtilis*, *B. coagulans*, *B. cereus*, *Staph. aureus*, *E. coli*, and *P. aeruginosa* [19]. Curcumin also exhibited inhibitory activity on methicillin-resistant *Staph. aureus* strains (MRSA) with MIC value of 125–250 $\mu\text{g}/\text{mL}$ [20]. The *in vitro* investigation of 3 new compounds of curcumin, namely, indium curcumin, indium diacetyl curcumin, and diacetyl curcumin, against *Staph. aureus*, *S. epidermidis*, *E. coli*, and *P. aeruginosa* revealed that indium curcumin had a better antibacterial effect compared to curcumin itself and it may be a good compound for further *in vivo* studies. However, diacetylcurcumin did not exhibit any antibacterial effect against tested bacteria [21]. These results demonstrated promising antibacterial activity for different curcumin derivatives as well. The stability and assembly of FtsZ protofilaments as a crucial factor for bacterial cytokinesis are introduced as a possible drug target for antibacterial agents. Curcumin suppressed the *B. subtilis* cytokinesis through induction of filamentation. It also without significantly affecting the segregation and organization of the nucleoids markedly suppressed the cytokinetic Z-ring formation in *B. subtilis* [22]. It was demonstrated that curcumin reduces the bundling of FtsZ protofilaments associated with the binding ability to FtsZ with a dissociation constant of 7.3 μM . It showed that curcumin via inhibition of assembly dynamics of FtsZ in the Z-ring can possibly suppress the bacterial cell proliferation as one of the probable antibacterial mechanisms of action [22]. The study on *E. coli* and *B. subtilis* demonstrated that curcumin by the inhibitory effect against FtsZ polymerization could suppress the FtsZ assembly leading to disruption of prokaryotic cell division [23].

Also, curcumin showed significant antibacterial activity with MIC values between 5 and 50 $\mu\text{g}/\text{mL}$ against 65 clinical isolates of *Helicobacter pylori* [41]. Curcumin also has an inhibitory effect on NF- κ B activation and as a result on the release of IL-8 and cell scattering which led to a reduction in inflammation of gastric tissue as the main consequence for *H. pylori* in stomach. It inhibits the I κ B α degradation, the activity of NF- κ B DNA-binding and I κ B kinase α and β (IKK α and β) [42]. Indeed, curcumin inhibited the matrix metalloproteinase-3 and metalloproteinase-9 activity (MMP-3 and MMP-9) as inflammatory molecules involved in *H. pylori* infection in mice and in cell culture with a dose dependent manner [43]. Curcumin showed more efficient

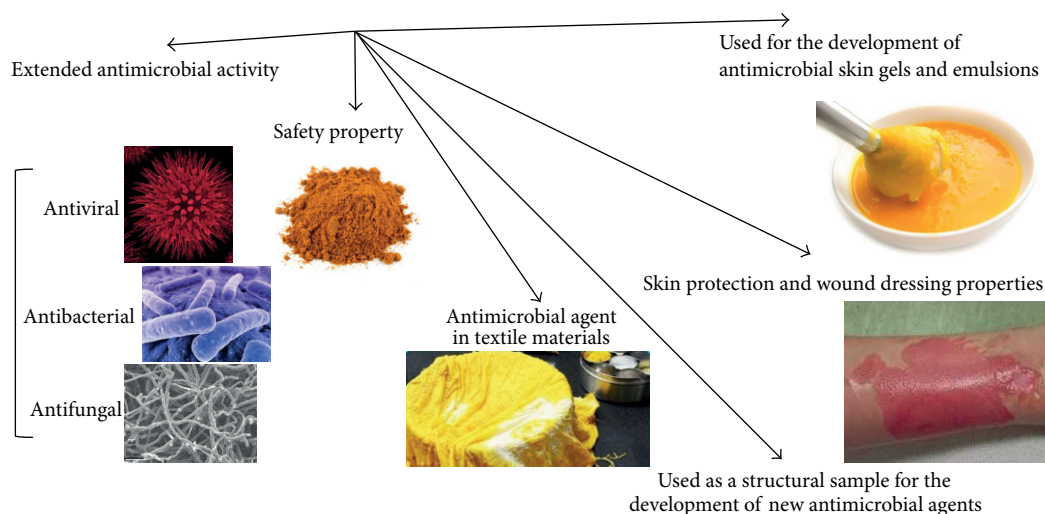


FIGURE 2: Importance of curcumin in antimicrobial studies.

therapeutic index than conventional triple therapy of *H. pylori* on MMP-3 and MMP-9 via reduction of activator protein-1 and proinflammatory molecule activation in *H. pylori* infected gastric tissues [43]. *In vivo* study of antibacterial effect of curcumin on *H. pylori* compared to OAM (Omeprazole, Amoxicillin, and Metronidazole) treatment revealed poor activity for eradication of *H. pylori* (5.9% versus 78.9% for OAM treatment). The reduction in inflammatory cytokine production was not reported from *pylori*-infected patients treated with curcumin [44]. The *in vivo* study of 1-week nonantibiotic therapy comprised of curcumin, pantoprazole, N-acetylcysteine, and lactoferrin against *H. pylori* infection was not effective for the eradication of *H. pylori*. However, the decrease in immunological criteria of gastric inflammation and dyspeptic symptoms was reported after 2 months of treatment schedule [45]. Nevertheless, the curcumin administration to the rats with *H. pylori*-induced gastric inflammation revealed a significant reduction in macromolecular leakage and NF- κ B activation [46]. In an *in vivo* study of *H. pylori*-infected C57BL/6 mice administered with curcumin exhibited immense therapeutic potential and pronounced eradication effect against *H. pylori* infection associated with restoration of gastric damage [41].

2.1. Synergistic Antimicrobial Activity. The outburst of drug resistant microbial strains necessitates the studies for synergistic effects of antibiotics in combination with plant's derivatives to develop the antimicrobial cocktail with a wider spectrum of activity and reduction of adverse side effects of antimicrobial agents. *Staph. aureus* resistance to the penicillin group of antibiotics is increasing associated with appearance of adverse side effects such as hypersensitivity and anaphylactic reactions [47]. The synergistic activity of curcuminoids and ampicillin combination demonstrated pronounced reduction in the MIC of ampicillin against either clinical strain or *Staph. aureus* ATCC 25923 strain. Bacteriocin subtilisin isolated from *B. amyloliquefaciens* in combination with encapsulated curcumin revealed partial synergism against

wild-type and nisin sensitive strains of *L. monocytogenes* Scott A [48]. In another *in vivo* study using 500 μ g/disc of curcumin against clinical isolate of *Staph. aureus* the synergistic activity with antibiotics of cefixime, cefotaxime, vancomycin, and tetracycline was demonstrated [49]. The results proved that consumption of turmeric during the treatment of *Staph. aureus* infections with these antibiotics especially cefixime can be possibly helpful. Curcumin also demonstrated a synergistic effect in combination with some antibiotics, including ampicillin, oxacillin, and norfloxacin against methicillin-resistant *Staph. aureus* strain (MRSA) [20]. The synergistic effect of curcumin with ciprofloxacin against MRSA has also been reported, although there is an evidence of its antagonistic activity against *S. typhi* and *S. typhimurium* in combination with ciprofloxacin [49, 50].

Strongly bound metal complexes to antimicrobial agents are introduced as another possible way for synergistic activity of respective antimicrobial agents through elevation of the binding effect of them to the bacterial walls. Complexes of curcumin with cobalt nanoparticles showed increased antibacterial activity against *E. coli* [51]. Additionally, fabrication of silver nanocomposite films impregnated with curcumin showed the stronger antibacterial activity against *E. coli*. It was shown that the bactericidal activity of sodium carboxymethyl cellulose silver nanocomposite films (SCMC SNCFs) as an effective antibacterial material was improved by loading of curcumin with SCMC SNCFs [52]. In another *in situ* investigation, the synergistic effect of curcumin encapsulated chitosan-[poly (vinyl alcohol)] silver nanocomposite films was shown. The novel antimicrobial films with pronounced antimicrobial exhibition against *E. coli* proved to be potential antibacterial material for treating infections or wound dressing [53].

2.2. Anti-Biofilm Activity. Secretion of exopolysaccharide alginate via different stimulators such as aminoglycosides and imipenem consumption caused the increase in biofilm volume of *P. aeruginosa*. Anti-biofilm activity of curcumin

against two strains of *P. aeruginosa* isolated from deep oropharyngeal swap samples of two cystic fibrosis patients with MIC values of 16 $\mu\text{g}/\text{mL}$ was investigated by crystal violet staining method. The curcumin treatment of the strains with MIC concentrations did not reveal noteworthy elevation in biofilm optical density [54]. In addition, in another study curcumin showed the potential for reduction of biofilm initiation genes, inhibition of 31 quorum sensing (QS) genes, and downregulation of virulence factors including acyl homoserine lactone (HSL) production, elastase/protease activity, and pyocyanin biosynthesis. The antimicrobial activities led to reduction of pathogenicity in *Arabidopsis thaliana* and *Caenorhabditis elegans* as whole plant and animal infected models with *P. aeruginosa* [7]. The results exhibited that curcumin can be a potential candidate for *P. aeruginosa* infections in special infections characterized by biofilm formation, although further comprehensive studies are needed for the approval.

In some cases the adverse effects of curcumin against different antibiotics were shown. Ciprofloxacin is the most effective antibiotic against typhoidal and nontyphoidal infection of *Salmonella*. The main mechanism for antibacterial activity of ciprofloxacin is through SOS response, induction of chromosome fragmentation, and the production of ROS in the bacterial cell. The *in vivo* and *in vitro* investigations on curcumin together with ciprofloxacin showed that, through interference with ciprofloxacin activity, it caused an elevation in proliferation of *Salmonella typhi* and *Salmonella enterica* serovar Typhimurium (*S. typhimurium*). Although curcumin could not suppress the ciprofloxacin-induced gyrase inhibition, it protected *Salmonella* against oxidative burst induced by interferon γ (IFN γ) or ciprofloxacin via owing strong antioxidant effect. The results demonstrated the curcumin by suppressing the antibacterial effect of IFN γ or ciprofloxacin might increase the *Salmonella* pathogenesis [55]. The study of curcumin activity in a murine model of typhoid fever exhibited an elevation of *Salmonella typhimurium* pathogenicity and increased resistance to antimicrobial agents including antimicrobial peptides, nitrogen species, and reactive oxygen. Upregulation of genes involved in antioxidative function like *mntH*, *sitA*, and *sodA* as well as other genes involved in resistance to antimicrobial peptides including *pmrD* and *pmrHFIJKLM* was considered as a possible cause for the mentioned elevated tolerance. Curcumin also induced upregulation effect on SPI2 genes involved in intracellular survival and downregulation activity on SPII genes involved for entry within epithelial cells. This information proved that the indiscriminate use of curcumin should probably inhibit the pathogenesis of *Salmonella* [55]. Additionally, curcumin also at a dose 500 $\mu\text{g}/\text{disc}$ showed antagonistic activity on the bactericidal effect of nalidixic acid against clinical strain of *Staph. aureus* investigated by disc diffusion method [49].

3. Antiviral Activity

Lack of effective therapeutics for the most of viral diseases, emergence of antiviral drug resistance, and high cost of some antiviral therapies necessitate finding new effective antiviral compounds [56, 57]. Additionally, the existing antiviral

therapies are not always well-tolerated or quite effective and satisfactory [58]. Hence, the increasing requirement for antiviral substances will be more highlighted. Plants as a rich source of phytochemicals with different biological activities including antiviral activities are in interest of scientists [59, 60]. It has been demonstrated that curcumin as a plant derivative has a wide range of antiviral activity against different viruses. Inosine monophosphate dehydrogenase (IMPDH) enzyme due to rate-limiting activity in the *de novo* synthesis of guanine nucleotides is suggested as a therapeutic target for antiviral and anticancer compounds. Among the 15 different polyphenols, curcumin through inhibitory activity against IMPDH effect in either noncompetitive or competitive manner is suggested as a potent antiviral compound via this process [61]. The study of different bioconjugates of curcumin, namely, di-*O*-tryptophanylphenylalanine curcumin, di-*O*-decanoyl curcumin, di-*O*-pamitoyl curcumin, di-*O*-bis-(γ,γ)folyl curcumin, C^4 -ethyl-*O*- γ -folyl curcumin, and 4-*O*-ethyl-*O*- γ -folyl curcumin, against variety of viruses including parainfluenza virus type 3 (PIV-3), feline infectious peritonitis virus (FIPV), vesicular stomatitis virus (VSV), herpes simplex virus (HSV), flock house virus (FHV), and respiratory syncytial virus (RSV) assessed by MTT test showed the potent antiviral activity of curcumin and its bioconjugates against different viral pathogens for further studies. Also, di-*O* tryptophanylphenylalanine curcumin and di-*O*-decanoyl curcumin revealed remarkable antiviral activity against VSV and FIPV/FHV with EC_{50} values of 0.011 μM and 0.029 μM , respectively. However, bioconjugates did not exhibit significant antiviral activity against III_B and ROD strains of type 1 human immunodeficiency virus (HIV-1) in MT-4 cells [62]. Table 1 summarizes the antiviral activity of *C. longa* and curcumin and possible mechanisms underlying inhibitory effects.

Viral long terminal repeat (LTR) has a critical role in transcription of type 1 human immunodeficiency virus (HIV-1) provirus. Inhibition of LTR activity can be a possible pathway for antiviral drug candidates in order to block HIV-1 replication [63, 64]. Curcumin proved to be an effective compound to inhibit the HIV-1 LTR-directed gene expression without any major effects on cell viability [24]. Curcumin and its derivatives, namely, reduced curcumin, allyl-curcumin, and tocopheryl-curcumin, revealed 70% to 85% inhibition in Tat protein transactivation of HIV-1 LTR measured by β -galactosidase activities of HeLa cells which in HIV-1 LTR was fused to the indicator of *lacZ* gene. Tocopheryl-curcumin demonstrated the most inhibition activity with 70% inhibition at 1 nM compared to 35% inhibition of curcumin at this concentration [25]. In addition, curcumin inhibited the acetylation of Tat protein of HIV significantly by p300 associated with suppression of HIV-1 multiplication. Curcumin by targeting the acetyltransferase proteins of p300/CREB-binding protein (CBP) can be a potent compound for combinatorial HIV therapeutics [28]. Curcumin was found to be an inhibitor of HIV-1 and HIV-2 protease with IC_{50} of 100 μM and 250 μM , respectively. The curcumin boron complexes exhibited noteworthy inhibition reduced to the IC_{50} value of 6 μM with time-dependent activity. The elevated affinity of

TABLE I: Antiviral activities of *Curcuma longa* L. and curcumin.

Virus	Antiviral substances	Description of antiviral activity type	Reference
HIV	Curcumin	Inhibition of HIV-1 LTR-directed gene expression	[24]
	Curcumin, reduced curcumin, allyl-curcumin, tocopheryl-curcumin	Inhibition of Tat-mediated transactivation of HIV-1 LTR	[25]
	Curcumin, curcumin boron complexes	Inhibition of HIV-1 and HIV-2 proteases	[26]
	Curcumin	Inhibition of HIV-1 Integrase	[27]
	Curcumin	Inhibition of Tat protein acetylation	[28]
	Curcumin	No antiviral effect in clinical trial	[29]
Influenza	Curcumin	Inhibition of haemagglutination	[30]
HSV-1	Curcumin, gallium-curcumin, Cu-curcumin	Reduction of HSV-1 replication	[31, 32]
HSV-2	Curcumin	Significant protection in mouse model	[33]
Coxsackievirus	Curcumin	Replication inhibition through UPS dysregulation	[34]
HBV	Aqueous extract	Suppression of HBV replication by increasing the p53 level	[35]
HCV	Curcumin	Decrease of HCV replication by suppressing the Akt-SREBP-1 pathway	[36]
HPV	Curcumin	Inhibition expression of viral oncoproteins of E6 and E7	[37]
HPV	Curcumin	Downregulation effect on the transcription of HPV-18	[38]
JEV	Curcumin	Reduction in production of infective viral particles	[39]
HTLV-1	Curcumin	Downregulation of JunD protein in HTLV-1-infected T-cell lines	[40]

boron derivatives of curcumin is possibly associated with the attachment of the orthogonal domains of the compound in intersecting sites within the substrate-binding cavity of the protease [26]. Integrase as another essential enzyme for HIV-1 replication was found to be inhibited by curcumin with IC_{50} value of $40 \mu M$. Inhibition of deletion mutant of integrase containing only amino acids 50–212 indicated that curcumin possibly interacts with catalytic core of the enzyme. The study of energy minimization and the structural analogs of curcumin elicited that an intramolecular stacking of two phenyl rings of curcumin is possibly responsible for anti-integrase activity via bringing the hydroxyl groups into close proximity [27]. However, rosmarinic acid and dicaffeoyl methane as two curcumin analogs showed noteworthy inhibitory activity against integrase of HIV-1 with IC_{50} values less than $10 \mu M$ with the slow rate of binding to the enzyme assessed by kinetic studies [65]. However, through a clinical trial investigation on curcumin as an anti-HIV compound in 40 patients in eight weeks it was shown that there is no reduction in viral load or elevation in CD4 counts. But patients claimed that they preferred to take the curcumin in order to tolerate the minor gastrointestinal sufferings and feel better [29]. This demonstrated that clinical trials can possibly show up with the results completely different from *in vitro* studies. The clinical trial of clear liquid soap containing 0.5% w/v ethanol extract of *C. longa* rhizome on HIV patients reduced the wound infections and 100% decrease in itching symptom and it also affected the abscess to convert to dryness scabs (78.6%) within 2 weeks [16].

Curcumin showed the anti-influenza activity against influenza viruses PR8, H1N1, and H6N1. The results showed

more than 90% reduction in virus yield in cell culture using $30 \mu M$ of curcumin. The plaque reduction test elicited the approximate EC_{50} of $0.47 \mu M$ for curcumin against influenza viruses [30]. In H1N1 and also H6N1 subtypes, the inhibition of haemagglutinin interaction reflected the direct effect of curcumin on infectivity of viral particles and this has proved by time of drug addiction experiment. Additionally, unlike amantadine, viruses developed no resistance to curcumin. The methoxyl derivatives of curcumin also did not show noteworthy role in the haemagglutination [30]. These results proved the significant potential of curcumin for inhibition of influenza.

In vitro study of curcumin and its derivatives, namely, gallium-curcumin and Cu-curcumin, exhibited remarkable antiviral activity against herpes simplex virus type 1 (HSV-1) in cell culture with IC_{50} values of 33.0 microg/mL, 13.9 microg/mL, and 23.1 microg/mL, respectively. The 50% cytotoxic concentration (CC_{50}) of the respective compounds on Vero cell line showed to be 484.2 $\mu g/mL$, 255.8 $\mu g/mL$, and 326.6 $\mu g/mL$, respectively [31]. Curcumin considerably decreased the immediate early (IE) gene expression and infectivity of HSV-1 in cell culture assays. Curcumin has an effect on recruitment of RNA polymerase II to IE gene promoters through mediation of viral transactivator protein VP16, by an independent process of p300/CBP histone acetyl transferase effect [32]. *In vitro* replication of HSV-2 could be decreased by curcumin with ED_{50} value of 0.32 mg/mL [32]. Moreover, an *in vivo* study on mouse model with intravaginal HSV-2 challenge showed significant protection against HSV-2 infection due to administration of curcumin. This study showed that curcumin can be a good candidate

for developing the antiviral products used intravaginally by women for protection against sexually transmitted herpes virus infection [33]. Indeed, a metallo-herbal complex of curcumin with copper (Cu^{2+}) demonstrated microbicidal effect for further studies of vaginal gel with antiviral activity [66].

Coxsackieviruses cause a variety of diseases such as dilated cardiomyopathy and myocarditis. Coxsackievirus B3 (CVB3) in spite of extensive investigations is still a major human pathogen without specific effective and approved treatment [67, 68]. Curcumin exhibited the antiviral activity against coxsackievirus by reduction of viral RNA expression, protein synthesis, and virus titer. In addition, it was found to have a protective effect on cells against virus-induced apoptosis and cytopathic activity. Analysis of different pathways showed that curcumin forced its potent antiviral effect in inhibition of coxsackievirus replication through dysregulation of the ubiquitin-proteasome system (UPS) [34]. The recent studies proved that the UPS-mediated protein modification or degradation is an essential factor in the regulation of coxsackievirus replication [69].

Liver diseases associated with viral infections are major pandemics [70]. The fact that hepatitis B virus (HBV) elevates the possibility for the hepatocellular carcinoma (HCC) development some 100-fold and 695,900 deaths occurred due to liver cirrhosis and HCC worldwide in 2008 makes the need to find new antivirals against hepatitis viruses [71, 72]. The study of antiviral effect of aqueous extract of *Curcuma longa* rhizoma against HBV in HepG 2.2.15 cells containing HBV genomes showed repression of HBsAg secretion from liver cells without any cytotoxic effect. It also suppressed the HBV particles production and the rate of mRNA production of HBV on infected cells. The *Curcuma longa* extract suppressed HBV replication by increasing the rate of p53 protein through enhancing the stability of the protein as well as transactivating the transcription of p53 gene. It was understood that the extract has suppressed HBV enhancer I and X promoter leading to repression of HBx gene transcription by affecting p53 [35]. *In vitro* investigation of the antiviral activity of curcumin Huh7 replicon cells expressing the hepatitis C virus (HCV) indicated that curcumin can be a potent anti-HCV compound. Results showed the decrease in HCV gene expression and replication through suppressing the Akt-SREBP-1 pathway. In addition, the mixture of curcumin and $\text{IFN}\alpha$ as the known anti-HCV therapy induced profound inhibitory activity on HCV replication and demonstrated that curcumin can be possibly used as a complementary therapy for HCV [36].

High-risk human papillomaviruses (HPVs) infection via the expression of E6 and E7 viral oncoproteins has a critical role for development of cervical carcinoma. Curcumin showed the inhibitory activity against the expression of E6 and E7 genes of HPV-16 and HPV-18 as two main highly oncogenic human papilloma viruses [37]. The transcription factor AP-1 is a critical factor for transcriptional regulation of high-risk HPVs such as HPV-16 and HPV-18. Curcumin downregulates the AP-1 binding activity in HeLa cells with decreasing effect on the transcription of HPV-18 [38]. The results showed that curcumin through apoptosis modulation

and also prevention of $\text{NF}\kappa\text{B}$ and AP-1 translocation associated with downregulation of viral oncogenes and decreasing the transcription of HPVs can be a good candidate for the management of highly oncogenic HPV infections [37, 38].

Japanese encephalitis virus (JEV) as an important endemic arbovirus in Southeast Asia is a major cause of acute encephalopathy which generally affects the children and leads to death in one third of patients. The permanent neuropsychiatric sequel is a complication for many survivors from JEV due to ineffective therapeutic measure [73]. The investigation of antiviral activity of curcumin on Neuro2a cell line infected with JEV showed reduction in production of infectious viral particles through inhibition of ubiquitin-proteasome system. The results of *in vitro* study indicated that curcumin through modulating cellular levels of stress-related proteins, reducing proapoptotic signaling molecules, restoration of cellular membrane integrity, and reduction in reactive oxygen species in cellular level imparts neuroprotection and can be a potential for further investigations [39].

Oncogenesis by human T-cell leukemia virus type 1 as an etiologic factor of adult T-cell leukemia (ATL) is critically dependent on the activation of the activator protein 1 (AP-1) [74]. The DNA binding and transcriptional effect of AP-1 in HTLV-1-infected T-cell lines were suppressed by curcumin treatment. Curcumin also inhibited the expression of JunD protein as an important factor in AP-1-DNA complex in HTLV-1-infected T-cells as well as HTLV-1 Tax-induced AP-1 transcriptional effect. Cell cycle arrest and inducing of apoptosis were found to be possible mechanisms against HTLV-1 replication in infected T-cell line by curcumin. Suppression of AP-1 activity possibly through decreasing the expression of JunD protein is introduced as a possible pathway for anti-ATL activity of curcumin [40].

4. Antifungal Activity

Substances and extracts isolated from different natural resources especially plants have always been a rich arsenal for controlling the fungal infections and spoilage. Due to extensive traditional use of turmeric in food products, various researches have been done in order to study the turmeric and curcumin with the aspect of controlling fungal related spoilage and fungal pathogens. The study of addition the turmeric powder in plant tissue culture showed that turmeric at the 0.8 and 1.0 g/L had appreciable inhibitory activity against fungal contaminations [75]. The methanol extract of turmeric demonstrated antifungal activity against *Cryptococcus neoformans* and *Candida albicans* with MIC values of 128 and 256 $\mu\text{g}/\text{mL}$, respectively [16]. The study of hexane extract of *C. longa* at 1000 mg/L demonstrated antifungal effect against *Rhizoctonia solani*, *Phytophthora infestans*, and *Erysiphe graminis*. It was also shown that 1000 mg/L of ethyl acetate extract of *C. longa* exhibited inhibitory effect against *R. solani*, *P. infestans*, *Puccinia recondita*, and *Botrytis cinerea*. Curcumin at 500 mg/L also showed antifungal activity against *R. solani*, *Pu. recondita*, and *P. infestans* [76]. Curcumin and turmeric oil exert antifungal effect against two phytophagous fungi, namely, *Fusarium solani* and *Helminthosporium oryzae*. Turmeric oil exhibited

the most effective antifungal activity against *F. solani* and *H. oryzae* with IC_{50} of 19.73 and 12.7 $\mu\text{g}/\text{mL}$, respectively [77]. The crude methanol extract of *C. longa* has inhibitory effect against some clinical isolates of dermatophytes. It was demonstrated that 18-month-old and freshly distilled oil isolated from rhizome of *C. longa* showed the most potent antifungal effect against 29 clinical isolates of dermatophytes with MIC values of 7.2 and 7.8 mg/mL , respectively [78]. *Trichophyton rubrum*, *T. mentagrophytes*, *Epidermophyton floccosum*, and *Microsporium gypseum* were suppressed by 1:40–1:320 dilutions of turmeric oil. An *in vivo* study on infected guinea pigs with *T. rubrum* demonstrated that dermal application of turmeric oil (dilution 1:80) induced an improvement in healing of the lesions after 2–5 days and it caused the lesions after 6–7 days of consumption to vanish. Turmeric oil also showed activity against pathogenic molds such as *Sporothrix schenckii*, *Exophiala jeanselmei*, *Fonsecaea pedrosoi*, and *Scedosporium apiospermum* with MIC values of 114.9, 459.6, 459.6, and 114.9 $\mu\text{g}/\text{mL}$, respectively [79]. However, curcumin showed more significant effect against *Paracoccidioides brasiliensis* than fluconazole, although it did not affect the growth of *Aspergillus* species [80]. The possible mechanism underlying the mentioned antifungal effect was found to be downregulation of $\Delta^{5,6}$ desaturase (ERG3) leading to significant reduction in ergosterol of fungal cell. Reduction in production of ergosterol results in accumulations of biosynthetic precursors of ergosterol which leads to cell death via generation of ROS [81]. Reduction in proteinase secretion and alteration of membrane-associated properties of ATPase activity are other possible critical factors for antifungal activity of curcumin [82].

Resistant strain development among the *Candida* species against existing antifungal drugs became a critical problem for therapeutic strategies. Thereby, finding new anti-*Candida* substances seems to be crucial [83]. The study of curcumin against 14 strains of *Candida* including 4 ATCC strains and 10 clinical isolates showed that curcumin is a potent fungicide compound against *Candida* species with MIC values range from 250 to 2000 $\mu\text{g}/\text{mL}$ [82]. In another study, anti-*Candida* activity of curcumin was demonstrated against 38 different strains of *Candida* including some fluconazole resistant strains and clinical isolates of *C. albicans*, *C. glabrata*, *C. krusei*, *C. tropicalis*, and *C. guilliermondii*. The MIC_{90} values for sensitive and resistant strains were 250–650 and 250–500 $\mu\text{g}/\text{mL}$, respectively. Intracellular acidification via inhibition of H^+ -extrusion was identified as possible mechanism for cell death of *Candida* species [84]. The development of hyphae was proved to be inhibited by curcumin through targeting the global suppressor thymidine uptake 1 (TUP1) [81, 85]. Curcumin also showed inhibitory effect on *Cryptococcus neoformans* and *C. dubliniensis* with MIC value of 32 mg/L [80]. One of the major complications during therapies against chronic asthma is oropharyngeal candidiasis. Curcumin as a potential candidate for the treatment of candidosis with anti-inflammatory activity was studied in a murine model of asthma. Oral administrator of Curcumin is more effective than dexamethasone in reducing fungal burden in BALB/c mice. It also significantly decreased pathological changes

in asthma [86]. Adhesion of *Candida* species isolated from AIDS patients to buccal epithelial cells is also markedly inhibited by curcumin and it was found to be more effective compared to fluconazole [80].

The investigation of curcumin mediation for photodynamic therapy can reduce the biofilm biomass of *C. albicans*, *C. glabrata*, and *C. tropicalis*. The results demonstrated that association of four LED fluences for light excitation with 40 μM concentration of curcumin at 18 J/cm^2 inhibited up to 85% metabolic activity of the tested *Candida* species. The use of curcumin with light proved to be an effective method for noteworthy improvement in the antifungal activity against planktonic form of the yeasts [87]. Photodynamic effect considerably decreased *C. albicans* viability in either planktonic or biofilm cultures probably through increasing the uptake of curcumin by cells. However, to a lesser extent, photodynamic therapy was found to be phototoxic to the macrophages. [88]. A study on a murine model of oral candidiasis was done for gathering reliable data for curcumin-mediated photodynamic therapy efficacy *in vivo*. Results proved that all exposures to curcumin with LED light markedly inhibited the *C. albicans* viability after photodynamic therapy without harming the host tissue of mice. However, 80 μM of curcumin in association with light showed the best decrease in colony counts of *C. albicans* [89]. These results showed that curcumin is a high potential photosensitizer compound for fungicidal photodynamic therapy especially against *Candida* species.

The strong antifungal activity of *C. longa* rhizome and its low side effect were the main reasons to investigate its probable synergistic effect with existing fungicides. The synergistic activity of curcumin with five azole and two polyene drugs including voriconazole, itraconazole, ketoconazole, miconazole, fluconazole, amphotericin B, and nystatin showed 10–35-fold reduction in the MIC values of the fungicides against 21 clinical isolates of *C. albicans*. The synergistic activity of curcumin with amphotericin B and fluconazole could be associated with the accumulation of ROS which will be suppressed by adding an antioxidant [85]. The study of 200 clinical isolates of *Candida* species including *C. tropicalis*, *C. kefyr*, *C. krusei*, *C. guilliermondii*, *C. glabrata*, *C. parapsilosis*, and *C. albicans* demonstrated fungicidal activity for curcumin with MIC value of 32–128 $\mu\text{g}/\text{mL}$. Combination of curcumin with amphotericin B also exhibited synergistic activity against tested *Candida* species, although fluconazole and curcumin in some cases showed additive effects rather than synergistic activity. These results proved that combination of curcumin with existing fungicidal agents can provide more significant effect against systemic fungal infections like candidemia and candidosis [90]. *In silico* analysis demonstrated that curcumin by attaching to albumin serum in a separate binding site of amphotericin B and forming the complex alleviated the adverse side effect of amphotericin B via delaying the red cell lysis. The stability and aqueous solubility of the complex of curcumin and amphotericin B with albumin serum can be a potential candidate for the treatment of visceral leishmaniasis and systemic fungal infections [91]. The *in vivo* study of combination of curcumin and piperine in

murine model of *Candida* infection also revealed synergistic effect with noteworthy fungal load reduction in kidney of Swiss mice [85]. The mixture of curcumin and ascorbic acid against different strains of *Candida* also exhibited 5- to 10-fold reduction of MIC values compared to the time that curcumin was tested alone [92]. These synergistic effects showed that curcumin in combination with different fungicide materials can significantly elicit synergistic activity to enhance the efficacy of existing antifungal strategies.

5. Enhancing the Bioavailability and Solubility of Curcumin to Improve Antimicrobial Activities

The optimum potential of curcumin is limited because of poor oral bioavailability and insufficient solubility in aqueous solvents leading to poor absorption, fast metabolism, and quick systemic elimination [5, 93]. For overcoming this obstacle, nanocarriers like curcumin-loaded PLGA (poly lactide-co-glycolide) and curcumin nanoparticle formulation were investigated and their better bioactivity and bioavailability as well as increased cellular uptake compared to curcumin were reported [5]. Another study revealed that heat-extracted curcumin elevated the solubility of curcumin 12-fold without significant disintegration due to heat treatment. Modification of 4-hydroxy-2-nonenal (HNE) as a critical oxidation by-product involved in disease pathogenesis via cytotoxicity, genotoxicity, and mutagenicity is inhibited 80% by heat-solubilized curcumin and suggested a possible mechanism for inducing bioactivity of curcumin [94]. The study of nanocurcumin as a nanoparticle of curcumin with the size of 2–40 nm processed by a wet-milling technique, showed curcumin to be more freely dispersible in water leading to more significant antimicrobial activity against *Staph. aureus*, *E. coli*, *P. aeruginosa*, *B. subtilis*, and two fungi of *P. notatum* and *A. niger* due to reduced particle size and enhanced bioavailability [95, 96]. However, nanocurcumin demonstrated more noteworthy activity against Gram-positive bacteria rather than Gram-negatives [95]. In another study to improve the stability and solubility of curcumin, microencapsulation process was investigated. Microcapsule of curcumin with improved solubility is suitable as a preservative and colorant in food industry and it exhibited potent antimicrobial effect against food-borne pathogens including *E. coli*, *Staph. aureus*, *B. subtilis*, *B. cereus*, *Yersinia enterocolitica*, *Penicillium notatum*, and *Saccharomyces cerevisiae* with MIC values ranging from 15.7 to 250 µg/mL. It was demonstrated that Gram-positive bacteria were more susceptible to the microcapsulated curcumin compared to Gram-negatives. However, antifungal effect was found to be stronger than the bactericidal effect [97, 98].

6. Conclusion

All previous investigations have shown the extensive antimicrobial activity of curcumin, although *in vivo* studies in some cases reported the less effective results of curcumin inhibitory effect. Among all former studies on antibacterial

activity of curcumin the most promising result is against *Helicobacter pylori*, at least for using the curcumin as a complementary compound in combination with other existing medicines to decrease the symptoms of gastritis. The extensive antiviral effects of curcumin against different viral pathogens nominate this compound as an antiviral drug candidate to develop new antivirals from natural resources against sensitive viruses especially by developing different curcumin derivatives. However, using curcumin or its derivatives as antiviral compounds needs further investigations. Regarding the studies on antifungal activities of curcumin the most significant effect was found against *Candida* species and *Paracoccidioides brasiliensis*, although curcumin revealed fungicide effect against various fungi. In spite of various biological activities of curcumin, no real clinical uses have been reported for this compound and still clinical trials are undergoing for different ailments and diseases, namely, colon and pancreatic cancers, multiple myeloma, myelodysplastic syndromes, Alzheimer, and psoriasis [99]. Until 2013, more than 65 clinical trials on curcumin have been carried out, and still more is underway. This polyphenol compound is now used as a supplement in several countries, namely, China, India, Japan, Korea, South Africa, the United States, Thailand, and Turkey [100].

Conflict of Interests

The authors declare that there is no conflict of interests regarding the publication of this paper.

Acknowledgment

The authors would like to thank University of Malaya for University Malaya Research Flagship Grant (UMRG) (FL001-13HTM) and Postgraduate Research Grant (PPP) (PG005-2012B).

References

- [1] H. P. T. Ammon and M. A. Wahl, "Pharmacology of *Curcuma longa*," *Planta Medica*, vol. 57, no. 1, pp. 1–7, 1991.
- [2] P. K. Lai and J. Roy, "Antimicrobial and chemopreventive properties of herbs and spices," *Current Medicinal Chemistry*, vol. 11, no. 11, pp. 1451–1460, 2004.
- [3] R. K. Maheshwari, A. K. Singh, J. Gaddipati, and R. C. Srimal, "Multiple biological activities of curcumin: a short review," *Life Sciences*, vol. 78, no. 18, pp. 2081–2087, 2006.
- [4] H. Hayakawa, Y. Minanyia, K. Ito, Y. Yamamoto, and T. Fukuda, "Difference of curcumin content in *Curcuma longa* L., (Zingiberaceae) caused by Hybridization with other *Curcuma* species," *American Journal of Plant Sciences*, vol. 2, no. 2, pp. 111–119, 2011.
- [5] P. Anand, H. B. Nair, B. Sung et al., "Design of curcumin-loaded PLGA nanoparticles formulation with enhanced cellular uptake, and increased bioactivity *in vitro* and superior bioavailability *in vivo*," *Biochemical Pharmacology*, vol. 79, no. 3, pp. 330–338, 2010.
- [6] C. A. C. Araújo and L. L. Leon, "Biological activities of *Curcuma longa* L.," *Memorias do Instituto Oswaldo Cruz*, vol. 96, no. 5, pp. 723–728, 2001.

- [7] T. Rudrappa and H. P. Bais, "Curcumin, a known phenolic from *Curcuma longa*, attenuates the virulence of *Pseudomonas aeruginosa* PAO1 in whole plant and animal pathogenicity models," *Journal of Agricultural and Food Chemistry*, vol. 56, no. 6, pp. 1955–1962, 2008.
- [8] P. LaColla, E. Tramontano, C. Musiu, M. E. Marongiu, E. Novellino, and G. Greco, "Curcumin-like derivatives with potent activity against HIV-1 integrase: synthesis, biological evaluation and molecular modeling," *Antiviral Research*, vol. 37, no. 3, pp. 57–57, 1998.
- [9] P. Anand, A. B. Kunnumakkara, R. A. Newman, and B. B. Aggarwal, "Bioavailability of curcumin: problems and promises," *Molecular Pharmaceutics*, vol. 4, no. 6, pp. 807–818, 2007.
- [10] L. Ammayappan and J. Jeyakodi Moses, "Study of antimicrobial activity of aloe vera, chitosan, and curcumin on cotton, wool, and rabbit hair," *Fibers and Polymers*, vol. 10, no. 2, pp. 161–166, 2009.
- [11] S. Han and Y. Yang, "Antimicrobial activity of wool fabric treated with curcumin," *Dyes and Pigments*, vol. 64, no. 2, pp. 157–161, 2005.
- [12] K. Varaprasad, K. Vimala, S. Ravindra, N. Narayana Reddy, G. Venkata Subba Reddy, and K. Mohana Raju, "Fabrication of silver nanocomposite films impregnated with curcumin for superior antibacterial applications," *Journal of Materials Science: Materials in Medicine*, vol. 22, no. 8, pp. 1863–1872, 2011.
- [13] C. H. Liu and H. Y. Huang, "Antimicrobial activity of curcumin-loaded myristic acid microemulsions against *Staphylococcus epidermidis*," *Chemical and Pharmaceutical Bulletin*, vol. 60, no. 9, pp. 1118–1124, 2012.
- [14] R. Wise, T. Hart, O. Cars et al., "Antimicrobial resistance. Is a major threat to public health," *British Medical Journal*, vol. 317, no. 7159, pp. 609–610, 1998.
- [15] N. Niamsa and C. Sittiwet, "Antimicrobial activity of *Curcuma longa* aqueous extract," *Journal of Pharmacology and Toxicology*, vol. 4, no. 4, pp. 173–177, 2009.
- [16] S. Ungphaiboon, T. Supavita, P. Singchangchai, S. Sungkarak, P. Rattanasuwan, and A. Itharat, "Study on antioxidant and antimicrobial activities of turmeric clear liquid soap for wound treatment of HIV patients," *Songklanakarinn Journal of Science and Technology*, vol. 27, no. 2, pp. 269–278, 2005.
- [17] O.-A. Lawhavit, N. Kongkathip, and B. Kongkathip, "Antimicrobial activity of curcuminoids from *Curcuma longa* L. on pathogenic bacteria of shrimp and chicken," *Kasetsart Journal—Natural Science*, vol. 44, no. 3, pp. 364–371, 2010.
- [18] I. M. Hosny, W. I. El Kholi, H. A. Murad, and R. K. El Dairouty, "Antimicrobial activity of Curcumin upon pathogenic microorganisms during manufacture and storage of a novel style cheese 'Karishcum'," *Journal of American Science*, vol. 7, pp. 611–618, 2011.
- [19] P. S. Negi, G. K. Jayaprakasha, L. J. M. Rao, and K. K. Sakariah, "Antibacterial activity of turmeric oil: a byproduct from curcumin manufacture," *Journal of Agricultural and Food Chemistry*, vol. 47, no. 10, pp. 4297–4300, 1999.
- [20] S. H. Mun, D. K. Joung, Y. S. Kim et al., "Synergistic antibacterial effect of curcumin against methicillin-resistant *Staphylococcus aureus*," *Phytotherapy Research*, vol. 19, no. 7, pp. 599–604, 2013.
- [21] S. Tajbakhsh, K. Mohammadi, I. Deilami et al., "Antibacterial activity of indium curcumin and indium diacetylcurcumin," *African Journal of Biotechnology*, vol. 7, no. 21, pp. 3832–3835, 2008.
- [22] D. Rai, J. K. Singh, N. Roy, and D. Panda, "Curcumin inhibits FtsZ assembly: an attractive mechanism for its antibacterial activity," *Biochemical Journal*, vol. 410, no. 1, pp. 147–155, 2008.
- [23] S. Kaur, N. H. Modi, D. Panda, and N. Roy, "Probing the binding site of curcumin in *Escherichia coli* and *Bacillus subtilis* FtsZ—a structural insight to unveil antibacterial activity of curcumin," *European Journal of Medicinal Chemistry*, vol. 45, no. 9, pp. 4209–4214, 2010.
- [24] C. J. Li, L. J. Zhang, B. J. Dezube, C. S. Crumpacker, and A. B. Pardee, "Three inhibitors of type 1 human immunodeficiency virus long terminal repeat-directed gene expression and virus replication," *Proceedings of the National Academy of Sciences of the United States of America*, vol. 90, no. 5, pp. 1839–1842, 1993.
- [25] S. Barthelemy, L. Vergnes, M. Moynier, D. Guyot, S. Labidalle, and E. Bahraoui, "Curcumin and curcumin derivatives inhibit Tat-mediated transactivation of type 1 human immunodeficiency virus long terminal repeat," *Research in Virology*, vol. 149, no. 1, pp. 43–52, 1998.
- [26] Z. Sui, R. Salto, J. Li, C. Craik, and P. R. Ortiz de Montellano, "Inhibition of the HIV-1 and HIV-2 proteases by curcumin and curcumin boron complexes," *Bioorganic & Medicinal Chemistry*, vol. 1, no. 6, pp. 415–422, 1993.
- [27] A. Mazumder, K. Raghavan, J. Weinstein, K. W. Kohn, and Y. Pommier, "Inhibition of human immunodeficiency virus type-1 integrase by curcumin," *Biochemical Pharmacology*, vol. 49, no. 8, pp. 1165–1170, 1995.
- [28] K. Balasubramanyam, R. A. Varier, M. Altaf et al., "Curcumin, a novel p300/CREB-binding protein-specific inhibitor of acetyltransferase, represses the acetylation of histone/nonhistone proteins and histone acetyltransferase-dependent chromatin transcription," *The Journal of Biological Chemistry*, vol. 279, no. 49, pp. 51163–51171, 2004.
- [29] J. S. James, "Curcumin: clinical trial finds no antiviral effect," *AIDS Treatment News*, no. 242, pp. 1–2, 1996.
- [30] D.-Y. Chen, J.-H. Shien, L. Tiley et al., "Curcumin inhibits influenza virus infection and haemagglutination activity," *Food Chemistry*, vol. 119, no. 4, pp. 1346–1351, 2010.
- [31] K. Zandi, E. Ramedani, K. Mohammadi et al., "Evaluation of antiviral activities of curcumin derivatives against HSV-1 in Vero cell line," *Natural Product Communications*, vol. 5, no. 12, pp. 1935–1938, 2010.
- [32] S. B. Kutluay, J. Doroghazi, M. E. Roemer, and S. J. Triezenberg, "Curcumin inhibits herpes simplex virus immediate-early gene expression by a mechanism independent of p300/CBP histone acetyltransferase activity," *Virology*, vol. 373, no. 2, pp. 239–247, 2008.
- [33] K. Z. Bourne, N. Bourne, S. F. Reising, and L. R. Stanberry, "Plant products as topical microbicide candidates: assessment of *in vitro* and *in vivo* activity against herpes simplex virus type 2," *Antiviral Research*, vol. 42, no. 3, pp. 219–226, 1999.
- [34] X. Si, Y. Wang, J. Wong, J. Zhang, B. M. McManus, and H. Luo, "Dysregulation of the ubiquitin-proteasome system by curcumin suppresses coxsackievirus B3 replication," *Journal of Virology*, vol. 81, no. 7, pp. 3142–3150, 2007.
- [35] H. J. Kim, H. S. Yoo, J. C. Kim et al., "Antiviral effect of *Curcuma longa* Linn extract against hepatitis B virus replication," *Journal of Ethnopharmacology*, vol. 124, no. 2, pp. 189–196, 2009.
- [36] K. Kim, K. H. Kim, H. Y. Kim, H. K. Cho, N. Sakamoto, and J. Cheong, "Curcumin inhibits hepatitis C virus replication via suppressing the Akt-SREBP-1 pathway," *FEBS Letters*, vol. 584, no. 4, pp. 707–712, 2010.

- [37] C. S. Divya and M. R. Pillai, "Antitumor action of curcumin in human papillomavirus associated cells involves downregulation of viral oncogenes, prevention of NFkB and AP-1 translocation, and modulation of apoptosis," *Molecular Carcinogenesis*, vol. 45, no. 5, pp. 320–332, 2006.
- [38] B. K. Prusty and B. C. Das, "Constitutive activation of transcription factor AP-1 in cervical cancer and suppression of human papillomavirus (HPV) transcription and AP-1 activity in HeLa cells by curcumin," *International Journal of Cancer*, vol. 113, no. 6, pp. 951–960, 2005.
- [39] K. Dutta, D. Ghosh, and A. Basu, "Curcumin protects neuronal cells from Japanese encephalitis virus-mediated cell death and also inhibits infective viral particle formation by dysregulation of ubiquitin-proteasome system," *Journal of Neuroimmune Pharmacology*, vol. 4, no. 3, pp. 328–337, 2009.
- [40] M. Tomita, H. Kawakami, J.-N. Uchihara et al., "Curcumin suppresses constitutive activation of AP-1 by downregulation of JunD protein in HTLV-1-infected T-cell lines," *Leukemia Research*, vol. 30, no. 3, pp. 313–321, 2006.
- [41] R. De, P. Kundu, S. Swarnakar et al., "Antimicrobial activity of curcumin against *Helicobacter pylori* isolates from India and during infections in mice," *Antimicrobial Agents and Chemotherapy*, vol. 53, no. 4, pp. 1592–1597, 2009.
- [42] A. Foryst-Ludwig, M. Neumann, W. Schneider-Brachert, and M. Naumann, "Curcumin blocks NF- κ B and the motogenic response in *Helicobacter pylori*-infected epithelial cells," *Biochemical and Biophysical Research Communications*, vol. 316, no. 4, pp. 1065–1072, 2004.
- [43] P. Kundu, R. De, I. Pal, A. K. Mukhopadhyay, D. R. Saha, and S. Swarnakar, "Curcumin alleviates matrix metalloproteinase-3 and -9 activities during eradication of *Helicobacter pylori* infection in cultured cells and mice," *PLoS ONE*, vol. 6, no. 1, Article ID e16306, 2011.
- [44] C. Koosirirat, S. Linpisarn, D. Changsom, K. Chawansuntati, and J. Wipasa, "Investigation of the anti-inflammatory effect of *Curcuma longa* in *Helicobacter pylori*-infected patients," *International Immunopharmacology*, vol. 10, no. 7, pp. 815–818, 2010.
- [45] F. Di Mario, L. G. Cavallaro, A. Nouvenne et al., "A curcumin-based 1-week triple therapy for eradication of *Helicobacter pylori* infection: something to learn from failure?" *Helicobacter*, vol. 12, no. 3, pp. 238–243, 2007.
- [46] K. Sintara, D. Thong-Ngam, S. Patumraj, N. Klaikeaw, and T. Chatsuwana, "Curcumin suppresses gastric NF- κ B activation and macromolecular leakage in *Helicobacter pylori*-infected rats," *World Journal of Gastroenterology*, vol. 16, no. 32, pp. 4039–4046, 2010.
- [47] F. C. Odds, "Synergy, antagonism, and what the checkerboard puts between them," *Journal of Antimicrobial Chemotherapy*, vol. 52, no. 1, p. 1, 2003.
- [48] T. Amrouche, K. S. Noll, Y. Wang, Q. Huang, and M. L. Chikindas, "Antibacterial activity of subtilisin alone and combined with curcumin, poly-L-lysine and zinc lactate against *Listeria monocytogenes* strains," *Probiotics and Antimicrobial Proteins*, vol. 2, no. 4, pp. 250–257, 2010.
- [49] K. M. Moghaddam, M. Iranshahi, M. C. Yazdi, and A. R. Shahverdi, "The combination effect of curcumin with different antibiotics against *Staphylococcus aureus*," *International Journal of Green Pharmacy*, vol. 3, no. 2, pp. 141–143, 2009.
- [50] S. A. Marathe, R. Kumar, P. Ajitkumar, V. Nagaraja, and D. Chakravorty, "Curcumin reduces the antimicrobial activity of ciprofloxacin against *Salmonella Typhimurium* and *Salmonella Typhi*," *Journal of Antimicrobial Chemotherapy*, vol. 68, no. 1, pp. 139–152, 2013.
- [51] S. Hatamie, M. Nouri, S. K. Karandikar et al., "Complexes of cobalt nanoparticles and polyfunctional curcumin as antimicrobial agents," *Materials Science and Engineering C*, vol. 32, no. 2, pp. 92–97, 2012.
- [52] K. Varaprasad, Y. M. Mohan, K. Vimala, and K. Mohana Raju, "Synthesis and characterization of hydrogel-silver nanoparticle-curcumin composites for wound dressing and antibacterial application," *Journal of Applied Polymer Science*, vol. 121, no. 2, pp. 784–796, 2011.
- [53] K. Vimala, Y. M. Mohan, K. Varaprasad et al., "Fabrication of curcumin encapsulated chitosan-PVA silver nanocomposite films for improved antimicrobial activity," *Journal of Biomaterials and Nanobiotechnology*, vol. 2, no. 1, pp. 55–64, 2011.
- [54] M. Karaman, F. Fırıncı, Z. Arıkan Ayyıldız, and I. H. Bahar, "Effects of Imipenem, Tobramycin and Curcumin on biofilm formation of *Pseudomonas aeruginosa* strains," *Mikrobiyoloji Bulteni*, vol. 47, no. 1, pp. 192–194, 2013.
- [55] S. A. Marathe, S. Ray, and D. Chakravorty, "Curcumin increases the pathogenicity of *Salmonella enterica* serovar typhimurium in Murine model," *PLoS ONE*, vol. 5, no. 7, Article ID e11511, 2010.
- [56] L. Tomei, S. Altamura, G. Paonessa, R. De Francesco, and G. Migliaccio, "HCV antiviral resistance: the impact of in vitro studies on the development of antiviral agents targeting the viral NS5B polymerase," *Antiviral Chemistry & Chemotherapy*, vol. 16, no. 4, pp. 225–245, 2005.
- [57] M. Lemoine, S. Nayagam, and M. Thursz, "Viral hepatitis in resource-limited countries and access to antiviral therapies: current and future challenges," *Future Virology*, vol. 8, no. 4, pp. 371–380, 2013.
- [58] E. De Clercq, "Strategies in the design of antiviral drugs," *Nature Reviews Drug Discovery*, vol. 1, no. 1, pp. 13–25, 2002.
- [59] S. A. A. Jassim and M. A. Naji, "Novel antiviral agents: a medicinal plant perspective," *Journal of Applied Microbiology*, vol. 95, no. 3, pp. 412–427, 2003.
- [60] S. Zorofchian Moghadamtousi, M. Hajrezaei, H. Abdul Kadir, and K. Zandi, "*Loranthus micranthus* Linn.: biological activities and phytochemistry," *Evidence-Based Complementary and Alternative Medicine*, vol. 2013, Article ID 273712, 9 pages, 2013.
- [61] I. Dairaku, Y. Han, N. Yanaka, and N. Kato, "Inhibitory effect of curcumin on IMP dehydrogenase, the target for anticancer and antiviral chemotherapy agents," *Bioscience, Biotechnology and Biochemistry*, vol. 74, no. 1, pp. 185–187, 2010.
- [62] R. K. Singh, D. Rai, D. Yadav, A. Bhargava, J. Balzarini, and E. De Clercq, "Synthesis, antibacterial and antiviral properties of curcumin bioconjugates bearing dipeptide, fatty acids and folic acid," *European Journal of Medicinal Chemistry*, vol. 45, no. 3, pp. 1078–1086, 2010.
- [63] G. J. Nabel, S. A. Rice, D. M. Knipe, and D. Baltimore, "Alternative mechanisms for activation of human immunodeficiency virus enhancer in T cells," *Science*, vol. 239, no. 4845, pp. 1299–1302, 1988.
- [64] B. R. Cullen and W. C. Greene, "Regulatory pathways governing HIV-1 replication," *Cell*, vol. 58, no. 3, pp. 423–426, 1989.
- [65] A. Mazumder, N. Neamati, S. Sunder et al., "Curcumin analogs with altered potencies against HIV-1 integrase as probes for biochemical mechanisms of drug action," *Journal of Medicinal Chemistry*, vol. 40, no. 19, pp. 3057–3063, 1997.

- [66] G. Chauhan, G. Rath, and A. K. Goyal, "In-vitro anti-viral screening and cytotoxicity evaluation of copper-curcumin complex," *Artificial Cells, Nanomedicine and Biotechnology*, vol. 41, no. 4, pp. 276–281, 2013.
- [67] C. Kawai, "From myocarditis to cardiomyopathy: mechanisms of inflammation and cell death: learning from the past for the future," *Circulation*, vol. 99, no. 8, pp. 1091–1100, 1999.
- [68] C.-K. Lee, K. Kono, E. Haas et al., "Characterization of an infectious cDNA copy of the genome of a naturally occurring, avirulent coxsackievirus B3 clinical isolate," *Journal of General Virology*, vol. 86, no. 1, pp. 197–210, 2005.
- [69] X. Si, B. M. McManus, J. Zhang et al., "Pyrrolidine dithiocarbamate reduces coxsackievirus B3 replication through inhibition of the ubiquitin-proteasome pathway," *Journal of Virology*, vol. 79, no. 13, pp. 8014–8023, 2005.
- [70] D. Ganem and A. M. Prince, "Hepatitis B virus infection—natural history and clinical consequences," *The New England Journal of Medicine*, vol. 350, no. 11, pp. 1118–1129, 2004.
- [71] D. M. Parkin, F. Bray, J. Ferlay, and P. Pisani, "Global cancer statistics, 2002," *CA: A Cancer Journal for Clinicians*, vol. 55, no. 2, pp. 74–108, 2005.
- [72] A. Jemal, F. Bray, M. M. Center, J. Ferlay, E. Ward, and D. Forman, "Global cancer statistics," *CA: A Cancer Journal for Clinicians*, vol. 61, no. 2, pp. 69–90, 2011.
- [73] C.-J. Chen, S.-L. Raung, M.-D. Kuo, and Y.-M. Wang, "Suppression of Japanese encephalitis virus infection by non-steroidal anti-inflammatory drugs," *Journal of General Virology*, vol. 83, no. 8, pp. 1897–1905, 2002.
- [74] M. Fujii, T. Niki, T. Mori et al., "HTLV-1 tax induces expression of various immediate early serum responsive genes," *Oncogene*, vol. 6, no. 6, pp. 1023–1029, 1991.
- [75] R. S. Upendra, P. Khandelwal, and A. H. M. Reddy, "Turmeric powder (*Curcuma longa* Linn.) as an antifungal agent in plant tissue culture studies," *International Journal of Engineering Science*, vol. 3, no. 11, pp. 7899–7904, 2011.
- [76] M.-K. Kim, G.-J. Choi, and H.-S. Lee, "Fungicidal property of *Curcuma longa* L. rhizome-derived curcumin against phytopathogenic fungi in a greenhouse," *Journal of Agricultural and Food Chemistry*, vol. 51, no. 6, pp. 1578–1581, 2003.
- [77] H. Chowdhury, T. Banerjee, and S. Walia, "In vitro screening of *Curcuma longa* L and its derivatives as antifungal agents against *Helminthosporium oryzae* and *Fusarium solani*," *Pesticide Research Journal*, vol. 20, no. 1, pp. 6–9, 2008.
- [78] M. Wuthi-udomlert, W. Grisanapan, O. Luanratana, and W. Caichompoo, "Antifungal activity of *Curcuma longa* grown in Thailand," *The Southeast Asian Journal of Tropical Medicine and Public Health*, vol. 31, no. 1, pp. 178–182, 2000.
- [79] A. Apisariyakul, N. Vanittanakom, and D. Buddhasukh, "Antifungal activity of turmeric oil extracted from *Curcuma longa* (Zingiberaceae)," *Journal of Ethnopharmacology*, vol. 49, no. 3, pp. 163–169, 1995.
- [80] C. V. B. Martins, D. L. Da Silva, A. T. M. Neres et al., "Curcumin as a promising antifungal of clinical interest," *Journal of Antimicrobial Chemotherapy*, vol. 63, no. 2, pp. 337–339, 2009.
- [81] M. Sharma, R. Manoharlal, N. Puri, and R. Prasad, "Antifungal curcumin induces reactive oxygen species and triggers an early apoptosis but prevents hyphae development by targeting the global repressor TUP1 in *Candida albicans*," *Bioscience Reports*, vol. 30, no. 6, pp. 391–404, 2010.
- [82] K. Neelofar, S. Shreaz, B. Rimple, S. Muralidhar, M. Nikhat, and L. A. Khan, "Curcumin as a promising anticandidal of clinical interest," *Canadian Journal of Microbiology*, vol. 57, no. 3, pp. 204–210, 2011.
- [83] W. Jianhua and W. Hai, "Antifungal susceptibility analysis of berberine, baicalin, eugenol and curcumin on *Candida albicans*," *Journal of Medical Colleges of PLA*, vol. 24, no. 3, pp. 142–147, 2009.
- [84] N. Khan, S. Shreaz, R. Bhatia et al., "Anticandidal activity of curcumin and methyl cinnamaldehyde," *Fitoterapia*, vol. 83, no. 3, pp. 434–440, 2012.
- [85] M. Sharma, R. Manoharlal, A. S. Negi, and R. Prasad, "Synergistic anticandidal activity of pure polyphenol curcumin in combination with azoles and polyenes generates reactive oxygen species leading to apoptosis," *FEMS Yeast Research*, vol. 10, no. 5, pp. 570–578, 2010.
- [86] M. Karaman, Z. Arıkan Ayyıldız, F. Fırınçlı et al., "Effects of curcumin on lung histopathology and fungal burden in a mouse model of chronic asthma and oropharyngeal candidiasis," *Archives of Medical Research*, vol. 42, no. 2, pp. 79–87, 2011.
- [87] L. N. Dovigo, A. C. Pavarina, J. C. Carmello, A. L. MacHado, I. L. Brunetti, and V. S. Bagnato, "Susceptibility of clinical isolates of *Candida* to photodynamic effects of curcumin," *Lasers in Surgery and Medicine*, vol. 43, no. 9, pp. 927–934, 2011.
- [88] L. N. Dovigo, A. C. Pavarina, A. P. D. Ribeiro et al., "Investigation of the photodynamic effects of curcumin against *Candida albicans*," *Photochemistry and Photobiology*, vol. 87, no. 4, pp. 895–903, 2011.
- [89] L. N. Dovigo, J. C. Carmello, C. A. de Souza Costa et al., "Curcumin-mediated photodynamic inactivation of *Candida albicans* in a murine model of oral candidiasis," *Medical Mycology*, vol. 51, no. 3, pp. 243–251, 2013.
- [90] S.-M. Tsao and M.-C. Yin, "Enhanced inhibitory effect from interaction of curcumin with amphotericin B or fluconazole against *Candida* species," *Journal of Food and Drug Analysis*, vol. 8, no. 3, pp. 208–212, 2000.
- [91] A. K. Kudva, M. N. Manoj, B. N. Swamy, and C. S. Ramadoss, "Complexation of amphotericin B and curcumin with serum albumin: solubility and effect on erythrocyte membrane damage," *Journal of Experimental Pharmacology*, vol. 3, pp. 1–6, 2011.
- [92] O. A. K. Khalil, O. M. M. de Faria Oliveira, J. C. R. Velloso et al., "Curcumin antifungal and antioxidant activities are increased in the presence of ascorbic acid," *Food Chemistry*, vol. 133, no. 3, pp. 1001–1005, 2012.
- [93] C. Mohanty, M. Das, and S. K. Sahoo, "Emerging role of nano-carriers to increase the solubility and bioavailability of curcumin," *Expert Opinion on Drug Delivery*, vol. 9, no. 11, pp. 1347–1364, 2012.
- [94] B. T. Kurien, A. Singh, H. Matsumoto, and R. H. Scofield, "Improving the solubility and pharmacological efficacy of curcumin by heat treatment," *Assay and Drug Development Technologies*, vol. 5, no. 4, pp. 567–576, 2007.
- [95] B. Bhawana, R. K. Basniwal, H. S. Buttar, V. K. Jain, and N. Jain, "Curcumin nanoparticles: preparation, characterization, and antimicrobial study," *Journal of Agricultural and Food Chemistry*, vol. 59, no. 5, pp. 2056–2061, 2011.
- [96] D. Shailendiran, N. Pawar, A. Chanchal, R. P. Pandey, H. B. Bohidar, and A. K. Verma, "Characterization and antimicrobial activity of nanocurcumin and curcumin," in *Proceedings of the International Conference on Nanoscience, Technology and Societal Implications (NSTSI '11)*, pp. 1–7, IEEE, December 2011.

- [97] Y. Wang, Z. Lu, H. Wu, and F. Lv, "Study on the antibiotic activity of microcapsule curcumin against foodborne pathogens," *International Journal of Food Microbiology*, vol. 136, no. 1, pp. 71–74, 2009.
- [98] Y.-F. Wang, J.-J. Shao, C.-H. Zhou et al., "Food preservation effects of curcumin microcapsules," *Food Control*, vol. 27, no. 1, pp. 113–117, 2012.
- [99] H. Hatcher, R. Planalp, J. Cho, F. M. Torti, and S. V. Torti, "Curcumin: from ancient medicine to current clinical trials," *Cellular and Molecular Life Sciences*, vol. 65, no. 11, pp. 1631–1652, 2008.
- [100] S. C. Gupta, G. Kismali, and B. B. Aggarwal, "Curcumin, a component of turmeric: from farm to pharmacy," *Biofactors*, vol. 39, no. 1, pp. 2–13, 2013.

Research Article

The Interaction Pattern between a Homology Model of 40S Ribosomal S9 Protein of *Rhizoctonia solani* and 1-Hydroxyphenazine by Docking Study

Seema Dharni,¹ Sanchita,² Abdul Samad,³ Ashok Sharma,² and Dharani Dhar Patra¹

¹ Agronomy and Soil Science Division, CSIR-Central Institute of Medicinal and Aromatic Plants, Lucknow 226015, India

² Biotechnology Division, CSIR-Central Institute of Medicinal and Aromatic Plants, Lucknow 226015, India

³ Crop Protection Division, CSIR-Central Institute of Medicinal and Aromatic Plants, Lucknow 226015, India

Correspondence should be addressed to Dharani Dhar Patra; ddpatra@rediffmail.com

Received 25 December 2013; Revised 19 February 2014; Accepted 19 February 2014; Published 22 April 2014

Academic Editor: José Carlos Tavares Carvalho

Copyright © 2014 Seema Dharni et al. This is an open access article distributed under the Creative Commons Attribution License, which permits unrestricted use, distribution, and reproduction in any medium, provided the original work is properly cited.

1-Hydroxyphenazine (1-OH-PHZ), a natural product from *Pseudomonas aeruginosa* strain SD12, was earlier reported to have potent antifungal activity against *Rhizoctonia solani*. In the present work, the antifungal activity of 1-OH-PHZ on 40S ribosomal S9 protein was validated by molecular docking approach. 1-OH-PHZ showed interaction with two polar contacts with residues, Arg69 and Phe19, which inhibits the synthesis of fungal protein. Our study reveals that 1-OH-PHZ can be a potent inhibitor of 40S ribosomal S9 protein of *R. solani* that may be a promising approach for the management of fungal diseases.

1. Introduction

Microorganisms are capable of synthesizing versatile chemical structures with diverse biological activities beyond the scope of synthetic organic chemistry [1] and can be directly used as fungicide products or as lead molecules for designing of novel synthetic products. Phenazine constitutes a large group of nitrogen containing heterocyclic compounds that are substituted at different sites of the core ring system and therefore displays a wide range of structural derivatives and are remarkable for the multiplex mechanism of their biological activities. More than 100 different phenazine structural derivatives have been identified and over 6,000 compounds that contain phenazine as a central moiety have been synthesized and 100 biologically active (antibacterial, antifungal, antiviral, and antitumor) phenazines from natural origin are known to date, synthesized mainly by *Pseudomonas* and *Streptomyces* species [2–4]. Fluorescent pseudomonades such as *Pseudomonas fluorescens* 2–79, *Pseudomonas chlororaphis* (previously named *P. aureofaciens* 30–84) [5], and *Pseudomonas aeruginosa* are the best studied phenazine producers [2].

Phenazines are site-specific inhibitors which target individual sites within the fungal cells or multisite inhibitors which target different sites in each fungal cell. Phenazine acts in three ways; one of the mechanisms is underlying those which inhibit energy production by blocking SH-groups, the glycolysis/citrate cycle, or the respiratory chain. Second that inhibits biosynthesis of proteins, nucleic acids, cell walls, and membrane lipids, or interfere with mitosis, and third which induces indirect effects which change host/pathogen interactions [6]. The enzymes involved in any of the above-mentioned processes can be considered as a target receptor and the metabolite as ligand. Molecular docking studies can also be performed for microbial fungicides to validate their inhibiting properties.

Clofazimine is a synthetic phenazine analogue belonging to the riminophenazines group of compounds which was originally discovered in lichens [2, 7] and another phenazine, bis (phenazine-1-carboxamide), acts as a potent cytotoxin and represents an interesting class of dual topoisomerase I/II directed anticancer activity [8]. The highlight of biological significance of phenazines is their ability to act as broad-spectrum antimicrobial, antiparasite, antimalarial, and

antifungal agents affecting a vast range of organisms [2, 9, 10]. Inhibition of DNA-dependent RNA synthesis in the absence of detected DNA intercalation has been observed for lomofungin during elongation, which has been shown to block the transcription complex at the initiation state as well as during elongation [11].

Phenyl amides (PA) fungicides affect nucleic acids synthesis by inhibiting the activity of the RNA polymerase I system which interferes with nucleic acid synthesis, thus blocking rRNA synthesis [12]. Phenylpyrrole fungicidal ingredient, fludioxonil, (4-(2,2-difluoro-1,3-benzodioxil-4-yl)-1H-pyrrole-3-carbonitrile), produced by *Pseudomonas pyrrocinia*, revealed inhibition of spore germination and germ tube elongation [13]. Tubericidin produced by *Streptomyces violaceoniger*, was highly active against *Phytophthora capsici* and *Rhizoctonia solani*. Tubericidin interferes the nucleic acid synthesis, including *de novo* purine synthesis, rRNA processing, and tRNA methylation [14]. The derivatives of phenazine—antibiotics iodine, muxin, and pyocyanin—are capable of interacting with DNA/RNA either by blocking the template (DNA intercalation), binding to RNA polymerase, or binding to a ribonucleoside 5'-triphosphate [15]. A new phenazine-1-carboxylic acid phenylamide (PCA-1-P) exhibited substantial growth retardation of three gram-positive and the strong inhibitory activity of PCA-1-P derivatives towards the RNA synthesis *in vitro* T7-RNA-polymerase [16].

In this study we have described the mode of action of 1-OH-PHZ inhibiting the 40S ribosomal protein S9 of *R. solani* through docking approaches. The 40S ribosomal protein S9 plays a central role in the initiation factors considered to be a primary rRNA-binding protein that facilitates scanning of messenger RNAs and initiation of protein synthesis. The ribosomal protein S9 is an essential protein located at the entrance tunnel of the mRNA into the ribosome and plays an accurate role in decoding. Lindström and Zhang reported that ribosomal protein S9 is required for normal cell growth and proliferation, as depletion of S9 resulted in decreased protein synthesis which is associated with G₁ cell cycle arrest [17]. A recent study has been shown that ribosomal protein S9 is located at the entrance tunnel of mRNA in the ribosomes and is involved in regulation of mRNA translation, possibly translation termination [18]. It will be of considerable interest in the future to further find out a specific antifungal agent targeting on inhibition of the translation step which has the effect of blocking protein production and ultimately its function.

2. Materials and Methods

2.1. Bacterial Strain. SD12 was isolated from metal polluted soil as previously described by Dharni et al. [19]. The strain was also deposited at Microbial Type Culture Collection (MTCC), IMTECH, Chandigarh, India (<http://mtcc.imtech.res.in/>), with accession number 106439.

2.2. 1-Hydroxyphenazine (1-OH-PHZ). As described previously by Dharni et al. [19], 1-OH-PHZ was purified from the

culture supernatant of *P.aeruginosa* SD12 by using stepwise gradient vacuum liquid chromatography.

2.3. Nucleotide Sequence Accession Number. The nucleotide sequence of 16S rRNA of strain SD-12 has been reported in the GenBank database of NCBI (<http://www.ncbi.nlm.nih.gov/>) having the accession number HQ268805.

2.4. Structure Prediction of Protein. The three-dimensional structure of 40S ribosomal protein S9 of *Rhizoctonia solani* is not available in any database. For deducing the structure, the protein sequence (176 amino acid) was obtained from NCBI database (acc. no. ABE68880) and uploaded in FASTA format in SWISS-MODEL via the ExPASy web server [20]. To obtain the closest match BLAST of query protein sequence was performed which searched against Protein Data Bank (PDB), <http://www.rcsb.org/pdb/home/home.do> [21]. The modeled structure of the protein was submitted to the PMDB database, <http://mi.caspar.it/PMDB/main.php>.

2.5. Structure Validation. After the model generation, its quality assessment was done, based on both geometric and energetic aspects. The SWISS PDB Viewer was used for minimizing the energy of modeled protein [22]. The stereochemical properties of obtained protein model were checked using RAMPAGE server [23]. The ramachandran plot provided the residue position in particular segments based on φ and ψ angles between N-C $_{\alpha}$ and C $_{\alpha}$ -C atoms of residues.

2.6. Ligand Structure. For docking study, 1-hydroxyphenazine was taken as a ligand compound. The structure of this compound was retrieved from Pubchem database maintained at NCBI, <http://pubchem.ncbi.nlm.nih.gov/>. The three-dimensional structure of ligand was converted from mol to pdb format to input into the Autodock. This conversion was done through Open Babel tool, <http://sourceforge.net/projects/openbabel/>.

2.7. Molecular Docking. The docking of ligand (1-OH-PHZ) with modeled 40S ribosomal S9 protein was performed by Autodock 4.2 using genetic algorithm approach [24]. The grid box dimension of 0.375 Å was selected in protein for docking with ligand. The blind docking approach was acquired as this gives good results in substrate binding site prediction [25]. In this approach, the full flexible ligand was used for docking while keeping the protein in a fixed orientation in space. The negative and lower value of binding energy as well as more numbers of hydrogen bonds showed favored binding between ligand and target.

3. Results and Discussion

3.1. 1-Hydroxyphenazine (1-OH-PHZ). Our previous studies demonstrated that 1-OH-PHZ showed antifungal activity against *R. solani*, a soilborne pathogen, at 40 µg/disc (Figure 1) [19]. 1-OH-PHZ earlier isolated from *P. aeruginosa* TISTR 781 [26] was reported to inhibit *Escherichia coli* and



FIGURE 1: Antifungal activity of 1-hydroxyphenazine at 40 µg/disc against *Rhizoctonia solani*.

TABLE 1: Docking results and K_i values for each conformation studied.

Conformations	Free energy of binding (kcal/mol)	Predicted inhibition constant, K_i (uM)	Ligand efficiency	Hydrogen bonding	Residues
1	-5.44	103.69	-0.36	1	LEU76
2	-5.94	44.45	-0.4	No	
3	-5.84	52.24	-0.39	1	ARG69
4	-5.44	103.62	-0.36	1	LEU76
5	-5.94	44.44	-0.4	No	
6	-5.84	52.06	-0.39	1	ARG69
7	-5.44	103.67	-0.36	1	LEU76
8	-5.84	52.12	-0.39	1	ARG69
9	-5.44	103.32	-0.36	1	LEU76
10	-5.84	52.12	-0.39	1	ARG69

Xanthomonas campestris pv. *vesicatoria*. Recently, phenazine-1-carboxylic acid (PCA) produced by *Pseudomonas* sp. M18G is being marketed as *Shenquinmycin* in China, which has gained a Pesticide Registration Certification (*Fusarium oxysporum*) issued by the Chinese Ministry of Agriculture, owing to its high efficiency against various phytopathogens, low toxicity, and good environmental compatibility. It is proved as an effective agent for the biocontrol of withering of watermelon sprout (code) and piemintoe epidemic disease (*Pythium capsici*) [27, 28]. 1-OH-PHZ was earlier isolated from *P. aeruginosa* TISTR 781 and known to inhibit *Escherichia coli* and *Xanthomonas campestris* pv. *vesicatoria* [26]. N-acrylamides of 9-substituted phenazine-1-carboxylic acids (PCA) have been reported as strong inhibitors of RNA synthesis [29, 30].

3.2. Secondary Structure Prediction. GOR4 server [12] was used for secondary structure prediction of modeled protein. Helix, sheet, and coils were the secondary structures found to occur in the protein. GOR4 server reveals 58.52% residues in α helices, 8.52% residues in β sheet, and 32.95% residues in random coils (Figure 2). The results revealed that α helices contributed more as compared to other structures. These structures were joined together to form a three-dimensional

structure of protein. The secondary structures were predicted by using default parameters. The results have been validated through Chou Fasman servers [31].

3.3. Homology Modeling of 40S Ribosomal S9 Protein. 40S ribosomal S9 protein is an important target responsible for fungal growth [32]. To predict the structure of this protein, homology modeling approach was performed. The query sequence of target protein was found homologous to the known structure of protein of the same family of *Thermomyces lanuginosus*. After BLAST search the high resolution crystal structure of homologous protein having PDB id 3JYV was considered as template for comparative modeling. The query and template sequences showed 78% identity and 6e - 87 Evaluate in sequence alignment and were taken as template for homology modeling (Figure 3). The structure was modeled on automated mode of SWISS-MODEL workspace, <http://swissmodel.expasy.org/>, with its default parameters. The residues ranging between 6 and 163 participated in homology modeling. The total energy -5238.173 KJ/mol of the model was converted to -7587.487 KJ/mol after minimizing the energy through SWISS PDB Viewer. The final predicted 3D structure

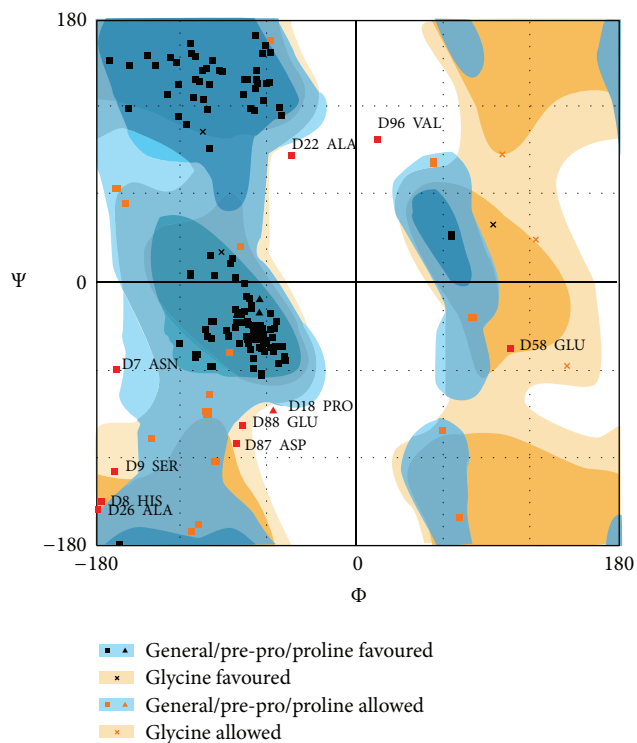


FIGURE 5: Modeled structure of 40S ribosomal S9 protein.

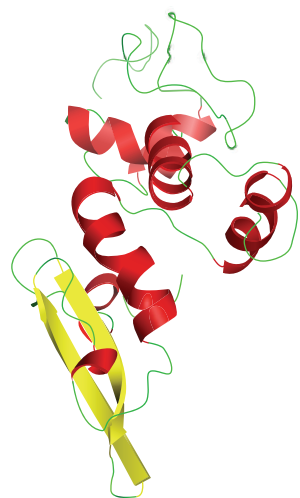


FIGURE 6: Ramachandran map of 40S ribosomal ligand moleS9 protein of *Rhizoctonia solani*.

against *Rhizoctonia solani*. A homology model of 40S ribosomal S9 protein of *R. solani* was built and validated through ramachandran plot. Validation by the software showed that the homology model energy score is similar to the crystal structure of the template. SWISS model was used to develop a reliable model for performing the docking study. This docking study of the 40S ribosomal S9 protein showed that out of 10 docked conformations, the 3rd conformation was the best because it has comparatively lower binding energy as well as hydrogen bonding. These observations may be of great

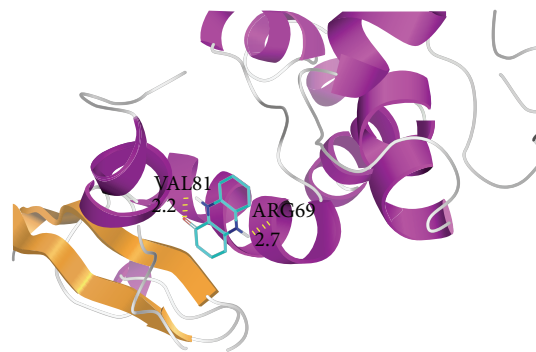


FIGURE 7: Docking of 1-OH-PHZ with 40S ribosomal S9 protein.

help in the QSAR based designing of fungicides from a very common, inexpensive, and nontoxic natural product, which is safe for humans, animals, and environment. This study will also facilitate the understanding of the structural and functional basis of ligand binding to the protein for further research.

Conflict of Interests

The authors declare that there is no conflict of interests regarding the publication of this paper.

Acknowledgment

This work was supported by Senior Research Fellowship Award to two of the authors, Seema Dharni and Sanchita, from CSIR, New Delhi.

References

- [1] N. Porter, "Physicochemical and biophysical panel symposium biologically active metabolites," *Journal of Pest Science*, vol. 16, no. 4, pp. 422–427, 1985.
- [2] D. V. Mavrodi, W. Blankenfeldt, and L. S. Thomashow, "Phenazine compounds in fluorescent *Pseudomonas* spp. biosynthesis and regulation," *Annual Review of Phytopathology*, vol. 44, pp. 417–445, 2006.
- [3] J. L. Arbiser and S. L. Moschella, "Clofazimine: a review of its medical uses and mechanisms of action," *Journal of the American Academy of Dermatology*, vol. 32, no. 2 I, pp. 241–247, 1995.
- [4] M. McDonald, D. V. Mavrodi, L. S. Thomashow, and H. G. Floss, "Phenazine biosynthesis in *Pseudomonas fluorescens*: branchpoint from the primary shikimate biosynthetic pathway and role of phenazine-1,6-dicarboxylic acid," *Journal of the American Chemical Society*, vol. 123, no. 38, pp. 9459–9460, 2001.
- [5] S. M. Delaney, D. V. Mavrodi, R. F. Bonsall, and L. S. Thomashow, "phzO, a gene for biosynthesis of 2-hydroxylated phenazine compounds in *Pseudomonas aureofaciens* 30-84," *Journal of Bacteriology*, vol. 183, no. 1, pp. 318–327, 2001.
- [6] L. Burpee, "Integrated disease management, an introduction to Fungicides," Courses Support, 2006.

- [7] V. M. Redd, J. F. O'Sullivan, and P. R. J. Gangadharam, "Antimycobacterial activities of riminophenazines," *Journal of Antimicrobial Chemotherapy*, vol. 43, no. 5, pp. 615–623, 1999.
- [8] J. A. Spicer, S. A. Gamage, G. W. Rewcastle et al., "Bis(phenazine-1-carboxamides): structure-activity relationships for a new class of dual topoisomerase I/II directed anticancer drugs," *Journal of Medicinal Chemistry*, vol. 43, no. 7, pp. 1350–1358, 2000.
- [9] H. Yang, P. M. Johnson, K.-C. Ko et al., "Cloning, characterization and expression of escapin, a broadly antimicrobial FAD-containing L-amino acid oxidase from ink of the sea hare *Aplysia californica*," *Journal of Experimental Biology*, vol. 208, part 18, pp. 3609–3622, 2005.
- [10] H. Cerecetto, M. González, M. Risso et al., "1,2,4-Triazine N-oxide derivatives: studies as potential hypoxic cytotoxins. Part III," *Archiv der Pharmazie*, vol. 337, no. 5, pp. 271–280, 2004.
- [11] H. Budzikiewicz, "Secondary metabolites from fluorescent pseudomonads," *FEMS Microbiology Reviews*, vol. 104, no. 3–4, pp. 209–228, 1993.
- [12] H. Buchenauer, *Chemistry of Plant Protection. Part 6: Controlled Release, Biochemical Effects of Pesticides, Inhibition of Plant Pathogenic Fungi*, Springer, New York, NY, USA, 1990.
- [13] N. Ochiai, M. Fujimura, M. Oshima et al., "Effects of iprodione and fludioxonil on glycerol synthesis and hyphal development in *Candida albicans*," *Bioscience, Biotechnology and Biochemistry*, vol. 66, no. 10, pp. 2209–2215, 2002.
- [14] R. J. Suhadolnik, *Nucleosides as Biological Probes*, Wiley-Interscience, New York, NY, USA, 1979.
- [15] U. Hollstein and R. J. Van Gemert Jr., "Interaction of phenazines with polydeoxyribonucleotides," *Biochemistry*, vol. 10, no. 3, pp. 497–504, 1971.
- [16] L. H. Paľchykovs'ka, I. V. Alexeeva, V. H. Kostina et al., "New amides of phenazine-1-carboxylic acid: antimicrobial activity and structure-activity relationship," *Ukrain'skyi Biokhimichnyi Zhurnal*, vol. 80, no. 3, pp. 140–147, 2008.
- [17] M. S. Lindström and Y. Zhang, "Ribosomal protein S9 is a novel B23/NPM-binding protein required for normal cell proliferation," *The Journal of Biological Chemistry*, vol. 283, no. 23, pp. 15568–15576, 2008.
- [18] L. Pnueli and Y. Arava, "Genome-wide polysomal analysis of a yeast strain with mutated ribosomal protein S9," *BMC Genomics*, vol. 8, article 285, 2007.
- [19] S. Dharni, M. Alam, K. Kalani et al., "Production, purification, and characterization of antifungal metabolite from *Pseudomonas aeruginosa* SD12, a new strain obtained from tannery waste polluted soil," *Journal Microbiology Biotechnology*, vol. 22, no. 5, pp. 674–683, 2012.
- [20] C. Combet, M. Jambon, G. Deléage, and C. Geourjon, "Geno3D: automatic comparative molecular modelling of protein," *Bioinformatics*, vol. 18, no. 1, pp. 213–214, 2002.
- [21] H. M. Berman, J. Westbrook, Z. Feng et al., "The protein data bank," *Nucleic Acids Research*, vol. 28, no. 1, pp. 235–242, 2000.
- [22] N. Guex and M. C. Peitsch, "SWISS-MODEL and the Swiss-PdbViewer: an environment for comparative protein modeling," *Electrophoresis*, vol. 18, no. 15, pp. 2714–2723, 1997.
- [23] S. C. Lovell, I. W. Davis, W. B. Arendall III et al., "Structure validation by $C\alpha$ geometry: φ, ψ and $C\beta$ deviation," *Proteins: Structure, Function and Genetics*, vol. 50, no. 3, pp. 437–450, 2003.
- [24] G. M. Morris, H. Ruth, W. Lindstrom et al., "AutoDock4 and AutoDockTools4: automated docking with selective receptor flexibility," *Journal of Computational Chemistry*, vol. 30, no. 16, pp. 2785–2791, 2009.
- [25] C. Hetényi and D. van der Spoel, "Blind docking of drug-sized compounds to proteins with up to a thousand residues," *FEBS Letters*, vol. 580, no. 5, pp. 1447–1450, 2006.
- [26] K. Saosoong, W. Wongphathanakul, C. Poasir, and C. Ruan-gviriyachai, "Isolation and analysis of antibacterial substance produced from *P. aeruginosa* TISTR 781," *KKU Science Journal*, vol. 37, pp. 163–172, 2009.
- [27] D.-Q. Wu, J. Ye, H.-Y. Ou et al., "Genomic analysis and temperature-dependent transcriptome profiles of the rhizosphere originating strain *Pseudomonas aeruginosa* M18," *BMC Genomics*, vol. 12, article 438, 2011.
- [28] Y. Li, X. Du, Z. J. Lu et al., "Regulatory feedback loop of two phz gene clusters through 5'-untranslated regions in pseudomonas sp. M18," *PLoS ONE*, vol. 6, no. 4, Article ID e19413, 2011.
- [29] L. G. Palchykovska, O. V. Vasylychenko, M. O. Plantonov et al., "T7 evaluation of antibacterial and antiviral activity of N-arylamides of 9-methyl- and 9-methoxyphenazine-1-carboxylic acids-inhibitors of the phage T7 model transcription," *Biopolymer and Cell*, vol. 28, no. 6, pp. 477–485, 2012.
- [30] R. P. Ricciardi, D. W. Hollomon, and D. Gottlieb, "Age dependent changes in fungi: ribosomes and protein synthesis in *Rhizoctonia solani* mycelium," *Archives of Microbiology*, vol. 95, no. 4, pp. 325–336, 1974.
- [31] P. Y. Chou and G. D. Fasman, "Conformational parameters for amino acids in helical, β -sheet, and random coil regions calculated from proteins," *Biochemistry*, vol. 13, no. 2, pp. 211–222, 1974.
- [32] J. Rabl, M. Leibundgut, S. F. Ataide, A. Haag, and N. Ban, "Crystal structure of the eukaryotic 40S ribosomal subunit in complex with initiation factor 1," *Science*, vol. 331, no. 6018, pp. 730–736, 2011.
- [33] B. S. Yadav, V. Tripathi, A. Kumar et al., "Molecular modeling and docking characterization of Dectin-1 (PAMP) receptor of *Bubalus bubalis*," *Experimental and Molecular Pathology*, vol. 92, no. 1, pp. 7–12, 2012.

Research Article

Biodegradation and Utilization of Organophosphorus Pesticide Malathion by Cyanobacteria

Wael M. Ibrahim,¹ Mohamed A. Karam,¹ Reda M. El-Shahat,² and Asmaa A. Adway¹

¹ Botany Department, Faculty of Science, Fayoum University, Fayoum, Egypt

² Agricultural Research Center, Ministry of Agriculture, Egypt

Correspondence should be addressed to Wael M. Ibrahim; wms01@fayoum.edu.eg

Received 20 February 2014; Accepted 3 April 2014; Published 17 April 2014

Academic Editor: José Carlos Tavares Carvalho

Copyright © 2014 Wael M. Ibrahim et al. This is an open access article distributed under the Creative Commons Attribution License, which permits unrestricted use, distribution, and reproduction in any medium, provided the original work is properly cited.

Three strains of filamentous Cyanobacteria were used to study their growth and utilization of organophosphorus pesticide malathion. A sharp decrease in the growth of the algal strains was observed by increasing the concentration of malathion. Amongst them *Nostoc muscorum* tolerated different concentrations and was recorded as the highest efficient strain for biodegradation (91%) of this compound. Moreover, carbohydrate and protein content of their cells overtopped the other strains especially at higher concentrations. The algal strains were further subjected to grow under P-limitation in absence and presence of malathion. Although, the algal growth under P-limitation recorded a very poor level, a massive enhanced growth and phosphorous content of cells were obtained when the P-limited medium was amended with malathion. This study clarified that *N. muscorum* with its capability to utilize malathion as a sole phosphorous source is considered as an inexpensive and efficient biotechnology for remediation of organophosphorus pesticide from contaminated wastewater.

1. Introduction

As a result of human impact, the levels of organic compounds found in surface water have increased in the recent decades. Of these organic compounds, pesticides are most commonly detected in all aquatic environments [1]. These pesticides are mainly used for agricultural purposes [2]. They enter the aquatic environment via runoff after being sprayed in agricultural fields and can potentially reach groundwater [3].

Malathion is a nonsystemic, wide spectrum organophosphate pesticide (OP), used to control insects on field crops, fruits, vegetables and also extensively used to prevent mosquitoes, flies, household insects, animal parasites, and head body lice [4].

Recent research shows that malathion has a variety of syndromes and effects including hepatotoxicity [5–7], human breast carcinoma [8], genetic damage [9], and disrupted normal hormone activity [10].

Not only are the chemical and physical methods of decontamination expensive and time-consuming, but also in most cases they do not provide a complete solution.

Bioremediation provides a suitable way to remove contaminants from the environment as, in most of the cases, OP compounds are totally mineralized by the microorganisms. Most OP compounds are degraded by microorganisms in the environment as a source of phosphorus or carbon or both [11].

Photoautotrophic microorganisms, such as Cyanobacteria, are used for wastewater treatment to remove nitrogen and phosphorus [12]. They have potential to remove various pollutants, such as dyes [13], heavy metals [14], and pesticides [15]. Therefore, this study is conducted to investigate the survival and tolerance of cyanobacterial isolates *Anabaena oryzae*, *Nostoc muscorum*, and *Spirulina platensis* with different concentrations of malathion, as well as evaluating their efficiency for removing and recovering this pesticide from contaminated wastewater.

2. Material and Methods

2.1. Algal Strains. The algal strains (*Anabaena oryzae* and *Nostoc muscorum*) were isolated from different water samples

collected from Al-Fayoum Governorate, Egypt. Whereas, *Spirulina platensis* was obtained from Agricultural Research Center, Ministry of Agriculture, Giza, Egypt.

2.2. Chemicals. The organophosphorus pesticide used in this study is commercially available as Malathion, chemical name (O,O-dimethyl-S-[1,2-di(ethoxycarbonyl)ethyl]phosphorodithioate) was obtained from Kafr Elzayyat company, Egypt (98% active ingredient).

2.3. Experimental Design. The selected algal isolates were batch-cultured in 500 mL Erlenmeyer flasks. Into each flask 200 mL of liquid culture media, BG11 medium [16] for *A. oryzae* and *N. muscorum* and Zarrouk medium [17] for *S. platensis*, was added. The initial inoculum was approximately 5×10^4 cell/mL. Malathion was added to the culture medium to the final concentrations 0.02, 0.2, 2, 20, 50, or 100 ppm. The culture flasks were kept under continuous illumination provided by daylight fluorescent tubes with an average light intensity of $40 \mu\text{Em}^{-2} \text{s}^{-1}$ maintained constantly during the experiment. The flasks were incubated in a culture room at $28 \pm 1^\circ\text{C}$ under continuous shaking of 80 rpm. Samples were taken after every four-day intervals up to fifty-two days for the estimation of the growth in terms of cell count. After 20 days, 50 mL of algal cultures was filtrated by centrifugation at 1500 rpm for 20 minutes. The algal filtrate was used to determine malathion residues in the culture medium.

To obtain phosphorus-limited cultures, exponentially growing cells were inoculated into flasks containing medium with 1/10th of the original phosphorus concentration. The phosphorus-limited cells were cultured in a medium without and with different concentrations of malathion. Samples were taken after 20 days for estimation of cell count and phosphorus content in the tested algal cells.

2.4. Analytical Analysis. Different algal cultures were sonicated with Ultrasonic Homogenizer (Model: cp100, USA) to make them short fragments; 10 mL of algal solution was placed on vials containing 0.1 mL Lugol's solution [18]. Cell count was carried out using a standard haemocytometer under an Olympus BH-2 light microscope. Protein content of algal biomass was determined according to Lowry et al. [19]. For the determination of carbohydrate content in algal cells, the anthrone sulphuric acid method which was carried out by Fales [20] and adopted by Irigoyen et al. [21] was used. The total phosphorus content in the algal biomass was measured spectrophotometrically at 720 nm according to Pierpoint [22]. Hewlett Packard Agilent GC System (Gas Chromatograph, USA) Model 6890 equipped with a flame photometric detector (FPD) with phosphorus filter was used for determination of malathion residues in the culture medium.

2.5. Statistical Analysis. Data were presented as mean of replicates from three runs and were analyzed statistically using Student's *t*-test for independent samples. Statements of significant differences were based on accepting $P \leq 0.05$. To validate the tolerance of algal strains, two identical

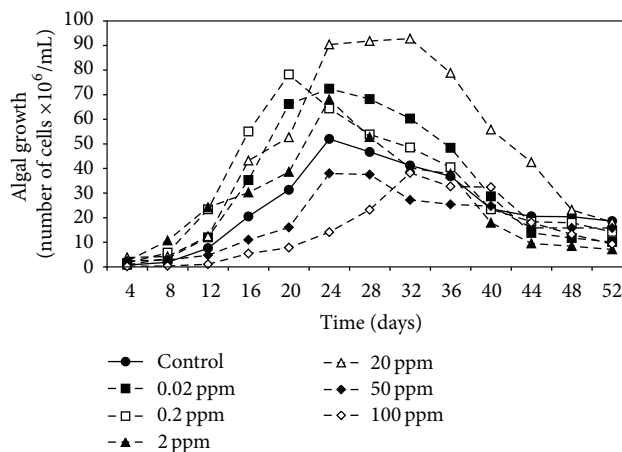


FIGURE 1: Effect of different malathion concentrations on the growth of *A. oryzae*.

series of linear regression curves were established for growth experiment.

3. Results

3.1. Effect of Malathion on Growth of Tested Algal Strains. Data in Figures 1, 2, and 3 demonstrated the effect of malathion concentrations on the growth of three cyanobacterial strains, *A. oryzae*, *N. muscorum*, and *S. platensis*. Obviously, an inverse relationship between malathion concentration and the algal growth was recorded. At low concentrations of malathion (0.02–20 ppm), the maximum growth of *A. oryzae* and *N. muscorum* was achieved within 24 days recording an increment of the total cell number by 41% and 75%, respectively, compared with the untreated culture. At the same time, different malathion concentrations dramatically reduced the growth of *S. platensis* recording a reduction of the total cell count by 19% compared with the control treatment. Regression lines (Figure 4) indicated that *N. muscorum* was more tolerant than the other algal strains with different concentrations of malathion.

3.2. Effect of Malathion on Carbohydrate and Protein Content of Algal Cells. Data present in Figure 5 indicated that the treatment of *A. oryzae* and *N. muscorum* with different malathion concentrations caused a very high significant increase in total carbohydrate content with increasing concentrations of malathion and the highest carbohydrate content (0.39 and 1.09 mg/g dry weight, resp.) was recorded at 50 ppm of malathion. At the same time, carbohydrate content of *S. platensis* was increased until 20 ppm of malathion and then dramatically decreased as malathion concentration increased further.

Concerning protein content of algal strains, it is clear from Figure 6 that treatment of *A. oryzae* and *N. muscorum* with malathion significantly increased protein content of cells especially at higher concentrations (50 and 100 ppm). In case of *S. platensis*, lower concentrations of malathion (0.2 and 20 ppm) caused significant increase in protein content of

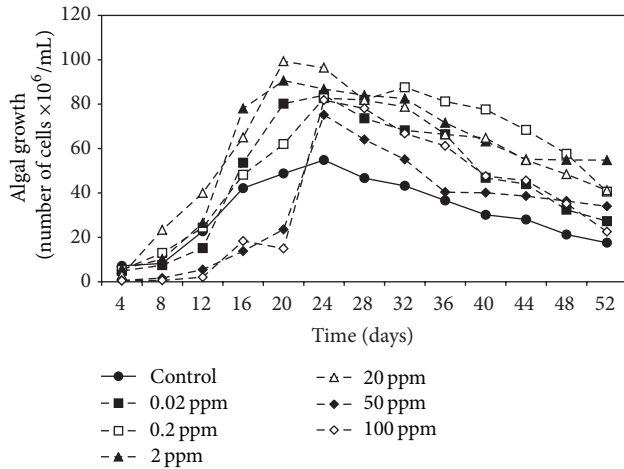


FIGURE 2: Effect of different malathion concentrations on the growth of *N. muscorum*.

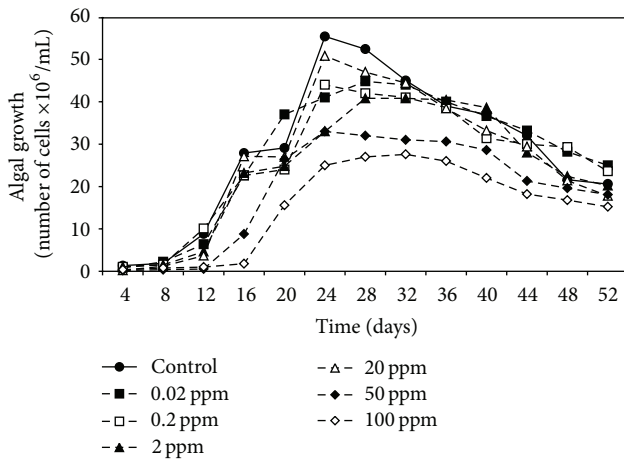


FIGURE 3: Effect of different malathion concentrations on the growth of *S. platensis*.

algal cells and high concentrations caused gradual decrease in protein content.

3.3. Biodegradation of Malathion by Different Algal Strains. Data present in Figure 7 illustrated that the three algal strains have the ability to biodegrade malathion at different concentrations. In general, *N. muscorum* was recorded as the highest efficient strain followed by *A. oryzae* and the lowest one was *S. platensis* with mean removal values of 91%, 65%, and 54%, respectively.

3.4. The Ability of Algal Strains to Utilise Malathion as Phosphorus Source. Algal strains were grown under phosphorus limitation condition in absence and presence of malathion in order to investigate their ability to utilise malathion as a sole phosphorus source. In absence of malathion, the growth of cells was markedly dwindled under phosphorus limitation recording a decrement in the total cell count by 75.5% compared with the unlimited cells (Table 1). On the other

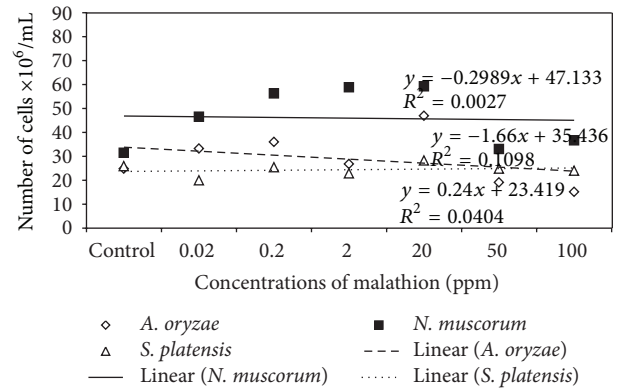


FIGURE 4: Regression lines of algal growth (expressed as cell count) of tested strains.

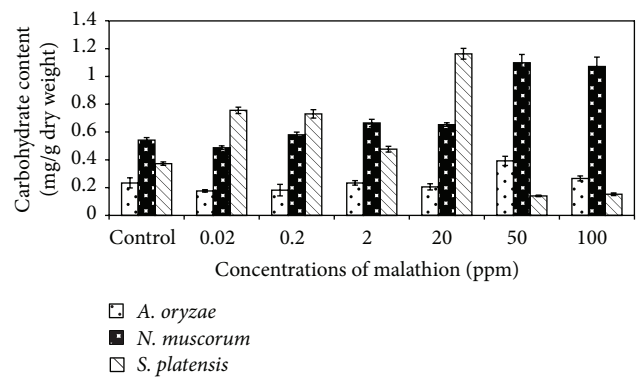


FIGURE 5: Effect of different concentrations of malathion on carbohydrate content of algal biomass. Data are the means of three replicates and error bars represent the standard errors of the means.

hand, when malathion was used as a sole phosphate source for the growth of algal strains under P-limitation condition, the greatest cell number was achieved recording 39%, 52%, and 20% increase more than the same conditions without the addition of malathion for *A. oryzae*, *N. muscorum*, and *S. platensis*, respectively.

The ability of algal strains to use malathion as phosphate source was confirmed by analysing the internal phosphorus content inside the algal biomass. Data in Table 2 revealed that the total phosphorus content of the cells that were cultured in media with P-limitation was very minor. When the limited culture was amended with malathion, the amounts of total phosphorus were increased to the same range spotted in the unlimited cells.

4. Discussion

It is clear from the results that the growth of algal strains was decreased as malathion concentration increased. This inverse correlation between malathion concentration and the algal growth agrees with Ibrahim and Essa [15] and Ghadai et al. [23] who studied the effect of different concentrations (1–400 ppm) of organophosphorus pesticides on the growth of seven cyanobacterial strains. They found that the low

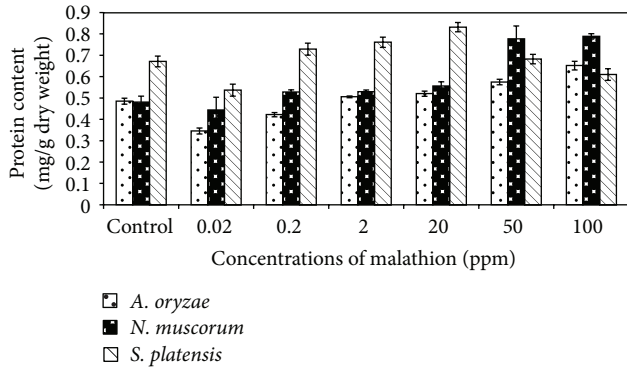


FIGURE 6: Effect of different concentrations of malathion on protein content of algal biomass. Data are the means of three replicates and error bars represent the standard errors of the means.

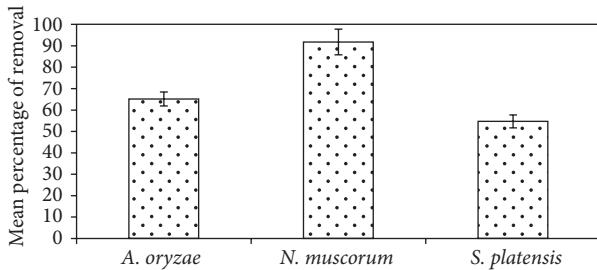


FIGURE 7: Efficiency of different algal strains to biodegrade malathion. Error bars represent the standard errors of the means.

TABLE 1: The growth of algal strains, expressed as cell count (number of cells $\times 10^6/\text{mL}$), under unlimitation and P-limitation conditions with the addition of malathion.

Algal strains	<i>A. oryzae</i>	<i>N. muscorum</i>	<i>S. platensis</i>
Unlimitation	24.7 ± 2.9	6.6 ± 0.5	8.8 ± 0.1
P-limitation	1.2 ± 0.3^a	1.4 ± 0.2^a	4.2 ± 0.4^a
P-limitation with different concentrations of malathion (ppm)			
0.02	4.4 ± 0.5^b	2.1 ± 0.3^b	6.4 ± 1.1^b
0.2	5.4 ± 1.2^b	4.3 ± 0.3^b	7.0 ± 0.9^b
2	5.6 ± 0.6^b	4.8 ± 0.5^b	7.2 ± 0.9^b
20	13.4 ± 0.6^b	4.9 ± 0.2^b	7.8 ± 0.7^b
50	22.6 ± 0.8^b	7.1 ± 0.1^b	8.2 ± 0.7^b
100	26.1 ± 2.4^b	7.6 ± 0.5^b	0.0 ± 0.0^b

Values are means of three replicates \pm standard errors.

^aSignificant decrease compared with unlimitation condition.

^bSignificant increase compared with P-limitation condition.

concentrations stimulated the growth in terms of cell number and the higher concentrations dramatically reduced the algal growth. In this respect, extensive studies have been made concerning the inhibitory effects of organophosphorus pesticides on the cell count of different algal species [24–27].

The inhibitory effect of malathion could be attributed to the adsorption of this compound on the rich-lipid plasma

TABLE 2: Total phosphorus content (mg/g dry weight) of algal biomass under unlimitation and P-limitation condition with the addition of malathion.

Algal strains	<i>A. oryzae</i>	<i>N. muscorum</i>	<i>S. platensis</i>
Unlimitation	10.1 ± 0.1	9.2 ± 0.1	19.8 ± 0.1
P-limitation	2.2 ± 0.1^a	3.6 ± 0.1^a	0.7 ± 0.1^a
P-limitation with different concentrations of malathion (ppm)			
0.02	6.9 ± 0.0^b	11.2 ± 0.0	1.0 ± 0.0
0.2	8.8 ± 0.1^b	4.3 ± 0.1^b	0.9 ± 0.1^b
2	11.6 ± 0.1^b	4.7 ± 0.1^b	0.9 ± 0.1^b
20	13.7 ± 0.1^b	5.8 ± 0.1^b	3.8 ± 0.1^b
50	14.0 ± 0.1^b	6.6 ± 0.1^b	4.1 ± 0.1^b
100	15.9 ± 0.1^b	10.4 ± 0.1^b	0.0 ± 0.0^b

Values are means of three replicates \pm standard errors.

^aSignificant decrease compared with unlimitation condition.

^bSignificant increase compared with P-limitation condition.

membranes of the algal cells, thus, altering the membranes permeability [28] and diminishing photosynthetic activity [29, 30] as well as increasing reactive oxygen species (ROS) during stress [25].

Figure 4 indicated that *N. muscorum* was more tolerant to different concentrations of malathion than the other algal strains. In agreement with these results Nayak et al. [27] reported that *Nostoc* sp. tolerated more than *Anabaena* sp. to organophosphorus pesticide monocrotophos and can grow up to 150 ppm. Also, Kumar et al. [31] study the tolerance of three cyanobacterial strains to endosulfan and record the tolerance in the order of *N. muscorum* > *A. variabilis* > *A. fertilissima*. Highest tolerance of *N. muscorum* could be as a result of its highest ability to biodegrade malathion (91%) at different concentrations (Figure 7).

In general, data obtained from Figures 5 and 6 indicated that the total carbohydrate and protein content of algal biomass increased significantly with increasing malathion concentrations. Such a phenomenon may be due to the presence of some enzymes which can hydrolyse this organophosphorus compound and utilize malathion as nutrient sources [15, 32]. Ghadai et al. [23] found that the organophosphorus pesticide diazinon stimulates carbohydrate content of blue green alga, *A. cylindrica*.

When algal strains were cultured in P-limited medium supplemented with different malathion concentrations, a highly significant growth was obtained compared with the cells that were grown under the same conditions without malathion addition which recorded a sharp reduction in their growth. In accordance with such results, Ibrahim and Essa [15] studied the effect of malathion on the growth of *A. oryzae* under phosphorus limited conditions. They found that the growth of *A. oryzae* under P-limitation recorded a very poor level and a massive enhanced growth was obtained when the P-limited medium was amended with malathion. The stimulative effect of malathion on growth could be as a result of the increment of the available phosphorus, resulting from

degradation of this compound by algal strains. Therefore, total phosphorus content of algal biomass was estimated in order to confirm their capability to utilise malathion as a phosphorus source. Results in Table 2 illustrated that the phosphorus content of the cells which grew under P-limitation and in presence of malathion was much higher than that found in cells cultured under the same conditions but without the addition of malathion revealing the capability of this strain to break down and utilize malathion as a sole phosphorus source. These findings agreed with Subramanian et al. [33] who attributed the growth enhancement of Cyanobacteria *Aulosira fertilissima* that was grown in the presence of malathion to their capability to utilize this compound as sole sources of phosphorus in the absence of inorganic phosphate from the medium.

5. Conclusions

The present study is the first evidence of the ability of *A. oryzae*, *N. muscorum*, and *S. platensis* to biodegrade and utilize malathion as a source of phosphorus. Overall, the data obtained highlight the efficiency of algal strains to grow under high concentrations of malathion with enhancement of biomass carbohydrate and protein content. Moreover, *N. muscorum* overtopped the other strains in removing more than 90% of malathion. Hence, work in this regard should continue to characterise the genetic and enzymatic components responsible for the utilization of malathion and other organophosphorus pesticides of this strain in order to evaluate its efficiency for the bioremediation of these environmental pollutants.

Conflict of Interests

The authors declare that there is no conflict of interests regarding the publication of this paper.

References

- [1] U. Ali, J. H. Syed, R. N. Malik et al., "Organochlorine pesticides (OCPs) in South Asian region," *Science of the Total Environment*, vol. 476-477, pp. 705-717, 2014.
- [2] M. A. Z. Chowdhury, I. Jahan, N. Karim et al., "Determination of carbamate and organophosphorus pesticides in vegetable samples and the efficiency of gamma radiation in their removal," *BioMed Research International*, vol. 2014, Article ID 145159, 9 pages, 2014.
- [3] K. Bunzel, M. Kattwinkel, and M. Liess, "Effects of organic pollutants from wastewater treatment plants on aquatic invertebrate communities," *Water Research*, vol. 47, no. 2, pp. 597-606, 2013.
- [4] V. L. Low, C. D. Chen, H. L. Lee et al., "Current susceptibility status of Malaysian *Culex quinquefasciatus* (Diptera: Culicidae) against DDT, propoxur, malathion, and permethrin," *Journal of Medical Entomology*, vol. 50, no. 1, pp. 103-111, 2013.
- [5] A. S. Derbalah, "Efficacy of some botanical extracts against *Trogoderma granarium* in wheat grains with toxicity evaluation," *The Scientific World Journal*, vol. 2012, Article ID 639854, 9 pages, 2012.
- [6] R. Josse, A. Sharaneck, C. C. Savary, and A. Guillouzo, "Impact of isomalathion on malathion cytotoxicity and genotoxicity in human HepaRG cells," *Chemico-Biological Interactions*, vol. 209, pp. 68-76, 2014.
- [7] R. Mesnage, N. Defarge, J. S. Vendômois, and G. E. Seralini, "Major pesticides are more toxic to human cells than their declared active principles," *BioMed Research International*, vol. 2014, Article ID 179691, 8 pages, 2014.
- [8] L. S. Kjeldsen, M. Ghisari, and E. C. Bonefeld-Jørgensen, "Currently used pesticides and their mixtures affect the function of sex hormone receptors and aromatase enzyme activity," *Toxicology and Applied Pharmacology*, vol. 272, no. 2, pp. 453-464, 2013.
- [9] S. Karami-Mohajeri, M. Hadian, S. Fouladdel et al., "Mechanisms of muscular electrophysiological and mitochondrial dysfunction following exposure to malathion, an organophosphorus pesticide," *Human & Experimental Toxicology*, vol. 33, no. 3, pp. 251-263, 2014.
- [10] C. Taxvig, N. Hadrup, J. Boberg et al., "In vitro-in vivo correlations for endocrine activity of a mixture of currently used pesticides," *Toxicology and Applied Pharmacology*, vol. 272, no. 3, pp. 757-766, 2013.
- [11] D. G. Karpouzias and B. K. Singh, "Microbial degradation of organophosphorus xenobiotics: metabolic pathways and molecular basis," *Advances in Microbial Physiology*, vol. 51, pp. 119-225, 2006.
- [12] H. Wang, Z. Hu, B. Xiao, Q. Cheng, and F. Li, "Ammonium nitrogen removal in batch cultures treating digested piggery wastewater with microalgae *Oedogonium sp.*," *Water Science and Technology*, vol. 68, no. 2, pp. 269-275, 2013.
- [13] S. Rangabhashiyam, E. Suganya, N. Selvaraju, and L. A. Varghese, "Significance of exploiting non-living biomaterials for the biosorption of wastewater pollutants," *World Journal of Microbiology and Biotechnology*, 2014.
- [14] W. M. Ibrahim, "Biosorption of heavy metal ions from aqueous solution by red macroalgae," *Journal of Hazardous Materials*, vol. 192, no. 3, pp. 1827-1835, 2011.
- [15] M. W. Ibrahim and M. A. Essa, "Tolerance and utilization of organophosphorus insecticide by nitrogen fixing Cyanobacteria," *Egyptian Journal of Botany*, vol. 27, pp. 225-240, 2010.
- [16] R. Rippka, J. Deruelles, and J. B. Waterbury, "Generic assignments, strain histories and properties of pure cultures of cyanobacteria," *Journal of General Microbiology*, vol. 111, no. 1, pp. 1-61, 1979.
- [17] C. Zarrouk, *Contribution a l'etude d'une cyanophyceae. Influence de divers facteurs physiques et chimiques sur la croissance et la photosynthese de Spirulina maxima (Stech. et Gardner)* Geitler [Ph.D. thesis], Universite de Paris, Paris, France, 1966.
- [18] G. W. Prescott, *How to Know the Freshwater Algae*, The Picture Key Nature Series, W.M.C. Brown Company Publishers, Dubuque, Iowa, USA, 3rd edition, 1978.
- [19] O. H. Lowry, N. J. Rosebrough, A. L. Farr, and R. J. Randall, "Protein measurement with the Folin phenol reagent," *The Journal of biological chemistry*, vol. 193, no. 1, pp. 265-275, 1951.
- [20] F. W. Fales, "The assimilation and degradation of carbohydrates by yeast cell," *Journal of Biological Chemistry*, vol. 193, pp. 113-124, 1951.
- [21] J. J. Irigoyen, D. W. Emericha, and S. Diaz, "Water stress induced changes in concentrations of praline and total soluble sugars in nodulated alfalfa (*Medicago sativa*) plants," *Physiology of Plant*, vol. 84, pp. 55-60, 1992.

- [22] W. S. Pierpoint, "The phosphatase and metaphosphatase activities of pea extracts," *The Biochemical journal*, vol. 65, no. 1, pp. 67–76, 1957.
- [23] A. K. Ghadai, S. Kumar, and D. K. Acharya, "Bio-Molecular assay of cyanobacteria on response to diazinon an Organophosphorus insecticide," *International Journal of Chemical Research*, vol. 2, no. 1, pp. 20–24, 2010.
- [24] J. Ma, R. Zheng, L. Xu, and S. Wang, "Differential sensitivity of two green algae, *Scenedesmus obliquus* and *Chlorella pyrenoidosa*, to 12 pesticides," *Ecotoxicology and Environmental Safety*, vol. 52, no. 1, pp. 57–61, 2002.
- [25] F. I. Y. Mostafa and C. S. Helling, "Impact of four pesticides on the growth and metabolic activities of two photosynthetic algae," *Journal of Environmental Science and Health B Pesticides, Food Contaminants, and Agricultural Wastes*, vol. 37, no. 5, pp. 417–444, 2002.
- [26] A. A. Fathi, "Some metabolic activities in the green alga *Scenedesmus bijuga* as affected by the insecticide trichlorfon," *Protistology*, vol. 3, pp. 92–98, 2003.
- [27] B. Nayak, S. Bhattacharyya, and J. Sahu, "Photosynthetic response of two rice field cyanobacteria to pesticides," in *Pesticides-Advances in Chemical and Botanical Pesticides*, P. R. Soundararajan, Ed., chapter 7, pp. 151–168, Agricultural and Biological Sciences, 2012.
- [28] C. Rioboo, O. González, C. Herrero, and A. Cid, "Physiological response of freshwater microalga (*Chlorella vulgaris*) to triazine and phenylurea herbicides," *Aquatic Toxicology*, vol. 59, no. 3-4, pp. 225–235, 2002.
- [29] Y. Yamamoto and H. Tsukada, "Measurement of in situ specific growth rates of microcystis (cyanobacteria) from the frequency of dividing cells," *Journal of Phycology*, vol. 45, no. 5, pp. 1003–1009, 2009.
- [30] N. Manikar, I. S. Kumar, K. Habib, and T. Fatma, "Biochemical analysis of *Anabaena variabilis* exposed to malathion pesticide with special reference to oxidative stress and osmolytes," *International Journal of Innovative Research in Science, Engineering and Technology*, vol. 2, no. 10, pp. 5403–5420, 2013.
- [31] S. Kumar, K. Habib, and T. Fatma, "Endosulfan induced biochemical changes in nitrogen-fixing cyanobacteria," *Science of the Total Environment*, vol. 403, no. 1–3, pp. 130–138, 2008.
- [32] S. XIE, J. LIU, L. LI, and C. QIAO, "Biodegradation of malathion by *Acinetobacter johnsonii* MA19 and optimization of cometabolism substrates," *Journal of Environmental Sciences*, vol. 21, no. 1, pp. 76–82, 2009.
- [33] G. Subramanian, S. Sekar, and S. Sampooram, "Biodegradation and utilization of organophosphorus pesticides by cyanobacteria," *International Biodeterioration and Biodegradation*, vol. 33, no. 2, pp. 129–143, 1994.

Research Article

Production and Cytotoxicity of Extracellular Insoluble and Droplets of Soluble Melanin by *Streptomyces lusitanus* DMZ-3

D. N. Madhusudhan,¹ Bi Bi Zainab Mazhari,¹ Syed G. Dastager,² and Dayanand Agsar¹

¹ A-DBT Research Laboratory, Department of Microbiology, Gulbarga University, Gulbarga 585 106, India

² NCIM Resource Centre, Biochemical Sciences Division, National Chemical Laboratory (CSIR), Pune 411008, India

Correspondence should be addressed to Dayanand Agsar; dayanandagsar@gmail.com

Received 21 February 2014; Revised 14 March 2014; Accepted 14 March 2014; Published 16 April 2014

Academic Editor: Leandro Rocha

Copyright © 2014 D. N. Madhusudhan et al. This is an open access article distributed under the Creative Commons Attribution License, which permits unrestricted use, distribution, and reproduction in any medium, provided the original work is properly cited.

A *Streptomyces lusitanus* DMZ-3 strain with potential to synthesize both insoluble and soluble melanins was detected. Melanins are quite distinguished based on their solubility for varied biotechnological applications. The present investigation reveals the enhanced production of insoluble and soluble melanins in tyrosine medium by a single culture. *Streptomyces lusitanus* DMZ-3 was characterized by 16S rRNA gene analysis. An enhanced production of 5.29 g/L insoluble melanin was achieved in a submerged bioprocess following response surface methodology. Combined interactive effect of temperature (50°C), pH (8.5), tyrosine (2.0 g/L), and beef extract (0.5 g/L) were found to be critical variables for enhanced production in central composite design analysis. An optimized indigenous slant culture system was an innovative approach for the successful production (264 mg/L) of pure soluble melanin from the droplets formed on the surface of the culture. Both insoluble and soluble melanins were confirmed and characterized by Chemical, reactions, UV, FTIR, and TLC analysis. First time, cytotoxic study of melanin using brine shrimps was reported. Maximum cytotoxic activity of soluble melanin was Lc_{50} -0.40 μ g/mL and insoluble melanin was Lc_{50} -0.80 μ g/mL.

1. Introduction

Melanin, a polyphenolic polymer formed by the oxidative polymerization of phenolic and/or indolic compounds, was generally produced from the oxidation of L-tyrosine by tyrosinase or laccase to L-DOPA and dopaquinones, finally to dihydroxyindole carboxylic acid and their reduced forms [1]. Melanins are commonly found in animals, plants, bacteria, and fungi [2]. In humans, they are found mainly in the skin and hair as dark colored pigments. In bacteria and fungi, melanins are found in their cell wall. The biological melanins are commonly known based on the color and the substrate from which they originate. Eumelanin is blackish brown, Pheomelanin is yellow to red, and Pyomelanin is brown in color [3]. Eumelanin is the predominant pigment synthesized in humans and microorganisms, especially in bacteria and fungi [2].

Melanin is commercially extracted from cuttlefish and depends on irregular supply of natural material and also is

expensive [4]. Plenty of literature is available regarding the synthesis and production of eumelanin by different bacteria [5, 6] and fungi [7, 8]. The production of melanin by recombinant *E. coli* under optimized submerged bioprocess was reported by Muñoz et al. [9]. Dastager et al. [10] and Quadri and Agsar [11] have reported the production of melanin by *Streptomyces* species. Manivasagan et al. [12] and Surwase et al. [13] have reported the production of melanin by *Actinoalloteichus sp.* and *Brevundimonas sp.*, respectively, employing Response Surface Method (RSM). RSM using different statistical designs is an important approach to optimize the process condition for the enhanced production of bioactive molecules [14]. Formation of droplets on the surface of the colonies of few sporulated microorganisms constituting mainly enzymes or antibiotics or pigments was reported [15–17].

Melanin plays an important role in humans and its lack leads to several abnormalities and diseases. The reduced

melanin in neurons causes Parkinson's disease [18]. Melanin also plays an important role in microorganisms against damages from high temperatures, chemical stress, and biochemical threats [19]. The role of biologically active melanin includes being cytotoxic, antitumor [20], antivenin [21], antiviral [22], and radio protective [23]. Sun-screens containing water soluble melanin protect against harmful UV radiations. Water soluble melanins are used in solid plastic films, lenses, paints, varnishes, and other surface protection formulations to provide greater UV protections [24]. AIDS treatment news [25] reveals the selective antiviral activity of synthetic soluble melanin against human immunodeficiency virus [22]. However, it is critical for melanin to be water soluble for a better commercial potential in biotechnological applications. Insoluble melanins require severe treatments such as boiling in strong alkali or the use of strong oxidants for making them water soluble, which often damages them [26]. The present investigation was undertaken to produce insoluble melanin and soluble melanin from droplets of *Streptomyces*, as no literature is available regarding this approach. The standardization of production of bioactive molecules from such droplets is a novel criterion explaining production of melanin by *Streptomyces* in unique form. Further, the cytotoxic activity of melanins was evaluated using brine shrimps. The brine shrimp cytotoxic activity has been found out as safe, practical, and economical to determine the bioactivity of the synthetic compounds [27], which showed a significant correlation with *in vitro* growth check for human solid tumor cell lines [28].

2. Materials and Methods

2.1. Screening of *Streptomyces*. *Streptomyces* collection preserved in our A-DBT (Actinomycetes-Diversity and Bioprocess Technology) research laboratory was screened by plate culture for the synthesis of melanin on starch tyrosine agar (STA): Starch 10 g, K₂HPO₄ 2 g, KNO₃ 2 g, NaCl 2 g, Tyrosine 4 g, MgSO₄ 0.05 g, CaCO₃ 0.3 g, FeSO₄ 0.01 g, Agar 20 g, deionized water 1 L, and pH 8.0 and also on tyrosine agar (TA): Gelatin 5 g, Tyrosine 5 g, beef extract 3 g, Agar 20 g, deionized water 1 L, and pH 8.0 [29]. The plates inoculated with test isolates were incubated at 40°C for 120 h and observed for synthesis of melanin based on the intensity of dark brown pigmentation and degree of zone of catalysis as reported by Nicolaus et al. [3] and Shivaveerakumar et al. [30].

2.2. Molecular Characterization of *Streptomyces*. Efficient isolate for melanin synthesis was characterized by 16S rRNA analysis [31]. Genomic DNA was prepared by using Chelex-100 (Sigma-Aldrich, USA) chelating ion exchange resin method [32]. Employing about 100 nanogram DNA, 16S rRNA amplified using universal F27 (5'AGAGTTTGATCM-TGGCTCAG-) and R1525 (5'TACGG(C/T) TACCTTGT-TACGACTT) primers. Accuracy of PCR product was visualized on agarose gel and sequenced using a BigDye Terminator kit, version 3.1, on an automatic ABI 3100 sequencer (Applied Biosystems Inc.). The sequences obtained were analyzed

using NCBI Blast search and EzTaxon [33] to restore closest relatives and phylogenetic tree was obtained.

2.3. Production of Insoluble Melanin. Submerged bioprocess in tyrosine broth was standardized for the production of melanin using *Streptomyces lusitanus* DMZ-3, employing important process variables one at a time and keeping others at a constant level [34]. pH (7.0, 7.5, 8.0 and 8.5) of the medium, inoculum size (from 1×10^6 to 1×10^9 with interval of 1×10^1), incubation temperature (35, 40, 45, 50 and 55°C), period of incubation (48, 72, 96, 120, 144 and 168 h), and rate of agitation (120, 140, 160, 180 and 200 rpm) were manually optimized. The influence of various carbon sources (Starch, glucose, sucrose, maltose, and beef extract at 0.2 to 2.0% concentrations), nitrogen sources (soyabean meal, ammonium nitrate, casein, and tyrosine at 0.2 to 2.0% concentrations), and mineral salts (CuSO₄, MgSO₄, FeSO₄, MnSO₄, and K₂HPO₄ at 0.05 to 0.25% concentrations) were also optimized.

Response Surface Method (RSM) with central composite design (CCD) was employed [12] to resolve the optimum combination and interactive effect of critical process variables on the enhanced production of melanin. The CCD of 30 runs was set using the Design Expert Software, USA (Version 7.0). All the experiments were carried out in duplicate and average of melanin production obtained was considered as the dependent variables or responses (Y). The predicted response was calculated from the second degree polynomial equation, which included all the terms. $Y = \beta_0 + \sum \beta_i X_i + \sum \beta_{ii} X_i^2 + \sum \beta_{ij} X_i X_j$, where Y stands for the response variable, β_0 is the intercept coefficient, β_i represents the coefficient of the linear effect, β_{ii} the coefficient of quadratic effect, and β_{ij} the *ij*th interaction coefficient effect. $X_i X_j$ are input variables which influence the response variable Y and β_i is the *i*th linear coefficient [35]. Other parameters which have no much role in production of melanin were kept constant. The statistical and numerical analysis of the model was performed with the analysis of variance (ANOVA). The statistical significance of the model was analyzed by the Fisher's F-test, its associated probability P(F), correlation coefficient R, and determination coefficient R², which explains the quality of polynomial model. The quadratic models were represented as contour plots (three-dimensional) and response surface curves were created for each variable. The model was validated for enhanced production of melanin, at specific level of optimized critical process variables.

The extraction and purification of the melanin were carried out as per the standard protocols described by Fava et al. [36] and Harki et al. [37], respectively. The incubated broth was centrifuged at 8,000 g for 15 minute to separate the cell mass and the pigment. Extracted dried pigment pellet was subjected to the dialysis in cellulose membrane against phosphate buffer of pH 7.0 and purified by column using Silica Gel material of 60–120 mesh size.

2.4. Production of Soluble Melanin. An indigenous method of slant culture system was standardized and operated for the synthesis and extraction of soluble pigment. Potential

isolate of *Streptomyces* was inoculated on the slants of tyrosine agar. The 50 mL capacity borosilicate glass tube with 15 mL medium was employed for the synthesis of melanin formed as clearly visible pigment droplets on the surface of the slant culture. The slants inoculated were incubated at 45°C for 120 h. The dark brown pigment droplets present on the entire surface of the culture were completely extracted using micropipette and dried in hot air oven at 60°C for 1 h. Replicates of three slants were considered to calculate a simple arithmetic mean of total soluble melanin produced per liter of tyrosine medium.

2.5. Confirmation of Melanin. The pigments obtained by both submerged bioprocess and slant culture were confirmed as insoluble and soluble melanin by following chemical method, UV-vis spectroscopy, FT-IR spectroscopy, and thin layer chromatographic techniques. The solubility of pigments in deionized water, 1 N HCl, 1 N NaOH, 1 N KOH, 1 N NH₄OH, ethanol, acetone, chloroform, and benzene was assessed [1, 38]. The reaction of the pigment with oxidizing agent H₂O₂ (30%), reducing agents H₂S, and sodium hydrosulfite (5%) was observed and recorded for the confirmation of the pigment as a melanin. The pigment was also subjected to precipitation reaction with FeCl₃ (1%), ammonical silver nitrate, and potassium ferricyanide. UV-visible absorption spectrum in the region of 200 to 600 nm was observed [39] for a characteristic property of a melanin using Systronics 2201 double beam UV-visible spectrophotometer. The pigments were directly subjected to FT-IR Spectroscopy analysis and spectrum was recorded at 4000 to 500 cm⁻¹ [40] using thermo Nicolet iS5 FT-IR Spectroscopy. The confirmation of the pigment as melanin was also performed by thin layer chromatography [41]. The pigment extracts were separated and compared with standard melanin using silica gel chromatography plate (Merck TLC Silica Gel 60 F₂₅₄). The separation was made using the different proportions of organic solvents such as chloroform, hexane, butanol, acetic acid, and methanol. After optimizing the solvent proportions, separate bands were observed staining with iodine.

2.6. Cytotoxic Activity of Melanin. The cytotoxic activities of insoluble and soluble melanins were determined by following the standard protocol of Meyer et al. [42] using brine shrimps (*Artemia salina*). Artificial sea/saline water was prepared, dissolving 20 g of NaCl per liter and pH was adjusted to 8.5 with 0.1 M Na₂CO₃. 1 g eggs of brine shrimp was added to the 1L seawater and incubated at 28°C for 48 h with constant air supply and light. The hatched brine shrimps were collected and rinsed in fresh seawater. The insoluble and soluble melanin concentrations (0, 1, 2, 4, 8, 16, 32, and 64 µg/mL) were diluted in 5 mL seawater in separate tubes and incubated at 28°C. Sample with zero concentration of melanins was considered as control. The mortality number of brine shrimps for every 6 h up to 24 h was recorded. The percentage of mortality and lethal concentration value (LC₅₀-µg/mL) of melanins were calculated. The mortality end point of the bioassay was referred to as the absence of controlled

forward motion during 30 seconds of observation and the concentration that killed 50% of brine shrimps as LC₅₀. Criterion of toxicity for fractions was categorized as nontoxic (LC₅₀ values > 1000 µg/mL), poor toxic (500–1000 µg/mL), and toxic (<500 µg/mL) according to Déciga-Campos et al. [43].

3. Results and Discussion

3.1. Screening and Characterization of *Streptomyces*. Seven isolates of *Streptomyces* were screened for the extracellular synthesis of melanin on starch tyrosine and tyrosine agar. Starch casein agar is a medium prescribed by Küster and Williams [44] for the isolation of actinobacteria. Casein was replaced by tyrosine and used for the isolation and screening of *Streptomyces* for the synthesis of melanin. Degree of coloration or intensity of color (brown) was conventional method prescribed [45] for the detection of melanin synthesis by microorganisms. A varied degree of synthesis of melanin by the test isolates of *Streptomyces* was clear from the visible (Figure 1(a)) brown pigment (melanin) intensity on starch tyrosine agar. In addition to the intensity of brown pigmentation, the formation of catalytic zone around the colonies of the test isolates on tyrosine agar (Figure 1(b)) significantly reveals the synthesis of melanin. However, tyrosine agar was reported earlier [29] to be used for the differentiation of *Streptomyces* but never recorded for the formation of catalytic zone indicating the melanin activity. Surprisingly, this medium exhibited both, high intensity of color and also catalytic zone (a clear zone around the colony catalyzing the tyrosine), indicating the synthesis of melanin. The degrees of catalytic zone developed can be considered as an innovative criterion for the selection of potential isolate targeting the production of melanin. An isolate *Streptomyces* DMZ-3 was selected as physiologically efficient and potential isolates (Figure 1(b)) for the maximum synthesis of melanin. A similar approach was reported by Shivaveerakumar et al. [30] as a novel criterion for the screening of actinobacteria aiming at the synthesis of extracellular tyrosinase.

Actinobacteria can be analyzed at various molecular levels to gain information suitable for constructing databases and effective identification. Sequence analysis of various genes provides a stable classification and accurate identification, which has become the cornerstone of modern phylogenetic taxonomy [46]. The region of 16S rRNA gene is highly variable and differs significantly between species where other areas are more conserved and suitable for identification at the generic level [47]. An almost complete 16S rRNA gene sequence of isolate DMZ-3 (1,401 nucleotides) was determined (Genbank, NCBI Accession number: KF486519). A phylogenetic tree was constructed based on 16S rRNA gene sequences to show the comparative relationship between isolate DMZ-3 and other related *Streptomyces* species (Figure 1(c)). The comparative analysis of 16S rRNA gene sequence and phylogenetic relationship reveals that isolate DMZ-3 lies in a subclade with *Streptomyces lusitanus*, sharing 99.7% of 16S rRNA gene sequence similarity.

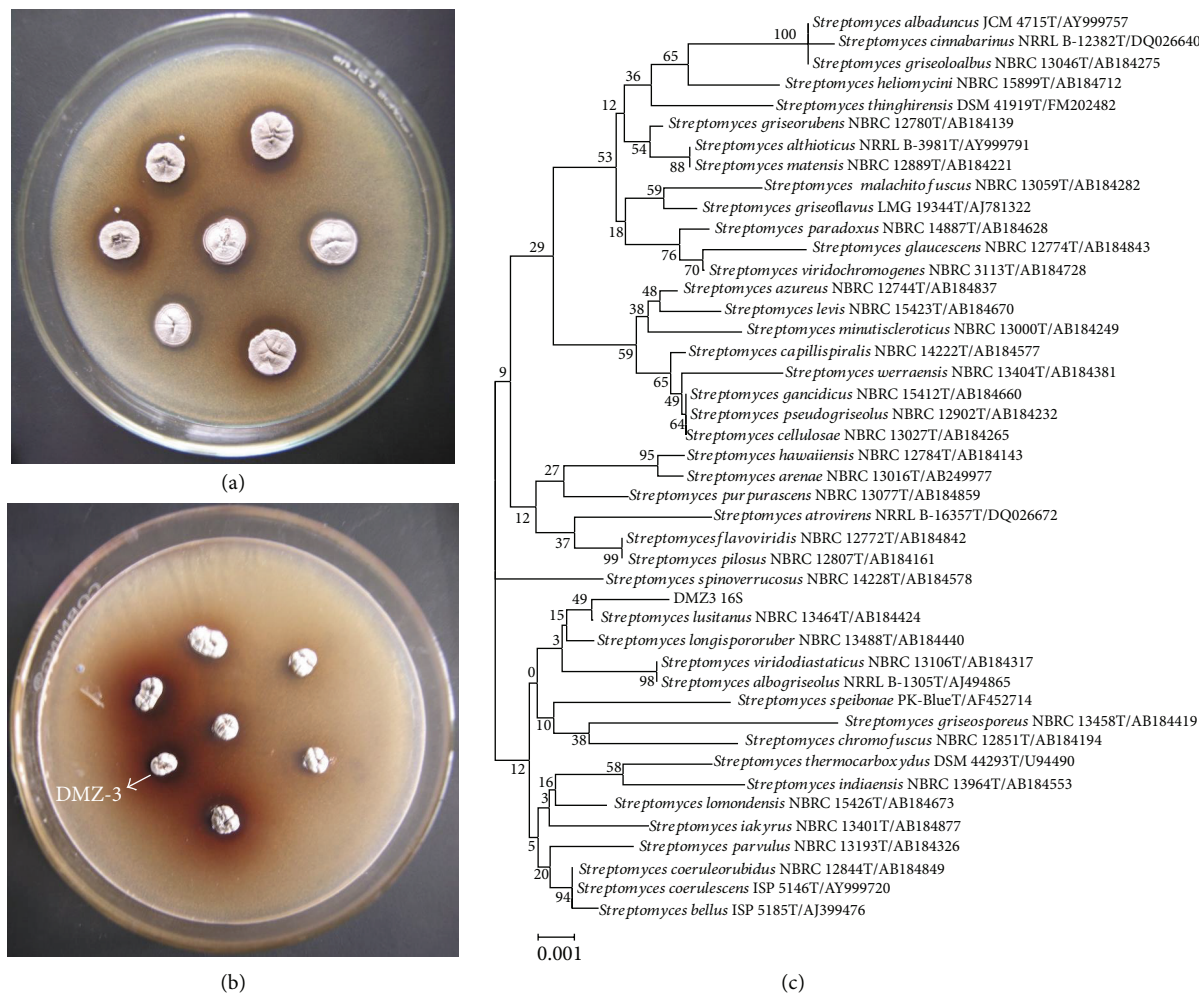


FIGURE 1: Screening of isolates for the synthesis of melanin on starch tyrosine (a), tyrosine agar (b), and phylogenetic tree (c) of *Streptomyces* DMZ-3.

3.2. Production of Insoluble and Soluble Melanin. Operation of process variables using manually one at a time and keeping others constant is a precondition to detect critical variables for the production of melanin employing response surface methodology. 4.2 g/L melanin was produced by *Streptomyces lusitanus* DMZ-3 in tyrosine medium under the optimized submerged bioprocess. Among all the optimized process variables, temperature, pH, tyrosine, and beef extract were identified as critical variables based on the level of the melanin production. Determination of important physiochemical and nutritional factors is an important criterion for the maximum production of melanin, in the development of a suitable bioprocess. Few reports are available regarding the production of extracellular and intracellular melanins. Santos and Stephanopoulos [5] and Muñoz et al. [9] reported 375 mg/L and 6 g/L of extracellular melanin production, respectively, by recombinant *E. coli*. Sajjan et al. [6] and Youngchim et al. [48] have reported the production of intracellular melanin by *Klebsiella sp.* and *Aspergillus fumigatus*, respectively. Dastager et al. [10] revealed the production of extracellular melanin by *Streptomyces* in synthetic media.

In the recent past, Response Surface Method, a software based statistical design, is the most validated method for the production of biomolecules, especially in the submerged fermentation. In the present investigation, an attempt was made to achieve the higher production of melanin by *Streptomyces lusitanus* DMZ-3 in submerged bioprocess. Actual and predicted values of the degree of melanin production with identified critical process variables employing RSM with CCD were shown in Table 1. Maximum response with 5.29 g/L of melanin was achieved at 9th run against a predicted value of 4.65 g/L. A polynomial equation regarding the production of melanin (Y) based on the regression analysis was as follows:

$$\begin{aligned} \text{Melanin production (Y)} = & 4.35 + 0.094X_1 \\ & + 0.17X_2 + 0.95X_3 \\ & - 0.050X_4 - 0.57X_1^2 \\ & - 0.34X_2^2 - 0.58X_3^2 \end{aligned}$$

TABLE 1: Optimization of critical process variables employing response surface method for the production of insoluble melanin by *Streptomyces lusitanus* DMZ-3.

Run	Critical process variables				Melanin production (g/L)	
	X_1 : A: Temperature °C	X_2 : B: pH	X_3 : C: Tyrosine %	X_4 : D: Beef extract %	Actual value	Predicted value
1	42.50	7.75	1.25	1.25	4.35	4.35
2	42.50	7.75	1.25	1.25	4.35	4.35
3	35.00	7.00	0.50	2.00	1.08	2.12
4	35.00	8.50	2.00	2.00	3.05	3.51
5	27.50	7.75	1.25	1.25	2.12	1.90
6	35.00	8.50	2.00	0.50	4.21	3.73
7	42.50	7.75	1.25	1.25	4.35	4.35
8	42.50	7.75	2.75	1.25	4.05	3.91
9	50.00	8.50	2.00	0.50	5.29	4.65
10	42.50	9.25	1.25	1.25	3.15	3.35
11	35.00	7.00	2.00	2.00	3.11	2.99
12	50.00	7.00	0.50	0.50	1.63	1.57
13	35.00	7.00	2.00	0.50	2.41	2.91
14	50.00	8.50	2.00	2.00	3.92	4.53
15	57.50	7.75	1.25	1.25	2.16	2.27
16	42.50	7.75	1.25	1.25	4.35	4.35
17	50.00	8.50	0.50	2.00	1.55	1.44
18	35.00	8.50	0.50	2.00	1.53	1.38
19	42.50	7.75	1.25	2.75	4.48	3.47
20	42.50	7.75	1.25	1.25	4.35	4.35
21	42.50	7.75	1.25	-0.25	2.78	3.67
22	50.00	8.50	0.50	0.50	1.89	1.72
23	35.00	8.50	0.50	0.50	1.55	1.75
24	50.00	7.00	2.00	2.00	3.20	3.40
25	42.50	7.75	-0.25	1.25	0.090	0.12
26	42.50	6.25	1.25	1.25	2.98	2.67
27	42.50	7.75	1.25	1.25	4.35	4.35
28	50.00	7.00	2.00	0.50	3.35	3.22
29	50.00	7.00	0.50	2.00	1.38	1.58
30	35.00	7.00	0.50	0.50	3.10	2.21

$$\begin{aligned}
 & - 0.19X_4^2 + 0.15X_1X_2 \\
 & + 0.24X_1X_3 + 0.024X_1X_4 \\
 & + 0.32X_2X_3 - 0.073X_2X_4 \\
 & + 0.041X_3X_4,
 \end{aligned}
 \tag{1}$$

where X was the response variables for melanin production with X_1 , X_2 , X_3 , and X_4 as coded values of temperature, pH, tyrosine, and beef extract, respectively. The model characteristic response for the production of melanin was statistically analyzed (Table 2) using ANOVA. The model showed a high coefficient R^2 value of 0.8832 where standard should be >0.75 and between 0 and 1. The model F value of 8.10 implies the model as significant and the lack of fit F value was 5.62 indicating the lack of fit was not significant in relation to the pure error. The ratio greater than 4 is desirable to confirm

the model as acceptable and the obtained ratio was 10.462. This revealed that the model can be used to navigate the design space. The response variables C , A^2 , B^2 , and C^2 were found to be as significant model terms. Each critical variable in the model with respect to incubation time was presented as response surface curves by contour plots (Figure 2). Every critical variable showed maximum melanin production at a constant middle level of the other variables. However, increase in the production of melanin was observed with increase in these variables. The validation of the statistical model and regression analysis considering $X_1(50^\circ\text{C})$, $X_2(8.5\text{ pH})$, $X_3(2\%)$, and $X_4(0.5\%)$ values were evident that the use of RSM with CCD can be effectively used and the conditions are ideal for the production of melanin.

Temperature, pH, tyrosine, and beef extract were the most critical factors to produce enhanced level (5.29 g/L) melanin by *Streptomyces lusitanus* DMZ-3 in submerged bioprocess. Manivasagan et al. [12] reported the production (85.37 $\mu\text{g/L}$)

TABLE 2: Analysis of variance (ANOVA) of model response data.

Source	Sum of squares	Df	Mean square	F value	P value prob > F
Model	42.50	14	3.04	8.10	0.0001
A: temperature	0.21	1	0.21	0.56	0.4647
B: pH	0.69	1	0.69	1.84	0.1948
C: tyrosine	21.57	1	21.57	57.55	<0.0001
D: beef extract	0.061	1	0.61	0.16	0.6923
AB	0.38	1	0.38	1.00	0.3329
AC	0.90	1	0.90	2.40	0.1425
AD	9.506E – 003	1	9.506E – 003	0.025	0.8756
BC	1.61	1	1.61	4.29	0.0561
BD	0.086	1	0.086	0.23	0.6397
CD	0.026	1	0.026	0.070	0.7943
A ²	8.81	1	8.81	23.51	0.0002
B ²	3.09	1	3.09	8.24	0.0117
C ²	9.36	1	9.36	24.99	0.0002
D ²	1.04	1	1.04	2.76	0.1173
Residual	5.62	15	0.37		
Lack of fit	5.62	10	0.56		
Pure error	0.000	5	0.000		
Cor total	48.12	29			

$R^2 = 0.8832$

of melanin from *Actinoalloteichus sp.* MA-32, with glycerol, L-tyrosine, NaCl, and trace salt solution as critical process variables employing response surface methodology with central composite design. However, Surwase et al. [13] revealed pH, tryptone, L-tyrosine, and copper sulphate as critical variables for the production (6.8 g/L) of melanin by a bacterium, *Brevundimonas sp.* SGJ employing response surface method with Box-Behnken method. It is evident from the present investigation and with reported literature that a critical process variable, either physicochemical or nutritional, does vary from one organism to another, irrespective of method being employed for the production of melanin. The physiological and metabolic nature of the organism involved might regulate the process variables required for the production of melanin in given bioprocess. The simple ingredients of the medium for an efficient production of melanin are the added advantage of the present investigation.

The preserved culture of *Streptomyces lusitanus* DMZ-3 on tyrosine agar, to our surprise, could show the formation of dark brown pigment droplets (Figure 3) on the entire surface of the slant culture. This natural phenomenon of synthesis of dark brown pigment in the form of droplets was explored and standardized for the production of melanin. It is a novel approach to progress the production of melanin employing a slant culture system. An entire slant culture grown on 15 mL medium could generate about 1 mL droplet and upon drying 3.96 mg of pigment was obtained. A simple experiment, designed statistically in triplicate, revealed the production of 264 mg pigment per liter of tyrosine medium by *Streptomyces lusitanus* DMZ-3. Early literature reports the formation of droplets on the surface of the colonies of fungi [17] and *Streptomyces* [49, 50], consisting broad range of enzymes,

antibiotics, and pigments. The present investigation reveals the formations of droplets on the surface of *Streptomyces lusitanus* and for the first time droplets were reported to contain exclusively pure soluble melanin. It is interesting to note that the formation of droplets occurred only when the isolate was grown at 45°C on tyrosine agar with a pH of 8.0. It confirms the earlier reports [51] indicating the formation of droplets by organisms under stress conditions. Martín et al. [52] reported that the gene for the secretion of this kind of metabolite droplets lies within the gene cluster for the corresponding biosynthesis. In depth investigations are essential to understand specific genes regulating the synthesis of soluble melanin droplets by *Streptomyces lusitanus* DMZ-3. A water soluble melanin has been reported [53] in a mutant strain of *Bacillus thuringiensis*. However, few patents reveal the production of water soluble synthetic [54] and fungal melanin [55].

3.3. Confirmation and Characterization of Melanins. The pigment obtained under submerged bioprocess was purified by chromatographic technique using silica gel columns. Thus purified pigment (pigment 1) and the pigment directly extracted from the slant culture system (pigment 2) were analyzed for their characteristic chemical features (Table 3). Interestingly, both pigments 1 and 2 produced by the same organism *Streptomyces lusitanus* DMZ-3 were revealed to be insoluble and soluble in water, respectively. However, solubility of both pigments in other alkaline solutions and organic solvents is one and the same. The other chemical reactions of both the pigments were also similar. In all, blackish brown color and total chemical reactions confirm

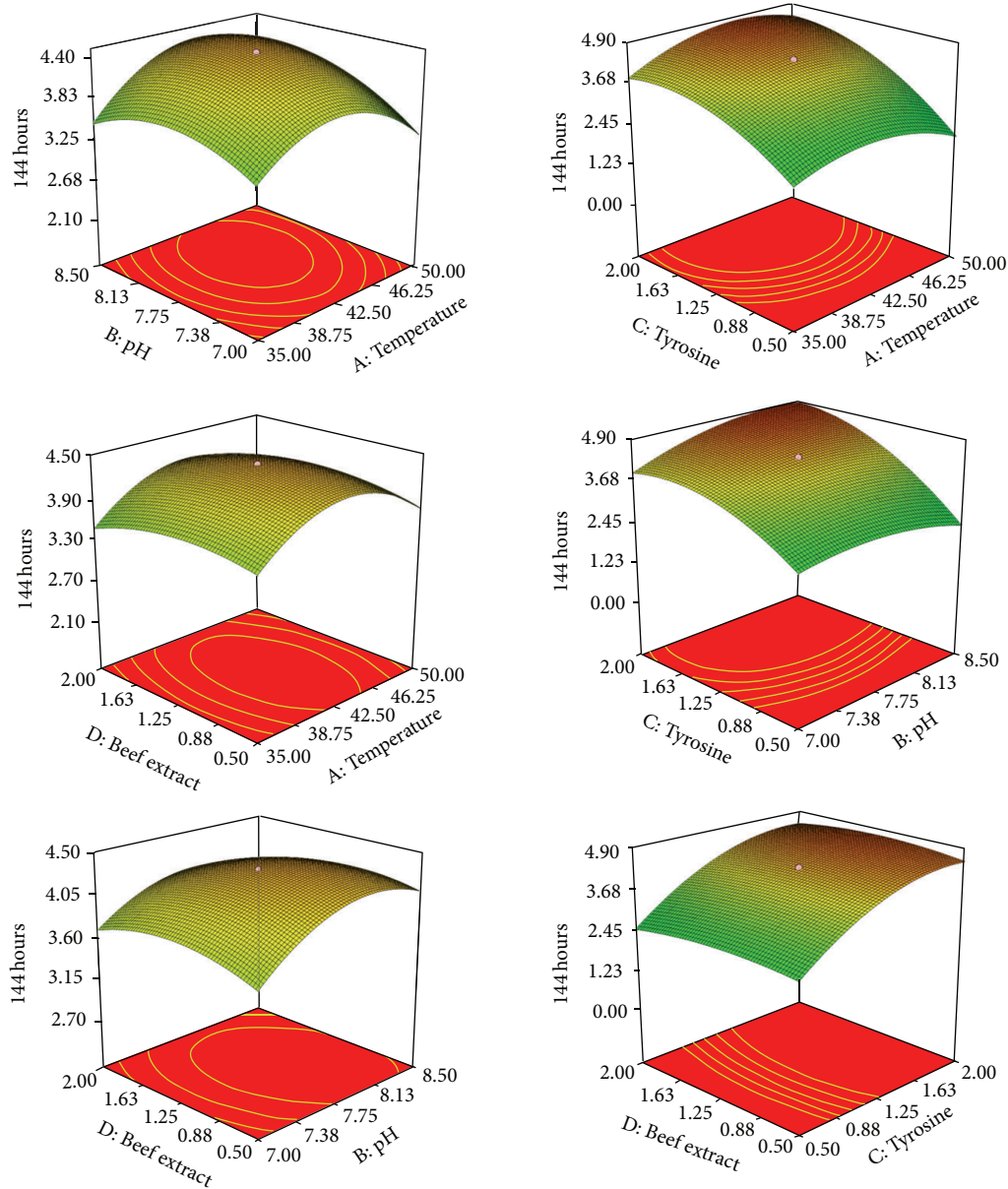


FIGURE 2: Contour plots and response surface curves of the production of insoluble melanin by *Streptomyces lusitanus*.

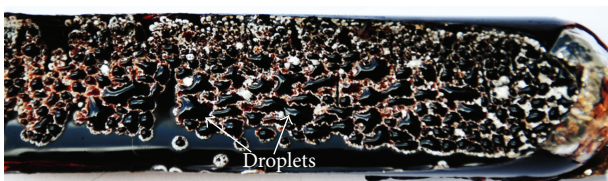


FIGURE 3: Formation of dark brown pigment droplets on the surface of the slant culture of *Streptomyces lusitanus* DMZ-3.

[1, 56] pigments 1 and 2 as insoluble and soluble melanin, respectively.

Both pigments gave maximum UV absorption between 200 and 300 nm but decreased towards visible range in the similar line of standard melanin under UV-Vis spectrophotometer (Figure 4), revealing [57] the typical nature

of the melanin absorbance. The FT-IR spectrophotometric (Figure 5) analysis of insoluble and soluble pigments showed the absorption at 3305.00 cm^{-1} ($-\text{OH}$ and $-\text{NH}$ bonds), 1651.41 cm^{-1} (aromatic stretch $\text{C}=\text{C}$), and 3386.47 cm^{-1} and 1644.48 cm^{-1} respectively. The absorbance at these ranges proves [58, 59] the pigments as melanins and the peaks in the soluble melanin indicate the purity. Finally, the pigments were separated after standardizing the solvent proportion with 1:4:1 ratio of 0.1 N NaOH, ethanol, and chloroform, respectively. The separated bands (Figure 6) reveal the equal R_f with standard melanin.

3.4. *Cytotoxicity of Melanins*. Assessment of cytotoxicity of chemicals using cell lines is not an uncommon procedure and is accurately correlated [60] with the assessment of

TABLE 3: Chemical analysis of the pigments.

Color and reactions	Observations	
	Pigment 1	Pigment 2
Color	Blackish brown	Blackish brown
Solubility in water	Insoluble	Soluble
Solubility in 0.1N NH ₄ OH	Readily soluble	Readily soluble
Solubility in 0.1N NaOH	Soluble	Soluble
Solubility in 0.1N KOH	Soluble	Soluble
Solubility in organic solvents (Ethanol, acetone, chloroform, benzene)	Insoluble	Insoluble
Reaction with sodium dithionite and with potassium ferricyanide	Decolorized and turned to brown	Decolorized and turned to brown
Reaction with H ₂ S	Reduced	Reduced

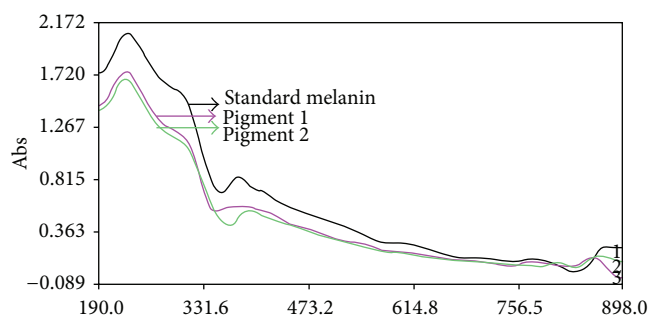


FIGURE 4: UV-visible spectrophotometric analysis of insoluble and soluble melanins.

cytotoxicity using brine shrimps. The brine shrimp assay method is considered as an excellent alternate option to assess the cytotoxic activity of the biological product [61]. From the beginning of its introduction to standardization [42], this *in vivo* test had successfully been adopted for the bioassay of active cytotoxic and antitumor agents [62]. Further the lethal concentration of brine shrimp can be correlated with the lethal dose in mice and was explained using medicinal plants earlier [63]. The number of brine shrimps survived and the percentage of mortality for 6 h, 12 h, and 24 h was summarized in Table 4. After 24 h, the total mortality was 100% in the highest concentration (64 $\mu\text{g}/\text{mL}$) of soluble melanin and 95% mortality was observed in insoluble melanin. The LC_{50} value was 0.40 $\mu\text{g}/\text{mL}$ for soluble melanin and 0.80 $\mu\text{g}/\text{mL}$ for insoluble melanin. Both pigments exhibit higher cytotoxic activity as LC_{50} value of both showed less than 500 $\mu\text{g}/\text{mL}$ [43]. However, soluble melanin could reveal 100% mortality and greater cytotoxic activity with half of the LC_{50} value, when compared to insoluble melanin.

4. Conclusions

A successful production of both insoluble and soluble melanins from a single isolate of *Streptomyces* is a significant

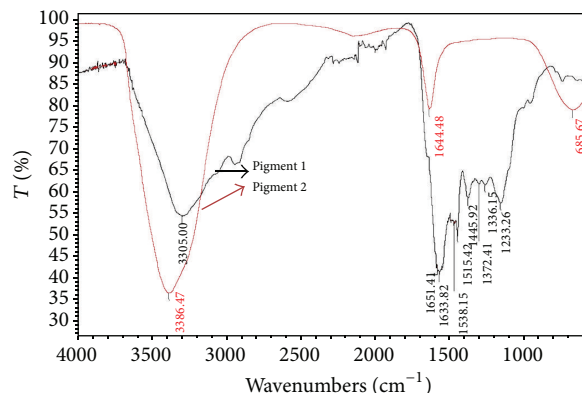


FIGURE 5: FT-IR Spectroscopic analysis of pigments 1 and 2.

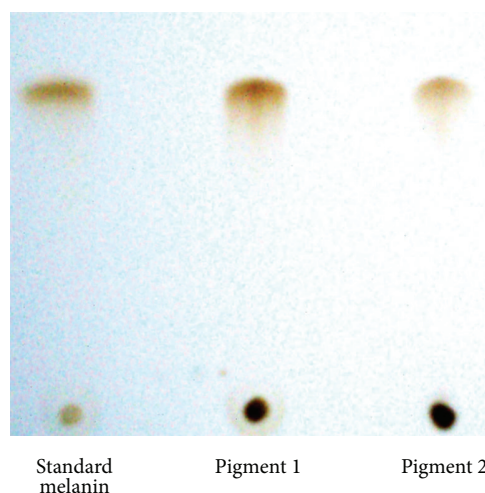


FIGURE 6: Thin layer chromatograph of insoluble and soluble melanins.

observation of the present investigation. *Streptomyces lusitanus* DMZ-3 characterized by 16S rRNA analysis was proved to be an efficient isolate for the synthesis of both melanins. An increased production (5.29 g/L) of insoluble melanin, in tyrosine medium under submerged bioprocess, was achieved by response surface methodology. The isolate had shown a greater consistency towards higher conditions of temperature (50°C) and pH (8.5) for the maximum production of insoluble melanin, using simple nutritional ingredients such as tyrosine and beef extract. An indigenous slant culture system designed and standardized for the production of pure soluble melanin from the droplets formed on the surface of the culture is a novel criterion. In an optimized slant culture system, we were able to harvest 0.264 g/L pure soluble melanin. Both melanin pigments produced by *Streptomyces lusitanus* DMZ-3 were confirmed and characterized with chemical reactions, UV, FTIR, and TLC analysis. Assessment of cytotoxicity of natural products is normally determined by either cell culture methods employing specific cell lines or using laboratory mice as experimental animals. In the present work, cytotoxicity of melanins was successfully investigated by using brine shrimps for the first time. Both insoluble and

TABLE 4: Cytotoxic activity of the insoluble and soluble melanins.

Concentration of melanin ($\mu\text{g/mL}$)	Log of concentration of melanin	Survived brine shrimps			Percent mortality			LC_{50} ($\mu\text{g/mL}$) at 24 h
		6 h	12 h	24 h	6 h	12 h	24 h	
Insoluble melanin								
01.0	0	19	11	06	10	45	70	0.80
02.0	0.301	17	11	07	15	45	65	
04.0	0.602	17	10	06	15	50	70	
08.0	0.903	17	09	04	15	55	80	
16.0	1.204	16	09	04	20	55	80	
32.0	1.505	16	09	03	20	55	85	
64.0	1.806	16	07	01	20	65	95	
Soluble melanin								
01.0	0	17	05	04	15	75	80	0.40
02.0	0.301	17	05	04	15	75	80	
04.0	0.602	16	05	04	20	75	80	
08.0	0.903	16	05	04	20	75	80	
16.0	1.204	15	05	03	25	75	85	
32.0	1.505	15	04	02	25	80	90	
64.0	1.806	15	03	00	25	85	100	

soluble melanins have been proved to be highly toxic but soluble melanin was more biologically active ($0.40 \mu\text{g/mL}$) as compared to insoluble melanin ($0.80 \mu\text{g/mL}$).

Conflict of Interests

The authors have no conflict of interests to declare.

Acknowledgment

The research Grant provided by Department of Biotechnology (BT/PR13864/PID/06/580/2010, Dt. 05.08.2011), Government of India, New Delhi, is sincerely acknowledged.

References

- [1] A. A. Bell and M. H. Wheeler, "Biosynthesis and functions of fungal melanins," *Annual Review of Phytopathology*, vol. 24, pp. 411–451, 1986.
- [2] K. Tarangini and S. Mishra, "Production, characterization and analysis of melanin from isolated marine *Pseudomonas* sp. using vegetable waste," *Research Journal of Engineering Sciences*, vol. 2, no. 5, pp. 40–46, 2013.
- [3] R. A. Nicolaus, M. Piattelli, and E. Fattorusso, "The structure of melanins and melanogenesis-IV. On some natural melanins," *Tetrahedron*, vol. 20, no. 5, pp. 1163–1172, 1964.
- [4] M. Magarelli, P. Passamonti, and C. Renieri, "Purification, characterization and analysis of sepia melanin from commercial sepia ink (*Sepia Officinalis*)," *CES Medicina Veterinaria y Zootecnia*, vol. 5, no. 2, pp. 18–28, 2010.
- [5] C. N. S. Santos and G. Stephanopoulos, "Melanin-based high-throughput screen for L-tyrosine production in *Escherichia coli*," *Applied and Environmental Microbiology*, vol. 74, no. 4, pp. 1190–1197, 2008.
- [6] S. Sajjan, G. Kulkarni, V. Yaligara, L. Kyoung, and T. B. Karegoudar, "Purification and physicochemical characterization of melanin pigment from klebsiella sp. GSK," *Journal of Microbiology and Biotechnology*, vol. 20, no. 11, pp. 1513–1520, 2010.
- [7] R. Romero-Martinez, M. Wheeler, A. Guerrero-Plata, G. Rico, and H. Torres-Guerrero, "Biosynthesis and functions of melanin in *Sporothrix schenckii*," *Infection and Immunity*, vol. 68, no. 6, pp. 3696–3703, 2000.
- [8] K. Rajagopal, G. Kathiravan, and S. Karthikeyan, "Extraction and characterization of melanin from *Phomopsis*: a phellyphytic fungi Isolated from *Azadirachta indica* A. Juss," *African Journal of Microbiology Research*, vol. 5, no. 7, pp. 762–766, 2011.
- [9] V. H. Muñoz, N. Cabrera-Valladares, F. Bolívar, G. Gosset, and A. Martínez, "Optimum melanin production using recombinant *Escherichia coli*," *Journal of Applied Microbiology*, vol. 101, no. 5, pp. 1002–1008, 2006.
- [10] S. G. Dastager, W.-J. Li, A. Dayanand et al., "Seperation, identification and analysis of pigment (melanin) production in Streptomyces," *African Journal of Biotechnology*, vol. 5, no. 11, pp. 1131–1134, 2006.
- [11] S. R. Quadri and D. Agsar, "Detection of melanin producing thermo-alkaliphilic Streptomyces from limestone quarries of the Deccan traps," *World Journal of Science and Technology*, vol. 2, no. 2, pp. 08–12, 2012.
- [12] P. Manivasagan, J. Venkatesan, K. Senthilkumar, K. Sivakumar, and S.-K. Kim, "Isolation and characterization of biologically active melanin from *Actinoalloteichus* sp. MA-32," *International Journal of Biological Macromolecules*, vol. 58, pp. 263–274, 2013.
- [13] N. S. Surwase, S. B. Jadhav, S. S. Phugare, and J. P. Jadhav, "Optimization of melanin production by *Brevundimonas* sp. SGJ using response surface methodology," *3 Biotech*, vol. 3, pp. 187–194, 2013.
- [14] M. Aghaie-Khouzani, H. Forootanfar, M. Moshfegh, M. R. Khoshayand, and M. A. Faramarzi, "Decolorization of some

- synthetic dyes using optimized culture broth of laccase producing ascomycete *Paraconiothyrium variabile*,” *Biochemical Engineering Journal*, vol. 60, pp. 9–15, 2012.
- [15] D. B. Johnstone and S. A. Waksman, “Production of streptomycin by *Streptomyces bikiniensis*,” *Journal of Bacteriology*, vol. 55, no. 3, pp. 317–236, 1948.
- [16] B. A. M. Rudd and D. A. Hopwood, “Genetics of actinorhodin biosynthesis by *Streptomyces coelicolor* A3(2),” *Journal of General Microbiology*, vol. 114, no. 1, pp. 35–43, 1979.
- [17] M. Gareis and E.-M. Gareis, “Guttation droplets of *Penicillium nordicum* and *Penicillium verrucosum* contain high concentrations of the mycotoxins ochratoxin A and B,” *Mycopathologia*, vol. 163, no. 4, pp. 207–214, 2007.
- [18] M. Fasano, S. Giraud, S. Coha, B. Bergamasco, and L. Lopiano, “Residual substantia nigra neuromelanin in Parkinson’s disease is cross-linked to α -synuclein,” *Neurochemistry International*, vol. 42, no. 7, pp. 603–606, 2003.
- [19] N. G. Allam and E. H. F. Abd El-Zaher, “Protective role of *Aspergillus fumigatus* melanin against ultraviolet (UV) irradiation and *Bjerkandera adusta* melanin as a candidate vaccine against systemic candidiasis,” *African Journal of Biotechnology*, vol. 11, no. 24, pp. 6566–6577, 2012.
- [20] R. C. R. De Goncalves and S. R. Pombeiro-Sponchiado, “Antioxidant activity of the melanin pigment extracted from *Aspergillus nidulans*,” *Biological and Pharmaceutical Bulletin*, vol. 28, no. 6, pp. 1129–1131, 2005.
- [21] Y.-C. Hung, V. Sava, M.-Y. Hong, and G. S. Huang, “Inhibitory effects on phospholipase A2 and antivenin activity of melanin extracted from *Theasinensis* Linn,” *Life Sciences*, vol. 74, no. 16, pp. 2037–2047, 2004.
- [22] D. C. Montefiori and J. Zhou, “Selective antiviral activity of synthetic soluble L-tyrosine and L-dopa melanins against human immunodeficiency virus *in vitro*,” *Antiviral Research*, vol. 15, no. 1, pp. 11–25, 1991.
- [23] E. Dadachova, R. A. Bryan, X. Huang et al., “Ionizing radiation changes the electronic properties of melanin and enhances the growth of melanized fungi,” *PLoS ONE*, vol. 2, no. 5, article e457, 2007.
- [24] J. Gallas and M. Eisner, “Melanin polyvinyl alcohol plastic laminates for optical applications,” US Patent 7029758, 2006.
- [25] J. S. James, “Soluble melanins-Potential HIV Treatment?” *Aids Treatment News*, pp. 139, November 1991.
- [26] G. Prota, *Melanins and Melanogenesis*, Academic Press, New York, NY, USA, 1992.
- [27] P. A. De Almeida, T. M. S. Da Silva, and A. Echevarria, “Mesoionic 5-alkyl-1,3-dithiolium-4-thiolates: synthesis and brine shrimp toxicity,” *Heterocyclic Communications*, vol. 8, no. 6, pp. 593–600, 2002.
- [28] T. M. S. Silva, R. J. B. Nascimento, M. M. Batista, M. F. Agra, and C. A. Camara, “Brine shrimp bioassay of some species of *Solanum* from Northeastern Brazil,” *Brazilian Journal of Pharmacognosy*, vol. 17, no. 1, pp. 35–38, 2007.
- [29] R. M. Atlas, *Tyrosine Agar: Hand Book of Microbiological Media*, ASM Press, Washington, DC, USA, 4th edition, 2010.
- [30] S. Shivaveerakumar, D. N. Madhusudhan, D. Agsar, and M. Kontro, “Catalytic zone, a novel screening approach for the extracellular tyrosinase by *Streptomyces vinaceusdrappus* DSV5,” *Journal of Pure and Applied Microbiology*, vol. 7, no. 4, pp. 2799–2808, 2013.
- [31] W. G. Weisburg, S. M. Barns, D. A. Pelletier, and D. J. Lane, “16S ribosomal DNA amplification for phylogenetic study,” *Journal of Bacteriology*, vol. 173, no. 2, pp. 697–703, 1991.
- [32] F. J. Laurent, F. Provost, and P. Boiron, “Rapid identification of clinically relevant *Nocardia* species to genus level by 16S rRNA gene PCR,” *Journal of Clinical Microbiology*, vol. 37, no. 1, pp. 99–102, 1999.
- [33] J. Chun, J.-H. Lee, Y. Jung et al., “EzTaxon: a web-based tool for the identification of prokaryotes based on 16S ribosomal RNA gene sequences,” *International Journal of Systematic and Evolutionary Microbiology*, vol. 57, no. 10, pp. 2259–2261, 2007.
- [34] B.-L. Liu and Y.-M. Tzeng, “Optimization of growth medium for the production of spores from *Bacillus thuringiensis* using response surface methodology,” *Bioprocess Engineering*, vol. 18, no. 6, pp. 413–418, 1998.
- [35] B. Sajeena Beevi, P. P. Jose, and G. Madhu, “Optimization of process parameters affecting biogas production from organic fraction of municipal solid waste via anaerobic digestion,” *World Academy of Science, Engineering and Technology, International Journal of Environmental, Earth Science and Engineering*, vol. 8, no. 1, 2014.
- [36] F. Fava, D. D. Gioia, and L. Marchetti, “Characterization of a pigment produced by *Pseudomonas fluorescens* during 3-chlorobenzoate co-metabolism,” *Chemosphere*, vol. 27, no. 5, pp. 825–835, 1993.
- [37] E. Harki, T. Talou, and R. Dargent, “Purification, characterization and analysis of melanin extracted from *Tuber melanosporum* Vitt,” *Food Chemistry*, vol. 58, no. 1-2, pp. 69–73, 1997.
- [38] M. Thomas, “Melanins,” in *Modern Methods of Plant Analysis*, pp. 661–675, Springer, Berlin, Germany, 1955.
- [39] G. M. Gadd, “Effects of media composition and light on colony differentiation and melanin synthesis in *Microdochium bolleyi*,” *Transactions of British Mycological Society*, vol. 78, no. 1, pp. 115–122, 1982.
- [40] J. P. Ravishankar, V. Muruganandam, and T. S. Suryanaryanan, “Isolation and characterization of melanin from a marine fungus,” *Botanica Marina*, vol. 38, no. 5, pp. 413–416, 1995.
- [41] O. A. Borowik and M. D. Engstrom, “Chromosomal evolution and biogeography of collared lemmings (*Dicrostonyx*) in the eastern and High Arctic of Canada,” *Canadian Journal of Zoology*, vol. 71, no. 8, pp. 1481–1493, 1993.
- [42] B. N. Meyer, N. R. Ferrigni, and J. E. Putnam, “Brine shrimp: a convenient general bioassay for active plant constituents,” *Planta Medica*, vol. 45, no. 1, pp. 31–34, 1982.
- [43] M. Déciga-Campos, I. Rivero-Cruz, M. Arriaga-Alba et al., “Acute toxicity and mutagenic activity of Mexican plants used in traditional medicine,” *Journal of Ethnopharmacology*, vol. 110, no. 2, pp. 334–342, 2007.
- [44] E. Küster and S. T. Williams, “Starch-casein medium for isolation of Streptomycetes,” *Nature*, vol. 202, pp. 928–929, 1964.
- [45] T. A. Nurudeen and D. G. Ahearn, “Regulation of melanin production by *Cryptococcus neoformans*,” *Journal of Clinical Microbiology*, vol. 10, no. 5, pp. 724–729, 1979.
- [46] G. Muyzer, S. Hottenträger, A. Teske, and C. Wawer, “Denaturing gradient gel electrophoresis of PCR-amplified 16S rDNA—a new molecular approach to analyze the genetic diversity of mixed microbial communities,” in *Molecular Microbial Ecology Manual*, A. D. L. Akkermans, J. D. van Elsas, and F. J. de Bruijn, Eds., pp. 1–23, Kluwer Academic Publishers, Dordrecht, The Netherlands, 1996.
- [47] R. Amann and W. Ludwig, “Ribosomal RNA-targeted nucleic acid probes for studies in microbial ecology,” *FEMS Microbiology Reviews*, vol. 24, no. 5, pp. 555–565, 2000.

- [48] S. Youngchim, R. Morris-Jones, R. J. Hay, and A. J. Hamilton, "Production of melanin by *Aspergillus fumigatus*," *Journal of Medical Microbiology*, vol. 53, no. 3, pp. 175–181, 2004.
- [49] "The family of Streptomycetaceae: part II molecular biology," in *The Prokaryotes*, H. Schrempf, M. Dworkin, S. Falkow, E. Rosenberg, K. H. Schleifer, and E. Stackebrandt, Eds., vol. 3, pp. 605–622, Springer, 2007.
- [50] K. F. Chater, S. Biró, K. J. Lee, T. Palmer, and H. Schrempf, "The complex extracellular biology of *Streptomyces*," *FEMS Microbiology Reviews*, vol. 34, no. 2, pp. 171–198, 2010.
- [51] D. H. Jennings, "The role of droplets in helping to maintain a constant growth rate of aerial hyphae," *Mycological Research*, vol. 95, no. 7, pp. 883–884, 1991.
- [52] J. F. Martín, J. Casqueiro, and P. Liras, "Secretion systems for secondary metabolites: how producer cells send out messages of intercellular communication," *Current Opinion in Microbiology*, vol. 8, no. 3, pp. 282–293, 2005.
- [53] A. E. Aghajanyan, A. A. Hambardzumyan, A. S. Hovsepyan, R. A. Asaturian, A. A. Vardanyan, and A. A. Saghiyan, "Isolation, purification and physicochemical characterization of water-soluble *Bacillus thuringiensis* melanin," *Pigment Cell Research*, vol. 18, no. 2, pp. 130–135, 2005.
- [54] S. J. Orlow and J. M. Pawelek, "Soluble melanin," US Patent no. 5218079A, June 2003.
- [55] R. K. Seshagiri, P. Jalmi, and P. Bodke, "A process for production of water soluble melanin using a strain of the fungus *Gliocephalo trichum*," Patent no. WO, 2010064262 A2, June 2010.
- [56] W. Yuan, S. H. Burleigh, and J. O. Dawson, "Melanin biosynthesis by *Frankia* strain Ce15," *Physiologia Plantarum*, vol. 131, no. 2, pp. 180–190, 2007.
- [57] V. E. Coyne and L. Al-Harthi, "Induction of melanin biosynthesis in *Vibrio cholerae*," *Applied and Environmental Microbiology*, vol. 58, no. 9, pp. 2861–2865, 1992.
- [58] S. L. Hoti and K. Balaraman, "Formation of melanin pigment by a mutant of *Bacillus thuringiensis* H-14," *Journal of General Microbiology*, vol. 139, no. 10, pp. 2365–2369, 1993.
- [59] P. Selvakumar, S. Rajasekar, K. Periasamy, and N. Raaman, "Isolation and characterization of melanin pigment from *Pleurotus cystidiosus* (telomorph of *Antromycopsis macrocarpa*)," *World Journal of Microbiology and Biotechnology*, vol. 24, no. 10, pp. 2125–2131, 2008.
- [60] J. L. Carballo, Z. L. Hernández-Inda, P. Pérez, and M. D. García-Grávalos, "A comparison between two brine shrimp assays to detect *in vitro* cytotoxicity in marine natural products," *BMC Biotechnology*, vol. 2, no. 17, pp. 1–5, 2002.
- [61] E. L. Quignard, A. M. Pohlit, S. M. Nunomura et al., "Screening of plants found in Amazonas state for lethality towards brine shrimp," *Acta Amazon*, vol. 33, no. 1, pp. 93–104, 2003.
- [62] S. Pisutthanan, P. Plianbangchang, N. Pisutthanan, S. Ruanruay, and O. Muanrit, "Brine shrimp lethality activity of Thai medicinal plants in the family Meliaceae," *Naresuan University Journal*, vol. 12, no. 2, pp. 13–18, 2004.
- [63] A. Lagarto Parra, R. Silva Yhebra, I. Guerra Sardiñas, and L. Iglesias Buela, "Comparative study of the assay of *Artemia salina* L. and the estimate of the medium lethal dose (LD50 value) in mice, to determine oral acute toxicity of plant extracts," *Phytomedicine*, vol. 8, no. 5, pp. 395–400, 2001.

Research Article

In Vitro and In Vivo Leishmanicidal Activity of *Astronium fraxinifolium* (Schott) and *Plectranthus amboinicus* (Lour.) Spreng against *Leishmania (Viannia) braziliensis*

Silvio César Gomes de Lima,¹ Maria Jania Teixeira,²
José Evaldo Gonçalves Lopes Júnior,¹ Selene Maia de Morais,³ Alba Fabiola Torres,¹
Milena Aguiar Braga,¹ Raphael Oliveira Rodrigues,¹ Gilvandete Maria Pinheiro Santiago,⁴
Alice Costa Martins,¹ and Aparecida Tiemi Nagao-Dias¹

¹ Departamento de Análises Clínicas e Toxicológicas, Faculdade de Farmácia, Universidade Federal do Ceará (UFC),
Rua Capitão Francisco Pedro 1210, 60430-370 Fortaleza, CE, Brazil

² Departamento de Patologia e Medicina Legal, Faculdade de Medicina, UFC, Rua Monsenhor Furtado S/N,
60430-350 Fortaleza, CE, Brazil

³ Departamento de Química, Universidade Estadual do Ceará, Avenida Paranjana 1700, 60000-001 Fortaleza, CE, Brazil

⁴ Departamento de Farmácia, Faculdade de Farmácia, UFC, Rua Capitão Francisco Pedro 1210, 60430-370 Fortaleza, CE, Brazil

Correspondence should be addressed to Aparecida Tiemi Nagao-Dias; tiemindi@yahoo.com.br

Received 20 February 2014; Accepted 20 March 2014; Published 16 April 2014

Academic Editor: José Carlos Tavares Carvalho

Copyright © 2014 Silvio César Gomes de Lima et al. This is an open access article distributed under the Creative Commons Attribution License, which permits unrestricted use, distribution, and reproduction in any medium, provided the original work is properly cited.

The aim of the present work was to evaluate antileishmanial activity of *Astronium fraxinifolium* and *Plectranthus amboinicus*. For the in vitro tests, essential oil of *P. amboinicus* (OEPA) and ethanolic extracts from *A. fraxinifolium* (EEAF) were incubated with 10^6 promastigotes of *L. (Viannia) braziliensis*. The OEPA was able to reduce the parasite growth after 48 h; nonetheless, all the EEAFs could totally abolish the parasite growth. For the in vivo studies, BALB/c mice were infected subcutaneously (s.c.) with 10^7 *L. braziliensis* promastigotes. Treatment was done by administering OEPA intralésionalmente (i.l.) for 14 days. No difference was found in lesion thickness when those animals were compared with the untreated animals. Further, golden hamsters were infected s.c. with 10^6 *L. braziliensis* promastigotes. The first protocol of treatment consisted of ethanolic leaf extract from *A. fraxinifolium* (ELEAF) administered i.l. for 4 days and a booster dose at the 7th day. The animals showed a significant reduction of lesion thickness in the 6th week, but it was not comparable to the animals treated with Glucantime. The second protocol consisted of 15 daily intralésionais injections. The profiles of lesion thickness were similar to the standard treatment. In conclusion, in vivo studies showed a high efficacy when the infected animals were intralésionalmente treated with leaf ethanolic extract from *A. fraxinifolium*.

1. Introduction

Leishmaniasis is a disease that affects human beings and animals and is caused by the protozoa parasite of the genus *Leishmania* which is transmitted by the bite of infected female phlebotomine sandflies and displays a spectrum of manifestations which goes from cutaneous involvement (CL) with late destruction of mucous membranes to generalized systemic visceral disease (VL) with fatal outcome if not

treated [1]. According to the World Health Organization [2], about 0.2 to 0.4 million of new VL cases and 0.7 to 1.2 million of CL occur in the world. Brazil and other nine countries, mostly situated in Africa and South America, are responsible for about 70 to 75% of global incidence of the disease [3]. Brazil has reported 23,793 CL cases in 2012 [4]. Various factors contribute to the increase of the disease incidence, for instance, the process of urbanization which alters the environment in recurrence of economic

and social pressures [5]. The main *Leishmania* species which cause the CL disease in Brazil are *L. (Viannia) braziliensis*, *L. (Leishmania) amazonensis*, and *L. (V.) guyanensis* [6]. *L. (V.) braziliensis* is the most common aetiologic agent of CL disease in Brazil and other countries in Latin America, and it can be found in endemic zones from the different regions of Brazil [6]. American cutaneous leishmaniasis is a form of disease that causes a single or various cutaneous lesions that can heal spontaneously. Nonetheless, in some cases when mucosa, such as nasal or oral mucosa, is injured, treatment is necessary; otherwise, permanent sequelae may occur [7]. The clinical form and severity of the disease may depend on the *Leishmania* species [8] and/or to the individual immune response [7]. HIV-positive individuals are probably at high risk of developing cutaneous leishmaniasis [9] probably at more severe forms of the disease. This reveals a new challenge in terms of treatment of the disease in immunocompromised individuals. Early diagnosis and treatment are important to prevent sequelae. Pentavalent antimonials are still the treatment of choice for over 50 years; however, they comprise several problems, such as endovenous use and prolonged and high-cost treatment [10]. Increased incidence of resistance to the drug has been described [8]. Another problem is related to the lower efficacy of the drugs in children compared to adults [11]. Alternatively, pentamidine and amphotericin B may be used. In general, these compounds are also expensive and require long-term treatment [8]. Another point to take into account is that the drugs available for CL treatment produce significant side effects due to their high toxicity and tissue drug accumulation, which includes myalgias, nausea, vomiting, cardiac arrhythmia, hepatitis, or pancreatitis [12, 13]. Miltefosine and fluconazole have recently showed effectiveness against CL [14, 15], but despite their lower toxicity, these second line drugs are not useful against other forms of leishmaniasis [13]. Furthermore, the continuous use of ineffective drugs has led to the development of resistance to their compounds [16], which have stirred an urgent need for novel, effective, and safe drugs for treatment of leishmaniasis. Several studies have been done in order to evaluate antileishmanicidal activity of medicinal plants [17, 18]. The species *Astronium fraxinifolium* Schott, popularly known as “gonçalo alves,” occurs in the tropical savannas of central Brazil (Cerrado Brasileiro), in soils with good fertility, and it can also be found in the northeastern region of the country. The *Myracrodruon urundeuva* species, a plant of the same family, native in northeastern Brazil, is widely used in folk medicine for treatment of various dermatological disorders and is known to have antimicrobial [19], antiulcer [20], and anti-inflammatory activities [21]. *Plectranthus amboinicus*, popularly known as malvarisco, a native aromatic plant of India and cultivated in many parts of the world, including Brazil, belongs to the Lamiaceae family and the genus *Plectranthus*. It is popularly used in the treatment of various diseases including skin, digestive tracts, urogenital, respiratory disorders, infections, and pain [22]. Several studies have been published confirming much of the popular use of *Plectranthus amboinicus*, such as anti-inflammatory and antimicrobial activities [23–27]. The aim of the present work was to demonstrate in vitro and in

vivo antileishmanial activity of *Astronium fraxinifolium* and *Plectranthus amboinicus*.

2. Methods

2.1. Parasites. The strain of *L. (V.) braziliensis* (MHOM-BR-94-H3227) was grown in Schneider culture medium (Sigma Chem. Co., St. Louis, Mo, USA), containing 10% heat-inactivated foetal bovine serum (Sigma), 200 U penicillin/mL, and 200 mg streptomycin/ μ L (Sigma). The strain of *L. braziliensis* (MHOM-BR-94-H3227) was isolated from a patient with cutaneous leishmaniasis and characterized by polymerase chain technique and by monoclonal antibodies [28].

2.2. Plant Materials. The ethanolic extracts of the bark, sapwood, and leaves of *A. fraxinifolium* were collected in the city of Lavras da Mangabeira (06° 45' 12" S 38° 57' 52" W 239 m), Ceara, Brazil. The extraction was obtained by Gonçalves Jr. and described elsewhere (Gonçalves Jr. et al., manuscript in preparation). All the extracts contained phenols and tannins. The essential oil of *P. amboinicus* was provided by Braga, MA, and description of the protocol was done according to Gonçalves et al., 2012 [26]. The major component of the essential oil was carvacrol.

2.3. In Vitro Studies

2.3.1. Antileishmanial Evaluation. The in vitro evaluation of the antileishmanial activity of the essential oil from *P. amboinicus* and of ethanolic extracts (bark, sapwood, and leaf) from *A. fraxinifolium* was performed in 48-well microplates. Each well received 200 μ L of medium containing 10^6 promastigotes of *L. braziliensis*, 200 μ L Schneider supplemented medium, and 2.5% essential oil of *P. amboinicus*. Ethanolic extracts from *A. fraxinifolium* were added at 2.5 mg/mL concentrations in 1% dimethyl sulfoxide or DMSO (VETEC, Brazil) to the wells. The plates were left at 26°C in a BOD incubator during 24, 48, and 72 h, without shaking. Then, the parasites were fixed with 2% formalin, stained with Trypan blue, and visualized using a light microscope at 400x magnification. The parasites were counted in a Neubauer chamber. As controls, 1% DMSO and amphotericin B (Sigma, USA) were used.

2.3.2. Cytotoxicity Assay. Macrophage cell line RAW 264.7, obtained from the Rio de Janeiro Cell Bank (BCRJ, Brazil), was grown in microculture plates containing Minimum Essential Media supplemented with 10% v/v foetal bovine serum, penicillin (100 U/mL), and streptomycin (100 μ g/mL). Cells were incubated at 37°C in a humidified 5% CO₂ atmosphere. Before each experiment, the cells were incubated in medium without foetal calf serum for 24 h to obtain cells in the G₀ phase of the cell cycle. For each experiment, cells were removed from the culture medium and incubated with 0.25% trypsin and 0.02% ethylenediaminetetraacetic acid (v/v) for approximately 10 min at 37°C. Trypsin

was inactivated by adding the same volume of medium containing foetal bovine serum. The suspension was centrifuged for 10 min at 1500 ×g. The supernatant was discarded, and the cells were resuspended in culture medium. The macrophages were quantified using a Neubauer chamber and subcultured (1×10^5 cells/mL) into a 96-well microplate for 24 h. The essential oil of *P. amboinicus* was tested from 0.125 to 4.0% v/v and the ethanolic extracts of *A. fraxinifolium* from 0.039 to 2.5 mg/mL concentrations. After an incubation of 24 h, 100 µL of the supernatant was discarded and 100 µL of 3-(4,5-dimethylthiazol-2-yl)-2,5-diphenyltetrazolium bromide (MTT) at 500 µg/mL dissolved in phosphate-buffered saline (PBS), pH 7.4, was added to the wells after incubation for 4 h at 37°C. Thereafter, 10% sodium dodecyl sulphate in 0.01 N HCl was added to solubilise the formazan crystals [29]. Plates were then incubated for 17 h, and readings were performed at 570 nm using a microplate reader. Assays were performed in triplicate.

2.4. In Vivo Studies

2.4.1. Animals. Three- to four-month adult male golden hamsters (*Mesocricetus auratus*) and BALB/c, male, 8 weeks, obtained from the Central Animal Facility of the Department of Pathology and Legal Medicine of the Federal University of Ceará, were housed in groups of six to eight per cage with free access to water and food. All procedures involving the uses of animals were approved by the Ethics Committee for Animal Research of the Federal University of Ceará (protocol number 75/2011).

2.4.2. Treatment with the Essential Oil of *P. amboinicus*. BALB/c mice were divided into 3 groups (5 animals per group), untreated, Glucantime, and test. The animals were injected subcutaneously in right hind footpad with 10^7 stationary phase *L. braziliensis* promastigotes in 20 µL of sterile saline. Lesion sizes were measured weekly with a dial gauge caliper (0.01 mm sensitivity, Mitutoyo, Japan) and expressed as the difference between the thicknesses (mm) of the infected and contralateral uninfected footpads.

The treatment was initiated when the lesions appeared (about the 27th day). Dosis of 20 µL of 5% essential oil of *P. amboinicus* in 1% DMSO was administered intralesionally once a day for 14 days. Meglumine antimoniate (Glucantime), injected intramuscularly at the dose of 60 mg/kg/day, 20 µL, was used as reference drug. Untreated animals were intralesionally injected with 1% DMSO. The uninfected contralateral footpad was also intralesionally injected with the same solution used for treatment. This procedure was done in order to check toxicity of the material used to treat the animals.

2.4.3. Treatment with Ethanolic Extracts of Leaves from *A. fraxinifolium*. Golden hamsters, weighing about 70 g, were divided into 8 groups with 5 animals per group (2 untreated, 2 Glucantime, 2 tests, 2 uninfected). The animals were injected subcutaneously in the right hind footpad with 10^6 stationary phase *L. braziliensis* promastigotes in 20 µL of sterile saline. Lesion sizes were measured weekly with a dial gauge caliper

(0.01 mm sensitivity, Mitutoyo, Japan) and expressed as the difference between the thicknesses (mm) of the infected and contralateral uninfected footpads. The treatment was initiated when the lesions appeared (about the 20th day after infection). Meglumine antimoniate (Glucantime), injected intramuscularly at the dose of 60 mg/kg/day, 20 µL, was used as reference drug. Untreated animals were intralesionally injected with 1% DMSO. For the test treatment, two protocols were used. The first treatment protocol consisted of 20 µL ethanolic leaf extract (at 2.5 mg/mL in 1% DMSO) administered intralesionally for 4 consecutive days. At the 7th day, a single booster (40 µL) was given. The second treatment protocol consisted of intralesional injections of 20 µL ethanolic leaf extract administered for 15 consecutive days. The animals were also weighed during this period. The animals were euthanized after the 8th week of infection.

2.5. Parasite Load. The number of parasites in the lesions was quantified by the limiting dilution technique as previously described [30]. Briefly, after the treatment, the animals were euthanized by inhalation of halothane (Sigma-Aldrich) and submerged in 3% iodized alcohol up to 3 minutes to allow decontamination. The infected footpads were removed aseptically and macerated in a Petri dish with 2 mL of Schneider medium and left to stand for 5 minutes. After homogenization, the material was tenfold serially diluted in Schneider medium supplement with 10% foetal bovine serum. One hundred microliters of these dilutions was distributed into 96-well flat bottom plates containing agar-blood in 6 replicates per concentration. The plates were incubated at 25°C and observed under an inverted microscope (Nikkon, Japan) every 3 days, up to a maximum of 30 days, to record the dilutions containing promastigotes. The final number of parasites per tissue was determined using the ELIDA software version 12c [31].

2.5.1. Statistical Analysis. The data relating to the parasite load were analyzed using the nonparametric Mann-Whitney test. The lesion sizes from treated and untreated animals were analysed by the one-way Anova and complemented by the Tukey-Kramer test for multiple comparisons. The analyses were performed using GraphPad Prism version 5.0 and the GraphPad InStat version 3.01 programs. The level of significance for a null hypothesis was 5% ($P < 0.05$).

3. Results and Discussion

In the present study we decided to evaluate two medicinal plants, *Plectranthus amboinicus* and *Astronium fraxinifolium*. *P. amboinicus* is original from India, but it has easily been adapted to the conditions of soil and climate of Brazilian northeastern region. As it was shown in our previous study [26], the major component in essential oil obtained from *P. amboinicus* was carvacrol (yield above 90%). Carvacrol is a monoterpene phenol, isomer to thymol, and presents various biological activities such as antimicrobial, antitumor, and anti-inflammatory activities [32]. *Astronium fraxinifolium* is original from the central-west region of Brazil, but it has also

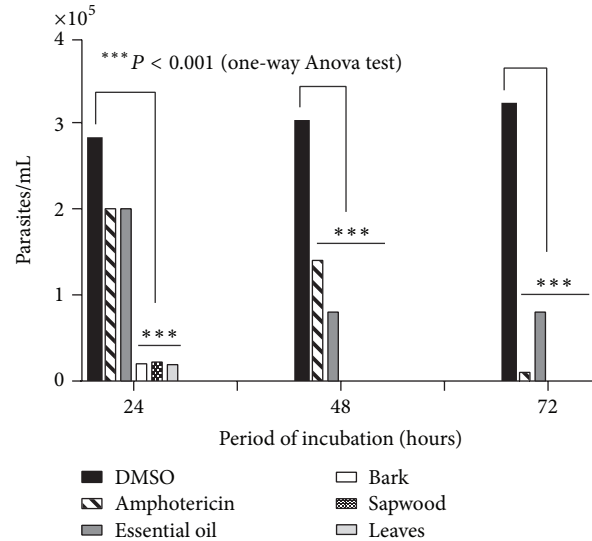


FIGURE 1: In vitro antileishmanial activity of essential oil of *P. amboinicus* at 2.5% in 1% DMSO and ethanolic extracts (from bark, stem bark, and leaf) of *A. fraxinifolium* at 2.5 mg/mL incubated with 10^6 promastigotes of *L. braziliensis* during 24 h, 48 h, and 72 h. The parasites were fixed in formaldehyde, stained with Trypan blue and visualized at light microscope at 400x magnification.

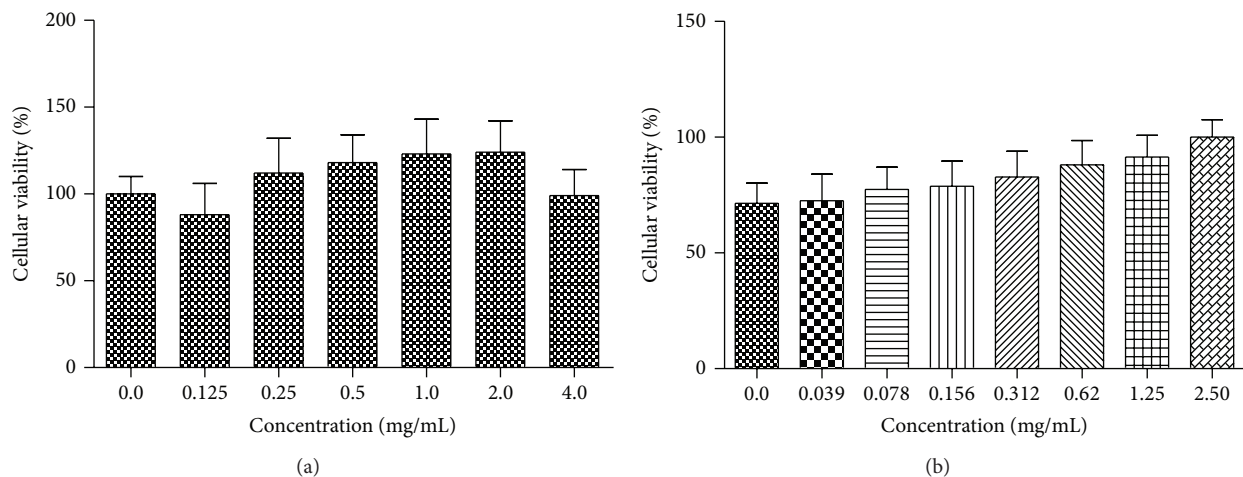


FIGURE 2: Cytotoxicity of the plant material. Percentage of cellular viability (mean \pm standard error mean) using RAW 264.7 macrophages after 24 h incubation with essential oil of *P. amboinicus* (a) or with ethanolic leaf extract of *A. fraxinifolium* (b) at various concentrations.

been found in various regions of the northeastern region of the country. Its activities are poorly known unlike the other plant from the same family, *M. urundeuva*, which is original from the northeastern region of Brazil. As *A. fraxinifolium* can be cultivable, it is not at extinction risk.

As it was shown in Figure 1, essential oil of *P. amboinicus* at 2.5% was able to reduce the viability of *L. braziliensis* promastigotes in the first 48 h, similar to the reference drug ($P < 0.001$) when compared to parasites incubated with 1% DMSO. However, at 72 h, no significant decrease was observed in comparison to the previous period of 48 h. On the other hand, all the ethanolic extracts (from bark, sapwood, and leaves) from *A. fraxinifolium* at 2.5 mg/mL totally abolished the parasite growth after 48 h. In vitro results showed that both essential oil of *P. amboinicus* (EOPA) and ethanolic

extracts from *A. fraxinifolium* (EEAF) presented potential activity against *L. braziliensis* promastigotes. However, EOPA did not cause 100% mortality in parasite when compared to EEAF. Nonetheless, we decided to test the EOPA treatment in animal models based on data from other researchers [33] who showed a good antileishmanial activity of essential oil, in the case of *Lippia sidoides* Cham., which contained 43.7% of carvacrol.

No cytotoxic activity of the plant materials was observed when they were incubated in different concentrations with RAW 267.4 macrophage at 24 hours (Figure 2).

Despite the promising in vitro results, in vivo experiments did not reveal a good efficacy of the treatment with EOPA in mouse model. No difference was found when the animals treated with the plant material and the untreated animals

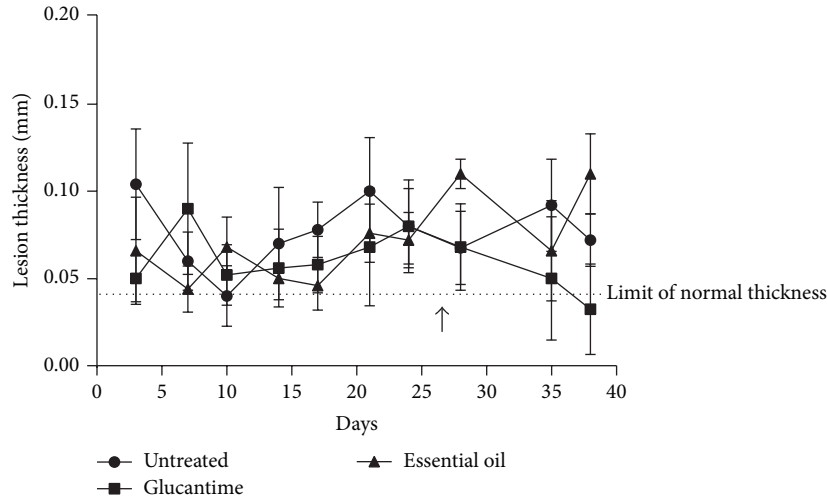


FIGURE 3: Lesion thickness of BALB/c mouse footpad infected with 10^7 promastigotes of *Leishmania braziliensis* and treated with essential oil of *Plectranthus amboinicus*. The protocol of treatment was 15 daily doses of $20 \mu\text{L}$ of 2.5% plant material. The arrow indicates start of treatment (about the 27th day).

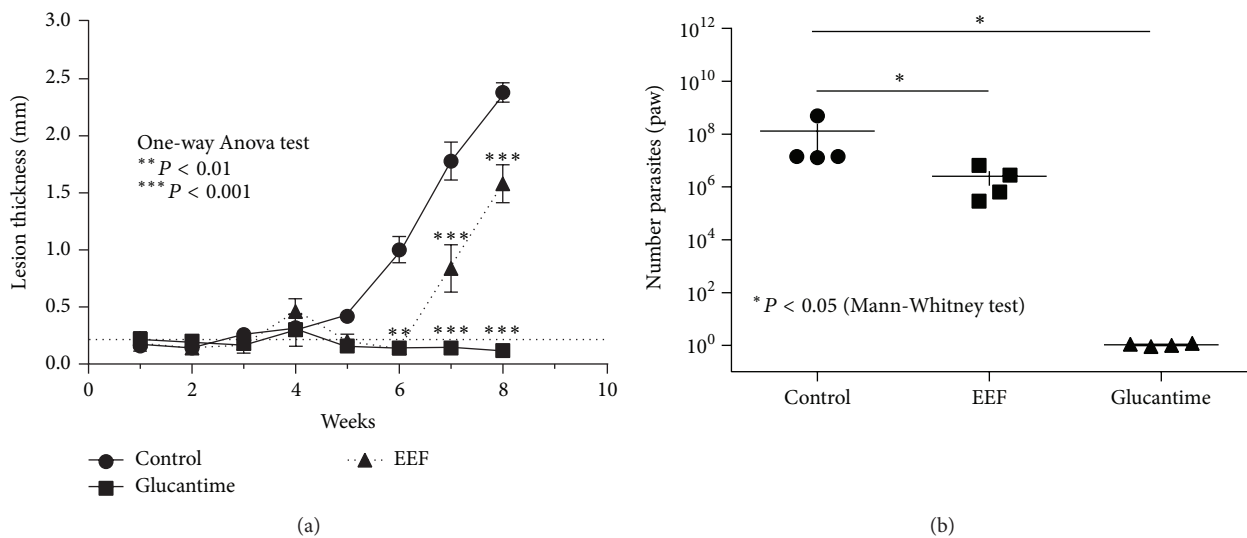


FIGURE 4: Lesion thickness (a) and number of parasites (b) in hamster footpad infected with 10^6 promastigotes of *Leishmania braziliensis*. The animals were treated with leaf ethanolic extract from *Astronium fraxinifolium* (EEF). The protocol of treatment was 4 dairy doses of $20 \mu\text{L}$ of 2.5 mg/mL plant material and 1 booster dose of $40 \mu\text{L}$ of the plant. The treatment started when the lesions appeared (3 weeks).

were compared in terms of lesion thickness (Figure 3). This fact could be related to the concentration of the essential oil, to the route of administration, or even to the period of treatment. Probably the essential oil of *P. amboinicus* should be associated with other plant materials in order to improve the efficacy of treatment. We have previously observed through in vitro experiments that the association of EEF with EOPA led to total inhibition of parasite growth after 48 h (data not shown). Monzote et al. [17] have demonstrated that essential oil from *Chenopodium ambrosioides* showed a synergic activity with pentamidine against *Leishmania amazonensis* promastigotes. In respect to the route of administration, Patrício et al. [34] have shown that the treatment administered via the intralesional route

was more effective than the oral route. According to their data, mice infected with *L. amazonensis* and treated with the hydroalcoholic crude extract from the leaves of *Chenopodium ambrosioides* administered via the intralesional route showed a greater reduction of the parasite load in various organs compared to the other route of administration.

Additionally, we decided to use the gold hamster model to evaluate the activity of our plant materials in vivo based on the fact that hamsters are known to be highly susceptible to *Leishmania* subgenus *Viannia* infection [35]. Also, male animals were tested because this gender is more susceptible to the *Leishmania* infection than the females, and this susceptibility seems to be related to the type of cytokine produced [35].

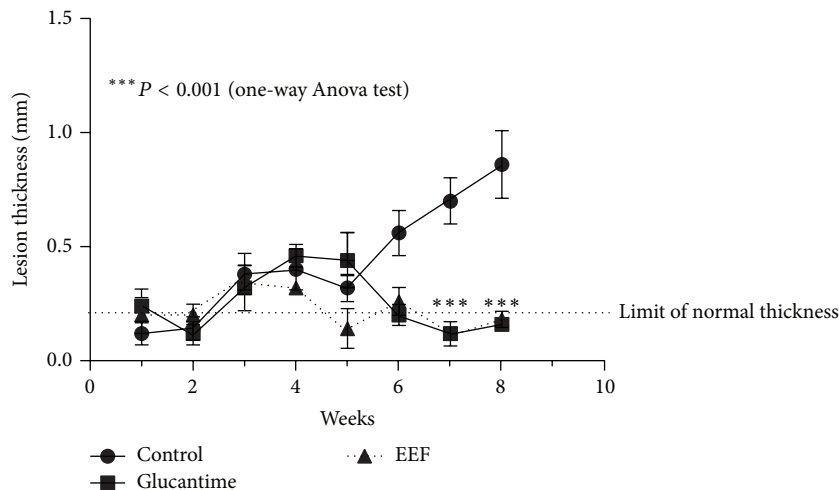


FIGURE 5: Lesion thickness of hamster footpad infected with 10^6 promastigotes of *Leishmania braziliensis*. The animals were treated with leaf ethanolic extract from *Astronium fraxinifolium* (EEF). The protocol of treatment was 15 dairy doses of $20 \mu\text{L}$ of 2.5 mg/mL plant material. The treatment started when the lesions appeared (3 weeks).

Hamsters treated with 4 daily doses of ethanolic leaf extract from *A. fraxinifolium* and 1 booster dose showed a significant reduction of lesion thickness after the 6th week after infection ($P < 0.001$) in comparison to the untreated animals, but it was not comparable to the reduction observed in the group of animals treated with Glucantime (Figure 4(a)). In respect to parasite growth, the animals treated with the plant material showed lower parasites in the infected footpad after treatment in comparison to the untreated animals (Figure 4(b), $P < 0.05$). However, a higher number of parasites were found when the group of animals treated with the plant material was compared with the group treated with Glucantime.

Hamsters treated with 15 daily doses of the plant material showed a profile of lesion thickness similar to those treated with Glucantime, much lower than that observed in the untreated animals (Figure 5, $P < 0.001$). After the 7th week of infection, the lesion thickness in the group treated with the plant material was below the limit of normal thickness. Any loss of weight was not observed in the animals treated with the plant material. No inflammation was found in the uninfected animals treated with the plant material.

In conclusion, both essential oil from *P. amboinicus* and ethanolic extracts from *A. fraxinifolium* were able to reduce parasite growth in vitro; however, studies in vivo showed a much higher efficacy when hamsters were intralesionally treated with leaf ethanolic extract from *A. fraxinifolium*. More studies with these plant materials are necessary to demonstrate the efficacy of the treatment administered in association with other plant materials and/or the reference drug.

Conflict of Interests

The authors declare that there is no conflict of interests regarding the publication of this paper.

Acknowledgments

This research was supported financially by the CNPq (Processes 579437/2008-6 and 554970/2010-4) and Fun-cap/PPSUS (Process 09100057-2).

References

- [1] P. Desjeux, "Leishmaniasis: current situation and new perspectives," *Comparative Immunology, Microbiology and Infectious Diseases*, vol. 27, no. 5, pp. 305–318, 2004.
- [2] WHO, "Status of endemicity of cutaneous leishmaniasis, worldwide, 2012," http://gamapserver.who.int/mapLibrary/Files/Maps/Leishmaniasis_CL.2013.png.
- [3] J. Alvar, I. D. Velez, C. Bern et al., "Leishmaniasis worldwide and global estimates of its incidence," *PLOS ONE*, vol. 7, no. 5, Article ID e35671, 12 pages, 2012.
- [4] WHO, "Leishmaniasis: number of cases of cutaneous leishmaniasis reported data by country," <http://apps.who.int/gho/data/node.main.NTDLEISHCNUM?lang=en>.
- [5] Secretaria da Saúde do Estado do Ceará (Ceara), "Leishmaniose visceral," Informe epidemiológico, pp. 1–11, September 2012.
- [6] B. Gontijo and M. D. L. R. de Carvalho, "American cutaneous leishmaniasis," *Revista da Sociedade Brasileira de Medicina Tropical*, vol. 36, no. 1, pp. 71–80, 2003.
- [7] L. Reveiz, A. N. S. Maia-Elkhoury, R. S. Nicholls, G. A. Sierra Romero, and Z. E. Yadon, "Interventions for American cutaneous and mucocutaneous leishmaniasis: a systematic review update," *PLOS ONE*, vol. 8, no. 4, Article ID e61843, 14 pages, 2013.
- [8] A. D. Haldar, P. Sen, and S. Roy, "Use of antimony in the treatment of leishmaniasis: current status and future directions," *Molecular Biology International*, vol. 2011, Article ID 571242, 23 pages, 2011.
- [9] A. Hozannah, M. Santos, A. Chrusciak-Talhari, and C. Talhari, "Leishmaniasis and AIDS coinfection," *Anais Brasileiros de Dermatologia*, vol. 88, no. 6, pp. 992–993, 2013.

- [10] O. L. S. Almeida and J. B. Santos, "Advances in the treatment of cutaneous leishmaniasis in the new world in the last ten years: a systematic literature review," *Anais Brasileiros de Dermatologia*, vol. 86, no. 3, pp. 497–506, 2011.
- [11] P. Layegh, S. Rahsepar, and A. A. Rahsepar, "Systemic meglumine antimoniate in acute cutaneous leishmaniasis: children versus adults," *American Journal of Tropical Medicine and Hygiene*, vol. 84, no. 4, pp. 539–542, 2011.
- [12] S. L. Croft, K. Seifert, and V. Yardley, "Current scenario of drug development for leishmaniasis," *Indian Journal of Medical Research*, vol. 123, no. 3, pp. 399–410, 2006.
- [13] E. Palumbo, "Current treatment for cutaneous leishmaniasis: a review," *American Journal of Therapeutics*, vol. 16, no. 2, pp. 178–182, 2009.
- [14] P. R. Machado, J. Ampuero, L. H. Guimarães et al., "Miltefosine in the treatment of cutaneous leishmaniasis caused by *Leishmania braziliensis* in Brazil: a randomized and controlled trial," *PLoS neglected tropical diseases*, vol. 4, no. 12, article e912, 2010.
- [15] A. Q. Sousa, M. S. Frutuoso, E. A. Moraes, R. D. Pearson, and M. M. L. Pompeu, "High-dose oral fluconazole therapy effective for cutaneous leishmaniasis due to *Leishmania (Viannia) braziliensis*," *Clinical Infectious Diseases*, vol. 53, no. 7, pp. 693–695, 2011.
- [16] P. Escobar, V. Yardley, and S. L. Croft, "Activities of hexadecylphosphocholine (miltefosine), ambisome, and sodium stibogluconate (pentostam) against *Leishmania donovani* in immunodeficient scid mice," *Antimicrobial Agents and Chemotherapy*, vol. 45, no. 6, pp. 1872–1875, 2001.
- [17] L. Monzote, A. M. Montalvo, R. Scull, M. Miranda, and J. Abreu, "Combined effect of the essential oil from *Chenopodium ambrosioides* and antileishmanial drugs on promastigotes of *Leishmania amazonensis*," *Revista do Instituto de Medicina Tropical de Sao Paulo*, vol. 49, no. 4, pp. 257–260, 2007.
- [18] V. Cechinel Filho, C. Meyre-Silva, R. Niero et al., "Evaluation of antileishmanial activity of selected Brazilian plants and identification of the active principles," *Evidence-Based Complementary and Alternative Medicine*, vol. 2013, Article ID 265025, 7 pages, 2013.
- [19] V. T. L. Gomes, T. P. Chaves, L. C. B. Alencar, I. C. Dantas, A. C. D. Medeiros, and D. C. Felismino, "Antimicrobial activity of natural products from *Myracrodruon urundeuva* Allemão (aroeira-do-sertão)," *Revista Cubana de Plantas Mediciniais*, vol. 18, no. 4, pp. 529–533, 2013.
- [20] E. A. Carlini, J. M. Duarte-Almeida, E. Rodrigues, and R. Tabach, "Antiulcer effect of the pepper trees *Schinus terebinthifolius* Raddi (aroeira-da-praia) and *Myracrodruon urundeuva* Allemão, Anacardiaceae (aroeira-do-sertão)," *Brazilian Journal of Pharmacognosy*, vol. 20, no. 2, pp. 140–146, 2010.
- [21] S. M. C. Souza, L. C. M. Aquino, A. C. Milach Jr., M. A. M. Bandeira, M. E. P. Nobre, and G. S. B. Viana, "Antiinflammatory and antiulcer properties of tannins from *Myracrodruon urundeuva* Allemão (Anacardiaceae) in rodents," *Phytotherapy Research*, vol. 21, no. 3, pp. 220–225, 2007.
- [22] C. W. Lukhoba, M. S. J. Simmonds, and A. J. Paton, "*Plectranthus*: a review of ethnobotanical uses," *Journal of Ethnopharmacology*, vol. 103, no. 1, pp. 1–24, 2006.
- [23] A. P. A. D. Gurgel, J. G. da Silva, A. R. S. Grangeiro et al., "In vivo study of the anti-inflammatory and antitumor activities of leaves from *Plectranthus amboinicus* (Lour.) Spreng (Lamiaceae)," *Journal of Ethnopharmacology*, vol. 125, no. 2, pp. 361–363, 2009.
- [24] J. Chang, C. Cheng, L. Hung, Y. Chung, and R. Wu, "Potential use of *Plectranthus amboinicus* in the treatment of rheumatoid arthritis," *Evidence-Based Complementary and Alternative Medicine*, vol. 7, no. 1, pp. 115–120, 2010.
- [25] Y. Chiu, T. Huang, C. Chiu et al., "Analgesic and antiinflammatory activities of the aqueous extract from *Plectranthus amboinicus* (Lour.) Spreng, both in vitro and in vivo," *Evidence-Based Complementary and Alternative Medicine*, vol. 2012, Article ID 508137, 11 pages, 2012.
- [26] T. B. Gonçalves, M. A. Braga, F. F. M. Oliveira et al., "Effect of subinhibitory and inhibitory concentrations of *Plectranthus amboinicus* (Lour.) Spreng essential oil on *Klebsiella pneumoniae*," *Phytomedicine*, vol. 19, no. 11, pp. 962–968, 2012.
- [27] F. M. Oliveira, A. F. Torres, T. B. Gonçalves et al., "Efficacy of *Plectranthus amboinicus* (Lour.) Spreng in a murine model of methicillin-resistant *Staphylococcus aureus* skin abscesses," *Evidence-Based Complementary and Alternative Medicine*, vol. 2013, Article ID 291592, 9 pages, 2013.
- [28] C. I. de Oliveira, M. J. Teixeira, C. R. Teixeira et al., "*Leishmania braziliensis* isolates differing at the genome level display distinctive features in BALB/c mice," *Microbes and Infection*, vol. 6, no. 11, pp. 977–984, 2004.
- [29] T. Mosmann, "Rapid colorimetric assay for cellular growth and survival: application to proliferation and cytotoxicity assays," *Journal of Immunological Methods*, vol. 65, no. 1–2, pp. 55–63, 1983.
- [30] R. G. Titus, M. Marchand, T. Boon, and J. A. Louis, "A limiting dilution assay for quantifying *Leishmania major* in tissues of infected mice," *Parasite Immunology*, vol. 7, no. 5, pp. 545–555, 1985.
- [31] C. Taswell, "Limiting dilution assays for the determination of immunocompetent cell frequencies. III. Validity tests for the single-hit poisson model," *Journal of Immunological Methods*, vol. 72, no. 1, pp. 29–40, 1984.
- [32] K. H. C. Baser, "Biological and pharmacological activities of carvacrol and carvacrol bearing essential oils," *Current Pharmaceutical Design*, vol. 14, no. 29, pp. 3106–3119, 2008.
- [33] P. A. Farias-Junior, M. C. Rios, A. Tauanny et al., "Leishmanicidal activity of carvacrol-rich essential oil from *Lippia sidoides*," *Biological Research*, vol. 45, no. 4, pp. 399–402, 2012.
- [34] F. J. Patrício, G. C. Costa, P. V. S. Pereira et al., "Efficacy of the intralésional treatment with *Chenopodium ambrosioides* in the murine infection by *Leishmania amazonensis*," *Journal of Ethnopharmacology*, vol. 115, no. 2, pp. 313–319, 2008.
- [35] B. L. Travi, Y. Osorio, P. C. Melby, B. Chandrasekar, L. Arteaga, and N. G. Saravia, "Gender is a major determinant of the clinical evolution and immune response in hamsters infected with *Leishmania* spp," *Infection and Immunity*, vol. 70, no. 5, pp. 2288–2296, 2002.

Research Article

Biologic Propensities and Phytochemical Profile of *Vangueria madagascariensis* J. F. Gmelin (Rubiaceae): An Underutilized Native Medicinal Food Plant from Africa

Nelvana Ramalingum and M. Fawzi Mahomoodally

Department of Health Sciences, Faculty of Science, University of Mauritius, 230 Réduit, Mauritius

Correspondence should be addressed to M. Fawzi Mahomoodally; f.mahomoodally@uom.ac.mu

Received 9 February 2014; Revised 19 February 2014; Accepted 5 March 2014; Published 10 April 2014

Academic Editor: José Carlos Tavares Carvalho

Copyright © 2014 N. Ramalingum and M. F. Mahomoodally. This is an open access article distributed under the Creative Commons Attribution License, which permits unrestricted use, distribution, and reproduction in any medium, provided the original work is properly cited.

Vangueria madagascariensis (VM), consumed for its sweet-sour fruits, is used as a biomedicine for the management of diabetes and bacterial infections in Africa. The study aims to assess the potential of VM on α -amylase, α -glucosidase, glucose movement, and antimicrobial activity. The antioxidant properties were determined by measuring the FRAP, iron chelating activity, and abilities to scavenge DPPH, HOCl, \cdot OH, and NO radicals. Leaf decoction, leaf methanol, and unripe fruit methanol extracts were observed to significantly inhibit α -amylase. Active extracts against α -glucosidase were unripe fruit methanol, unripe fruit decoction, leaf decoction, and ripe fruit methanol, which were significantly lower than acarbose. Kinetic studies revealed a mixed noncompetitive type of inhibition. Leaf methanolic extract was active against *S. aureus* and *E. coli*. Total phenolic content showed a strong significant positive correlation ($r = 0.88$) with FRAP. Methanolic leaf extract showed a more efficient NO scavenging potential and was significantly lower than ascorbic acid. Concerning \cdot OH-mediated DNA degradation, only the methanol extracts of leaf, unripe fruit, and ripe fruit had IC₅₀ values which were significantly lower than α -tocopherol. Given the dearth of information on the biologic propensities of VM, this study has established valuable primary information which has opened new perspectives for further pharmacological research.

1. Introduction

Vangueria madagascariensis (VM) J. F. Gmelin (Rubiaceae), also commonly known as Vavangue, Voavanga, or Tamarind of the Indies, is a perennial plant which is native to tropical Africa and Madagascar [1]. Some species of genus *Vangueria* are widely studied *in vitro* and used in traditional medicine in various countries. For instance, in Tanzania, different parts of the species *Vangueria infausta* have traditionally been used for the treatment and/or management of malaria, wounds, menstrual, and uterine problems [2].

With respect to VM, available folk data suggest its use as an anthelmintic against roundworms, as antimicrobial, as astringent against cholagogue, and as expectorant, for the treatment of smallpox and sores, herpes labialis, and in the management of diabetes [3]. Preliminary phytochemical screening of the leaves and stems has shown the presence of alkaloids, terpenes, and cyanogenetic heterosides as well

as phenols, tannins, and saponosides which may likely be responsible for its antimicrobial effects [1]. According to Musa et al. [4] roots of VM are macerated and administered orally for the treatment of diabetes mellitus. In Mauritius, an infusion of the leaves of VM, ingested once a week, has also been reported for the same purpose [1]. Moreover, a study carried out among Islanders of the Indian Ocean, which also included Mauritians, reported that leaf decoction is taken mainly to treat skin infections and abscesses [5].

There is currently a dearth of scientific validation of the purported traditional uses of VM as a biomedicine and previous evidence may still be considered as insufficient to support its folkloric use [5–7]. Additional research work is needed to probe into the antidiabetic, antimicrobial, and antioxidant properties of VM which may help validate its traditional claims and delineate further health benefits. Therefore, the main aim of this study was to investigate the

antidiabetic, antimicrobial, and antioxidant properties of the leaves, ripe and unripe fruits, and the seeds of VM. To the best of our knowledge this is the first study to report the biological activity of VM *in vitro*. Given the dearth of updated information on the biological properties of VM, this work can provide an opportunity to establish valuable primary information on the bioactivity of VM and hence open new perspectives for further pharmacological research.

2. Materials and Methods

2.1. Preparation of Plant Materials. Fresh leaves and both unripe and ripe fruits of VM were collected from Black River, Mauritius. They were authenticated at the National Herbarium of the Mauritius Sugar Industry Research Institute, Réduit. Fruits were cut into small pieces and seeds were removed on the day of collection. The mesocarp and epicarp pieces of fruits were lyophilized overnight whilst the seeds were crushed to remove the endocarp. The endocarp was discarded and the seeds along with the leaves were air dried under shade for 5–7 days till constant mass was obtained. The dried leaves, seeds, and pieces of fruits were homogenized in an electrical food grinder to a fine powder and were stored in air-tight containers.

2.2. Extraction Process. Methanol (Sigma-Aldrich, St. Louis, USA) and decoction extracts were used in the current study. It was important to assess the therapeutic properties of the crude extract in order to validate the medicinal uses of the different parts of the plants, as this is the way in which the local population uses them. All extracts were concentrated *in vacuo* until a constant weight was obtained and the percentage (%) yield was calculated [8]. The gummy material was collected and stored in tightly closed bottles in the dark at 4°C for biological assays.

2.3. In Vitro α -Amylase Assay. The activity of α -amylase was carried out according to the starch-iodine colour changes with minor modifications [7]. Briefly, 0.1 mL of α -amylase solution (15 μ g/mL in 0.1 M acetate buffer, pH 7.2 containing 0.0032 M sodium chloride) was added to a mixture of 3 mL of 1% soluble starch solution (1 g soluble potato starch, suspended in 10 mL water was boiled for exactly 2 min. After cooling, water was added to a final volume of 100 mL. The solution was kept in the refrigerator and was used within 2–3 days) and 2 mL acetate buffer (0.1 M, pH 7.2) preequilibrated at 30°C in a water bath. Substrate and α -amylase blank determinations were undertaken under the same conditions. At zero time and at the end of the incubation period, 0.1 mL of reaction mixture was withdrawn from each tube after mixing and discharged into 10 mL of an iodine solution (0.245 g iodine and 4.0 g Potassium Iodide in 1 liter). After mixing, the absorbency of the starch-iodine mixture was measured spectrophotometrically at 565 nm. The absorbency of the starch blank was subtracted from the sample reading. One unit of amylase activity was arbitrarily defined as $[A_0 - A_t/A_0] \times 100$, where A_0 and A_t were absorbances of the iodine complex of the starch digest at zero time and after

60 min of hydrolysis. Specific activity of amylase was defined as units/mg protein/60 min. Extract (0.10 mL) was incubated with 0.1 mL of the enzyme and substrate solution for 15 min at 30°C. The assay was conducted as described above; one unit of amylase inhibitor was defined as that which reduced the activity of the enzyme by one unit. Assays were replicated three times and the mean values were used. The percentage α -amylase inhibition was calculated according to the formula [9]:

% inhibition

$$= \frac{\{\text{absorbance (control)} - \text{absorbance (sample)}\}}{\text{absorbance (control)}} \times 100\% \quad (1)$$

2.4. In Vitro α -Glucosidase Assay. The α -glucosidase inhibitory activity was determined as described previously [10, 11]. The inhibition was measured spectrophotometrically (405 nm) in the presence of the extracts or positive control (20 μ L at varying concentrations) at pH 6.9. In a 96-microtitre plate, a reaction mixture containing extracts, 20 μ L of 1 mM *p*-nitrophenyl α -D-glucopyranoside as a substrate and 1 unit/mL glucosidase enzyme, in 50 μ L of 0.1 M sodium phosphate buffer was preincubated for 30 min at 37°C. After incubation the reaction was stopped by adding 50 μ L of sodium carbonate (0.1 M). Acarbose (400 μ g/mL) was used as a positive control. The IC₅₀ value was defined as the concentration of α -glucosidase inhibitor to inhibit 50% of its activity under the assay conditions.

2.5. Kinetic Studies. Kinetic studies were carried out according to Kotowaroo et al. [7] with minor modifications. A concentration of 0.10 g/mL of the extracts was used and a calibration curve was constructed using a modified glucose-based colorimetric assay [7]. A 1% dinitrosalicylic solution (DNS) was prepared by mixing 10 g of dinitrosalicylic, 0.5 g sodium disulphite and 10 g NaOH in 1 L distilled water. 3 mL of this solution was then added to glucose solution at different concentration (10, 5, 2.5, 1.25 and 0.625 g/L). The test tubes, covered with paraffin film were heated at 90°C for 5–15 min until a red brown coloration developed. 1 mL of 40% Rochelle salt solution was then added. The test tubes were cooled under tap water and the absorbance was measured at 575 nm. A double reciprocal plot (1/V versus 1/[S]) where V is reaction velocity and [S] is substrate concentration was plotted. The kinetic constants (K_m and V_{max}) were calculated [12], where K_m is the Michaelis-Menten constant, V_{max} is the maximal velocity, [S] is the substrate concentration, and V is the rate of reaction.

Evaluation of the kinetics parameters of α -glucosidase inhibition by the plant extracts was conducted as described previously [10, 13] with minor modifications. Enzyme activity was measured with increasing concentrations of *p*-nitrophenyl α -D-glucopyranoside (PNPG) (0.0625, 0.125, 0.25, 0.5, and 1 mM) as substrate in the absence or presence of the plant extracts at a single concentration. Plant extract was incubated with 10 μ L α -glucosidase solution (1 U/mL), 50 μ L sodium phosphate buffer (0.1 M, pH 6.9), and 20 μ L graded

concentrations of PNPG for 30 min at 37°C. The reaction was terminated by adding 50 µL sodium carbonate (0.1 M). The velocity of the reaction was defined as the rate of formation of the product, *p*-nitrophenol, which was determined using a calibration curve constructed by measuring the absorbance of varying concentration of *p*-nitrophenol.

2.6. Glucose Movement In Vitro. A simple model system was used to evaluate effects of VM extracts on glucose movement *in vitro* based on a modified method [14]. This method involved the use of a dialysis tube (10 cm × 15 cm) into which 2 mL of a solution of glucose (22 mM) and NaCl (0.15 M) and 1 mL of plant extract (20 mg/mL) were introduced and sealed. The tube was placed in a conical flask containing 40 mL of 0.15 M NaCl solution with 10 mL distilled water. The conical flask was then placed in an orbital shaking incubator at 37°C on 100 rpm. The appearance of glucose in the external solution was measured at set time intervals. The effects of plant extract on glucose diffusion were compared to control tests conducted in the absence of plant extracts. All tests were carried out in triplicate.

2.7. Antimicrobial Screening. The procedures used for the antimicrobial screening in the present study are as described previously [15, 16]. The disc diffusion method was used as a preliminary test to find out if plant extracts were active. Clear inhibition zones around discs indicated the presence of antimicrobial activity. Inhibition zones less than 7 mm were not evaluated. If extracts show antimicrobial activity by disc diffusion, MIC (minimum inhibitory concentration) was then determined. MIC which is the least concentration of antimicrobial agent that will inhibit visible growth of an organism after an overnight incubation was determined using microtitre dilution broth method in 96-well microplates [17]. Streptomycin sulphate and gentamicin sulphate were used as positive control for testing against *S. aureus* and *E. coli*, respectively.

2.8. Antioxidant Activities

DPPH Free Radical Scavenging Assay. Assay was carried as described previously [18]. Stock solutions of crude extracts and the positive control, ascorbic acid (400 µg/mL), were prepared in methanol at appropriate concentrations and added to DPPH (200 µL at 100 µM prepared in methanol) in a 96-microtitre plate. The plate was then incubated for 30 min at 37°C. Absorbance of each solution was measured at 517 nm. The extracts and standard were analysed in triplicate at different concentrations and the IC₅₀ values were determined as follows [19]:

$$\% \text{ inhibition} = \frac{\text{absorbance blank sample} - \text{absorbance extract}}{\text{absorbance blank sample}} \times 100. \quad (2)$$

Ferric Reducing Antioxidant Power (FRAP) Assay. The FRAP assay was adapted from the method of Benzie and Strain [20]. The stock solutions included acetate buffer (300 mM, pH 3.6), TPTZ (10 mM) solution in HCl (40 mM), and FeCl₃·6H₂O solution (20 mM). The fresh working solution was prepared by mixing 25 mL acetate buffer, 2.5 mL TPTZ solution, and 2.5 mL FeCl₃·6H₂O solution and then equilibrating at 37°C for 15 min before using. Plant extracts (0.15 mL) at known concentrations were allowed to react with FRAP solution (2.85 mL) for 30 min in the dark. Analysis of extracts and positive control trolox (200 mM) were done in triplicate. Readings of the Persian blue complex were then taken at 593 nm. Results were expressed in mM trolox equivalent (TE)/g fresh mass using the following equation based on the calibration curve: $y = 0.0016x$, $R^2 = 0.8336$.

Hypochlorous Acid (HOCl) Scavenging Assay. HOCl was measured by the chlorination of taurine [21]. Sample cuvettes contained HOCl (100 µL; 600 µmol/L), taurine (100 µL; 150 mmol/L), and 100 µL of plant extracts at various concentrations in a total volume of 1 mL of PBS at a pH of 7.4. The reaction mixtures were thoroughly mixed and then allowed to stand for 10 min at room temperature. After incubation, potassium iodide solution (100 µL; 20 mmol/L) was added and absorption was measured against reference blank cuvette (100 µL PBS instead of extract; absorbance corresponding to 100% HOCl) at 350 nm. The absorbance of the reaction mixture was read both before and after the addition of potassium iodide. The results were expressed as the percentage HOCl inhibitions for each extract and the positive control; ascorbic acid (400 µg/mL). The IC₅₀ was calculated.

Hydroxyl Radical (•OH) Scavenging/Deoxyribose Assay. •OH scavenging activity was assessed by determining its ability to oxidise deoxyribose [22]. The reaction mixture consisted of 100 µL of hydrogen peroxide (15 µmol/L), 100 µL iron chloride (3 mmol/L), 100 µL EDTA (3 mmol/L), 100 µL ascorbic acid (3 mmol/L), and 100 µL extracts at various concentrations. 2-Deoxy-ribose (100 µL) was then added followed by PBS (pH 7.4) in a total volume of 1 mL. After 30 min of incubation at 37°C, 60% trichloroacetic acid (1 mL) and thiobarbituric acid (0.5 mL; 1 g in 100 mL of 0.05 mol/L sodium hydroxide) were added to the reaction mixture. The reaction mixture was boiled for 20 min to observe the development of light pink chromogen. After boiling the absorbance was measured at 532 nm and the •OH scavenging activity of the extract was reported as the percentage of inhibition of deoxyribose degradation against α-tocopherol (400 µg/mL) as positive standard. The IC₅₀ was calculated.

Nitric Oxide Radical (NO) Scavenging Assay. At physiological pH, nitric oxide generated from aqueous sodium nitroprusside solution (SNP) interacts with oxygen to produce nitrite ions, which may be quantified by Griess Illosvay reaction [23]. The reaction mixture (3 mL) contained SNP (2 mL 10 mM), PBS (0.5 mL), and extract and standard solution at various concentrations (0.5 mL). The mixture was incubated for 25°C for 150 min after which 0.5 mL was transferred and mixed

with 1 mL sulphanic acid reagent (0.33% in 20% glacial acetic acid) and allowed to stand for 5 min for complete diazotization. Naphthyl Ethylenediamine dihydrochloride (1 mL; 0.1% w/v) was added, mixed, and allowed to stand for a further 30 min. The pink-coloured chromophore was measured spectrophotometrically at 540 nm against a blank sample. All tests were performed in triplicates and ascorbic acid (400 µg/mL) was used as positive standard. The IC₅₀ was calculated.

Iron Chelating Activity. The ability of the various extracts to chelate Fe (II) was investigated using a modified method [24]. The principle is based on the formation of a purple coloured complex, which is inhibited in the presence of chelating agents. The reaction mixture contained 200 µL of the plant extract of varied concentration and 50 µL of ferric chloride/FeCl₂·4H₂O (2.5 mM), which was made up to 1 mL by the addition of deionised water and was incubated for 5 min at room temperature. Ferrozine (50 µL of 2.5 mM) was then added, and the absorbance was read at 562 nm. EDTA (400 µg/mL) was used as positive control. Percentage chelating activity was calculated using the formula shown below. The IC₅₀ was calculated

$$\begin{aligned} & \% \text{ chelating activity} \\ & = \frac{\text{absorbance blank} - \text{absorbance sample}}{\text{absorbance blank}} \times 100. \end{aligned} \quad (3)$$

2.9. Quantitative Phytochemical Determination

Total Phenol Content. The total phenolic content was determined according to the Folin and Ciocalteu's method [25] with slight modifications. The extracts (0.5 mL; stock solution 1 mg/mL) were mixed with ten-fold diluted Folin-Ciocalteu's reagent (2.5 mL) into test tubes and aqueous sodium carbonate (2 mL, 7.5%) was added. The mixture was thoroughly mixed and allowed to stand for 30 min at room temperature. The resulting blue coloration was measured at 760 nm. All determinations were performed and results expressed in mg gallic acid equivalent (GAE)/g fresh weight using the calibration graph: $y = 0.0036x$, $R^2 = 0.9341$.

Total Flavonoid Content. Total flavonoid content was determined using a method of Amaeze et al. [25]. 2 mL plant extract was added to 2 mL of 2% AlCl₃ solution which was prepared in ethanol. The absorbance was measured at 420 nm after being allowed to stand 1 hr at room temperature. All determinations were performed in triplicates and total flavonoid content was calculated as rutin equivalent (RE) in mg/g fresh weight based on the calibration curve: $y = 0.0088x$, $R^2 = 0.9003$.

Total Proanthocyanidin Content. Determination of proanthocyanidin content was carried out as reported previously [25]. The extract (0.5 mL) at various concentrations was mixed with 1.5 mL of 4% vanillin-methanol solution and 0.75 mL concentrated hydrochloric acid. The mixture was allowed to stand for 15 min after which the absorbance was measured at 500 nm. Total proanthocyanidin contents were expressed as

TABLE 1: Inhibitory activity of VM extracts on α-amylase and α-glucosidase.

Extracts	IC ₅₀ ^a (mg/mL)	
	α-amylase	α-glucosidase
Decoction		
Leaf	1.12 ± 0.17 ^a	0.61 ± 0.21 ^b
Unripe fruit	5.25 ± 15.69 ^a	0.50 ± 6.01 ^b
Ripe fruit	29.62 ± 13.73 ^a	15.73 ± 4.19 ^a
Seed	6.81 ± 2.95 ^a	182.14 ± 103.36 ^a
Methanol		
Leaf	1.70 ± 0.10 ^a	6.19 ± 1.87
Unripe fruit	1.23 ± 0.24 ^a	0.36 ± 0.07 ^b
Ripe fruit	7.74 ± 1.56 ^a	3.28 ± 0.45 ^b
Seed	3.75 ± 1.18 ^a	46.28 ± 6.01 ^a
Acarbose	0.11 ± 0.03	5.03 ± 0.14

^aIC₅₀ is defined as the concentration sufficient to obtain 50% of maximum inhibitory activity, expressed as mean ± SD ($n = 3$). ^a $P < 0.05$ is considered as significantly higher from positive control acarbose (400 µg/mL). ^b $P < 0.05$ is considered as significantly lower from positive control acarbose.

catechin equivalents (CE) (stock solution 400 µg/mL) using the following equation based on the calibration curve: $y = 0.0015x$, $R^2 = 0.9025$.

2.10. Qualitative Phytochemical Screening. The preliminary screening for different phytochemicals was based on the intensity of colour development formation of any precipitate on addition of specific reagents screening using modified standard protocols [26]. Results were reported as low amount (+), moderate amount (++), and high amount (+++) depending on intensity of colour formation [27].

2.11. Statistical Analysis. All data were expressed as means ± SD for three experiments. Statistical analyses were performed using SPSS version 16.0. Normality test was performed before using parametric tests (ANOVA or Pearson correlation). Normality tests were based on Shapiro Wilk's test where a P value >0.05 translates into normal data. ANOVA with Tukey multiple comparisons were carried out to test for any significant differences between the means. Correlations were obtained by Pearson correlation coefficient. The significance level was at 0.05 ($P < 0.05$) [28].

3. Results

Extraction of 50.0 g of powered plant materials with methanol resulted in slightly higher yield compared to decoction. The percentage yields of decoction were leaf extract (19.4%), unripe fruit extract (26.8%), ripe fruit extract (29.4%), and seed extract (8.2%). In contrast, the percentage yields for the methanolic extracts were leaf (20.0%), unripe fruit (24.2%), ripe fruit (29.8%), and seeds (19.8%).

3.1. Inhibitory Activity on Key Carbohydrate Hydrolyzing Enzymes. Leaf decoction (IC₅₀ = 1.12 ± 0.17 mg/mL), leaf methanol (IC₅₀ = 1.70 ± 0.10 mg/mL), and unripe fruit

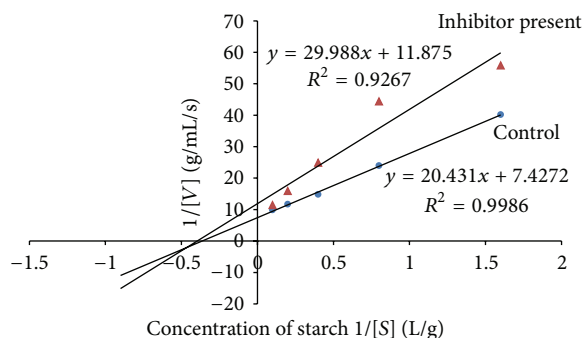


FIGURE 1: The Lineweaver-Burk plots for amylase in the presence or absence of leaf decoction extract (10 mg/mL). Each point represents values in the presence of the inhibitor: red triangle or control blue circle.

methanol ($IC_{50} = 1.23 \pm 0.24$ mg/mL) extracts displayed the highest inhibitory activity (Table 1). However, the values were significantly higher than the positive control acarbose ($IC_{50} = 0.11 \pm 0.03$ mg/mL). The weakest activity was observed in the ripe fruit ($IC_{50} = 29.62 \pm 13.73$ mg/mL) and seed ($IC_{50} = 6.81 \pm 2.95$ mg/mL) decoction extracts. Additionally, Table 1 also summarizes the effects of the different extracts of VM on α -glucosidase activity. The most active extracts (1 mg/mL) were unripe fruit methanolic extract ($IC_{50} = 0.36 \pm 0.07$ mg/mL), unripe fruit decoction ($IC_{50} = 0.50 \pm 6.0$ mg/mL), leaf decoction ($IC_{50} = 0.61 \pm 0.21$ mg/mL), and ripe fruit methanol ($IC_{50} = 3.28 \pm 0.45$ mg/mL), where values were significantly lower than acarbose ($IC_{50} = 5.03 \pm 0.14$ mg/mL).

3.2. Kinetic Studies. The leaf decoction, leaf methanolic, and unripe fruit methanolic extracts were assessed through kinetic studies to determine the type of enzyme-inhibition. The Lineweaver-Burk plots (Figures 1, 2, and 3) were generated using the calibration curve of glucose ($y = 0.1254x + 0.4313$). The double reciprocal Lineweaver-Burk plots showed a decrease in both V_{max} (leaf decoction from 0.13 to 0.084 g/mL/s; leaf methanol extract from 0.13 to 0.055 g/mL/s; unripe methanol extract from 0.13 to 0.030 g/mL/s) and K_m (leaf decoction from 2.75 to 2.53 g/L; leaf methanol extract from 2.75 to 0.87 g/mL/s; unripe methanol extract from 2.75 to 0.94 g/mL/s) values when the inhibitor was added to the reaction mixture, confirming a mixed noncompetitive type of inhibition.

Figures 4–7 show Lineweaver-Burk plots obtained by evaluating the leaf decoction, unripe fruit decoction, unripe fruit, and ripe fruit methanolic extracts through kinetic studies against α -glucosidase. The double reciprocal Lineweaver-Burk plots showed a decrease in both V_{max} and K_m values when the extract was added. Such results suggest a mixed noncompetitive type of inhibition. From Figure 4, V_{max} was observed to decrease from 0.0025 to 0.0021 mM/min while K_m decreased from 0.38 to 0.22 mM in the presence of leaf decoction extract. Also, V_{max} decreased from 0.0025 to 0.0024 Mm/min while K_m decreased from 0.38 to 0.29 mM in the presence of unripe fruit decoction extract (Figure 5).

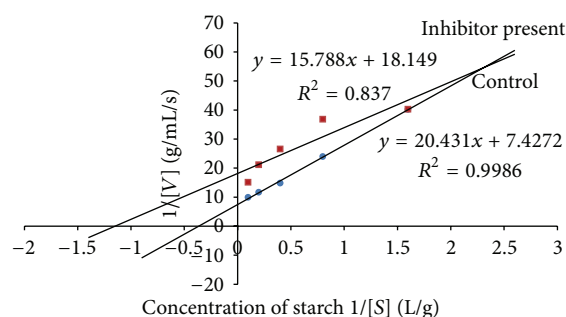


FIGURE 2: The Lineweaver-Burk plots for amylase in the presence or absence of leaf methanolic extract (10 mg/mL). Each point represents values in the presence of the inhibitor: red square or control blue circle.

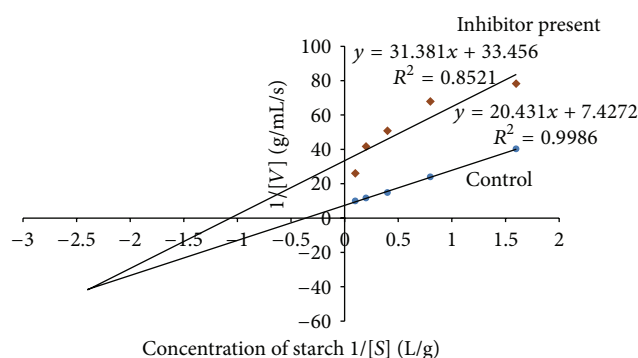


FIGURE 3: The Lineweaver-Burk plots for amylase in the presence or absence of unripe methanolic extract (10 mg/mL). Each point represents values in the presence of the inhibitor: brown diamond or control blue circle.

With regard to unripe methanol extract, V_{max} was found to decrease from 0.0025 to 0.0017 mM/min while K_m decreased from 0.38 to 0.16 mM (Figure 6). In the presence of ripe methanol extract, V_{max} value was found to decrease from 0.0025 to 0.0019 Mm/min while K_m decreased from 0.38 to 0.32 mM (Figure 7).

3.3. Correlation of Carbohydrate Enzymes Inhibitory Effects with Phytochemical Constituents. The relationship between key carbohydrate enzymes inhibitory effects of extracts with total phenolic, flavonoid, and proanthocyanidin contents was investigated using Pearson correlation. As displayed in Table 2, there was no significant correlation ($P > 0.05$) with total phenolic, flavonoid, or proanthocyanidin content. However, the percentage shared variance for α -amylase was as follows: 4.0% for total phenolic content, 98.0% for total flavonoid content, and 31.4% for total proanthocyanidins. For α -glucosidase, the percentage shared variance was 96.0% for total phenolic content, 32.5% for flavonoid, and 98.0% for proanthocyanidin content.

3.4. Effect of VM Extracts on Glucose Movement In Vitro. Results in Table 3 revealed that most of the extracts did

TABLE 2: Relationship between phytochemical constituents and key carbohydrate enzymes inhibitory effects of extracts.

Phytochemical constituent	α -amylase IC ₅₀ ^a (μ g/mL)		α -glucosidase IC ₅₀ ^a (μ g/mL)	
	<i>r</i>	Sig. (2-tailed) value	<i>r</i>	Sig. (2-tailed) value
Total phenolic content ¹	-0.20	>0.05	0.98	>0.05
Total flavonoid ²	-0.99	>0.05	0.57	>0.05
Total proanthocyanidins ³	-0.56	>0.05	0.99	>0.05

^aIC₅₀ is defined as the concentration sufficient to obtain 50% of maximum scavenging activity, expressed as mean \pm SD (*n* = 3). *r* = Pearson correlation. ¹mg GAE/g fresh weight; ²mg RE/g fresh weight; ³mg CE/g fresh weight.

TABLE 3: Effect of VM on the movement of glucose over 3 hrs incubation.

Extracts	Concentration of glucose in external solution (mM/L) after 1 hr incubation period						
	0	0.5	1	1.5	2	2.5	3
Decoction							
Leaf	2.17 \pm 0.087	2.89 \pm 0.15 ^b	3.68 \pm 0.07 ^b	4.63 \pm 0.093 ^{ab}	4.22 \pm 0.097*	4.04 \pm 0.035 ^{*a}	3.76 \pm 0.080 ^{*a}
Unripe fruit	2.18 \pm 0.061	3.06 \pm 0.22	3.73 \pm 0.08	3.79 \pm 1.89	4.39 \pm 0.16	4.20 \pm 0.046 ^{*b}	4.54 \pm 0.046 ^{*b}
Ripe fruit	2.23 \pm 0.046	3.42 \pm 0.14	3.87 \pm 0.05	4.31 \pm 0.31	5.53 \pm 0.076	5.96 \pm 0.063	8.37 \pm 0.61 ^b
Seed	2.25 \pm 0.035	3.51 \pm 0.076 ^b	3.99 \pm 0.046	4.68 \pm 0.063	5.09 \pm 0.061	5.67 \pm 0.08	6.49 \pm 0.122
Methanol							
Leaf	2.22 \pm 0.087	2.72 \pm 0.25	3.37 \pm 0.093*	3.75 \pm 0.063 ^{*ab}	4.13 \pm 0.046*	4.70 \pm 0.380 ^{*ab}	5.04 \pm 0.046 ^{*a}
Unripe fruit	2.33 \pm 0.052	2.79 \pm 0.061	4.37 \pm 0.12 ^b	4.47 \pm 0.076	4.91 \pm 0.061 ^b	5.68 \pm 0.046	8.02 \pm 0.23 ^b
Ripe fruit	2.31 \pm 0.076	3.10 \pm 0.076	3.54 \pm 0.19	4.39 \pm 0.061	5.88 \pm 0.24 ^b	6.54 \pm 0.11	8.42 \pm 0.24 ^{*b}
Seed	2.28 \pm 0.017	2.81 \pm 0.061	3.55 \pm 0.061	4.34 \pm 0.076	4.93 \pm 0.178	5.41 \pm 0.070	7.30 \pm 0.33 ^b
Blank	2.26 \pm 0.017	2.85 \pm 0.03 ^b	4.03 \pm 0.091 ^b	4.48 \pm 0.080 ^b	5.30 \pm 0.052 ^b	6.01 \pm 0.24 ^b	7.16 \pm 0.16 ^b

All data are shown as mean \pm SD; each run in triplicates; **P* < 0.05 is considered as statistically significant (one way ANOVA with post hoc analysis) compared to blank/negative control at respective time interval. ^aSignificant difference (*P* < 0.05) exists between leaf decoction and leaf methanol extracts at respective time interval. ^b*P* > 0.05 compared with glucose concentration at a previous time of incubation.

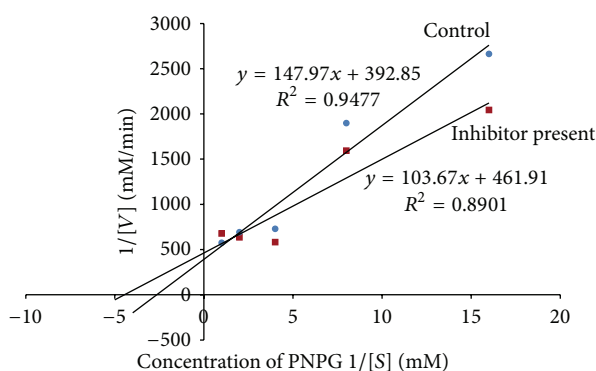


FIGURE 4: The Lineweaver-Burk plots for glucosidase in the presence or absence of leaf decoction extract (1 mg/mL). Each point represents values in the presence of the inhibitor: red square or control blue circle.

not significantly retard glucose movement across the dialysis tube. However, leaf decoction extract was the most active inhibitor of glucose movement in the model system where glucose diffusion was significantly decreased after 2 hr incubation period compared to control and external glucose concentration was 3.76 \pm 0.080 mmol/L after 3 hr. In contrast, leaf methanol extract could decrease glucose movement earlier at a 1 h period of incubation but the overall decrease by a 3 hr period was significantly less (5.04 \pm

0.046 mmol/L) compared to the decoction extract. Unripe fruit decoction extract (4.54 \pm 0.046 mmol/L) could also significantly decrease glucose movement after 3 hr compared to control (7.16 \pm 0.16 mmol/L) as well as leaf methanol extract (5.04 \pm 0.046 mmol/L). However, though the movement of glucose was slow at the beginning and increased with time, such movement was not time dependent for the different extracts since overall no significant differences were noted in glucose concentrations between incubation times.

Results obtained for the antimicrobial tests performed on both the decoction and methanolic extracts of VM are presented in Table 4. It was found that the extracts showed a narrow spectrum of activity, being active only to the Gram positive *S. aureus* and to the Gram negative *E. coli*. Highest inhibitory activity was noted for *E. coli* using unripe fruit decoction extract (12.67 \pm 0.58 mm), whereas for *S. aureus*, leaf methanol extract produced highest inhibition (11.67 \pm 1.53 mm). However, no comparable zones of inhibition to respective standard antibiotic were obtained since mean inhibitory zones of inhibition for all active extracts were significantly lower (*P* < 0.05) than the mean standard.

3.5. Antimicrobial Screening by Disc Diffusion. The extracts showing antibacterial activities by disc diffusion method were tested by broth dilution assay to determine the MICs (Table 5). The lowest MIC value (6.25 mg/mL) was recorded for the methanolic leaf extract against *S. aureus* which can

TABLE 4: Results of preliminary antimicrobial screening of the plant extracts (50 mg/mL) using disc diffusion method.

Test microorganisms	Gram stain +/-	Standard ^b	Diameter of zone of inhibition (mm) ^a								
			Decoction ^c				Methanol ^c				
			S1	S2	S3	S4	S1	S2	S3	S4	
<i>Staphylococcus aureus</i>	G+	26.33 ± 0.58	—	—	10.67 ± 1.15 ^d	—	—	11.67 ± 1.53 ^d	—	—	8.33 ± 1.53 ^d
<i>Escherichia coli</i>	G-	21.67 ± 3.79	—	12.67 ± 0.58 ^d	—	—	10.00 ± 2.00 ^d	—	—	—	—
<i>Pseudomonas aeruginosa</i>	G-	15.33 ± 1.53	—	—	—	—	—	—	—	—	—
<i>Aspergillus niger</i>	F	23.00 ± 1.00	—	—	—	—	—	—	—	—	—
<i>Candida albicans</i>	F	20.67 ± 0.58	—	—	—	—	—	—	—	—	—

^aNo. of replicates (n = 3) for each sample; values are given as mean ± SD. ^bTested at a concentration of 10 µg/disk (Oxoid), bacteria, ampicillin; fungi, nystatin. ^cS1: leaf, S2: unripe fruit, S3: ripe fruit, S4: seed. ^dValues significantly lower (P < 0.05) from positive control, standard antibiotic (One way ANOVA, post hoc Tukey). G+, Gram positive; G-, Gram negative; F, fungi; (-), no distinct zone of inhibition.

TABLE 5: Minimum inhibitory concentrations (mg/mL) of the plant extracts.

Test microorganisms	Gram stain +/-	Standard antibiotic ^b (mg/mL)	Plant extracts ^c [MIC ^a (mg/mL)]								
			Decoction				Methanol				
			S1	S2	S3	S4	S1	S2	S3	S4	
<i>Staphylococcus aureus</i>	G+	0.078	—	—	12.50	—	—	6.25	—	—	25.00
<i>Escherichia coli</i>	G-	0.078	—	25.00	—	—	—	12.50	—	—	—

^aMIC: minimum inhibitory concentration; average of 3 independent experiments; ^bStreptomycin sulphate and gentamicin sulphate tested at a concentration of 20 mg/mL; ^cS1: leaf, S2: unripe fruit S3: ripe fruit, S4: seed; G+, Gram positive; G-, Gram negative.

TABLE 6: DPPH scavenging activity of plant extracts.

Samples	IC ₅₀ ^a (µg/mL)		F	One way ANOVA P value (post hoc)
	Decoction	Methanol		
Leaf	132.78 ± 11.38 ^a	9.04 ± 0.66		<0.05*
Unripe fruit	612.46 ± 47.21 ^a	10.01 ± 0.93	349.97	<0.05*
Ripe fruit	602.54 ± 39.53 ^a	48.46 ± 0.63		<0.05*
Seed	612.46 ± 47.22 ^a	105.86 ± 2.82 ^a		<0.05*

^aIC₅₀ is defined as the concentration sufficient to obtain 50% of maximum scavenging activity, expressed as mean ± SD (n = 3). *P < 0.05 is considered as statistically significant (post hoc Tukey HSD). ^aValues significantly higher (P < 0.05) from positive control, ascorbic acid (IC₅₀ = 0.001 ± 0.0006 µg/mL).

be considered as poor activity compared to the standard antibiotic.

3.6. Antioxidant Activities of Plant Extracts

3.6.1. DPPH Radical Scavenging Assay. DPPH radical scavenging activity of the methanol extracts was higher compared to decoction extracts as the overall concentration of extracts needed to scavenge 50% DPPH radical was lower (Table 6). One way ANOVA analysis revealed that a significant difference exists between the different extracts (F = 349.97; P < 0.05). Post hoc comparison using Tukey HSD shows that the activity of all decoctions extracts was significantly different from their respective methanol extracts (P < 0.05). Moreover, only the activity of methanol extracts of leaf and unripe and ripe fruit was comparable to the positive control ascorbic acid (IC₅₀ = 0.001 ± 0.0006 µg/mL).

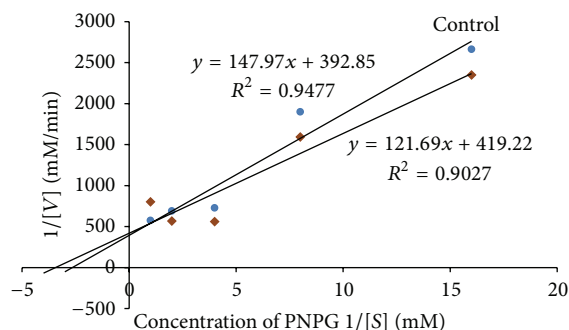


FIGURE 5: The Lineweaver-Burk plots for glucosidase in the presence or absence of unripe fruit decoction extract (1 mg/mL). Each point represents values in the presence of the inhibitor: brown diamond or control blue circle.

3.6.2. Ferric Reducing Antioxidant Power of Extracts. Table 7 shows that there is a significant difference (F = 186.81; P < 0.05) between the antioxidant capacity of the extracts as assessed by FRAP. The different extracts were found to be active in the reduction of Fe⁴⁺ to Fe²⁺, indicating their antioxidant activity as reducing agents. The order of activity is as follows: leaf_{methanol} → unripe fruit_{methanol} → ripe fruit_{methanol} → seed_{methanol} → leaf_{decoction} → unripe fruit_{decoction} → ripe fruit_{decoction} → seed_{decoction}. Furthermore, a significant difference (P < 0.05) was noted between the unripe and ripe fruit decoction extracts and between the unripe fruit and ripe fruit methanolic extracts.

3.6.3. Correlation between Antioxidant Activity and Phytochemical Content. The relationship between antioxidant

TABLE 7: Ferric reducing antioxidant power of extracts.

Samples	mM trolox equivalent (TE)/g fresh weight ^a		F	One way ANOVA P value (post hoc)
	Decoction	Methanol		
Leaf	350.42 ± 1.91	372.5 ± 2.17	186.81	<0.05*
Unripe fruit	330.83 ± 2.83 ^b	361.25 ± 1.25		<0.05*
Ripe fruit	322.93 ± 0.72 ^b	357.08 ± 0.72		<0.05*
Seed	319.17 ± 5.05	346.67 ± 1.91		<0.05*

^aData are expressed as mM trolox equivalent (TE)/g fresh weight, mean ± SD ($n = 3$). ^bSignificant difference ($P < 0.05$) exists between unripe fruit and ripe fruit extracts within same extraction solvent. * $P < 0.05$ is considered as statistically significant (post hoc Tukey HSD).

TABLE 8: Relationship between phenolic content and antioxidant activity of extracts.

Phytochemical constituent	Pearson correlation			
	DPPH ^a		FRAP ^a	
	r	IC ₅₀ ^b ($\mu\text{g}/\text{mL}$) Sig. (2-tailed) value	r	mM trolox equivalent (TE)/g fresh weight Sig. (2-tailed) value
Total phenolic content (mg GAE/g fresh weight)	-0.78	<0.05*	0.88	<0.05*
Total flavonoid (mg RE/g fresh weight)	-0.28	>0.05	0.49	>0.05
Total proanthocyanidins (mg CE/g fresh weight)	-0.40	>0.05	0.54	>0.05

^bIC₅₀ is defined as the concentration sufficient to obtain 50% of maximum scavenging activity, expressed as mean ± SD ($n = 3$). * $P < 0.05$ is considered as statistically significant. ^aCorrelation coefficient of DPPH-FRAP: $r = -0.94$, $P < 0.05$.

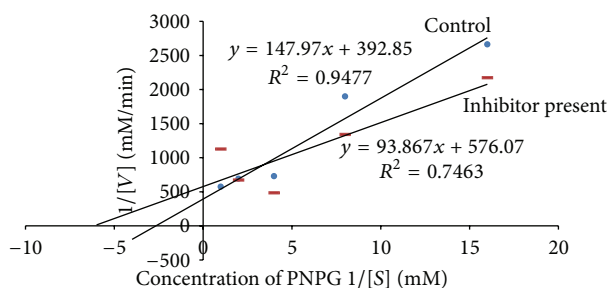


FIGURE 6: The Lineweaver-Burk plots for glucosidase in the presence or absence of unripe fruit methanol extract (1 mg/mL). Each point represents values in the presence of the inhibitor: red dash or control blue circle.

activity with total phenolic, flavonoid, and proanthocyanidin contents was investigated using Pearson correlation. As displayed in Table 8, there was a strong, significant, negative correlation between total phenolic content and DPPH radical scavenging activity ($r = -0.77$, $P < 0.05$), implying that higher total phenolic content resulted in a lower concentration of extracts needed to achieve 50% scavenging activity. On the other hand, no statistically significant correlations were found between DPPH activity and total flavonoids and proanthocyanidins contents. The percentage of shared variance was only 8.0% and 16.3% between DPPH and total flavonoid and between DPPH and total proanthocyanidins, respectively. Also, with respect to FRAP assay, a strong significant positive relationship was found only with total phenolic content ($r = 0.88$, $P < 0.05$). The percentage of shared variance was 23.8% between FRAP and total flavonoid, whereas between FRAP and total proanthocyanidins it was 29.4%. Correlation between the DPPH method and FRAP

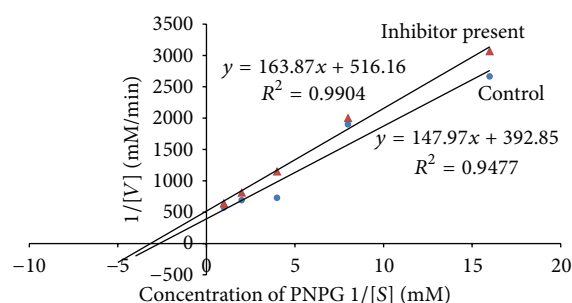


FIGURE 7: The Lineweaver-Burk plots for glucosidase in the presence or absence of ripe fruit methanol extract (1 mg/mL). Each point represents values in the presence of the inhibitor: red triangle or control blue circle.

method, however, revealed a strong significant negative relationship ($r = -0.94$, $P < 0.05$), meaning that these methods were reliable in assessing the antioxidant power of the extracts.

3.6.4. HOCl Scavenging Activity. Table 9 shows the HOCl scavenging activity of the different extracts of VM. Significant differences were only obtained between methanol and decoction extracts of ripe fruit and seed. Methanol unripe fruit extract had the highest scavenging action in view of its low IC₅₀ value (IC₅₀ = 222.99 ± 3.15 $\mu\text{g}/\text{mL}$). However, none of the extracts had IC₅₀ value that was greater than the control ascorbic acid (IC₅₀ = 46.00 ± 2.35 $\mu\text{g}/\text{mL}$). Also, seed decoction extract had the lowest value since its IC₅₀ value (IC₅₀ = 6656.35 ± 390.40 $\mu\text{g}/\text{mL}$) was significantly higher than ascorbic acid. Correlation of this assay results with phytochemical content of the extracts (Figure 8) showed the

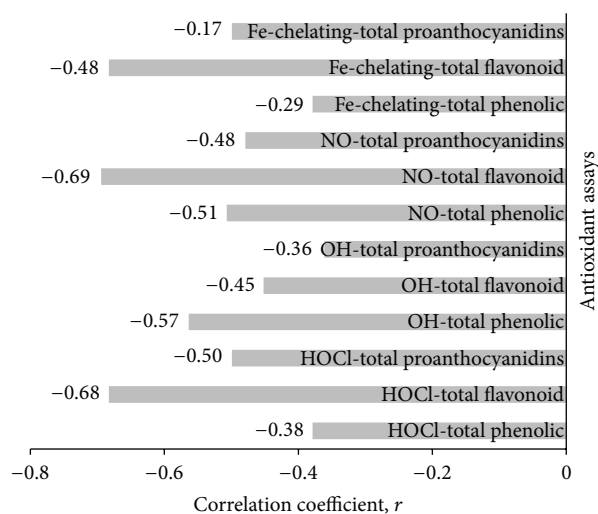


FIGURE 8: Correlation coefficients between iron-chelating activity, $\cdot\text{OH}$, NO, and HOCl assays, with total phenolic, flavonoid, and proanthocyanidins contents.

strongest association with total flavonoid content ($r = -0.68$; 46.6% shared variance).

3.6.5. $\cdot\text{OH}$ Scavenging Activity. All decoction extracts were significantly different ($P < 0.05$) from their respective methanol extracts in inhibiting $\cdot\text{OH}$ -mediated deoxyribose degradation (Table 9). The ripe fruit decoction extract was also significantly less active ($P < 0.05$) in scavenging $\cdot\text{OH}$ compared to the unripe decoction extract since a higher IC_{50} value was obtained ($\text{IC}_{50} = 260.96 \pm 4.29 \mu\text{g/mL}$). Moreover, compared to the positive control α -tocopherol, only the methanol extracts of leaf ($\text{IC}_{50} = 0.09 \pm 0.04 \mu\text{g/mL}$), unripe ($\text{IC}_{50} = 0.29 \pm 0.08 \mu\text{g/mL}$), and ripe ($\text{IC}_{50} = 0.26 \pm 0.02 \mu\text{g/mL}$) fruits which had IC_{50} values which were smaller than that of α -tocopherol ($\text{IC}_{50} = 0.50 \pm 0.11 \mu\text{g/mL}$). This suggests that they exhibited more efficient inhibitory activity than α -tocopherol. From Figure 8, correlation of $\cdot\text{OH}$ scavenging activity with quantitative evaluation of phytochemical content revealed a moderate negative relationship ($r = -0.57$) with total phenolics which translates into 32.5% of shared variance with total phenolic content.

3.6.6. NO Scavenging Activity. As per Table 9, significant differences ($P < 0.05$) were only found between methanol and decoction extracts of ripe fruit and seed. Methanol leaf extract had an IC_{50} value ($\text{IC}_{50} = 43.22 \pm 0.59 \mu\text{g/mL}$) significantly lower than the control ascorbic acid ($\text{IC}_{50} = 546.54 \pm 9.79 \mu\text{g/mL}$) demonstrating a more efficient scavenging potential than the latter. The NO scavenging potential of decoction extracts of ripe fruit and unripe fruit was also significantly different. Strong negative correlation ($r = -0.69$; 47.6% shared variance) was also obtained with total flavonoid content (Figure 8).

3.6.7. Iron Chelating Activity. From Table 9 it can also be observed that all the extracts had considerable iron chelating

activity as demonstrated by their IC_{50} values (expressed in mg/mL) which are comparable to the positive control EDTA ($\text{IC}_{50} = 0.001 \pm 0.0003 \mu\text{g/mL}$). The strongest correlation ($r = -0.48$) was with total flavonoid content which resulted in 23.0% of shared variance.

3.7. Quantitative Phytochemical Analysis. Table 10 shows the overall mean concentration of total phenol, flavonoids, and proanthocyanidins. According to Tawaha et al. [29] plant species having GAE greater than 20 mg/mL dry weight were considered as having high phenolic content. It was noted that all samples were high in total phenol content, with VM leaf methanol extract having the greatest concentration. Post hoc analysis demonstrated that all decoction extracts were significantly different from their respective methanolic extracts. With regard to total flavonoid content, the concentration was found to vary between $6.72 \pm 0.04 \text{ mg RE/g}$ fresh weight and $8.90 \pm 0.35 \text{ mg RE/g}$ fresh weight for the decoction extracts and between $7.13 \pm 0.13 \text{ mg RE/g}$ fresh weight and $9.00 \pm 0.05 \text{ mg RE/g}$ fresh weight for methanol extracts. Significant difference ($P < 0.05$) was noted between flavonoid content of decoction and methanol extracts of unripe fruit. Also, the methanol unripe fruit sample shows significant difference ($P < 0.05$) compared to the methanol ripe fruit sample.

For total proanthocyanidins ($F = 563.37$; $P < 0.05$), comparison of mean within extraction solvent revealed that ripe fruit methanol extract significantly differed from the unripe fruit methanol extract ($P < 0.05$) as well as their respective decoction extracts. Proanthocyanidins content of all decoction extracts was also found to be significantly different from their respective methanol extracts.

3.8. Qualitative Phytochemical Screening. Table 11 shows the qualitative phytochemical screening of the different plant parts. Results were expressed as low amount (+), moderate amount (++), high amount (+++), or absence (-) to report the presence or absence of bioactive components. Phenolic compounds, flavonoids, and anthocyanins were present in all extracts.

4. Discussion

In the present series of *in vitro* experiments, the antidiabetic properties of the decoction and methanol extracts of different parts of VM were assessed in terms of their propensity to inhibit key intestinal carbohydrate digesting enzymes, namely, α -amylase and α -glucosidase. Consequently, the mode of enzyme inhibition for the most active extracts was determined using the Michaelis-Menten constant and maximal velocity in the presence and absence of the plant extracts. Findings in this study tend to demonstrate that only the leaf decoction, leaf methanol, and unripe methanol extracts exhibited significant inhibitory effects on α -amylase and α -glucosidase activity comparable to acarbose. Acarbose, being structurally analogous to an oligosaccharide derived from starch digestion, has an affinity for binding site of key carbohydrate hydrolysing enzymes. Such affinity is 10 000 to 100 000-fold higher than that of regular oligosaccharides

TABLE 9: Scavenging of reactive oxygen species and iron chelating activity (IC₅₀ values) of extracts and reference compounds.

Activity	Extract	IC ₅₀ ^a (μg/mL)		One way ANOVA	
		Decoction extracts	Methanolic extracts	F	P value (post hoc)
HOCl	Leaf	235.55 ± 10.61	382.06 ± 4.35	682.92	>0.05
	Unripe fruit	275.27 ± 18.21 ^c	222.99 ± 3.15		>0.05
	Ripe fruit	982.44 ± 70.66 ^{bc}	418.91 ± 39.22		<0.05*
	Seed	6656.35 ± 390.40 ^b	941.50 ± 120.40 ^b		<0.05*
OH	Leaf	289.04 ± 5.29 ^d	0.09 ± 0.04	3.03	<0.05
	Unripe fruit	157.21 ± 1.19 ^{cd}	0.29 ± 0.08		<0.05*
	Ripe fruit	260.96 ± 4.29 ^{cd}	0.26 ± 0.02		<0.05*
	Seed	803.76 ± 23.72 ^d	22.43 ± 3.97		<0.05*
NO	Leaf	241.22 ± 34.74	43.22 ± 0.59 ^f	434.23	>0.05
	Unripe fruit	436.24 ± 2.99 ^c	91.36 ± 3.26		>0.05
	Ripe fruit	2367.36 ± 198.63 ^{ce}	219.14 ± 39.78		<0.05*
	Seed	6092.38 ± 443.32 ^e	1103.20 ± 11.80 ^e		<0.05*
Iron chelating ^g	Leaf	2.52 ± 1.76 ^h	0.002 ± 0.0005	4.96	<0.05*
	Unripe fruit	0.95 ± 0.40	0.07 ± 0.03		>0.05
	Ripe fruit	0.57 ± 0.52	0.06 ± 0.04		>0.05
	Seed	0.25 ± 0.42	0.0009 ± 0.0003		>0.05

^aIC₅₀ expressed as mean ± SD (n = 3). ^bValues significantly higher (P < 0.05) from ascorbic acid (400 μg/mL; IC₅₀ = 46.00 ± 2.35 μg/mL). ^cSignificant difference (P < 0.05) exists between unripe fruit and ripe fruit extracts within same extraction solvent. ^dValues significantly higher (P < 0.05) from α-tocopherol (400 μg/mL; IC₅₀ = 0.50 ± 0.11 μg/mL). ^eValues significantly higher (P < 0.05) from ascorbic acid (400 μg/mL; IC₅₀ = 546.54 ± 9.79 μg/mL). ^fValue significantly lower (P < 0.05) from ascorbic acid (400 μg/mL; IC₅₀ = 546.54 ± 9.79 μg/mL). ^gIC₅₀ values expressed in mg/mL. ^hValues significantly higher (P < 0.05) from EDTA (400 μg/mL; IC₅₀ = 0.001 ± 0.0003 μg/mL). *P < 0.05 is considered as statistically significant (post hoc Tukey HSD).

TABLE 10: Total phenolic, flavonoid, and proanthocyanidin contents of extracts.

Plant extracts	Decoction	Methanol	F	One way ANOVA P value (post hoc)
	Total phenolic content (mg GAE/g fresh weight) ^a			
Leaf	58.56 ± 1.17	122.22 ± 1.02	1.16	<0.05*
Unripe fruit	35.00 ± 0.33 ^d	70.33 ± 0.33 ^d		<0.05*
Ripe fruit	37.00 ± 0.88 ^d	61.22 ± 1.07 ^d		<0.05*
Seed	35.67 ± 0.33	67.33 ± 3.53		<0.05*
	Total flavonoid content (mg RE/g fresh weight) ^b			
Leaf	8.90 ± 0.35	9.00 ± 0.05	61.06	>0.05
Unripe fruit	8.43 ± 0.18	7.55 ± 0.26 ^d		<0.05*
Ripe fruit	8.00 ± 0.13	8.20 ± 0.07 ^d		>0.05
Seed	6.72 ± 0.04	7.13 ± 0.13		>0.05
	Total proanthocyanidins (mg CE/g fresh weight) ^c			
Leaf	159.32 ± 5.43	185.72 ± 1.14	563.37	<0.05*
Unripe fruit	78.65 ± 2.86 ^d	154.92 ± 3.54 ^d		<0.05*
Ripe fruit	159.50 ± 2.75 ^d	134.57 ± 2.60 ^d		<0.05*
Seed	60.87 ± 4.41	42.53 ± 6.06		<0.05*

All data are shown as mean ± SD in triplicates; ^adata are expressed as mg gallic acid equivalent (GAE)/g fresh weight; ^bdata are expressed as mg rutin equivalent (RE)/g fresh weight; ^cdata are expressed as mg catechin equivalent (CE)/g fresh weight; ^dsignificant difference (P < 0.05) exists between ripe fruit and unripe fruit samples extracted using same solvent. Refer to text. *P < 0.05 is considered as statistically significant.

from nutritional carbohydrates, and C–N linkage present cannot be cleaved, thus acting as a potent blocker of enzymatic hydrolysis [30]. These outcomes were in contrast to the study of Kotowaroo et al. [7], where increasing concentration of aqueous VM leaf extracts did not result in significant inhibitory action on the enzyme. Thus, it can be postulated

that such significant inhibitory activity of the VM leaf decoction extract on α-amylase might be one reason that would validate its traditional use for diabetic management [1].

One could argue that various tested extracts of VM contain bioactive compounds that affect the activity of the two carbohydrate-hydrolyzing enzymes in several ways like

TABLE 11: Qualitative phytochemical screening of the plant extracts.

Bioactive compounds	Plant extracts ^a							
	Decoction				Methanolic			
	S1	S2	S3	S4	S1	S2	S3	S4
Alkaloids	-	+	+	-	++	+	+	-
Saponins	-	+	-	+	-	-	-	-
Phenolic compounds	+++	++	++	++	+++	+++	++	++
Flavonoids	+	+	+	+	++	+	+	+
Antraquinones	+	+	-	-	+	+	+	-
Steroids	-	-	-	+	+	-	-	+
Anthocyanins	++	+	++	+	++	++	++	+

(-): Absence, (+): low presence, (++) : moderate presence, (+++) : high presence. ^aS1: leaf sample, S2: unripe fruit sample, S3: ripe fruit sample, S4: seed sample.

competing with the substrate to bind with the active site of the enzyme or it might also work by binding to another region or to an enzyme substrate complex. Thus, kinetics parameters were calculated from the double reciprocal plot for the most active extracts. The trend lines revealed that both the maximal velocity of the enzyme-substrate reaction (V_{max}) and the affinity (K_m) are decreased in the presence of the plant extracts, suggesting a mixed noncompetitive type of inhibition against both α -amylase and α -glucosidase. Mixed inhibition is a mode of enzyme inhibition whereby the inhibitor binds to the enzyme irrespective of whether the enzyme is already bound to the substrate or not, but it has a greater affinity for one state or the other. The noncompetitive inhibition exhibited by the extracts implies that they had different affinities for both the free enzymes and the enzyme-substrate complexes. Consequently, this suggests that the active component of the extract binds to a region other than the active site of the enzymes or combines with either free enzymes or enzyme-substrate complex possibly interfering with the action of both [31]. Therefore, this type of inhibition is said to result from an allosteric effect where the inhibitor binds to a different site on an enzyme, causing conformational changes that ultimately decrease affinity of the substrate to the active site. When the inhibitor favours binding to the enzyme-substrate complex, an increase in the $1/K_m$ value is noted which consequently suggest that affinity is reduced, causing decrease in velocity of the enzyme-substrate reaction [32]. In the same line of argument, the decrease in K_m and V_{max} observed from the experimental data implied that the present kinetics study tends to suggest that the bioactive compounds in the extracts bind preferably to the enzyme-substrate complex. It is also worth highlighting that the plant inhibitors having mechanism of action of not occupying the active site or not competing with a substrate to bind to the active site of α -amylase offer major advantage over acarbose which is a competitive inhibitor. This also means that the action of the plant inhibitors would not be affected at higher concentration of substrate and would still be effective at

lower concentration. In contrast, higher concentration of the acarbose would be needed to produce the same effect [33].

Published research suggests that there is a significant relationship between phenolic content, flavonoids, and other phytochemical compounds like condensed tannins in extract and the ability to inhibit α -amylase and α -glucosidase [34]. For instance, studies have found that flavonoids could demonstrate the highest inhibitory activities depending on the number of hydroxyl groups in the molecule of the compound. It was shown that the potency of inhibition is correlated with the number of hydroxyl groups on the B ring of the flavonoid skeleton [35]. In the present study, no correlation between neither total phenolic, flavonoid nor proanthocyanidins contents of the different extracts and the inhibition of α -glucosidase or pancreatic α -amylase was observed. Consequently, it can be assumed that active extracts may have other chemical components which play an important role in inhibition of α -glucosidase or α -amylase activities. None of the extracts, however, showed inhibitory effects in a dose response manner on increasing concentrations probably because of saturation at high concentrations thereby causing no further increase in inhibition [7].

Recently, many investigators have focused on the potential of different plant extracts on the diffusion of glucose across the semipermeable membrane or dialysis tube [36]. Such attention has probably been aroused by the fact that in recent years, national and international diabetes associations have consistently emphasized the need to increase intake of a high dietary fibre diet. The viscous and gel-forming properties of soluble dietary fibre like guar gum or β -glucan have been documented to be able to reduce macronutrient absorption, specifically postprandial glucose response after carbohydrate-rich meals and beneficially influence certain blood lipids [37]. In the present study, the *in vitro* dialysis-based model revealed that most of the different extracts did not significantly retard glucose movement across the dialysis tube. Though the exact mechanism of retardation was not investigated, it can be suggested that the concentration, pH, osmolarity, or water retention ability of soluble fibre present in the extract might act as important factors in the antihyperglycemic activity [38, 39]. It was also brought forward by Ahmed et al. [40] that the retardation in glucose diffusion might also be attributed to the physical obstacle presented by high molecular weight fiber particles towards glucose molecules and the entrapment of glucose within the network formed by fibers.

The present investigation has also endeavored to probe into the antimicrobial properties of VM using the disk diffusion assay and the determination of minimum inhibitory concentration. Results clearly demonstrate that out of the 8 extracts of VM investigated, only antimicrobial properties of the unripe decoction extract were active against the Gram negative *E. coli* whereas ripe decoction and seed methanol extracts were on the other hand active against Gram positive *S. aureus*. Leaf methanol extracts having the highest percentage activity were active against both bacteria. According to EUCAST [41], the antibiotic breakpoint assessed by the disc diffusion method was >26 mm for *S. aureus*, >14 mm for *E. coli*, and >15 mm for *P. aeruginosa* for detection of

susceptible bacteria. Thus, results obtained concerning zone of inhibition of standard antibiotic used in this study fell within respective range and this confirmed susceptibility of these strains of bacteria. However, though certain extracts were active, zones of inhibition obtained were significantly less compared to the standard antibiotic used. None of the active extracts had antimicrobial potency comparable to the standard antibiotic. The plant extracts were less effective against the Gram negative bacteria probably because of their resistant multilayered structure of the Gram negative cell wall and their ability to form biofilms. *Per se*, it is documented that in the biofilms, the bacteria are embedded in an extracellular polymeric matrix and are protected against environmental stresses and antimicrobial treatment as well as against the host immune system [42]. Moreover, reports from the Centers for Disease Control and Prevention (CDC) and National Institutes of Health (NIH) estimated that the frequency of infections caused by biofilms, especially in the developed world, lies between 65% and 80%, respectively, [43]. Also, no activity was detected against fungi, which probably points out that antibacterial agents are more common in plants studied than antifungal agents [16].

Differences in antimicrobial property of the plant extracts probably related to the presence of bioactive compounds since an arsenal of phytochemicals originally serve as defense mechanisms against microbial predation [44]. Interestingly, phytochemical screening of the current investigation revealed that the active extracts possessed different amounts of at least 7 classes of bioactive metabolites: alkaloids, saponins, phenolic compounds, flavonoids, anthraquinones, anthocyanins, and to a lesser extent, steroids and saponins. For this case, toxicity of phenolic compounds to microorganisms is directly proportional to the degree of hydroxylation. The oxidised compounds can cause bacterial enzyme inhibition possibly through interaction with sulphhydryl groups or bacterial proteins [44]. Quinones and flavonoids have the ability to complex irreversibly with nucleophilic amino acids in bacterial proteins like adhesions, cell wall envelope transport proteins, thereby causing their inactivation [44].

Studies have long established that ROS have potent oxidative effects on many cellular constituents (e.g., protein, lipids, and DNA), which leads to impairments of various cellular functions; thus they are directly and indirectly associated with the pathogenesis of insulin resistance via the inhibition of insulin signals and the dysregulation of adipocytokines/adipokines which have been implicated in the pathogenesis and progression of diabetes, hypertension, atherosclerosis, and cancer [45] or metabolic syndrome and the collection of cardiometabolic risk factors that include obesity, insulin resistance, hypertension, and dyslipidemia [46]. The scavenging of free radicals is thought to be a valuable measure to depress the level of oxidative stress in tissues for prevention and treatment of these chronic and degenerative diseases [47]. As a result, to further delineate any antioxidant effects of the 8 extracts of VM, 6 standard antioxidant assays were carried out.

Six standard antioxidant assays were performed to assess the various mechanisms of the antioxidant potential of VM. A strong significant correlation between FRAP and DPPH

values suggested that antioxidant components in different VM extracts were capable of both reducing oxidants and scavenging free radicals. When considering the ferric reducing power, the methanol extracts had overall higher trolox equivalence which significantly differed from respective decoction extracts. Similar results were also noted with DPPH assay. The methanol extracts had significantly higher antioxidant capacity compared to decoction extracts which was probably due to the fact that methanol is more efficient in extracting polyphenols and anthocyanidins rather than a single-compound solvent system like water [48]. Methanol extracts had indeed the highest amount of total phenol content while the amounts of proanthocyanidins were also considerable. It is also worth noting that the presence of reducing sugars such as sucrose and fructose, ascorbic acid, aromatic amines, and some amino acids in extracts might also react with the Folin-Ciocalteu reagent, therefore leading to an overestimation of phenols [49]. Furthermore, to confirm whether the antioxidant potential of VM extracts is dependent on either total phenol, flavonoid, or proanthocyanidins contents, results revealed strong correlation between antioxidant capacities assessed by DPPH and FRAP and total phenolic content. It has been found that phenolics can scavenge DPPH radicals by their hydrogen donating ability [50].

Another important observation from the present study is the significant difference between the antioxidant property of unripe and ripe fruits when extracted with the same solvent. These results tend to corroborate with previous investigations, where they reported parallel results when comparing antioxidant activity of fruit extracts at different stages of ripening [50, 51]. Phenolic compounds are documented to synthesize rapidly during the early stages of fruit maturity. As the fruit matures, decline in phenolic compounds concentration is simultaneously observed due to the dilution caused by cell growth [50]. In fact, there is also a decrease of primary metabolism in the ripe fruit resulting in a lack of substrates essential for the biosynthesis of phenolic compounds. Besides transformation reactions like polymerisation, oxidation, and conjugation of bound phenolics during maturation could also result in the decrease of phenolic composition [51].

In the present study, methanol unripe fruit extract had the highest scavenging action but none comparable to ascorbic acid. Although no significant difference was obtained, flavonoids were shown to have a considerable percentage of shared variance with HOCl scavenging effect demonstrating moderate association. Indeed, according to Ribeiro et al. [52], flavonoids have the ability to modulate the neutrophil's oxidative burst. It was also demonstrated that flavonoids with either the catechol moiety or a *p*-unsaturated carbonyl with the free hydroxyl group at C-3 have shown the best myeloperoxidase inhibitory properties [53].

With regard to $\cdot\text{OH}$, these are singlet oxygen species, which are highly reactive and have the capacity to damage DNA, which appears to represent the major target, involved in mutagenesis, carcinogenesis, diabetes, and so forth [23]. VM was found to remove the hydroxyl radicals from the sugar and prevented the reaction. The data proved that methanol extracts had better scavenging activity than

decoction extracts with overall lower IC₅₀ values. However, they were not a stronger scavenger of [•]OH compared to the α -tocopherol. Highest percentage of shared variance was obtained with total phenolic content which established that the scavenging effect was probably due to these bioactive compounds.

High concentration of nitric oxide produced by inducible nitric-oxide synthase in macrophages can result in oxidative damage through the conversion of peroxynitrite [54]. Sustained accumulation of this radical directly contributes to the vascular collapse associated with septic shock, whereas chronic expression of the NO radical is associated with a range of carcinomas and inflammatory conditions like juvenile diabetes, multiple sclerosis, arthritis, and ulcerative colitis [23]. The scavenging effect of plants extracts on NO was more pronounced in the methanol extracts. More specifically, methanol leaf extract had an IC₅₀ value significantly lower than the control ascorbic acid, and thus, it might be suggested that it has a more potent NO scavenging activity than the standard.

With respect to iron chelating activity, only leaf decoction extracts had a scavenging effect significantly higher than the positive control EDTA. On the other hand, other extracts can be deemed to have comparable strong effects in stabilizing the oxidised form of the metal ion. Indeed, the two oxidation states of iron, Fe²⁺ and Fe³⁺, can donate or accept electrons through redox reactions that are important for normal metabolic reactions, but in excess they also may be harmful to cells by aiding in the conversion of superoxide anion (O^{2•-}) and H₂O₂ to the extremely reactive [•]OH [55]. Such activity in this study has been mildly associated with flavonoids present in the extracts. As per Symonowicz and Kolanek [56] structural composition of several flavonoids revealed that there are three potential coordination sites to chelate metal ions, namely, between 5-hydroxy and 4-carbonyl groups, between 3-hydroxy and 4-carbonyl groups, and between 3',4'-hydroxy groups in B ring.

5. Conclusions

Though being an underutilized food plant, VM can be considered as a promising medicinal food plant that deserves to be further explored for the management of diabetes and related complications. Indeed, impeding the absorption of glucose through the inhibition of the carbohydrate-hydrolyzing enzymes such as α -amylase and α -glucosidase in the digestive tract could enable overall smooth glucose management in diabetic patients. VM extracts being more of the noncompetitive type inhibitor implies that the bioactive components responsible for such action would rather bind to a region beside the active site which is a major advantage over acarbose which is a competitive inhibitor. As a result, it is evident that, with higher intake of dietary carbohydrates, higher concentration of acarbose would be needed to show the same effect. This would not be the case with VM which is still effective at lower concentration. Given the dearth of updated information on the biological properties of VM, this study has provided an opportunity to establish

valuable primary information on the bioactivity of VM and has opened new perspectives for further pharmacological research.

Conflict of Interests

The authors declare that there is no conflict of interests regarding the publication of this paper.

References

- [1] A. Gurib-Fakim and T. Brendler, *Medicinal and Aromatic Plants of Indian Ocean Islands: Madagascar, Comoros, Seychelles and Mascarenes*, Medpharm, Stuttgart, Germany, 2004.
- [2] T. Abeer, "Flavonoidal content of *Vangueria infausta* extract grown in Egypt: investigation of its antioxidant activity," *International Research Journal of Pharmacy*, vol. 2, no. 3, pp. 157–161, 2011.
- [3] H. J. de Boer, A. Kool, A. Broberg, W. R. Mziray, I. Hedberg, and J. J. Levenfors, "Anti-fungal and anti-bacterial activity of some herbal remedies from Tanzania," *Journal of Ethnopharmacology*, vol. 96, no. 3, pp. 461–469, 2005.
- [4] M. S. Musa, F. E. Abdelrasool, E. A. Elsheikh, L. A. M. N. Ahmed, A. L. E. Mahmoud, and S. M. Yagi, "Ethnobotanical study of medicinal plants in the Blue Nile State, South-eastern Sudan," *Journal of Medicinal Plant Research*, vol. 5, no. 17, pp. 4287–4297, 2011.
- [5] S. K. Jain and S. Srivastava, "Traditional uses of some Indian plants among islanders of Indian Ocean," *Indian Journal of Traditional Knowledge*, vol. 4, no. 4, pp. 345–357, 2005.
- [6] C. Orwa, A. Mutua, R. Kindt, R. Jamnadass, and S. Anthony, "Agroforestry Database: a tree reference and selection guide version 4.0," 2009, <http://www.worldagroforestry.org/sites/treedbs/treedatabases.asp>.
- [7] M. I. Kotowaroo, M. F. Mahomoodally, A. Gurib-Fakim, and A. H. Subratty, "Screening of traditional antidiabetic medicinal plants of Mauritius for possible α -amylase inhibitory effects *in vitro*," *Phytotherapy Research*, vol. 20, no. 3, pp. 228–231, 2006.
- [8] F. Amelia, G. N. Afnani, A. Musfiroh, A. N. Fikriyani, S. Ucche, and M. Murrulkimahi, "Extraction and stability test of anthocyanin from Buni fruits (*Antidesma bunius* L.) as an alternative natural and safe food colorants," *Journal of Food and Pharmaceutical Sciences*, vol. 1, no. 2, pp. 49–53, 2013.
- [9] R. Sangeetha and N. Vedaasree, "*In vitro* α -amylase inhibitory activity of the leaves of *Thespesia populnea*," *ISRN Pharmacology*, vol. 2012, Article ID 515634, 4 pages, 2012.
- [10] J. A. Bachhawat, M. S. Shihabudeen, and K. Thirumurugan, "Screening of fifteen Indian Ayurvedic plants for alpha-glucosidase inhibitory activity and enzyme kinetics," *International Journal of Pharmacy and Pharmaceutical Sciences*, vol. 3, no. 4, pp. 267–274, 2011.
- [11] M. F. Mahomoodally, A. H. Subratty, A. Gurib-Fakim, I. M. Choudhary, and S. N. Khan, "Traditional medicinal herbs and food plants have the potential to inhibit key carbohydrate hydrolyzing enzymes *in vitro* and reduce postprandial blood glucose peaks *in vivo*," *The Scientific World Journal*, vol. 2012, Article ID 285284, 9 pages, 2012.
- [12] R. K. Murray, D. K. Granner, P. A. Mayes, and V. W. Rodwell, *Harper's Illustrated Biochemistry*, Lange Medical Books, New York, NY, USA, 26th edition, 2003.

- [13] S. Gurudeeban, K. Satyavani, and T. Ramanathan, "Alpha glucosidase inhibitory effect and enzyme kinetics of coastal medicinal plants," *Bangladesh Journal of Pharmacology*, vol. 7, pp. 186–191, 2012.
- [14] A. M. Gallagher, P. R. Flatt, G. Duffy, and Y. H. A. Abdel-Wahab, "The effects of traditional antidiabetic plants on *in vitro* glucose diffusion," *Nutrition Research*, vol. 23, no. 3, pp. 413–424, 2003.
- [15] M. K. Kinoo, M. F. Mahomoodally, and D. Puchooa, "Antimicrobial and physico-chemical properties of processed and raw honeys of Mauritius," *Advances in Infectious Diseases*, vol. 2, no. 2, pp. 25–36, 2012.
- [16] M. F. Mahomoodally, A. Gurib-Fakim, and A. H. Subratty, "Antimicrobial activities and phytochemical profiles of endemic medicinal plants of Mauritius," *Pharmaceutical Biology*, vol. 43, no. 3, pp. 237–242, 2005.
- [17] R. M. Mariita, C. K. P. O. Ogol, N. O. Oguge, and P. O. Okemo, "Methanol extract of three medicinal plants from Samburu in northern Kenya show significant antimycobacterial, antibacterial and antifungal properties," *Research Journal of Medicinal Plant*, vol. 5, no. 1, pp. 54–64, 2011.
- [18] K. K. Parekh, A. M. Patel, A. J. Modi, and H. R. Chandrashekar, "Antioxidant and cytotoxic activities of few selected *Ipomoea* species," *Pharmacologia*, vol. 3, no. 9, pp. 377–386, 2012.
- [19] A. Rohman, S. Riyanto, N. Yuniarti, W. R. Saputra, R. Utami, and W. Mulatsih, "Antioxidant activity, total phenolic, and total flavonoid of extracts and fractions of red fruit (*Pandanus conoideus* Lam.)" *International Food Research Journal*, vol. 17, no. 1, pp. 97–106, 2010.
- [20] I. F. F. Benzie and J. J. Strain, "The ferric reducing ability of plasma (FRAP) as a measure of "antioxidant power": the FRAP assay," *Analytical Biochemistry*, vol. 239, no. 1, pp. 70–76, 1996.
- [21] L. Wang, M. Bassiri, R. Najafi et al., "Hypochlorous acid as a potential wound care agent," *Journal of Burns and Wounds*, vol. 6, pp. 65–79, 2007.
- [22] P. Thirunavukkarasu, T. Ramanathan, L. Ramkumar, R. Shanmugapriya, and G. Renugadevi, "The antioxidant and free radical scavenging effect of *Avicennia officinalis*," *Journal of Medicinal Plant Research*, vol. 5, no. 19, pp. 4754–4758, 2011.
- [23] B. Hazra, S. Biswas, and N. Mandal, "Antioxidant and free radical scavenging activity of *Spondias pinnata*," *BMC Complementary & Alternative Medicine*, vol. 8, article 63, 2008.
- [24] D. Ramful, T. Bahorun, E. Bourdon, E. Tarnus, and O. I. Aruoma, "Bioactive phenolics and antioxidant propensity of flaved extracts of Mauritian citrus fruits: potential prophylactic ingredients for functional foods application," *Toxicology*, vol. 278, no. 1, pp. 75–87, 2010.
- [25] O. U. Amaeze, G. A. Ayoola, M. O. Sofidiya, A. A. Adepoju-Bello, A. O. Adegoke, and H. A. B. Coker, "Evaluation of antioxidant activity of *Tetracarpidium conophorum* (Müll. Arg) Hutch & Dalziel leaves," *Oxidative Medicine and Cellular Longevity*, vol. 2011, Article ID 976701, 7 pages, 2011.
- [26] M. F. Mahomoodally, *Biochemical investigation into the antidiabetic potential of medicinal plants in Mauritius [Ph.D. thesis]*, University of Mauritius, Moka, Mauritius, 2008.
- [27] Y. Vaghasiya and S. Chanda, "Antimicrobial and free radical scavenging activity of different solvent extracts of *Mangifera indica* L. seeds," *Research Journal of Microbiology*, vol. 5, no. 12, pp. 1207–1212, 2010.
- [28] J. Pallant, *SPSS Survival Manual: A Step by Step Guide to Data Analysis Using SPSS*, Allen and Unwin, Sydney, Australia, 4th edition, 2011.
- [29] K. Tawaha, F. Q. Alali, M. Gharaibeh, M. Mohammad, and T. el-Elimat, "Antioxidant activity and total phenolic content of selected Jordanian plant species," *Food Chemistry*, vol. 104, no. 4, pp. 1372–1378, 2007.
- [30] R. Rhabasa-Lhoret and J. L. Chiasson, "Alpha-glucosidase inhibition," in *International Textbook of Diabetes Mellitus*, R. A. Defronzo, E. Ferrannini, H. Keen, and P. Zimmet, Eds., pp. 901–914, John Wiley & Sons, Chichester, UK, 2004.
- [31] M. I. Kazeem, T. V. Dansu, and S. A. Adeola, "Inhibitory effect of *Azadirachta indica* A. juss leaf extract on the activities of α -amylase and α -glucosidase," *Pakistani Journal of Biological Sciences*, vol. 16, no. 21, pp. 1358–1362, 2013.
- [32] K. B. Storey, *Functional Metabolism: Regulation and Adaptation*, John Wiley & Sons, Hoboken, NJ, USA, 2004.
- [33] V. Ghadyale, S. Takalikar, V. Haldavnekar, and A. Arvindekar, "Effective control of postprandial glucose level through inhibition of intestinal alpha glucosidase by *Cymbopogon martinii* (Roxb.)," *Evidence-Based Complementary and Alternative Medicine*, vol. 2012, Article ID 372909, 6 pages, 2012.
- [34] S. Adisakwattana, P. Jiphimai, P. Prutanopajai, B. Chanathong, S. Sapwarabol, and T. Ariyapitipan, "Evaluation of α -glucosidase, α -amylase and protein glycation inhibitory activities of edible plants," *International Journal of Food Sciences and Nutrition*, vol. 61, no. 3, pp. 295–305, 2010.
- [35] P. M. de Sales, P. M. de Souza, L. A. Simeoni, P. D. O. Magalhães, and D. Silveira, " α -amylase inhibitors: a review of raw material and isolated compounds from plant source," *Journal of Pharmacy and Pharmaceutical Sciences*, vol. 15, no. 1, pp. 141–183, 2012.
- [36] S. K. Basha and V. S. Kumari, "*In vitro* antidiabetic activity of *Psidium guajava* leaves extracts," *Asian Pacific Journal of Tropical Diseases*, vol. 2, supplement 1, pp. S98–S100, 2012.
- [37] M. O. Weickert and A. F. H. Pfeiffer, "Metabolic effects of dietary fiber consumption and prevention of diabetes," *The Journal of Nutrition*, vol. 138, no. 3, pp. 439–442, 2008.
- [38] P. J. Wood, M. U. Beer, and G. Butler, "Evaluation of role of concentration and molecular weight of oat β -glucan in determining effect of viscosity on plasma glucose and insulin following an oral glucose load," *British Journal of Nutrition*, vol. 84, no. 1, pp. 19–23, 2000.
- [39] J. W. Anderson, W. R. Midgley, and B. Wedman, "Fiber and diabetes," *Diabetes Care*, vol. 2, no. 4, pp. 369–379, 1979.
- [40] F. Ahmed, N. S. Siddaraju, and A. Urooj, "*In vitro* hypoglycemic effects of *Gymnema sylvestre*, *Tinospora cordifolia*, *Eugenia jambolana* and *Aegle marmelos*," *Journal of Natural Pharmaceuticals*, vol. 2, no. 2, pp. 52–55, 2011.
- [41] European Committee on Antimicrobial Susceptibility Testing (EUCAST), "Breakpoint tables for interpretation of MICs and zone diameters," 2013, http://www.eucast.org/fileadmin/src/media/PDFs/EUCAST_files/Breakpoint_tables/Breakpoint_table_v.3.1.pdf.
- [42] C. Heilmann and F. Gotz, "Cell—cell communication and biofilm formation in Gram-positive bacteria," in *Bacterial Signaling*, R. Krämer and K. Jung, Eds., chapter 1, pp. 7–22, Wiley-VCH, Weinheim, Germany, 2010.
- [43] R. Sawhney and V. Berry, "Bacterial biofilm formation, pathogenicity, diagnostics and control: an overview," *Indian Journal of Medical Sciences*, vol. 63, no. 7, pp. 313–321, 2009.
- [44] M. M. Cowan, "Plant products as antimicrobial agents," *Clinical Microbiology Reviews*, vol. 12, no. 4, pp. 564–582, 1999.

- [45] M. Matsuda and I. Shimomura, "Increased oxidative stress in obesity: implications for metabolic syndrome, diabetes, hypertension, dyslipidemia, atherosclerosis, and cancer," *Obesity Research & Clinical Practice*, vol. 7, no. 5, pp. e330–e341, 2013.
- [46] C. K. Roberts and K. K. Sindhu, "Oxidative stress and metabolic syndrome," *Life Sciences*, vol. 84, no. 21-22, pp. 705–712, 2009.
- [47] L. Fu, B.-T. Xu, X.-R. Xu et al., "Antioxidant capacities and total phenolic contents of 62 fruits," *Food Chemistry*, vol. 129, no. 2, pp. 345–350, 2011.
- [48] J. Jakopič, R. Veberič, and F. Štampar, "Extraction of phenolic compounds from green walnut fruits in different solvents," *Acta Agriculturae Slovenica*, vol. 93, no. 1, pp. 11–15, 2009.
- [49] K. N. Prasad, L. Y. Chew, H. E. Khoo, K. W. Kong, A. Azlan, and A. Ismail, "Antioxidant capacities of peel, pulp, and seed fractions of *Canarium odontophyllum* Miq. fruit," *Journal of Biomedicine and Biotechnology*, vol. 2010, Article ID 871379, 8 pages, 2010.
- [50] K. N. Prasad, B. Yang, K. W. Wong et al., "Phytochemicals and antioxidant capacity from *Nypa fruticans* Wurmb. fruit," *Evidence-Based Complementary and Alternative Medicine*, vol. 2013, Article ID 154606, 9 pages, 2013.
- [51] J. Gruz, F. A. Ayaz, H. Torun, and M. Strnad, "Phenolic acid content and radical scavenging activity of extracts from medlar (*Mespilus germanica* L.) fruit at different stages of ripening," *Food Chemistry*, vol. 124, no. 1, pp. 271–277, 2011.
- [52] C. Ribeiro, M. Freitas, S. M. Tomé, A. M. S. Silva, G. Porto, and E. Fernandes, "Modulation of human neutrophils' oxidative burst by flavonoids," *European Journal of Medicinal Chemistry*, vol. 67, pp. 280–292, 2013.
- [53] L. O. Regasini, J. C. R. Velloso, D. H. S. Silva et al., "Flavonols from *Pterogyne nitens* and their evaluation as myeloperoxidase inhibitors," *Phytochemistry*, vol. 69, no. 8, pp. 1739–1744, 2008.
- [54] R. J. Nijveldt, E. van Nood, D. E. C. van Hoorn, P. G. Boelens, K. van Norren, and P. A. M. van Leeuwen, "Flavonoids: a review of probable mechanisms of action and potential applications," *The American Journal of Clinical Nutrition*, vol. 74, no. 4, pp. 418–425, 2001.
- [55] S. Mandal, B. Hazra, R. Sarkar, S. Biswas, and N. Mandal, "Assessment of the antioxidant and reactive oxygen species scavenging activity of methanolic extract of *Caesalpinia crista* leaf," *Evidence-Based Complementary and Alternative Medicine*, vol. 2011, Article ID 173768, 11 pages, 2011.
- [56] M. Symonowicz and M. Kolanek, "Flavonoids and their properties to form chelate complexes," *Biotechnology Food Sciences*, vol. 76, no. 1, pp. 35–41, 2012.

Research Article

Arrabidaea chica Hexanic Extract Induces Mitochondrion Damage and Peptidase Inhibition on *Leishmania* spp.

Igor A. Rodrigues,¹ Mariana M. B. Azevedo,² Francisco C. M. Chaves,³ Celuta S. Alviano,⁴ Daniela S. Alviano,⁴ and Alane B. Vermelho⁴

¹ Departamento de Produtos Naturais e Alimentos, Centro de Ciências da Saúde, Faculdade de Farmácia, Universidade Federal do Rio de Janeiro, 219491-590 Rio de Janeiro, RJ, Brazil

² Programa de Pós Graduação Ciências dos Alimentos, Instituto de Química, Universidade Federal do Rio de Janeiro, 21941-590 Rio de Janeiro, RJ, Brazil

³ Embrapa Amazônia Ocidental, CP 319, 69010-970 Manaus, AM, Brazil

⁴ Departamento de Microbiologia Geral, Centro de Ciências da Saúde, Instituto de Microbiologia Paulo de Góes, Universidade Federal do Rio de Janeiro, 21941-590 Rio de Janeiro, RJ, Brazil

Correspondence should be addressed to Alane B. Vermelho; abvermelho@micro.ufrj.br

Received 21 February 2014; Accepted 23 March 2014; Published 9 April 2014

Academic Editor: José Carlos Tavares Carvalho

Copyright © 2014 Igor A. Rodrigues et al. This is an open access article distributed under the Creative Commons Attribution License, which permits unrestricted use, distribution, and reproduction in any medium, provided the original work is properly cited.

Currently available leishmaniasis treatments are limited due to severe side effects. *Arrabidaea chica* is a medicinal plant used in Brazil against several diseases. In this study, we investigated the effects of 5 fractions obtained from the crude hexanic extract of *A. chica* against *Leishmania amazonensis* and *L. infantum*, as well as on the interaction of these parasites with host cells. Promastigotes were treated with several concentrations of the fractions obtained from *A. chica* for determination of their minimum inhibitory concentration (MIC). In addition, the effect of the most active fraction (B2) on parasite's ultrastructure was analyzed by transmission electron microscopy. To evaluate the inhibitory activity of B2 fraction on *Leishmania* peptidases, parasites lysates were treated with the inhibitory and subinhibitory concentrations of the B2 fraction. The minimum inhibitory concentration of B2 fraction was 37.2 and 18.6 $\mu\text{g}/\text{mL}$ for *L. amazonensis* and *L. infantum*, respectively. Important ultrastructural alterations as mitochondrial swelling with loss of matrix content and the presence of vesicles inside this organelle were observed in treated parasites. Moreover, B2 fraction was able to completely inhibit the peptidase activity of promastigotes at pH 5.5. The results presented here further support the use of *A. chica* as an interesting source of antileishmanial agents.

1. Introduction

Among individual infectious diseases leishmaniasis is in the ninth position of the global burden of diseases. This illness has two main clinical manifestations which are cutaneous lesions (cutaneous leishmaniasis—CL) and visceral impairments (visceral leishmaniasis—VL) [1]. CL and VL represent a serious public health problem in 98 countries and 3 territories on 5 continents where the disease can be found. According to World Health Organization (WHO), there are more than 220,000 CL cases and 58,000 VL cases per year [2]. In Brazil, CL and VL are widespread and can be found

not only in rural areas but also in urban areas mainly due to deforestation and new settlements [3].

Despite the large number of both synthetic and natural antileishmanial agents described in the literature, only a few drugs have reached the clinical stage with approval for human use. This fact could be partly explained by the lack of investments in drug research for poverty-related diseases, which includes leishmaniasis [4]. The current chemotherapy for leishmaniasis treatment still relies on the use of pentavalent antimonials and amphotericin B, although liposomal amphotericin B, paromomycin, and miltefosine have been introduced for the treatment of the disease in several

countries. However, most of these drugs are expensive, present toxic effects, and are able to induce parasite resistance [5]. Consequently, the search for new and more effective antileishmanial agents remains crucial.

Arrabidaea chica (HBK) Verlot, Bignoniaceae, is a scrambling shrub native to tropical America, more particularly in the Amazon basin where it is also known as “Pariri,” “Crajirú,” “Carajuru,” or “Carajiru.” The leaves of *A. chica* have been traditionally used by Brazilian Indians as a dye for body painting in rituals and to protect the skin against sunlight as well as an insect repellent. Chemical investigations have been carried out since the beginning of this century to determine the composition of the *A. chica* dye, which used to be commercialized as such [6]. Nowadays *A. chica* is used by the regional population as an anti-inflammatory and astringent agent as well as a remedy for intestinal colic, diarrhea, leucorrhea, anemia, and leukemia [7]. The present study aimed to evaluate the antileishmanial effects of the hexanic extract of the *A. chica* leaves.

2. Materials and Methods

2.1. Chemicals. Resazurin, RPMI 1640 medium, and bovine serum albumin were purchased from Sigma Chemical Co., USA. Amphotericin B was purchased from Fontoura-Wyeth, Brazil. Fetal bovine serum (FBS) was purchased from Cripion Biotecnologia Ltda, Brazil. All solvents used were spectroscopic grade from Tedia (Fairfield, OH, USA). Column chromatographic product was purchased from Merck (Darmstadt, Germany).

2.2. Plant Material and Acquisition of the Hexanic Extract. The sample of *A. chica* was kept in a germplasm bank under the same cultivation practices at the EAFM Herbarium from Federal Institute of Amazonas (Manaus, AM), where a voucher specimen was deposited (registry EAFM 6791). Leaves of *A. chica* were collected between 08:00 and 09:00 AM.

A. chica crude extract was obtained by 1 week extraction in hexane. Then, the extract was carefully filtered, dried, and stored in opaque glass vials at -10°C . Afterwards, the crude extract was subjected to silica gel column chromatography with an increasing gradient of polarity, starting with 100% *n*-hexane and 100% ethyl acetate to 100% ethanol, affording five fractions (B1, B2, B3, B4, and B5).

2.3. Analysis of the Hexanic Extract of *A. chica* by GC-MS. The B2 fraction of the hexanic extract from “crajirú” was analyzed by a gas chromatograph (GC) interfaced to a mass spectrometer (MS) employing the following conditions: the oven temperature was programmed from 60°C to 300°C at $10^{\circ}\text{C}/\text{min}$, and helium was the carrier gas (at $1.0\text{ mL}/\text{min}$). One microliter of 1% solution of the B2 fraction in dichloromethane was injected in split mode (1:50). Mass spectra were obtained in an Agilent 5973N system, fitted with a low bleeding 5% phenyl/95% methyl silicone (HP-5 MS, $30\text{ m} \times 0.25\text{ mm} \times 0.25\text{ }\mu\text{m}$) fused silica capillary column, operating in the electronic ionization mode (EI) at 70 eV , with a scan mass range of 40–500 *m/z*. Sampling

rate was 3.15 scan/s. The ion source was kept at 230°C , mass analyzer at 150°C , and transfer line at 260°C . Linear retention indices (LRI) were measured by injection of a series of *n*-alkanes (C_{10} – C_{30}) in the same column and conditions as described above and compared with reference data. The identification of the B2 fraction constituents was made based on the retention indexes and by comparison of mass spectra with computer search using NIST21 and NIST107 libraries. Compound concentrations were calculated from the GC peak areas, and they were arranged in order of GC elution.

2.4. Parasite Strains and Cell Cultures. Promastigote forms of two *Leishmania* species, *Leishmania* (*L.*) *amazonensis* (IFLA/BR/1967/PH8) and *L. (L.) infantum* (MHOM/BR/1974/PP75) from the *Leishmania* Type Culture Collection of Oswaldo Cruz Institute/Fiocruz (Rio de Janeiro/RJ/Brazil) were used in all experiments. Parasites were axenically cultured in PBHIL medium as previously described [8]. In order to assure infectiveness of the parasites, periodical infection of mice peritoneal macrophages was performed.

2.5. Evaluation of *Leishmania* Inhibitory Concentrations. The assay was carried out in a 96-well microtiter plate where the hexanic extract from *A. chica* was serially diluted in duplicate to final test concentrations (1–500 $\mu\text{g}/\text{mL}$). Then 5.0×10^5 promastigote forms of *L. amazonensis* or *L. infantum* were harvested at the early stationary phase, added to each well, and plated at 26°C for 120 h. At the end of incubation period, 25 μL of resazurin solution (5 mg/100 mL of phosphate buffer saline, pH 7.2) was added and the viability of parasites was determined in accordance with the protocol previously described [9]. The minimal inhibitory concentration (MIC) was considered the lowest concentration of the hexanic extract that completely prevented the growth of *Leishmania in vitro*. Alternatively, 120 h-treated parasites were centrifuged (1,000 *g*/5 min), washed twice in PBS, and then reincubated in fresh PBHIL culture medium in order to evaluate the leishmanicidal effect. The lowest concentration able to inhibit parasite growth was considered the minimal leishmanicidal concentration (MLC). The 50% inhibitory concentration (IC_{50}) was determined by logarithmic regression analysis of the data obtained as described above.

2.6. Ultrastructure Analysis. Alterations in the ultrastructure of the parasites were analyzed by transmission (TEM) electron microscopy. First, promastigote forms of *L. infantum* were harvested at the early stationary phase of growth, washed twice with PBS, and incubated in the presence of a subinhibitory concentration (subMIC) of *A. chica* hexanic extract at 28°C for 24 hours. After the parasites were washed twice in PBS they were fixed with glutaraldehyde solution (2.5% glutaraldehyde in 0.1 M sodium cacodylate buffer containing 3.5% sucrose, pH 7.4) at 4°C for 60 min. Samples of treated cells and their controls (untreated cells) were sent to Plataforma Rudolf Barth (Instituto Oswaldo Cruz/Fiocruz/RJ) and processed as previously mentioned [10]. The photomicrographs were obtained using an electron microscope Jeol JEM1011.

TABLE 1: Antileishmanial activity and cytotoxic effect of the *A. chica* hexanic extract fractions.

Hexanic extract fraction	<i>L. amazonensis</i>		<i>L. infantum</i>		Macrophages	SI
	MIC ($\mu\text{g/mL}$)	IC ₅₀ ($\mu\text{g/mL}$)	MIC ($\mu\text{g/mL}$)	IC ₅₀ ($\mu\text{g/mL}$)	MCC ($\mu\text{g/mL}$)	
B1	na	nd	na	nd	nd	nd
B2	37.2	31.8	18.6	14.7	297.6	8.0 ^a /16 ^b
B3	186.7	152.2	186.7	139.6	nd	nd
B4	368	198.5	368	179.7	nd	nd
B5	na	nd	na	nd	nd	nd
Amphotericin B	1.01	0.07	0.625	0.01	14.6	14.4 ^a /23.4 ^b

MIC: minimum inhibitory concentration; IC₅₀: 50% inhibitory concentration; MCC: minimum cytotoxic concentration.

na: not active at the highest concentration tested (500 $\mu\text{g/mL}$); nd: not determined.

SI: selective index; ^aselective index for *L. amazonensis*; ^bselective index for *L. infantum*.

2.7. Peptidase Inhibition Assay. *L. amazonensis* and *L. infantum* promastigotes (10^6 parasites/mL) were harvested at the log phase, washed twice by centrifugation (1,500 \times g/5 min) with PBS pH 6.8, and then disrupted through seven cycles of freezing and thawing ($-80^\circ\text{C}/37^\circ\text{C}$). The cellular extracts were then centrifuged (12,000 \times g/10 min) and the supernatant aliquots preserved at 0°C . Peptidase (gelatinase) activity was analyzed through the protocol adapted from Cedrola et al. [11]. Briefly, 100 μL of the cellular lysates was incubated with different concentrations of the hexanic extract in a PBS 0.1M pH 5.5, or pH 10, and gelatin 1% mixture. E64 (cysteine peptidase inhibitor) and 1,10-phenanthroline (metallopeptidase inhibitor) were used as positive controls. After the 30 min incubation period at 37°C , enzymatic activity was stopped with isopropanol and the samples were refrigerated at 4°C for 15 min. Next, the samples were centrifuged (2,500 \times g/15 min) and 100 μL supernatant was collected and the absorbance was measured as previously described [12]. One unit of gelatinase activity was defined as the amount of enzyme required to produce 1 μg of peptides under the described assay conditions.

2.8. Peritoneal Mouse Macrophages and Cytotoxicity Assay. Nonelicited peritoneal macrophages from female Balb/c mice were collected in cold RPMI 1640 medium and plated in 96-well culture plates at the concentration of 10^5 cells/100 μL . Different concentrations, ranging from 1 to 500 $\mu\text{g/mL}$, of the hexanic extract were added to each well and the cells were incubated at 37°C in 4% CO_2 atmosphere for 48 h. The minimum cytotoxic concentration (MCC) was determined as previously described by Al-Musayeb et al. using resazurin as the cellular viability indicator [13]. The selective index (SI) was calculated using the MIC/MCC ratios. The animals used for macrophage acquisition were killed according to the federal guidelines and institutional policies by cervical dislocation.

2.9. Infection of Macrophages, Anti-Intracellular Amastigote Activity, and Nitric Oxide Production. Peritoneal mouse macrophages were obtained as described above. The infection assays were carried out following the protocol described by Passero et al. with slight modifications [14]. Briefly, peritoneal macrophages (10^5 cells/100 μL) were plated in 96-well culture

plates and a ratio of 5 stationary phase promastigotes (*L. amazonensis* or *L. infantum*) to 1 macrophage was used for the infection procedure. The parasite-macrophage interactions were carried out in RPMI 1640 medium supplemented with 10% of FBS at 35°C for 24 hours in 4% CO_2 atmosphere. After interaction assays were completed free promastigotes and nonadherent macrophages were removed by extensive washing with PBS and the hexanic extract was added to each well at inhibitory and subinhibitory concentrations for *L. amazonensis* and *L. infantum*. After 48 hours of treatment the supernatants from *L. amazonensis*- and *L. infantum*-infected macrophages were analyzed for their nitrite contents by Griess reaction [15]. Then the plates were washed four times with PBS and cultures were incubated in PBHIL medium supplemented with 10% of FBS for 72 hours at 26°C to evaluate the number of promastigote forms differentiated into the medium. The number of viable promastigotes was determined using a hemocytometer chamber.

3. Results and Discussion

In the present study we investigated the antileishmanial effects of the hexanic extract from *A. chica* against two *Leishmania* species, the causative agents of cutaneous and visceral leishmaniasis, *L. amazonensis* and *L. infantum*, respectively. Table 1 summarizes the inhibitory activity of five fractions obtained from the crude hexanic extract on the growth of the parasites tested. B2 (1:1 *n*-hexane/ethyl acetate) was the most active fraction with MIC values of 37.2 and 18.6 $\mu\text{g/mL}$ for *L. amazonensis* and *L. infantum* promastigotes, respectively. Recently, the antimicrobial activity of a hydroethanolic extract from *A. chica* was reported against *Helicobacter pylori* and *Enterococcus faecalis* demonstrating the potential of this plant as a source of biologically active molecules [16]. Only a few species from the *Arrabidaea* genus have been investigated for their antiprotozoal activity. In a study conducted by Barbosa et al. the ethanol extract from *A. chica* and fractions were active against *Trypanosoma cruzi* trypomastigotes, but high concentrations were needed to cause parasite lyses (4.0 and 2.0 mg/mL, resp.) [6]. Triterpenoids isolated from an *A. triplinervia* ethanol extract have been shown to present anti-*T. cruzi* activity [17]. However, the crude ethanol extract as well as the isolated compounds, ursolic acid and oleanolic acid, caused *in vitro* elimination of trypomastigotes at high

TABLE 2: Chemical characterization of the B2 fraction obtained from the *A. chica* hexanic extract.

RT	LRI	Components	%
15.876	1968	<i>n</i> -Hexadecanoic acid	19.61
17.294	2114	Phytol	3.05
17.508	2143	Linoleic acid	6.36
17.575	2150	Linolenic acid, methyl ester	25.38
17.777	2173	Octadecanoic acid	14.10
19.517	2363	Eicosanoic acid	1.31
25.290	3031	Vitamin E	4.94
26.244	3176	Campesterol	1.60
26.491	3206	Stigmasterol	4.02
27.135	3417	Gamma-sitosterol	12.85
% total			93.22

RT: retention time.

LRI: linear retention indices.

concentrations of 5.0, 0.4, and 1.6 mg/mL, respectively. In the present study, the reincubation of parasites treated at MIC values in fresh medium revealed that those cells were no longer able to grow. Thus, the inhibitory activity observed was leishmanicidal for the promastigote forms of *L. amazonensis* and *L. infantum* (MIC values = MLC values).

Leishmania promastigotes were shown to be more sensitive to B2, and therefore the chemical analysis of this fraction was carried out and the main components identified were linolenic acid, methyl ester (25.38%) *n*-hexadecanoic acid (19.61%), octadecanoic acid (14.10%), and gamma-sitosterol (12.85%) as shown in Table 2. Fatty acids have been reported to be active against *Leishmania*; however the activity of such compounds seems to be related mainly to unsaturated fatty acids rather than their saturated analogues [18]. The fatty acid-rich methanol extract from *Ulva lactuca* displayed antitrypanosomal and antileishmanial activities through parasite motility inhibition at low concentrations (<100 µg/mL). In that work, *n*-decanoic acid, *n*-dodecanoic acid, and *n*-hexadecanoic acid were described as the main active compounds [19]. More recently, the action mechanism of some fatty acids has been related to topoisomerase IB inhibition as demonstrated by Carballeira et al., during the evaluation of the antileishmanial activity of α -methoxylated fatty acids [20]. Here, the B2 fraction demonstrated significant peptidase inhibition when tested on cellular lysates of *Leishmania* (Figure 1). After incubation of the cellular lysates treated at MIC (37.2 and 18.6 µg/mL) and twice MIC (74.4 and 37.2 µg/mL) of B2 with phosphate buffer 5.5 pH at 37°C, peptidase activity was completely inhibited for *L. amazonensis* and *L. infantum*, respectively (Figure 1(a)). E64 (cysteine peptidase inhibitor) was used as the positive control completely inhibiting peptidase activity when incubated with *Leishmania* lysates under the same conditions. In order to evaluate the effect of the B2 fraction on metallopeptidases, cellular lysates from *L. amazonensis* and *L. infantum* were also incubated with phosphate buffer 10.0 pH (Figure 1(b)). Despite the decrease in peptidase activity the results show that B2 was less effective against those peptidases.

Naturally occurring sterols also present antileishmanial activity. In a study conducted by Pan et al. sterols obtained from the roots of *Pentalimon andrieuxii* displayed the best inhibitory activities (IC₅₀) at concentrations ranging from 9.2 to 30.0 µM and 0.03 to 3.5 µM against promastigote and amastigote forms of *L. mexicana*, respectively [21]. The authors attributed the antileishmanial activity of the sterols tested to membrane alterations caused by cholesterol replacement during its biosynthesis. In the present study, important alterations on the ultrastructure of *L. infantum* promastigotes were also observed on B2-treated parasites (Figure 2). Parasites presented abnormal cell body shapes after 24 h exposure to the B2 fraction at 18.6 µg/mL (MIC), when compared to untreated parasites (Figure 2(b)). Mitochondrial dilatation with loss of matrix contents and Golgi complex alterations followed by a cytoplasm vacuolization process were also observed (Figure 2(c)). In addition, an intense exocytic process of cytoplasmic content into the flagellar pocket was noted. Mitochondrion seems to be a common target for several natural products, crude extracts, or isolated compounds, as has been reported by several researchers [10, 22–24]. The mode of action of most natural products that cause mitochondrial damage and parasite death has been attributed mainly to sterol biosynthesis inhibition and mitochondrial membrane potential dysfunction [25–27]. Here, the *L. infantum* mitochondrion was drastically damaged by the B2 fraction obtained from *A. chica* hexanic extract as shown in Figure 2. An intense swelling of the mitochondrion with the presence of vesicles was observed in the parasites. In some cases, the mitochondrion membrane appears to be disrupted.

The B2 fraction from the *A. chica* hexanic extract demonstrated antileishmanial activity during the infection of peritoneal mice macrophages. After a 48-hour treatment with B2 at MIC and subMIC values, the number of promastigotes recovered in the supernatants of *L. amazonensis*- and *L. infantum*-infected macrophage cultures was drastically reduced when compared to controls (Figure 3). According to Passero et al. only viable amastigotes are able to differentiate to promastigotes under established conditions [14]. Besides, after treatment with 37.2 and 18.6 µg/mL of the B2 fraction, the nitrite contents detected in the supernatant of *L. amazonensis*-infected macrophages was higher than those found on untreated cells cultures, about 7.6 and 1.16 µM, respectively. With the *L. infantum* model of infection, the nitrite content detected on MIC and subMIC-treated cultures was about 12.5 and 2.0 µM, respectively (Figure 4). These results give additional evidence of the enhancement of macrophage killing mechanism elicited by *A. chica* against the intracellular form of *Leishmania*. Moreover, *A. chica* has been described as a potent wound healing agent able to stimulate fibroblast growth and collagen synthesis at 30 µg/mL (EC₅₀) and 250 µg/mL, respectively. *In vivo* assays demonstrated an impressive reduction of lesion size of about 96% [28]. In addition, Lima de Medeiros et al. reported the hepatoprotective activity of the hydroethanolic extract of *A. chica* based on the suppression of hepatic markers such as serum glutamic oxaloacetate transaminase (GOT) and glutamic pyruvate transaminase (GPT) and decreasing levels of plasma

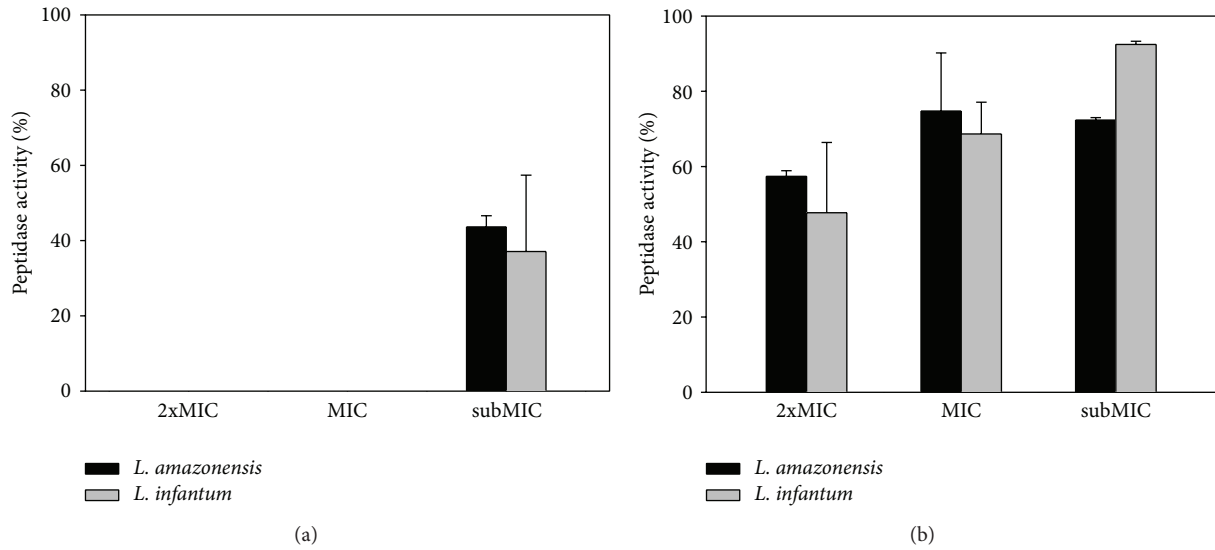


FIGURE 1: Inhibitory activity of the B2 fraction obtained from the *A. chica* hexanic extract on *Leishmania* peptidases. (a) Peptidase inhibitory activity at pH 5.5; (b) peptidase inhibitory activity at pH 10. 2xMIC, MIC, and subMIC values for *L. amazonensis* and *L. infantum* were 74.4, 37.2, and 18.6 $\mu\text{g}/\text{mL}$ and 37.2, 18.6, and 9.3 $\mu\text{g}/\text{mL}$, respectively.

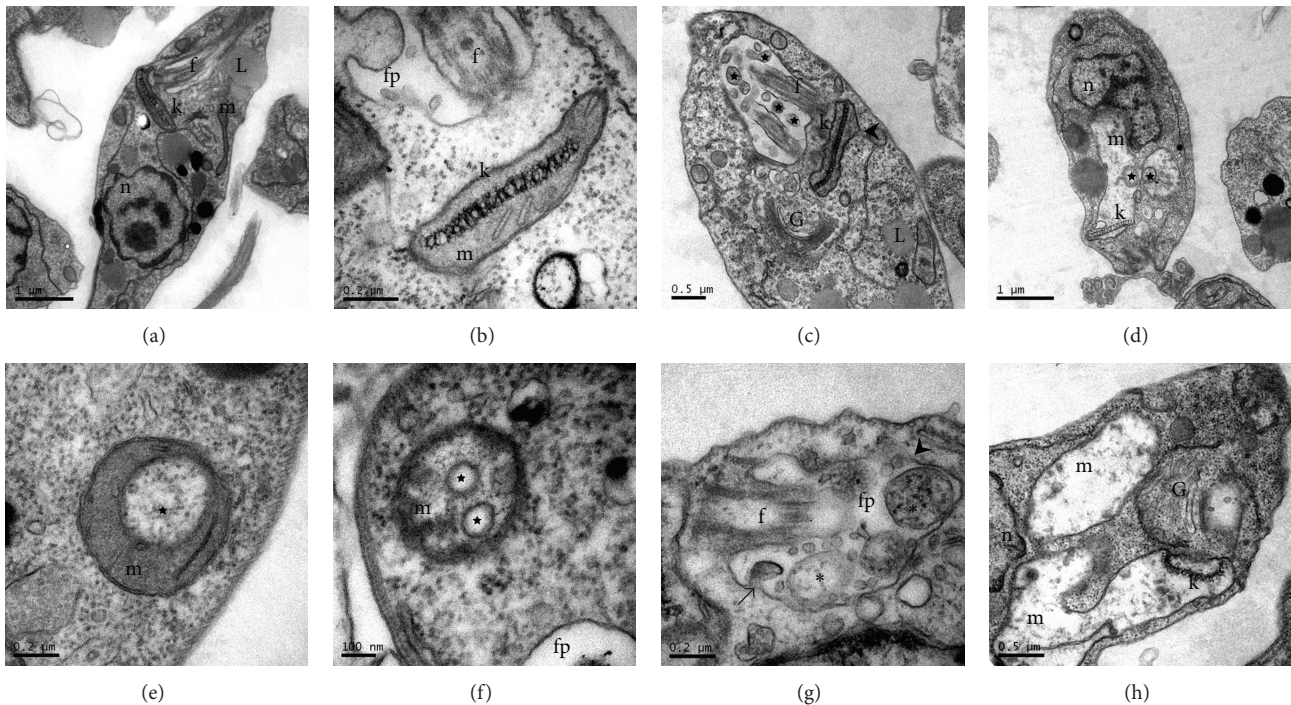


FIGURE 2: Transmission electron microscopy of *L. infantum* promastigotes treated with the B2 fraction from the *A. chica* hexanic extract. ((a)-(b)) Thin sections of untreated promastigote forms displaying normal morphology and intracellular structures. (b) Detail of the mitochondrion containing the kinetoplast (k). ((c)-(h)) Parasites treated for 24 hours with subMIC (9.3 $\mu\text{g}/\text{mL}$) or MIC (18.6 $\mu\text{g}/\text{mL}$) of the B2 fraction, showing serious cellular damage. (c) Parasite treated with subMIC value of the B2 fraction presenting a dilated flagellar pocket with the presence of several vacuoles (*). Note the rupture of the mitochondrion membrane (arrowhead in (c)). (d) Parasite treated with the B2 fraction at MIC value (18.6 $\mu\text{g}/\text{mL}$) presenting mitochondrial swelling and some vesicles (\star) inside this organelle; (details of intramitochondrial vesicles in (e) and (f)); (g) in detail, parasite flagellar pocket showing intense release of vesicles with cytoplasmic content (*); (h) in detail, increased mitochondrial volume and Golgi complex alterations. n, nucleus; m, mitochondrion; k, kinetoplast; f, flagellum; fp, flagellar pocket; G, Golgi complex; L, lipid.

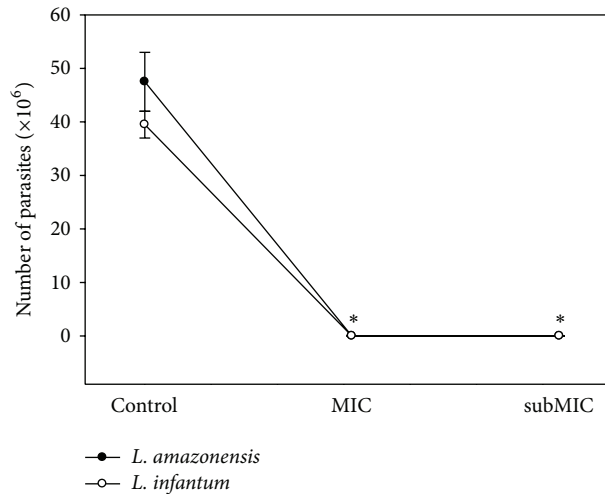


FIGURE 3: Anti-intracellular amastigote activity of the B2 fraction from the *A. chica* hexanic extract. B2-treated macrophages previously infected with *Leishmania* were incubated in fresh medium at 28°C for 72 hours. The number of promastigote forms obtained from macrophages cultures was counted using a hemocytometer chamber. Each point represents the mean ± S.E. of 2 independent experiments performed in triplicate. MIC and subMIC values for *L. amazonensis* and *L. infantum* were 37.2 and 18.6 µg/mL and 18.6 and 9.3 µg/mL, respectively. Asterisks indicate that treated parasites were statistically different ($P < 0.05$) from control parasites.

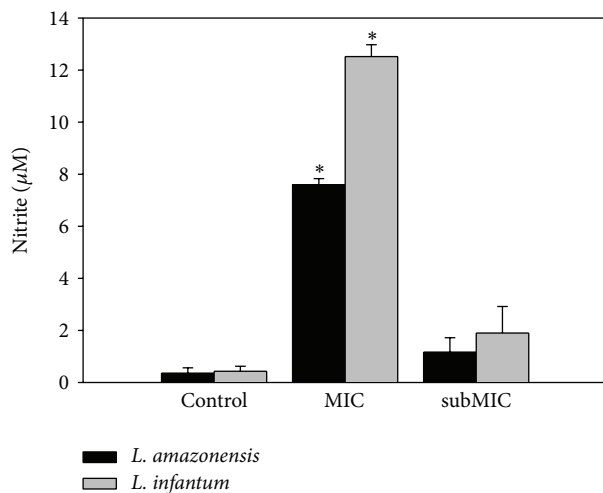


FIGURE 4: Nitric oxide synthesis by *Leishmania*-infected macrophages treated with the B2 fraction. After 48 hours treatment with the B2 fraction the supernatant from *L. amazonensis*- and *L. infantum*-infected macrophages was collected and the nitrite content determined through Griess reaction. Each point represents the mean ± S.E. of 2 independent experiments performed in triplicate. MIC and subMIC values for *L. amazonensis* and *L. infantum* were 37.2 and 18.6 µg/mL and 18.6 and 9.3 µg/mL, respectively. Asterisks indicate that treated parasites were statistically different ($P < 0.05$) from control parasites.

bilirubin [29]. Considering the clinical manifestations related to cutaneous and visceral leishmaniasis, such as skin lesions and hepatic damage, respectively, *A. chica* could represent a promising phytotherapeutic agent.

In conclusion, the hexanic extract from *A. chica*, especially the B2 fraction, possesses activity against *L. amazonensis* and *L. infantum*. Fatty acids and sterols probably are the main components involved in the antileishmanial activity, but further investigation will be necessary in order to evaluate the isolated compounds. Taken together, the results presented herein in addition to those reported in literature concerning tissue healing effects and liver protection of *A. chica* are motivation for further investigation of this plant using *in vivo* models of *Leishmania* spp. infection.

Conflict of Interests

The authors declare that there is no conflict of interests regarding the publication of this paper.

Acknowledgments

The authors thank Luciana T. Zimmermann for her technical assistance. They also thank the *Plataforma Rudolf Barth do Instituto Oswaldo Cruz* (Fiocruz/RJ) for the acquisition of the transmission electron microscopy images. This work was financially supported by the Brazilian agencies MCT/CNPq, CAPES, and FAPERJ.

References

- [1] M. P. Barrett and S. L. Croft, "Management of trypanosomiasis and leishmaniasis," *British Medical Bulletin*, vol. 104, pp. 175–196, 2012.
- [2] WHO, "Leishmaniasis: epidemiology and access to medicines—an update based on the outcomes of WHO regional meetings, literature review and experts' opinion," World Health Organization, Geneva, Switzerland, 2012.
- [3] J. Alvar, I. D. Vélez, C. Bern et al., "Leishmaniasis worldwide and global estimates of its incidence," *PLoS ONE*, vol. 7, no. 5, Article ID e35671, 2012.
- [4] J. P. Ehrenberg and S. K. Ault, "Neglected diseases of neglected populations: thinking to reshape the determinants of health in Latin America and the Caribbean," *BMC Public Health*, vol. 5, article 119, 2005.
- [5] M. den Boer, D. Argaw, J. Jannin, and J. Alvar, "Leishmaniasis impact and treatment access," *Clinical Microbiology and Infection*, vol. 17, no. 10, pp. 1471–1477, 2011.
- [6] W. L. R. Barbosa, L. D. N. Pinto, E. Quignard, J. M. D. S. Vieira, J. O. C. Silva Jr., and S. Albuquerque, "Arrabidaea chica (HBK) Verlot: phytochemical approach, antifungal and trypanocidal activities," *Revista Brasileira de Farmacognosia*, vol. 18, no. 4, pp. 544–548, 2008.
- [7] J. T. G. Siraichi, D. F. Felipe, L. Z. S. Brambilla et al., "Antioxidant capacity of the leaf extract obtained from *Arrabidaea chica* cultivated in Southern Brazil," *PLoS ONE*, vol. 8, no. 8, Article ID e72733, 2013.
- [8] I. A. Rodrigues, B. A. da Silva, A. L. S. dos Santos, A. B. Vermelho, C. S. Alviano, and M. do Socorro Santos Rosa, "A new experimental culture medium for cultivation of *Leishmania*

- amazonensis*: its efficacy for the continuous in vitro growth and differentiation of infective promastigote forms," *Parasitology Research*, vol. 106, no. 5, pp. 1249–1252, 2010.
- [9] M. Rolón, C. Vega, J. A. Escario, and A. Gómez-Barrio, "Development of resazurin microtiter assay for drug sensibility testing of *Trypanosoma cruzi* epimastigotes," *Parasitology Research*, vol. 99, no. 2, pp. 103–107, 2006.
- [10] I. A. Rodrigues, M. M. Azevedo, F. C. Chaves et al., "In vitro cytotoxic effects of the essential oil from *Croton cajucara* (red sacaca) and its major constituent 7-hydroxycalamenene against *Leishmania chagasi*," *BMC Complementary and Alternative Medicine*, vol. 13, article 249, 2013.
- [11] S. M. L. Cedrola, A. C. N. de Melo, A. M. Mazotto et al., "Keratinases and sulfide from *Bacillus subtilis* SLC to recycle feather waste," *World Journal of Microbiology and Biotechnology*, vol. 28, no. 3, pp. 1259–1269, 2012.
- [12] O. H. Lowry, N. J. Rosebrough, A. L. Farr, and R. J. Randall, "Protein measurement with the Folin phenol reagent," *The Journal of Biological Chemistry*, vol. 193, no. 1, pp. 265–275, 1951.
- [13] N. M. Al-Musayeb, R. A. Mothana, A. Matheussen, P. Cos, and L. Maes, "In vitro antiplasmodial, antileishmanial and antitrypanosomal activities of selected medicinal plants used in the traditional Arabian Peninsular region," *BMC Complementary and Alternative Medicine*, vol. 12, article 49, 2012.
- [14] L. F. D. Passero, A. Bonfim-Melo, C. E. P. Corbett et al., "Antileishmanial effects of purified compounds from aerial parts of *Baccharis uncinella* C. DC. (Asteraceae)," *Parasitology Research*, vol. 108, no. 3, pp. 529–536, 2011.
- [15] S. J. Green, M. S. Meltzer, J. B. Hibbs Jr., and C. A. Nacy, "Activated macrophages destroy intracellular *Leishmania major* amastigotes by an L-arginine-dependent killing mechanism," *Journal of Immunology*, vol. 144, no. 1, pp. 278–283, 1990.
- [16] L. Mafioleti, I. F. da Silva Junior, E. M. Colodel, A. Flach, and D. T. Martins, "Evaluation of the toxicity and antimicrobial activity of hydroethanolic extract of *Arrabidaea chica* (Humb. & Bonpl.) B. Verl," *Journal of Ethnopharmacology*, vol. 150, no. 2, pp. 576–582, 2013.
- [17] J. P. V. Leite, A. B. Oliveira, J. A. Lombardi, J. D. S. Filho, and E. Chiari, "Trypanocidal activity of triterpenes from *Arrabidaea triplinervia* and derivatives," *Biological and Pharmaceutical Bulletin*, vol. 29, no. 11, pp. 2307–2309, 2006.
- [18] N. M. Carballeira, M. M. Cartagena, C. F. Prada, C. F. Rubio, and R. Balaña-Fouce, "Total synthesis and antileishmanial activity of the natural occurring acetylenic fatty acids 6-heptadecynoic acid and 6-icosynoic acid," *Lipids*, vol. 44, no. 10, pp. 953–961, 2009.
- [19] L. V. Cunningham, B. H. Kazan, and S. S. Kuwahara, "Effect of long-chain fatty acids on some trypanosomatid flagellates," *Journal of General Microbiology*, vol. 70, no. 3, pp. 491–496, 1972.
- [20] N. M. Carballeira, M. Cartagena, F. Li et al., "First total synthesis of the (±)-2-methoxy-6-heptadecynoic acid and related 2-methoxylated analogs as effective inhibitors of the leishmania topoisomerase IB enzyme," *Pure and Applied Chemistry*, vol. 84, no. 9, pp. 1867–1875, 2012.
- [21] L. Pan, C. M. Lezama-Davila, A. P. Isaac-Marquez et al., "Sterols with antileishmanial activity isolated from the roots of *Pentalinon andrieuxii*," *Phytochemistry*, vol. 82, pp. 128–135, 2012.
- [22] M. D. S. S. Rosa, R. R. Mendonça-Filho, H. R. Bizzo et al., "Antileishmanial activity of a linalool-rich essential oil from *Croton cajucara*," *Antimicrobial Agents and Chemotherapy*, vol. 47, no. 6, pp. 1895–1901, 2003.
- [23] N. Sen, B. B. Das, A. Ganguly et al., "Camptothecin induced mitochondrial dysfunction leading to programmed cell death in unicellular hemoflagellate *Leishmania donovani*," *Cell Death and Differentiation*, vol. 11, no. 8, pp. 924–936, 2004.
- [24] M. A. Brenzan, A. O. Santos, C. V. Nakamura et al., "Effects of (-) mammea A/BB isolated from *Calophyllum brasiliense* leaves and derivatives on mitochondrial membrane of *Leishmania amazonensis*," *Phytomedicine*, vol. 19, no. 3-4, pp. 223–230, 2012.
- [25] F. Fonseca-Silva, J. D. F. Inacio, M. M. Canto-Cavaleiro, and E. E. Almeida-Amaral, "Reactive oxygen species production and mitochondrial dysfunction contribute to quercetin induced death in *Leishmania amazonensis*," *PLoS ONE*, vol. 6, no. 2, Article ID e14666, 2011.
- [26] J. M. Medina, J. C. Rodrigues, W. de Souza, G. C. Atella, and H. Barrabin, "Tomatidine promotes the inhibition of 24-alkylated sterol biosynthesis and mitochondrial dysfunction in *Leishmania amazonensis* promastigotes," *Parasitology*, vol. 139, no. 10, pp. 1253–1265, 2012.
- [27] L. Monzote, M. García, J. Pastor et al., "Essential oil from *Chenopodium ambrosioides* and main components: activity against *Leishmania*, their mitochondria and other microorganisms," *Experimental Parasitology*, vol. 136, pp. 20–26, 2014.
- [28] M. P. Jorge, C. Madjarof, A. L. Gois Ruiz et al., "Evaluation of wound healing properties of *Arrabidaea chica* Verlot extract," *Journal of Ethnopharmacology*, vol. 118, no. 3, pp. 361–366, 2008.
- [29] B. Lima de Medeiros, K. dos Santos Costa, J. F. Alves Ribeiro, J. O. Carrera Silva Jr., W. L. Ramos Barbosa, and J. C. Tavares Carvalho, "Liver protective activity of a hydroethanolic extract of *Arrabidaea chica* (Humb. and Bonpl.) B. Verl. (pariri)," *Pharmacognosy Research*, vol. 3, no. 2, pp. 79–84, 2011.

Research Article

Antioxidant Activity of Essential Oil and Extracts of *Valeriana jatamansi* Roots

Sakshima Thusoo, Sahil Gupta, Rasleen Sudan, Jaspreet Kour, Sahil Bhagat, Rashid Hussain, and Madhulika Bhagat

School of Biotechnology, University of Jammu, Jammu 180006, India

Correspondence should be addressed to Madhulika Bhagat; madhulikasbt@gmail.com

Received 21 February 2014; Accepted 8 March 2014; Published 6 April 2014

Academic Editor: José Carlos Tavares Carvalho

Copyright © 2014 Sakshima Thusoo et al. This is an open access article distributed under the Creative Commons Attribution License, which permits unrestricted use, distribution, and reproduction in any medium, provided the original work is properly cited.

Valeriana jatamansi is an indigenous medicinal plant used in the treatment of a number of diseases. In the present study, chemical composition of the essential oil was determined by GC-MS. Seven major components were identified in *Valeriana jatamansi* essential oil, namely, β -vatiene, β -patchoulene, dehydroaromadendrene, β -gurjunene, patchoulic alcohol, β -guaiene, and α -muurolene. Methanolic, aqueous, and chloroform extracts of *Valeriana jatamansi* roots were also prepared and analyzed for their polyphenols and flavonoid content. Antioxidant activity of essential oil and different extracts of *Valeriana jatamansi* roots was determined by DPPH radical scavenging and chelation power assay. A linear correlation has been obtained by comparing the antioxidant activity and polyphenols and flavonoid content of the extracts. Results indicated that antioxidant activity of methanolic extract could be attributed to the presence of rich amount of polyphenols and flavonoid. Essential oil of *Valeriana jatamansi* roots showed moderate antioxidant activity.

1. Introduction

Valeriana jatamansi Jones syn. *V. wallichii* popularly known as Indian Valerian (Mushkibala in Hindi/Kashmiri, Suganthdhawal or Tagara in Sanskrit) belongs to family Valerianaceae [1]. *Valeriana* is a major genus of the family Valerianaceae and is represented in all the temperate and subtropical areas of the world. In India, about 16 species and two subspecies have been reported [2].

Valeriana jatamansi is a small, perennial dwarf, hairy, rhizomatous herb having thick roots covered with fibers. The plant grows at an altitude of 1220–3000 m [1]. *Valeriana jatamansi* is regarded as an aphrodisiac, antispasmodic, tranquilizer, antiseptic, expectorant, febrifuge, nerve tonic, ophthalmic, sedative, and tonic useful in hysteria, cholera, snakebite, scorpion sting, asthma, and eurosia [3]. Roots are acrid and bitter which are used as carminative, laxative and are also used for curing blood diseases, burning sensation, cholera, skin disease, throat troubles, and ulcers [3]. The therapeutic properties of the plant are attributed to a class of compounds called valepotriates. The valepotriates are

a group of monoterpenoids of iridoid type having epoxy group and β -acetoxy isovaleric acids [4]. The root of *V. jatamansi* is a source of effective antileishmanial agent [5]. Root extract of *V. jatamansi* also exhibits larvicidal and adulticidal activity against different mosquito species [6]. The aqueous and methanolic extracts of rhizomes possess anti-inflammatory activity. This could be attributed to the high amount of flavonoids and tannins in the plant [7]. The objective of this study was to verify the phytochemicals and antioxidant potential of both essential oil and extracts of *Valeriana jatamansi* roots.

2. Materials and Methods

2.1. Collection of Plant Material. Fresh plant material (roots) was collected from the high altitude of Patnitop in Jammu and Kashmir, India, and identified at the herbarium of the department of Botany, Jammu University. The material was shade dried and ground to a fine texture in a grinding machine.

2.2. Isolation of Essential Oil. Essential oil was extracted by hydrodistillation for 4 h using a Clevenger-type apparatus. The oil was stored at 4°C in the dark until analyzed.

2.3. Preparation of Extracts. The finely powdered roots were extracted with three different solvents on the basis of their polarity, that is, from nonpolar to polar. Chloroform, methanol, and water were used as solvents. 15 g of the given powdered plant material was mixed in 75 mL of each solvent and the mixture was stirred for 24 hours. The suspended mixture was filtered through whatman's filter paper and filtrate was collected. This procedure was performed thrice to get three filtrates and residue. The filtrates were then dried at room temperature. Gummy solid thus obtained after evaporation of each of the solvents was labelled and stored for further use.

2.4. GC-MS Analysis of Essential Oil. Analysis of the oil using gas chromatography and mass spectrometry was carried out at Indian Institute of Integrative Medicine (CSIR, India), Canal Road, Jammu, India. GC-MS 4000 (Varian, USA) system with a HP-5MS agilent column (30 m × 0.25 mm i.d., 0.25 μ film thickness) was used for analysis. Injector temperature was 280°C. Oven temperature programme used was holding at 50°C for 5 min, heating to 280°C at 3°C/min, and keeping the temperature constant at 280°C for 7 min. Helium was used as a carrier gas at a constant flow of 1.0 mL/min and an injection volume of 0.20 μL was employed.

The MS scan parameters included electron impact ionization voltage of 70 eV, a mass range of 40–500 m/z. The identification of components of the essential oil was based on comparison of their mass spectra with those stored in NIST05 library or with mass spectra from literature [8].

2.5. Determination of Total Phenols and Flavonoids in Extracts. Total phenolic content was determined according to Folin-Ciocalteu method [9]. 0.5 mL of extract solution was mixed with 0.5 mL of 1N Folin-Ciocalteu reagent. The mixture was kept for 5 min, followed by the addition of 1 mL of 20% Na₂CO₃. After 10 min of incubation at room temperature, the absorbance was measured at 750 nm using a spectrophotometer. The concentration of phenolic compounds was calculated according to the following equation obtained from the standard gallic acid:

$$\text{Absorbance} = 0.0364 \text{ gallic acid } (\mu\text{g}) + 0.009. \quad (1)$$

Flavonoid content in the extract/fractions was determined by a colorimetric method [10]. Plant extracts were diluted with distilled water to a volume of 3.5 mL and 150 μL of a 5% NaNO₂ solution. After 5 min, 300 μL of 10% AlCl₃·H₂O solution was added. After 6 min, 300 μL of 1M NaOH and 550 μL of distilled water were added to prepare the mixture. The solution was mixed well and the absorbance was observed at 510 nm using UV-VIS spectrophotometer. The concentration of flavonoid compounds was calculated

TABLE 1: Chemical composition of essential oil of *Valeriana jatamansi* roots analysed by GC-MS.

Compounds	Nature of compound	Amount in % age
β-patchoulene	Sesquiterpene	20.18
β-gurjunene	Sesquiterpene	13.0
β-vatirenene	Sesquiterpene	28.07
α-murolene	Sesquiterpene	5.20
β-guaiene	Sesquiterpene	5.88
Dehydroaromadendrene	Sesquiterpene	15.92
Patchoulic alcohol	Sesquiterpene	11.72

according to the following equation obtained from the standard quercetin graph:

$$\text{Absorbance} = 0.001 \text{ quercetin } (\mu\text{g}) + 0.032. \quad (2)$$

2.6. DPPH Radical Scavenging Assay. The radical scavenging activity of extracts was determined with slight modifications in the method [11]. 1 mL from a 0.5 mM methanol solution of the DPPH radical was mixed to 2.0 mL sample and to this 2.0 mL of 0.1 M sodium acetate buffer (pH 5.5) was added. The mixtures were well shaken and kept at room temperature in the dark for 30 min. The absorbance was measured at 517 nm using a double beam UV-VIS spectrophotometer. Methanol was used as a negative control.

The radical scavenging activity of essential oil was determined [12]. 1 mL of different concentrations of the essential oil or bioactive fraction was mixed with 1 mL of a 90 μM DPPH solution in methanol, and final volume was made to 4 mL with methanol. The mixtures were well shaken and kept at 25°C in the dark for 1 h. The absorbance was measured at 517 nm. Oil concentration providing 50% inhibition (IC₅₀) was calculated from the graph by plotting inhibition% against oil concentration. BHT was used as reference.

2.7. Chelating Power on Ferrous (Fe²⁺) Ions. The chelating effect on ferrous ions of *Valeriana jatamansi* extracts was estimated by slight modifications in the method [13]. Different dilutions of extract/fractions were made to a volume of 3 mL with methanol. 60 μL of 2 mM FeCl₂ was added. The reaction was initiated by the addition of 120 μL of 5 mM ferrozine into the mixture, which was then left at room temperature for 10 min before determining the absorbance of the mixture at 562 nm. The ratio of inhibition of ferrozine-Fe²⁺ complex formation was calculated using the following equation:

$$\begin{aligned} & \% \text{ inhibition} \\ & = \left(\frac{[\text{absorbance of control} - \text{absorbance of test sample}]}{\text{absorbance of control}} \right) \\ & \times 100. \end{aligned} \quad (3)$$

2.8. Statistical Analysis. For all the experiments, three samples were analysed and all the assays were carried out in triplicates. The results were expressed as mean values with standard deviation.

TABLE 2: Showing total phenol and flavonoid content of different extracts of *Valeriana jatamansi* roots.

S. no.	Test sample	Total phenols (mg GAEs/g dry wt.)	Total flavonoids (mg QEs/g dry wt.)
1	Methanolic extract	187.13 ± 6.8	257.69 ± 9.8
2	Aqueous extract	77.66 ± 2.1	452.30 ± 12.4
3	Chloroform extract	9.89 ± 0.3	25.38 ± 2.0

Data is represented as mean ± SD of three triplicate experiments.

TABLE 3: Showing the antioxidant activity of the essential oil and different extracts of *Valeriana jatamansi* roots.

S. no.	Test sample	DPPH activity (IC ₅₀ in µg/mL)	Chelation power on ferrous ions (% age at 100 µg)
1	Essential oil	876 ± 12.8 µg/mL	31%
2	Methanolic extract	78 ± 2.9 µg/mL	76%
3	Aqueous extract	154 ± 4.6 µg/mL	43%
4	Chloroform extract	—	12%
5	BHT	28 ± 0.8 µg/mL	—

Data is represented as mean ± SD of three triplicate experiments.

3. Results and Discussions

3.1. GC-MS Analysis of Essential Oil. Hydrodistillation of roots of *Valeriana jatamansi* produced greenish yellow essential oil with the yield of 0.8%. Chemical composition of the essential oil was determined by gas chromatography and mass spectrometry (Table 1). Seven major components were identified in essential oil viz., β-vatirenene, β-patchoulene, Dehydroaromadendrene, β-gurjunene, patchoulic alcohol, β-guaiene and α-muurolene. The chemical analysis of essential oil shows that *V. jatamansi* roots contain only sesquiterpenes in its essential oil.

3.2. Total Phenols and Flavonoids. Phenolic compounds have been reported to exhibit various biological activities like, antioxidant, antimicrobial etc. Total phenolic compounds in extracts were determined by Folin-Ciocalteu method and expressed as Gallic acid equivalents (GAEs). As shown in Table 2, highest amount of phenolic compound was observed in methanolic extract (187.13 ± 6.8 mg GAEs/g), followed by aqueous extract (77.66 ± 2.1 mg GAEs/g). Least amount of phenolic compounds was observed in chloroform extract (9.89 ± 0.3 mg GAEs/g). Many studies have revealed that the phenolic contents in the plants are associated with their antioxidant activities probably due to their redox properties, which allow them to act as reducing agents, hydrogen donors, and singlet oxygen quenchers [9, 14].

Total amount of flavonoids was expressed in quercetin equivalent (QE). Aqueous extract of *Valeriana jatamansi* had relatively high amount of flavonoids (452.30 ± 12.4 mg QEs/g) followed by methanolic extract (257.69 ± 9.8 mg QEs/g) and very less amount was observed in chloroform extract (5.38 ± 0.3 mg QEs/g).

3.3. DPPH Radical Scavenging Activity. DPPH assay has been extensively used for screening plant extracts because many samples can be accommodated in short period and are sensitive enough to detect active ingredients at low concentrations [15]. The antioxidant activity of *Valeriana jatamansi*

roots essential oil and extracts is summarized in Table 3. Among all the test samples, methanolic extract of *Valeriana jatamansi* was found to be the most potent antioxidant (IC₅₀ 78 ± 2.9 µg/mL), followed by aqueous extract (IC₅₀ values 154 ± 4.6 µg/mL). Essential oil of *Valeriana jatamansi* roots showed poor radical scavenging activity (IC₅₀ values 876 ± 12.8 µg/mL), whereas chloroform extract showed negligible activity. BHT was taken as reference antioxidant (IC₅₀ 28 ± 0.8 µg/mL). A linear correlation has been obtained by comparing the antioxidant activity and polyphenols and flavonoid content of the extracts. The extracts containing good amount of phenols and flavonoids possess potential antioxidant activity. Previous studies have also reported positive correlation between phenolic and flavonoid content and DPPH radical scavenging activity of plant extracts [16]. The moderate antioxidant activity of essential oil could be attributed to the presence of sesquiterpenes.

3.4. Chelation Power. Chelation activity is also one of the important mechanisms of antioxidant activity. Result of chelation activity of the essential oil and different root extracts is shown in Table 3. It is evident by the data that the methanolic extract of *Valeriana jatamansi* possesses good chelation activity (76%) followed by aqueous extracts (43%) and essential oil (31%) at 100 µg/mL concentration. Chloroform extract showed poor chelation activity (12%).

4. Conclusions

Methanol extract of roots of *Valeriana jatamansi* possesses remarkable antioxidant activity as compared to its essential oil. Thus root extract of *V. jatamansi* can prove beneficial in food and pharmaceutical industry.

Conflict of Interests

The authors declare that there is no conflict of interests regarding the publication of this paper.

References

- [1] A. M. Rather, I. A. Nawchoo, A. H. Ganie, H. Singh, B. Dutt, and A. A. Wani, "Bioactive compounds & medicinal properties of *Valeriana jatamansi* Jones-a review," *Life Science Journal*, vol. 9, pp. 2–10, 2012.
- [2] S. Sati and C. S. Mathela, "Essential oil composition of *Valeriana hardwickii* var. *arnottiana* from the Himalayas," *Flavour and Fragrance Journal*, vol. 20, no. 3, pp. 299–301, 2005.
- [3] R. N. Chopra, S. O. Nayyar, and I. C. Chopra, *Glossary of Indian Medicinal Plants*, CSIR Publication, New Delhi, India, 1956.
- [4] R. Kaur, M. Sood, S. Chander, R. Mahajan, V. Kumar, and D. R. Sharma, "In Vitro propagation of *Valeriana jatamansi*," *Plant Cell, Tissue and Organ Culture*, vol. 59, no. 3, pp. 227–229, 1999.
- [5] S. Ghosh, S. Debnath, S. Hazra et al., "Valeriana wallichii root extracts and fractions with activity against *Leishmania* spp.," *Parasitology Research*, vol. 108, no. 4, pp. 861–871, 2011.
- [6] V. K. Dua, M. F. Alam, A. C. Pandey et al., "Insecticidal activity of *Valeriana jatamansi* (valerianaceae) against mosquitoes," *Journal of the American Mosquito Control Association*, vol. 24, no. 2, pp. 315–318, 2008.
- [7] F. Subhan, N. Karim, and M. Ibrar, "Anti-inflammatory activity of methanolic and aqueous extracts of *Valeriana wallichii* DC rhizome," *Pakistan Journal of Plant Sciences*, vol. 13, pp. 103–108, 2007.
- [8] R. P. Adams, *Identification of Essential Oil Components by Gas Chromatography/Mass Spectrometry*, Allured Publishing Corporation, Carol Stream, Ill, USA, 4th edition, 2007.
- [9] S. T. Chang, J. H. Wu, S. Y. Wang, P. L. Kang, N. S. Yang, and L. F. Shyur, "Antioxidant activity of extracts from *Acacia confusa* Bark and Heartwood," *Journal of Agricultural and Food Chemistry*, vol. 49, no. 7, pp. 3420–3424, 2001.
- [10] J. Zhishen, T. Mengcheng, and W. Jianming, "The determination of flavonoid contents in mulberry and their scavenging effects on superoxide radicals," *Food Chemistry*, vol. 64, no. 4, pp. 555–559, 1999.
- [11] N. Abe, T. Murata, and A. Hirota, "Novel DPPH Radical Scavengers, Bisorbicillinol and Demethyltrichodimerol, from a Fungus," *Bioscience, Biotechnology and Biochemistry*, vol. 62, no. 4, pp. 661–666, 1998.
- [12] B. Bozin, N. Mimica-Dukic, N. Simin, and G. Anackov, "Characterization of the volatile composition of essential oils of some lamiaceae spices and the antimicrobial and antioxidant activities of the entire oils," *Journal of Agricultural and Food Chemistry*, vol. 54, no. 5, pp. 1822–1828, 2006.
- [13] T. C. P. Dinis, V. M. C. Madeira, and L. M. Almeida, "Action of phenolic derivatives (acetaminophen, salicylate, and 5-aminosalicylate) as inhibitors of membrane lipid peroxidation and as peroxy radical scavengers," *Archives of Biochemistry and Biophysics*, vol. 315, no. 1, pp. 161–169, 1994.
- [14] S. Guleria, A. K. Tikku, and S. Rana, "Antioxidant activity of acetone extract/fractions of *Terminalia bellerica* Roxb.fruit," *Indian Journal of Biochemistry and Biophysics*, vol. 47, no. 2, pp. 110–116, 2010.
- [15] C. Sánchez-Moreno, "Review: methods used to evaluate the free radical scavenging activity in foods and biological systems," *Food Science and Technology International*, vol. 8, no. 3, pp. 121–137, 2002.
- [16] F. Shahidi and P. K. Wanasundara, "Phenolic antioxidants," *Critical Reviews in Food Science and Nutrition*, vol. 32, no. 1, pp. 67–103, 1992.

Research Article

Antioxidants, Phytochemicals, and Cytotoxicity Studies on *Phaleria macrocarpa* (Scheff.) Boerl Seeds

Ma Ma Lay,¹ Saiful Anuar Karsani,^{1,2} Behrooz Banisalam,¹
Sadegh Mohajer,¹ and Sri Nurestri Abd Malek¹

¹ Institute of Biological Sciences, Faculty of Science, University of Malaya, 50603 Kuala Lumpur, Malaysia

² University of Malaya Centre for Proteomics Research (UMCPR), University of Malaya, 50603 Kuala Lumpur, Malaysia

Correspondence should be addressed to Ma Ma Lay; mamalayster@gmail.com

Received 30 November 2013; Revised 6 February 2014; Accepted 18 February 2014; Published 27 March 2014

Academic Editor: Fabio Ferreira Perazzo

Copyright © 2014 Ma Ma Lay et al. This is an open access article distributed under the Creative Commons Attribution License, which permits unrestricted use, distribution, and reproduction in any medium, provided the original work is properly cited.

In recent years, the utilization of certain medicinal plants as therapeutic agents has drastically increased. *Phaleria macrocarpa* (Scheff.) Boerl is frequently used in traditional medicine. The present investigation was undertaken with the purpose of developing pharmacopoeial standards for this species. Nutritional values such as ash, fiber, protein, fat, and carbohydrate contents were investigated, and phytochemical screenings with different reagents showed the presence of flavonoids, glycosides, saponin glycosides, phenolic compounds, steroids, tannins, and terpenoids. Our results also revealed that the water fraction had the highest antioxidant activity compared to the methanol extract and other fractions. The methanol and the fractionated extracts (hexane, chloroform, ethyl acetate, and water) of *P. macrocarpa* seeds were also investigated for their cytotoxic effects on selected human cancer cells lines (MCF-7, HT-29, MDA-MB231, Ca Ski, and SKOV-3) and a normal human fibroblast lung cell line (MRC-5). Information from this study can be applied for future pharmacological and therapeutic evaluations of the species, and may assist in the standardization for quality, purity, and sample identification. To the best of our knowledge, this is the first report on the phytochemical screening and cytotoxic effect of the crude and fractionated extracts of *P. macrocarpa* seeds on selected cells lines.

1. Introduction

Herbal medicine plays a key role in the development of pharmaceuticals and thus there is a high demand in natural medicine for the global market. Although there are thousands of species listed as medicinal plants, only a small number are commercially used in traditional treatments. In this respect, there are very few in-depth scientific studies on the medicinal properties of plants. However, traditional herbal medicine is still prominent and is considered an important alternative to conventional medicine particularly in developing countries. Despite its well-known benefits, *Phaleria macrocarpa* (Scheff.) Boerl is still relatively unknown in terms of its biochemical constituents and biological activity. *P. macrocarpa* is a plant commonly used in East Asian herbal medicines. *P. macrocarpa* is used as a remedy for a variety of ailments such as cancer, diabetes mellitus, allergies, liver and heart diseases, kidney failure, blood diseases, high blood

pressure, and stroke. It is also used to treat various skin diseases including acne [1, 2].

P. macrocarpa plants have round, oval shaped seeds that have a diameter of approximately 1 cm. The seed is the most poisonous part of the plant, having higher toxicity levels than the stem, roots, and leaves. *P. macrocarpa* fruits and leaves are used in traditional medicine as a concoction. The seeds which have an unpleasant odor are usually used for the treatment of skin diseases. The compounds quercetin and naringin have been found in the seeds [3]. The essential oils of the seeds consist of heptadecane, octadecane, diclosan, triclosan, vinyl laurate, and dioctyl ester [4]. Another study reported the presence of Mahkoside A and kaempferol 3-O- β -D-glucoside in the seeds [5]. Two novel compounds, 29-norcucurbitacin and desacetylfevicordin A, and three known 29-norcucurbitacin derivatives have also been isolated from the ethyl acetate fraction of *P. macrocarpa* seeds [6].

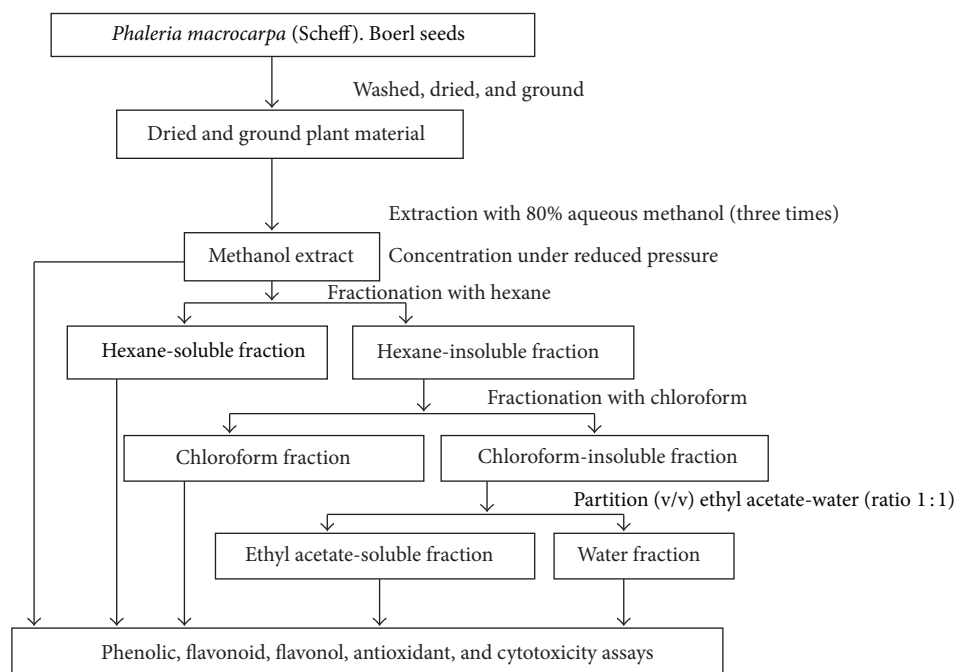


FIGURE 1: Extraction procedure and its fractionations of *P. macrocarpa* (Scheff.) Boerl seeds.

The ethanol extract of *P. macrocarpa* seeds exhibited toxicity towards T47D breast cancer cell lines ($LC_{50} 15.12 \pm 3.21 \mu\text{g/mL}$) through COX-2 inhibition [7]. Additionally, the ethanol extract of the seeds and the fruits' flesh have been shown to increase *p53* gene expression but had no effect on Bcl-2 gene expression. Moreover, the n-hexane extract of the seeds had a greater effect in increasing *p53* gene expression than that of the flesh of the fruit, but had no effect on Bcl-2 gene expression [8]. The ethanol extracts of *P. macrocarpa* seeds and fruits have been found to be nontoxic to human mononuclear peripheral normal cells but were slightly toxic to Vero cell lines [9].

Although *P. macrocarpa* has been used extensively in Indonesia, there is limited scientific research available on the biological properties of this plant in relation to its medicinal benefits. The present research investigated the total phenolic and flavonoid content and the antioxidative and cytotoxic activities of the crude and fractionated extracts of *P. macrocarpa* seeds.

2. Material and Methods

2.1. Plant Materials. Seeds of *Phaleria macrocarpa* (Scheff.) Boerl were collected from Yogyakarta, Indonesia, in December 2011. A voucher specimen (ID no. KLU 47923) was deposited into a repository at the Institute of Biological Sciences, Faculty of Science, University of Malaya, Malaysia. Samples were washed and dried in an oven at approximately 50°C . The seeds were then ground into powder and stored in airtight containers.

2.2. Preparation for Extraction. The dried powder was macerated with 80% aqueous methanol and extracted for 72 h

before filtration (three times). The filtrate obtained was concentrated under reduced pressure (60 rpm at 37°C). This crude methanol extract was then fractionated, initially with hexane followed by chloroform. The chloroform insoluble fraction was subjected to partition with ethyl acetate and water (Figure 1). The methanol extract and its fractions (hexane, chloroform, ethyl acetate and water) were refiltered and evaporated at low pressure (60 rpm at 37°C) to remove excess solvent.

2.3. Phytochemical Screening Analysis. In order to classify the types of organic constituents present in the plant samples, preliminary phytochemical screening tests were carried out on the plant samples according to the qualitative and quantitative methods of Trease and Evans [10] and Sofowora [11]. The organic constituents that were investigated were those listed in Table 2. α -Amino acids, carbohydrates, cyanogenic glycosides, organic acids, reducing sugars, saponin glycosides, and starch content determination were carried out on water extracts. Alkaloids tests were used with 1% HCl extract. Determination of flavonoids, glycosides, phenolic compounds, and tannins were performed on the ethanol extract. Test for steroids was performed on the petroleum-ether extract.

2.4. Physiochemical Determination. The nutritional values of the *P. macrocarpa* seeds, including moisture, ash, fiber, protein, fat, carbohydrate contents, and energy value, were determined by using the methods of AOAC [12], Trease and Evans [10], and Harbone [13].

2.5. Determination of Moisture Content. The moisture content of the dried powder samples was determined by using

the oven drying method [14, 15]. A clean dried crucible was weighed and 10 g of the dried *P. macrocarpa* seeds powder was placed in a beaker. The sample was dried in an electric oven at 105°C until all the moisture was removed from the sample and constant weight was achieved. The crucible containing the dried sample was weighed again and the loss of weight was recorded as the moisture content of the dried powdered *P. macrocarpa* seeds. The experiment was repeated three times. The moisture content (%) was calculated by using the following equation:

$$\text{Moisture percentage (\%)} = \frac{W_2 - W_1}{W_0} \times 100, \quad (1)$$

where W_1 = weight of sample after drying (g), W_2 = weight of sample before drying (g), and W_0 = weight of the sample (g)

2.6. Determination of Ash Content. Ash content was determined by using the method of A.O.C.S [12]. Briefly, the ash value of the samples represented the inorganic residue when the organic matter has been burnt away. An accurately weighted amount (10 g) of the sample was placed in a pre-heated, cooled and weighed porcelain crucible. The crucible was heated carefully on a hot plate until the organic matter was dried and burnt off without flaming and finally heated in a furnace at $550 \pm 50^\circ\text{C}$.

The percentage of ash content was calculated using the following formula:

$$\text{Percentage of Ash (\%)} = \frac{\text{Weight of Ash}}{\text{Weight of sample}} \times 100. \quad (2)$$

2.7. Determination of Crude Fiber Content. The crude fiber content was determined by using the method of A.O.A.C [16]. Dried powdered sample was weighed (10 g) and extracted with petroleum ether (100 mL) three times. The extracted sample was air-dried and transferred to a round-bottomed flask. In the flask, 30 mL of sulphuric acid (0.1275 M) was added, followed by 170 mL of hot sulphuric acid. The solution was then refluxed for approximately 30 minutes and filtered through a Buchner funnel. The insoluble matter was washed with boiling water until the final filtrate was free from acid.

The residue was placed back into the flask with 30 mL of sodium hydroxide (0.313 M), and 170 mL of hot sodium hydroxide (0.313 M) was then added. The mixture was again refluxed for about 30 minutes and filtered using sintered glass. The residue was washed with 1% HCl and then washed again with boiling water until there was no acid present. The residue was finally washed with ethanol and ether and dried in an oven at 100°C and then weighed. This procedure was repeated until the fiber content was constant. The fiber content was calculated using the following equation:

$$\text{Percentage of Crude fiber (\%)} = \frac{\text{Loss in weight}}{\text{Weight of sample}} \times 100. \quad (3)$$

2.8. Determination of Carbohydrate Content. Carbohydrate content was calculated by multiplying the reducing sugar

content. The reducing sugar content was determined using the Fehling's reducing method of Lane and Eynon's [16]. Weighted sample (10 g) was placed into a 250 mL round-bottomed flask and 20 mL of sulphuric acid (0.5 M) was added. Reflux was then performed in a sand bath for 2.5 hours. The residue was washed after filtration with warm distilled water. The solution was then neutralized with sodium carbonate powder and the mixture's volume was made up to 100 mL with distilled water. This was followed by titration with Fehling's solution, equal amounts of solution A (copper sulphate solution) and solution B (sodium potassium tartrate and sodium hydroxide solution) using methylene blue as indicator. The mixed Fehling's solution (5 mL) was pipetted into a conical flask and distilled water (5 mL) was added. The solution was then boiled for 15 seconds. Methylene blue indicator (a few drops) was then titrated with the solution until the colour changed from blue to green. The carbohydrate content was then calculated according to following equation:

$$\begin{aligned} \text{Percentage of carbohydrate content (\%)} \\ = \frac{5 \times 0.005 \times 100 \times 100 \times 100}{V \times 10 \times W} \times 0.9\%, \end{aligned} \quad (4)$$

where V = volume of sample solution (titration volume) and W = weight of powdered sample

2.9. Determination of Fat Content. Fat content of *P. macrocarpa* seeds was determined using the soxhlet extraction method [12]. A seed sample (10 g) was placed in a soxhlet extractor. Petroleum ether was then poured into the extractor and extraction was performed for 12 hours. The volume of the petroleum ether extract was reduced to 15 mL by evaporation. This was then dried at 105°C in an oven until constant weight was achieved. The fat content was then calculated by using the following equation:

$$\begin{aligned} \% \text{ of Fat content} \\ = \frac{\text{Weight of fat obtained from sample} \times 100}{\text{Weight of sample}}. \end{aligned} \quad (5)$$

2.10. Determination of Protein Content. Protein content was determined using the A.O.A.C method [12]. Briefly, powdered samples (1 g), 50 mL of distilled water, 5 g of copper sulphate, and 15 mL of concentrated sulphuric acid were added to a Kjeldahl flask. The flask was partially closed by means of a funnel, and the content was digested by heating the flask at an inclined position in the digester. The mixture was heated for 30 minutes until there was 40 mL of clear 0.1 M standard sulphuric. A few drops of methyl red indicator were mixed into the clear solution. The flask was then placed below the condenser and the end of the adapter tube was dipped in the acid. The flasks were set up for Kjeldahl distillation and 70 mL of 40% sodium hydroxide was added through the funnel. The funnel was washed twice with 50 mL of distilled water. Distillation was then performed for one hour. The distilled ammonia was then nitrated with 0.1 M standard solution until the color changed from yellow to colorless. The experiment was repeated three times. The nitrogen content

and protein content in the sample were calculated using the following relation:

$$\begin{aligned} & \text{Percentage of Nitrogen (\%)} \\ & = \frac{(V_s - V_b) \times M_A \times 0.0140 \times 100}{\text{Weight of sample (W)}} \end{aligned} \quad (6)$$

Protein content = percentage of Nitrogen \times 6.25,

where V_s = volume in cm^3 of standard acid used in the titration of sample, V_b = volume in cm^3 of standard acid used in the blank titration, M_A = molarity of standard acid solution in mol dm^{-3} , and W = weight of the sample in grams.

2.11. Determination of Phenolic Content. The total phenolic content of the crude methanol and the fractionated extracts (hexane, chloroform, ethyl acetate, and water) was determined using the Folin-Ciocalteu method [17–20]. Briefly, 200 μL of each extract solution of different concentrations was mixed with 1 mL of Folin-Ciocalteu reagent (1:10 diluted with H_2O) and 800 μL of Na_2CO_3 (75.05 g/L). The mixture was thoroughly shaken for 15 minutes and then held in a water bath at a temperature of 37°C . The solution was allowed to stand for 1 hour at room temperature in a dark place and the absorption was measured at 750 nm using a spectrophotometer. Distilled water was used as blank, and gallic acid (0–250 mg/L) was used to construct a standard calibration curve. Gallic acid concentration was established from the calibration curve, $y = 0.0221x + 0.2189$; $R^2 = 0.9914$.

2.12. Determination of Flavonoid Content. Total flavonoid content of *P. macrocarpa* seeds was measured using the methods of Ebrahimzadeh, Nabavi, and Ordonez [20–22] with minor modifications. To determine the flavonoid content, 1 mL of each sample was added to 0.1 mL of 10% $\text{Al}(\text{NO}_3)_3$ solution, 0.1 mL of 1 M potassium acetate, and 3.8 mL of methanol. The solution was thoroughly mixed using a vortex mixer for two to three minutes and then stood untouched for 10 minutes at room temperature. Absorbance was determined at 415 nm using a spectrophotometer. The total content of flavonoids was measured and expressed as quercetin equivalent on a dry weight basis ($y = 0.0855x + 0.2004$; $R^2 = 0.9813$).

2.13. Determination of Flavonol Content. The method of Kumaran [23] and Mbaebie [24] with slight modifications was used to measure the total flavonol content of the methanol extract. Briefly, 1 mL of extract was added to a centrifuge tube with 2 mL of prepared AlCl_3 in ethanol and 3 mL of sodium acetate (50 g/L) solution. The mixture was stirred thoroughly with a vortex and was then incubated for 1 hour. The absorbance was measured with a spectrophotometer at 440 nm. A calibration curve was constructed using quercetin (1, 5, 10, 15, and 20 mg/mL). The total flavonol content was calculated using the calibration curve with the following equation, $y = 0.0353x + 0.1456$; $R^2 = 0.9807$.

2.14. Antioxidant DPPH Assay. Screenings of antioxidant activity of the crude methanol extract, chloroform, hexane, ethyl acetate, and water fractions of *P. macrocarpa* seeds were carried out by determination of DPPH free radical scavenging property using UV spectrophotometric methods [21, 25]. Based on this protocol, 50 μL of test solutions from different dry extracts and concentrations (1, 5, 10, 15, and 20 mg/mL) was dissolved in water. This solution was then combined with 1.95 mL of DPPH methanol solution. After being mixed, solutions were kept at room temperature, in the dark for 30 minutes. After the reaction, the increase in absorbance was recorded at 517 nm. Methanol was used as a blank, DPPH solution was used as negative control (A_0), and gallic acid was used as positive control. The antioxidant activity was expressed as an IC_{50} value. All experiments were carried out in triplicate. The scavenging effect was obtained from the following relation:

$$\text{Scavenging effect (\%)} = \frac{(A_0 - A_1) \times 100}{A_0}, \quad (7)$$

where A_0 was the absorbance of the control reaction and A_1 was the absorbance of the sample of the tested extracts. Gallic acid was used as standard. Percentage of inhibition was calculated using the following formula: % inhibition = $[(A_{\text{negative}} - A_{\text{test}})/A_{\text{negative}}] \times 100$ (A is absorbance).

2.15. Cytotoxicity Screening

2.15.1. Cell Culture and Culture Medium. Human cervical carcinoma cells (Ca Ski), hormone-dependent breast carcinoma cells (MCF-7), human breast adenocarcinoma cells (MDA-MB231), human ovarian carcinoma cells (SKOV-3), human colon carcinoma cells (HT-29), and noncancer human fibroblast cells (MRC-5) were purchased from the American Tissue Culture Collection (ATCC, USA).

HT 29, Ca Ski, and MCF-7 cells were maintained in RPMI 1640 medium (Sigma), MDA-MB231 and SKOV-3 cells in Dulbecco's Modified Eagle's medium (DMEM, Sigma), and MRC-5 cells in Eagle's Minimum Essential medium (EMEM, Sigma), supplemented with 10% fetal bovine serum (FBS, PAA Lab, Austria), 100 $\mu\text{g}/\text{mL}$ penicillin or streptomycin (PAA Lab, Austria), and 50 $\mu\text{g}/\text{mL}$ kanamycin/amphotericin B (PAA Lab, Austria). The cells were cultured in a CO_2 incubator (5%) and kept at 37°C in a humidified atmosphere. The cultures were subcultured every 2–3 days and checked frequently under an inverted microscope (Leica, Germany) for any contamination.

2.15.2. MTT Cell Proliferation Assay. MTT [3-(4, 5-dimethylthiazol-2-yl)-5-diphenyl tetrazolium bromide] assay was performed on the cultured cells in 96-well plates according to the method of Mosmann [26, 27]. Briefly, cells were cultured to confluence. They were then centrifuged at 1,000 rpm for 5 minutes and resuspended with 1.0 mL of growth medium. The density of the viable cells was counted using 0.4% trypan blue exclusion dye in a haemocytometer with a microscope. The cells were then seeded into microtiter plates and incubated in a CO_2 incubator at 37°C for 24 hrs. After reaching 70–80%

TABLE 1: Yield of methanol extract and its fractions from *P. macrocarpa* of seeds.

Extract and fractions	Yield (g)	Percentage of yield (%)
Methanolic extract (ME)	198.7	11.99
Hexane fraction (HF)	158.7	9.47
Chloroform fraction (CF)	7.2	0.43
Ethyl acetate fraction (EAF)	6.2	0.37
Water fraction (WF)	Freeze dry	

confluence, each extract at concentrations of 1, 10, 25, 50, and 100 $\mu\text{g}/\text{mL}$ (in 200 μL of 10% media) was added to the respective wells containing the cells. Wells with untreated cells were used as the negative control and cells exposed to doxorubicin were used as positive control. After 24, 48, and 72 hours, 10 μL MTT stock solution was added to each well. OD was then determined by measuring absorbance at 540 nm using an ELISA microplate reader. The percentage of inhibition (%) was calculated according to the following formula:

$$\text{Percentage of inhibition (\%)} = \frac{\text{OD control} - \text{OD sample} \times 100\%}{\text{OD control}} \quad (8)$$

Cytotoxicity of each sample is expressed as $\pm\text{IC}_{50}$ value. The extract that gave IC_{50} of 30 $\mu\text{g}/\text{mL}$ or less was considered active [26].

2.16. Gas Chromatography-Mass Spectrometry (GC-MS). GC-MS was used to determine the molecular weight of the components collected and the purity of the collected extracts. Running conditions were as follows: oven temperature was programmed with an initial temperature of 100°C and increased at a ramp rate of 5°C/min and reached a final temperature of 300°C. The carrier gas or mobile phase used was helium and a flow rate of 1 mL/min was programmed. The mass spectrometry mode used was electron ionization (EI) mode with a current of 70 eV. The injection mode was programmed with a sample injection volume of 1 μL with a split mode at a ratio of 1:20. The injection port temperature was set to 230°C and the detector/interface temperature was set to 250°C. The results were collected for 40 minutes. The total ion chromatogram obtained was autointegrated using ChemStation and the chemical compounds or components were analysed by comparison with the supplied mass spectral database (NIST 05 Mass Spectral Library, USA).

2.17. Statistical Analysis. All data for each test are the average of triplicate experiments for comparison of values and were recorded as the mean \pm standard deviation using Microsoft Excel software and statistical data analyses were performed using SPSS software.

3. Results

3.1. Extraction. The extracts were concentrated using a rotary evaporator (Buchi, USA) under reduced pressure at 35°C. The

yield of extracts from *P. macrocarpa* seeds is shown in Table 1. The highest yield from *P. macrocarpa* seeds was the hexane fraction (9.47%).

3.2. Preliminary Phytochemical Studies. In order to determine the types of phytoorganic constituents present in *P. macrocarpa* seeds, a preliminary phytochemical investigation was carried out according to conventional methods. The results obtained from these experiments are summarized in Table 2.

The phytochemical tests showed that there were secondary metabolites, including carbohydrate, flavonoids, glycosides, saponin glycosides, phenolic compounds, steroids, tannins, and terpenoids, present in different extracts of *P. macrocarpa* seeds. Small amounts of alkaloids, α -amino acids, cyanogenic glycosides, organic acids, reducing sugars, and starches were also found to be present.

The main constituents such as flavonoids, glycosides, saponin glycosides, phenolic compounds, steroids, tannins, and terpenoids present in *P. macrocarpa* seeds may contribute to the presence of bioactivities such as antibacterial, an analgesic, an antifungal, an anti-inflammatory agent, and cytotoxicity. Moreover, the toxic chemical constituents, cyanogenic glycosides, were also present in the seeds.

3.3. Physicochemical Studies. The determination of nutritional values such as moisture, ash, fiber, protein, fat, and carbohydrate contents was carried out using the A.O.A.C method as well as the Lane and Eynon titration method and the results obtained are shown in Figure 2(a) and Table 3. Different physicochemical parameters for the purpose of standardization such as moisture ($6.31 \pm 1.43\%$), ash ($2.96 \pm 1.86\%$), protein ($20.73 \pm 2.44\%$), crude fiber ($22.76 \pm 2.79\%$), crude fat ($18.4 \pm 3.11\%$), and carbohydrate ($29.34 \pm 1.98\%$) were determined.

3.4. Flavonoid, Flavonol, and Phenolic Determinations. It was found that the methanol extract had the highest flavonoid content ($9.33 \pm 0.8 \text{ mg/mL}$), followed by ethyl acetate, water, chloroform, and hexane fractions, which were 8.38 ± 1.0 , 8.08 ± 0.3 , 6.78 ± 1.1 , and $4.18 \pm 1.5 \text{ mg/mL}$, respectively.

The methanol extract ($8.93 \pm 1.1 \text{ mg/mL}$) of *P. macrocarpa* seeds exhibited the highest amount of total flavonol content, followed by water, ethyl acetate, chloroform, and hexane fractions, which were 8.93 ± 1.0 , 6.13 ± 0.5 , 4.29 ± 0.9 , and $4.29 \pm 0.7 \text{ mg/mL}$, respectively.

The total phenolic content of the *P. macrocarpa* seeds extracts and fractions was expressed as gallic acid equivalents. The methanol extract of *P. macrocarpa* seeds exhibited the highest amount ($7.20 \pm 0.7 \text{ mg/mL}$) of total phenolics, followed by water, ethyl acetate, chloroform, and hexane fractions, which were 5.12 ± 1.4 , 3.58 ± 1.1 , 3.26 ± 1.0 , and $2.63 \pm 0.1 \text{ mg/mL}$, respectively.

These data are shown in Figure 2(b) and Table 4.

3.5. DPPH (2, 2-Diphenyl-1-picryl-hydazyl) Antioxidant Assay. DPPH assay was used to determine the free radical scavenging ability of extracts and fractions of *P. macrocarpa* seeds and to determine the antioxidant activity of its

TABLE 2: Results of chemical constituents of *P. macrocarpa* seeds.

No.	Tests	Reagents	Observation
1	Alkaloids	Wagner's reagent	+
		Mayer's reagent	+
		Dragendorff's reagent	+
		Sodium picrate solution	+
2	α -Amino acids	Ninhydrin reagent	+
3	Carbohydrates	10% α -naphthol and conc: H_2SO_4	++
4	Cyanogenic glycosides	Sodium picrate solution	+
5	Flavonoids	Mg and conc: HCl	++
6	Glycosides	10% lead acetate	++
7	Organic acids	Bromothymol blue	+
8	Phenolic compounds	1% $FeCl_3$	++
9	Reducing sugars	Fehling's solutions A and B	+
10	Saponin glycosides	Distilled water	++
11	Starch	Iodine solution	+
12	Steroids	Acetic anhydride and conc: H_2SO_4	++
13	Tannins	1% Gelatin	++
14	Terpenoids	Acetic anhydride and conc: H_2SO_4	++

+++ : large amount; ++ : medium amount; + : small amount; - : absent; + : present.

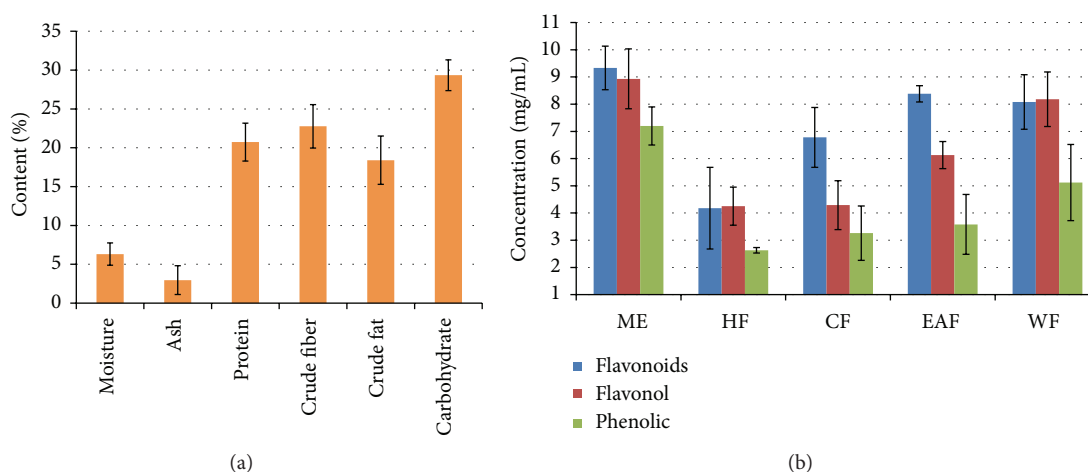


FIGURE 2: (a) The percentage of moisture, ash, protein, crude fiber, crude fat, and carbohydrate contents on *P. macrocarpa* Boerl seeds (b) Total amount of concentration of flavonoid, flavonol, and phenolic contents of *P. macrocarpa* seeds. ME: methanol extract, HF: hexane fraction, EAF: ethyl acetate fraction, CF: chloroform fraction, WF: water fraction.

phytoconstituents. It is important to note that a lower IC_{50} value equals a higher scavenging activity. The scavenging activity was presented as the percentage of inhibition of DPPH free radicals (Figure 3 and Table 4). Based on IC_{50} values, the samples can be ranked in the following descending order: water fraction > methanol extract > ethyl acetate fraction > hexane fraction > chloroform fraction. The results revealed that the water fraction was most active for antioxidant activity compared to other fractions. The radical

scavenging effect was found to increase with increasing concentrations.

3.6. Cytotoxicity Screening of MTT Cell Proliferation Assay.

The methanol and fractionated extracts (hexane, chloroform, ethyl acetate, and water) were investigated for cytotoxic effects in human cervical adenocarcinoma cells (Ca Ski), human hormone-dependent breast carcinoma (MCF-7),

TABLE 3: The percentage of moisture, ash, protein, crude fiber, crude fat, and carbohydrate contents and the amount of nutrition values on *P. macrocarpa* seeds.

Tests parameter	Percentage of contents (%)
Moisture	6.31 ± 1.43
Ash	2.96 ± 1.86
Protein	20.73 ± 2.44
Crude fiber	22.76 ± 2.79
Crude fat	18.40 ± 3.11
Carbohydrate	29.34 ± 1.98

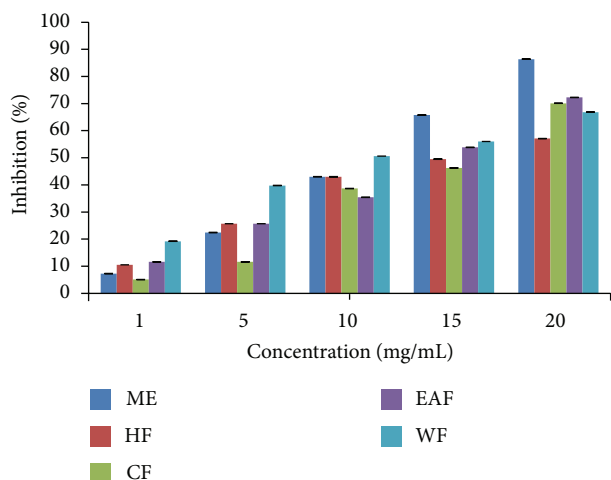


FIGURE 3: Percentage of inhibition of DPPH free radical scavenging of *P. macrocarpa* seeds. ME: methanol extract, HF: hexane fraction, EAF: ethyl acetate fraction, CF: chloroform fraction, WF: water fraction.

human colon adenocarcinoma cells (HT-29), human ovarian carcinoma cells (SKOV-3), human hormone-dependent breast carcinoma (MDA-MB231), and normal cells (MRC-5) using MTT cells proliferation assay at 24 hrs, 48 hrs, and 72 hrs, respectively.

The methanol extract of *P. macrocarpa* seeds showed excellent cytotoxic effects with IC_{50} value of $8.2 \pm 4.66 \mu\text{g/mL}$ in Ca Ski cells at 24 hrs and 12.0 ± 2.2 , 8.5 ± 1.68 , and $3.0 \pm 2.50 \mu\text{g/mL}$ in MCF-7 cells at 24 hrs, 48 hrs, and 72 hrs, respectively. The methanol extract also showed good cytotoxic activity in HT-29 cells with IC_{50} values of 29.3 ± 2.26 , 25.0 ± 1.35 , and $21.5 \pm 3.30 \mu\text{g/mL}$ at 24 hrs, 48 hrs, and 72 hrs, respectively, in Ca Ski cells with IC_{50} values of $19.7 \pm 0.92 \mu\text{g/mL}$, and in SKOV-3 cells with IC_{50} values of 16.5 ± 2.52 , 22.1 ± 2.47 , and $36.0 \pm 3.55 \mu\text{g/mL}$ at 24 hrs, 48 hrs, and 72 hrs, respectively. However, this extract had no cytotoxic effect in MDA-MB231 cells with $IC_{50} > 100 \mu\text{g/mL}$, and the extract also had low cytotoxic effect in the MRC-5 cells with $IC_{50} > 50 \mu\text{g/mL}$.

The hexane fraction of *P. macrocarpa* seeds showed moderate cytotoxic effects with IC_{50} values of 45.2 ± 1.49 and $55.5 \pm 1.97 \mu\text{g/mL}$ at 24 hrs and 48 hrs on MCF-7, $40.0 \pm 3.15 \mu\text{g/mL}$ in HT-29 cells at 24 hrs, and 40.5 ± 3.52 and $50.0 \pm 3.02 \mu\text{g/mL}$ in SKOV-3 at 24 hrs and 48 hrs. In addition, the

hexane fraction also displayed low cytotoxic effect in MCF-7 at 72 hrs, HT-29 at 48 hrs and 72 hrs, and in SKOV-3 at 72 hrs. The IC_{50} value of treatment with hexane fraction in MCF-7 was $72.5 \pm 1.52 \mu\text{g/mL}$ for 72 hrs exposure. IC_{50} values in HT-29 were 64.0 ± 2.03 and $75.0 \pm 3.14 \mu\text{g/mL}$ at 48 hrs and 72 hrs, while IC_{50} value in SKOV-3 was $70.3 \pm 3.53 \mu\text{g/mL}$ at 72 hrs. In contrast, the hexane fraction exhibited no cytotoxic effects in MDA-MB231 cells or MRC-5 cells.

The chloroform fraction of *P. macrocarpa* seeds exhibited the highest cytotoxic effect with IC_{50} value of 10.0 ± 1.31 , 8.2 ± 1.04 , and $22.0 \pm 1.86 \mu\text{g/mL}$ at 24 hrs, 48 hrs, and 72 hrs in Ca Ski cells, 9.5 ± 2.95 , 8.7 ± 1.59 , and $21.0 \pm 1.98 \mu\text{g/mL}$ at 24 hrs, 48 hrs, and 72 hrs on HT29, and 24.8 ± 2.06 , 16.5 ± 3.21 , and $9.00 \pm 2.6 \mu\text{g/mL}$ in SKOV-3 cells. The chloroform fraction exhibited moderate cytotoxic effect in MCF-7 with IC_{50} value of 57.5 ± 2.64 , 40.0 ± 1.48 , and $46.5 \pm 3.45 \mu\text{g/mL}$ for 24 hrs, 48 hrs, and 72 hrs, respectively. In contrast, the chloroform fraction had no cytotoxic effect against the MDA-MB231 cells and normal MRC-5 cells with $IC_{50} > 100 \mu\text{g/mL}$.

The ethyl acetate fraction of *P. macrocarpa* seeds exhibited the highest cytotoxic effect with $IC_{50} < 25 \mu\text{g/mL}$ in SKOV-3 cells, MDA-MB 231 cells, MCF-7 cells, and Ca Ski cells. On the other hand, the ethyl acetate fraction exhibited low cytotoxic effect in MRC-5 normal cells with IC_{50} value of $35 \mu\text{g/mL}$. The ethyl acetate fraction exhibited the highest cytotoxic effect in all selected cells (Ca Ski, MCF-7, HT-29, and MDA-MB231). The water extract showed no cytotoxic effect against all selected cancer cell lines with $IC_{50} > 100 \mu\text{g/mL}$ and exhibited a mild cytotoxic effects against MRC-5 cells. The corresponding data is shown in Figure 4 and Table 5.

3.7. Characterization and Identification of Hexane and Chloroform Fractions. Six compounds were identified from the hexane fraction of *P. macrocarpa* seeds using GC-MS. They were methyl stearate, oleic acid, methyl oleate, linoleic acid, methyl linolenate, and palmitic acid. Moreover, a GC/MS analysis of the chloroform fraction of *P. macrocarpa* seeds showed the presence of methyl myristate, palmitic acid, methyl oleate, methyl linoleate, oleic acid, and (z)- and 9,17-octadecadienal, (z). A comparison with the NIST mass spectral library (NIST 05 MS library, 2002) and Adams (2001) confirmed the identity of the compounds. The chemical structures of the identified compounds in the hexane and chloroform fractions of *P. macrocarpa* seeds are as shown in Figure 5.

4. Discussion

A longer shelf life can be achieved by reducing moisture content. Thus, moisture content is a critical factor for the stability of an extract. Moisture enhances fungal and bacterial growth, therefore decreasing the longevity of the extract. The time it takes for plant material to deteriorate depends on how much water the plant material contains.

Carbohydrates play a vital role in the immune system, fertilization, pathogenesis, blood clotting, and human development. Foods that contain carbohydrates can raise blood glucose and the three main types of carbohydrate are

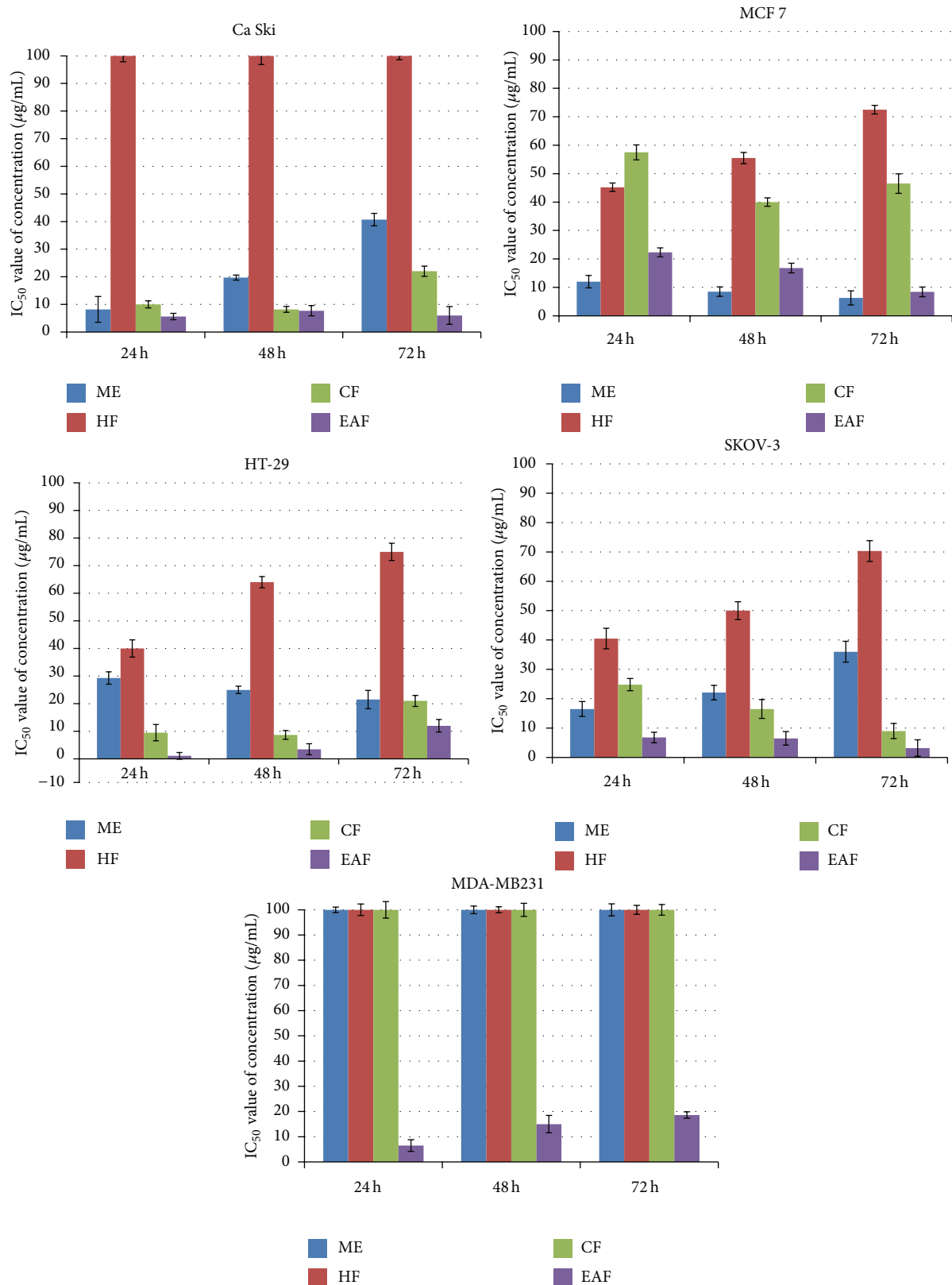


FIGURE 4: *In vitro*, cytotoxic effects of *P. macrocarpa* seedson Ca Ski, MCF-7, HT-29, SKOV-3, and MDA-MB231 cell lines. ME: methanol extract, HF: hexane fraction, EAF: ethyl acetate fraction, CF: chloroform fraction, WF: water fraction. Each value is expressed as mean ± standard deviation of three measurements.

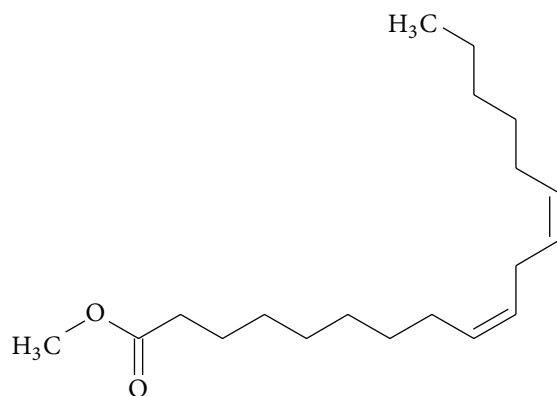
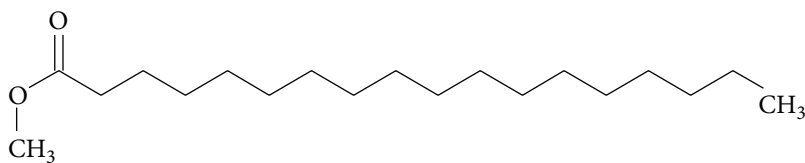
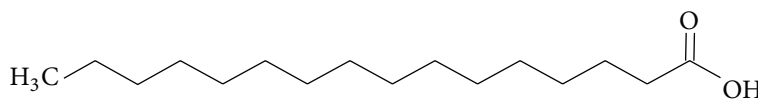
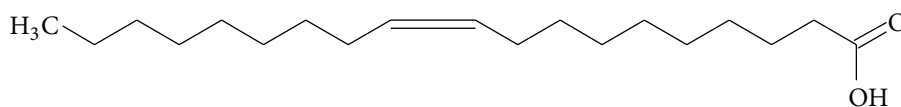
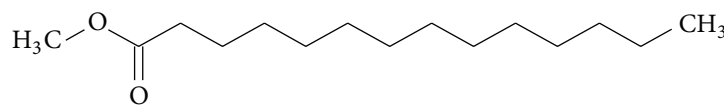
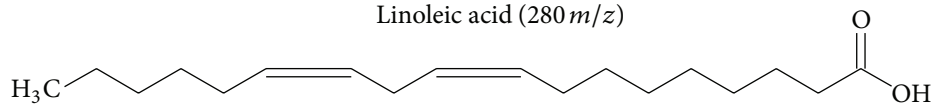
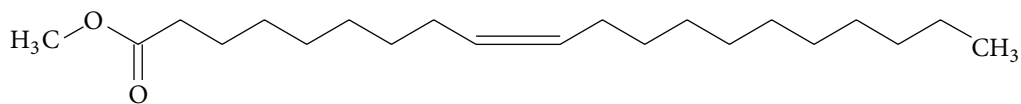
Methyl linoleate (294 *m/z*)Methyl stearate (298 *m/z*)Palmitic acid (256 *m/z*)Oleic acid (282 *m/z*)Methyl myristate (242 *m/z*)Linoleic acid (280 *m/z*)Methyl oleate (298 *m/z*)

FIGURE 5

TABLE 4: Total flavonoid, total flavonol, total phenolic contents, and result of DPPH free radical scavenging property of *P. macrocarpa* seeds.

Tests	ME (mg/mL)	HF (mg/mL)	CF (mg/mL)	EAF (mg/mL)	WF (mg/mL)
Flavonoid	9.33 ± 0.8	4.18 ± 1.5	6.78 ± 1.1	8.38 ± 0.3	8.08 ± 1.0
Flavonol	8.93 ± 1.1	4.25 ± 0.7	4.29 ± 0.9	6.13 ± 0.5	8.18 ± 1.0
Phenolic	7.20 ± 0.7	2.63 ± 0.1	3.26 ± 1	3.58 ± 1.1	5.12 ± 1.4
DPPH	11.50 ± 0.03	15.00 ± 0.04	15.75 ± 0.04	14.00 ± 0.05	9.75 ± 0.03

ME: methanol extract; HF: hexane fraction; EAF: ethyl acetate fraction; CF: chloroform fraction; WF: water fraction.

TABLE 5: *In vitro*, cytotoxic effects of methanol extract and its fractions of *P. macrocarpa* cancer cells lines and normal human fibroblast breast cells line.

Cell line	Incubation periods (hours)	ME	HF	CF	EAF	Doxorubicin
Ca Ski	24	8.2 ± 4.66	≥100	10.0 ± 1.31	5.6 ± 1.17	0.92 ± 0.64
	48	19.7 ± 0.92	≥100	8.2 ± 1.04	7.7 ± 1.85	0.69 ± 1.05
	72	40.7 ± 2.26	≥100	22.0 ± 1.86	6.0 ± 3.22	0.45 ± 0.99
MCF7	24	12.0 ± 2.2	45.2 ± 1.49	57.5 ± 2.64	22.3 ± 1.58	1.05 ± 1.08
	48	8.5 ± 1.68	55.5 ± 1.97	40.0 ± 1.48	16.8 ± 1.70	0.12 ± 0.69
	72	6.3 ± 2.50	72.5 ± 1.52	46.5 ± 3.45	8.4 ± 1.71	0.92 ± 1.70
HT29	24	29.3 ± 2.26	40.0 ± 3.15	9.5 ± 2.95	1.1 ± 1.20	0.92 ± 0.72
	48	25.0 ± 1.35	64.0 ± 2.03	8.7 ± 1.59	3.5 ± 2.00	0.32 ± 2.16
	72	21.5 ± 3.30	75.0 ± 3.14	21.0 ± 1.98	12 ± 2.28	0.88 ± 0.94
SKOV-3	24	16.5 ± 2.52	40.5 ± 3.52	24.8 ± 2.06	6.8 ± 1.8	1.02 ± 1.79
	48	22.1 ± 2.47	50.0 ± 3.02	16.5 ± 3.21	6.5 ± 2.3	0.32 ± 0.97
	72	36.0 ± 3.55	70.3 ± 3.53	9.0 ± 2.6	3.2 ± 2.81	0.62 ± 0.98
MDA-MB231	24	≥100	≥100	≥100	6.5 ± 2.3	0.43 ± 0.50
	48	≥100	≥100	≥100	15 ± 3.43	0.59 ± 1.01
	72	≥100	≥100	≥100	18.6 ± 1.26	0.95 ± 1.32

ME: methanol extract; HF: hexane fraction; EAF: ethyl acetate fraction; CF: chloroform fraction; WF: water fraction. Doxorubicin was used as positive control. Each value is expressed as mean ± standard deviation of three measurements.

starches, sugars, and fiber. A macronutrient protein consists of amino acids which is required for proper growth and human body function. The seeds were found to contain a high level of crude fiber which is a potential source of phenolic antioxidants. The major components of fibers are cellulose, hemicelluloses, lignin, β -glucans, gums, and pectin and hydrocolloids. These components can behave as pro-antioxidants [28, 29]. In our present physicochemical study, *P. macrocarpa* seeds were mainly made up of carbohydrates, followed by crude fiber, proteins, fat, moisture, and ash. High-protein and low-carbohydrate diets are often effective for weight loss. Dietary fiber can aid in digestion, is helpful for weight management, and reduces constipation. However, many high-protein and low-carbohydrate foods are low in fiber. Women aged 50 and older need at least 21 grams of fiber daily, whilst those aged 19 to 50 require 25 grams, men aged 50 and older need 30 grams, and those between the age of 19 to 50 should consume at least 38 grams of fiber.

Steroids possess biological activities which are insecticidal, cardiotoxic, and antimicrobial activities and these are potentially useful for development into therapeutic drugs. Tannins are known to be important for their antiviral, antibacterial, antiparasitic effects, anti-inflammatory, antiulcer, and antioxidant properties [30–33]. Saponins have been found to have antimicrobial, anti-inflammatory, antifeedant, and hemolytic effects [34, 35]. Some alkaloids

have been reported to have anticancer and antiviral activity and saponins have been reported to be cardiotoxic, while flavonoids have anticancer and anti-inflammatory activity [10, 36]. The presence of tannins may be responsible for the ability of *P. macrocarpa* seeds to be used in the treatment of diseases such as diabetes, diarrhea, and dysentery. Our preliminary phytochemical studies revealed that the chemical components of *P. macrocarpa* seeds also include flavonoids, phenolics, steroids, tannins, terpenoids, glucosides, saponins, and carbohydrates.

Previous researchers reported that kaempferol, myricetin, naringin, quercetin, rutin [3], 29-norcucurbitacin derivatives, fevicordin A, fevicordin A glucoside, fevicordin D glucoside [6], mahkocide A, dodecanoic acid, palmitic acid, des-acetyl flavicordin-A, flavicordin-A, flavicordin-D flavicordin-A glucoside, ethyl stearate, lignans and sucrose [37, 38], mangiferin (a C-glucosylxanthone), kaempferol-3- β -D-glucoside, dodecanoic acid, palmitic acid, ethyl stearate, sucrose [5], pinoselinol, lariciresinol, matairesinol, alkaloids and saponins [37, 39], saponins, alkaloids, polyphenolics, phenols, flavonoids, lignans, tannins [40–42], icarisiside C3, mangiferin, gallic acid, phalerin, glycoside (3,4,5-trihydroxy-4-methoxy-benzophenone-3-O- β -D-glucoside) [43], and 2,4',6, trihydroxy-4-methoxy-benzophenone-3-O- β -D-glucoside [44] were isolated from different parts of *P. macrocarpa*. The hexane extract of the seeds was

found to contain methyl myristate, methyl stearate, oleic acid, methyl oleate, linoleic acid, methyl linoleate, palmitic acid, methyl palmitate, 6-octadecenoic acid, and 9,17-octadecadiol, β -sitosterol as major components. A further 30% to 40% of components were not identified as these were polar compounds that require HPLC analysis. Other compounds reported in the literature for the seeds, leaves, and fruits were not identified in this investigation. It is probable that the components reported in the literature may be present in other fractions (methyl acetate, CHCl_3 , and water fractions).

Phenolics are able to transfer protons to radicals [45]. DPPH, which provides free radicals, is normally a blue-violet color. However, the DPPH turned yellow after it was converted to 1, 1-diphenyl-2-picrylhydrazine, which has less free-radical activity. Hendra et al. reported that the IC_{50} values of free radical and reducing power in methanol with HCl of *P. macrocarpa* seeds were 245.0 ± 1.94 and 150.2 ± 1.28 [42]. In our investigation using DPPH assay, the water fraction displayed the highest IC_{50} value followed by methanol, ethyl acetate, hexane, and chloroform fraction.

The presence of flavonoids in *P. macrocarpa* seeds may be responsible for the traditional use of the plants in treating cancer, inflammations, and allergies. Recently, it has been shown that phenolic compounds in crude methanol and ethyl acetate extract of *P. macrocarpa* leaves displayed good antioxidant and antimicrobial activities [46]. Hendra et al. (2011) examined the amount of total phenolic (47.7 ± 1.04 mg gallic acid equivalent/g DW) and the amount of flavonoid (35.9 ± 2.47 mg rutin equivalent/g DW) contents in the methanol extract with HCl of *P. macrocarpa* seeds [42]. In this study, the total flavonoids content was higher than that in the results previously reported by Rohyami [47] and phenol, flavonol, and flavonoid contents were the highest in the aqueous methanol extract followed by ethyl acetate, water, chloroform, and hexane extracts

MTT assay is a sensitive and reliable colorimetric assay that uses quantitative measurements to calculate the viability, proliferation, and activation of cells. This method is commonly applied to screen anticancer agents [48]. The most well-known methods used to calculate cytotoxicity are the neutral red (NR) uptake and dimethylthiazole-diphenyl tetrazolium bromide (MTT) metabolism [27, 49]. Earlier investigations showed that the ethanol extract of *P. macrocarpa* seeds and fruit meat were not toxic to normal human cells, but slightly toxic to a Vero cell line [9]. The ethanol extract of *P. macrocarpa* seed fruit also showed toxicity towards T47D breast cancer cell line through COX-2 expression inhibition [7]. Desacetylfevicordin A has been isolated from the ethyl acetate extract of *P. macrocarpa* seeds and this compound displayed excellent cytotoxicity in brine shrimp [43]. The ethyl acetate of *P. macrocarpa* seeds exhibited mild cytotoxic effect against HepG2 cells (IC_{50} values between 30 and 60 $\mu\text{g}/\text{mL}$) [46]. Previous studies showed that the cytotoxic activity of the seeds on HT-29, MCF-7, Hela, and Chang liver cells lines were 38.4 ± 0.37 , 25.5 ± 1.37 , 29.5 ± 1.0 and 67.8 ± 0.27 , respectively [42]. In our study, the methanolic extract of *P. macrocarpa* seeds was found to pose cytotoxic effect against HT-29, MCF-7, Cas Ki,

and SKOV-3 cell lines (IC_{50} values giving from 1.1 ± 1.20 to 36.0 ± 3.55) and mild toxicity on normal cell lines. There were significant cytotoxic effects on selected cancer cells lines that were both time- and dose-dependent manner due to the presence of many secondary metabolites.

The phytochemical screening also indicated the presence of a small amount of cyanogenic glycosides. Cyanogenic glucosides which can cause acute cyanide poisoning cause rapid respiration and pulse, decrease the blood pressure, and induce vomiting, diarrhea, headache, dizziness, and so on. Thus, these components have to be removed (usually by boiling) prior to consumption for therapeutic purposes.

5. Conclusion

P. macrocarpa seeds exhibited antioxidant and cytotoxic activities. It is highly probable that these activities are due to the presence of phenolic and flavonoid compounds in appreciable amounts in the plant. Furthermore, the cytotoxicity activity suggested that the seed may contain a potential anticancer agent. The outcome of this study is encouraging, demonstrating the potential for the *P. macrocarpa* as a source of multiple therapeutic agents.

Abbreviations

EAF: Ethyl acetate fraction
ME: Methanol extract
HF: Hexane fraction
CF: Chloroform fraction
WF: Water fraction
g: Gram
mg: Milligram
mL: Milliliter.

Conflict of Interests

The authors declare that there is no conflict of interests regarding the publication of this paper.

Authors' Contribution

Ma Ma Lay was involved in all experiments and Behrooz Banisalam was involved in antioxidant assay. All authors read and approved the submitted version of the paper.

Acknowledgments

This work was supported by grants from the Malaysian Ministry of Higher Education (nos. PS286/2009C and PS470/2010B). Ma Ma Lay is a scholarship recipient from the "Islamic Development Bank, Saudi Arabia." The authors would like to thank Professor Dr. Amru Bin Nasrullah Boyce for generously allowing the use of his laboratory for this research.

References

- [1] N. Harmanto, *Mahkota Dewa Obat Pusaka Para Dewa*, Cetakan keempat, Agromedia Pustaka, Jakarta, Indonesia, 2002.
- [2] A. Jemal, R. Siegel, E. Ward, T. Murray, J. Xu, and M. J. Thun, "Cancer statistics, 2007," *Ca: A Cancer Journal for Clinicians*, vol. 57, no. 1, pp. 43–66, 2007.
- [3] R. Hendra, S. Ahmad, A. Sukari, M. Y. Shukor, and E. Oskoueian, "Flavonoid analyses and antimicrobial activity of various parts of *Phaleria macrocarpa* (Scheff.) Boerl fruit," *International Journal of Molecular Sciences*, vol. 12, no. 6, pp. 3422–3431, 2011.
- [4] W. Wijayani, *Sitotoksitas Minyak Atsiri Biji Dan Daging Buah Mahkota Dewa (Phaleria Macrocarpa [Scheff.] Boerl.) Terhadap Myeloma Cell Line Dan HeLa Cell Line Serta Identifikasi Senyawa Minyak Atsiri Dengan Kromatografi Gas-Spektrometri Massa (GC-MS)*, Skripsi FMIPA UGM, Yogyakarta, Indonesia, 2005.
- [5] Y.-B. Zhang, X.-J. Xu, and H.-M. Liu, "Chemical constituents from Mahkotadewa," *Journal of Asian Natural Products Research*, vol. 8, no. 1-2, pp. 119–123, 2006.
- [6] D. Kurnia, K. Akiyama, and H. Hayashi, "29-Norcucurbitacin derivatives isolated from the Indonesian medicinal plant, *Phaleria macrocarpa* (Scheff.) Boerl," *Bioscience, Biotechnology and Biochemistry*, vol. 72, no. 2, pp. 618–620, 2008.
- [7] M. Bakhriansyah, *Pengaruh Ekstrak Etanol Biji Mahkota Dewa (Phaleria Macrocarpa [Scheff.] Boerl.) Pada Sel Kanker Payudara T47D: Kajian Aktivitas Sitotoksik Dan Penghambatan Ekspresi Siklooksigenase-2*, Program Pascasarjana UGM, 2004.
- [8] L. Wardani, *The Effect of Phaleria Macrocarpa [Scheff.] Boerl.) Seed and Flesh Fruit Extract to P53 and Bcl-2 Gene Expression in Hela Cell Line*, FMIPA UGM, 2005.
- [9] A. Endang, R. Tri Joko, and E. Dewi, "Cytotoxicity of *Phaleria macrocarpa* (Scheff) boerl fruits flesh and seed extract of ethanol and its effect against p53 and Bcl-2 genes expression of normal," in *Proceedings of the International Conference on Computational Science (ICCS '07)*, 2007.
- [10] C. Evans, *Trease and Evans Pharmacognosy*, Saunder, 2002.
- [11] A. Sofowora, *Medicinal Plants and Traditional Medicine in Africa*, Spectrum Books Ltd, Ibadan, Nigeria, 2nd edition, 1993.
- [12] AOAC, *Official Methods of Analysis*, Association of Official Analytical Chemists, Arlington, Tex, USA, 2002.
- [13] J. Harborne, *Phytochemical Methods*, Chapman and Hall, London, UK, 1973.
- [14] AOAC, *Official Methods of Analysis*, Association of Official Analytical Chemists, Gaithersburg, Md, USA, 17th edition, 2000.
- [15] J. Lako, V. C. Trenerry, M. Wahlqvist, N. Wattanapenpaiboon, S. Sotheeswaran, and R. Premier, "Phytochemical flavonols, carotenoids and the antioxidant properties of a wide selection of Fijian fruit, vegetables and other readily available foods," *Food Chemistry*, vol. 101, no. 4, pp. 1727–1741, 2007.
- [16] W. Horwitz, *Official Method of Analysis*, AOAC Interantional, Gaithersburg, Md, USA, 17th edition, 2000.
- [17] A. A. Adedapo, F. O. Jimoh, S. Koduru, P. J. Masika, and A. J. Afolayan, "Assessment of the medicinal potentials of the methanol extracts of the leaves and stems of *Buddleja saligna*," *BMC Complementary and Alternative Medicine*, vol. 9, article 21, 2009.
- [18] M. Zovko Končić, D. Kremer, J. Gruz et al., "Antioxidant and antimicrobial properties of *Moltkia petraea* (Tratt.) Griseb. flower, leaf and stem infusions," *Food and Chemical Toxicology*, vol. 48, no. 6, pp. 1537–1542, 2010.
- [19] S. McDonald, P. D. Prenzler, M. Antolovich, and K. Robards, "Phenolic content and antioxidant activity of olive extracts," *Food Chemistry*, vol. 73, no. 1, pp. 73–84, 2001.
- [20] S. M. Nabavi, M. A. Ebrahimzadeh, S. F. Nabavi, A. Hamidinia, and A. R. Bekhradnia, "Determination of antioxidant activity, phenol and flavonoid content of *Parrotia persica* Mey," *Pharmacologyonline*, vol. 2, pp. 560–567, 2008.
- [21] M. A. Ebrahimzadeh, S. F. Nabavi, and S. M. Nabavi, "Antioxidant activities of methanol extract of *Sambucus ebulus* L. flower," *Pakistan Journal of Biological Sciences*, vol. 12, no. 5, pp. 447–450, 2009.
- [22] A. A. L. Ordoñez, J. D. Gomez, M. A. Vattuone, and M. I. Isla, "Antioxidant activities of *Sechium edule* (Jacq.) Swartz extracts," *Food Chemistry*, vol. 97, no. 3, pp. 452–458, 2006.
- [23] A. Kumaran and R. Joel Karunakaran, "In vitro antioxidant activities of methanol extracts of five *Phyllanthus* species from India," *Food Science and Technology*, vol. 40, no. 2, pp. 344–352, 2007.
- [24] B. O. Mbaebie, H. O. Edeoga, and A. J. Afolayan, "Phy to chemical analysis and antioxidants activities of aqueous stem bark extract of *Schotia latifolia* Jacq," *Asian Pacific Journal of Tropical Biomedicine*, vol. 2, no. 2, pp. 118–124, 2012.
- [25] L. I. Mensor, F. S. Menezes, G. G. Leitao et al., "Screening of Brazilian plants extracts for antioxidants activity by the use of DPPH free radical method," *Phytotherapy Research*, vol. 15, pp. 127–130, 2001.
- [26] F. Denizot and R. Lang, "Rapid colorimetric assay for cell growth and survival: modifications to the tetrazolium dye procedure giving improved sensitivity and reliability," *Journal of Immunological Methods*, vol. 89, no. 2, pp. 271–277, 1986.
- [27] T. Mosmann, "Rapid colorimetric assay for cellular growth and survival: application to proliferation and cytotoxicity assays," *Journal of Immunological Methods*, vol. 65, no. 1-2, pp. 55–63, 1983.
- [28] P. Maisuthisakul, R. Pongsawatmanit, and M. H. Gordon, "Antioxidant properties of Teaw (*Cratoxylum formosum* Dyer) extract in soybean oil and emulsions," *Journal of Agricultural and Food Chemistry*, vol. 54, no. 7, pp. 2719–2725, 2006.
- [29] P. Maisuthisakul, S. Pasuk, and P. Ritthiruangdej, "Relationship between antioxidant properties and chemical composition of some Thai plants," *Journal of Food Composition and Analysis*, vol. 21, no. 3, pp. 229–240, 2008.
- [30] H. Kolodziej and A. F. Kiderlen, "Antileishmanial activity and immune modulatory effects of tannins and related compounds on *Leishmania* parasitised RAW 264.7 cells," *Phytochemistry*, vol. 66, no. 17, pp. 2056–2071, 2005.
- [31] T. Nakagawa and T. Yokozawa, "Direct scavenging of nitric oxide and superoxide by green tea," *Food and Chemical Toxicology*, vol. 40, no. 12, pp. 1745–1750, 2002.
- [32] V. Schulz, R. Hansel, and V. Tyler, *Fitoterapia Racional Um Guia de Fitoterapia Para as ciencias da saude*, Manole, Barueri, Brazil, 2002.
- [33] S. D. Kapu, Y. B. Ngwai, O. Kayode, P. A. Akah, C. Wambebe, and K. Gamaniel, "Anti-inflammatory, analgesic and anti-lymphocytic activities of the aqueous extract of *Crinum giganteum*," *Journal of Ethnopharmacology*, vol. 78, no. 1, pp. 7–13, 2001.
- [34] G. Francis, Z. Kerem, H. P. S. Makkar, and K. Becker, "The biological action of saponins in animal systems: a review," *British Journal of Nutrition*, vol. 88, no. 6, pp. 587–605, 2002.

- [35] R. Xu, W. Zhao, J. Xu, B. Shao, and G. Qin, "Studies on bioactive saponins from Chinese medicinal plants," *Advances in Experimental Medicine and Biology*, vol. 404, pp. 371–382, 1996.
- [36] J. A. Manthey, N. Guthrie, and K. Grohmann, "Biological properties of citrus flavonoids pertaining to cancer and inflammation," *Current Medicinal Chemistry*, vol. 8, no. 2, pp. 135–153, 2001.
- [37] P. Hendra, Y. Fukushi, and Y. Hashidoko, "Synthesis of benzophenone glucopyranosides from *Phaleria macrocarpa* and related benzophenone glucopyranosides," *Bioscience, Biotechnology and Biochemistry*, vol. 73, no. 10, pp. 2172–2182, 2009.
- [38] A. Rabia, Z. B. A. Mohammad, D. Aidiahmad, S. Amirin, and I. U. Muhammad, "Phytochemistry and medicinal properties of *Phaleria macrocarpa* (Scheff.) Boerl. extracts," *Pharmacognosy Review*, vol. 7, no. 13, pp. 73–80, 2013.
- [39] A. Saufi, C. B. I. Von Heimendahl, A. W. Alfermann, and E. Fuss, "Stereochemistry of lignans in *Phaleria macrocarpa* (Scheff.) Boerl.," *Zeitschrift fur Naturforschung C*, vol. 63, no. 1-2, pp. 13–16, 2008.
- [40] S. C. Chong, M. A. Dollah, P. P. Chong, and A. Maha, "*Phaleria macrocarpa* (Scheff.) Boerl fruit aqueous extract enhances LDL receptor and PCSK9 expression in vivo and in vitro," *Journal of Ethnopharmacology*, vol. 137, no. 1, pp. 817–827, 2011.
- [41] R. R. Tjandrawinata, D. Nofiarny, L. W. Susanto, P. Hendra, and A. Clarissa, "Symptomatic treatment of premenstrual syndrome and/or primary dysmenorrhea with DLBS1442, a bioactive extract of *Phaleria macrocarpa*," *International Journal of General Medicine*, vol. 4, pp. 465–476, 2011.
- [42] R. Hendra, S. Ahmad, E. Oskoueian, A. Sukari, and M. Y. Shukor, "Antioxidant, anti-inflammatory and cytotoxicity of *Phaleria macrocarpa* (Boerl.) Scheff fruit," *BMC Complementary and Alternative Medicine*, vol. 11, article 110, 2011.
- [43] D. Kurnia, K. Akiyama, and H. Hayashi, "29-Norcucurbitacin derivatives isolated from the Indonesian medicinal plant, *Phaleria macrocarpa* (Scheff.) Boerl.," *Bioscience, Biotechnology and Biochemistry*, vol. 72, no. 2, pp. 618–620, 2008.
- [44] S. Oshimi, K. Zaima, Y. Matsuno et al., "Studies on the constituents from the fruits of *Phaleria macrocarpa*," *Journal of Natural Medicines*, vol. 62, no. 2, pp. 207–210, 2008.
- [45] C. Sanchez-Moreno, J. A. Larrauri, and F. Saura-Calixto, "A procedure to measure the antiradical efficiency of polyphenols," *Journal of the Science of Food and Agriculture*, vol. 76, pp. 270–276, 1998.
- [46] Y. Andriani, M. A. W. Effendy, T. M. T. Sifzizul, and H. Mohamad, "Antibacterial, radical-scavenging activities and cytotoxic properties of *Phaleria macrocarpa* (Scheff.) Boerl. Leaves in HepG2 cell lines," *International Journal of Pharmaceutical Sciences and Research*, vol. 2, no. 7, pp. 1700–1706, 2011.
- [47] Y. Rohyami, "Penentuan Kandungan Flavonoid dari Ekstrak Metanol Daging Buah Mahkota Dewa (*Phaleria macrocarpa* Scheff Boerl.)," *Jurnal Logika*, vol. 5, 2009.
- [48] R. D. Petty, L. A. Sutherland, E. M. Hunter, and I. A. Cree, "Comparison of MTT and ATP-based assays for the measurement of viable cell number," *Journal of Bioluminescence and Chemiluminescence*, vol. 10, no. 1, pp. 29–34, 1995.
- [49] J. R. Sellers, S. Cook, and V. S. Goldmacher, "A cytotoxicity assay utilizing a fluorescent dye that determines accurate surviving fractions of cells," *Journal of Immunological Methods*, vol. 172, no. 2, pp. 255–264, 1994.

Research Article

Mitogenic Effects of Phosphatidylcholine Nanoparticles on MCF-7 Breast Cancer Cells

Yamila B. Gándola,¹ Sebastián E. Pérez,² Pablo E. Irene,¹ Ana I. Sotelo,¹
Johanna G. Miquet,¹ Gerardo R. Corradi,¹ Adriana M. Carlucci,² and Lorena Gonzalez¹

¹ Instituto de Química y Fisicoquímica Biológicas (UBA-CONICET), Facultad de Farmacia y Bioquímica, Junín 956, 1113 Buenos Aires, Argentina

² Departamento de Tecnología Farmacéutica, Facultad de Farmacia y Bioquímica, Junín 956, 1113 Buenos Aires, Argentina

Correspondence should be addressed to Lorena Gonzalez; lgonza74@yahoo.com.ar

Received 20 December 2013; Revised 14 February 2014; Accepted 14 February 2014; Published 20 March 2014

Academic Editor: Leandro Rocha

Copyright © 2014 Yamila B. Gándola et al. This is an open access article distributed under the Creative Commons Attribution License, which permits unrestricted use, distribution, and reproduction in any medium, provided the original work is properly cited.

Lecithins, mainly composed of the phospholipids phosphatidylcholines (PC), have many different uses in the pharmaceutical and clinical field. PC are involved in structural and biological functions as membrane trafficking processes and cellular signaling. Considering the increasing applications of lecithin-based nanosystems for the delivery of therapeutic agents, the aim of the present work was to determine the effects of phosphatidylcholine nanoparticles over breast cancer cellular proliferation and signaling. PC dispersions at 0.01 and 0.1% (w/v) prepared in buffer pH 7.0 and 5.0 were studied in the MCF-7 breast cancer cell line. Neutral 0.1% PC-derived nanoparticles induced the activation of the MEK-ERK1/2 pathway, increased cell viability and induced a 1.2 fold raise in proliferation. These biological effects correlated with the increase of epidermal growth factor receptor (EGFR) content and its altered cellular localization. Results suggest that nanoparticles derived from PC dispersion prepared in buffer pH 7.0 may induce physicochemical changes in the plasma membrane of cancer cells which may affect EGFR cellular localization and/or activity, increasing activation of the MEK-ERK1/2 pathway and inducing proliferation. Results from the present study suggest that possible biological effects of delivery systems based on lecithin nanoparticles should be taken into account in pharmaceutical formulation design.

1. Introduction

Lecithins are a mixture of phospholipids where phosphatidylcholines are the main components (up to 98% w/w). Egg or soy lecithin as well as purified phospholipids is used for pharmaceutical purposes as dispersing, emulsifying, and stabilizing agents included in intramuscular and intravenous injectables or parenteral nutrition [1–3]. Lecithins have been used to form liposomes, mixed micelles, and submicron emulsions for pharmaceutical purposes. Moreover, aqueous lecithin dispersions (water-lecithin-dispersion (WLD)) alone or in combination with cationic molecules have been proposed as carriers of lipophilic drugs and even as oligonucleotides delivery systems for cancer treatment [4, 5]. Actually, nanoparticles designed from lecithin-in-water emulsions were successfully used to deliver docetaxel to tumor cells

in vitro and even in a tumor model in mice [6]. Moreover, lecithin-based nanoparticles have demonstrated to deliver siRNA to breast cancer cells [7].

Phosphatidylcholines, the main components of lecithins, are glycerophospholipids that incorporate choline as the head group. The fatty acids bound to the glycerophosphatidic acid can vary but generally one of them is unsaturated and the other one is saturated. Phosphatidylcholine (PC) is a major constituent of the cell membranes which is more commonly found in the exoplasmic or outer leaflet of the plasma membrane. PC also plays a role in membrane-mediated cell signaling. The phospholipase D-mediated catabolism of PC yields phosphatidic acid (PA) and choline, which are important lipid second messengers involved in several signaling pathways [8–10]. PA binds to Raf-1 and promotes its recruitment to the plasma membrane where it is activated by direct

interaction with Ras [11, 12]. Ras-mediated Raf-1 activation leads to mitogen-activated protein kinase (MAPK) and PI3K/Akt activation [13]. Therefore, PA would have a pivotal role in the amplification of signaling cascades required for survival and growth [14]. PA also binds the mammalian target of rapamycin (mTOR), a protein kinase that regulates cell cycle progression and cell growth regulating several cellular events like translation, transcription, membrane trafficking, and protein degradation [15].

Phosphatidylcholine is also a substrate of the phosphatidylcholine-specific phospholipase C (PC-PLC). This enzyme has been implicated in proliferation, differentiation, and apoptosis of mammalian cells. PC-PLC-mediated hydrolysis of PC yields PC-derived diacylglycerol (DAG) and phosphocholine (P-chol) [8, 16]. DAG and P-chol, in turn, activate a variety of kinases involved in cell proliferation, including MAPKs, in different cell types [17, 18].

The lipid second messengers PA and DAG that are generated as a result of PLD and PC-PLC activity, respectively, can also affect membrane trafficking, directly by altering membrane curvature or indirectly by recruiting and/or activating signaling mediators [19]. PLD-derived PA has been linked to vesicular trafficking processes including Golgi transport, endocytosis, and exocytosis [19]. Moreover, aberrant phosphatidylcholine metabolism in cancer cells was reported to downmodulate the membrane expression of specific receptors or proteins relevant for cell proliferation and survival [20, 21]. Particularly, inhibition of phosphatidylcholine-specific phospholipase C downregulates Human Epidermal Growth Factor Receptor 2 (HER2) overexpression on plasma membrane of breast cancer cells [21]. Likewise, membrane phospholipid composition was demonstrated to affect epidermal growth factor receptor (EGFR) endocytosis [22]. Lipid composition not only affects EGFR trafficking but also has relevant regulatory effects on its kinase domain activation and signaling [22, 23].

Membrane phospholipids as well as their fatty acid profile are altered in tumor cells. The choline metabolite profile of cancer cells is characterized by an elevation of phosphocholine and total choline-containing compounds. Indeed, total cellular phosphatidylcholine (PC) can be used as a marker for membrane proliferation in neoplastic mammary gland tissues [24] or as a predictive biomarker for monitoring tumor response [25].

Phosphatidylcholines are therefore not inert vehicles but biological active compounds; phospholipids and their derived second messengers are involved in cell proliferation and trafficking, and the increase of phosphocholine and choline-containing compounds has been described in tumor cells. It has been recently highlighted that certain excipients have a role as active pharmaceutical components of formulations because they can modify the pharmacological activity of an active drug or produce biological effects [26]. Considering that phosphatidylcholines are the main components of lecithins and taking into account the increasing applications of lecithin-based formulations in nanomedicine and for the delivery of antineoplastic agents, the aim of the present work was to determine the biological effects of phosphatidylcholine nanoparticles over breast cancer cell signaling and proliferation.

2. Material and Methods

2.1. Reagents. Purified phosphatidylcholine from soybean lecithin (Phospholipon 90G, CAS-number 97281-47-5) was purchased from Lipoid (Ludwigshafen, Germany). Trizma base, HEPES, Tween 20, Triton X-100, sodium dodecyl sulfate (SDS), glycine, ammonium persulfate, aprotinin, phenylmethylsulfonyl fluoride (PMSF), sodium orthovanadate, 2-mercaptoethanol, Hoechst 33258, and BSA-fraction V were obtained from Sigma Chemical Co. (St. Louis, MO, USA). PVDF membranes, high performance chemiluminescence film, and enhanced chemiluminescence- (ECL-) Plus are from Amersham Biosciences (GE Healthcare, Piscataway, NY, USA). Mini-Protean apparatus for SDS-polyacrylamide electrophoresis, miniature transfer apparatus, acrylamide, bis-acrylamide, and TEMED were obtained from Bio-Rad Laboratories (Hercules, CA, USA). Anti-EGFR (1005) antibody and secondary antibodies conjugated with HRP were purchased from Santa Cruz Biotechnology Laboratories (Santa Cruz, CA, USA). Antibodies anti-phospho-mTOR Ser2448, anti-mTOR, anti-p44/42 MAP kinase (ERK 1/2), and anti-phospho-p44/42 MAP kinase Thr202/Tyr204 were from Cell Signaling Technology Inc. (Beverly, MA, USA). Cy3-conjugated secondary antibody against rabbit polyclonal immunoglobulins was from Jackson ImmunoResearch Laboratories, Inc. Bicinchoninic acid (BCA) protein assay kit was obtained from Thermo Scientific, Pierce Protein Research Products (Rockford, IL, USA).

2.2. Preparation of Phosphatidylcholine Nanoparticles. Dispersions of Phospholipon 90G 0.01 and 0.1% (w/v) in two different diluents (66 mM isotonic phosphate buffer pH 7.0 and 50 mM isotonic acetate buffer pH 5.0) were prepared. Buffers were isotonized by adding sodium chloride when necessary according to Sørensen and White-Vincent methods. Phosphatidylcholine was first dispersed in the appropriate diluent with means of extensive mixing at 60°C by use of a thermostated magnetic stirrer in order to obtain good hydration. Next, the dispersion was stirred for 2 minutes at the same temperature with a high-shear mixer (Ultra-Turrax T18 basic, IKA Werke, Staufen, Germany) and sonicated at 20 kHz for 10 minutes. It was then sterilized by autoclaving (121°C, 15 minutes). The sizes of the resulting particles in the dispersions were determined by photon correlation spectroscopy (PCS) using a Zetasizer (Malvern Nano ZS, Malvern Instruments Ltd., UK). The zeta potential of the samples was measured by the same instrument and the zeta potential values were calculated according to Smoluchowski equation (Table 1). As shown in Table 1, particles in the range of the nanometric size were obtained.

2.3. Cell Culture. MCF-7 human breast cancer cell line was obtained from the American Type Culture Collection (ATCC) (Rockville, MD, USA). Cells were maintained in Dulbecco's minimum essential medium (DMEM) supplemented with 10% fetal bovine serum (FBS), 50 µg/mL gentamycin (Invitrogen, Life technology), and 2 mM L-glutamine (Invitrogen, Life technology). Cells were cultured in 75 cm² culture flasks at 37°C in a humidified atmosphere of 5% CO₂.

TABLE 1: Effect of pH on the particle size and zeta potential of the phosphatidylcholine nanoparticles.

Formulation	Particle size (d .nm) \pm SD	PdI	Z-Pot (mV) \pm SD
pH 5.0	232.7 \pm 19.6	0.494	13.8 \pm 2.1
pH 7.0	189.1 \pm 11.9	0.544	-40.3 \pm 3.0

d .nm: diameter expressed in nm; PdI: polydispersion index.

Phosphatidylcholine (PC) nanoparticles were prepared in pH 5.0 and pH 7.0 buffers and analyzed by Dynamic Light Scattering (DLS). The size and zeta potential of the particles were measured and reported as mean \pm S.E.M. ($n = 4$).

2.4. Culture Cells Treatment. To perform immunoblotting assays, cells were seeded in clear 6-well plates (Corning Costar, Fisher Scientific, USA) at a density of 300,000 cells/well, while for immunofluorescence assays cells were seeded at a density of 20,000 cells/well in covers placed in 24-well plates. Phosphatidylcholine nanoparticles at 0.1 and 0.01% were added in the presence or absence of serum. Cells were further incubated at 37°C for 24 hours in a 5% CO₂ atmosphere. After incubation, cells were washed with phosphate saline buffer and dishes were kept at -80°C until cell solubilization to prepare cells extracts, while covers were immediately processed for specific immunofluorescence labeling.

2.5. Preparation of Cell Extracts and Immunoblotting. Cells were homogenized in buffer composed of 1% v/v Triton, 0.1M Hepes, 0.1M sodium pyrophosphate, 0.1M sodium fluoride, 0.01M EDTA, 0.01M sodium vanadate, 0.002M PMSE, and 0.035 trypsin inhibitory units/mL aprotinin (pH 7.0) at 4°C. Cell homogenates were centrifuged at 15,000 \times g for 40 minutes at 4°C to remove insoluble material. Protein concentration of supernatants was determined by the BCA protein assay kit. Equal protein aliquots of solubilized cells were diluted in Laemmli buffer, boiled for 5 minutes, and stored at -20°C until electrophoresis.

Samples were subjected to electrophoresis in SDS-polyacrylamide gels. Electrotransference of proteins from gel to PVDF membranes and incubation with antibodies were performed as already described [27]. Immunoreactive proteins were revealed by enhanced chemiluminescence. Band intensities were quantified using Gel-Pro Analyzer 4.0 software (Media Cybernetics, Silver Spring, MD, USA).

To reprobe with other antibodies, the membranes were washed with acetonitrile for 10 minutes and then incubated in stripping buffer (2% w/v SDS, 0.100 M 2-mercaptoethanol, 0.0625 M Tris/HCl, pH 6.7) for 40 minutes at 50°C while shaking, washed with deionized water, and blocked with BSA.

2.6. Cell Viability Assay. Cells were seeded in clear 96-well plates (Corning Costar, Fisher Scientific, USA) at a density of 10,000 cells/well. Phosphatidylcholine at 0.1 and 0.01% was added in 100 μ L of medium in the presence or absence of serum. Cells were further incubated at 37°C for 24 and 48 hours in a 5% CO₂ atmosphere. After incubation with the phosphatidylcholine nanoparticles, cell number was evaluated using the CellTiter 96 aqueous nonradioactive cell proliferation assay (Promega, Madison, WI, USA). Triplicates were run for each treatment. Values were expressed in terms of percent of untreated control cells.

2.7. BrdU Incorporation Assay. DNA synthesis in proliferating cells was determined by measuring BrdU incorporation with a BrdU ELISA assay [28]. For this purpose, the cells were seeded in 96-well culture plates at a density of 10,000 cells/well. Phosphatidylcholine nanoparticles at 0.1 and 0.01% were added in 100 μ L of medium in absence of serum. Cells were further incubated at 37°C for 48 hours in a 5% CO₂ atmosphere. BrdU (0.01 M final concentration) was added to the cells 16 hs before the end of incubation with PC nanoparticles. At the conclusion of labeling, cultures were rinsed with phosphate buffered saline (PBS), pH 7.0, fixed with 70% EtOH, denatured with 2 M HCl (100 μ L/well, 10 minutes, 37°C), and neutralized with 0.1 M Trizma buffer, pH 9. Cells were then incubated with monoclonal anti-BrdU antibody (50 μ L/well; 1 μ g/mL final; Roche, USA) at 37°C for 60 minutes, washed with PBS, and incubated with goat anti-mouse IgG horseradish peroxidase (HRP) conjugate at 37°C for 30 minutes. Afterwards, cells were washed and labeling evidenced with tetramethylbenzidine (TMB). Triplicates were run for each treatment. Values were expressed in terms of percent of untreated control cells.

2.8. Immunofluorescence. Cells were washed twice in PBS, pH 7.0, fixed in 2% formaldehyde in PBS for 10 minutes at room temperature. After three washes with PBS (5 minutes each), fixed cells were permeabilized with 0.5% Triton X-100 in PBS for 15 minutes and incubated in blocking solution (10% FBS in PBS) for 30 minutes to decrease nonspecific binding of the antibodies. Cells were then incubated for 1 hour at 37°C with anti-EGFR, then washed, and incubated with Cy3-conjugated secondary antibody against rabbit polyclonal immunoglobulins. After a final washing step (3 washes 5 minutes each in PBS), cells were incubated with Hoechst 33258 (2 μ g/mL) for ten minutes. Finally, covers were mounted on glass slides and fluorescence stained cells were imaged by epifluorescent microscopy on a Leica DM2000 with a \times 40 objective (Numerical Aperture =0.65) or by an Olympus Fluoview FV1000 spectral laser scanning confocal microscope with a \times 60 oil immersion objective (Numerical Aperture =1.35) using dual excitation (473 nm for Cy3 and 405 nm for Hoesch). At least 10 fields were examined and representative images were photographed.

2.9. Statistical Analysis. Experiments were performed analyzing the phosphatidylcholine dispersions and vehicle (control) in parallel, n representing the number of different experiments. Results are presented as mean \pm S.E.M. Statistical analyses were performed by ANOVA followed by the Newman-Keuls Multiple Comparison Test using the GraphPad Prism 4 statistical program by GraphPad Software, Inc. (San Diego, CA, USA). Data were considered significantly different if $P < 0.05$.

3. Results

3.1. Phosphatidylcholine Nanoparticles Activate Cell Signaling Molecules Involved in Cell Proliferation. Previous results from our research group have demonstrated that nanoparticles prepared from phosphatidylcholine dispersed at 0.01 and

0.1% (w/v) in buffer pH 5.0 and buffer pH 7.0 are able to bind oligonucleotides and deliver them to breast cancer cells [7]. To determine oligonucleotide internalization, transfection experiments were performed either in absence or presence of serum and after a 24-hour incubation period [7]. That study suggested that lecithin-based delivery systems might represent feasible novel formulations for anticancer gene therapies. However, phosphatidylcholines, the main components of lecithin, are involved in several biological processes like cell proliferation and dynamics of the cell membrane. To ascertain if PC nanoparticles have *per se* promitogenic activity, the effects of phosphatidylcholine-based nanoparticles over signal transduction pathways involved in cell proliferation and survival were studied in the previously described experimental conditions [7]. Considering that PC-derived second messengers are involved in the activation of cellular signaling mediators like mTOR and MAPKs [9, 29, 30], activation of the Akt-mTOR and MEK1/2-ERK1/2 signaling pathways by phosphatidylcholine was analyzed in the MCF-7 breast cancer cell line.

3.1.1. Akt and mTOR Phosphorylation and Protein Content.

Akt is activated by many types of cellular stimuli and regulates fundamental cellular functions such as transcription, translation, proliferation, growth, and survival. Its dysregulation has been associated with the development of diseases such as cancer [31, 32]. Akt phosphorylation and protein content of MCF-7 cells previously treated with aqueous phosphatidylcholine dispersions were analyzed by western blotting. Akt phosphorylation at Ser473, an activating residue, was not statistically different in control and treated cells neither in absence (Figure 1(a)) nor in presence (Figure 1(b)) of serum. Incubation with phosphatidylcholine had no effects on Akt protein content from MCF-7 cells (Figures 1(a) and 1(b)).

Mammalian target of rapamycin complex is a Ser/Thr kinase of the phosphatidylinositol 3-kinase-related kinase protein family. Akt phosphorylates and activates mTOR, thus inducing protein synthesis and cell growth [15, 33]. mTOR activation and protein content were studied by western blotting in cells treated with phosphatidylcholine nanoparticles (Figures 1(c) and 1(d)). Resembling the results obtained for Akt, mTOR phosphorylation was not induced by PC either in absence or in presence of serum, even when cells were incubated with the highest concentrations of phosphatidylcholine dispersions (Figures 1(c) and 1(d)).

3.1.2. MEK and ERK 1/2 Phosphorylation and Protein Content.

The Ras/Raf/MEK/ERK cascade couples signals from cell surface receptors to transcription factors, which can regulate cell cycle progression, apoptosis, or differentiation [34]. This signaling cascade is often activated in certain tumors by chromosomal translocations, mutations in cytokine receptors, or overexpression of wild type or mutated receptors.

MAP kinase kinase (MEK) is a dual-specificity kinase that phosphorylates tyrosine and threonine residues on extracellular-signal-regulated kinases 1 and 2 (ERK 1/2) [35]. Two related genes encode MEK1 and MEK2. Under basal conditions, MEK binds the inactive serine/threonine kinase ERK

and restricts it to the cytosol. The MEK/ERK complex dissociates when MEK is activated and phosphorylates ERK, which may then dimerize. An activated ERK dimer can regulate targets in the cytosol and also translocate to the nucleus where it phosphorylates a variety of transcription factors regulating gene expression.

Phosphorylation of MEK1/2 and ERK1/2 was studied in the MCF-7 cells incubated with PC nanoparticles. Results showed that MEK1/2 and ERK1/2 phosphorylation was significantly increased when cells were treated with phosphatidylcholine dispersed in pH 7.0 solution at high concentration independently of the absence (Figures 2(a) and 2(c)) or presence (Figures 2(b) and 2(d)) of serum. PC nanoparticles dispersed in buffer pH 7.0 at low concentration (0.01%) showed a slight tendency to stimulate ERK1/2 phosphorylation; however, this difference did not achieve statistical significance (Figures 2(a) and 2(b)). MEK1/2 and ERK1/2 protein levels did not vary either in absence or in presence of serum.

3.2. Phosphatidylcholine Nanoparticles Induce MCF-7 Cell Proliferation.

As it was previously mentioned, MEK1/2-ERK 1/2 signaling pathway is involved in cell growth and proliferation promotion, so the effects of phosphatidylcholine nanoparticles over breast cancer cell viability were studied. For this purpose, MCF-7 cells were seeded in 96-well plates and incubated during 24 hours (Figures 3(a) and 3(b)) or 48 hours (Figures 3(c) and 3(d)) with phosphatidylcholine dispersed at 0.1 and 0.01% in the absence (Figures 3(a) and 3(c)) or presence (Figures 3(b) and 3(d)) of serum. Results showed that only high concentration of PC nanoparticles dispersed in buffer pH 7.0 significantly increased cell viability of MCF-7 breast cancer cells either in absence (Figures 3(a) and 3(c)) or presence of serum (Figures 3(b) and 3(d)) at both time periods. Phosphatidylcholine dispersed in buffer pH 5.0 or in buffer pH 7.0 at low concentration (0.01%) had moderate effects on cell viability but results were not statistically significant (Figure 3).

To ascertain if the increased cell viability induced by phosphatidylcholine nanoparticles 0.1% at pH 7.0 was a consequence of cell proliferation induction, BrdU incorporation assay was performed. Considering that the differences between viability of basal cells and PC-treated cells were better evidenced when cells were treated in the medium without serum, BrdU incorporation was assessed after 48 hours of treatment with phosphatidylcholine nanoparticles in absence of serum. Results demonstrated that increased cell viability correlated with increased incorporation of BrdU (Figure 4). When fold induction of BrdU incorporation was calculated it was observed that PC 0.1% at pH 7.0 induces a 20% increment in cell proliferation (Figure 4(b)).

The effects of phosphatidylcholine 0.1% dispersed in buffer pH 7.0 over MCF-7 cell proliferation correlated with the increased phosphorylation levels observed for MEK 1/2 and ERK1/2. Results suggest that high concentration of phosphatidylcholine nanoparticles at pH 7.0 induces activation of the MEK1/2-ERK1/2 pathway and cell proliferation of the breast cancer cells.

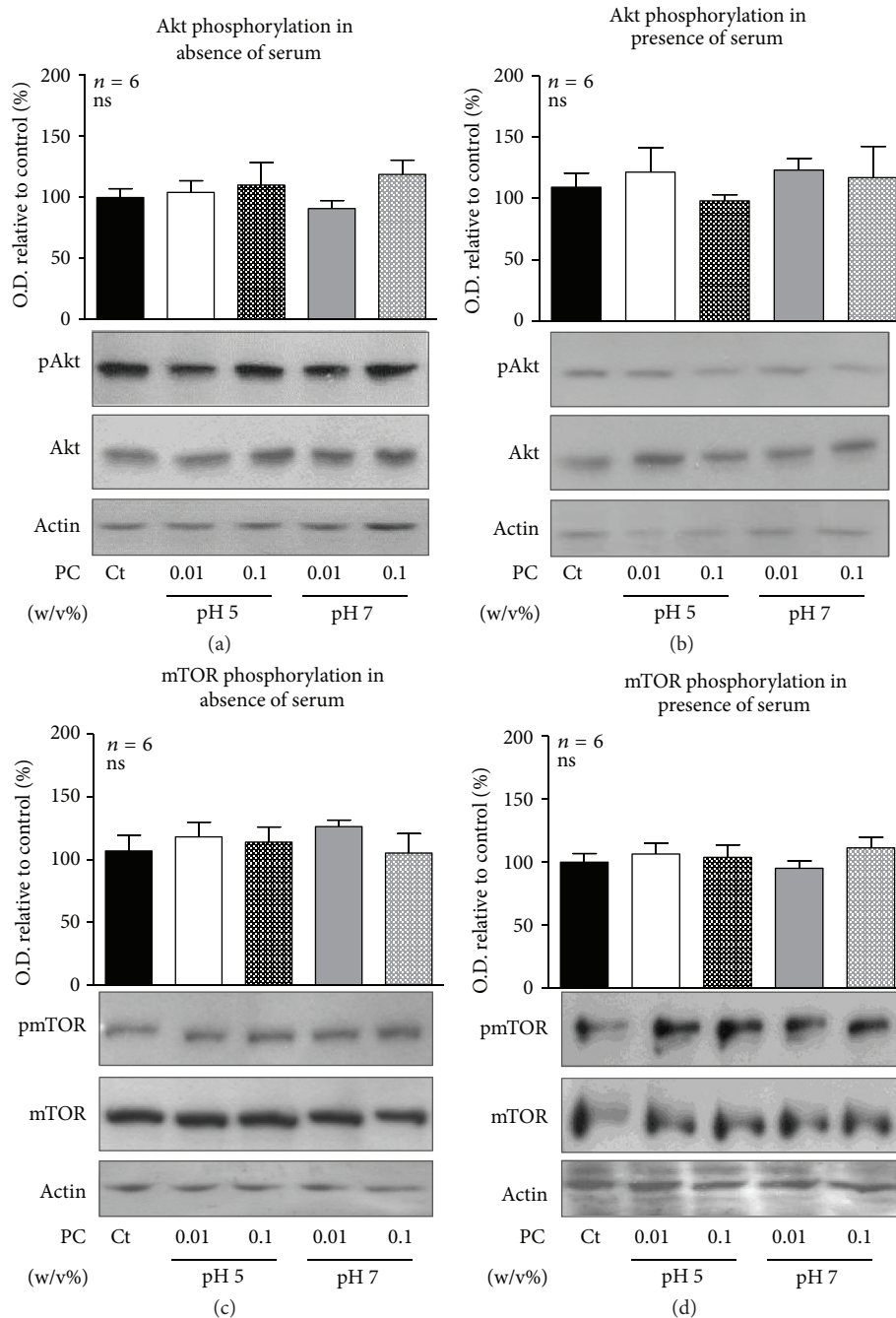


FIGURE 1: Akt and mTOR phosphorylation and protein content. MCF-7 breast cancer cells were incubated for 24 hs with PC nanoparticles dispersed at 0.1 and 0.01% (w/v) in buffer pH 5.0 and buffer pH 7.0 or vehicle (Ct) in the absence ((a) and (c)) or presence ((b) and (d)) of serum. Representative results of immunoblots with anti-Akt and anti-phospho-Akt S473 ((a) and (b)) and anti-mTOR and anti-phospho-mTOR S2448 ((c) and (d)) are shown. Reprobing with anti-actin antibody demonstrated uniformity of protein loading in all lanes. Quantification of phosphorylated proteins was performed by scanning densitometry and expressed as percent of values measured for control, nonstimulated breast cancer cells (Ct). Data are expressed as the mean \pm S.E.M. of the indicated number (*n*) of different experiments. Statistical analysis was performed by ANOVA.

3.3. EGFR Levels Are Increased in Breast Cancer Cells Treated with High Concentration of Phosphatidylcholine Nanoparticles. Molecular aspects of cell signaling are controlled by receptor/ligand localization and trafficking [36, 37]. Endocytosis and subsequent delivery of endosomal cargos to lysosomes are essential for the degradation of many membrane-associated proteins [38–40]. This process determines the

amplitude of growth factor signaling, and it is therefore tightly regulated.

As previously mentioned, PC and second messengers derived from these phospholipids are fundamental components of the cell membrane and affect its dynamics and protein trafficking. Particularly, previous studies have demonstrated that phospholipid membrane composition affects

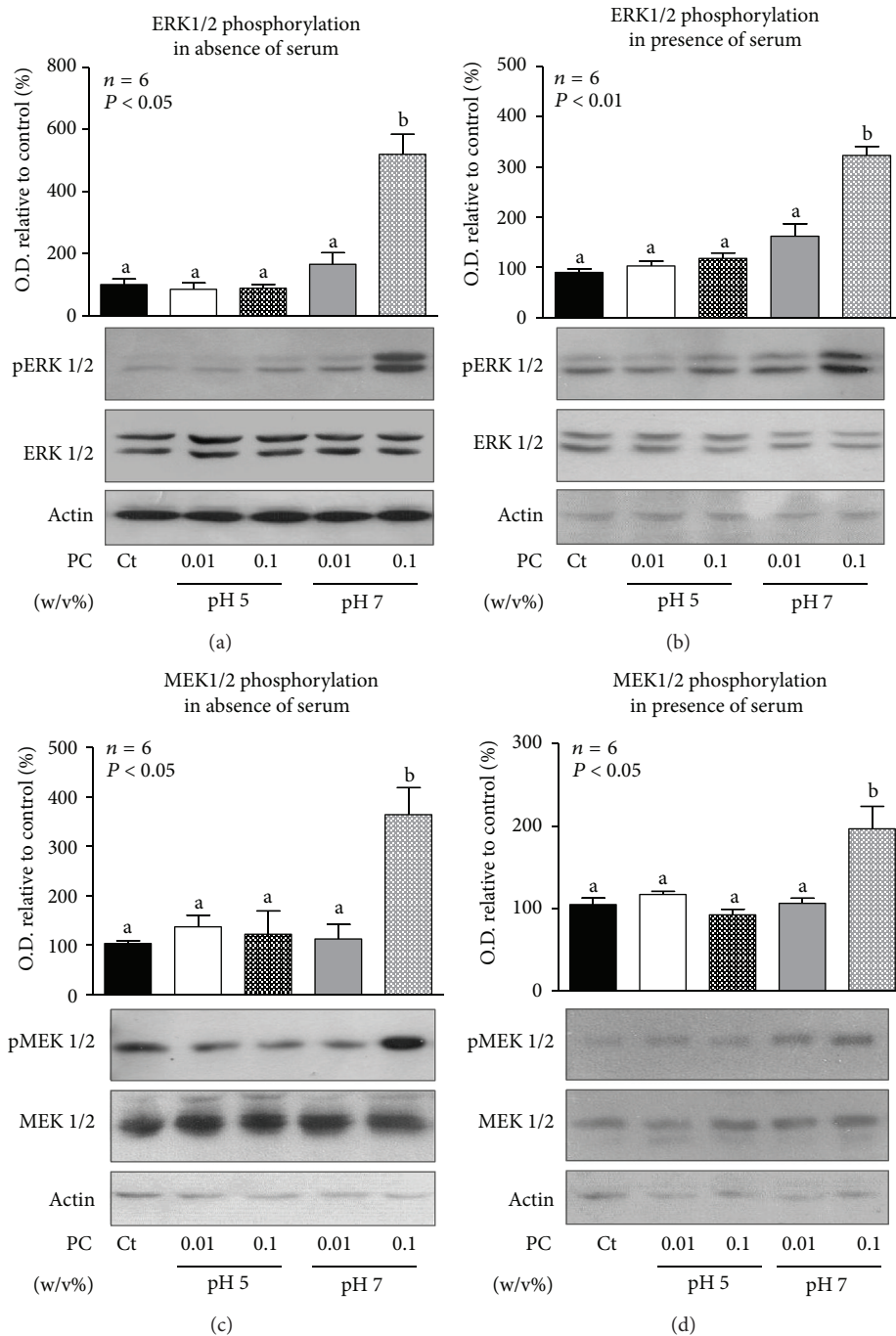


FIGURE 2: ERK1/2 and MEK1/2 phosphorylation and protein content. MCF-7 breast cancer cells were incubated for 24 hs with PC nanoparticles dispersed at 0.01 and 0.01% (w/v) in buffer pH 5.0 and buffer pH 7.0 or vehicle (Ct) in absence ((a) and (c)) or presence ((b) and (d)) of serum. Representative results of immunoblots with anti-p44/42 MAP kinase (ERK1/2) and anti-phospho-p44/42 MAP kinase Thr202/Tyr204 ((a) and (b)) and anti-MEK1/2 and antiphospho MEK ((c) and (d)) are shown. Reprobing with anti-actin antibody demonstrated uniformity of protein loading in all lanes. Quantification of phosphorylated proteins was performed by scanning densitometry and expressed as percent of values measured for control, nonstimulated breast cancer cells (Ct). Data are expressed as the mean \pm S.E.M. of the indicated number (n) of different experiments. Statistical analysis was performed by ANOVA. Different letters denote significant difference at $P < 0.05$, whereas results with the same letter are not statistically different from each other.

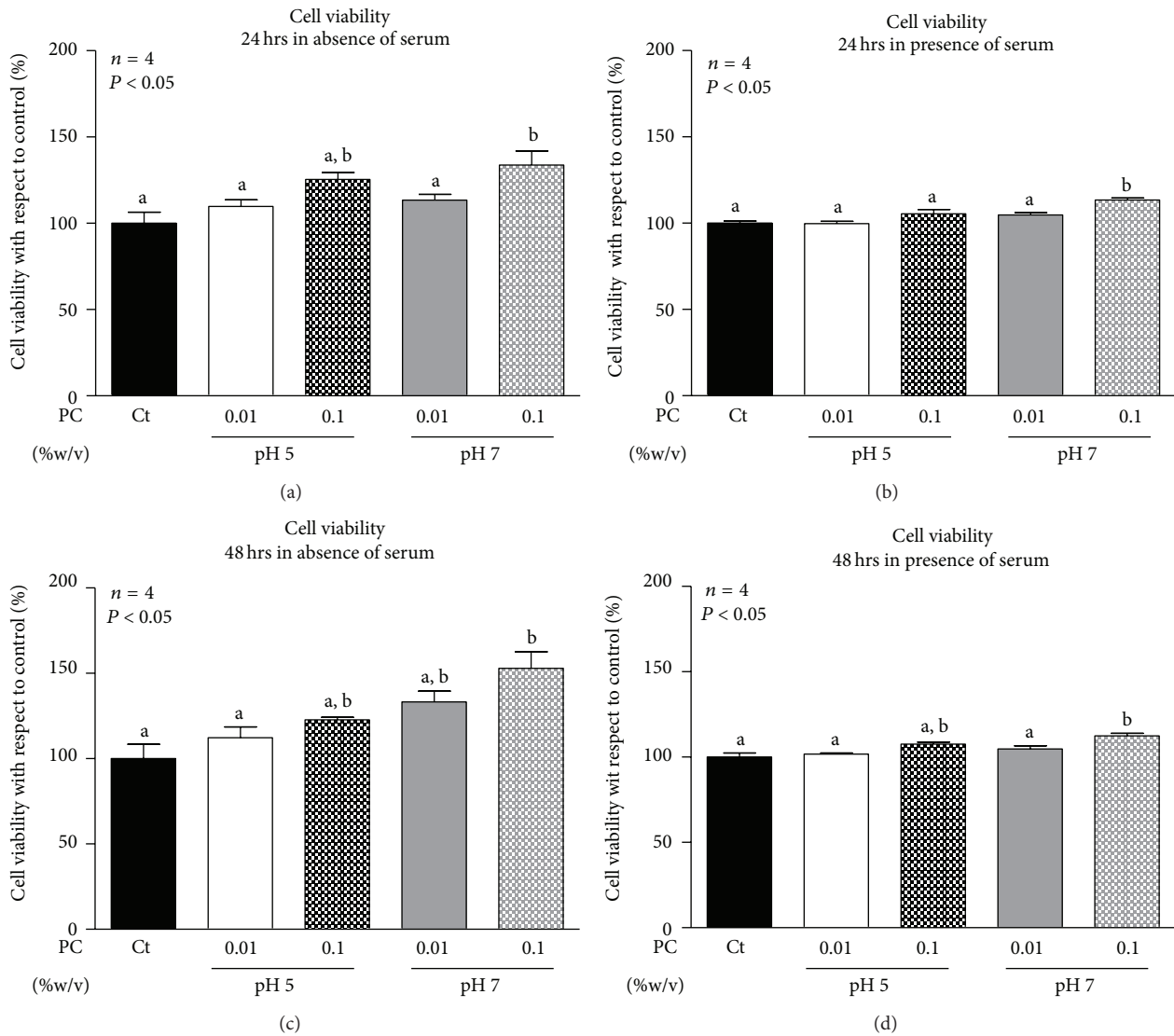


FIGURE 3: Viability of MCF-7 breast cancer cells incubated with phosphatidylcholine (PC) nanoparticles. Breast cancer cells were incubated for 24 hours ((a) and (b)) and 48 hours ((c) and (d)) with PC nanoparticles dispersed at 0.01 and 0.1% (w/v) or vehicle (Ct) in buffer pH 5.0 and buffer pH 7.0 in the absence ((a) and (c)) or the presence ((b) and (d)) of serum. After incubation, cell viability was evaluated using the CellTiter 96 aqueous nonradioactive cell proliferation assay (Promega). Triplicates were run for each treatment. Values were expressed in terms of percent of untreated control cells set as 100%. Data are expressed as the mean \pm S.E.M. of the indicated number (*n*) of independent experiments. Statistical analysis was performed by ANOVA. Different letters denote significant difference at $P < 0.05$, whereas results with the same letter are not statistically different from each other.

EGF receptor endocytosis and signaling [22, 23]. When purified EGFR was reconstituted into proteoliposomes of specific lipid compositions, the lipid environment did not affect EGF binding but EGFR tyrosine kinase function was indeed modified [23]. Moreover, mutants in the *Drosophila* phosphocholine cytidyltransferase 1 (CCT1), the rate-limiting enzyme in PC biosynthesis, result in altered phospholipid composition of cell membranes and affect the endocytic pathway of EGFR [22].

Endosomal trafficking of EGFR is crucial for determining the amplitude and duration of EGFR signaling. Actually, endocytosis of the EGFR is required for EGF-induced MAP kinase activation. This was evidenced in experiments in

which EGF induction of MAPKs was reduced in dynamin mutant cells which showed defects in clathrin-dependent receptor-mediated endocytosis [41]. Treatment of breast cancer cells with high concentration of phosphatidylcholine nanoparticles could affect membrane composition and consequently trafficking of EGFR and signaling through MAPKs. Therefore, EGFR levels were determined by western blotting and EGFR cellular localization was studied by immunofluorescence of cells treated with the PC nanoparticles.

Results showed that EGFR levels increased when cells were treated with PC nanoparticles dispersed in buffer pH 7.0 at high concentration both in absence or presence of serum (Figures 5(a) and 5(b)). Afterwards, immunofluorescence

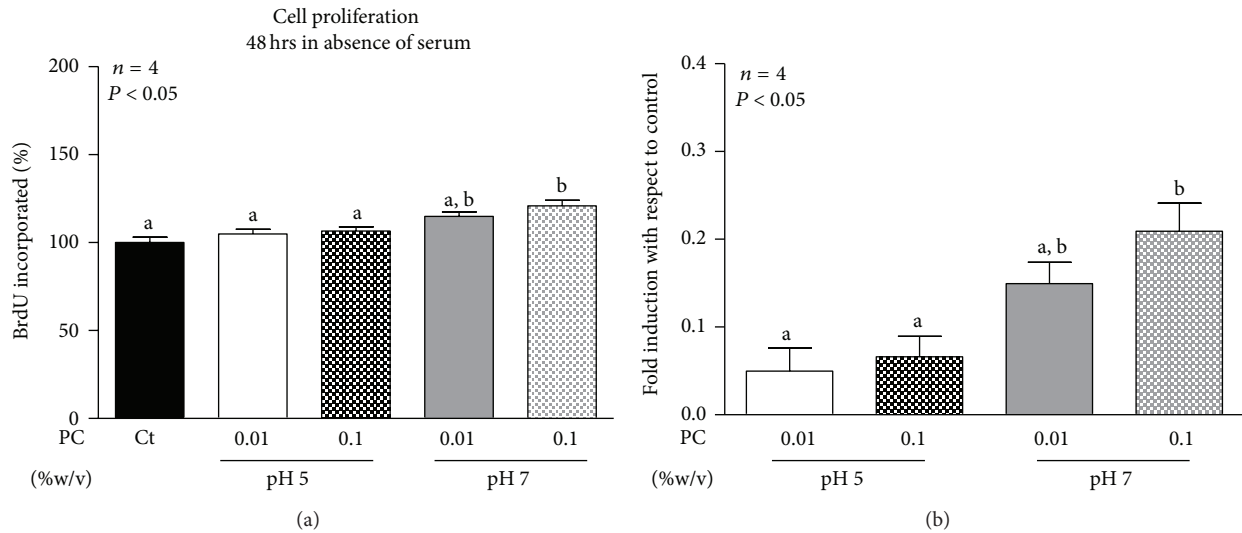


FIGURE 4: Proliferation of MCF-7 breast cancer cells incubated with phosphatidylcholine (PC) nanoparticles. Breast cancer cells were incubated for 48 hours with PC nanoparticle prepared in buffer pH 7.0 at 0.01 and 0.1% (w/v) or vehicle (Ct) in the absence of serum (a). Proliferation was determined by measuring BrdU incorporation with a BrdU ELISA. Triplicates were run for each treatment. Values were expressed in terms of percent of untreated control cells set as 100% (a). Data are expressed as the mean \pm S.E.M. of the indicated number (n) of independent experiments. Fold induction with respect to control was calculated (b). Statistical analysis was performed by ANOVA. Different letters denote significant difference at $P < 0.05$, whereas results with the same letter are not statistically different from each other.

studies were conducted to ascertain the cellular localization of increased EGFR in cells treated with PC 0.1% in pH 7.0. For comparison, EGFR-immunofluorescence was performed in control and phosphatidylcholine-treated cells. Observation of stained cells by epifluorescence microscopy showed that EGFR was uniformly distributed in control cells, while a significant proportion of PC-treated cells showed an increase in perinuclear EGFR staining (Figure 5(c)). However, PC-treated cells exhibited an increased percentage of rounded cells which might account for an increased proliferation rate. These morphological changes could explain the pattern of EGFR labeling observed when analyzed by epifluorescent microscopy. Therefore, confocal microscopy studies were performed to analyze possible alterations in EGFR cellular localization produced by treatment with PC nanoparticles (Figure 6). According to images obtained by epifluorescent microscopy, a significant proportion of PC-treated cells showed increased nuclear and perinuclear distribution of the EGFR (Figure 6).

4. Discussion

Despite the multiple and different uses of lecithin with pharmaceutical and therapeutic purposes, the possible biological consequences of phosphatidylcholine administration should be considered. They are important phospholipids involved not only in structural functions in the cell but also in membrane trafficking processes and signaling. Moreover, increased levels of phosphocholine and choline-containing compounds have been associated with progression and bad prognosis of tumors. Considering the increasing use of lecithin-based formulations for the delivery of antineoplastic agents, the biological effects of nanoparticles derived from

aqueous phosphatidylcholine dispersions over breast cancer cells proliferation and signaling were studied. Previously characterized phosphatidylcholine nanoparticles proposed as oligonucleotide delivery systems were used for that purpose [7]. Results showed that PC nanoparticles prepared in neutral buffer induced the activation of the MEK-ERK1/2 pathway and increased cell viability and proliferation of the MCF-7 breast cancer cell line. In accordance, Erkl/2 activation by phosphatidylcholine liposomes has been described to mediate neuronal differentiation [42, 43].

Incubation with the phosphatidylcholine nanoparticles prepared in neutral buffer was associated with increased EGFR content in the cancer cells and with its altered cellular localization. High phosphatidylcholine concentrations might induce physicochemical changes in the plasma membrane that affect receptor trafficking and turnover. Moreover, a process has been recently described, dependent on sustained stimulation of cPCK and PLD activities, that leads to EGFR sequestration near the perinuclear region, in the pericentron [44]. Accumulation of EGFR, reflected by increased EGFR content and perinuclear localization of the receptor, would result in increased activation of ERK1/2 and increased cell proliferation. Besides interfering with EGFR trafficking, PC nanoparticles might also have effects over EGFR activity [22, 23, 45]. Ligand-independent dimerization of EGFR occurs with reasonable frequency; however, it is not activated until the binding of the ligand. An autoinhibitory mechanism involving the EGFR C-terminal tail would explain the lack of activity of the dimer [45]. Interaction of phosphatidylcholine nanoparticles with inactive EGFR dimers could be proposed as a possible mechanism that disables such regulatory mechanisms and leads to EGFR activation even in absence of the specific ligand. Moreover, activation of the dimer involves

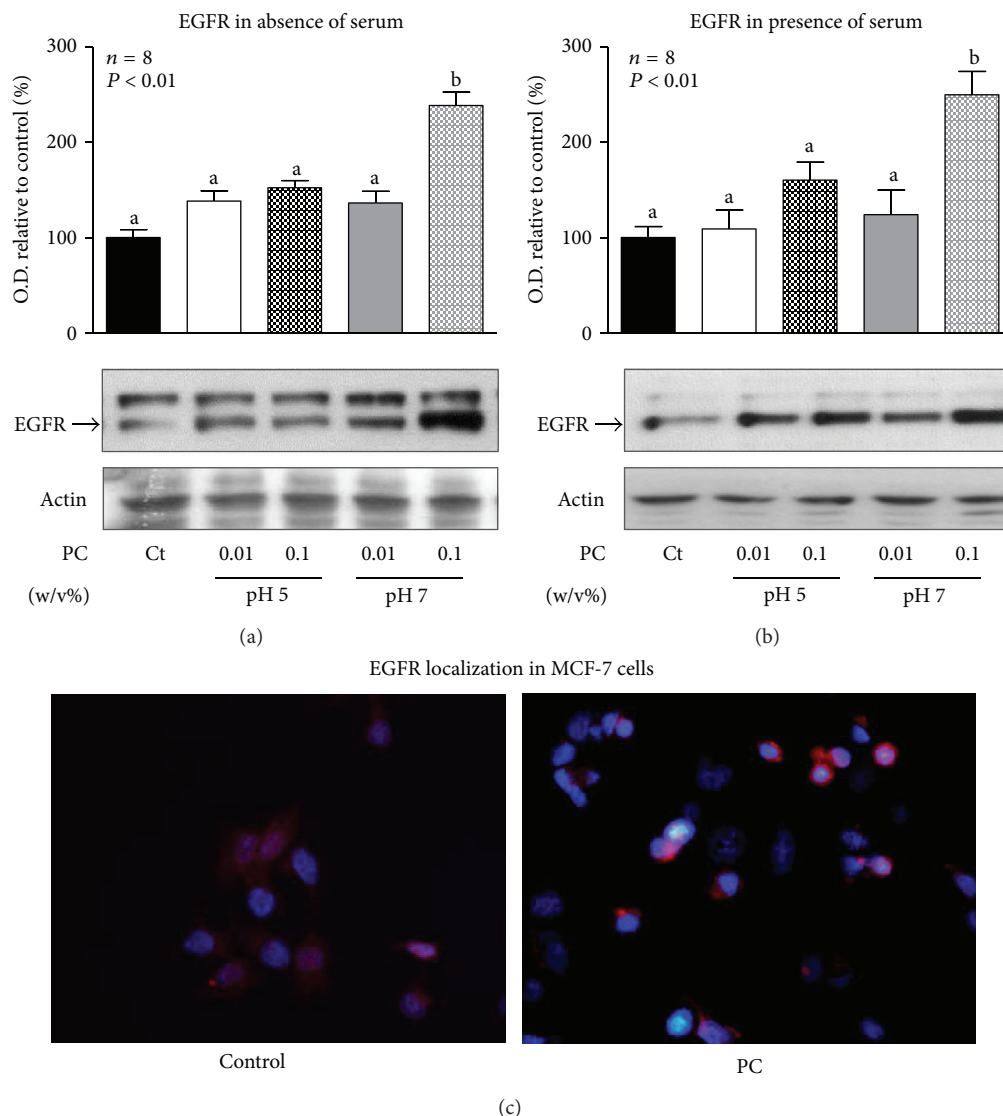


FIGURE 5: EGFR protein content and immunocytochemistry. MCF-7 breast cancer cells were incubated for 24 hours with PC nanoparticles dispersed at 0.1 and 0.01% (w/v) in buffer pH 5.0 and buffer pH 7.0 or vehicle (Ct) in absence (a) or presence (b) of serum for immunoblot studies, but only with PC dispersions at 0.1%, pH 7.0, or vehicle (control) in absence of serum for immunocytochemistry (c). Western blotting was performed as described in M & M. Membranes were re-probed to assess actin content and demonstrate equal protein loading in all lanes. Representative immunoblots are shown ((a) and (b)). EGFR quantification was performed by scanning densitometry and expressed as percent of values measured for control, nonstimulated breast cancer cells. Data are expressed as the mean \pm S.E.M. of the indicated number (*n*) of independent experiments. Statistical analysis was performed by ANOVA. Different letters denote significant difference at $P < 0.05$, whereas results with the same letter are not statistically different from each other. For EGFR immunocytochemistry (c), cells were washed, fixed, permeabilized, blocked, and incubated with the anti-EGFR antibody, the Cy3-conjugated secondary antibody, and Hoechst. Finally covers were mounted and examined by epifluorescence microscopy. Representative merged images of control and PC-nanoparticles-treated cells are shown (c).

reorganization of hydrophobic regions of the EGFR [46]; nanoparticles obtained from dispersed PC at buffer pH 7.0 might favor such reorganization facilitating the formation of the active conformation.

Increased concentration of phosphatidylcholine nanoparticles dispersed in buffer pH 7.0 had significant effects over cell proliferation, EGFR levels, and activation of the MEK1/2-ERK1/2 pathways; however, such effects were not observed for PC nanoparticles dispersed in pH 5.0 buffer. The main differences between both PC preparations is the charge

associated with the particles (zeta potential) (Table 1) and the final adopted form [7], while the size of the particles did not show important differences (Table 1). The nanoparticles were in the range of 180–250 nm for all the studied conditions (Table 1). At pH 5.0, small, isolated particles with irregular shape were observed while at pH 7.0 more elongated, locally cylindrical structures were described [7]. As expected, the zeta potential of the particles was positive when using pH 5.0 buffer as diluent and negative when using pH 7.0 buffer (Table 1). This fact can be related to changes

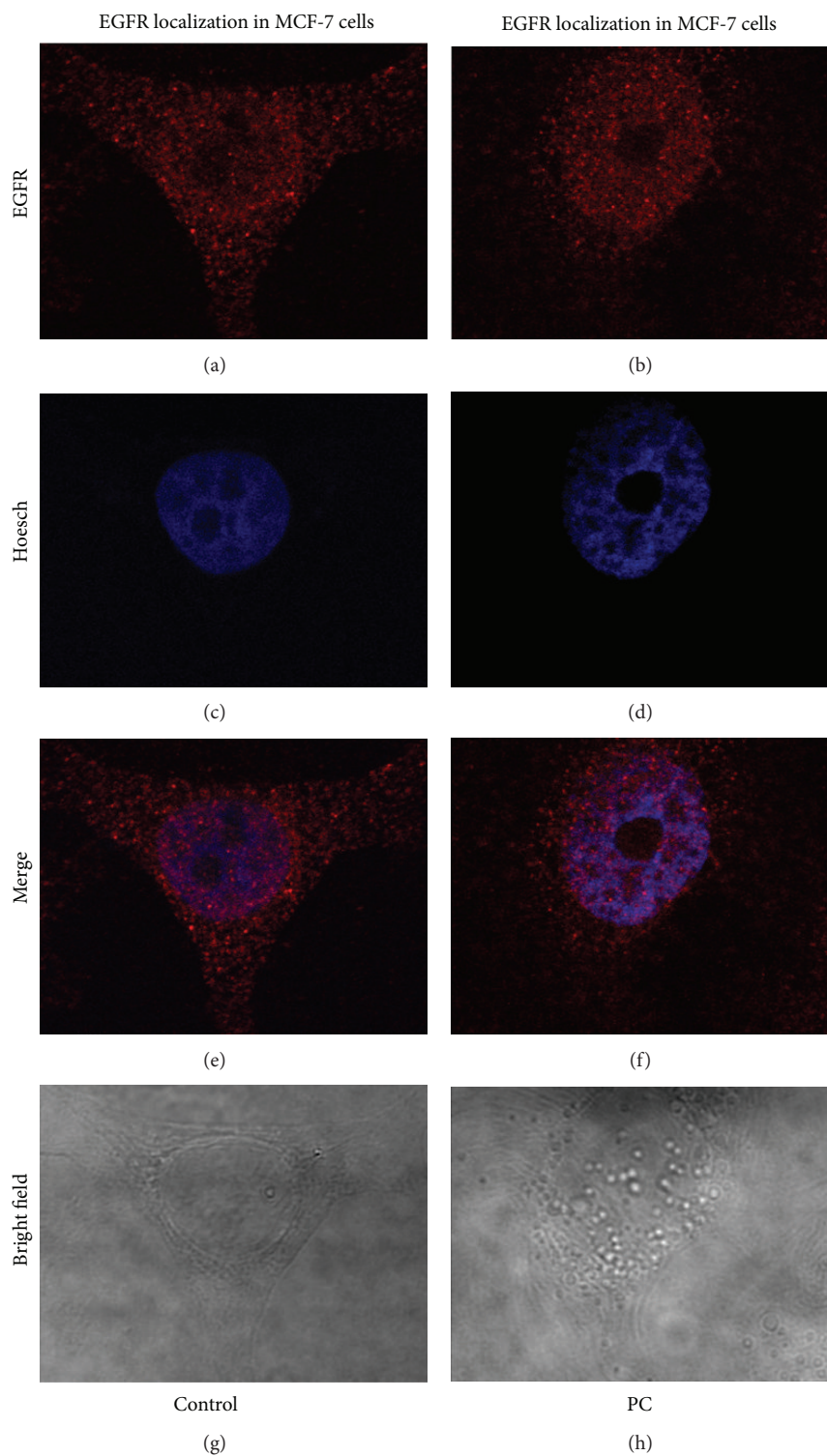


FIGURE 6: EGFR immunocytochemistry. MCF-7 breast cancer cells were incubated for 24 hours with PC nanoparticles dispersed at 0.1 in buffer pH 7.0 or vehicle (Ct) in absence of serum. For EGFR immunocytochemistry, cells were washed, fixed, permeabilized, blocked, and incubated with the anti-EGFR antibody, the Cy3-conjugated secondary antibody, and Hoechst. Finally covers were mounted and examined by confocal microscopy. Images were obtained using sequential scanning. Representative images of EGFR, nuclear staining, merge, and bright field are shown.

in the proportion of the differently charged forms of the zwitterionic phosphocholine polar head within the selected pH range and the conformational organization the molecules acquire as a result.

In spite of the studies accomplished using lipid-based nanocarriers for drug and gene delivery, the relationship between their physicochemical characteristics and activation of membrane receptors remains as an area of knowledge with incipient development. In this regard, cationic liposomal lipids have been described to modify cellular pathways and stimulate immune or anti-inflammatory responses [47]. However, the mechanisms responsible for those biological effects are poorly understood. Contrary to previous reports concerning cationic lipids, the present study shows that biological effects are induced when cells are incubated with the negatively charged phosphatidylcholine nanoparticles but not when positively charged PC nanoparticles are administered. Nevertheless, the mechanisms involved could be similar to that proposed for cationic lipids; insertion of a negatively charged phospholipid-derived nanoparticle in the biological membrane might modify the lipid environment of membrane proteins, the lipid-protein interaction and, therefore, membrane functioning.

5. Conclusion

Results from the present study suggest that high phosphatidylcholine concentrations, assembled in negatively charged nanoparticles, may induce physicochemical changes in the plasma membrane that affect EGFR cellular localization and/or its activity, therefore facilitating accumulation of the receptor in the cytoplasm, which would be associated with increased activation of the MEK-ERK1/2 pathway and induction of cell cycle progression. It is interesting that the described effects were specifically observed for the phosphatidylcholine nanoparticles prepared in pH 7 buffer but not at pH 5; so we propose that this might be related to the different net charge and morphology associated with the particles, as no significant differences in size between nanoparticles obtained from dispersion at pH 7.0 and 5.0 were observed. Considering that the PC nanoparticles prepared in a pH 5.0 buffer showed no significant biological effects over the breast cancer cells, these would be safer than those prepared in a pH 7.0 buffer to deliver antimetabolic agents.

The interpretation of the interaction between nanocarriers with membrane receptors is a matter that must be elucidated for a more appropriate understanding of the biological effects that are promoted. The present study highlights the importance of the research on the effects of vehicles broadly used in the pharmaceutical area and demonstrates that possible biological effects of formulations based on phosphatidylcholine nanoparticles should be considered. Moreover, studies about the possible biological action of PC nanoparticles on normal cells would be useful to expand our knowledge about their potential pharmaceutical uses. Excipient effects over normal physiology and cell biology represent important factors to be concerned about in rational formulation design.

Conflict of Interests

The authors declare that there is no conflict of interests regarding the publication of this paper.

Acknowledgments

Support for these studies was provided by the National Agency of Scientific and Technological Promotion (ANPCyT, PICT 595) and the University of Buenos Aires (UBACYT 20020090200186).

References

- [1] C. de Muynck, C. Cuvelier, and J. P. Remon, "Evaluation of rectal mucosal irritation in rabbits after sub-chronic administration of lecithin-containing suppositories," *Journal of Pharmacy and Pharmacology*, vol. 46, no. 1, pp. 78–79, 1994.
- [2] K. Drejer, A. Vaag, K. Bech, P. Hansen, A. R. Sorensen, and N. Mygind, "Intranasal administration of insulin with phospholipid as absorption enhancer: pharmacokinetics in normal subjects," *Diabetic Medicine*, vol. 9, no. 4, pp. 335–340, 1992.
- [3] J. H. Growdon and A. J. Gelenberg, "Choline and lecithin administration to patients with tardive dyskinesia," *Transactions of the American Neurological Association*, vol. 103, pp. 95–99, 1978.
- [4] M. Sznitowska, E. A. Dabrowska, and S. Janicki, "Solubilizing potential of submicron emulsions and aqueous dispersions of lecithin," *International Journal of Pharmaceutics*, vol. 246, no. 1-2, pp. 203–206, 2002.
- [5] M. Sznitowska, M. Klunder, and M. Placzek, "Paclitaxel solubility in aqueous dispersions and mixed micellar solutions of lecithin," *Chemical & Pharmaceutical Bulletin*, vol. 56, no. 1, pp. 70–74, 2008.
- [6] N. Yanasarn, B. R. Sloat, and Z. Cui, "Nanoparticles engineered from lecithin-in-water emulsions as a potential delivery system for docetaxel," *International Journal of Pharmaceutics*, vol. 379, no. 1-2, pp. 174–180, 2009.
- [7] S. E. Perez, Y. Gandola, A. M. Carlucci, L. Gonzalez, D. Turyn, and C. Bregni, "Formulation strategies, characterization, and *in vitro* evaluation of lecithin-based nanoparticles for siRNA delivery," *Journal of Drug Delivery*, vol. 2012, Article ID 986265, 9 pages, 2012.
- [8] J. H. Exton, "Phosphatidylcholine breakdown and signal transduction," *Biochimica et Biophysica Acta*, vol. 1212, no. 1, pp. 26–42, 1994.
- [9] M. Rizzo and G. Romero, "Pharmacological importance of phospholipase D and phosphatidic acid in the regulation of the mitogen-activated protein kinase cascade," *Pharmacology & Therapeutics*, vol. 94, no. 1-2, pp. 35–50, 2002.
- [10] W. Su, Q. Chen, and M. A. Frohman, "Targeting phospholipase D with small-molecule inhibitors as a potential therapeutic approach for cancer metastasis," *Future Oncology*, vol. 5, no. 9, pp. 1477–1486, 2009.
- [11] M. A. Rizzo, K. Shome, C. Vasudevan et al., "Phospholipase D and its product, phosphatidic acid, mediate agonist-dependent Raf-1 translocation to the plasma membrane and the activation of the mitogen-activated protein kinase pathway," *The Journal of Biological Chemistry*, vol. 274, no. 2, pp. 1131–1139, 1999.

- [12] M. A. Rizzo, K. Shome, S. C. Watkins, and G. Romero, "The recruitment of Raf-1 to membranes is mediated by direct interaction with phosphatidic acid and is independent of association with Ras," *The Journal of Biological Chemistry*, vol. 275, no. 31, pp. 23911–23918, 2000.
- [13] B. F. Clem, A. L. Clem, A. Yalcin et al., "A novel small molecule antagonist of choline kinase- α that simultaneously suppresses MAPK and PI3K/AKT signaling," *Oncogene*, vol. 30, no. 30, pp. 3370–3380, 2011.
- [14] J. Gomez-Cambronero, "New concepts in phospholipase D signaling in inflammation and cancer," *TheScientificWorldJournal*, vol. 10, pp. 1356–1369, 2010.
- [15] M. Laplante and D. M. Sabatini, "mTOR signaling in growth control and disease," *Cell*, vol. 149, no. 2, pp. 274–293, 2012.
- [16] A. Cuadrado, A. Carnero, F. Dolfi, B. Jimenez, and J. C. Lacal, "Phosphorylcholine: a novel second messenger essential for mitogenic activity of growth factors," *Oncogene*, vol. 8, no. 11, pp. 2959–2968, 1993.
- [17] M. C. van Dijk, F. J. Muriana, J. de Widt, H. Hilkmann, and W. J. van Blitterswijk, "Involvement of phosphatidylcholine-specific phospholipase C in platelet-derived growth factor-induced activation of the mitogen-activated protein kinase pathway in Rat-1 fibroblasts," *The Journal of Biological Chemistry*, vol. 272, no. 17, pp. 11011–11016, 1997.
- [18] I. Plo, D. Lautier, T. Levade et al., "Phosphatidylcholine-specific phospholipase C and phospholipase D are respectively implicated in mitogen-activated protein kinase and nuclear factor κ B activation in tumour-necrosis-factor- α -treated immature acute-myeloid-leukaemia cells," *Biochemical Journal*, vol. 351, part 2, pp. 459–467, 2000.
- [19] J. G. Donaldson, "Phospholipase D in endocytosis and endosomal recycling pathways," *Biochimica et Biophysica Acta*, vol. 1791, no. 9, pp. 845–849, 2009.
- [20] S. Cecchetti, F. Spadaro, L. Lugini, F. Podo, and C. Ramoni, "Functional role of phosphatidylcholine-specific phospholipase C in regulating CD16 membrane expression in natural killer cells," *European Journal of Immunology*, vol. 37, no. 10, pp. 2912–2922, 2007.
- [21] L. Paris, S. Cecchetti, F. Spadaro et al., "Inhibition of phosphatidylcholine-specific phospholipase C downregulates HER2 overexpression on plasma membrane of breast cancer cells," *Breast Cancer Research*, vol. 12, no. 3, article R27, 2010.
- [22] U. Weber, C. Eroglu, and M. Mlodzik, "Phospholipid membrane composition affects EGF receptor and Notch signaling through effects on endocytosis during *Drosophila* development," *Developmental Cell*, vol. 5, no. 4, pp. 559–570, 2003.
- [23] U. Coskun, M. Grzybek, D. Drechsel, and K. Simons, "Regulation of human EGF receptor by lipids," *Proceedings of the National Academy of Sciences of the United States of America*, vol. 108, no. 22, pp. 9044–9048, 2011.
- [24] A. Ghosh, J. Akech, S. Mukherjee, and S. K. Das, "Differential expression of cholinephosphotransferase in normal and cancerous human mammary epithelial cells," *Biochemical and Biophysical Research Communications*, vol. 297, no. 4, pp. 1043–1048, 2002.
- [25] K. Glunde and N. J. Serkova, "Therapeutic targets and biomarkers identified in cancer choline phospholipid metabolism," *Pharmacogenomics*, vol. 7, no. 7, pp. 1109–1123, 2006.
- [26] J. Goole, D. J. Lindley, W. Roth et al., "The effects of excipients on transporter mediated absorption," *International Journal of Pharmaceutics*, vol. 393, no. 1–2, pp. 17–31, 2010.
- [27] L. Gonzalez, M. E. Diaz, J. G. Miquet et al., "GH modulates hepatic epidermal growth factor signaling in the mouse," *Journal of Endocrinology*, vol. 204, no. 3, pp. 299–309, 2010.
- [28] D. Muir, S. Varon, and M. Manthorpe, "An enzyme-linked immunosorbent assay for bromodeoxyuridine incorporation using fixed microcultures," *Analytical Biochemistry*, vol. 185, no. 2, pp. 377–382, 1990.
- [29] D. A. Foster and L. Xu, "Phospholipase D in cell proliferation and cancer," *Molecular Cancer Research*, vol. 1, no. 11, pp. 789–800, 2003.
- [30] Y. Fang, M. Vilella-Bach, R. Bachmann, A. Flanigan, and J. Chen, "Phosphatidic acid-mediated mitogenic activation of mTOR signaling," *Science*, vol. 294, no. 5548, pp. 1942–1945, 2001.
- [31] K. M. Nicholson and N. G. Anderson, "The protein kinase B/Akt signalling pathway in human malignancy," *Cellular Signalling*, vol. 14, no. 5, pp. 381–395, 2002.
- [32] T. W. Miller, B. N. Rexer, J. T. Garrett, and C. L. Arteaga, "Mutations in the phosphatidylinositol 3-kinase pathway: role in tumor progression and therapeutic implications in breast cancer," *Breast Cancer Research*, vol. 13, no. 6, article 224, 2011.
- [33] R. O'Regan and N. N. Hawk, "mTOR inhibition in breast cancer: unraveling the complex mechanisms of mTOR signal transduction and its clinical implications in therapy," *Expert Opinion on Therapeutic Targets*, vol. 15, no. 7, pp. 859–872, 2011.
- [34] L. S. Steelman, S. C. Pohnert, J. G. Shelton, R. A. Franklin, F. E. Bertrand, and J. A. McCubrey, "JAK/STAT, Raf/MEK/ERK, PI3K/Akt and BCR-ABL in cell cycle progression and leukemogenesis," *Leukemia*, vol. 18, no. 2, pp. 189–218, 2004.
- [35] D. R. Alessi, Y. Saito, D. G. Campbell et al., "Identification of the sites in MAP kinase kinase-1 phosphorylated by p74raf-1," *The EMBO Journal*, vol. 13, no. 7, pp. 1610–1619, 1994.
- [36] J. R. Lee, S. Urban, C. F. Garvey, and M. Freeman, "Regulated intracellular ligand transport and proteolysis control EGF signal activation in *Drosophila*," *Cell*, vol. 107, no. 2, pp. 161–171, 2001.
- [37] T. E. Lloyd, R. Atkinson, M. N. Wu, Y. Zhou, G. Pennetta, and H. J. Bellen, "Hrs regulates endosome membrane invagination and tyrosine kinase receptor signaling in *Drosophila*," *Cell*, vol. 108, no. 2, pp. 261–269, 2002.
- [38] D. J. Katzmann, G. Odorizzi, and S. D. Emr, "Receptor downregulation and multivesicular-body sorting," *Nature Reviews Molecular Cell Biology*, vol. 3, no. 12, pp. 893–905, 2002.
- [39] P. G. Woodman and C. E. Futter, "Multivesicular bodies: coordinated progression to maturity," *Current Opinion in Cell Biology*, vol. 20, no. 4, pp. 408–414, 2008.
- [40] C. Raiborg and H. Stenmark, "The ESCRT machinery in endosomal sorting of ubiquitylated membrane proteins," *Nature*, vol. 458, no. 7237, pp. 445–452, 2009.
- [41] A. V. Vieira, C. Lamaze, and S. L. Schmid, "Control of EGF receptor signaling by clathrin-mediated endocytosis," *Science*, vol. 274, no. 5295, pp. 2086–2089, 1996.
- [42] A. Montaner, J. Girardini, and C. Banchio, "Phosphatidylcholine: role during embryonic neural stem cells differentiation," *Biocell*, vol. 37, supplement, article CB-P07, 2013.
- [43] L. Paoletti, P. Domizi, C. di Benedetto, and C. Banchio, "Phosphatidylcholine turn over induces neuronal differentiation in Neuro-2A cells," *Biocell*, vol. 37, supplement, article CB-P08, 2013.

- [44] J. Idkowiak-Baldys, A. Baldys, J. R. Raymond, and Y. A. Hannun, "Sustained receptor stimulation leads to sequestration of recycling endosomes in a classical protein kinase C- and phospholipase D-dependent manner," *The Journal of Biological Chemistry*, vol. 284, no. 33, pp. 22322–22331, 2009.
- [45] G. Pines, P. H. Huang, Y. Zhwang, F. M. White, and Y. Yarden, "EGFRvIV: a previously uncharacterized oncogenic mutant reveals a kinase autoinhibitory mechanism," *Oncogene*, vol. 29, no. 43, pp. 5850–5860, 2010.
- [46] X. Zhang, J. Gureasko, K. Shen, P. A. Cole, and J. Kuriyan, "An allosteric mechanism for activation of the kinase domain of epidermal growth factor receptor," *Cell*, vol. 125, no. 6, pp. 1137–1149, 2006.
- [47] C. Loney, M. Vandenbranden, and J. M. Ruyschaert, "Cationic liposomal lipids: from gene carriers to cell signaling," *Progress in Lipid Research*, vol. 47, no. 5, pp. 340–347, 2008.

Research Article

Chemical Constituents from the Fruits of *Forsythia suspensa* and Their Antimicrobial Activity

Ping-Chung Kuo,¹ Guo-Feng Chen,^{1,2} Mei-Lin Yang,² Ya-Hua Lin,¹ and Chi-Chung Peng¹

¹ Department of Biotechnology, National Formosa University, Yunlin 632, Taiwan

² Department of Chemistry, National Chung-Hsing University, Taichung 402, Taiwan

Correspondence should be addressed to Ping-Chung Kuo; pcckuo@sunws.nfu.edu.tw

Received 22 December 2013; Revised 6 February 2014; Accepted 9 February 2014; Published 12 March 2014

Academic Editor: José Carlos Tavares Carvalho

Copyright © 2014 Ping-Chung Kuo et al. This is an open access article distributed under the Creative Commons Attribution License, which permits unrestricted use, distribution, and reproduction in any medium, provided the original work is properly cited.

Lignans and phenylethanoid glycosides purified from *Forsythia suspensa* were reported to display various bioactivities in the previous literature, including the antimicrobial activity. Therefore, the present research is aimed to purify and identify the chemical constituents of the methanol extracts of fruits of *F. suspensa*. The methanol extracts of fruits of *F. suspensa* were fractionated and further purified with the assistance of column chromatography to afford totally thirty-four compounds. Among these isolates, 3 β -acetoxy-20 α -hydroxyursan-28-oic acid (**1**) was reported from the natural sources for the first time. Some of the purified principles were subjected to the antimicrobial activity examinations against *Escherichia coli* to explore new natural lead compounds.

1. Introduction

Food safety is an important public health issue continuously attracting researchers from various fields. The use of biopreservatives and pathogen antagonists had been completed as a means of protecting the microbiological safety of fresh and processed products [1–4]. Lignans and phenylethanoid glycosides are widely distributed among plant bioresources and those purified from *Forsythia suspensa* have already been reported to exhibit antimicrobial bioactivities in the previous literature [5–13]. Although these natural compounds did not exhibit better inhibition of the bacterial growth, they were not very toxic while compared with the synthetic antibiotics. *F. suspensa* (Oleaceae) is an important original plant of the crude drug “rengyo” (*Forsythiae Fructus*) which has been used for anti-inflammatory, diuretic, drainage, and antimicrobial purposes in Oriental medicine [6, 8]. Previous phytochemical investigations of *Forsythia* genus afforded a series of steroids, triterpenoids, lignans, and phenylethanoid glycosides [5–16]. In our continuous program aimed to the bioactive principles from natural sources, the fruits of *F. suspensa* were selected as the target due to their antimicrobial potential in our preliminary bioassay (Table 1). In the present study, we wished to report the structural characterization

of one new triterpene, 3 β -acetoxy-20 α -hydroxyursan-28-oic acid (**1**), along with thirty-three known compounds, as well as their antimicrobial effects against *E. coli*. We hoped to explore new lead compounds which could be performed for further investigation of the new antibiotic agents.

2. Materials and Methods

2.1. General Procedure. Melting point was determined by a Fisher Scientific melting point measuring apparatus without corrections. The IR spectrum was obtained, as a KBr disc, on a Bruker Tensor 27 FT-IR spectrometer. Optical rotation was measured with an Atago AP-300 automatic polarimeter. ¹H- and ¹³C-NMR, COSY, HMQC, HMBC, and NOESY spectra were recorded on the Varian Unity 400 and Bruker AV 500 NMR spectrometers, using tetramethylsilane (TMS) as the internal standard. Standard pulse sequences and parameters were used for the NMR experiments and all chemical shifts were reported in parts per million (ppm, δ). The low and high-resolution FAB mass spectra were obtained on a JEOL JMS-700 spectrometer operated in the positive-ion mode. All the chemicals were purchased from Merck KGaA (Darmstadt, Germany) unless specifically indicated. Column

TABLE 1: The minimum inhibitory concentrations (MICs) of the crude extract and partial purified fractions of *F. suspensa* against *E. coli* (BCRC-11634).

Sample	MIC (mg/mL)
FS (crude extracts)	4.25
FSC (chloroform fraction)	6.25
FSW (water fraction)	12.50

chromatography was performed on silica gels (Kieselgel 60, 70–230 mesh, Merck KGaA). Thin layer chromatography (TLC) was conducted on precoated Kieselgel 60 F 254 plates (Merck) and the compounds were visualized by UV light or spraying with 10% (v/v) H₂SO₄ followed by heating at 110°C for 10 min.

2.2. Plant Materials. The fruits of *Forsythia suspensa* were purchased from the herbal markets in Yunlin, Taiwan, and authenticated by Dr. C. S. Kuoh (Department of Bioscience, National Cheng Kung University, Tainan, Taiwan). A voucher specimen (PCKuo_2007001) was deposited in the herbarium of the Department of Biotechnology, National Formosa University, Yunlin, Taiwan.

2.3. Extraction and Isolation. The fruits of *Forsythia suspensa* (6.0 Kg) were powdered and refluxed with methanol (20 L × 7), and the combined extracts were concentrated under reduced pressure to give a brown syrup (1.4 Kg). The crude extract was suspended into water and partitioned with chloroform, successively to afford chloroform (450 g) and water soluble fractions (950 g), respectively.

The chloroform soluble extracts were purified by silica gel column chromatography (SiO₂ CC) eluted with *n*-hexane and acetone gradients (100:1 to 1:1) to afford 8 fractions as monitored by TLC. Fractions 4, 5, and 8 display significant spots and therefore were subjected to the further purification. Fraction 4 was purified by SiO₂ CC eluted with *n*-hexane/ethyl acetate (50:1) to yield three subfractions (F4.1~4.3). The subfraction F4.2 displayed significant spots and was applied to SiO₂ CC, eluted with *n*-hexane and acetone gradients (100:1 to 1:1), to afford β-amyrin acetate (2) (10 mg) and taraxasterol acetate (3) (6 mg). The subfraction F4.3 was purified with SiO₂ CC eluted with *n*-hexane and acetone gradients (300:1 to 1:1) to yield three minor fractions (F4.3.1~4.3.3). The minor fraction F4.3.1 was further applied to SiO₂ CC with benzene: ethyl acetate (50:1) solvent system to afford 3β-acetyl-20,25-epoxy-dammarane-24α-ol (4) (25 mg). F4.3.2 was repeatedly subjected to SiO₂ CC and preparative TLC (pTLC) (eluted with benzene: acetone, 20:1) to yield 3β-acetoxy-20α-hydroxyursan-28-oic acid (1) (10 mg). F4.3.3 was recrystallized with acetone to produce acetyl oleanolic acid (5) (20 mg). Fraction 5 was purified by SiO₂ CC eluted with *n*-hexane/ethyl acetate (50:1) to yield ten subfractions (F5.1~5.10). Subfractions F5.5, 5.6, 5.8, and 5.10 were major fractions and displayed significant spots by TLC monitoring. F5.5 was further isolated by SiO₂ CC with a mixed eluent of benzene and acetone (200:1) to afford 3β-acetyl-20,25-epoxy-dammarane-24α-ol (4) (20 mg). F5.6

was also subjected to SiO₂ CC with a mixed eluent of benzene and acetone (200:1) and further recrystallization of the minor fractions with chloroform/methanol to yield betulinic acid (6) (30 mg) and labda-8(17),13E-dien-15,18-dioic acid 15-methyl ester (7) (5 mg), respectively. F5.8 was recrystallized with chloroform/methanol to produce mixture of β-sitosterol (8) and stigmasterol (9) (630 mg). F5.10 was repeatedly subjected to SiO₂ CC and pTLC (eluted with benzene: acetone, 20:1) to yield ψ-taraxasterol (10) (8 mg).

Fraction 8 was subjected to SiO₂ CC eluted with chloroform/methanol gradients (50:1 to 1:1) and monitored by TLC to afford five subfractions (F8.1~8.5). Subfraction F8.1 was further recrystallized with chloroform/methanol to yield betulinic acid (6) (2 mg). F8.2 was repeatedly subjected to SiO₂ CC and pTLC (eluted with chloroform: methanol, 50:1) to afford ψ-taraxasterol (10) (2 mg) and 3β-hydroxyanticopalic acid (11) (12 mg), respectively. The subfraction F8.3 was purified with SiO₂ CC eluted with chloroform and methanol gradients (50:1 to 1:1) to yield three minor fractions (F8.3.1~8.3.3). The minor fraction F8.3.2 was further applied to pTLC eluted with benzene/acetone (10:1) to yield agatholic acid (12) (9 mg). F8.3.3 was repeatedly subjected to SiO₂ CC (eluted with chloroform/acetone, 50:1) and pTLC (eluted with benzene/acetone, 30:1) to yield 3,4-dimethoxybenzoic acid (13) (6 mg). Subfraction F8.4 was applied to SiO₂ CC eluted with chloroform and methanol gradients (50:1 to 1:1) to yield four minor fractions (F8.4.1~8.4.4). The minor fractions F8.4.2 and 8.4.3 were major fractions and displayed significant spots by TLC monitoring. F8.4.2 was further repeatedly subjected to SiO₂ CC and pTLC (eluted with *n*-hexane/acetone, 1:1) to yield vanillic acid (14) (12 mg) and syringic acid (15) (3 mg). F8.4.3 was further recrystallized with chloroform/methanol to yield phillyrin (16) (30 mg). Subfraction F8.5 was purified by SiO₂ CC eluted with chloroform and methanol gradients (50:1 to 1:1) to yield three minor fractions (F8.5.1~8.5.3). The minor fraction F8.5.1 was further repeatedly subjected to SiO₂ CC and pTLC (eluted with chloroform/ethyl acetate, 10:1) to afford *p*-hydroxyphenylacetic acid (17) (10 mg). F8.5.2 was isolated by pTLC eluted with chloroform/acetone (4:1) to produce *p*-hydroxybenzoic acid (18) (15 mg). F8.5.3 was further recrystallized with acetone to yield benzoic acid (19) (16 mg).

The water extracts were applied to a reversed-phase Diaion HP-20 column eluted with water and methanol gradients to afford six fractions as monitored by C-18 TLC; however, no constituents were identified from fractions 1–3. Fraction 4 (wF4) was subjected to SiO₂ CC eluted with chloroform/methanol gradients (100:1 to 1:1) and monitored by TLC to afford five subfractions (wF4.1~4.5). The subfraction wF4.1 was purified with SiO₂ CC eluted with chloroform and acetone gradients (100:1 to 1:1) to yield *p*-hydroxyphenylacetic acid methyl ester (20) (5 mg). Subfraction wF4.2 was applied to SiO₂ CC eluted with chloroform and acetone gradients (200:1 to 1:1) to yield four minor fractions (wF4.2.1~wF4.2.4). The minor fraction wF4.2.1 was further recrystallized with chloroform/methanol to afford *p*-tyrosol (21) (10 mg). The minor fractions wF4.2.2 and wF4.2.3 were further repeatedly subjected to SiO₂ CC and

pTLC (eluted with chloroform/methanol, 30:1) to afford *p*-hydroxybenzoic acid (**18**) (5 mg) and *p*-hydroxyphenylacetic acid (**17**) (4 mg), respectively. The minor fraction wF4.2.4 was subjected to SiO₂ CC and further purified by pTLC (eluted with chloroform/methanol, 20:1) to yield hydroxytyrosol (**22**) (3 mg). Subfraction wF4.4 was subjected to SiO₂ CC eluted with chloroform and acetone gradients (100:1 to 1:1) to yield five minor fractions (wF4.4.1~wF4.4.5). The minor fractions wF4.4.2, wF4.4.4, and wF4.4.5 displayed significant spots and were applied to SiO₂ CC, eluted with chloroform/methanol (10:1) to afford 2-furancarboxylic acid (**23**) (15 mg), salidroside (**24**) (18 mg), and (6*S*,9*R*)-roseoside (**25**) (10 mg), respectively. Subfraction wF4.5 was repeatedly subjected to SiO₂ CC (eluted with chloroform/methanol, 10:1) and further recrystallization of the minor fractions with chloroform/methanol to result in forsythoside D (**26**) (8 mg), methyl- α -D-glucopyranoside (**27**) (10 mg), and adoxosidic acid (**28**) (15 mg), respectively.

Fraction 5 (wF5) was subjected to SiO₂ CC eluted with chloroform/methanol gradients (200:1 to 1:1) and monitored by TLC to afford five subfractions (wF5.1~5.5). Subfractions wF5.1, wF5.3, and wF5.4 displayed significant spots and therefore were subjected to the further purification. Subfraction wF5.1 was repeatedly subjected to SiO₂ CC (eluted with chloroform/acetone, 300:1 to 1:1) and further recrystallized with chloroform/methanol to result in *p*-hydroxyphenylacetic acid methyl ester (**20**) (3 mg). Subfraction wF5.3 was applied to SiO₂ CC (eluted with chloroform/acetone, 300:1 to 1:1) and further recrystallized with chloroform/methanol to yield *p*-hydroxyphenylacetic acid (**17**) (5 mg) and protocatechualdehyde (**29**) (5 mg). Subfraction wF5.4 was repeatedly purified by SiO₂ CC (eluted with chloroform/acetone, 200:1 to 1:1) and further recrystallization of the minor fractions with chloroform/methanol to yield esculetin (**30**) (3 mg) and caffeic acid (**31**) (12 mg), respectively. Fraction 6 (wF6) was isolated by SiO₂ CC eluted with chloroform/methanol gradients (100:1 to 1:1) and monitored by TLC to result in five subfractions (wF6.1~6.5). Only subfractions wF6.2 and wF6.3 displayed significant spots and therefore were subjected to the further purification. Subfraction wF6.2 was repeatedly purified by SiO₂ CC (eluted with chloroform/acetone, 200:1 to 1:1) and further recrystallization of the minor fractions with acetone to yield *trans*-coumaric acid (**32**) (5 mg) and *trans*-ferulic acid (**33**) (5 mg). Subfraction wF6.3 was further recrystallized with acetone to result in quercetin (**34**) (45 mg).

2.3.1. Spectral Data of 1. White powder (CHCl₃), mp 238–245°C; $[\alpha]_D^{25}$ –118.0 (*c* 0.09, CHCl₃); IR (Neat) ν_{\max} : 3442, 2948, 1760, 1727, 1444, 1375, 1250 cm⁻¹; ¹H NMR (CDCl₃, 400 MHz) δ 0.83 (15H, m, CH₃-23, 24, 25, 27, 29), 0.94 (3H, s, CH₃-26), 1.35 (3H, s, CH₃-30), 2.05 (3H, s, CH₃-32), 2.10 (1H, m, H-15), 2.60 (2H, m, H-16), 4.48 (1H, dd, *J* = 10.4, 5.6 Hz, H-3 α); ¹³C NMR (CDCl₃, 125 MHz) δ 15.5 (C-26), 16.2 (C-23, 24, 25), 16.5 (C-27), 18.1 (C-6), 21.3 (C-32), 21.4 (C-11), 23.7 (C-2), 25.0 (C-12), 25.4 (C-30), 26.8 (C-22), 28.0 (C-29), 29.2 (C-16), 31.2 (C-15, 21), 35.1 (C-7), 37.1 (C-10), 37.9 (C-4), 38.7 (C-1), 40.4 (C-8), 43.2 (C-14, 18), 49.4 (C-13), 50.2 (C-17),

50.5 (C-9), 55.9 (C-5), 80.9 (C-3), 90.1 (C-20), 171.0 (C-31), 176.8 (C-28); FAB-MS *m/z* (*rel. int.*) 517 ([M+H]⁺, 100); HR-FAB-MS *m/z* 517.3896 [M+H]⁺ (calcd for C₃₂H₅₃O₅, 517.3893).

2.4. Antimicrobial Activity

2.4.1. Microorganisms. The antimicrobial activity was evaluated against *Escherichia coli* (BCRC-II634). The strains were kept at –70°C in Luria-Bertani agar (LBA), activated by transferring into nutritive agar and incubating at 37 ± 1.0°C for 18 h. The bacterial suspension of each strain was prepared in a sterile tube with glass pearls and turbidity adjusted with distilled water, according to McFarland scale number 1 tube, which corresponds to approximately 3 × 10⁸ CFU/mL [13].

2.4.2. Determination of the In Vitro Antimicrobial Activity. The antimicrobial activities against *E. coli* of different concentrations of tested samples were determined by the microtiter plate method described by the United States Pharmacopeia [17]. A twofold microdilution broth method was used to determinate the minimum inhibitory concentrations (MIC) value for each test substance [18–21]. Each well contained 10⁶ CFU/mL of test bacteria and LB medium (100 μ L). 100 μ L of MeOH solutions of tested samples (5 mg/mL for pure compounds and 20 mg/mL for the fractions) was added to wells of the first row. Dilutions were used to dispense 100 μ L into the other sterile 96 wells of an ELISA plate using a multichannel micropipette, resulting in eight concentrations to be tested for each compound. A negative control containing inoculated growth medium and methanol was prepared. Each experiment was performed in triplicate.

2.4.3. Minimum Inhibitory Concentration (MIC) Determination. The MIC value is a measure to define the antibacterial activity of a compound and is defined as the lowest concentration of drug that inhibits visible growth. The amount of growth in the wells containing test samples was compared with the amount of growth in the control wells when determining the growth end points. When a single skipped well occurred, the highest MIC was read.

3. Results and Discussion

3.1. Isolation and Characterization of Compounds. Dried and powdered fruits of *F. suspensa* were extracted with methanol, and the combined extracts were concentrated under reduced pressure to give deep brown syrup. The crude extract was suspended into water and partitioned with chloroform to afford chloroform and water soluble fractions, respectively. Purification of the chloroform fraction of the methanol extracts of fruits of *F. suspensa* by a combination of chromatographic techniques yielded one new triterpene, 3 β -acetoxy-20 α -hydroxyursan-28-oic acid (**1**) (Figure 1), β -amyryn acetate (**2**) [22], taraxasterol acetate (**3**) [23], 3 β -acetyl-20,25-epoxy-dammarane-24 α -ol (**4**) [24], acetyl oleanolic acid (**5**) [25], betulinic acid (**6**) [26], labda-8(17),13*E*-dien-15,18-dioic acid 15-methyl ester

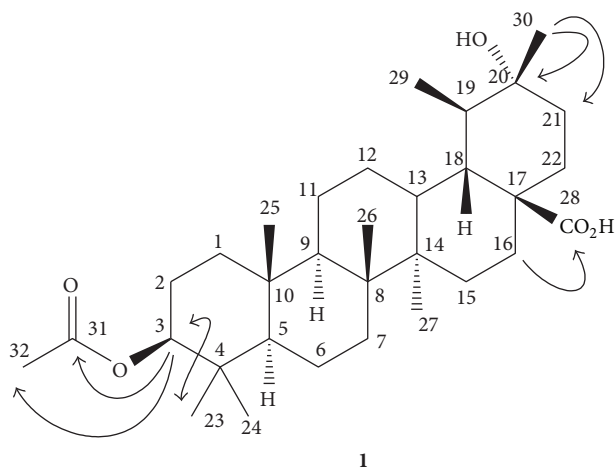


FIGURE 1: Chemical structure, significant HMBC (→) and NOESY (↔) correlations of compound 1.

(7) [27], mixture of β -sitosterol (8) and stigmasterol (9) [28], ψ -taraxasterol (10) [29], 3 β -hydroxyanticipalic acid (11) [30], agatholic acid (12) [31], 3,4-dimethoxybenzoic acid (13) [32], vanillic acid (14) [33], syringic acid (15) [33], phillyrin (16) [15], *p*-hydroxyphenylacetic acid (17) [34], *p*-hydroxybenzoic acid (18) [33], and benzoic acid (19) [35], respectively. The water fraction was subjected to the reversed-phase Diaion HP-20 column chromatography and successive isolation to afford *p*-hydroxyphenylacetic acid (17), *p*-hydroxybenzoic acid (18), *p*-hydroxyphenylacetic acid methyl ester (20) [36], *p*-tyrosol (21) [37], hydroxytyrosol (22) [38], 2-furancarboxylic acid (23) [39], salidroside (24) [40], (6*S*,9*R*)-roseoside (25) [41], forsythoside D (26) [8], methyl- α -D-glucopyranoside (27) [42], adoxosidic acid (28) [43], protocatechualdehyde (29) [44], esculetin (30) [45], caffeic acid (31) [46], *trans*-coumaric acid (32) [47], *trans*-ferulic acid (33) [48], and quercetin (34) [49], respectively. The chemical structures of known compounds 2–34 were identified by comparison of their physical and spectroscopic data with those reported in the literature. Among the isolates, compounds 2, 4, 6, 8, 14, 16, 17, 24, 26, 28, 31, and 34 had been identified from the titled plant. Other compounds were reported from *F. suspensa* for the first time. Compound 1 was a new compound and its structure was established by the spectral analysis.

3.2. Structural Elucidation of Compound 1. The purified white powder 1 was visualized by spraying with 1% (w/v) $\text{Ce}(\text{SO}_4)_2$ in 10% (v/v) aqueous H_2SO_4 followed by heating at 120°C and displayed purplish black spots on TLC plate. It also displayed positive responses against the Liebermann-Burchard test. These results suggested compound 1 to be a triterpenoid [50]. The molecular formula of 1 was established as $\text{C}_{32}\text{H}_{52}\text{O}_5$ by the pseudomolecular $[\text{M}+\text{H}]^+$ ion peak at m/z 517.3896 in HR-FAB-MS analysis and was further supported by its ^{13}C -NMR spectrum which showed signals for all the 32 carbons of the molecule including one set of acetyl group (δ_{C} 171.0,

TABLE 2: The minimum inhibitory concentrations (MICs) of the purified samples from *F. suspensa* against *E. coli* (BCRC-11634).

Compound	MIC (mg/mL)
1	4.55
2	5.00
6	1.20
10	1.20
11	3.42
12	2.62
16	3.94

21.3), one carboxylic acid group (δ_{C} 176.8), one oxygenated quaternary carbon (δ_{C} 90.1), and one acetoxy oxygenated carbon (δ_{C} 80.9), respectively. In the ^1H -NMR spectrum of 1, there were proton signals for seven methyl groups at δ 0.83 (15H, m, and CH_3 -23, -24, -25, -27, and -29), 0.94 (3H, s, and CH_3 -26), and 1.35 (3H, s, and CH_3 -30), and one acetyl methyl group at δ 2.05 (3H, s, and CH_3 -32), respectively. The spectroscopic data indicated compound 1 to possess oleanane type basic skeleton. In the downfield region, one oxygenated proton at δ 4.48 (1H, dd, $J = 10.4, 5.6$ Hz, H-3 α) was located at C-3 which was further established by the NOESY correlations between CH_3 -23 and H-3. The $^2J, ^3J$ -HMBC correlations from δ 4.48 (H-3) to δ_{C} 21.3 (C-32) and 171.0 (C-31) also evidenced the presence of acetoxy group at C-3. The substitution of tertiary alcohol at C-20 was also determined with the HMBC analysis of correlations from CH_3 -30 to C-21 (δ_{C} 31.2) and C-20 (δ_{C} 90.1). The $^2J, ^3J$ -HMBC correlation peak between δ 2.60 (m, H-16) and δ_{C} 176.8 (C-28) supported the carboxylic acid group to be attached at C-17. The complete assignments of ^1H and ^{13}C NMR signals of 1 were furnished from the NOESY and HMBC spectra. Therefore the chemical structure of 1 was established as 3 β -acetoxy-20 α -hydroxyursan-28-oic acid and shown in Figure 1.

3.3. The Antimicrobial Effects of Isolated Compounds against *Escherichia coli*. The crude extracts, partially purified fractions, and some of the purified principles (Figure 2) were subjected to the examinations for the inhibitory effects against *E. coli* [17–21]. The MIC data of the fractions were presented in Table 1. The MIC value of crude extracts (FS) was 4.25 mg/mL and demonstrated inhibition of the bacterial growth. Comparatively, the chloroform fraction (FSC) displayed more significant inhibitory effects against *E. coli* (BCRC-11634) than the water fraction (FSW) with MIC values of 6.25 and 12.50 mg/mL, respectively. When studying the influence of the concentration of compounds on the antimicrobial activities against *E. coli*, twofold microdilution broth method was used for the purified principles from the chloroform fraction (FSC), including triterpenoids 1, 2, 6, and 10; diterpenoids 11 and 12; and lignan 16. It was observed that as the concentration increased, the inhibition of the bacterial growth was also increased. All of the tested samples demonstrated the inhibitory effects in a concentration-dependent manner. The MIC data of the examined compounds were presented in Table 2. The MIC values were in the range

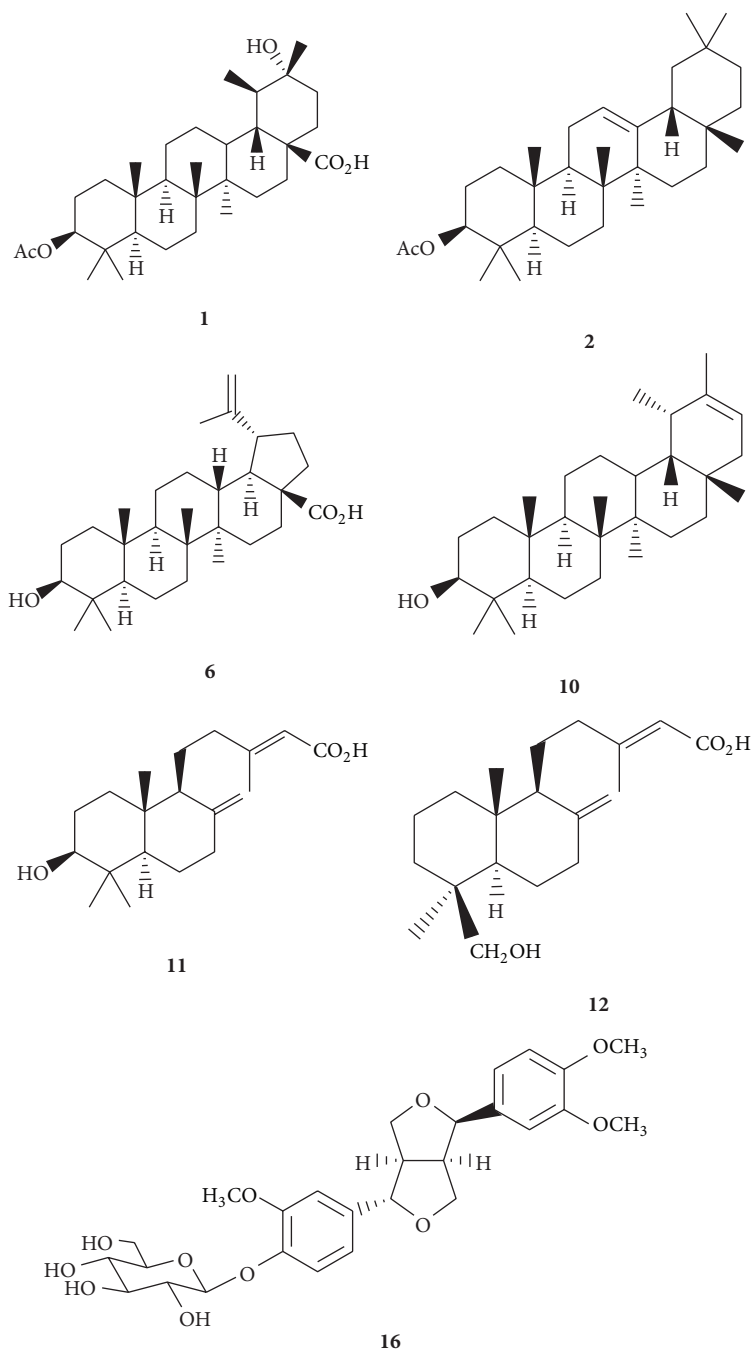


FIGURE 2: Structures of the isolated compounds subjected to the antimicrobial assay.

between 1.20 and 5.00 mg/mL against *E. coli* (BCRC-11634). Among the tested compounds, triterpenoids betulinic acid (6) and ψ -taraxasterol (10) exhibited the most significant inhibition against *E. coli* with MIC values of 1.20 mg/mL. These principles should be responsible for the bioactivity of the chloroform fraction (FSC). The results exhibited that the triterpenoids from the methanol extracts of fruits of *F. suspensa* possessed antibacterial activities against the common bacteria. It also provided evidence for the traditional uses of the fruits of *F. suspensa* as herbal medicines in the treatment

of bacterial diseases. Although these purified compounds did not display better inhibition of the bacterial growth compared with the reported synthetic antibiotics, the extracts and principles from the natural sources usually possessed lower toxicity. Further structural modification could be performed to improve the activity and maintain the safety of these compounds. Therefore, it would be potentially useful in developing new antimicrobial therapeutic agents.

Conflict of Interests

The authors declare that there is no conflict of interests regarding the publication of this paper.

Acknowledgment

The authors are grateful to the National Science Council, Taiwan, for the financial support of this research.

References

- [1] T. Abuladze, M. Li, M. Y. Menetrez, T. Dean, A. Senecal, and A. Sulakvelidze, "Bacteriophages reduce experimental contamination of hard surfaces, tomato, spinach, broccoli, and ground beef by *Escherichia coli* O157:H7," *Applied and Environmental Microbiology*, vol. 74, no. 20, pp. 6230–6238, 2008.
- [2] A. Allende, B. Martínez, V. Selma, M. I. Gil, J. E. Suárez, and A. Rodríguez, "Growth and bacteriocin production by lactic acid bacteria in vegetable broth and their effectiveness at reducing *Listeria monocytogenes* in vitro and in fresh-cut lettuce," *Food Microbiology*, vol. 24, no. 7-8, pp. 759–766, 2007.
- [3] A. L. Brown, J. C. Brooks, E. Karunasena, A. Echeverry, A. Laury, and M. M. Brashears, "Inhibition of *Escherichia coli* O157:H7 and *Clostridium sporogenes* in spinach packaged in modified atmospheres after treatment combined with chlorine and lactic acid bacteria," *Journal of Food Science*, vol. 76, no. 6, pp. M427–M432, 2011.
- [4] B. Leverentz, W. S. Conway, W. Janisiewicz, M. Abadias, C. P. Kurtzman, and M. J. Camp, "Biocontrol of the food-borne pathogens *Listeria monocytogenes* and *Salmonella enterica* serovar poona on fresh-cut apples with naturally occurring bacterial and yeast antagonists," *Applied and Environmental Microbiology*, vol. 72, no. 2, pp. 1135–1140, 2006.
- [5] C. L. Yui, "A study of the bacteriostatic principle isolated from *Forsythia suspensa* Vahl. (Lien-chiao)," *Yaoxue Xuebao*, vol. 8, no. 6, pp. 241–244, 1960.
- [6] K. Endo, K. Takahashi, T. Abe, and H. Hikino, "Structure of forsythoside A, an antibacterial principle of *Forsythia suspensa* leaves," *Heterocycles*, vol. 16, no. 8, pp. 1311–1314, 1981.
- [7] S. Nishibe, K. Okabe, and H. Tsukamoto, "Studies on the Chinese crude drug "*Forsythiae fructus*". VI: the structure and antibacterial activity of suspensaside isolated from *Forsythia suspensa*," *Chemical and Pharmaceutical Bulletin*, vol. 30, no. 12, pp. 4548–4553, 1982.
- [8] K. Endo and H. Hikino, "Structures of forsythoside C and D, antibacterial principles of *Forsythia suspensa* fruits," *Heterocycles*, vol. 19, no. 11, pp. 2033–2036, 1982.
- [9] S. Kitagawa, S. Nishibe, and H. Baba, "Studies on the Chinese crude drug "*Forsythiae fructus*". VIII: on isolation of phenylpropanoid glycosides from fruits of *Forsythia koreana* and their antibacterial activity," *Yakugaku Zasshi*, vol. 107, no. 4, pp. 274–278, 1987.
- [10] S. Nishibe, S. Kitagawa, S. Hisada et al., "Phenolic compounds from *Forsythiae fructus* and their biological activities," *Journal of Pharmacobio-Dynamics*, vol. 10, no. 3, s-48, 1987.
- [11] H. X. Kuang, N. Zhang, and Z. B. Lu, "Antibacterial constituents of the unripe fruit of *Forsythia suspensa* (Thunb.) Vahl," *Zhongyao Tongbao*, vol. 13, no. 7, pp. 32–63, 1988.
- [12] H. Qu, Y. Zhang, Y. Wang, B. Li, and W. Sun, "Antioxidant and antibacterial activity of two compounds (forsythiaside and forsythin) isolated from *Forsythia suspensa*," *Journal of Pharmacy and Pharmacology*, vol. 60, no. 2, pp. 261–266, 2008.
- [13] H. Qu, Y. Zhang, X. Chai, and W. Sun, "Isoforsythiaside, an antioxidant and antibacterial phenylethanoid glycoside isolated from *Forsythia suspensa*," *Bioorganic Chemistry*, vol. 40, no. 1, pp. 87–91, 2012.
- [14] S. Kitagawa, S. Nishibe, R. Benecke, and H. Thieme, "Phenolic compounds from *Forsythia* leaves. II," *Chemical & Pharmaceutical Bulletin*, vol. 36, no. 9, pp. 3667–3670, 1988.
- [15] M. M. A. Rahman, P. M. Dewick, D. E. Jackson, and J. A. Lucas, "Lignans of *Forsythia intermedia*," *Phytochemistry*, vol. 29, no. 6, pp. 1971–1980, 1990.
- [16] A. S. S. Rouf, Y. Ozaki, M. A. Rashid, and J. Rui, "Dammarane derivatives from the dried fruits of *Forsythia suspensa*," *Phytochemistry*, vol. 56, no. 8, pp. 815–818, 2001.
- [17] *The United States Pharmacopeia*, USP29-NF24, 2006.
- [18] S. Burt, "Essential oils: their antibacterial properties and potential applications in foods—a review," *International Journal of Food Microbiology*, vol. 94, no. 3, pp. 223–253, 2004.
- [19] M. Friedman, P. R. Henika, and R. E. Mandrell, "Bactericidal activities of plant essential oils and some of their isolated constituents against *Campylobacter jejuni*, *Escherichia coli*, *Listeria monocytogenes*, and *Salmonella enterica*," *Journal of Food Protection*, vol. 65, no. 10, pp. 1545–1560, 2002.
- [20] L. S. M. Ooi, Y. Li, S. L. Kam, H. Wang, E. Y. L. Wong, and V. E. C. Ooi, "Antimicrobial activities of Cinnamon oil and cinnamaldehyde from the Chinese medicinal herb *Cinnamomum cassia* Blume," *American Journal of Chinese Medicine*, vol. 34, no. 3, pp. 511–522, 2006.
- [21] B. Shan, Y. Z. Cai, J. D. Brooks, and H. Corke, "The in vitro antibacterial activity of dietary spice and medicinal herb extracts," *International Journal of Food Microbiology*, vol. 117, no. 1, pp. 112–119, 2007.
- [22] S. Matsunaga, R. Tanaka, and M. Akagi, "Triterpenoids from *Euphorbia maculata*," *Phytochemistry*, vol. 27, no. 2, pp. 535–537, 1988.
- [23] K. K. Bhutani, D. K. Gupta, and R. S. Kapil, "Occurrence of D/E *trans* stereochemistry isomeric to ursane (*cis*) series in a new pentacyclic triterpene from *Calotropis procera*," *Tetrahedron Letters*, vol. 33, no. 49, pp. 7593–7596, 1992.
- [24] H. Jing, J. S. Lee, W. Cao, C. F. Fang, and P. Lu, "Determination of forsythoside A from *Forsythia suspensa* by HPLC," *Xibei Yaoyue Zazhi*, vol. 18, no. 4, pp. 156–157, 2003.
- [25] K. Umehara, R. Takagi, M. Kuroyanagi, A. Ueno, T. Taki, and Y. J. Chen, "Studies on differentiation-inducing activities of triterpenes," *Chemical and Pharmaceutical Bulletin*, vol. 40, no. 2, pp. 401–405, 1992.
- [26] A. Nick, A. D. Wright, T. Rali, and O. Sticher, "Antibacterial triterpenoids from *Dillenia papuana* and their structure-activity relationships," *Phytochemistry*, vol. 40, no. 6, pp. 1691–1695, 1995.
- [27] C. Zdero, F. Bohlmann, and H. M. Niemeyer, "Friedolabdanes and other constituents from Chilean *Haplopappus* species," *Phytochemistry*, vol. 30, no. 11, pp. 3669–3677, 1991.
- [28] Y. H. Kuo and Y. C. Li, "Constituents of the Bark of *Ficus microcarpa* L.f.," *Journal of the Chinese Chemical Society*, vol. 44, no. 3, pp. 321–325, 1997.
- [29] H. Y. Ding, "Phytochemical and pharmacological studies on Chinese changzhu," *Journal of the Chinese Chemical Society*, vol. 47, no. 3, pp. 561–566, 2000.

- [30] S. Braun and H. Breitenbach, "Strukturaufklärung einer neuen diterpensäure aus *Metasequoia glyptostroboides* mit Hilfe der ^{13}C -NMR-spektroskopie," *Tetrahedron*, vol. 33, no. 1, pp. 145–150, 1977.
- [31] J. de Paiva Campello and S. F. Fonseca, "Diterpenes from *Araucaria angustifolia*," *Phytochemistry*, vol. 14, no. 10, pp. 2299–2300, 1975.
- [32] M. Trincado, H. Grützmacher, F. Vizza, and C. Bianchini, "Domino rhodium/palladium-catalyzed dehydrogenation reactions of alcohols to acids by hydrogen transfer to inactivated alkenes," *Chemistry*, vol. 16, no. 9, pp. 2751–2757, 2010.
- [33] C. Y. Chen, F. R. Chang, C. M. Teng, and Y. C. Wu, "Cheritamine, a new N-fatty acyl tryptamine and other constituents from the stems of *Annona cherimola*," *Journal of the Chinese Chemical Society*, vol. 46, no. 1, pp. 77–86, 1999.
- [34] K. Zhang, J. E. T. Corrie, V. R. N. Munasinghe, and P. Wan, "Mechanism of photosolvolytic rearrangement of p-hydroxyphenacyl esters: evidence for excited-state intramolecular proton transfer as the primary photochemical step," *Journal of the American Chemical Society*, vol. 121, no. 24, pp. 5625–5632, 1999.
- [35] P. Laurent, B. Lebrun, J. C. Braekman, D. Daloz, and J. M. Pasteels, "Biosynthetic studies on adaline and adalinine, two alkaloids from ladybird beetles (Coleoptera: Coccinellidae)," *Tetrahedron*, vol. 57, no. 16, pp. 3403–3412, 2001.
- [36] D. S. Bose and A. V. Narsaiah, "An efficient asymmetric synthesis of (S)-atenolol: using hydrolytic kinetic resolution," *Bioorganic and Medicinal Chemistry*, vol. 13, no. 3, pp. 627–630, 2005.
- [37] Y. Takaya, T. Furukawa, S. Miura et al., "Antioxidant constituents in distillation residue of Awamori spirits," *Journal of Agricultural and Food Chemistry*, vol. 55, no. 1, pp. 75–79, 2007.
- [38] L. Pouységu, T. Sylla, T. Garnier et al., "Hypervalent iodine-mediated oxygenative phenol dearomatization reactions," *Tetrahedron*, vol. 66, no. 31, pp. 5908–5917, 2010.
- [39] M. N. Preobrazhenskaya, I. I. Rozhkov, E. I. Lazhko, L. N. Yudina, and A. M. Korolev, "Reaction of vanilmandelic acid and 4-Hydroxybenzyl alcohol derivatives with L-ascorbic acid," *Tetrahedron*, vol. 53, no. 20, pp. 6971–6976, 1997.
- [40] H. Kuwajima, Y. Takai, K. Takaishi, and K. Inoue, "Synthesis of ^{13}C -labeled possible intermediates in the biosynthesis of phenylethanoid derivatives, cornoside and rengyosides," *Chemical and Pharmaceutical Bulletin*, vol. 46, no. 4, pp. 581–586, 1998.
- [41] Y. Yamano and M. Ito, "Synthesis of optically active vomifoliol and roseoside stereoisomers," *Chemical and Pharmaceutical Bulletin*, vol. 53, no. 5, pp. 541–546, 2005.
- [42] L. Albertin, M. Stenzel, C. Barner-Kowollik, L. J. R. Foster, and T. P. Davis, "Well-defined glycopolymers from RAFT polymerization: poly(methyl 6-O-methacryloyl- α -D-glucoside) and its block copolymer with 2-hydroxyethyl methacrylate," *Macromolecules*, vol. 37, no. 20, pp. 7530–7537, 2004.
- [43] S. Suciati, L. K. Lambert, B. P. Ross, M. A. Deseo, and M. J. Garson, "Phytochemical study of *Fagraea* spp. Uncover a new terpene alkaloid with anti-inflammatory properties," *Australian Journal of Chemistry*, vol. 64, no. 4, pp. 489–494, 2011.
- [44] H. Chiji, S. Tanaka, and M. Izawa, "Phenolic germination inhibitors in the seed balls of red beet (*Beta vulgaris* L. var. *rubra*)," *Agricultural and Biological Chemistry*, vol. 44, no. 1, pp. 205–207, 1980.
- [45] Y. Masamoto, H. Ando, Y. Murata, Y. Shimoishi, M. Tada, and K. Takahata, "Mushroom tyrosinase inhibitory activity of esculetin isolated from seeds of *Euphorbia lathyris* L.," *Bioscience, Biotechnology and Biochemistry*, vol. 67, no. 3, pp. 631–634, 2003.
- [46] V. D. S. Bolzani, L. M. V. Trevisan, and M. C. M. Young, "Caffeic acid esters and triterpenes of *Alibertia macrophylla*," *Phytochemistry*, vol. 30, no. 6, pp. 2089–2091, 1991.
- [47] Y. M. Chiang, H. K. Liu, J. M. Lo et al., "Cytotoxic constituents of the leaves of *Calocedrus formosana*," *Journal of the Chinese Chemical Society*, vol. 50, no. 1, pp. 161–166, 2003.
- [48] S. Prachayasittikul, S. Suphapong, A. Worachartcheewan, R. Lawung, S. Ruchirawat, and V. Prachayasittikul, "Bioactive metabolites from *Spilanthes acmella* Murr," *Molecules*, vol. 14, no. 2, pp. 850–867, 2009.
- [49] Y. Hua and H. Q. Wang, "Chemical components of *Anaphalis sinica* Hance," *Journal of the Chinese Chemical Society*, vol. 51, no. 2, pp. 409–415, 2004.
- [50] A. Srivastava and Y. N. Shukla, "Aryl esters and a coumarin from *Aygyreia speciosa*," *Indian Journal of Chemistry B*, vol. 37, no. 2, pp. 192–194, 1998.

Research Article

Antioxidant Activity of Extract and Its Major Constituents from Okra Seed on Rat Hepatocytes Injured by Carbon Tetrachloride

Lianmei Hu,¹ Wenlan Yu,¹ Ying Li,¹ Nagendra Prasad,² and Zhaoxin Tang¹

¹ College of Veterinary Medicine, South China Agricultural University, Guangzhou 510642, China

² Chemical Engineering Discipline, School of Engineering, Monash University, 46150 Bandar Sunway, Malaysia

Correspondence should be addressed to Nagendra Prasad; nagendra.prasad@monash.edu and Zhaoxin Tang; zxtangscu@gmail.com

Received 2 January 2014; Accepted 16 January 2014; Published 27 February 2014

Academic Editor: José Carlos Tavares Carvalho

Copyright © 2014 Lianmei Hu et al. This is an open access article distributed under the Creative Commons Attribution License, which permits unrestricted use, distribution, and reproduction in any medium, provided the original work is properly cited.

The antioxidant activities and protective effects of total phenolic extracts (TPE) and their major components from okra seeds on oxidative stress induced by carbon tetrachloride (CCl₄) in rat hepatocyte cell line were investigated. The major phenolic compounds were identified as quercetin 3-O-glucosyl (1 → 6) glucoside (QDG) and quercetin 3-O-glucoside (QG). TPE, QG, and QDG from okra seeds exhibited excellent reducing power and free radical scavenging capabilities including α , α -diphenyl- β -picrylhydrazyl (DPPH), superoxide anions, and hydroxyl radical. Overall, DPPH radical scavenging activity and reducing power of QG and QDG were higher than those of TPE while superoxide and hydroxyl radical scavenging activities of QG and TPE were higher than those of QDG. Furthermore, TPE, QG, and QDG pretreatments significantly alleviated the cytotoxicity of CCl₄ on rat hepatocytes, with attenuated lipid peroxidation, increased SOD and CAT activities, and decreased GPT and GOT activities. The protective effects of TPE and QG on rat hepatocytes were stronger than those of QDG. However, the cytotoxicity of CCl₄ on rat hepatocytes was not affected by TPE, QG, and QDG posttreatments. It was suggested that the protective effects of TPE, QG, and QDG on rat hepatocyte against oxidative stress were related to the direct antioxidant capabilities and the induced antioxidant enzymes activities.

1. Introduction

Oxidation is essential for living organisms. Reactive oxygen species (ROS) also are produced during oxidation [1]. Organisms can maintain a dynamic equilibrium between production and elimination of ROS in normal conditions. However, when organisms are subjected to stress conditions, this equilibrium is disrupted. Excessive accumulation of ROS will result in cellular injuries, including lipid peroxidation, protein oxidation, and DNA damage, which are involved in development of a variety of diseases including cellular aging, mutagenesis, carcinogenesis, hepatopathies, diabetes, and neurodegeneration [2]. Therefore, cellular antioxidant defense systems play important roles in counteracting these deleterious effects of ROS.

Almost all organisms possess antioxidant defense systems including antioxidant enzymes and nonenzymatic antioxidants. However, these systems are insufficient to prevent the

damage entirely in some cases [3]. Plants are the most important source of natural antioxidants [4]. Phenolic compounds or polyphenols, which consist of secondary metabolites, constitute a wide and complex array of phytochemicals that exhibit antioxidant actions. Epidemiological studies have indicated that regular consumption of foods rich in phenolic compounds is associated with reduced risk of cardiovascular diseases, neurodegenerative diseases, and certain cancers [5, 6]. These phenolic compounds hold promising potentials in the development of health foods, nutritional supplements, and herbal medicines for the application as antioxidants and ROS-related disease chemopreventive agents.

Okra (*Hibiscus esculentus* L.), also known as lady's finger and gumbo, belongs to Malvaceae family, which is distributed widely in Africa, Asia, Southern Europe, and America [7]. The plant is a common vegetable in most regions for its nutrition value. Okra pod contains thick slimy polysaccharides, which are used to thicken soups and stews,

as an egg white substitute, and as a fat substitute in chocolate bar cookies and in chocolate frozen dairy dessert [7]. Okra seed is rich in protein and unsaturated fatty acids such as linoleic acid [8]. In some countries, okra also is used in folk medicine as antiulcerogenic, gastroprotective, diuretic agents [9]. In addition, Arapitsas [10] reported that okra seed was rich in phenolic compounds, mainly composed of flavonol derivatives and oligomeric catechins, suggesting that it might possess some antioxidant properties. However, little information on antioxidant capabilities of major phenolic compounds from okra seed is available.

Carbon tetrachloride (CCl₄), a well-known environmental biohazard, can be particularly toxic to liver. CCl₄-induced hepatic injury, a classic experimental model, has been extensively used to evaluate the potential of drugs and dietary antioxidants against the oxidative damage [11, 12]. The objectives of the study were to evaluate the antioxidant activity of major phenolic compounds *in vitro* and their effects on oxidative stress induced by carbon tetrachloride (CCl₄) in rat hepatocyte cell line.

2. Materials and Methods

2.1. Plant Materials. Okra pods (*Hibiscus esculentus* L.) were harvested from a commercial orchard in Guangzhou, Guangdong, China. The fruit were manually separated, and the seeds were collected, sun-dried, and pulverized to a powder. The materials were stored at room temperature in a desiccator until use.

2.2. Extraction, Isolation, and Purification. Dried seed powder of *H. esculentus* was exhaustively extracted with methanol at temperature (25–32°C) for 3 days. The extracts were concentrated with a rotary evaporator (RE52AA, Yarong Equipment Co., Shanghai, China) under reduced pressure at 55°C and then fractionated sequentially by petroleum ether and EtOAc. The extraction with petroleum ether was to eliminate the pigments. EtOAc extract was obtained by evaporation under reduced pressure and then subjected to purification by silica gel column using CHCl₃-MeOH solvent system with increased polarity (0:100–60:40) to yield eight fractions. We were only interested in the major phenolic compounds. Therefore, the largest fractions were further purified by silica gel column and Sephadex LH-20 to yield compound 1 and compound 2, respectively. Compound 1 and compound 2 were identified as quercetin 3-O-glucosyl (1 → 6) glucoside and quercetin 3-O-glucoside (Figure 1), by comparison of experimental and literature NMR data [13].

2.3. Determination of Total Phenol Content. Total phenol content of TPE in *H. esculentus* was determined by the Folin-Ciocalteu method [14]. Chlorogenic acid was used as a standard. The total phenol content was determined in triplicate and expressed as chlorogenic acid equivalents in mg/g of plant material.

2.4. Evaluation of Antioxidant Activities. Antioxidant capabilities of total phenolic extracts and their major component

from okra were evaluated according to the described methods by Duan et al. [15] with minor modifications. To evaluate DPPH scavenging, 0.1 mL various concentrations of samples were mixed with 2.9 mL 0.1 mM DPPH-methanol solution. After 30 min of incubation at 25°C in the dark, the absorbance at 517 nm was measured. DPPH radical scavenging activity of the samples was calculated using the following formula: DPPH scavenging activity (%) = [1 – (absorbance of sample – absorbance of blank)/absorbance of control] × 100.

Superoxide radicals were generated by illuminating a solution containing riboflavin. The photoinduced reactions were performed at about 4000 lux. 25 μL various concentrations of sample were mixed with 3 mL reaction buffer [1.3 μM riboflavin, 13 mM methionine, 63 μM nitroblue tetrazolium (NBT), and 100 μM EDTA, pH 7.8]. The reaction solution was illuminated at 25°C for 15 min. The reaction mixture without sample was used as a control. The scavenging activity was calculated as follows: scavenging activity (%) = (1 – absorbance of sample/absorbance of control) × 100.

Hydroxyl radical scavenging activity was determined by evaluating inhibitory effect of samples on deoxyribose degradation. 0.2 mL different concentrations of samples were incubated with 1 mL reaction buffer (100 μM FeCl₃, 104 μM EDTA, 1.5 mM H₂O₂, 2.5 mM deoxyribose, and 100 μM L-ascorbic acid, pH 7.4) for 1 h at 37°C. After adding 1 mL 0.5% 2-thiobarbituric acid and 1 mL 2.8% trichloroacetic acid, the mixture was heated for 30 min at 80°C and then cooled on ice. The absorbance at 532 nm was measured. Percent inhibition of deoxyribose degradation was calculated as (1 – absorbance of sample/absorbance of control) × 100.

For the reducing power, 0.2 mL various concentrations of samples were incubated with 2.0 mL 200 mM sodium phosphate buffer (pH 6.6) and 2.0 mL 1% potassium ferricyanide at 50°C for 20 min. After adding 2.0 mL 10% trichloroacetic acid (w/v), the mixture was centrifuged at 4000 ×g for 5 min. 2.0 mL supernatant was mixed with 2.4 mL 0.016% ferric chloride, and the absorbance at 700 nm was measured. A higher absorbance indicates a higher reducing power.

2.5. Cell Culture and Cell Treatment. BRL-3A (rat hepatocyte) cell culture was obtained from Experimental Animal Center of Southern Medical University (Guangzhou, China). The cell line was cultured in RPMI-1640 medium containing 10% foetal bovine serum (FBS), 100 U/mL penicillin, and 100 mg/mL streptomycin at 37°C in an incubator of humidified air with 5% CO₂. Hepatocytes were seeded onto 24-well plates at 1 × 10⁵ cells/well and cultured for 24 h at 37°C under 5% CO₂. Later, the medium was removed and the hepatocytes were subjected to the following treatments: (1) pretreatment, the hepatocytes were first incubated with growth medium containing 100 μg/mL TPE, QG, or QDG for 4 h, and then the cells were washed and incubated with fresh growth medium containing 10 mM CCl₄ for another 4 h; (2) posttreatment, the hepatocytes were first incubated with growth medium containing 10 mM CCl₄ for 4 h, and then the cells were washed and incubated with fresh growth medium containing 100 μg/mL TPE, QG, or QDG for another 4 h.

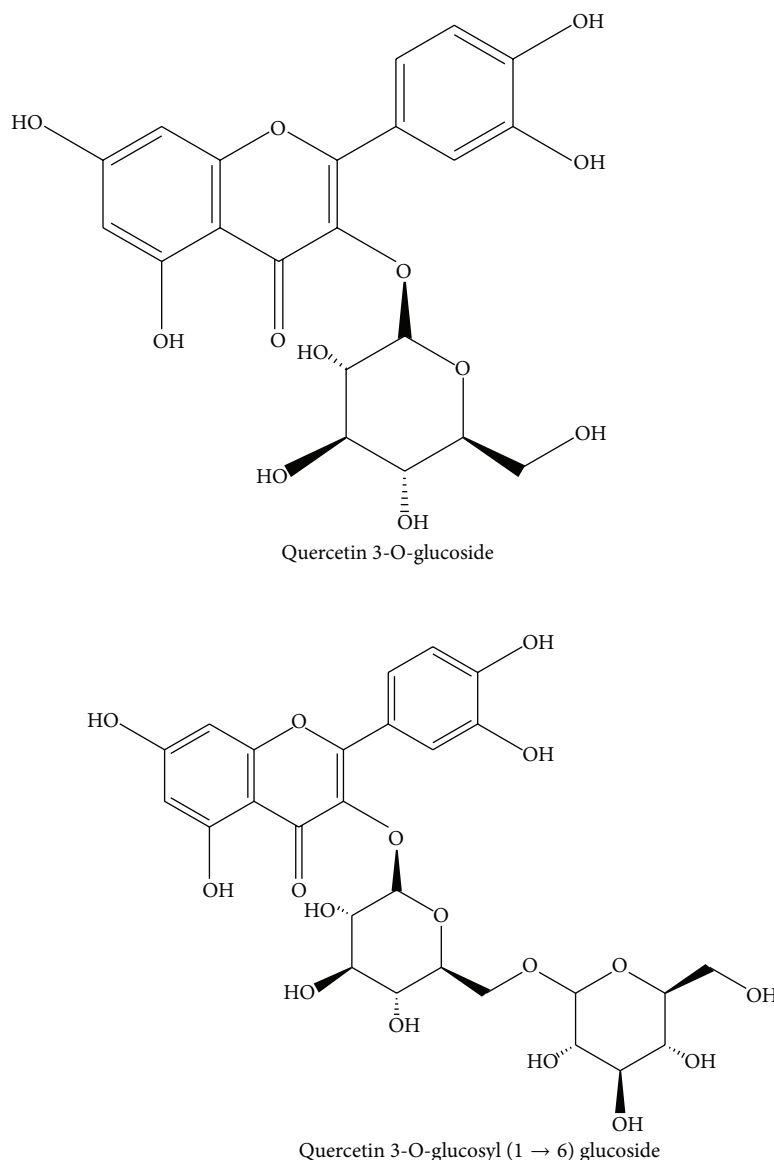


FIGURE 1: The chemical structures of the isolated compounds from *Hibiscus esculentus*. 1, quercetin 3-O-glucoside; 2, quercetin 3-O-glucosyl (1 → 6) glucoside.

2.6. Cell Viability. Cell viability of the hepatocytes was evaluated by MTT assay. After the cells were treated according to the above-mentioned method, the medium was removed and 20 μ L MTT solution (5 g/L) was added to each well of the 96-well plate. After 4 h of incubation at 37°C, the MTT solution was removed and 100 μ L dimethylsulphoxide (DMSO) was added to resolve the formazan generated from MTT. The absorbance of each well was recorded on a microplate reader (Thermo, MA, USA) at the wavelength of 490 nm. Cell viability in each test group and model group was expressed as percentage of the control group. The viability of cells in control group was considered as 100%.

2.7. MDA Content and Activities of GPT, GOT, SOD, and CAT. After the cells were treated according to the above-mentioned method, the supernatants were collected and assayed for malondialdehyde (MDA) content and

activities of glutamate pyruvate transaminase (GPT), glutamate oxalate transaminase (GOT), superoxide dismutase (SOD), and catalase (CAT) using commercial enzymatic kits from Nanjing Jiancheng Bioengineering Research Institute (Nanjing, China).

2.8. Statistical Analysis. All data were expressed as mean \pm standard deviation (SD). SPSS was used to analyze and report the data. The differences between the mean values of multiple groups were analyzed by one-way analysis of ANOVA with Duncan's Multiple Range Test. ANOVA data with $P < 0.05$ were classified as statistically significant.

3. Results and Discussions

3.1. Extraction of TPE and Purification of Major Constituent from *Hibiscus esculentus* Seed. *Hibiscus esculentus*

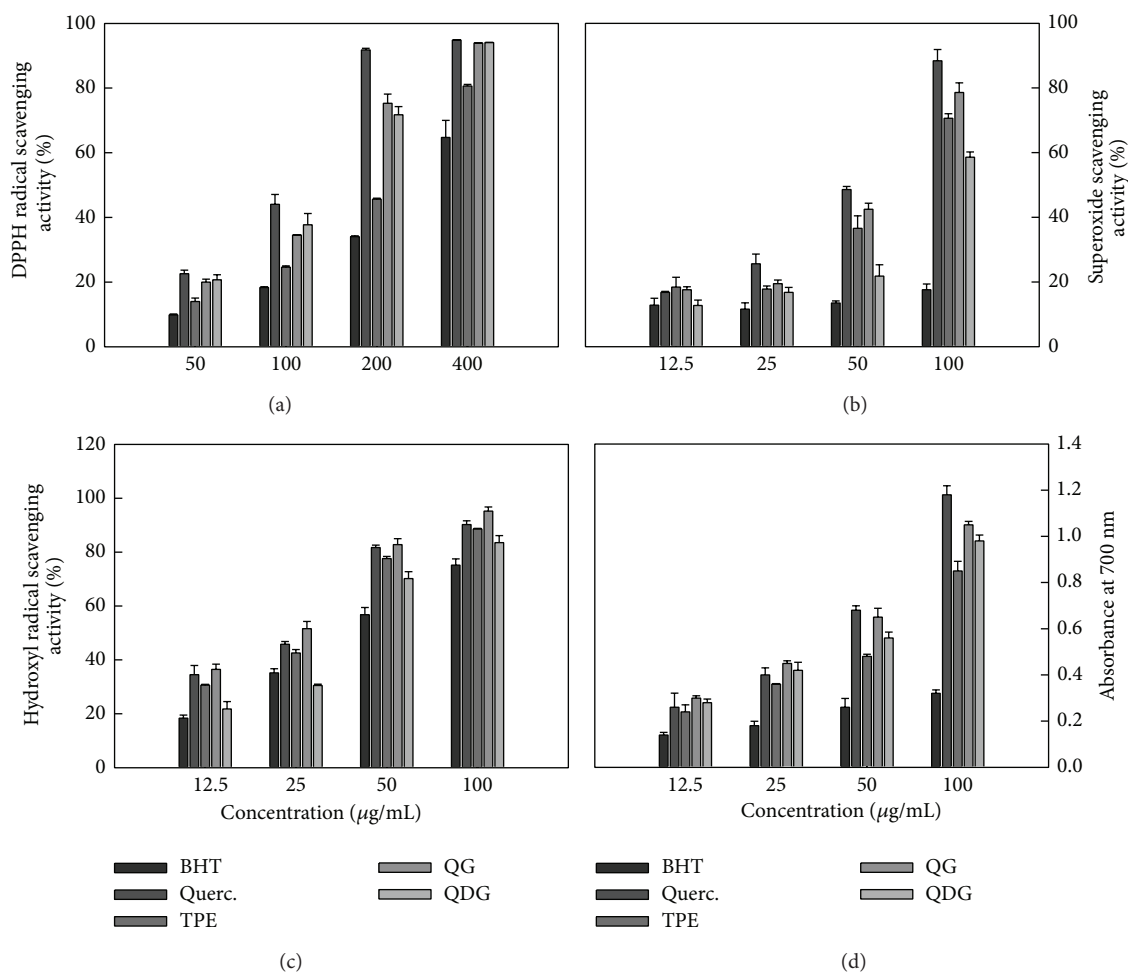


FIGURE 2: Free radical scavenging activities against DPPH radical (a), superoxide radical (b), and hydroxyl radical (c) and reducing power (d) of extract and isolated quercetin 3-O-glucoside and quercetin 3-O-diglucoside from *Hibiscus esculentus*.

seed was subjected to extraction with methanol and then sequential fractionation by petroleum ether and EtOAc. The extraction with petroleum ether was to eliminate the pigments. The EtOAc-soluble fraction was designated as total phenol extracts (TPE). The content of phenolic compounds in dry okra seed was 28.1 mg/g. Further, total phenol extracts (TPE) were purified and two major phenolic compounds were obtained and identified as quercetin 3-O-glucosyl (1 \rightarrow 6) glucoside (QDG) and quercetin 3-O-glucoside (QG) (Figure 1), by comparison of experimental and literature NMR data [13], which was consistent with the result reported by Arapitsas [10]. However, Atawodi et al. reported that quercetin glucoside was the only major polyphenol composition in okra seed [16]. The inconsistency might be associated with the differences in climate conditions of cultivation and/or the variety analyzed.

3.2. Antioxidant Activity of Total Phenolic Extracts (TPE) and Their Major Components from Okra Seeds In Vitro. Free radical scavenging activity is the most important mechanism by which antioxidants inhibit lipid peroxidation [1]. In this study, free radical scavenging activity against DPPH radical,

superoxide anions, and hydroxyl radical was analyzed to evaluate the antioxidant activities of total phenolic extracts (TPE) and their major components from okra seeds. In addition, reducing power, which exerts antioxidant action by breaking the free radical chain by donating a hydrogen atom, was investigated [15].

DPPH is a stable, purple, nitrogen-centered, and synthetic-free radical with the maximum wavelength of 517 nm. When the DPPH free radical is quenched, the color will fade away. The scavenging activity against DPPH free radical has been extensively used to evaluate antioxidant activity of plant extracts [17]. Figure 2(a) shows the scavenging activities against DPPH free radical of TPE, QG, and QDG from okra seed and BHT and quercetin. All tested samples exhibited the scavenging activities against DPPH free radical in a dose-dependent manner. The positive control quercetin and BHT had the highest and lowest scavenging activity against DPPH free radical, respectively. QG and QDG have almost an equivalent scavenging activity against DPPH free radical, but higher than TPE. At 100 $\mu\text{g/mL}$, the scavenging effects were 18.3%, 44.1%, 24.6%, 34.5%, and 37.3% for BHT, quercetin, TPE, QG, and QDG, respectively.

Superoxide anion, produced by a number of cellular reactions or enzymes, including iron-catalyzed Fenton reaction, lipoxygenases, peroxidase, NADPH oxidase, and xanthine oxidase, is the most important in organisms and is involved in the formation of other cell-damaging free radicals [1]. In the present study, TPE, QG, and QDG showed higher scavenging activity against superoxide anion than DPPH radical scavenging activity. Similarly, superoxide anion scavenging activities of TPE, QG, and QDG were stronger than that of BHT, but weaker than that of quercetin. At 50 $\mu\text{g/mL}$ and 100 $\mu\text{g/mL}$ of concentrations, the free radical scavenging activity of TPE was higher than that of QDG, but lower than that of QG (Figure 2(b))

Hydroxyl radical can be formed by the Fenton reaction in the presence of reduced transition metals and H_2O_2 , which is known to be the most reactive radical and is thought to initiate cell damage *in vivo* [18]. Similar to superoxide anion scavenging activity, TPE, QG, and QDG from okra seeds exhibited excellent hydroxyl radical scavenging activity in the following order: QG > TPE > QDG > BHT (Figure 2(c)).

Reducing power is widely used to evaluate the antioxidant activity of plant extracts. The reducing property indicates that the antioxidant compounds are electron donors and reduce the oxidized intermediates of lipid peroxidation process [19]. As shown in Figure 2(d), TPE, QG, and QDG from okra seeds showed much higher reducing power than BHT, suggesting that TPE, QG, and QDG possessed a stronger electron donating capacity. However, the reducing power of TPE, QG, and QDG was lower than that of quercetin at 100 $\mu\text{g/mL}$ of concentration. Furthermore, the reducing power of the extract and its major constituents from okra seed were in the following order: QG > QDG > TPE.

Overall, DPPH radical scavenging activity and reducing power of QG and QDG were higher than those of TPE; superoxide and hydroxyl radical scavenging activities of QG and TPE were higher than those of QDG; reducing power, superoxide anion, and hydroxyl radical scavenging activities of QG were higher than those of QDG. Moreover, the antioxidant activities investigated, except hydroxyl radical scavenging activity of quercetin, were higher than those of QG and QDG. It appeared that addition of glycosyl decreased the scavenging activity against DPPH free radical of quercetin and its derivatives. Some similar results were obtained by other researchers. Omololu et al. reported that quercetin had stronger scavenging activity against DPPH free radical than its rhamnosyl glucoside derivative [20]. Hopia and Heinonen investigated the antioxidant activities of quercetin and its selected glycosides in bulk methyl linoleate oxidized at 40°C and found that the order of activity of quercetin and its derivatives was quercetin > isoquercitrin > rutin [21]. Sun et al. also found that rhamnosidase could change rutin in asparagus juice to quercetin-3-glucoside, which has a higher antioxidant activity than rutin [22]. The possible reasons are as follows: (1) the steric effect by increased glycosylation decreased the accessibility of free radicals to flavonoid antioxidants; (2) the presence of a free 3-hydroxyl group in the C-ring is a requirement for the maximal radical scavenging activity of flavonoids and the substitution of the hydroxyl group by glycoside resulted in the decreases in free radical

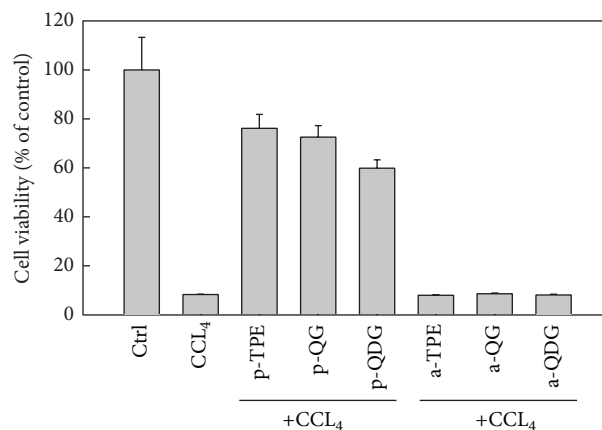


FIGURE 3: Effect of extract and isolated quercetin 3-O-glucoside and quercetin 3-O-diglucoside from *Hibiscus esculentus* on CCl_4 -induced cytotoxicity in rat hepatocytes. In the tick label, p means pretreatment while a means posttreatment.

scavenging ability and chelating activity to transition metal ions [21, 23]. In addition, QG and QDG played a dominant role in scavenging activity against superoxide anion and hydroxyl radical of total phenolic compounds of okra seed. In some plant flavonoids, quercetin 3-O-glucoside contributed to the major of antioxidant activities [24–27].

3.3. Effect of TPE, QG, and QDG on Cell Viability of Hepatocytes Injured by CCl_4 . It is well known that cell damage induced by reactive oxygen species (ROS) is an important mechanism of hepatotoxicity [28]. Tetrachloride (CCl_4) has been widely used to study liver injury induced by ROS in the mouse model. The mechanism is involved in free radicals generated during CCl_4 metabolism by hepatic cellular cytochrome P450, including trichloromethyl (CCl_3 and/or CCl_3O_2) and oxygen-centered lipid radicals (LO and/or LOO), which initiate the process of lipid peroxidation [29]. Kikkawa et al. suggested that *in vitro* primary cell culture system would be sufficient to detect hepatotoxicity in the early stage of drug discovery according to the relevance of *in vitro* system to *in vivo* system from some biomarkers related to oxidative stress by carbon tetrachloride [12]. In the present study, CCl_4 treatment resulted in a significant decrease in cell viability of the hepatocytes. After 4 h of incubation, the cell viability decreased to 8.3% compared with the control, indicating that the hepatocytes were severely injured. TPE, QG, and QDG pretreatments efficiently alleviated oxidative injury of the cell induced by CCl_4 . The cell viabilities of hepatocytes pretreated with TPE, QG, and QDG were 76.2%, 72.5%, and 59.9%, respectively (Figure 3). However, posttreatment with TPE, QG, and QDG had no significant protective effect on oxidative injury of the cells caused by CCl_4 . These results suggest that the extract and its major constituents can be potentially used for preventing rather than curing liver diseases in mammals. A similar result also was reported in fish hepatocytes by Yin et al. [30].

Antioxidants play an important role in protecting against CCl_4 -induced liver injury. There were some reports on the

protective effects of various natural products against CCl_4 -induced liver injury [30–36]. The protective effects might be related to the directed superoxide anion and hydroxyl radical scavenging activity. In our study, superoxide anion and hydroxyl radical scavenging activities were in the following order: $\text{QG} > \text{TPE} > \text{QDG}$, which was inconsistent with the protective effects. Possibly, the discrepancy could be related to differential uptake by hepatocytes or synergistic effects. Boyer et al. [37] reported that there existed a great difference in uptake of quercetin aglycon and quercetin 3-glucoside as purified compounds and from whole onion and apple peel extracts by Caco-2 cells. Yang and Liu [38] also found that apple extracts plus quercetin 3- β -D-glucoside combination possess a synergistic effect in MCF-7 cell proliferation.

3.4. Effect of TPE, QG, and QDG on Lipid Peroxidation and Activities of GPT and GOT in Hepatocytes Injured by CCl_4 . Malondialdehyde (MDA), a lipid peroxidized product, can reflect the extent of lipid peroxidation induced by oxidative stress. As shown in Figure 4, a significant increase in MDA level was observed in the CCl_4 -treated hepatocytes compared with the control hepatocytes. However, TPE, QG, and QDG treatments at $100 \mu\text{g}/\text{mL}$ significantly decreased the level of lipid peroxidation induced by CCl_4 . The results were in accordance with the cell viability, indicating that the protective effects of TPE, QG, and QDG on CCl_4 -induced hepatocytes injury were related to the alleviated lipid peroxidation.

GPT and GOT were widely used to evaluate liver damage by CCl_4 [30]. In the present study, significantly elevated GPT and GOT activities were observed in the supernatants of the CCl_4 -treated hepatocytes, which might be associated with the increased permeability of the hepatocytes and cellular leakage. Pretreatments with TPE, QG, and QDG significantly decreased the values of GPT and GOT activities (Figure 5), indicating that the extract and its major constituents from okra seed could maintain the functional integrity of the hepatocyte membrane, thus protecting the hepatocytes against CCl_4 -mediated toxicity.

3.5. Effect of TPE, QG, and QDG on Activities of SOD and CAT in Hepatocytes Injured by CCl_4 . Lipid peroxidation is the result of the excessive accumulation of ROS due to the altered balance between ROS generation and elimination in organism [39]. To control the level of ROS and protect cells against oxidative injury, organisms have developed an enzymatic antioxidant system and low molecular antioxidants [1]. Superoxide dismutase (SOD) is an important defense enzyme that catalyzes the dismutations of superoxide radicals to hydrogen peroxide while catalase (CAT) is involved in eliminating H_2O_2 . As shown in Figure 6(a), CCl_4 treatment alone resulted in a significant decrease in SOD activity of hepatocytes, as compared with the control. However, TPE, QG, and QDG pretreatments restored SOD activities in contrast to the CCl_4 -treated hepatocytes, which were beneficial in scavenging the superoxide anion and alleviating lipid peroxidation. There were no significant differences in SOD activities among TPE, QG, and QDG pretreated hepatocytes. Moreover, TPE, QG, and QDG posttreatments

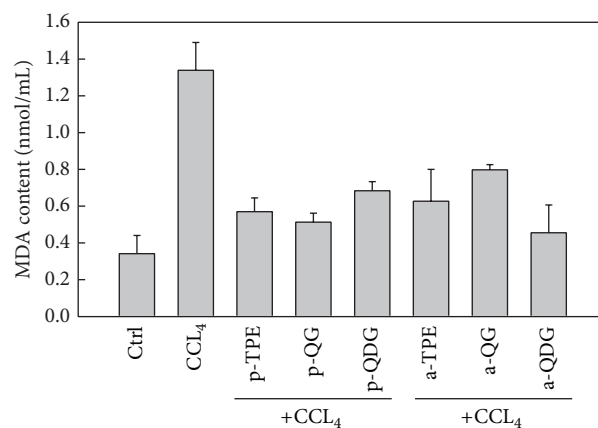


FIGURE 4: Effect of extract and isolated quercetin 3-O-glucoside and quercetin 3-O-diglucoside from *Hibiscus esculentus* on lipid peroxidation in the cell culture of hepatocytes injured by addition of CCl_4 *in vitro*. In the tick label, p means pretreatment while a means posttreatment.

also induced SOD activities in the CCl_4 pretreated hepatocytes (Figure 6(a)). Similarly, CAT activities in the CCl_4 -treated hepatocytes also were restored by TPE, QG, and QDG pretreatments. Even the same level of CAT activity, as compared with the control, was found in TPE-treated hepatocytes, which was higher than those in QG and QDG pretreated hepatocytes. CAT activities were partially restored by these treatments (Figure 6(b)).

Possibly, the alleviated biomacromolecule oxidation and elevated cell viability require synergic action of different antioxidant enzymes. There were some reports on the induced activities of antioxidant enzymes by natural products that played an important role in alleviating lipid peroxidation and decreasing the injury caused by CCl_4 [30, 31, 34, 36]. In the present study, both SOD and CAT activities were induced by pretreatments or posttreatments with TPE, QG, and QDG. However, posttreatment with TPE, QG, and QDG had no significant protective effect on oxidative injury of the cells caused by CCl_4 . Therefore, it is considered that the induced SOD and CAT activities by posttreatment with TPE, QG, and QDG could not repair the damaged hepatocytes.

4. Conclusions

Two major flavonoids, quercetin 3-O-diglucoside (QDG) and quercetin 3-O-glucoside (QG), were isolated and identified from okra seeds. QG, QDG, and the total phenolic extracts (TPE) from okra seeds showed excellent antioxidant activity *in vitro*, including reducing power and free radical scavenging capabilities against α, α -diphenyl- β -picrylhydrazyl (DPPH) radical, superoxide anion, and hydroxyl radical, which were much stronger than those of BHT, a widely used synthetic antioxidant. DPPH radical scavenging activity and reducing power of QG and QDG were higher than those of TPE while superoxide and hydroxyl radical scavenging activities of QG and TPE were higher than those of QDG. Moreover, reducing power, superoxide anion, and hydroxyl radical

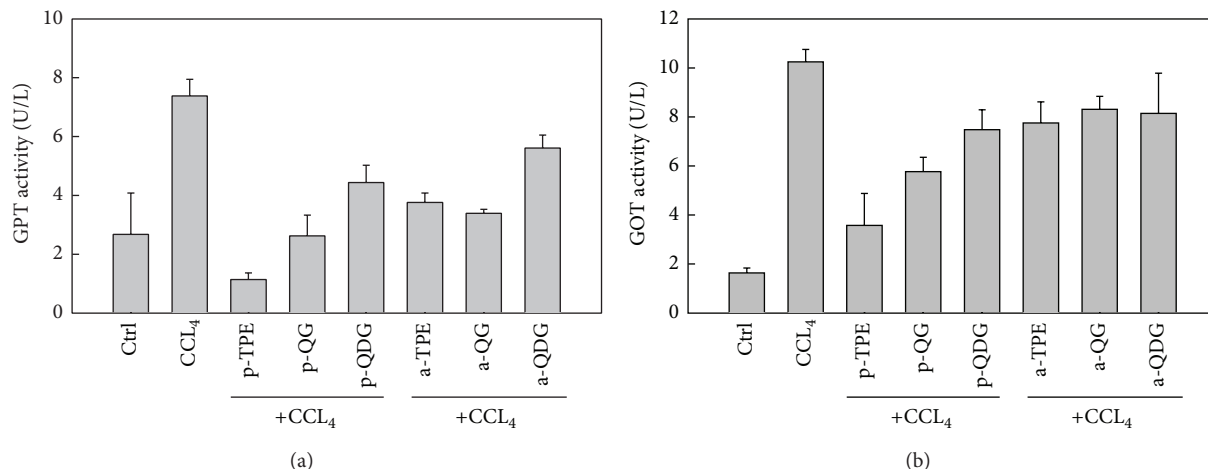


FIGURE 5: Effect of extract and isolated quercetin 3-O-glucoside and quercetin 3-O-diglucoside from *Hibiscus esculentus* on the activities of GPT (a) and GOT (b) in the cell culture of hepatocytes injured by addition of CCl₄ *in vitro*. In the tick label, p means pretreatment while a means posttreatment.

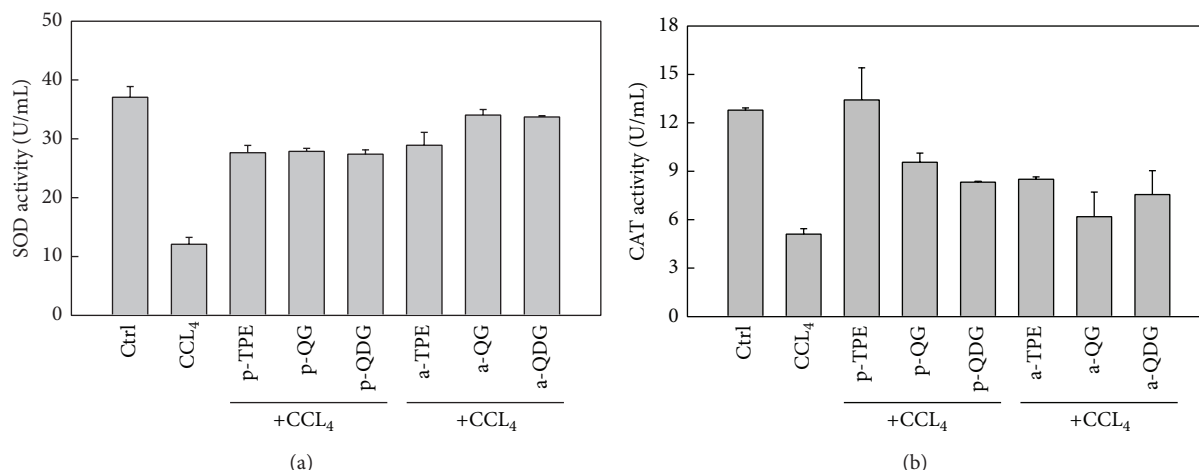


FIGURE 6: Effect of extract and isolated quercetin 3-O-glucoside and quercetin 3-O-diglucoside from *Hibiscus esculentus* on the activities of SOD (a) and CAT (b) in the cell culture of hepatocytes injured by addition of CCl₄ *in vitro*. In the tick label, p means pretreatment while a means posttreatment.

scavenging activities of QG were higher than those of QDG. Furthermore, TPE, QG, and QDG pretreatments significantly alleviated the cytotoxicity of CCl₄ on rat hepatocytes, with attenuated lipid peroxidation, increased SOD and CAT activities, and decreased GPT and GOT activities. The protective effects of TPE and QG on rat hepatocytes were stronger than that of QDG. However, the cytotoxicity of CCl₄ on rat hepatocytes was not affected by TPE, QG, and QDG posttreatments. It was suggested that the protective effects of TPE, QG, and QDG on rat hepatocyte against oxidative stress were related to the direct antioxidant activity and the induced activities of antioxidant enzymes. However, further investigation is required to evaluate protective effects of total phenolic extracts (TPE) and their major components from okra seeds on carbon tetrachloride-induced hepatotoxicity *in vivo*.

Conflict of Interests

The authors declare that there is no conflict of interests regarding the publication of this paper.

Authors' Contribution

Lianmei Hu and Wenlan Yu contributed equally to this work.

Acknowledgments

This work was supported by Science and Technology Planning Project of Guangdong Province, China (Grant no. 2011B020306009), the Knowledge Innovation Program of the Chinese Academy of Sciences (Grant no. KSCX2-EW-Q-8-1), and National Natural Science Foundation of China (Grant no. 31171778).

References

- [1] O. Blokhina, E. Virolainen, and K. V. Fagerstedt, "Antioxidants, oxidative damage and oxygen deprivation stress: a review," *Annals of Botany*, vol. 91, no. 2, pp. 179–194, 2003.
- [2] J. Moskovitz, M. B. Yim, and P. B. Chock, "Free radicals and disease," *Archives of Biochemistry and Biophysics*, vol. 397, no. 2, pp. 354–359, 2002.
- [3] M. G. Simic, "Mechanisms of inhibition of free-radical processes in mutagenesis and carcinogenesis," *Mutation Research*, vol. 202, no. 2, pp. 377–386, 1988.
- [4] K. N. Prasad, H. H. Xie, J. Hao et al., "Antioxidant and anticancer activities of 8-hydroxy-psoralen isolated from wampee [*Clauseria lansium* (Lour.) Skeels] peel," *Food Chemistry*, vol. 118, no. 1, pp. 62–66, 2010.
- [5] M. Soory, "Nutritional antioxidants and their applications in cardiometabolic diseases," *Infectious Disorders*, vol. 12, no. 5, pp. 388–401, 2012.
- [6] H. Y. Aboul-Enein, P. Berczynski, and I. Kruk, "Phenolic compounds: the role of redox regulation in neurodegenerative disease and cancer," *Mini-Reviews in Medicinal Chemistry*, vol. 13, no. 3, pp. 385–398, 2013.
- [7] N. Sengkhamparn, R. Verhoef, H. A. Schols, T. Sajjaanantakul, and A. G. J. Voragen, "Characterisation of cell wall polysaccharides from okra (*Abelmoschus esculentus* (L.) Moench)," *Carbohydrate Research*, vol. 344, no. 14, pp. 1824–1832, 2009.
- [8] O. J. Oyelade, B. I. O. Ade-Omowaye, and V. F. Adeomi, "Influence of variety on protein, fat contents and some physical characteristics of okra seeds," *Journal of Food Engineering*, vol. 57, no. 2, pp. 111–114, 2003.
- [9] I. Gürbüz, O. Üstün, E. Yesilada, E. Sezik, and O. Kutsal, "Anti-ulcerogenic activity of some plants used as folk remedy in Turkey," *Journal of Ethnopharmacology*, vol. 88, no. 1, pp. 93–97, 2003.
- [10] P. Arapitsas, "Identification and quantification of polyphenolic compounds from okra seeds and skins," *Food Chemistry*, vol. 110, no. 4, pp. 1041–1045, 2008.
- [11] S. Basu, "Carbon tetrachloride-induced lipid peroxidation: eicosanoid formation and their regulation by antioxidant nutrients," *Toxicology*, vol. 189, no. 1-2, pp. 113–127, 2003.
- [12] R. Kikkawa, M. Fujikawa, T. Yamamoto, Y. Hamada, H. Yamada, and I. Horii, "In vivo hepatotoxicity study of rats in comparison with in vitro hepatotoxicity screening system," *The Journal of Toxicological Sciences*, vol. 31, no. 1, pp. 23–34, 2006.
- [13] G. H. Shui and L. L. Peng, "An improved method for the analysis of major antioxidants of *Hibiscus esculentus* Linn," *Journal of Chromatography A*, vol. 1048, no. 1, pp. 17–24, 2004.
- [14] V. L. Singleton and J. A. Rossi, "Colorimetry of total phenolics with phosphomolybdic-phosphotungstic acid reagents," *American Journal of Enology and Viticulture*, vol. 16, no. 3, pp. 144–158, 1965.
- [15] X. W. Duan, Y. M. Jiang, X. G. Su, Z. Q. Zhang, and J. Shi, "Antioxidant properties of anthocyanins extracted from litchi (*Litchi chinensis* Sonn.) fruit pericarp tissues in relation to their role in the pericarp browning," *Food Chemistry*, vol. 101, no. 4, pp. 1365–1371, 2007.
- [16] S. E. Atawodi, J. C. Atawodi, G. A. Idakwo et al., "Polyphenol composition and antioxidant potential of *Hibiscus esculentus* L. fruit cultivated in Nigeria," *Journal of Medicinal Food*, vol. 12, no. 6, pp. 1316–1320, 2009.
- [17] C. Sánchez-Moreno, "Review: methods used to evaluate the free radical scavenging activity in foods and biological systems," *Food Science and Technology International*, vol. 8, no. 3, pp. 121–137, 2002.
- [18] E. Rollet-Labelle, M.-J. Grange, C. Elbim, C. Marquetty, M.-A. Gougerot-Pocidalo, and C. Pasquier, "Hydroxyl radical as a potential intracellular mediator of polymorphonuclear neutrophil apoptosis," *Free Radical Biology and Medicine*, vol. 24, no. 4, pp. 563–572, 1998.
- [19] K. H. S. Farvin and C. Jacobsen, "Phenolic compounds and antioxidant activities of selected species of seaweeds from Danish coast," *Food Chemistry*, vol. 138, no. 2-3, pp. 1670–1681, 2013.
- [20] P. A. Omololu, J. B. T. Rocha, and I. J. Kade, "Attachment of rhamnosyl glucoside on quercetin confers potent iron-chelating ability on its antioxidant properties," *Experimental and Toxicologic Pathology*, vol. 63, no. 3, pp. 249–255, 2011.
- [21] A. Hopia and M. Heinonen, "Antioxidant activity of flavonol aglycones and their glycosides in methyl linoleate," *Journal of the American Oil Chemists' Society*, vol. 76, no. 1, pp. 139–144, 1999.
- [22] T. Sun, J. R. Powers, and J. Tang, "Enzyme-catalyzed change of antioxidants content and antioxidant activity of asparagus juice," *Journal of Agricultural and Food Chemistry*, vol. 55, no. 1, pp. 56–60, 2007.
- [23] K. E. Heim, A. R. Tagliaferro, and D. J. Bobilya, "Flavonoid antioxidants: chemistry, metabolism and structure-activity relationships," *The Journal of Nutritional Biochemistry*, vol. 13, no. 10, pp. 572–584, 2002.
- [24] M. J. Piao, E. S. Yoo, Y. S. Koh et al., "Antioxidant effects of the ethanol extract from flower of *Camellia japonica* via scavenging of reactive oxygen species and induction of antioxidant enzymes," *International Journal of Molecular Sciences*, vol. 12, no. 4, pp. 2618–2630, 2011.
- [25] M. de Nisco, M. Manfra, A. Bolognese et al., "Nutraceutical properties and polyphenolic profile of berry skin and wine of *Vitis vinifera* L. (cv. Aglianico)," *Food Chemistry*, vol. 140, no. 4, pp. 623–629, 2013.
- [26] R. Garcia-Mateos, L. Aguilar-Santelises, M. Soto-Hernandez, and R. Nieto-Angel, "Flavonoids and antioxidant activity of flowers of Mexican *Crataegus* spp.," *Natural Product Research*, vol. 27, no. 9, pp. 834–836, 2013.
- [27] A. M. Mendoza-Wilson, M. E. Armenta-Vazquez, S. I. Castro-Arredondo et al., "Potential of polyphenols from an aqueous extract of apple peel as inhibitors of free radicals: an experimental and computational study," *Journal of Molecular Structure*, vol. 1035, pp. 61–68, 2013.
- [28] E. A. Ferreira, E. F. Gris, K. B. Felipe et al., "Potent hepatoprotective effect in CCl₄-induced hepatic injury in mice of phloracetophenone from *Myrcia multiflora*," *Libyan Journal of Medicine*, vol. 5, no. 1, 2010.
- [29] X.-W. Li, R. Zhu, B. Li et al., "Mechanism underlying carbon tetrachloride-inhibited protein synthesis in liver," *World Journal of Gastroenterology*, vol. 16, no. 31, pp. 3950–3956, 2010.
- [30] G. J. Yin, L. P. Cao, P. Xu, G. Jeney, and M. Nakao, "Hepatoprotective and antioxidant effects of *Hibiscus sabdariffa* extract against carbon tetrachloride-induced hepatocyte damage in *Cyprinus carpio*," *In Vitro Cellular and Developmental Biology*, vol. 47, no. 1, pp. 10–15, 2011.
- [31] Y. Wu, L. Li, T. Wen, and Y.-Q. Li, "Protective effects of echinacoside on carbon tetrachloride-induced hepatotoxicity in rats," *Toxicology*, vol. 232, no. 1-2, pp. 50–56, 2007.
- [32] J.-Y. Zhong, H.-Q. Cong, and L.-H. Zhang, "Inhibitory effects of grape procyanidins on free radical-induced cell damage in

- rat hepatocytes *in vitro*," *World Journal of Gastroenterology*, vol. 13, no. 19, pp. 2752–2755, 2007.
- [33] J.-F. Ye, H. Zhu, Z.-F. Zhou et al., "Protective mechanism of andrographolide against carbon tetrachloride- induced acute liver injury in mice," *Biological and Pharmaceutical Bulletin*, vol. 34, no. 11, pp. 1666–1670, 2011.
- [34] S. Ilavenil, B. Kaleeswaran, and S. Ravikumar, "Protective effects of lycorine against carbon tetrachloride induced hepatotoxicity in Swiss albino mice," *Fundamental & Clinical Pharmacology*, vol. 26, no. 3, pp. 393–401, 2012.
- [35] W. Jiang, M. Gao, S. A. Sun et al., "Protective effect of L-theanine on carbon tetrachloride-induced acute liver injury in mice," *Biochemical and Biophysical Research Communications*, vol. 422, no. 2, pp. 344–350, 2012.
- [36] S. Zhang, B. N. Lu, X. Han et al., "Protection of the flavonoid fraction from *Rosa laevigata* Michx fruit against carbon tetrachloride-induced acute liver injury in mice," *Food and Chemical Toxicology*, vol. 55, pp. 60–69, 2013.
- [37] J. Boyer, D. Brown, and H. L. Rui, "Uptake of quercetin and quercetin 3-glucoside from whole onion and apple peel extracts by Caco-2 cell monolayers," *Journal of Agricultural and Food Chemistry*, vol. 52, no. 23, pp. 7172–7179, 2004.
- [38] J. Yang and R. H. Liu, "Synergistic effect of apple extracts and quercetin 3- β -D-glucoside combination on antiproliferative activity in MCF-7 human breast cancer cells *in vitro*," *Journal of Agricultural and Food Chemistry*, vol. 57, no. 18, pp. 8581–8586, 2009.
- [39] D. Trachootham, W. Lu, M. A. Ogasawara, N. R.-D. Valle, and P. Huang, "Redox regulation of cell survival," *Antioxidants & Redox Signaling*, vol. 10, no. 8, pp. 1343–1374, 2008.